

30th Annual Meeting North American Skull Base Society

Rapid Evolution in the Healthcare Ecosystem: Becoming Frontiers

February 7–9, 2020

La Cantera Resort & Spa

San Antonio, Texas

EXECUTIVE COMMITTEE

Ricardo Carrau, MD
President

John Golfinos, MD
President-Elect

Lee Zimmer, MD
Vice President

Siviero Agazzi, MD, MBA
Secretary

Adam Zanation, MD
Treasurer

James Evans, MD
Immediate Past President

SCIENTIFIC PROGRAM COMMITTEE

Ricardo Carrau, MD
President

Adam Zanation, MD
Co-Chair

Daniel Prevedello, MD
Co-Chair

Paul Gardner, MD
Pre Meeting Course Co-Chair

Arturo Solares, MD
Pre Meeting Course Co-Chair

James Evans, MD
Immediate Past President

Moises Arriaga, MD
Christine Klatt-Cromwell, MD

Derrick Lin, MD

Kibwei McKinney, MD

Carlos Pinheiro-Neto, MD

Christopher Rassekh, MD

Shaan Raza, MD

Deanna Sasaki-Adams, MD

Tonya Stefko, MD

Brian Thorp, MD

Jamie Van Gompel, MD

DIRECTORS AT LARGE

Amir Dehdashti, MD

Anderson Eloy, MD

Rick Freidman, MD

Derrick Lin, MD

Erin McKean, MD

Kris Moe, MD

Danny Prevedello, MD

Shaan Raza, MD

Zoukaa Sargi, MD

Jeff Sorenson, MD

Allan Vescan, MD

BOARD OF ADVISORS

Ehab Hanna, MD

Michael Link, MD

Jacques Morcos, MD

Carl Snyderman, MD

Ian Witterick, MD



The North American Skull Base Society would like to recognize and thank the following companies for their support:

Educational Grant Support

<i>Diamond Sponsor</i>	<i>Platinum Sponsor</i>	<i>Gold Sponsor</i>	<i>Silver Sponsors</i>
Mizuho America, Inc.	Medtronic	DePuy Synthes	KARL STORZ Endoscopy-America, Inc. Olympus America, Inc.

Bronze Sponsors
SPIWay, LLC

Educational Grant
Cook Medical

Marketing Support
Diamond Level
Stryker

Equipment

Apex Medical, Inc.	KLS Martin	Stryker
Carl Zess Meditec, Inc.	Medtronic	
	Mizuho America, Inc.	

2020 Exhibitors

ACE Medical Company	KARL STORZ Endoscopy- America, Inc.	Olympus America, Inc.
Acoustic Neuroma Association	Kelyniam Global, Inc.	OssDsign USA, Inc.
American Surgical Company	Kirwan Surgical Products LLC	Peter Lazic US, Inc.
Apex Medical, Inc.	KLS Martin	SPIWay, LLC
Brainlab	Koven Technology, Inc.	Stryker
Black Forest Medical Group	Medtronic	Surgical Theater
Cook Medical	Mizuho America, Inc.	Sutter Medical USA
DePuy Synthes	NICO Corporation	Synaptive Medical
Elliquence	Nova Surgical Innovations, Inc.	TAKAYAMA/MUTOH
Haag-Streit USA	NSK America Corp.	Thieme Medical Publishers, Inc.
Inomed, Inc.		Zimmer Biomet
Integra LifeSciences		

s1 Presentation Abstracts

I-1 Author Index

Some of the product names, patents, and registered designs referred to in this publication are in fact registered trade marks or proprietary names even though specific reference to this fact is not always made in the text. Therefore, the appearance of a name without designation as proprietary is not to be construed as a representation by the Publisher that it is in the public domain.

All rights, including the rights of publication, distribution, and sales, as well as the right to translation, are reserved. No part of this work covered by the copyrights hereon may be reproduced or copied in any form or by any means—graphic, electronic, or mechanical, including photocopying, recording, taping, or information and retrieval systems—without written permission of the Publisher.

Important Note: Medical knowledge is ever-changing. As new research and clinical experience broaden our knowledge, changes in treatment and drug therapy may be required. The authors and editors of the material herein have consulted sources believed to be reliable in their efforts to provide information that is complete and in accord with the standards accepted at the time of publication. However, in view of the possibility of human error by the authors, editors,

or publisher of the work herein, or changes in medical knowledge, neither the authors, editors, or publisher, nor any other party who has been involved in the preparation of this work, warrants that the information contained herein is in every respect accurate or complete, and they are not responsible for any errors or omissions or for the results obtained from use of such information. Because of rapid advances in the medical sciences, independent verification of diagnoses and drug dosages should be made. Readers are encouraged to confirm the information contained herein with other sources. For example, readers are advised to check the product information sheet included in the package of each drug they plan to administer to be certain that the information contained in this publication is accurate and that changes have not been made in the recommended dose or in the contraindications for administration. This recommendation is of particular importance in connection with new or infrequently used drugs.

Although all advertising material is expected to conform to ethical (medical) standards, inclusion in this journal does not constitute a guarantee or endorsement of the quality or value of such product or of claims made by its manufacturer.

Presentation Abstracts

J Neurol Surg B 2020;81(suppl S1):S1–S272.

Oral Presentations

A001. Primary Visual Cortical Thickness Correlates with Visual Field Defects in Patients with Pituitary Macroadenomas: A Structural 7-Tesla Retinotopic Analysis

John W. Rutland¹, Bradley N. Delman¹, Kuang-Han Huang¹, Gaurav Verma¹, Noah C. Benson², Dillan F. Villavisanis¹, Hung-Mo Lin¹, Joshua B. Bederson¹, James Chelnis¹, Priti Balchandani¹, Raj K. Shrivastava¹

¹Icahn School of Medicine at Mount Sinai, New York, New York, United States

²New York University, New York, New York, United States

Introduction: Vision loss remains a debilitating complication of pituitary adenomas, although there is considerable variability in visual impairment before and after decompression surgery. Growing evidence suggests secondary damage to remote visual structures may contribute to vision loss in patients with chiasmatic compression. The present study leverages ultrahigh field 7-T MRI to study the retinotopic organization of the primary visual cortex (V1), and correlates visual defects with cortical thinning in V1 to characterize consequences of pituitary adenomas on the posterior visual system.

Methods: Eight patients (four males, mean age = 44.3 years) with pituitary adenomas, and eight matched healthy controls (four males, mean = 43.3 years) were scanned at 7-T MRI for prospective study. Whole-brain cortical thickness was calculated using an automated algorithm. A previously published surface-based algorithm was applied to associate the eccentricity and polar angle with each position in V1 (Fig. 1). Cortical thickness was calculated at each point in the retinotopic organization, and cortical thickness ratio was generated against matched controls for each point in the visual fields. Adenoma patients additionally underwent neurophthalmological examination including 24–2 Humphrey's automated visual field perimetry. Pattern deviation (PD) of each point in the visual field, the deviation in point-detection compared with normals, was correlated with cortical thickness at corresponding polar and eccentricity angles in V1.

Results: Whole-brain cortical thickness was successfully derived for all patients and controls. The mean tumor volume was 19.4 cm³. The median global thickness of V1 did not differ between patients (mean ± SD = 2.21 ± 0.12 cm), compared with controls (2.06 ± 0.13 cm), $p > 0.05$. Surface morphometry-based retinotopic maps revealed that all eight adenoma patients showed a significant positive correlation between PD and V1 thickness ratios (r -values range, 0.31–0.46), $p < 0.05$ (Figs. 2 and 3). Mixed procedure analysis revealed that $PD = -8.0719 + 5.5873 \times (\text{median V1 thickness ratio})$.

Conclusion: All eight patients showed significant positive correlations between V1 thickness and visual defect. These findings provide retinotopic of localized V1 cortical

neurodegeneration spatially corresponding to impairments in the visual field (Fig. 4). These results further characterize changes in the posterior visual pathway associated with chiasmatic compression, and may prove useful in the neuro-ophthalmological workup for patients with pituitary macroadenoma.

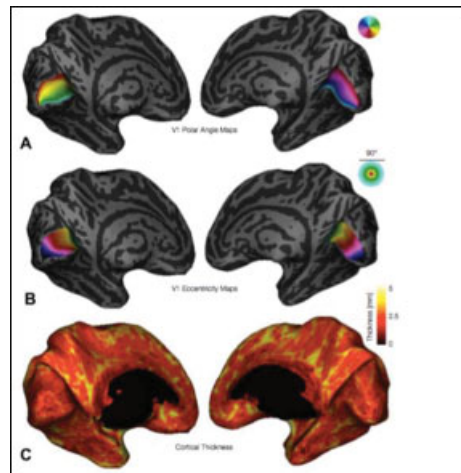


Figure 1. Inflated 3D cortical surfaces showing (A) polar angles, (B) eccentricities, and (C) cortical thickness. Legends for polar angle and eccentricity (upper right corner of panels A and B) plot the visual field, up to 45° of eccentricity, centered at the fovea; colors plotted on cortex indicate the position in the visual field of the cortical population receptive field center; for example, in panel A (polar angle maps) the lower vertical meridian / dorsal lip of V1 is colored red while the upper vertical meridian / ventral lip of V1 is cyan.

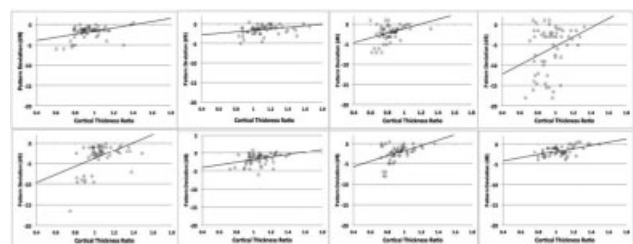


Figure 2. Pearson correlations showing the relationship between median V1 thickness ratio and pattern deviation in the eight patients with pituitary adenomas.

Subject No.	Pearson Coefficient	p-value
1	0.39	0.003
2	0.311	0.02
3	0.366	0.006
4	0.306	0.022
5	0.462	< 0.001
6	0.34	0.001
7	0.445	< 0.001
8	0.53	< 0.001

Figure 3. Pearson correlation coefficients and corresponding p-values between primary visual cortical thickness ratios and pattern deviation values in the eight patients with pituitary adenoma.

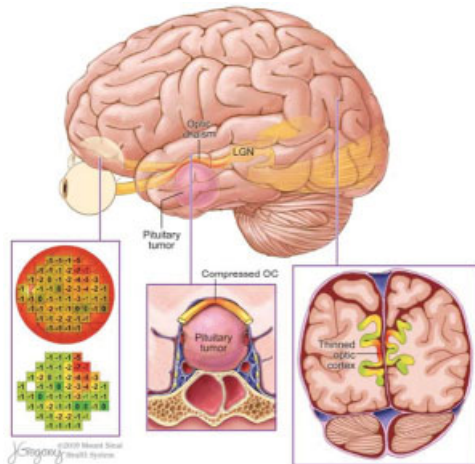


Figure 4. Rendering of a pituitary adenoma causes optic chiasm compression and retinotopic thinning in V1. Areas of visual field defect and corresponding regions of V1 thinning are shown in red.

A002. 7-Tesla Diffusion-Weighted MRI Apparent Diffusion Coefficient for Preoperative Evaluation of Pituitary Adenoma Consistency

John W. Rutland¹, Joshua Loewenstern¹, Daniel Ranti¹, Nadejda Tsankova¹, Joshua B. Bederson¹, Bradley N. Delman¹, Priti Balchandani¹, Raj K. Shrivastava¹

¹Icahn School of Medicine at Mount Sinai, New York, New York, United States

Background: Endoscopic surgery is an effective treatment strategy for pituitary adenomas; however, intrinsic tumor properties, including tumor consistency, can preclude gross total resection. Preoperative characterization of tumor consistency is useful and can guide surgical approach and help predict extent of resection. Advanced radiological modalities, such as 7-Tesla (T) diffusion-weighted imaging (DWI), may be useful in probing biological tissue properties of pituitary adenomas. The objective of the present study was to examine 7-T DWI as a novel method of measuring pituitary adenoma consistency (Fig. 1).

Methods: Thirteen patients with pituitary adenoma were scanned at 7-T MRI, which included a DWI acquisition. Regions of interest were drawn to calculate average tumor apparent diffusion coefficient (ADC). Tumor ADC was normalized to adjacent temporal gray matter ADC. All patients underwent surgical resection, and a single neurosurgeon rated tumor firmness from 1 (least firm) to 5 (most firm). Tumor specimens were evaluated for cellularity (H&E), collagen content (trichrome), and vascularity (CD31 stain) by a

neuropathologist. Extent of resection was determined through intraoperative observation and postoperative MRI. Tumor ADC was correlated with intraoperative consistency rating, histopathology, and extent of resection (Fig. 2).

Results: Corrected ADC values were significantly correlated with both tumor firmness ($r = -0.60$, $p = 0.029$) and extent of trichrome staining ($r = -0.72$, $p = 0.009$) such that greater ADC values were associated with decreased tumor firmness and decreased staining, respectively. Correlations between ADC values and tumor vascularity were not significant ($r = -0.09$, $p = 0.78$). Corrected ADC values in totally resected tumors (1.54) were greater than in subtotaly resected tumors (0.85; $p = 0.02$) and greater for moderate cellularity (1.51) relative to high tumor cellularity (0.8; $p = 0.035$). There was a trend-level association for partial resections to exhibit greater tumor firmness rating (3 vs. 1.7; $p = 0.051$). Finally, the degree of trichrome staining was also found to correlate positively with tumor firmness ($r = 0.60$; $p = 0.04$; Figs. 3 and 4).

Conclusion: Our results suggest that high resolution ADC of pituitary adenomas is a sensitive measure of tumor consistency. The 7-T DWI may hold clinical value in the preoperative workup and surgical management of patients with pituitary adenomas.

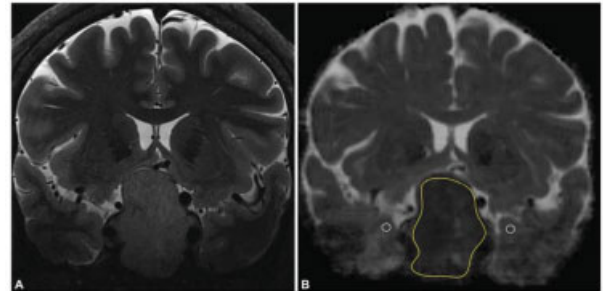


Figure 1. T2-TSE image of a patient with pituitary macroadenoma (A). ADC image with the pituitary tumor ROI in yellow and left and right temporal gray matter ROIs marked in white (B).

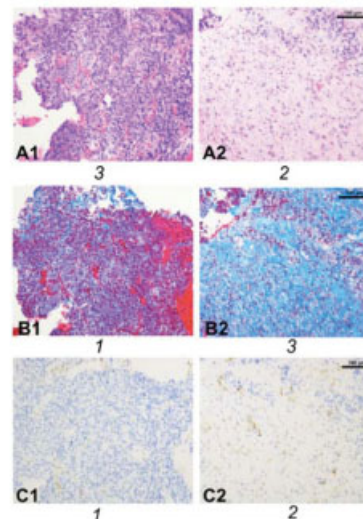


Figure 2. Histopathology scoring criteria. Representative histological images and their corresponding scores shown below. Cellularity was assessed on H&E (A1, A2). Collagen content was assessed with trichrome stain (B1, B2). Vascularity was assessed with CD31 stain (C1, C2).

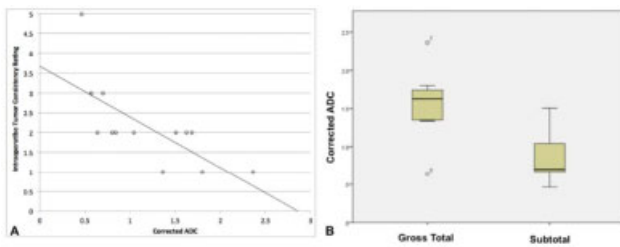


Figure 3. Pearson correlation showing a significant negative correlation between corrected tumor ADC values and intraoperative tumor consistency rating (A). Plot showing corrected tumor ADC in pituitary adenomas that were partially and totally resected (B).

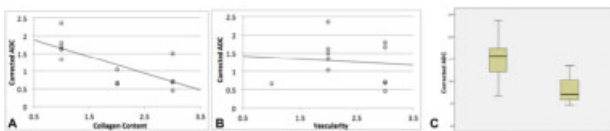


Figure 4. Pearson correlation showing a significant negative correlation between corrected tumor ADC values and tumor collagen content (A). Pearson correlation showing a non-significant negative correlation between corrected tumor ADC values and tumor vascularity (B). Plot showing higher corrected tumor ADC in tumors with moderate (2) compared with high (3) cellularity (C).

A003. Postoperative Pain Management and Perceived Patient Outcomes following Endoscopic Pituitary Surgery

Austin T. Hoke¹, Madison Malfitano¹, Lucas Frickey¹, Adam J. Kimple², Adam M. Zanation², Charles S. Ebert², Brent A. Senior², Brian D. Thorp²

¹UNC School of Medicine, Chapel Hill, North Carolina, United States

²UNC Otolaryngology/Head and Neck Surgery, Chapel Hill, North Carolina, United States

Purpose: Pain management has emerged as a point of emphasis in recent years given the ongoing opioid crisis in the United States. To date, there are no studies in the literature evaluating prescribing patterns and utilization of postoperative pain medication following endoscopic pituitary surgery. The goal of this study is to determine provider prescribing tendency, patient usage of pain medications, and perceived patient outcome regarding postoperative pain management. Such data will guide future prescribing methodologies and provide data for thoughtful prospective studies.

Methods: A total of 100 patients undergoing endoscopic pituitary surgery at one institution from 2016 to 2018 were identified. Postoperative pain medication regimens were obtained and patients were queried on the state narcotic database to determine if their narcotic prescription was filled. Patients were contacted via phone interview to determine the utilization and perceived outcome of their pain management regimen.

Results: A total of 54 different pain control regimens were prescribed to the 100 study patients. Also, 92% of study patients were prescribed an opioid upon discharge from the hospital and 85.9% of those patients filled the prescription. The average quantity of opioids prescribed per patient was 636 morphine milligram equivalents (MME), or the equivalent of 85 5 mg oxycodone tablets, with a standard deviation of 580 MME (equivalent to 77 5 mg oxycodone tablets) and a

range of 30 to 4,200 MME (equivalent to 4–560 5 mg oxycodone tablets). But 44% of study patients participated in a subsequent telephone survey. Again, 93.2% of surveyed patients received an opioid prescription of whom 87.8% filled that prescription. While 83.3% of the patients who filled their opioid prescription reported utilization of the opioids, 70% of users reported using less than 25% of their total prescription. Among them, 60% of survey responders who utilized their opioid prescription reported that the majority of their use was within the first 24 to 48 hours following surgery. Also, 83.3% of surveyed patients who utilized prescription opioids found that the narcotic adequately controlled pain and aided in recovery while 100% of surveyed patients who used either alternative prescription analgesics or over-the-counter agents reported adequate pain control and aided recovery.

Conclusion: There is significant variability in the prescribing patterns of analgesic medication type, dose, and quantity even within a single institution following endoscopic pituitary surgery. Though opioid prescriptions in our patient population are typically filled and consumed in some capacity, patients who used their prescription opioids were nearly three times more likely to use less than 25% of their total regimen than they were to use the entire prescription. The substantial variability in postoperative pain management prescribing patterns and likely overprescribing of opioids in this patient population warrant further investigation into the topic of analgesic decision making in patients undergoing endoscopic pituitary surgery everywhere.

A004. A Highly Sensitive and Specific ACTH-Based Predictor of Long-Term Remission after Surgery for Cushing's Disease

Marcus A. Zachariah¹, Santino G. Cua¹, Bradley A. Otto¹, Ricardo L. Carrau¹, Luma Ghalib¹, Russel R. Lonser¹, Daniel M. Prevedello¹

¹The Ohio State University, Columbus, Ohio, United States

Over 70% of cases of Cushing's syndrome are caused by an ACTH-secreting pituitary tumor, known as Cushing's disease.¹ An early predictor for long-term remission of Cushing's disease after surgery has received substantial interest in the neurosurgical and endocrinological literatures.² While previous studies have examined the predictive value of early postoperative ACTH levels, intraoperative ACTH levels have not been evaluated. We examined intraoperative ACTH levels and describe a highly sensitive and specific predictor for long-term remission in a subset of Cushing's patients.

The medical records of 46 consecutive patients who underwent surgery for Cushing's disease from July 21, 2011 to June 14, 2018 were retrospectively reviewed. Peripheral blood ACTH levels were drawn preoperatively, intraoperatively, and on the first day after surgery (POD1). Intraoperative ACTH levels were drawn during exposure, during manipulation of the tumor, and during closure.

Patients' demographics, pathology results, and long-term outcomes are described in **Table 1**. Preoperative, intraoperative, and postoperative ACTH levels are shown in **Fig. 1**. Confirming previous work, POD1 ACTH level was a sensitive and specific measure of long-term remission (**Fig. 2**; area under the curve = 0.765; mean follow-up = 3.048 years; range, 0.41–7.8 years).

Next, we compared ACTH levels in the patients who underwent purely extracapsular resection and those in whom the tumor was removed in piecemeal fashion. We saw a higher intraoperative maximum ACTH level in the piecemeal group (299.54 ± 304.62 pg/mL) compared with the extracapsular group (112.37 ± 96.72 pg/mL; p -value = 0.008). We reasoned that in the patients who underwent piecemeal resection, an intraoperative ACTH spike is

associated with tumor identification and physical disruption, which could be related to long-term remission. Notably, in the piecemeal group of patients, the ratio of the intraoperative maximum divided by the intraoperative minimum ACTH level was higher in those with long-term remission (4.83 – 4.25 pg/mL) compared with those with recurrence (2.55 ± 0.52 pg/mL), suggesting that in this subset of patients, an intraoperative ACTH spike associated with a low ACTH level during closure could be predictive of long-term remission. Thus, we hypothesized that combining the intraoperative ACTH ratio with the POD1 postoperative ACTH level ([intraoperative ACTH maximum/intraoperative ACTH minimum]/POD1 ACTH) would be a sensitive and specific predictor of long-term remission. In fact, in the subset of patients who underwent piecemeal dissection, this showed to be highly specific and sensitive, with an area under the curve of 0.904 (Fig. 3).

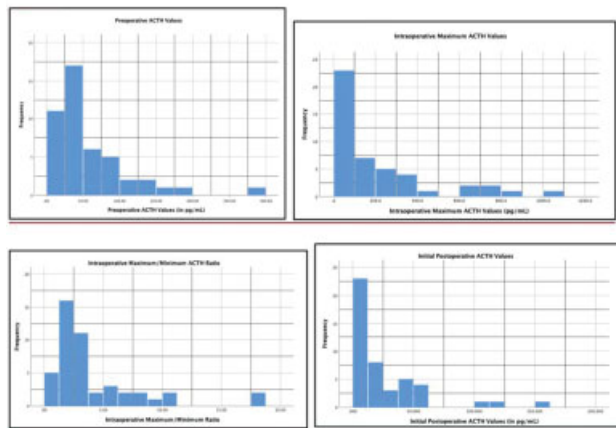


Fig. 1 Preoperative, intraoperative, and postoperative ACTH levels.

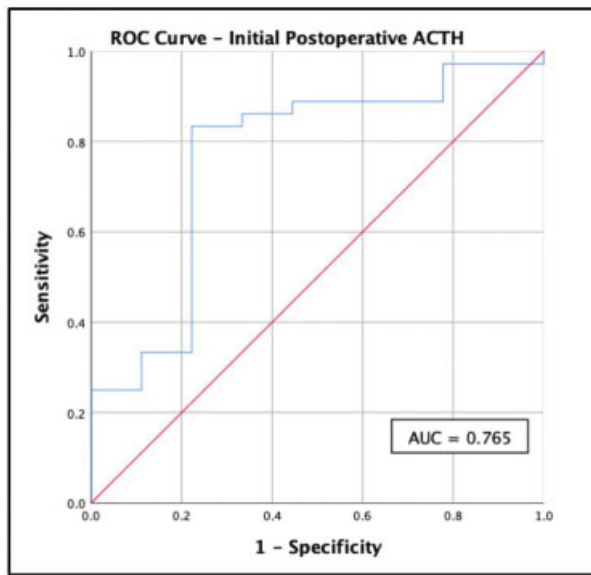


Fig. 2 A sensitive and specific measure of long-term remission.

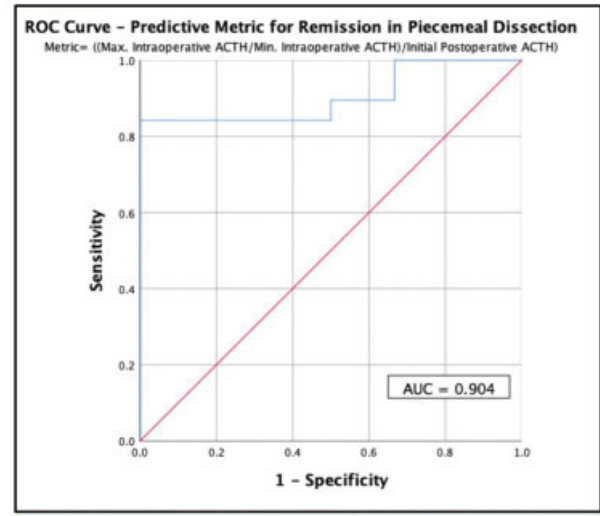


Fig. 3 The subset of patients.

a.

	Age
Mean	43.2
Standard Dev.	13.1

b.

	Gender		Tumor Pathology	
	Male	Female	Negative or weak positive for ACTH	Diffuse Positive for ACTH
Percentage	0.174	0.826	0.326	0.674
n	8	38	15	31

c.

	Resection Approach		Cushing's Disease Remission	
	Extracapsular	Intracapsular	Remission	No Remission
Percentage	0.435	0.565	0.804	0.196
n	20	26	37	9

Table 1 Patient demographics, pathology results, and long-term outcomes

References

1. Lonser RR, Nieman L, Oldfield EH. Cushing's disease: pathobiology, diagnosis, and management. *J Neurosurg* 2017;126(2):404–417
2. Pendharkar AV, Sussman ES, Ho AL, Hayden Gephart MG, Katznelson L. Cushing's disease: predicting long-term remission after surgical treatment. *Neurosurg Focus* 2015;38(2):E13

A005. Repeat Serum Sodium Values over 145 Predict Diabetes Insipidus after Endoscopic Transphenoidal Pituitary Tumor Resection

Rebecca Breese¹, Avinash Chandran², Sebastian Gil³, Weston Northam², Elizabeth Harris², Brian Thorp², Adam Zanation², Deanna Sasaki-Adams², Matthew Ewend², Carolyn Quinsey¹
¹Wake Forest Baptist Health, Winston-Salem, North Carolina, United States
²University of North Carolina, North Carolina, United States
³University of North Carolina School of Medicine, North Carolina, United States

Background: Central diabetes insipidus (DI) is a common complication following pituitary surgery caused by

damage or irritation to the posterior pituitary, pituitary stalk, or hypothalamic osmoregulatory centers. Most cases of postoperative DI are reported as transient, resolving within 1 week of surgery, though a small proportion of patients develop nontransient DI. Although there are generally accepted risk factors to DI development after surgery, such as Rathke's cleft cyst, craniopharyngioma, craniotomy, and tumor size, other risk factors may contribute and have not been clearly defined. Elevated serum sodium values are a known characteristic of DI; however, few studies have looked at the association between the development of this condition and postoperative sodium values.

Objective: This study was aimed to determine if DI is associated with sodium values within the first 48 hours after endoscopic transsphenoidal pituitary surgery and whether other perioperative variables may be associated with the development of DI.

Methods: A total of 347 patients undergoing 366 surgeries were included for analysis. Medical records were reviewed for demographics, repeat surgery, tumor pathology, extent of resection, intraoperative or postoperative CSF leak, hospital stay, follow-up, and maximum serum sodium concentration within the first 48 hours postoperatively. Bivariate associations between each explanatory variable of interest and postoperative DI was examined using Wald χ^2 tests. Multivariable logistic regression models were used to evaluate the association between postoperative 48-hour serum sodium concentrations and DI, after covariate adjustment.

Results: Of 360 resections, 52 patients (14.4%) showed evidence of DI postoperatively. Transient postoperative DI (lasting less than 7 days) occurred in 23 patients (6.4%), and nontransient DI occurred in 29 patients (8.1%). Of those with nontransient DI, 10 patients were deamino-8-D-arginine vasopressin (ddAVP)-independent within 6 months, 1 patient after 1 year, and 18 patients remained ddAVP-dependent with permanent DI (5.0%). Odds of DI were higher with higher recorded 48-hour maximum serum sodium measurements (OR = 1.86; 95% CI = 1.59–2.17; indicating differential odds with unit increases in serum sodium measurements). Odds of DI were also higher with higher frequencies of serum sodium concentration measurements over 145 (OR = 9.22; 95% CI = 5.11–16.63). Two serum sodium values above 145 predicted DI with 99.03% specificity and 50% sensitivity and had a 98.09% PPV and 66.45% NPV. In bivariate analyses, statistically significant associations were observed between patient age and DI (OR = 0.98, 95% CI = 0.96–0.99 for unit increases in age). There were no significant associations observed between sex, CSF leaks, extent of resection, or prior surgery and DI.

Conclusion: Higher maximum recorded values of serum sodium, and multiple serum sodium over 145, within 48 hours of postsurgery were associated with higher odds of DI. While elevated serum sodium is a known feature of diabetes insipidus, the positive and negative predictive values presented are useful resources for clinicians in medication decision making, safe discharge, and patient counseling.

A006. Readmission after Endoscopic Transsphenoidal Pituitary Surgery: Analysis of 584 Consecutive Cases
Iyan Younus¹, Georgiana Dobri¹, Rohan Ramakrishna¹, Theodore H. Schwartz¹

¹Weill Medical College/Cornell University, New York, New York, United States

Objective: Hospital readmission is a key component in value-based health care models but there is limited data about the 30-day readmission rate after endonasal endoscopic transsphenoidal surgery (EETS) for pituitary adenoma. The

objective of this study is to determine the incidence and identify factors associated with 30-day readmission after EETS for pituitary adenoma.

Methods: The authors analyzed a prospectively acquired database of EETS for pituitary adenoma from 2005 to 2018 at New York Presbyterian Hospital, Weill Cornell Medicine. We identified cases of unplanned readmission within 30 days of surgery. As a control group, we reviewed clinical and radiographic data of all other patients in the cohort that were not readmitted. Statistical significance was determined with $\alpha < 0.05$ using Pearson's Chi-square and Fisher's exact tests for categorical variables and the independent-samples *t*-test for continuous variables.

Results: Of 584 patients undergoing EETS for pituitary adenoma, 27 (4.6%) cases had unplanned readmission within 30 days. Most readmissions occurred within the first week after surgery with a mean time to readmission of 6.6 ± 3.9 days. The majority of readmissions (59%) were for hyponatremia. These patients had a mean sodium level of 120.6 ± 4.6 mEq/L at presentation. Other causes of readmission were epistaxis (11%), spinal headache (11%), sellar hematoma (7.4%), **cerebrospinal** fluid leak (CSF) leak (3.7%), nonspecific headache (3.7%), and pulmonary embolism (3.7%). The postoperative length of stay was significantly shorter for patients that were readmitted compared with the control (2.7 ± 1.0 days vs. 3.9 ± 3.2 days; $p < 0.05$). The mean body mass index (BMI) was significantly lower for readmitted patients compared with the control (26.4 ± 3.9 vs. 29.3 ± 6.1 kg/m²; $p < 0.05$).

Conclusion: Readmission after EETS for pituitary adenoma is a relatively rare phenomenon with delayed hyponatremia being the primary cause. We found that a shorter postoperative length of stay and lower BMI were associated with 30-day readmission.

A007. Long-Term Hypocortisolism after Pituitary Surgery: Can POD1 Stress Response Predict Long-Term Outcome?

Pascal Lavergne¹, Prachi Patel¹, Chandala Chitguppi¹, Tawfik Khouri¹, Mindy Rabinowitz¹, Gurston G. Nyquist¹, Marc R. Rosen¹, Christopher J. Farrell¹, James J. Evans¹

¹Thomas Jefferson University, Philadelphia, Pennsylvania, United States

Introduction: Long-term function of the hypothalamic-pituitary-adrenal (HPA) axis is an important metric following pituitary surgery. Although universal stress dose and postoperative steroids have been a common practice for pituitary surgery, many centers now tailor postoperative steroid therapy based on patients' individual pre- and early postoperative cortisol values. Previous studies have identified the predictive value of cortisol levels drawn on postoperative days (POD) 1, 2, and 6 as useful tool to predict immediate and long-term hypocortisolism. While a low value should prompt steroid replacement, a normal value early in the postoperative course has not traditionally been viewed as a strong predictor of long-term normal function. Cortisol levels drawn on POD 1 can show high values which are not seen on POD2, likely representing a normal stress response to surgery. The predictive value of POD 1 cortisol levels on long-term HPA axis function remains to be elucidated.

Methods: A single-institution retrospective review of patients who underwent endoscopic transnasal transsphenoidal surgery for a pituitary adenoma between 2014 and 2017 (ongoing recruitment) was performed. Patients with preoperative hypocortisolism or insufficient data in the medical record were excluded from the study. Baseline demographic data, tumor characteristics, and endocrine results were collected. Chi-squared, Kendall's tau and

Spearman's rho, and *t*-tests were used to assess relationships between categorical and continuous variables and long-term hypocortisolism. Long-term hypocortisolism was defined as the need for exogenous steroids more than 6 months after surgery.

Results: One hundred and twenty-six nonsecretory pituitary adenoma patients were included in this review. Twenty-seven of the 126 (21%) patients needed steroid replacement 6 months or more after surgery. Male patients were more likely to require long-term replacement with an odds ratio of 2.065 (1.005–4.241). POD 1, POD 2, and PO 3 months' cortisol values were highly correlated with the need for long-term steroids. POD 1 morning cortisol had the highest correlation with long-term hypocortisolism with a hazard ratio (HR) of 17.996 (7.558–28.435) compared with POD 2 values (HR = 8.980 [1.910–16.051]). Mean POD 1 cortisol value for patients without long-term hypocortisolism was significantly higher compared with the patient with long-term hypocortisolism (37.32 [11.77–62.88] vs. 19.33 [0.99–37.66] ng/mL). Tumor size and recurrent tumor were not associated with long-term hypocortisolism.

Conclusion: POD 1 cortisol is a strong predictor of long-term hypocortisolism. Although a combination of POD 1 and POD 2 has been advocated to accurately predict the need for steroid replacement therapy, our results suggest that a POD 1 level alone can be sufficient. Stress response on POD 1 with high morning cortisol value seems to be correlated with long-term normal function of the HPA axis. These results suggest that the evaluation of the cortisol level alone should not be a criterion to keep patients in the hospital past the first POD. Outpatient cortisol monitoring will still be needed to identify the low percentage of patients that may develop long-term hypocortisolism with a normal POD1 value. This study also emphasizes the previous finding that stress dose steroids are not uniformly required postoperatively.

A009. Dural Sealants Do Not Reduce Postoperative Cerebrospinal Fluid Leaks after Endoscopic Endonasal Skull Base Surgery

Michael McDowell¹, Rachel Jacobs¹, Benita Valappil¹, Eric Wang¹, Carl Snyderman¹, Paul A. Gardner¹

¹University of Pittsburgh Medical Center, Pittsburgh, Pennsylvania, United States

Introduction: The application of cranial tissue sealants to assist with dural closure is widespread, but data are lacking regarding its utility in endoscopic endonasal surgery (EES).

Objectives: Based on a null hypothesis that the use of cranial sealants after EES does not prevent postoperative cerebrospinal fluid (CSF) leaks. A prospective study was conducted to assess the effect of sealant usage on postoperative CSF leaks following standard reconstruction.

Methods: A prospective, case-control trial of sealant usage after EES was performed from April 2017 to June 2018. The mean follow-up time was 8 months. This study accrued 200 consecutive adult and pediatric patients with skull base pathology who underwent EES. From April 2017 to November 2017, sealant was used as part of standard closure on all EES cases. From November 2017 to June 2018, no sealant was used.

Results: Two hundred consecutive adult and pediatric patients, with a mean age of 52.7 years (range, 10–87 years) were enrolled in the study. In the first 100 patients where sealant was used in the reconstruction, 48 patients had an intraoperative CSF leak. Of these 48, 26 patients had high-flow leaks. The rate of postoperative CSF leaks was 5% in the sealant group. In the subsequent 100 patients, no sealant was used with 59 intraoperative CSF leaks of which 36 were high

flow leaks. The overall rate of postoperative CSF leak in this group was 3% ($p = 0.64$ when comparing overall leak rates). When examining the subset of high flow CSF leaks, the rate of postoperative CSF leak was 12% in the sealant group and 6% in the group without sealant ($p < 0.64$). One hundred seven patients within this group had a documented intraoperative CSF leak, of which 59 did not receive sealant and 48 received sealant ($p = 0.16$). Sixty-two of the CSF leaks were high flow. The cohort with sealant had five postoperative CSF leaks (5% rate) compared with a three leaks (3% rate) in the cohort without sealant ($p = 0.72$). No patient without an intraoperative leak had a postoperative CSF leak. Five of the eight patients with CSF leaks had a high-flow leak. There was no significant difference in sex, age, body mass index, smoking status, surgical pathology, or prior EES in patients with a postoperative CSF leak (**Table 1**). The only significant difference between the two groups was that there were more patients with sinonasal pathology in the no sealant cohort (nine patients, one leak) than the sealant cohort (one patient, 0 leaks; $p = 0.04$).

Conclusion: Perioperative dural sealant usage as a supplement to standard EES closure techniques does not reduce the rate of postoperative CSF leak.

A010. Transorbital Endoscopic Approach for Repair of Frontal Sinus Cerebrospinal Fluid Leaks: A Single-Institutional Experience

Raywat Noiphithak¹, Pree Nimmanitya¹, Vich Yindeedej¹, Pataravit Rukskul¹

¹Division of Neurosurgery, Department of Surgery, Faculty of Medicine, Thammasat University, Bangkok, Thailand

Background: Management of frontal sinus cerebrospinal fluid (CSF) leak is challenging because of its complex anatomy. Recently, transorbital endoscopic approach (TOEA) has been reported as one of minimally invasive surgeries to repair defect in the frontal sinus.

Objective: This study was aimed to describe surgical technique and our experience in TOEA for the frontal sinus leak repair.

Methods: We reviewed patients with CSF leaks from the frontal sinus who were treated with TOEA in our institution during 2016 to 2019. The surgery began with superior eye lid incision (**Fig. 1**). After exposure of superomedial part of the orbit, entry site of the frontal sinus was located medially to supraorbital nerve with neuronavigator guidance (**Fig. 2**). The defect was identified under endoscopic visualization (**Fig. 3**) and was repaired with multilayered reconstruction technique. Clinical data, location and size of the defect, reconstruction material, patency of the frontal sinus, and follow-up were analyzed.

Results: Sixteen patients (21–61 years) were successfully repaired the leaks with a mean follow-up of 11 months. Etiologies were trauma (75%) and iatrogenic (4%). Eleven patients (68.8%) were recurrent cases from previous surgical repair by either endoscopic endonasal or conventional transcranial approaches. All patients had the defects located in superior or lateral part of the frontal sinus with defect size ranging 2.0 to 30.8 mm in diameter. Drainage of the frontal sinus was preserved in 10 cases (62.5%; **Fig. 4**). There were no complications in this clinical series.

Conclusion: This clinical series revealed that the use of TOEA for the frontal CSF leak repair was effective and can be applied as an alternative minimally invasive technique for management this condition.



Fig. 1 Superior eye lid incision and instrument handling in tranorbital endoscopic approach.

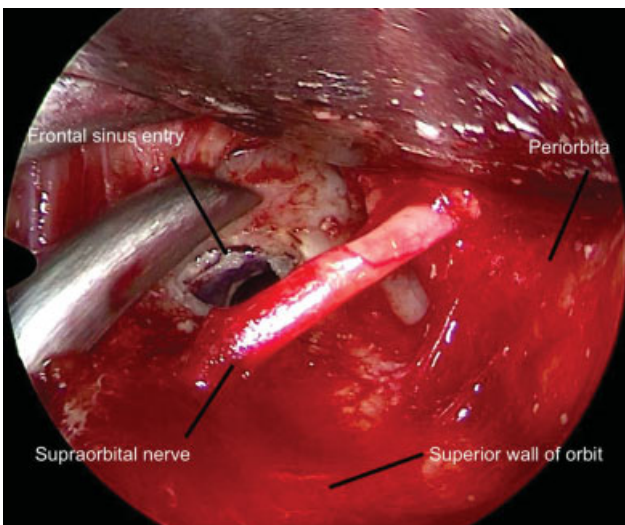


Fig. 2 Entry site of frontal sinus.

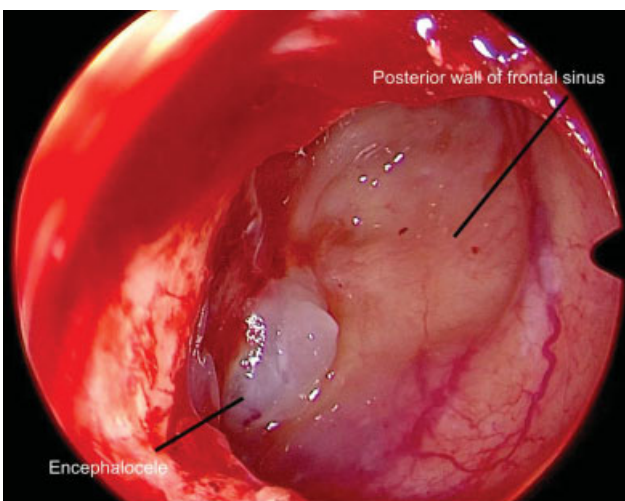


Fig. 3 Defect and encephalocele in right frontal sinus was identified under endoscopic visualization.

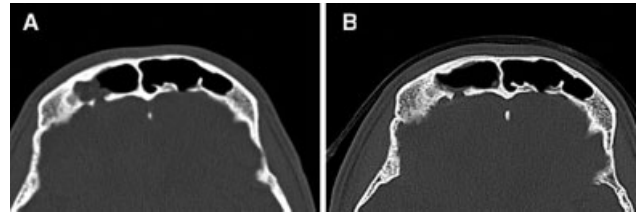


Fig. 4 Pre-operative CT scan (A) demonstrated defect in posterior wall of right frontal sinus with encephalocele which was repaired by transorbital endoscopic approach. At 6 months, there was no evidence of CSF leak. The defect was completely reconstructed with patency of the frontal sinus shown in the follow-up CT scan (B).

A011. A Novel Scoring System for Complexity and Operative Success of Osteocutaneous Free-Flap Reconstruction of the Midface and Orbit

Brian Swendseid¹, Swar Vimawala¹, Matthew Stewart¹, Tony Richa¹, Ryan Heffelfinger¹, Howard Krein¹, Adam Luginbuhl¹, Richard Goldman¹, Joseph Curry¹

¹Thomas Jefferson University Hospitals, Philadelphia, Pennsylvania, United States

Background: Reconstructing the bony midface and orbit is challenging due to complex anatomy and proximity to vital structures. Use of an osteocutaneous free flap can restore osseous continuity, support the orbit to prevent diplopia, allow for dental rehabilitation, and improve cosmesis. Osteocutaneous free-flap success has historically been evaluated based on patient symptoms, return to normal diet, radiographic union, and/or avoidance of complications. However, these methods do not account for the postoperative position of the reconstructed bone. Classification systems exist for midface defects (e.g., Brown and Cordeiro); however, no scoring system has described the successful or unsuccessful reconstruction of these defects and restoration of normal anatomy. This project proposes an anatomic-based scoring system for midface free-flap reconstruction and compares the results from the three most commonly used free flaps.

Methods: Review of a retrospective free flap database at a single tertiary-care institution identified 46 patients who underwent osteocutaneous reconstruction of the midface or orbit. Postoperative imaging scans were reviewed and scored based on three factors: (1) subunit score was the number of independent subunits of the midface or orbit that were resected during the ablative surgery and successfully reconstructed with the osseous portion of the free flap; (2) contact score was the number of different bony appositions that were found to have successful bony contact; (3) position score was the number of separate osseous segments that were placed in an anatomic position. The three scores were treated separately, then added together to produce an overall complexity score. The scores of patients who underwent scapula, fibula and osteocutaneous radial forearm free flaps were compared using ANOVA testing.

Results: The mean Subunit Score was 3.9, with a significantly higher score for scapula free flaps compared with fibula or osteocutaneous radial forearm flaps (mean, 5.1 vs. 2.9 and 2.8, $p < 0.0001$). The mean contact score was 2.0, without a significant difference between flap types ($p = 0.14$). The mean position score was 1.4, without a significant difference between flap types ($p = 0.34$). The mean combined overall complexity score was 7.3, without a significant difference between flap types ($p = 0.31$)

Discussion: Standardized scoring systems are valuable tools. They help to guide management decisions, allow for

better comparison of data across institutions, and can provide stratification of operative complexity to guide reimbursement. Optimal scoring systems should be quick and easy to perform. We propose a novel scoring system for osseous midface reconstruction based on postoperative imaging scans that can be completed in less than 1 minute. Other measures of free flap success focus on patient outcomes and complications, rather than successful restoration of normal anatomy. As such, our system could be a valuable tool to assess operative success and complexity in midface and orbital reconstruction. At our institution, the scapula free flap was able to successfully reconstruct a higher number of separate anatomic subunits compared with fibula or osteocutaneous radial forearm free flaps.

A012. Heterogeneity in Outcomes Reporting in Endoscopic Endonasal Skull Base Reconstruction: A Systematic Review
 Christina Dorismond¹, Griffin D. Santarelli², Brian D. Thorp¹, Adam J. Kimple¹, Charles S. Ebert¹, Adam M. Zanation¹

¹University of North Carolina School of Medicine, Chapel Hill, North Carolina, United States

²Barrow Neurological Institute, Phoenix, Arizona, United States

Background: There are currently no reporting standards for intraoperative or perioperative outcomes following endoscopic endonasal skull base surgery. This is problematic as it makes performing systematic reviews and meta-analysis impossible, impairing our ability to practice evidence-based medicine.

Objective: The goal of this study was to describe patterns of reporting outcomes in endoscopic endonasal skull base reconstruction.

Study Design: This study is a systematic review.

Methods: PubMed, EMBASE, CINAHL, Cochrane Review Databases, and Web of Science (2005 to June 21, 2019) were systematically searched for all publications on skull base reconstruction. Articles were limited to those with ≥ 25 patients and a focus on skull base reconstruction via an endoscopic endonasal approach. Articles with $>20\%$ of cases on primary CSF leaks (spontaneous, traumatic, or congenital) were excluded. Initial screening was based on review of title and abstract and those studies not meeting the above criteria were excluded. Full-text review was then performed to select the final studies. Subsequently, reported outcomes data was extracted from all included studies.

Results: A total of 111 studies were included in the review, including 20,548 patients undergoing skull base surgery. There was heterogeneity for pathologies treated, with 107 (96.4%) studies reporting the indication for reconstruction, among which sellar pathology was the most common. All studies reported some demographic data, but 17 (15.3%) did not report the gender distribution of patients and 16 (14.4%) did not report the age of patients. A total of 105 studies (94.6%) presented grouped or both grouped and individual patient data, while 6 (5.4%) studies presented solely individual patient data. Also, 48 studies (43.2%) reported patients' history of prior surgery or radiotherapy and fewer studies (27, 24.3%) reported mean tumor size. Reporting of cerebrospinal fluid (CSF) findings had greater heterogeneity. Only 77 (69.4%) studies reported the presence or absence of intraoperative CSF leaks, with 42 of these studies (54.5%) providing a scaling system for these leaks. An even smaller number of studies (26, 23.4%) reported lumbar drain status. With regards to postoperative outcomes, few studies reported mean or median length of hospital stay (19, 17.1%) or of follow-up (51, 45.9%). The most commonly reported outcome was rate of postoperative CSF leak (108, 97.3%). Reporting of other surgical complications was less

consistent, including meningitis (53, 47.7%), epistaxis (23, 20.7%), pneumocephalus (20, 18.0%), septal perforation (15, 13.5%), and flap necrosis (13, 11.7%). The rates of other general complications were rarely reported within the studies, including stroke (8, 7.2%), pulmonary embolism or deep vein thrombosis (14, 12.6%), and mortality (21, 18.9%).

Conclusion: There is significant heterogeneity in the outcomes reported in studies relating to endoscopic endonasal skull base surgery reconstruction. This highlights the need for the development of standard reporting outcomes to minimize bias and improve the execution of systematic reviews on the subject.

A013. Sinonasal Quality-of-Life Outcomes after Endoscopic Endonasal Transphenoidal Surgery with Free Mucosal Graft Reconstruction

Tara J. Wu¹, Angela Chen¹, Marvin Bergsneider², Jivianne T. Lee¹, Jeffrey D. Suh¹, Marilene B. Wang¹

¹UCLA Department of Head and Neck Surgery, Los Angeles, California, United States

²UCLA Department of Neurosurgery, Los Angeles, California, United States

Objectives: The literature suggests that after endoscopic endonasal transphenoidal surgery (EETS) without formal reconstruction of the sella, sinonasal quality of life (QOL) recovers by 3 to 6 months postoperatively. An option for sellar reconstruction, in the absence of a significant intraoperative cerebrospinal fluid (CSF) leak, is a free mucosal graft (FMG) taken from the posterior septum. In this study we analyze sinonasal quality of life (QOL) outcomes in patients undergoing EETS with FMG reconstruction.

Design: Present study is a retrospective review.

Setting: This study was conducted at a tertiary care academic center.

Participants: Patients undergoing sellar reconstruction with a FMG after EETS from 2013 to 2018.

Main Outcome Measures: Patient, tumor, and surgical factors were included, along with postoperative complications. Patients completed sinonasal outcome test 22 (SNOT-22) scores during the preoperative visit, as well as first two postoperative visits. SNOT-22 scores were further categorized into five domains, as previously described in the literature.

Results: A total of 115 patients underwent sellar reconstruction with a FMG during EETS. Most surgeries were performed for pituitary adenomas (82%). Among the patients, 104 (90%) had no intraoperative CSF leak, while 11 patients (10%) had a low-grade intraoperative CSF leak. There was one patient (<1%) who developed a postoperative CSF leak. Three patients (3%) developed epistaxis, requiring an emergency room visit or operative intervention. The median time from surgery until the first postoperative visit was 13 days (95% CI: 6–22). The median time from surgery until the second postoperative visit was 57 days (95% CI: 15–126). The average preoperative SNOT-22 score was 17.5; first postoperative SNOT-22 score was 32.9; and second postoperative SNOT-22 score was 21.3 (**Fig. 1**), suggesting near normalization of sinonasal QOL by the second postoperative visit. After categorizing by SNOT-22 domains, there were significant improvements in SNOT-22 scores for almost all domains, including domain 1 (rhinologic symptoms), domain 2 (extranasal rhinologic symptoms), domain 3 (ear/facial symptoms), and domain 4 (sleep dysfunction) symptoms (**Fig. 2**).

Conclusion: During EETS, FMG reconstruction of sellar defects is an effective and well-tolerated option for patients without significant intraoperative CSF leaks. Patients

demonstrated early recovery of baseline sinonasal QOL by 2 months postoperatively.

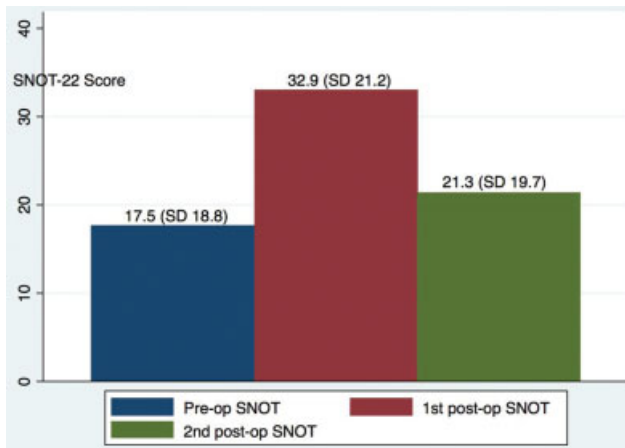


Fig. 1 Comparison of average preoperative and first two postoperative visit SNOT-22 scores.

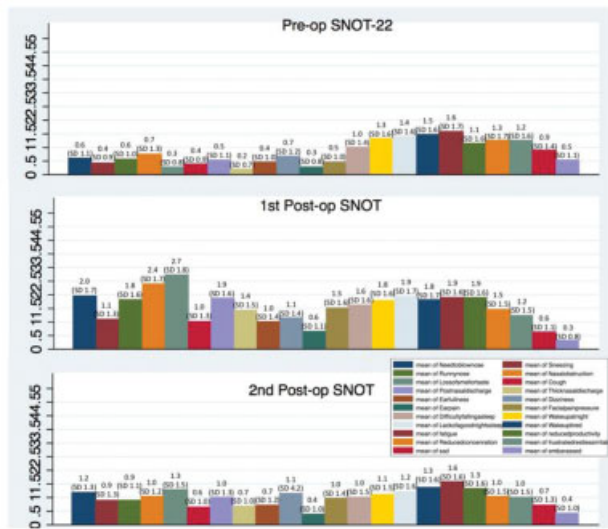


Fig. 2 Comparison of individualized preoperative and first two postoperative visit SNOT-22 scores

A014. Correlation of Skull Base CSF Leak Flow Rates with Fluid Pattern on Early, Delayed, and Subtraction Volumetric Extended Echo Train T2 MRI

John W. Rutland¹, Satish Govindaraj¹, Corey M. Gill¹, Michael Shohet¹, Alfred Illoreta¹, Joshua B. Bederson¹, Raj K. Shrivastava¹, Bradley N. Delman¹

¹Icahn School of Medicine at Mount Sinai, New York, New York, United States

Introduction: Cerebrospinal fluid (CSF) leak is a potentially fatal condition that occurs when a dural defect in the skull base permits CSF communication between the cranial vault and sinonasal cavities. Flow rate is an important property of CSF leaks that can effect surgical decision making and predispose a certain patient population to complications and inferior outcomes. However, predicting CSF flow rate preoperatively is challenging with current diagnostic tools. The present study employs early and late T2-weighted MRI and

volumetric subtraction as a novel method of quantifying CSF flow rate, and correlates radiological results with intra-operative findings and clinical outcomes.

Methods: A total of 45 patients met inclusion criteria for this study and underwent 3-Tesla MRI, which included two identical T2-CUBE sequences that were 45 minutes apart. Semiautomated volumetric segmentation of CSF leak volumes was performed on early and late acquisitions using 3D-Slicer, and volumes were subtracted to obtain accumulated CSF volume. CSF volumes were compared between high- and low-flow patients and correlated with treatment outcomes including recurrence.

Results: Out of the 45 patients, 25 (55.6%) had definitive evidence of CSF leak, and 22 (88%) underwent surgical repair. High-flow patients (**Fig. 1**) had higher early (4,057.4 vs. 982.0 mm³, *p* = 0.04), late (4,584 vs. 1,095.6 mm³, *p* = 0.04), and accumulated (526.6 vs. 113.6 mm³, *p* = 0.01) CSF volumes than low-flow patients (**Fig. 2**). The five (22.7%) patients that exhibited postoperative CSF leak recurrence, had significantly greater early (6,296.9 vs. 1,227.8 mm³, *p* = 0.008) and late (6,874.4 vs. 1,447.9 mm³, *p* = 0.008) CSF leak volume. Accumulated CSF volume was not significantly greater in patients with leak recurrence (577.5 vs. 220.1 mm³, *p* = 0.07). Early, late, and accumulated CSF leak volume were significantly correlated with postoperative hospital stay as well as duration of postoperative lumbar drain placement, *p* < 0.05 for all (**Table 1**). Accumulated CSF volume was the most significant factor for predicting flow rate. For every one standard deviation increase in volume difference, the odds of high flow leak increased by 11.0 (95% CI: 1.5–238.8; *p* = 0.008). Early CSF volume was the most significant predictor for postoperative leak recurrence. For every one standard deviation increase in early volume, the odds of recurrence increased by 4.6 (95% CI: 1.5–22.0; *p* = 0.005).

Conclusion: High resolution T2-CUBE MRI coupled with precise volumetric segmentation and subtraction of CSF leak demonstrated predictive value in differentiating low- and high-flow CSF leaks, as well as identifying patients with postoperative complications, such as leak recurrence. These findings may be useful in the clinical workup and management of patients with anterior skull base CSF leak.

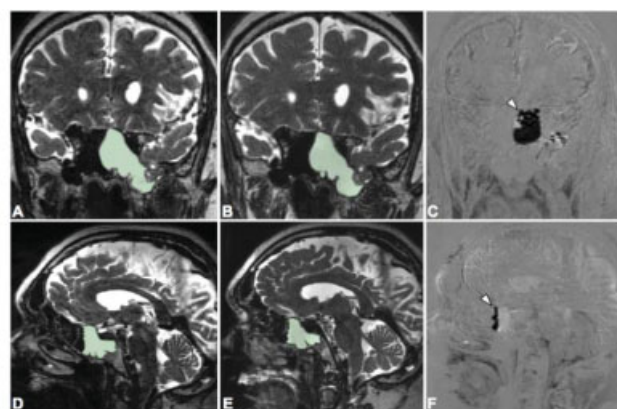


Figure 1. Coronal depiction of CSF volumetric measurement in early (A) and late (B) T2-CUBE acquisitions in a patient with a high-flow leak with CSF pooling from a left sphenoid encephalocele. Image subtraction (C) between early and late acquisitions reveals signal hypointensity (denoted by white arrow head), representing considerable CSF accumulation between scans. Sagittal depiction of CSF volumetric measurement in early (D) and late (E) acquisitions, with image subtraction revealing CSF accumulation (F).

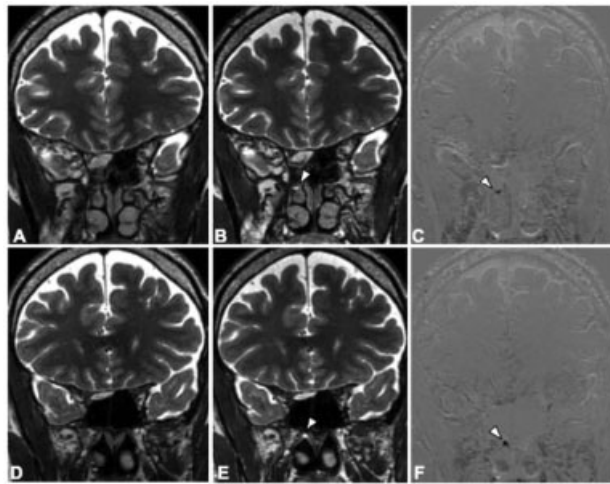


Figure 2. MRI of a patient with a low-flow CSF leak from a cribriform meningoencephalocele. No pooling CSF is observed in the early acquisitions (A and D), however, CSF volume (denoted by white arrow heads) is seen on the late acquisition (B and E). Image subtraction (C and F) between the early and late acquisitions shows signal hypointensities, representing accumulated CSF (denoted by white arrow heads).

	Early CSF Volume (mm ³)	Late CSF Volume (mm ³)	Accumulated CSF Volume (mm ³)
Flow Rate			
Low-Flow (N = 12)	982.0 (1527.8)	1095.6 (1601.7)	113.6 (139.6)
High-Flow (N = 10)	4057.4 (4325.5)	4584 (4817.5)	526.6 (579.6)
p-value	0.04	0.04	0.01
Recurrence			
Non-Recurrence (N = 17)	1227.8 (2582.9)	1447.9 (2952.4)	220.1 (392.1)
Recurrence (N = 5)	6296.9 (3148)	6874.4 (3543.9)	577.5 (551.1)
p-value	0.008	0.0008	0.07
Subsequent Repair			
No subsequent repair (N = 18)	1699.0 (3211.3)	1934.6 (3548.4)	235.6 (391.9)
Subsequent repair (N = 4)	5443.7 (2854.8)	6040.8 (3378.3)	597.1 (613.4)
p-value	0.03	0.03	0.12
Rhinorrhea Flow			
Intermittent rhinorrhea (N = 11)	2471.1 (3133.3)	2717 (3343.5)	246 (267)
Constant rhinorrhea (N = 5)	2013.4 (2539.2)	2227.2 (2678.7)	213.7 (214.1)
p-value	> 0.05	> 0.05	> 0.05

Table 1. Early, late, and accumulated CSF leak volume based on flow properties and surgical outcomes. Boldface values denote significance.

A015. Decreased Rate of CSF Leaks after Skull Base Fractures in the 21st Century: A Two-Institution Experience

Brittany M. Stopa¹, Oscar A. Leyva¹, Cierra Harper¹, Kyla A. Truman¹, Carleton E. Corrales², Timothy R. Smith¹, William B. Gormley¹

¹Department of Neurosurgery, Computational Neuroscience Outcomes Center at Harvard, Brigham and Women’s Hospital, Boston, Massachusetts, United States

²Division of Otolaryngology, Brigham and Women’s Hospital, Boston, Massachusetts, United States

Introduction: Cerebrospinal fluid (CSF) leaks are among the possible complications in patients with skull base fractures. CSF leaks can lead to meningitis so proper detection and management is crucial. Historically, the literature reports a rate of CSF leaks in skull base fracture patients of 10 to 30%. However, with the advent of advanced imaging modalities, such as thin slice computed tomography (CT) scanning, detection of skull base fractures has become more refined and accessible. A 2013 report from a statewide patient database of over 10,000 patients found a rate of CSF leaks in adult skull base fracture patients of <2%. To investigate further the proposed potential decrease in the rate of CSF leaks, we conduct here an institutional retrospective review.

Methods: A retrospective chart review of two major academic medical centers was conducted for the time period January 2000 through July 2018. Patients with skull base fracture were identified using ICD9/10 codes. Variables included age, gender, CSF leak within 90 days, management regimen (conservative vs. lumbar drain vs. surgical repair), meningitis within 90 days, and 1-year mortality. When ICD9/10 codes did not indicate CSF leak, but did indicate meningitis, lumbar drain, and/or surgical repair, CSF leak was considered to be present. Patients under the age of 18 years were excluded from analysis. Analysis was done in R v.3.0.1 software.

Results: Overall, there were 4,944 patients with skull base fractures, of which 202 (4.1%) developed a CSF leak within 90 days. Mean age was 49.2 (±21.9) years and 1,586 (32%) were female. Age distribution is given in Fig. 1. Incidence of skull base fractures by year is given in Fig. 2. Among CSF leaks, 85 (42%) were conservatively managed, 104 (52%) were treated with lumbar drain, and 12 (6%) required surgical repair. Meningitis developed within 90 days in 58 (29%) patients. Among meningitis patients, 32 were conservatively managed, 23 required lumbar drain, and 3 required surgical repair. The 1-year mortality for all skull base fracture patients was 535 (11%), for patients with CSF leaks was 23 (11%), and for patients with meningitis was 9 (16%).

Conclusion: In this 18-year, two-institution retrospective review of 4,944 skull base fracture patients, we found the rate of CSF leaks to be 4.1%. This is lower than the historically-cited range of 10 to 30%. Given the increased incidence of skull base fractures over recent decades, as illustrated in Fig. 1, this decreased rate of CSF leaks may actually represent a relative decrease. This may be an effect of the advances in modern imaging modalities making it easier to more readily detect and diagnose skull base fractures. The rate of meningitis in this population was 29%, and for those who developed meningitis the 1-year mortality was 16%. This suggests that while the relative rate of CSF leaks may be decreasing in the skull base fracture population, they remain a clinically important complication.

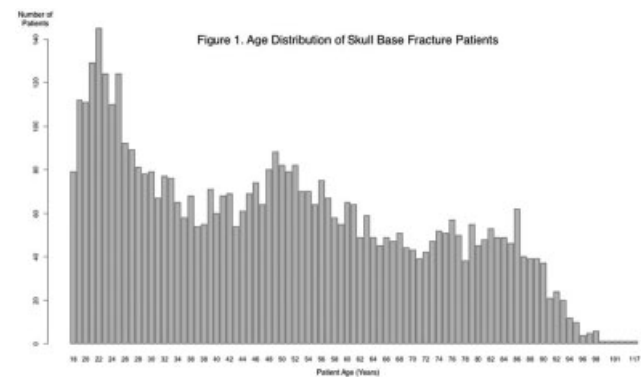


Fig. 1 Age distribution of skull base fracture patients.

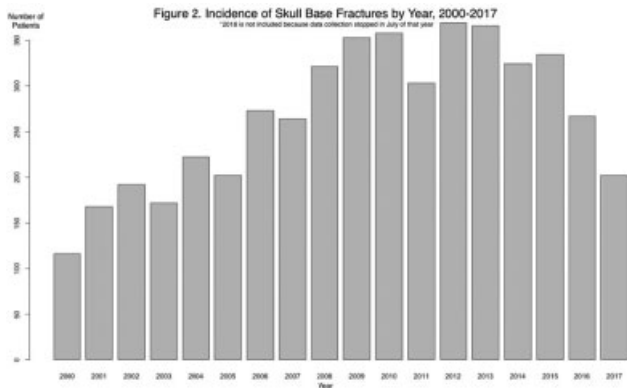


Fig. 2 Incidents of skull base fractures by year 2000 to 2007.

A017. Multicenter Analysis of Clinical Outcomes and Biomarkers of Esthesioneuroblastoma

Matt Lechner¹, Mario Hermsen², Mario Turri-Zanoni³, Volker H. Scharfetter⁴, Sam Helman⁵, Jordan Varghese⁵, C. Arturo Solares⁵, Kelly Magliocca⁶, Simon Wang⁷, Susanne Sprung⁸, David Howard⁹, Nils Engel¹⁰, David Capper¹¹, Ulrich Schueller¹², Martin Forster¹³, Amrita Jay¹⁴, Cillian Forde¹³, Jozsef Dudas⁴, Herbert Riechelmann⁴, R. Peter Manes¹⁵, Wendell G. Yarbrough¹⁶, Jose L. Llorente², Sarah K. Wise⁵, Paolo Castelnovo³, Valerie J. Lund¹⁷

¹UCL Cancer Institute, University College London, London, United Kingdom

²Instituto de Investigación Sanitaria del Principado de Asturias (ISPA), Instituto Universitario de Oncología del Principado de Asturias (IUOPA), Centro de Investigación Biomédica en Red (CIBER-ONC), Oviedo, Spain

³Unit of Otorhinolaryngology - Head & Neck Surgery, University of Insubria, Varese, Italy

⁴Department of Otorhinolaryngology-Head and Neck Surgery, Medical University of Innsbruck, Innsbruck, Austria

⁵Department of Otorhinolaryngology-Head and Neck Surgery, Emory University, Atlanta, Georgia, United States

⁶Department of Pathology, Emory University, Atlanta, Georgia, United States

⁷Institute of Nuclear Medicine, University College Hospital, London, United Kingdom

⁸Institute of Pathology, Medical University of Innsbruck, Innsbruck, Austria

⁹Head and Neck Cancer Unit, Imperial College Healthcare NHS Trust, London, United Kingdom

¹⁰Ludwig-Maximilians University, Munich, Germany

¹¹Department of Neuropathology, Charite University, Berlin, Germany

¹²University Medical Center Hamburg-Eppendorf, Hamburg, Germany

¹³Head and Neck Centre, University College London Hospitals NHS Trust, London, United Kingdom

¹⁴Department of Histopathology, University College London Hospitals NHS Trust, London, United Kingdom

¹⁵Division of Otolaryngology, Department of Surgery, Yale School of Medicine, New Haven, Connecticut, United States

¹⁶Department of Otolaryngology/Head and Neck Surgery and Department of Pathology, University of North Carolina, Chapel Hill, North Carolina, United States

¹⁷Royal National Throat, Nose and Ear Hospital and Head and Neck Centre, University College London Hospitals NHS Trust, London, United Kingdom

Background and Objectives: Esthesioneuroblastoma is a rare nasal neoplasm which usually originates from the

olfactory neuroepithelium in the upper portion of the nasal cavity adjacent to the cribriform plate.¹⁻³ Our objectives were to analyze multicenter clinical data from esthesioneuroblastoma patients to inform on outcomes and to identify novel diagnostic and prognostic biomarkers.

Material and Methods: For this multicenter analysis we included clinical data from 113 esthesioneuroblastoma patients (54 males; mean age: 49.4 years) from various centers in the United States and Europe, in particular data on clinical presentation, diagnosis, treatment and clinical outcomes. We also analyzed immunohistochemical data (SSTR2) and imaging data (68Ga-DOTA-TOC PET-CT-scanning and 68Ga-DOTA-TOC PET-MRI-scanning) where available to inform about diagnostic and prognostic potential. Statistical testing was performed in SPSS version 24.

Results: At initial presentation patients complained of nasal obstruction (77.4%), rhinorrhea (40.7%), epistaxis (39%), anosmia (30%), headache (13.8%), epiphora (5%), and diplopia (1.3%). With regard to age at presentation, we did not observe a bimodal distribution, but a peak between 37 and 58 years of age. The most useful poor prognostic indicators were bony skull base involvement and dural infiltration, each associated with significantly worse outcomes ($p = 0.024$ and $p < 0.001$, respectively). A total of 86.6% of patients received adjuvant radiotherapy and had a significantly improved survival ($p = 0.012$). Mean follow-up was 64.7 (± 51.6) months. 5-year overall survival was 88.2%. The most common location for recurrent/residual disease was the neck, followed by dura/brain. 83% of samples stained positive for SSTR2 and expression was associated with 68Ga-DOTA-TOC uptake both in 68Ga-DOTA-TOC PET-CT-scanning and 68Ga-DOTA-TOC PET-MRI-scanning.

Conclusion: Less than a third of esthesioneuroblastoma patients present with anosmia. Our analysis also shows that the most significant prognostic indicators in our set of samples are bony skull base involvement and dural infiltration rather than stage based on commonly used staging systems. The high rate of expression of Somatostatin receptor 2 (SSTR2) with 68Ga-DOTA-TOC uptake in both 68Ga-DOTA-TOC PET-CT-scans and 68Ga-DOTA-TOC PET-MRI-scans shows the enormous translational potential of this marker with regard to imaging and novel targeted therapies.

References

1. Lund VJ, Howard D, Wei W, Spittle M. Olfactory neuroblastoma: past, present, and future? *Laryngoscope* 2003;113(3):502-507
2. Dulguerov P, Allal AS, Calcaterra TC. Esthesioneuroblastoma: a meta-analysis and review. *Lancet Oncol* 2001;2(11):683-690
3. Rimmer J, Lund VJ, Beale T, Wei WI, Howard D. Olfactory neuroblastoma: a 35-year experience and suggested follow-up protocol. *Laryngoscope* 2014;124(7):1542-1549

A018. Treatment Modality Role in Survival of Patients with Advanced Squamous Cell Carcinoma of the Sinonasal Cavity: A National Cancer Database Study

Chris Johnson¹, Camilo Reyes¹

¹Augusta University, Augusta, Georgia, United States

Background: Squamous cell carcinoma (SCCa) is the most common paranasal sinus malignancy and commonly presents in advanced stages. Unfortunately, survival is strongly influenced by tumor stage at presentation leading to universally poor outcomes for many patients with advanced

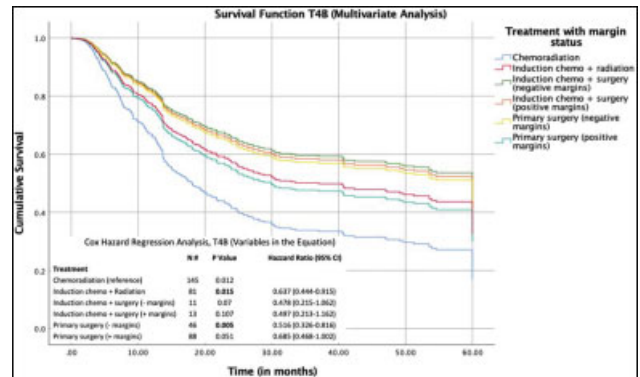
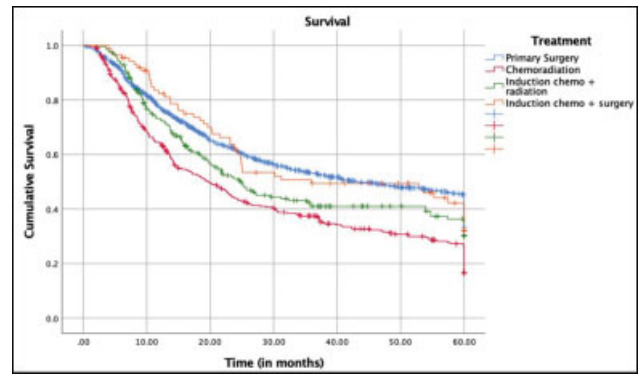
disease. Current data regarding treatment of advanced T-stage paranasal sinus SCCa is lacking and limited to small, retrospective, single institution studies. Over the past two decades of studies have been conducted that investigated the role of neoadjuvant therapy to improve outcomes.

Objective: Review treatment modalities survival of advanced T-stage SCCa of the paranasal sinus.

Methods: Using the National Cancer Database (NCDB), we analyzed over 2,000 cases of paranasal sinus malignancy. Patients were selected for age 18 years or older; first malignancy; tumor stage 4A or 4B; malignancy of the maxillary, ethmoid, sphenoid, and frontal sinus; and complete data regarding treatment, staging, and margin status. Patients were grouped according to the following treatment modalities: primary surgery, concurrent chemoradiation, neoadjuvant chemotherapy followed by surgery, and induction chemotherapy followed by surgery. Groups were compared for difference in patient demographics, comorbidities, and disease specific factors. Kaplan–Meier analysis was used to assess overall survival. Cox’s hazard ratio (HR) analysis was used to assess factors affecting overall survival.

Results: A total of 2,711 patients were included in the analysis. The mean age was 62 years and 67.5% of patients were male. The most common subsite was the maxillary sinus (59.3%), followed by the nasal cavity (29.3%), and the ethmoid sinuses (11.3%). The most common treatment modalities were chemoradiation (16.5%), surgery followed by chemoradiation (16%), surgery followed by radiation (15.9%), surgery alone (9.8%), induction chemotherapy followed by radiation (9.3%), and radiation only (7.4%). Kaplan–Meier analysis demonstrated a 5-year overall survival of 45% for primary surgery patients, 42% for neoadjuvant therapy followed by surgery, 36% for induction chemotherapy followed by radiation, and 27% for chemoradiation alone. On Cox’s hazard analysis maxillary sinus (HR = 1.39), cN2 disease (HR = 1.48), SCCa spindle cell variant (HR = 2.160), advanced age (HR = 1.76), and chemoradiation (HR = 1.27) were found to have a statistically significant impact on the risk of death. Negative margins were associated with a lower risk of death (HR = 0.74). Specifically for T4B tumors, advanced age and chemoradiation remained risk factors for death. When surgically treated patients were grouped according to margin status and compared with the aforementioned treatment groups the difference in survival curves was more pronounced but only achieved statistical significance for worse survival in the chemoradiation treatment group.

Conclusion: In our analysis, surgery was a common treatment modality both in the setting of surgery plus adjuvant treatment and neoadjuvant treatment followed by surgery. Overall the surgically treated patients had a trend toward improved survival when compared with other treatment groups but only reached statistical significance when compared with patients treated with chemoradiation alone. The survival differences more pronounced when negative margins were achieved during surgery.



A019. Survival Outcomes in Sinonasal Poorly Differentiated Squamous Cell Carcinoma

Feras Y. Ackall¹, Ian Barak², Khalil Issa¹, Jordan Teitelbaum¹, David W. Jang¹, Sin-Ho Jung², Ralph Abi Hachem¹

¹Duke University Medical Center, Durham, North Carolina, United States

²Duke University, Durham, North Carolina, United States

Introduction: Primary sinonasal malignancies are rare with squamous cell carcinoma (SCC) representing the most common type. Histological differentiation of SCC has been shown to determine its biological behavior. Multimodality treatment is often employed in management of these tumors, though there is no consensus on treatment regimen and sequence of therapy. Our goal is to analyze treatment outcomes in poorly differentiated SCC (PDSCC) using a large national database.

Methods: The National Cancer Database (NCDB) was queried for sinonasal invasive SCC, grade 3 (poorly differentiated) from 2004 to 2014. Patient demographics (age, sex, and race), tumor characteristics (TNM stage, primary site, grade, and histological subtype), and treatment characteristics (year, treatment modalities, facility volume, and surgical margin status) were tabulated. Kaplan–Meier (KM) analysis was performed to compare overall survival (OS) between tumor histology subtype as well as primary tumor site. Multivariable Cox’s proportional hazards regression was performed for statistical analysis of treatment regimen on OS.

Results: A total of 1,074 patients were identified. Most patients were white (82%) males (67%) with a median age of 64 years. The maxillary sinus was the most common site

(45%) and SCC, NOS the most common subtype (72%). T4 tumors were observed in 50% of patients with most patients treated at high volume facilities (77%) with radiation therapy alone (25.2%) followed by surgical resection with adjuvant radiation (24.4%). Among them, 626 patients underwent surgical resection as part of their treatment and in 63% of these cases, negative margins were obtained. In KM analysis, spindle cell SCC histological subtype was associated with worse OS (median OS: 15.1 months, $p = 0.028$) as were primary tumors of the maxillary sinus (median OS: 25 months, $p < 0.001$). In our Cox-PH model, higher T-stage (HR = 1.92, 2.61, and 3.60 for T2, T3 and T4 patients, respectively; $p < 0.001$) and age (HR = 1.02, $p < 0.001$) was associated with worse survival. Treatment at a high-volume facility (HR = 0.68, $p = 0.01$) and those who underwent surgical resection followed by adjuvant radiation (HR = 0.68, $p = 0.01$) had improved OS. Chemotherapy within the treatment regimen did not confer survival benefit overall (NS). In a model of only surgical patients, surgery plus adjuvant radiation when negative margins were obtained (HR = 0.71, $p = 0.09$), and surgery plus chemoradiation when positive margins were present (HR = 0.63, $p = 0.08$) trended toward improved survival.

Conclusion: Sinonasal PDSCC appears to be best treated at high-volume centers with surgical resection plus adjuvant radiation. Chemotherapy may have a role in patients with positive surgical margins along with adjuvant radiation. A prospective, multicenter, randomized controlled trial is necessary to confirm these findings.

A020. Management of Soft Tissue Sarcomas of the Skull Base: Factors Impacting Tumor Control and Disease-Specific Survival

Idara Edem¹, Franco Demonte¹, Ahmed Habib¹, Shirley Su¹, Ehab Hanna¹, Paul Gidley¹, Marcelie Nader¹, Michael Kupferman¹, Jack Phan¹, Shaan Raza¹

¹The University of Texas M.D. Anderson Cancer Center, Houston, Texas, United States

Background: Soft tissue sarcomas (STS) of the skull base are rare and, as such, there is limited published knowledge and data to guide the surgical management of patients with these tumors.

Objective: This study was aimed to determine the factors that affect tumor control rates and survival in patients undergoing surgical resection of soft tissue sarcomas of the skull base.

Methods: Retrospective review of prospectively collected data for 60 patients with soft tissue sarcomas of the skull base, surgically treated at our institution between 1969 and 2016. Tumor and treatment-related factors were collected and assessed for impact on progression-free survival (PFS) and disease-specific survival (DSS). Tumors were graded according to the Federation Nationale des Centes de Lutte Contre Le Cancer (FNCLCC) system, which is used to categorize STS subtypes according to histologic features predictive of biologic behavior. Kaplan–Meier estimates of PFS and DSS were calculated and survival curves were compared using the log rank test. The Cox proportional hazards model was used in the univariate and multivariate analyses to identify predictive factors.

Results: Sixty patients with a mean age of 35 (range, 2–75) years and a median presenting Karnofsky's performance score (KPS) of 90 were identified for study inclusion. Six (10%) patients were FNCLCC grade 1, 18 (30%) were FNCLCC grade 2, and 36 (60%) were FNCLCC grade 3. The most common histologic diagnoses represented were hemangiopericytoma (23.3%), rhabdomyosarcoma (20%),

malignant fibrous histiocytoma (10%) and liposarcoma (10%). Mean length of follow-up was 73.7 months \pm 57.6 (SD). Five-year PFS and DSS rates were 45 and 60%, respectively. Ten-year PFS and DSS rates were 29 and 32%, respectively. Recurrence occurred in 19 (31.7%) patients. The most common cause of treatment failure was local recurrence, in 12 of 60 patients (20%). In the multivariate analysis for the entire cohort, metastasis on presentation was an independent predictor of poor DSS (hazard ratio [HR] = 3.76, 95% confidence interval [CI]: 1.53–9.21). For patients who presented without metastasis ($n = 52$), prior radiation treatment (HR = 0.009, CI: 0.023–0.590), cavernous sinus involvement (HR = 0.051, CI: 0.010–0.270) were negative predictors while gross total resection (GTR) with negative margins (HR = 9.416, CI: 1.276–69.514) was a positive predictor of PFS. For DSS, brain invasion (HR = 0.254, CI: 0.089–0.729) was the only independent predictor of survival.

Conclusion: The most common cause of treatment failure for patients with soft tissue sarcomas of the skull base is local recurrence, which defines the goals of treatment. Metastasis at presentation was an independent predictor of poor DSS. For patients presenting with local disease only, prior radiation treatment, cavernous sinus involvement, and GTR with negative margins were independent predictors of PFS whereas brain invasion was an independent predictor of poor DSS. This data can be used to inform surgical decision making and counseling for patients with soft tissue sarcomas of the skull base.

A021. Treatment of Sinonasal Squamous Cell Carcinoma: The Experience at a Single Tertiary Care Facility Over 32 Years

Michael J. Sylvester¹, Rachel Fenberg¹, Erin L. McKean¹, Kyle K. VanKoeveering¹

¹University of Michigan, Ann Arbor, Michigan, United States

Background and Objective: Relative to many other head and neck cancers, sinonasal squamous cell carcinoma (SNSCC) is a rare malignancy of the head and neck with notably poor prognosis. Although it is the most common carcinoma of the sinonasal cavity, it comprises only 3 to 5% of all head and neck cancers. Treatment of SNSCC classically entails surgical resection followed by adjuvant radiotherapy. A trend toward endoscopic over open tumor resection has resulted in fewer postoperative complications and surgical morbidity, unfortunately with seemingly no significant improvement in survival. Prognosis for SNSCC remains poor with reports of 5-year survival of as low as 50%. Current knowledge and further research of this malignancy is limited by small sample sizes. Thus, we aimed to evaluate the patient characteristics and outcome data among patients with SNSCC treated at a single tertiary care facility.

Methods: We performed retrospective review to analyze the epidemiologic patient characteristics and comorbidities, pathological characteristics, staging, treatment modality, and complications, and survival among patients treated with SNSCC at a single tertiary care hospital from 1987 through 2019.

Results: We identified a total of 59 patients meeting our search criteria. Of them, 17 (28.8%) were female and 42 (71.2%) were male. Average age at diagnosis of our cohort was 60.3 years with a minimum age of 28.7 years and a maximum age of 90.6 years. Of those that had documented smoking history, 42 out of 58 (72.4%) had documented smoking history. Overall 5-year survival for our cohort was 59%.

Conclusion: Here, we report the experience of patients treated for SNSCC at a single tertiary care facility including

analysis of patient characteristics, pathological characteristics, staging, treatment modality and complications, and survival.

A022. Aneurysmal Bone Cysts of the Paranasal Sinuses: The Mayo Clinic Experience and Review of the Literature

Alyssa J. Smith¹, Kathryn V. Abel¹, Garret Choby¹

¹Mayo Clinic, Rochester, Minnesota, United States

Background/Purpose: Aneurysmal bone cysts (ABCs) are benign, lytic bone lesions that commonly arise in long bones and vertebral column, and more rarely in the head and neck. Presentation in the paranasal sinuses is an even rarer entity and there is no consensus in the literature on the appropriate diagnostic or treatment approaches for these patients. The purpose of this study was to elucidate the clinical behavior, treatment, and outcomes for patients presenting with ABCs of the paranasal sinuses.

Methods: A literature search was performed to identify reports of ABCs of the paranasal sinuses (psABC) in the literature. Additionally, a retrospective chart review was performed to identify patients evaluated at the authors' center with a histopathologically confirmed diagnosis of psABC.

Results: A total of 90 patients (82 cases from the literature search and 8 cases from the author's institution) met inclusion criteria. The median age at diagnosis was 14 years (range, 4 months–90 years) and median symptom duration prior to presentation was 4 months (range, 3 days–6 years). The most common presenting symptom was painless facial swelling ($n = 35$, 38.9%). The ethmoid sinuses were the most likely subsite involved ($n = 55$, 61.1%) followed by unilateral maxillary sinus involvement ($n = 24$, 26.7%). Also, 86 patients (95.6%) underwent surgical treatment. The surgical approach was reported in 75 cases, with 20 cases (26.7%) done completely endoscopically and 55 (73.3%) requiring an open or combined approach. Further, 61 patients (70.9%) underwent an R0 resection of their tumor, 23 patients (26.7%) underwent an R1 resection, and 2 patients did not have any data reported for the amount of tumor resected. 10 patients (11.1%) underwent adjuvant radiation therapy. Follow-up data were reported for 68 patients. Median follow-up time was 14 months (range, 1 month–10 years). But 16 patients (23.5%) were found to have a poor outcome (recurrence or progression of their disease) at follow-up. Only 11 of these patients (68.8%) had recurrence or progression within the first 12 months after treatment. Based on univariate Cox's proportional hazard models, patients were more likely to have a poor outcome if they presented with proptosis (HR = 3.73) or orbital involvement on imaging (HR = 3.22). Factors that did not have a statistically significant effect on outcome included age at diagnosis, sex, medical comorbidity, diagnosis of fibrous dysplasia, adjuvant treatment with radiation or medical therapy, or presence of bilateral or multi-sinus disease (**Fig. 1**).

Conclusion: psABCs typically present with symptoms of painless swelling or nasal obstruction. Orbital involvement at the time of presentation is a negative prognostic indicator with these patients being more likely to have recurrence after treatment. Recurrence or progression of disease is most likely to occur in the first year after treatment and therefore patients should be monitored closely during this time period.

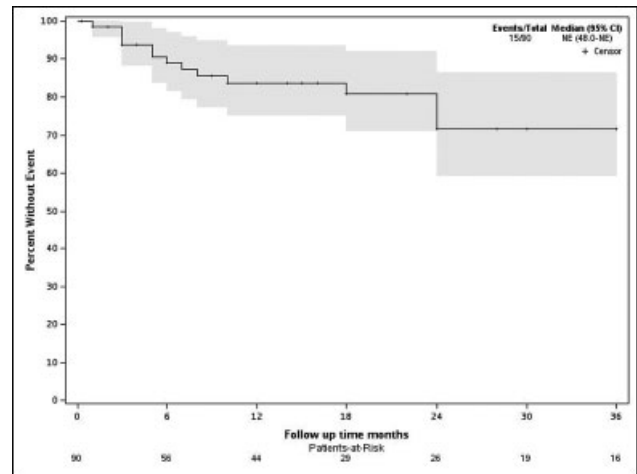


Fig. 1 Kaplan–Meier estimate of time to event (recurrence or progression).

A023. Sinonasal Undifferentiated Carcinoma: An Institutional Trend towards Induction Chemotherapy followed by Definitive Chemoradiation

Nyall London¹, Ahmed Mohyeldin², Georges Daoud³, Dukagjin Blakaj³, Mauricio Gamez³, Ricardo Carrau³

¹Johns Hopkins University, Baltimore, Maryland, United States

²Stanford University, Stanford, California, United States

³The Ohio State University, Columbus, Ohio, United States

Background: Sinonasal undifferentiated carcinoma (SNUC) is an aggressive locally invasive malignancy of the sinonasal cavity treated by multimodality therapy. Recent reports have investigated the role of induction chemotherapy in the treatment of SNUC. The goal of our study was to ascertain the effects of the addition of induction chemotherapy in the treatment paradigm of SNUC at our institution.

Methods: A retrospective chart analysis of 21 cases of SNUC from 2010 to 2018 at a single institution was performed. A retrospective chart review was conducted including demographic information, disease pathology, patient presenting symptoms, smoking/alcohol history, and surgical, chemotherapy, and radiation treatments utilized. A treatment algorithm was developed based on the data presented in this study and past experience.

Results: The average age at diagnosis was 58.9 years. The most common presenting symptom included nasal obstruction/congestion (47.6%), epistaxis (38.1%), and visual changes/diplopia (38.1%). The average SUV on PET-CT was 35.3. Of the 21 patients in this cohort, 18 (85.7%) presented with T4 disease, 7 (33.3%) presented with nodal disease, and 3 (14.3%) presented with distant metastasis. Six patients underwent surgery, three of six as definitive management, and two of six for decompression of the visual apparatus. Prior to 2016, patients at this institution were managed by multiple Head and Neck teams and multimodality treatment varied from initial surgical management, various combinations of cisplatin and etoposide, and radiotherapy approaches. In 2016, management trended to transfer to a single team that preferred induction chemotherapy consisting of three cycles of docetaxel and cisplatin at 75 mg/m² and fluorouracil at 3,000 to 3,750 mg/m² followed by concurrent chemoradiation. Since 2016, all patients with SNUC were managed using the latter paradigm. To this point, patients treated with TPF induction chemotherapy followed by concurrent chemoradiation show no evidence of disease (mean follow-up of 16.8 months). Of the 17 patients in this study who have

completed a full course of chemoradiation, 5 (29.4%) required surgical lysis of adhesions due to synechiae of the nasal cavity. Based on the results of this study and past experience, a treatment algorithm was developed incorporating induction chemotherapy and indications for surgical management (Fig. 1).

Conclusion: Multimodality treatment for SNUC has recently begun transitioning, as highlighted by this study, toward increased use of induction chemotherapy rather than initial surgery. Induction chemotherapy may aid in selecting for patients who will respond well to definitive concurrent chemoradiation. This study contributes to a growing body of literature highlighting the use of induction chemotherapy for SNUC.

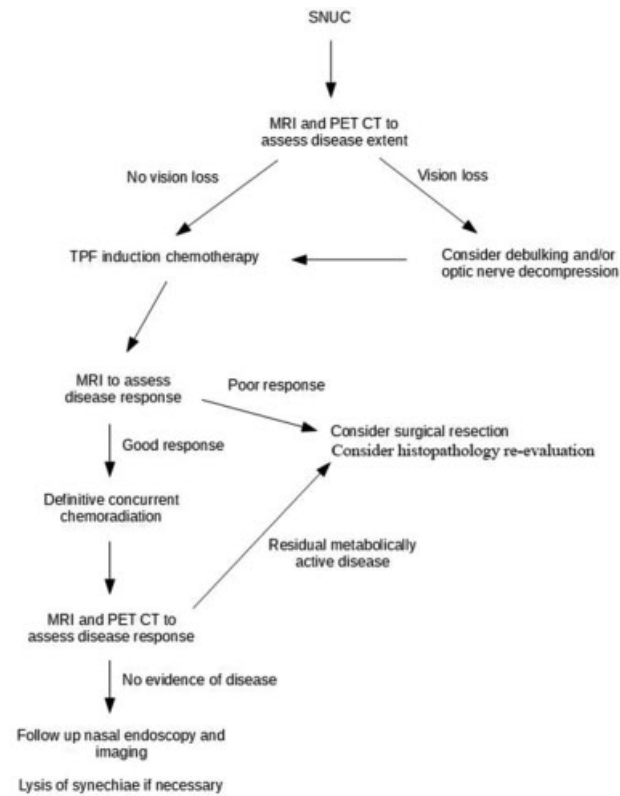


Fig. 1 Treatment algorithm.

A024. Sinonasal Squamous Cell Carcinoma Outcomes: Does Treatment at a High-Volume Center Confer Survival Benefit?

Jordan I. Teitelbaum¹, Ian Barak¹, Khalil Issa¹, Feras Ackall¹, Sin-Ho Jung¹, David Jang¹, Ralph Abi-Hachem¹

¹Duke University Medical Center, Durham, North Carolina, United States

Background: Sinonasal squamous cell carcinoma (SCC) is a rare tumor. Treatment involves multiple modalities, as well as a multidisciplinary team of specialists. Due to the complexity and infrequency of sinonasal SCC, clinical volume, and experience of the treating center may contribute to patient outcomes.

Methods: The National Cancer Database (NCDB) dataset from 2004 to 2014 was analyzed. Patients with sinonasal SCC were identified. Patient demographics, tumor characteristics including primary site, tumor classification (T-stage), resection margins, treatment regimen (surgery, radiation, chemotherapy, and multimodality), and facility case-specific volume averaged per year and grouped in tertiles as low (0–

33%), medium (33–67%), and high (67–100%) were compared. Overall survival was compared using Cox’s proportional hazards regression analysis.

Results: A total of 3,835 patients who were treated for sinonasal SCC between 2004 and 2014 were identified. Therapeutic options for patients included surgery alone (18.6%), radiotherapy (RT) alone (29.1%), definitive chemoradiation (15.4%), surgery with adjuvant RT (22.8%), and combinations (14.1%) of the aforementioned treatments. On multivariate analysis, patients who underwent surgery with adjuvant RT had better overall survival (HR = 0.74, $p < 0.001$, CI: 0.63–0.86). As for treatment volume per facility, 7.4% of patients were treated at a low-volume center, 17.5% at a medium-volume center, and 75.1% at a high-volume center. For all patients who underwent treatment, univariable analysis showed that treatment at a high-volume facility conferred a significantly better overall survival (HR = 0.77, $p = 0.002$). Multivariable Cox-PH regression analysis adjusting for age, sex, tumor classification, and treatment regimen demonstrated that patients who underwent treatment at a high-volume facility (HR = 0.81, $p < 0.001$) had statistically significantly improved survival.

Conclusion: This study shows a better overall survival for sinonasal SCC treated at high volume centers. Further study may be needed to understand the effect of case volume on the paradigms of sinonasal SCC management.

A025. 1,000 Consecutive Endonasal Endoscopic Skull Base Cases: How Long is the Learning Curve?

Iyan Younus¹, Rafael Uribe-Cardenas¹, Peter Morgenstern¹, Mahmoud ElJalby¹, Ashutosh Kacker¹, Vijay K. Anand¹, Theodore H. Schwartz¹

¹Weill Cornell Medicine, New York, New York, United States

Introduction: Endoscopic endonasal approaches (EEA) to the skull base have evolved over the past 20 years to become an essential component of a comprehensive skull base practice at most major academic medical centers. Given its relative infancy, large series of cases with detailed analysis of the indications, results and complications of this rapidly changing field are lacking. Many case series show a learning curve from the earliest cases, where the authors were inexperienced or were not using advanced closure techniques. We eliminated early cases to examine the alterations in practice and outcomes in a more mature series.

Methods: We reviewed a prospectively acquired database of all EEA cases performed by the senior authors at Weill Cornell Medicine/New York Presbyterian Hospital. Although the first cases were performed in 2004, we eliminated the first 200 cases and included 1,000 consecutive cases from January 2008 to December 2018 to avoid the bias created by the early learning curve. Data entered prospectively into the database included pathology, approach, closure technique and materials, intraoperative CSF leak, use of lumbar drainage and post-operative CSF leak. Other demographics and extent of resection were determined retrospectively by chart and MRI review.

Results: Of the 1,000 cases, the most common pathologies included pituitary adenoma (51%), meningoencephalocele or CSF leak repair (8.6%), meningioma (8.4%), craniopharyngioma (7.3%), odontoid (3.1%), RCC (2.8%), chordoma (2.4%), other malignancies (2.3%), and metastasis (1.6%). More procedures for craniopharyngioma (56%), odontoid (81%), RCC (68%), and metastasis (70%) were performed in the latter half of the cohort compared with the first half (44, 19, 32, and 30%, respectively). Lumbar drains were used in 24% of our cases, 32% in the first half and 16% in the second half of cases ($p < 0.05$). GTR increased from 40% in the first

half to 73% in the second half ($p < 0.005$). GTR increased most dramatically for chordoma (56 vs. 100%; $p < 0.05$) and craniopharyngioma (41 vs. 71%; $p < 0.05$). The rate of any complication was 6.4% in the first half and 6.2% in the latter half of cases and vascular injury occurred in only 0.3% of cases. Post-operative CSF leak occurred in 2% of cases (meningioma 7.1%, chordoma 4.2%, RCC 3.6%, craniopharyngioma 2.7%, pituitary adenoma 0.8%) and was overall unchanged between the first and second half of the series.

Conclusion: EEA for a variety of skull base pathologies is becoming increasingly safe and effective over time. With practice, experience and an algorithm for closure based on pathology, location and presence of a leak, rates of CSF leak and complications can be quite low. Nevertheless, even after several hundred cases, there are noticeable improvements in outcome, particularly extent of resection for more complex tumors indicating a long, albeit flatter learning curve.

A026. Complications following 1,002 Endoscopic Endonasal Approaches at a Single Tertiary Center: Lessons Learned 2010 to 2018

Douglas A. Hardesty¹, Alaa Montaser¹, Daniel Kreatsoulas¹, Varun Shah¹, Brad A. Otto¹, Ricardo Carrau¹, Daniel M. Prevedello¹

¹Ohio State University, Columbus, Ohio, United States

Introduction: The endoscopic endonasal approach (EEA) has evolved into a mainstay of skull base surgery over the last two decades. Publications examining intraoperative and perioperative complications of this technique remain scarce, and the landmark series of 800 patients published by Kassam in 2011 examined the first era of EEA (1998–2007). We sought to examine our single-institution series of over 1,000 patients undergoing EEA neurosurgery procedures since year 2010, to elucidate safety and risk factors for complication in the perioperative and postoperative setting.

Methods: We retrospectively reviewed perioperative and postoperative complications in patients undergoing EEA between 2010 and 2018 at our institution, after IRB approval.

Results: We identified 1,002 patients meeting inclusion criteria. Pituitary adenoma was the most common pathology (38%), followed by meningioma (11%). Almost half ($n = 477$, 47.6%) of patients underwent an operation more complex than simple transsellar. Two patients (0.2%) suffered intraoperative carotid artery injury: one had no neurological sequelae, and one suffered permanent hemiparesis after a remote hemorrhage from antiplatelet agents. No patients died intraoperatively. Postoperatively, transient sodium/water hemostasis derangements were not uncommon (8.7%) but rarely permanent (1.5%). Sixty-one patients (6.1%) had postoperative cerebrospinal fluid leaks; 45 of which occurred within the surgical hospitalization. Six patients (0.6%) suffered meningitis, one of whom died. Three other patients died of medical complications, yielding a total mortality of 0.4%. Expanded intradural-level operations were a risk factor for complications (OR = 2.7, level IVa and OR = 6.1 for IVb, each $p < 0.0001$), as were anatomically expanded operations (OR = 2.3 extended sagittal plane, OR = 1.7 sagittal/coronal combined, each $p < 0.002$). From our data, a complicated predicted risk model is proposed.

Conclusion: Our study represents one of the largest cohorts of modern EEA, and demonstrates that even complex EEA have an acceptable safety profile at experienced centers, with low morbidity and mortality. Intraoperative and postoperative complications are nevertheless correlated with increasingly complex procedures and pathologies.

A027. DVT/PE Rates and Etiologies after Endoscopic Endoscopic-Assisted Skull Base Surgery

Kawinyarat Jitaroon¹, Sun H. Song¹, Michael T. Chang¹, Yossawee Wongworawut¹, Nour Ibrahim¹, Juan C. Fernandez-Miranda¹, Zara M. Patel¹, Robert L. Dodd¹, Peter H. Hwang¹, Griffith R. Harsh², Jayakar V. Nayak¹

¹Stanford University, Stanford, California, United States

²University of California, Davis, California, United States

Introduction: Endonasal/endoscopic-assisted (endo-assisted) skull base surgery is associated with protracted operative times, often followed by prolonged periods without ambulation, possibly increasing the risks of postoperative deep vein thrombosis (DVT) and pulmonary embolism (PE). However, perioperative DVT/PE prophylaxis is rarely administered for these procedures due to concern for intracranial hemorrhage. We therefore sought to establish the first evidence regarding incidence of DVT/PE after endoscopic/endo-assisted skull base surgery, and define any predisposing factors for DVT/PE following endoscopic skull base procedures.

Methods: Single institution, retrospective review of all endoscopic/endo-assisted skull base surgeries in patients >15 years old, over a 10-year period from 2009 to 2019, was conducted. Patient demographics, DVT/PE incidence and risk factors, hospital course, comorbidities, and Caprini's score were enumerated. Skull base tumor properties including malignancy, functional adenomas, were also assessed. Revision surgeries performed in the same patient were each counted as separate events.

Results: A total of 1,122 patients met inclusion criteria. Overall incidence of DVT and/or PE in endoscopic/endo-assisted skull base surgery was 2.32% (26/1,122), including 1.6% (18/1,122) who experienced DVT only, and 1.25% (14/1,122) who had DVT with PE. With malignancies excluded, the absolute rate of DVT/PE for associated with endonasal skull base procedures was 1.9% (18/966). The overall mean, median and most frequent postoperative durations prior to DVT/PE occurrence were 5, 4.5, and 2 days respectively for the entire patient cohort, and 9, 6, and 4 days when malignant pathologies are excluded. For all patients, an increased risk of DVT and/or PE was associated with (1) decreased mobility ($p < 0.000001$); (2) recent pneumonia ($p < 0.00001$); (3) extended lumbar drain use ($p < 0.0001$); (4) recent stroke ($p < 0.00018$); (5) recent prior DVT/PE ($p = 0.011$); (6) malignant skull base tumor ($p = 0.016$); (7) varicose vein presence ($p = 0.022$); (8) hypertension ($p = 0.024$); (9) recent prior major surgery ($p = 0.033$); (10) hyperlipidemia (0.034); and (11) male gender ($p = 0.037$). Several preoperative endocrinopathies were also independent risk factors for postoperative development of DVT/PE: SIADH ($p = 0.014$), adrenal insufficiency ($p = 0.002$), hypothyroidism ($p = 0.005$), and Cushing's syndrome ($p = 0.013$). For every 10 hours of inpatient admission, postoperative risk of DVT/PE incrementally increased (OR = 1.03, $p = 0.003$). Prolonged duration of hospitalization over 5 days from any condition also significantly augmented the risk of DVT/PE (OR = 4.47, $p = 0.008$). Finally, a mild elevation in the Caprini score (5.92 vs. 4.39) also increased the risk of DVT/PE (OR = 1.39, $p = 0.003$) following endoscopic/endo-assisted skull base surgery.

Conclusion: The incidence of DVT/PE following endoscopic/endo-assisted skull base surgery is approximately 2% (1.9–2.3%), with numerous associated risk factors also identified. A low-to-moderate Caprini's score is still associated with increased DVT/PE risk after these advanced endonasal procedures. These data provide evidence to assist treatment teams in the design of DVT/PE prophylaxis guidelines for endoscopic/endo-assisted skull base surgery, and suggest

that post-operative DVT/PE prophylaxis be considered following completion of postoperative days 3 and 4 in patients with preoperative risk factors or who require prolonged inpatient admission where appropriate.

A028. Impact of Frailty on Outcomes following Endoscopic Endonasal Skull Base Surgery: A Prospective Cohort Analysis of 152 Patients

Ezequiel Goldschmidt¹, Nitin Agarwal¹, Tavis Taylor¹, Stefanie Altieri¹, Andrew Bilderback¹, Carl H. Snyderman¹, Paul Gardner¹, Daniel Hall¹

¹University of Pittsburgh, Pittsburgh, Pennsylvania, United States

Introduction: With an aging population, elderly patients with multiple comorbidities are more frequently undergoing surgical intervention and are at an increased risk for complications. Therefore, developing strategies to preoperatively identify patients who may be at an increased risk of perioperative complications is essential. To this end, the objective measurement of a frailty score may predict the incidence of postoperative adverse events by using a previously validated simple and inexpensive questionnaire.

Methods: A retrospective review of prospectively collected cohort was performed. A quality improvement project was implemented that assessed clinical outcomes after elective endoscopic endonasal approaches (EEAs) to the cranial base from a quaternary care institution between May 2016 and October 2017. Frailty was assessed with the Risk Analysis Index (RAI), and patients were categorized as nonfrail (RAI 0–29) or prefrail/frail (RAI \geq 30). Both the RAI considering the cancer status (C-RAI) and not considering it (NC-RAI) were analyzed. Blood loss, length of stay (LOS), surgical site infections, readmissions, and mortality were analyzed.

Results: Nonfrail patients had a shorter hospitalization compared with prefrail/frail patients (3.2 ± 3.3 days vs. 3.9 ± 3.5 days, $p < 0.001$). Prefrail and frail patients were more likely to require admission to the ICU after surgery than nonfrail patients (17.4 vs. 11.4%, respectively, $p < 0.05$). The C-RAI showed a significant difference in mortality between nonfrail and prefrail/frail patients at 90 days (0 vs. 4.9%, $p < 0.001$) and 1 year (0 vs. 9.8%, $p < 0.001$), whereas the NC-RAI elicited a difference at 60 days (0 vs. 8.3%, $p < 0.05$), 90 days (0.7 vs. 8.3%, $p < 0.05$), and 1 year (1.4 vs. 16.7%, $p < 0.05$).

Conclusion: Frailty, measured using RAI, predicts mortality, length of stay and ICU requirement after endoscopic endonasal approaches, and is a useful and objective tool to assess perioperative risk in elderly patients undergoing this type of surgery.

A029. Clinical Outcomes and Complications following Internal Neurolysis for the Treatment of Trigeminal Neuralgia: An Institutional Case Series

Jacob Mazza¹, Victor Sabourin¹, Pascal Lavergne¹, Jeffery Head¹, Tomas Garzon¹, Donald Ye¹, Anthony Stefanelli¹, Fadi Al-Saiegh¹, James J. Evans¹

¹Thomas Jefferson University, Philadelphia, Pennsylvania, United States

Introduction: Treatment for trigeminal neuralgia (TN) has evolved over the years. Although medication, particularly carbamazepine, remains the primary option, many surgical interventions are available to provide pain relief. Microvascular decompression (MVD) has been the cornerstone of surgical therapy in the last decades. However, fewer options are available for patients without neurovascular compression (NVC) or with low-grade NVC. For those patients with limited

surgical options, internal neurolysis (IN) is now being considered an option to provide pain relief. However, the longevity of pain relief and complications accompanying IN has yet to be established.

Methods: We conducted a retrospective review of patients treated at Thomas Jefferson University Hospital (TJUH) for TN who received IN as either stand-alone treatment or in conjunction with MVD. Through retrospective chart review, we collected data variables including pain scores using the Barrow Neurologic Institute (BNI) facial pain scale, and pre- and postoperative facial numbness scores using the BNI facial hypoesthesia scale, as well as general complications, following surgery. Facial numbness scores were collected during patient clinic visits and recorded in the electronic medical record (EMR). Postoperative complications were assessed through patient follow-up clinic visits and recorded in the EMR.

Results: A total of 23 patients treated at TJUH for TN via IN were identified via retrospective chart review. Fifteen patients received combination IN + MVD, and eight patients received IN alone. Preoperatively, 100% of patients rated their facial pain as IV or V on the BNI facial pain scale. Pain relief was obtained in 73% of patients receiving IN as stand-alone therapy and 93% of patients receiving IN + MVD at last follow-up. But 18 (78%) patients had no facial numbness and 5 (22%) had mild, nonbothersome facial numbness preoperatively. At last follow-up, 16 (70%) patients had mild, nonbothersome numbness and 6 (26%) had no facial numbness. Only one (4%) patient rated their facial numbness as mild, bothersome at last follow-up. Additional complications related to trigeminal nerve manipulation included corneal hypoesthesia seen in one (4%) individual. There were no reported incidents of anesthesia dolorosa. Incidence of eye dryness, tongue numbness and wound erosion were also reported.

Conclusion: IN shows promising pain-relief outcomes in a patient population with limited treatment options. While there is an increased rate of facial hypoesthesia, it doesn't seem to affect patient quality of life. Serious adverse events remain rare, with very few cases of severe trigeminal nerve dysfunction. Further studies on IN are necessary to define the long-term pain and complication outcomes, and to determine its exact role in the armamentarium of TN therapies.

A030. Clinical Analysis of 11 Cases of Pseudoaneurysm Hemorrhage of Internal Carotid Artery after Radiotherapy for Nasopharyngeal Carcinoma

Houyong Li¹, Dehui Wang¹, Huabin Li¹, Yurong Gu¹, Xicai Sun¹, Huapeng Yu¹, Quan Liu¹, Huankang Zhang¹

¹Department of Otolaryngology, Eye, Ear, Nose and Throat Hospital, Shanghai Medical College of Fudan University, Shanghai, China

Objective: To investigate the treatment of ruptured pseudoaneurysm of internal carotid artery after radiotherapy for nasopharyngeal carcinoma.

Methods: From June 2012 to May 2019, 11 patients with pseudoaneurysmal hemorrhage of internal carotid artery diagnosed after radiotherapy for nasopharyngeal carcinoma were reviewed, including 8 males and 3 females, with an average age of 53.7 years.

Result: Three patients died of massive hemorrhage after nasal packing and not receiving DSA treatment in time. One patient died of massive hemorrhage during DSA treatment without nasal packing. Three patients underwent anterior and posterior nasal packing and DSA was implanted with covered stent to survive. Two patients were treated with DSA spring coil occlusion because they could not implant the covered stent after nasal packing. One patient survived and

one died of brain edema. One case underwent DSA examination after anterior and posterior nasal packing. It was found that the pseudoaneurysm of internal carotid artery was ruptured and the covered stent could not be implanted. BOT test was positive. After superficial temporal artery bypass with middle cerebral artery, the internal carotid artery was embolized and survived.

Conclusion: Internal carotid artery hemorrhage after radiotherapy for nasopharyngeal carcinoma can be effectively treated by DSA implantation after nasal packing.

A031. Postoperative Nasal Debridement in the Operating Room after Endoscopic Skull Base Surgery: When is it Indicated?

Adedamola Adepoju¹, Kent Curran², Maria Peris-Celda¹, Tyler Kenning¹, Carlos Pinheiro-Neto³

¹Department of Neurologic Surgery, Albany Medical Center, Albany, New York, United States

²Albany Medical College, Albany, New York, United States

³Division of Otolaryngology and Head and Neck Surgery, Department of Surgery, Albany Medical Center, Albany, New York, United States

Introduction: The nasal debridement after endoscopic endonasal skull base surgery is a fundamental step in the overall postoperative patient care. The debridement aims to decrease the risk of infections improving the drainage of the sinuses and nasal breathing after the surgery. Depending on the degree of nasal structures resected for the approach, the type of reconstruction and comorbidities, some patients may require several office visits for the nasal cleaning. Most adult patients often tolerate the outpatient debridement with topical local anesthesia. However, some patients cannot tolerate debridement in the clinic and the procedure is performed in the operating room under general anesthesia or deep sedation. There is no study in the literature that clarifies this issue. The main objectives of the study are to determine the incidence of debridement performed in the operating room (inpatient) and to elucidate the factors associated with it. In addition, we sought to determine factors that are associated with increased nasal crusting, and the frequency of debridement in the outpatient setting.

Methods: The medical data of adult patients who had endoscopic endonasal skull base surgery at Albany Medical Center from January 2014 to December 2018 were reviewed retrospectively. Premorbid and operative data including the type of endoscopic approach and the type of reconstruction (none, mucosal grafts, and pedicled flap) were recorded. Postoperative data including the number of outpatient and inpatient debridement was recorded. Chi-square, *t*-test, Fisher's analysis were used for statistical analysis

Results: Two hundred and thirty-five (235) patients who met the inclusion criteria had 246 surgeries. The average age was 55 years (range, 18–87 years). Female comprised 57.0%. Majority of the disease 65.4% was sella/suprasellar lesions including pituitary adenoma, and craniopharyngioma. Eleven percent of the cases involved anterior cranial skull base resections. Free mucosal graft from the nasal floor was used for reconstruction in 53.2% and a pedicled flap including either nasoseptal or pericranial flap was used in 22.8%. Fifty-eight cases (23.7%) were extradural procedures and did not require reconstruction. The rate of postoperative inpatient debridement was 4.90% with average of 37.6 ± 15.3 days from the primary surgery. The harvesting of pedicled flaps showed a statistical association with the need of inpatient debridement compared with free mucosal graft and no reconstruction (12.5 vs. 3.8 vs. 0.0% $p < 0.05$). Pedicled flap patients also required more outpatient nasal debridement than nonpedicled flap patients (2.6 vs. 1.7 vs. 1.5 debride-

ment; $p < 0.001$). History of psychiatric disorder was also associated with need for inpatient debridement (9.52 vs. 3.30%, $p < 0.05$). Current tobacco smoking had higher rate of inpatient debridement but was not statistically significant (9.09 vs. 4.22%, $p > 0.05$).

Conclusion: Nasal debridement performed in the operating room is a low occurrence in postoperative management of patients who underwent endoscopic skull base surgery. The harvesting of pedicled flaps, history of psychiatric disorders, and possibly smoking are the main factors associated with increased risk of need for inpatient debridement in the adult population. Patients with these risk factors should be counseled about that possibility during the initial evaluation.

A032. The Expanded Endonasal Approach: Does Greater Exposure Change Rhinologic Outcomes?

John M. Byrne IV¹, Ari Stone², Margaret Tallmadge¹, Krista Brackman¹, Bhavani Kura², Juanita Celix², Amin Kassam², Sammy Khalili²

¹Aurora Research Institute, Inuvik, Canada

²Aurora Neuroscience Innovation Institute, Milwaukee, Wisconsin, United States

Objective: This study was aimed to investigate the postoperative sinonasal outcomes of patients who have undergone a widely expansive expanded endonasal approach.

Methods: A retrospective chart review of patients who had undergone a widely expansive expanded endonasal approach procedure by a single skull base surgery team between June 1, 2016 and June 1, 2019 was completed. Inclusion criteria were only those patients that completed a Sinonasal outcome test-22 (SNOT-22). Our approach was characterized by either a uninostril or a binostril technique with a posterior septectomy, depending on the lesion location. If a skull base defect was present, a nasoseptal or pericranial flap was used. An abdominal fat graft was also employed as a biologic dressing when an intraoperative cerebrospinal fluid (CSF) leak presented. Patients were seen preoperatively and 1, 2, and 4 weeks postoperatively. They were also seen for follow-up at 3, 6, and 12 months postoperatively. Postoperative care included debridements at 1-, 2-, and 4-week follow-up clinic visits. Each patient had nasal packing and antibiotics postoperatively. Packing was removed within the first week after surgery. Once packing was removed, patients were instructed to use a NeilMed rinse bottle with saline rinse at minimum six times per day until advised to discontinue usage. Fat grafts were removed at the third postoperative visit, 4 weeks after surgery. Preoperative SNOT scores were compared with scores collected at each postoperative clinic visit. The patient population was divided between individuals that underwent a uninostril approach or a binostril approach to determine if there was any difference between the two groups 6 months post-surgery. Chi-squared analysis was also used to compare possible differences in patient outcomes based on collected patient demographic information including gender, age, whether they were diabetic, depressed, anxious, and using immunocompromising or topical medications.

Results: Only 139 skull base surgeries with an associated SNOT score were completed during the 3-year review period. There was no significant difference in total, rhinological or quality of life patient outcomes, measured via SNOT-22 scores, at least 6 months postoperatively when compared with preoperative scores ($p = 0.157$). Comparison of uninostril vs. binostril approaches also did not show any significant difference in outcomes at least 6 months after

surgery ($p = 0.5353$). There was no statistical difference between groups based on reconstruction method.

Conclusion: The widely expansive expanded endonasal approach with active postoperative care does not appear to affect long-term rhinological or quality of life patient outcomes. The benefits of our approach include increased operative dexterity, topical delivery of postoperative medication, and visualization of pathology.

A034. Distal Vascular Compression (Beyond the Obersteiner Redlich Zone) during Fully Endoscopic Microvascular Decompression for Trigeminal Neuralgia

Rachel Blue¹, John Y. K. Lee¹

¹University of Pennsylvania, Philadelphia, Pennsylvania, United States

Objective: Proximal vascular decompression of the trigeminal nerve at the Obersteiner Redlich zone has become the neurosurgical standard of care since Dr. Jannetta introduced microvascular decompression in 1967. Fifty years later, the introduction of the endoscope into the CP angle provides the surgeon the ability to identify distal vascular compression at the entrance into Meckel's cave. In this study, we catalog the incidence of distal (beyond the Obersteiner Redlich zone) vascular compression during endoscopic MVD.

Methods: A retrospective review and analysis of operative videos of endoscopic microvascular decompression (E-MVD) for TN. A 6-year interval review, from 2013 to 2019, yielded 233 consecutive patients undergoing E-MVD by a single surgeon for TN. Start date of 2013 chosen because of institution of centralized server for surgical video backup. Patients undergoing E-MVD for neoplasia or E-MVD for hemifacial spasm/glossopharyngeal neuralgia were excluded. Patients without recorded operative videos were excluded. Trigeminal nerve was always visualized in full from pontine exit zone to its entry into Meckel's cave, and then divided into anatomic half. Vascular compression was categorized into one of four groups: (1) proximal (majority of compression from dorsal root entry zone (DREZ) to midpoint of the trigeminal nerve), (2) distal (majority of compression from midpoint of trigeminal nerve to Meckle's cave), (3) both proximal and distal (separate and distinct proximal and distal compression), and 4) no discernable compression. Additionally, petrosal tubercle (PT) bone anatomy was analyzed and determined as either obstructive (obstructing visualization of >50% of trigeminal nerve during surgical approach when 0-degree endoscope is in view of both PT and trigeminal nerve) or non-obstructive (obstructing <50% of trigeminal nerve during surgical approach when 0-degree endoscope is in view of both PT and trigeminal nerve).

Results: Proximal vascular compression of the trigeminal nerve was noted in 143/233 (61%) of patients. Distal vascular compression of the trigeminal nerve was noted in 36/233 (15%) of patients (**Fig. 1**). Proximal and distal vascular compression of the trigeminal nerve was noted in 50/233 (21%). No discernable compression was noted in 4/233 (2%) of patients. Petrosal tubercle anatomy noted to be obstructive in 42/233 (18%) of patients (**Fig. 2**) and non-obstructive in 191/233 (82%) of patients.

Conclusion: E-MVD offers benefits compared with conventional microscopic microvascular decompression by way of enhanced visualization, particularly with distal structures and around corners. Two factors directly related to decreased visualization of vascular compression are an obstructive PT and distal compression of the trigeminal nerve near Meckle's cave. This study demonstrates the rate of subsets of patients with obstructive PT and with distal/proximal and distal vascular compression that would have greater difficulty with visualization in a microscopic versus

endoscopic approach. Future work will correlate anatomic findings with outcome.

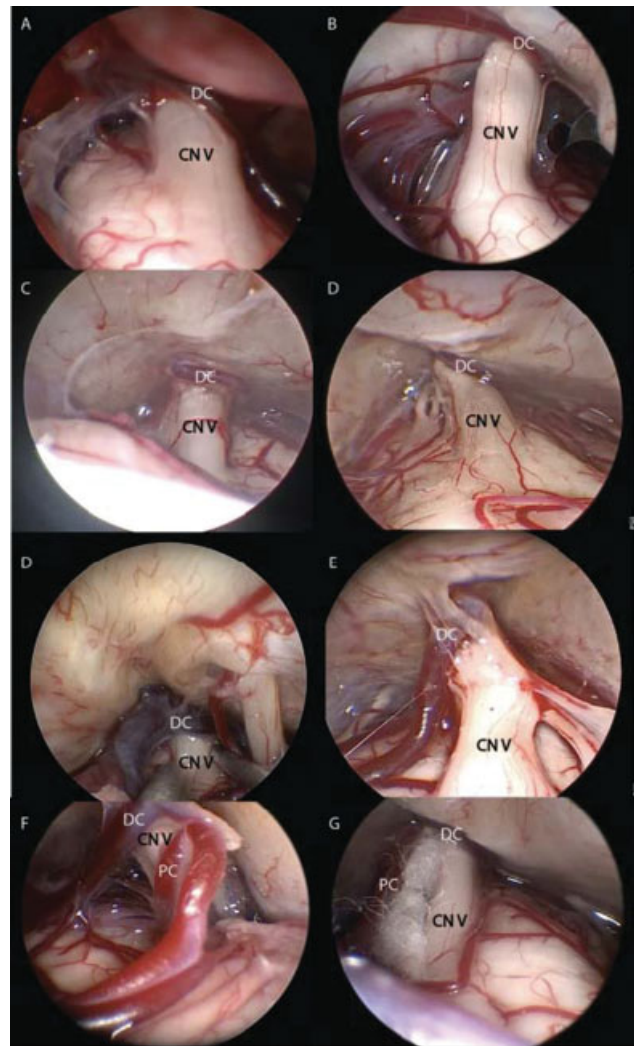


Figure 1: Endoscopic view of distal vascular compression of the trigeminal nerve (A-E) and both proximal and distal vascular compression of the trigeminal nerve (F&G). CNV = trigeminal nerve, DC=distal compression, PC=proximal compression

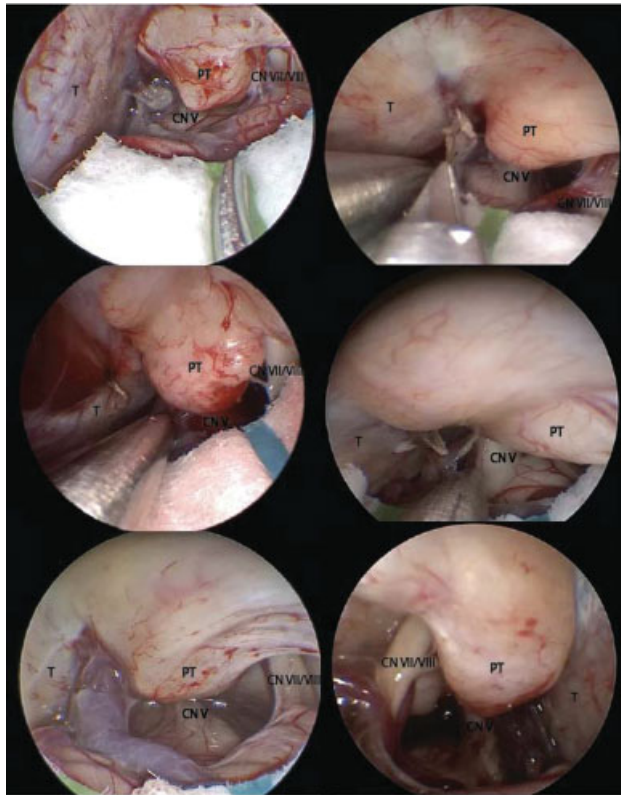


Figure 2. Endoscopic view of obstructive petrosal tubercle (obstructing visualization of >50% of the trigeminal nerve). PT=petrosal tubercle, T=tentorium, CN V=trigeminal nerve, CN VII/VIII= facial nerve and vestibulocochlear nerve.

A035. Comparative Analysis of Endoscopic Transorbital Approach and Extended Minipterional Approach for Sphenoid Wing Meningiomas with Osseous Involvement: Preliminary Surgical Results

Hun Ho Park¹, Jihwan Yoo¹, In-Sik Yun², Chang-Ki Hong¹

¹Department of Neurosurgery, Gangnam Severance Hospital, Yonsei University, Seoul, South Korea

²Department of Plastic surgery, Gangnam Severance Hospital, Yonsei University, Seoul, South Korea

Objective: Sphenoid wing meningiomas (SWMs) with osseous involvement are slow-growing benign tumors that can be cured with complete surgical resection. The majority of symptoms arise from adjacent hyperostosis and recurrences occur from inadequate resection of sphenoid bone infiltration. Sufficient resection of these tumors requires extensive surgical exposure, but recent endoscopic transorbital approach (ETOA) offers one of minimally invasive alternatives. The authors assess the feasibility of ETOA and compare the surgical outcome of ETOA and extended minipterional approach (eMPTA) for SWMs with osseous involvement.

Methods: From October 2015 to May 2019, a total of 24 patients underwent surgery for SWMs with osseous involvement. Among them, tumor resection was performed by ETOA for 11 patients (45.8%) and eMPTA for 13 patients (54.2%). The tumor characteristics, extent of resection, surgical outcome, and morbidity, and approach-related aesthetic outcome were analyzed and compared retrospectively between ETOA and eMPTA based on SWM classification.

Results: The location of SWMs was middle sphenoid ridge (group III) for 15 patients (45.8%), lateral or greater sphenoid wing (group IV) for 7 patients (29.2%), medial or

lesser sphenoid wing (group I) for 3 patients (12.5%), and medial with cavernous sinus (CS) infiltration (group II) for 3 patients (12.5%). Gross total resection was achieved in 9 of 11 patients (81.8%) with ETOA and 11 of 13 patients (84.6%) with eMPTA. There were no differences in tumor classification, histology, size, consistency, peritumoral edema, and adhesion, CS lateral wall invasion, and internal carotid artery displacement between the two approaches. Surgery time, surgical bleeding, and hospital length of stay were significantly shorter with ETOA. Three patients had newly developed symptoms, such as diplopia ($n = 1$), ptosis ($n = 1$), and cerebrospinal fluid leak ($n = 1$) after ETOA, with full recovery later. There were two patients with vasospasm ($n = 1$) and ptosis ($n = 1$) after eMPTA. No differences could be seen in surgical morbidities between ETOA and eMPTA.

Conclusion: The preliminary surgical results suggest that ETOA can be a reasonable alternative to eMPTA for SWMs with osseous involvement. ETOA provides direct access to the sphenoid bone and resectability with a more rapid and minimally invasive exposure than eMPTA. Maximal subtotal resection with extensive sphenoid bone decompression for tumors with CS infiltration is the key to a good clinical outcome, regardless of the surgical approach.

A036. Extent of Surgical Resection of Epidermoid Tumors Affects Risk of Recurrence: Results of the Largest Meta-analysis of 691 Patients

Brian Shear¹, Lan Jin², Yawei Zhang², Wyatt David¹, Elena Fomchenko¹, E. Zeynep Erson-Omay¹, Anita Huttner³, Robert K. Fulbright⁴, Jennifer Moliterno¹

¹Yale Department of Neurosurgery, New Haven, Connecticut, United States

²Yale Department of Surgery, New Haven, Connecticut, United States

³Yale Department of Pathology, New Haven, Connecticut, United States

⁴Yale Department of Radiology, New Haven, Connecticut, United States

Introduction: Neurosurgical resection of epidermoid tumors can be quite challenging and potentially morbid, leading to questions surrounding extent of resection. In the largest meta-analysis to date of patients with epidermoid tumors, we compared recurrence rates for STR and GTR and the associated complications.

Methods: A systemic literature review following the PRISMA guidelines was completed followed by a proportional meta-analysis to compare the pooled recurrence rates between STR and GTR in epidermoid tumors. Fixed- and mixed-effect models were used to compare the pooled proportions of recurrence after STR or GTR. The relationship between recurrence rate and follow-up time was studied using linear regression and natural cubic spline models.

Results: Twenty-seven studies with 691 patients met our inclusion criteria, among whom, 293 (42%) underwent STR, while 398 (58%) received GTR. The average recurrence rate of all procedures was 11%. The proportional meta-analysis showed that the pooled recurrence rate after STR (21%) was seven times that after GTR (3%). The most common surgical complications were transient cranial nerve palsies, occurring equally in STR and GTR cases when reported. The average recurrence rate for studies with longer follow-up time (>4.4 years) (17.4%) was significantly higher than the average recurrence rate for studies with shorter follow-up time (<4.4 years; 5.7%).

Conclusion: STR of epidermoid tumors is associated with a significantly higher rate of recurrence (~ seven times) compared with GTR and correlates with time such that more recurrences, on average, are observed after longer

postoperative periods of time. Types of complications, and their frequencies, do not seem to differ between STR and GTR. Attempts at GTR, when appropriate, should be made during the initial surgery with efforts to optimize success. In all postoperative epidermoid tumor cases, but particularly following STR, close follow-up with serial MRIs, even years after surgery, is recommended.

A037. Choroid Plexus Papillomas of the Cerebellopontine Angle and Fourth Ventricle: Cohort Study

Amanda M. Casabella¹, Avital Perry¹, Christopher S. Graffeo¹, Lucas P. Carlstrom¹, Michael J. Link¹

¹Mayo Clinic, Rochester, Minnesota, United States

Introduction: Choroid plexus papilloma (CPP) is a benign WHO grade-I lesion, which accounts for 1% of adult and 2.5% of pediatric intracranial tumors. CPP predominantly arise in the lateral ventricle, while posterior fossa CPP involving the cerebellopontine angle (CPA) or fourth ventricle are rare, with incompletely understood natural history and optimal treatment.

Methods: Single-institution cohort study of CPP arising within the CPA or fourth ventricle, 1990 to 2018.

Results: A total of 11 CPP were identified in the CPA, and 28 within the fourth ventricle. The most common presentations were headache (89%), imbalance (67%), and dizziness (44%). Cystic components were observed exclusively in CPA tumors (57 vs. 0%), while calcification was comparably prevalent in both groups (27 vs. 25%). Gross total resection (GTR) was achieved in 73% overall, 72.7% in the CPA and 73.1% in the fourth ventricle. Recurrence/progression was observed in five CPA tumors (46%) and nine intraventricular CPP (32%), which were treated with various combinations of radiosurgery ($n = 14$), radiotherapy ($n = 4$), repeated surgery ($n = 3$), and chemotherapy ($n = 9$). Multiple instances of recurrence/progression were observed in six patients (15%). Atypical (WHO grade II) CPP were diagnosed in one CPA tumors (9%) and three fourth ventricle CPP (11%), while metastatic lesions were subsequently identified in three patients, only one of which was classified as atypical on initial histopathologic diagnosis.

Conclusion: CPP are benign tumors that are rarely encountered in the posterior fossa, where they typically present with characteristic signs of mass effect. Although generally amenable to resection, CPP are frequently adherent to cranial nerves, potentially predisposing to increased risk of recurrence in the CPA. Atypical CPP are exceedingly uncommon, but require aggressive, multi-modality oncologic therapy, and metastatic tumors

A038. Endoscopic Endonasal versus Transcranial Approach to Resection of Olfactory Groove Meningiomas: A Systematic Review

Aarti Purohit¹, Roshani Jha¹, Adham M. Khalafallah¹, Carrie Price¹, Nicholas R. Rowan¹, Debraj Mukherjee¹

¹Johns Hopkins School of Medicine, Baltimore, Maryland, United States

Background: Despite the increasing utility of the endoscopic endonasal approach (EEA) for the management of anterior skull base (ASB) pathologies, the optimal treatment strategy for olfactory groove meningiomas (OGM) remains unclear.

Objective: This project sought to systematically compare outcomes of EEA management to the conventional transcranial approach (TCA) for the treatment of OGMs.

Methods: A systematic review was performed to identify studies that compared outcomes following EEA and TCA for OGMs. Data extracted from each study included gross total resection (GTR), incidence of cerebrospinal fluid (CSF) leaks, and postoperative complications including anosmia.

Results: The results of the search yielded five studies that met the criteria for inclusion and analysis. All studies compared TCA ($n = 922$) to EEA ($n = 141$) outcomes for OGMs. Overall, the rate of gross total resection (GTR) was lower among the endoscopic group (70.9%) relative to the transcranial group (91.5%). The rate of postoperative CSF leak were 6.3% versus 25.5% for the transcranial and endoscopic groups, respectively. Postoperative anosmia was higher for patients undergoing EEA (95.9%) compared with patients in the transcranial group (37.4%).

Conclusion: In this analysis, EEA was associated with a lower rate of GTR and higher incidences of CSF leaks and postoperative anosmia. However, with increasing surgeon familiarity with the endoscopic anatomy and technique for managing ASB pathologies, a nuanced approach may be used to minimize patient morbidity and widen the spectrum of skull base surgery.

A039. High Variability of Outside Radiologist Reports in Trigeminal Neuralgia Patients Undergoing Endoscopic Microvascular Decompression

Rachel Blue¹, Denise Miller¹, Carrie Li¹, John Y. K. Lee¹

¹University of Pennsylvania, Philadelphia, Pennsylvania, United States

Objective: Preoperative MRI studies are routinely ordered as workup for patients with trigeminal neuralgia (TN). In this study, we catalog the incidence of neurovascular compression reported by "outside radiologists" on preoperative MRI imaging.

Methods: A retrospective review and analysis of operative videos, medical charts, and MRI imaging of endoscopic microvascular decompression (E-MVD) for TN. A 6-year interval review, from 2013 to 2019, yielded 186 consecutive patients undergoing E-MVD by a single surgeon for TN. Start date of 2013 chosen because of institution of centralized server for surgical video backup. Patients undergoing E-MVD for neoplasia were excluded. Patients without recorded operative videos or preoperative MRI's read by a radiologist were excluded. Patient were initially categorized to have neurovascular compression or no compression based on operative video and chart review. Each group was then further categorized to either compression or no compression noted on preoperative MRI, as read by "outside radiologist." Additional variables collected include: magnet strength (3/1.5 T), FIESTA/CISS/heavy T2-weighted imaging. Patients were offered surgery based on clinical characteristics (sharp, shooting, Burchiel's criteria, medication refractory, etc.) and not based on radiology reports or preoperative MRI findings.

Results: Outside radiologists reported vascular compression in 65 (35%) of all patients who underwent E-MVD. They reported no vascular compression in 39 (21%) patients. Outside radiologists made no mention of having searched or analyzed the study for vascular compression in 82 (44%) patients. Use of higher strength magnet 3T did not influence radiologist reports of vascular compression (30 vs. 29%; $n = 71$ because most did not report type of magnet). Use of FIESTA/CISS sequences did improve likelihood of reporting vascular compression (65 vs. 35%; $p < 0.05$). Intraoperative neurovascular compression was noted in 183 (98%) patients, 4 (2%) patients had no discernable compression. None of the four patients without discernable compression had compression was found on preoperative MRI.

Conclusion: MRIs are routinely ordered preoperatively for patients with TN, largely to rule out other possibly pathologies causing TN. Overall, the frequency of radiographic neurovascular compression reported by outside radiologists is quite low, despite the very high intraoperative findings of neurovascular compression. In our study, we did not find a clear difference between 3T and 1.5T MRI but it does appear that dedicated FIESTA/CISS imaging significantly increases the frequency of neurovascular compression found on preoperative imaging.

A040. Surgical Tips and Pitfalls of Endoscopic Superior Eyelid Transorbital Surgery for Orbit, Middle Fossa, and Meckel's Cave Lesions

Doosik Kong¹, Minsoo Kim¹

¹Samsung Medical Center, Sungkyunkwan University, Seoul, South Korea

Objective: The tumors involving the orbit and Meckel's cave remain extremely challenging because of the surrounding complex neurovascular structures and which involve the deep orbit, floor of the frontal bone and lesser and greater wing of sphenoid bone. We introduce a new minimal-access technique using the endoscopic transorbital approach (eTOA) to cranioorbital lesions, Meckel's cave and the middle cranial fossa lesions and review the surgical tips and pitfalls of this approach.

Methods: Between September 2016 and September 2019, we performed eTOA in 45 patients with tumors involving the sphenoorbital areas, Meckel's cave lesions and middle cranial fossa or petrous apex lesions. The pathologies included schwannoma (14), meningioma (20), dermoid (2), trauma (2), and other malignancies. We evaluated the clinical outcome, associated morbidities, and limitations of this novel surgical technique.

Results: Among 45 patients, 32 (71.1%) underwent gross total or near total resection of tumor. Four patients underwent extended eTOA (with lateral orbital rim osteotomy). For meningioma, GTR/NTR rate was 35% but patients with schwannoma had 92% of GTR/NTR rate. Of them, 14 patients (46.7%) had preoperative proptosis on the ipsilateral side and all of 14 patients had improvement in exophthalmos. Among 10 patients, 6 were with preoperative optic neuropathy had postoperative improvement. Drilling of the trapezoid sphenoid floor, a middle fossa "peeling" technique, and full visualization of the Meckel's cave were applied to access the lesions. There was no postoperative cerebrospinal fluid leak and postoperative optic neuropathy. To access the lateral and inferior margin of the tumor, the emphasis should be placed on the importance of adequately removing the greater sphenoidal wing and lateral orbital rim, when needed. However, eTOA may still have a limitation in approaching posterior fossa lesions and infratemporal fossa because of the limited working space.

Conclusion: The eTOA affords a direct route to access orbit, Meckel's cave and the middle cranial fossa lesions. With experience, this novel approach will be successfully applied to selected skull base lesions.

A041. The Endonasal Endoscopic Perspective of Paraclinoid Aneurysms a Cadaveric Anatomical Analysis

Huy Q. Truong¹, Salomon Cohen-Cohen², Nathan T. Zwagerman¹, Juan C. Fernandez-Miranda³, Paul A. Gardner⁴

¹Medical College of Wisconsin, Milwaukee, Wisconsin, United States

²Mayo Clinic Rochester, Rochester, Minnesota, United States

³Stanford University Medical Center, Stanford, California, United States

⁴University of Pittsburgh Medical Center, Pittsburgh, Pennsylvania, United States

Background: Aneurysms on the paraclinoid segment of the internal carotid artery (ICA) are a rare but challenging to fully assess and treat. Due to the complicated anatomy of the area, several classification systems and terminologies have been proposed focusing on different aspects of the disorder. During endoscopic endonasal dissection of anatomical specimens, several incidental paraclinoid aneurysms were discovered. The anatomical findings of the aneurysms and a literature review on the topic are presented herein.

Materials and Methods: Four anatomical specimens with incidental aneurysms at the paraclinoid segment were used for endoscopic endonasal dissection. All specimens' vasculature was injected with colored latex. A literature review on the topic was performed.

Results: Aneurysm 1: the aneurysm was tightly wrapped by the carotid collar membrane and contained between the proximal (PDR) and distal dural ring (DDR), with the dome projected medially. There was no perforator in the vicinity of the aneurysm and no apparent connection to subarachnoid space was found as the DDR adhered tightly to the wall of ICA. Aneurysm 2: the aneurysm arose at the origin of the secondary superior hypophyseal artery (SHA), and was located in a pouch-like carotid cave with a medially-oriented dome and subarachnoid access. Aneurysm 3: a inferoposteriorly pointing aneurysm that was associated with a primary SHA and was covered with carotid collar, within a slit-type carotid cave, with potential dissection into the intradural space. Aneurysm 4: the aneurysm had no association with ICA perforator, dome projected inferoposteriorly, with no carotid cave and no intradural access.

Discussion: With the complex and highly variant anatomy of the paraclinoid segment of the ICA, associated perforators, the clinoid space, and carotid cave, the classification systems of paraclinoid aneurysm available on current literature seem insufficient in guiding assessment and management of these medially directed aneurysms. Angiographic classifications cannot predict the aneurysm's relationship to dural structures (and therefore risk of hemorrhage) and small perforators. Several authors highlighted the use of MRI for determining the intradural/extradural nature of the aneurysm and the risk of intracranial extension and bleeding of paraclinoid aneurysm by assessing its spatial relationship to DDR and diaphragm sellae. However, the presence of SHA and the slit-type carotid cave makes the distinction not definitive, as demonstrated by cases of aneurysms 2 and 3 in our series. Most of paraclinoid aneurysms have medially or inferiorly projecting domes which offer a favorable angle for clipping through EEA. Several successful clippings of paraclinoid aneurysms through an endoscopic endonasal approach (EEA) have been recently reported in the literature. It is critical for surgeons to understand the risk of subarachnoid hemorrhage indication for surgery, and the dural structures that may tightly adhere to the aneurysm to impact safety and necessity of the surgery (**Fig. 1**).

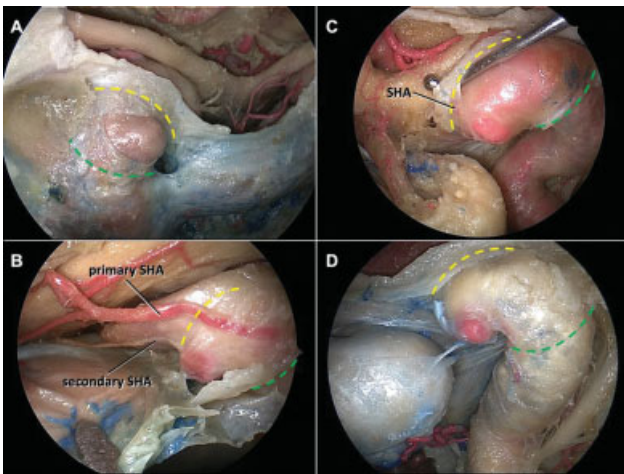


Fig. 1 (A) Aneurysm 1. (B) Aneurysm 2. (C) Aneurysm 3. (D) Aneurysm 4. Green dash line, approximation of proximal dural ring; yellow dash line, approximation of distal dural ring.

A042. Endoscopic Endonasal Approach for Craniopharyngiomas with Intraventricular Extension: Long-Term Outcomes and Meta-analysis

Hanna Algattas¹, Pradeep Setty¹, Ezequiel Goldschmidt¹, Eric W. Wang¹, Elizabeth Tyler-Kabara¹, Carl H. Snyderman¹, Paul A. Gardner¹
¹UPMC

Background: Traditionally, skull base tumors with intraventricular extension are approached via open craniotomy or transventricular approaches. However, craniopharyngiomas are increasingly resected via an endoscopic endonasal approach (EEA); yet those with intraventricular extension are of increased complexity and EEA with this degree of extension is not well studied.

Methods: Patients undergoing EEA for resection of craniopharyngioma with third ventricular involvement between 2002 and 2015 were retrospectively reviewed. Tumor characteristics and outcomes were reviewed and compared with previously published EEA and transcranial approach (TCA) studies for all craniopharyngioma locations. Comparison of these groups was done via meta-analysis and a random effects model.

Results: Sixty-two patients were included. Average tumor volume was 13.93 cm³ with an average 2.61 cm³ (17.3%) intraventricular volume. Patients presented with visual impairment (75.8%), panhypopituitarism (29.0%), headache (16.1%), and diabetes insipidus (16.1%). Gross total resection (GTR) was achieved in 47% of all cases (56% of cases where GTR was the goal); after 2012 the overall GTR rate increased to 77%. Of those presenting with visual impairment, 97.9% experienced improvement or stability of vision. The rates of postoperative cerebrospinal fluid (CSF) leak and meningitis was 19 and 8.1%, respectively. When nasoseptal flap reconstruction (since 2006) was used, the CSF leak rate dropped to 10%. Two patients had tumor bed/intraventricular hemorrhage requiring reoperation and one patient had an epidural hematoma requiring evacuation. There were no postoperative mortalities. Six (9.6%) patients required shunting prior to tumor resection. Overall, 25% underwent postoperative shunt placement with 7 out of 10 patients (70%) treated prior to introduction and routine use of the nasoseptal flap and only 7 of 46 (15%) required a shunt following routine use of nasoseptal flap reconstruction.

Meta-analysis demonstrated overall similarity in presenting features and outcomes between the present cohort for intraventricular lesions, EEA, and TCA for all craniopharyngiomas. TCA demonstrated a higher GTR rate, however, with heterogeneity in the model (sizable study variation). EEA for craniopharyngioma with intraventricular extension showed improved visual outcomes compared with TCA but also increased incidence of CSF leaks without concomitant increase in rates of meningitis (again with heterogeneity in the random effects model).

Conclusion: EEA for craniopharyngiomas with intraventricular extension shows similar outcomes to those of TCA and EEA for all craniopharyngiomas and expands one of the potential anatomic limits of this approach. Given involvement of the ventricle, CSF leak/shunt rates are expectedly high. GTR rates increased and CSF leak/shunt rates decreased dramatically with time and the introduction of the nasoseptal flap. These outcomes reflect the importance of an experienced team and demonstrate a clear learning curve.

A043. Clinical Outcomes of Endoscopic Endonasal Odontoid Resection: A Single Center Experience

Elysia Grose¹, Ioana Moldovan², Shaun Kilty³, Charles Agbi⁴, Andre Lamothe⁵, Fahad Alkherayf⁴

¹Faculty of Medicine, University of Ottawa, Ottawa, Ontario, Canada

²Division of Neurosurgery, Department of Surgery, The Ottawa Hospital Research Institute, Ottawa, Canada

³Department of Otolaryngology- Head & Neck Surgery, University of Ottawa, Ottawa, Canada

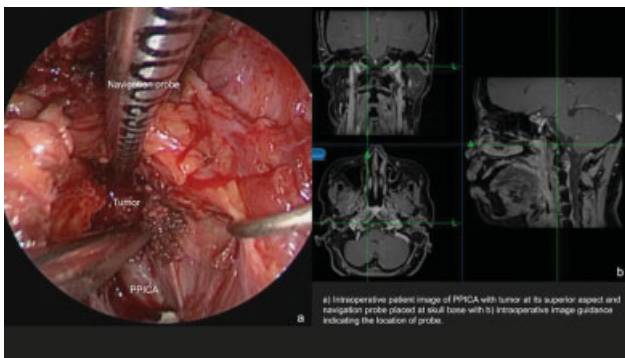
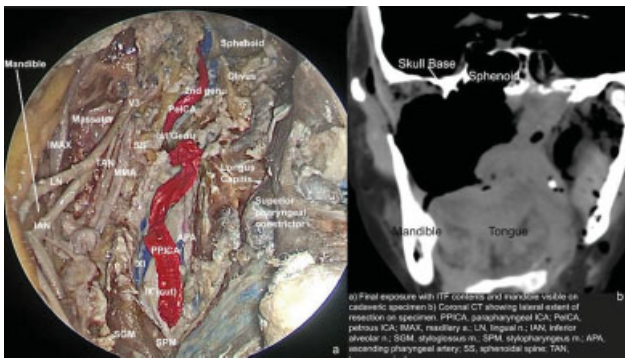
⁴Division of Neurosurgery, Department of Surgery, University of Ottawa, Ottawa, Ontario, Canada

⁵Department of Otolaryngology- Head & Neck Surgery, The Ottawa Hospital, Ottawa, Canada

Introduction: The advent of endoscopic endonasal skull base techniques has enabled safe and effective access to the anterior craniocervical junction which offers several advantages over the traditional transoral approach. Recent literature comparing the endonasal and transoral approach showed that the endonasal approach reduces the length of hospital stay, ventilation time, and the incidence of postoperative tracheostomy, allows earlier extubation and postoperative feeding. Some risks that exist with the transnasal approach, including cerebrospinal fluid (CSF) leakage, cervical instability, and vascular injury, can be effectively managed through the endonasal approach. The objective of this study is to review the intra- and postoperative complications associated with endoscopic endonasal odontoid resection.

Methods: This study is a retrospective chart review of all adult patients who underwent an endoscopic endonasal odontoid resection at a single tertiary care center between January 2011 and May 2019. Demographic, clinical, surgery, and pathology data were collected. Patients' intra- and postoperative complications were analyzed.

Results: Seventeen patients who underwent endoscopic endonasal odontoid resection were included in the study. The median age at admission was 67 years (range, 33–84 years) and 61% of the patients were female. The median follow up duration was 9 months (range, 4–47 months). Indications for surgery included basilar invagination (8/17, 47%), rheumatoid arthritis (3/17, 18%), congenital osseous malformation (2/17, 12%), odontoid fracture (1/17, 6%), and compression of cervicomedullary area (3/17, 18%). Presenting symptoms included difficulty with fine hand movements (10/17, 59%), myelopathy (9/17, 53%), lower cranial nerve symptoms (3/17, 18%), difficulty walking (8/17, 47%), and sensory symptoms (5/17, 29%). Four patients (4/17, 24%) had a syrinx on MRI. In terms of intraoperative complications, one patient



Background: In the past decade, minimal access endoscopic endonasal approaches (EEA) to the nasopharynx have been developed. For large nasopharyngeal tumors extending below the palatal plane and laterally beyond the pterygoid musculature, maxillary swing, and Fisch's type C infratemporal fossa approaches are necessary. The purpose of this study is to evaluate the possibility of achieving an endoscopic transoral nasopharyngectomy (ETON) for resection of large nasopharyngeal lesions as a natural orifice alternative to open approaches.

Study Design: Present study is a cadaveric study with clinical correlate.

Methods: ETON was completed in a fresh cadaveric specimen under endoscopic guidance. The resection extended superiorly to the sphenoid sinus, inferiorly to the same axial plane as the tongue, laterally to the mandible and posteriorly to the prevertebral musculature. Surgical freedom and angles of attack were also measured at the first genu, and the second genu of the internal carotid artery (ICA).

Results: The resection can be completed in two steps. First, parapharyngeal space (PPS) dissection with or without infratemporal fossa (ITF) dissection. An incision is made 2 cm from the maxillary alveolar ridge along the hard palate and carried down to the lateral floor of mouth. Exposure and resection of the posterior hard palate, maxillary tuberosity, pterygoid hamulus, pterygoid plates, and prestyloid PPS was performed followed by identification of the parapharyngeal ICA with subsequent ITF dissection. Second, eustachian tube (ET) removal and sphenoidotomy. The ET is identified superomedially and dissected off the skull base followed by the removal of petrous bone and exposure of petrous ICA with subsequent sphenoidotomy. Full exposure of the parapharyngeal and petrous ICA was achieved. The anterior and posterior genu were accurately identified with accurate dissection and identification of surrounding neurovascular structures. Surgical freedom (cm²) at the first genu and second genu were 20.54 and 26.4 cm², respectively. The angles of attack (degrees) for the first genu were 65.7 and 29.1 degrees on the axial and sagittal planes, respectively. The angles of attack for the second genu were 78.25 and 29.61 degrees on the axial and sagittal planes, respectively. A patient with recurrent nasopharyngeal carcinoma (rNPC) with apparent recurrence surrounding the ICA at the skull base was managed with a pure transoral approach. PPS dissection without ITF dissection was undertaken. The parapharyngeal ICA was successfully identified and followed to the skull base. The tumor was biopsied and the diagnosis was confirmed.

Discussion: ETON is a feasible technique. Resection can extend laterally to the mandible and inferiorly to the level of the tongue, or inclusively lower. ETON may be indicated for the management of nasopharyngeal tumors that extend laterally into ITF and extend inferiorly below the palatal plane. ETON also provides adequate visualization and manipulation of the ICA, as well as accurate dissection of surrounding tissues, thus, making it an attractive approach for tumors in direct contact with the ICA.

A046. Endoscopic Endonasal Optic Canal Decompression: Case Series

Meaghan S. Hodson¹, Jeffrey Glicksman², Tyler Kenning², Maria Peris-Celda², Carlos Pinheiro-Neto²

¹Albany Medical College, Albany, New York, United States

²Albany Medical Center, Albany, New York, United States

Background: Optic nerve decompression surgery has been used for several indications. There is documented use of optic nerve decompression for treatment of papilledema from pseudotumor cerebri, nonarteritic ischemic optic neuropathy, and traumatic optic neuropathy. Prior studies have demonstrated the efficacy of optic nerve decompression in improving vision for these patients. The purpose of this study is to evaluate the demographics of patients who underwent endoscopic endonasal optic nerve decompression, the indication for the surgery, presence of intraoperative complications, outcomes of the surgery in the form of vision improvement, and postoperative complications.^{1,2}

Methods: Medical records were reviewed and data were collected on 13 patients who underwent endoscopic endonasal optic nerve decompression by a single surgical team at a tertiary care medical center between April 2, 2015 and May 8, 2019. Data were analyzed using simple statistical techniques including sums, ratios and averages.^{3,4}

Results: Patients underwent optic nerve decompression surgery for various pathologies including one patient for skull fracture impinging on the optic nerve, six patients for meningiomas extending into the optic canal, one patient for intracranial metastatic breast cancer, one patient for disseminated blastomycosis into the orbital apex, one patient for fibrous dysplasia with optic nerve compression, one patient for orbital and posterior frontal table dehiscence, one patient for optic apicitis, and one patient for plasmacytoma causing compression of the optic canal. The patient population included an age ranged from 37 to 67 years, with the average age of 52 years. The patient population included 7 males and 6 females. The ethnicities of the patient population included 10 Caucasian patients, 1 African American patient, and 2 patients who preferred not to answer. Out of the 13 patients, 2 had intraoperative CSF leaks during the operation which were treated with either a free mucosal graft or a nasoseptal

flap. 62% of the patients had a subjective improvement in vision at their first postoperative visit. Postoperatively, no patients developed a CSF leak but two patients developed sphenoid retention cysts in the postoperative period.

Conclusion: Endoscopic endonasal optic nerve decompression surgery is an effective method of addressing multiple different pathologies involving the optic canal. The surgery does have the potential for postoperative development of a sphenoid retention cyst.

References

1. Kelman SE, Heaps R, Wolf A, Elman MJ. Optic nerve decompression surgery improves visual function in patients with pseudotumor cerebri. *Neurosurgery* 1992;30(3):391–395
2. Sergott RC, Cohen MS, Bosley TM, Savino PJ. Optic nerve decompression may improve the progressive form of nonarteritic ischemic optic neuropathy. *Arch Ophthalmol* 1989;107(12):1743–1754
3. Joseph MP, Lessell S, Rizzo J, Momose KJ. Extracranial optic nerve decompression for traumatic optic neuropathy. *Arch Ophthalmol* 1990;108(8):1091–1093
4. Levin LA, Joseph MP, Rizzo JF III, Lessell S. Optic canal decompression in indirect optic nerve trauma. *Ophthalmology* 1994;101(3):566–569

A047. Impact of Medicaid Insurance on Outcomes following Endoscopic Transsphenoidal Pituitary Surgery

Iyan Younus¹, Rohan Ramakrishna¹, Ashutosh Kacker¹, Abtin Tabaei¹, Vijay K. Anand¹, Theodore H. Schwartz¹

¹Weill Cornell Medicine, New York, New York, United States

Introduction: Despite the rise of studies in the neurosurgery literature suggesting that patients with Medicaid insurance have inferior outcomes, there remains a paucity of data on the impact of insurance on outcomes after endonasal endoscopic transsphenoidal surgery (EETS). Given the increasing importance of complications in quality based health care metrics, the objective of this study is to assess whether Medicaid insurance type influences outcomes in EETS for pituitary adenoma.

Methods: The authors analyzed a prospectively acquired database of EETS for pituitary adenoma from 2005 to 2018 at NewYork Presbyterian Hospital, Weill Cornell Medicine. We identified all patients with Medicaid insurance. As a control group, we also reviewed clinical, socioeconomic, and radiographic data of all other patients in the series with all other insurance types. Statistical significance was determined with an $\alpha < 0.05$ using Pearson's Chi-square and Fisher's exact tests for categorical variables and the independent-samples *t*-test for continuous variables.

Results: Of 584 patients undergoing EETS for pituitary adenoma, 57 (10%) had Medicaid insurance. The median postoperative length of stay was significantly longer for patients with Medicaid insurance compared with the control (4.5 vs. 3 days; $p < 0.05$). Maximum tumor diameter was significantly larger for Medicaid patients compared with the control (26.1 ± 12 vs. 23.1 ± 11 mm; $p < 0.05$). Baseline comorbidities were not significantly different between Medicaid cases and the control. Patients with Medicaid insurance had a significantly higher rate of any complication and long-term neurological deficit. The overall complication rate for Medicaid cases was 14% compared with 7% for the control ($p < 0.05$). The rate of neurologic deficit was 5.3% in Medicaid cases compared with 1.1% of the control ($p < 0.05$).

Conclusion: The impact of insurance type on EETS for pituitary adenoma has not previously been reported in the literature. We found that larger maximum tumor diameter, longer postoperative length of stay, and higher rate of complications were associated with Medicaid insurance.

A049. Development of Clinically Applicable Molecular Markers Distinguishing Sinonasal Undifferentiated Carcinoma from Sinonasal Squamous Cell Carcinoma

Yoko Takahashi¹, Frederico O. Gleber-Netto¹, Diana Bell¹, Dianna Roberts¹, Tong-Xin Xie¹, Ahmed S. Abdelmeguid¹, Curtis Pickering¹, Jeffrey N. Myers¹, Ehab Y. Hanna¹

¹The University of Texas MD Anderson Cancer Center, Houston, Texas, United States

Background: Sinonasal undifferentiated carcinoma (SNUC) is a rare, highly aggressive cancer. Moreover, reliable histopathologic markers that distinguish SNUC from poorly differentiated sinonasal squamous cell carcinoma (SNSCC) are lacking. Distinguishing between SNSCC and SNUC has significant clinical importance since the prognosis and treatment strategies are different. Therefore, new diagnostic molecular markers for SNUC are needed. Previously, we have reported gene expression levels of seven markers completely distinguished SNUCs from SNSCCs. However, the use of those single transcripts as biomarkers has many limitations, since measurement of absolute transcript expression is methodology dependent and relies on normalization through housekeeping genes. To enhance the potential clinical relevance of our finding, we introduced the top scoring pairs algorithm to identify molecular markers that distinguish the two tumor types regardless of the gene expression assay platform.

Methods: Formalin-fixed paraffin-embedded tumor specimens obtained from 15 treatment-naïve SNUC and 6 treatment-naïve SNSCC were used in this study. Gene expression analysis of the specimens was performed using an HTG oncology biomarker panel. To identify pairs of genes that distinguish SNUCs from SNSCCs, the top-scoring-pair analysis was employed on 132 differentially expressed genes between SNUCs and SNSCCs.

Results: We identified 104 gene pairs that separated SNUCs from SNSCC perfectly (area under the curve = 1.00). Among these pairs, the following gene pairs can be used as potential diagnostic markers to distinguish SNUCs from SNSCCs because of their great difference of gene expression levels between two genes and easy availability of their detection probes in the market; the gene pairs whose expression of the first gene is lower than the second gene in SNUC are *KRT16CLCA2*, *STMN1* > *NDRG1* and *FANCL* > *ITGB6*.

Conclusion: We successfully identified new diagnostic pairs of markers that distinguish SNUCs from SNSCCs. Since these gene pairs can be measured regardless of the gene expression assay platform, they might serve as clinically applicable diagnostic markers.

A050. Sinonasal Mucosal Melanoma: A Comparison of Outcomes between Surgical Resection and Immune Checkpoint Inhibition

Shivangi Lohia¹, Stephanie Flukes¹, Alexander N. Shoushtari¹, Akash D. Shah¹, Ian Ganly¹, Snehal G. Patel¹, Jennifer R. Cracchiolo¹, Christopher Barker¹, Jatin P. Shah¹, Viviane S. Tabar¹, Marc Cohen¹

¹Memorial Sloan Kettering Cancer Center, New York, New York, United States

Introduction: Mucosal melanoma of the head and neck is rare with a poor prognosis. The NCCN suggested management paradigm coincides with the historically utilized recommendation of surgical resection with adjuvant radiation for all surgically resectable tumors. With the introduction and integration of immune checkpoint inhibition (ICI) durable treatment responses and improvement in overall survival have been observed. Using retrospective data, we sought to evaluate the relative roles of surgery and checkpoint inhibition for mucosal melanoma of the paranasal sinuses.

Patients and Methods: A retrospective review of 102 patients with malignant mucosal melanoma of the sinonasal region was conducted at a single institution from 1997 to 2018. Patients were separated into three cohorts based on whether they were treated with surgical resection, ICI (either single agent CTLA-4, PD-1, or combination CTLA-4 and PD-1 blockade), or surgery and ICI together. Radiotherapy was used as adjuvant treatment for an equal proportion of patients within each group. Outcomes of interest were disease specific and overall survival at 5 years calculated using the Kaplan-Meier method. Multivariate analysis was performed using Cox regression. Patients were excluded if duration of follow-up was less than 24 months.

Results: A total of 94 patients (67 patients undergoing surgical excision, 10 undergoing ICI, and 17 undergoing surgery plus ICI) were included in the analysis. Overall, 79.8% patients received radiation with no difference among the three groups. In the surgical group the mean age at presentation was 67 years with 34 (51%) patients staged as T4 at diagnosis. In the ICI group the mean age was 71 years with 9 (90%) patients staged as T4. In the surgery plus ICI group, the mean age at presentation was 68 years with seven (41%) patients presenting at stage T4. But 30% of patients in the ICI group had distant metastases at presentation, while 4.4 and 17.6% of patients presented with metastases in the surgery and surgery plus ICI groups, respectively. Disease specific survival (DSS) and overall survival (OS) at 5 years was 36, 30, and 58% in the surgery, ICI, and surgery plus ICI group and 33, 30, and 42% for the surgery, ICI, and surgery plus ICI group, respectively. OS was not statistically significant between the three groups, though there was a trend toward better OS in patients receiving both surgery and ICI ($p = 0.075$), whereas DSS was significantly improved in patients receiving surgery plus ICI ($p = 0.05$). In multivariate analysis, increasing T-stage was the only variable associated with worse survival (hazard ratio = 1.682, CI: 1.134–2.494, $p = 0.01$).

Conclusion: There was a significant improvement in disease-specific survival and a trend toward improved overall survival for patients undergoing both surgery and ICI compared with either modality alone. Despite those patients receiving ICI having a higher rate of advanced disease and distant metastases, their survival outcomes were not significantly different to those receiving surgery alone. Prospective research should evaluate the optimal treatment paradigm for mucosal melanoma. Until we have further data, we recommend a combination of surgery, immune checkpoint inhibition, and radiation when feasible.

A051. Surgical Management of Skull Base/Infratemporal Fossa Malignancies: Predictors of Postoperative Performance

Patrick J. Hunt¹, Moran Amit¹, Mohamed Aashiq¹, Franco DeMonte¹, Ehab Y. Hanna¹, Michael E. Kupferman¹, Shirley Y. Su¹, Paul W. Gidley¹, Marc-Elie Nader¹, Shaan M. Raza¹
¹M. D. Anderson, Houston, Texas, United States

Background: Infratemporal fossa (ITF) tumors are difficult to treat due to nearby vital structures and cranial nerves, necessitating aggressive multimodal strategies balanced with efforts to avoid treatment-associated decline in performance.

Objective: We sought to assess factors that predict better postoperative performance in patients undergoing surgery for ITF tumors.

Methods: We reviewed all patients surgically treated for ITF malignancy between 1999 and 2017 at our institution. One hundred patients had sufficient pre- and posttreatment data for evaluation and were included. Patient demographics, preoperative performance, tumor stage, tumor characteristics, treatment modalities, pathologic data, and postoperative performance were collected. Postoperative performance scores were collected between 3 and 13 months following surgery.

Results: The 5-year survival rate was 62.2%. Ages ranged from 6 to 84 years, 61% were male, and 62% had a diagnosis of sarcoma. We found that higher preoperative KPS ($p < 0.001$), short length of stay ($p = 0.004$), and a diagnosis of sarcoma (62 patients; $p = 0.0243$) are predictors of higher postoperative KPS. Additionally, we found that soft tissue tumor origin (57 patients; $p = 0.0036$), high-pathology grade (75 patients; $p = 0.0136$), and percutaneous endoscopic gastrotomy (nine patients; $p = 0.0247$), but not age at presentation ($p = 0.4$), intracranial tumor spread ($p = 0.6375$), perineural invasion (40 patients; $p = 0.5699$), or tracheostomy tube placement (21 patients; $p = 0.0552$) were predictors of lower postoperative KPS. Male patients, patients with sarcomas, and patients with high-grade tumors were all groups that demonstrated greater decreases in KPS scores between pre- and posttreatment.

Conclusion: Our findings will guide difficult treatment decisions in patients with tumors of the ITF, including the decisions to pursue surgery, radiotherapy, and chemotherapy. Additionally, this work will allow treatment teams to better describe expected patient outcomes during patient consultations.

A052. Identification of Epithelial Membrane Protein 2 (EMP2) as a Molecular Marker and Correlate for Angiogenesis in Meningioma

Kunal S. Patel¹, Sameer Kejrwal¹, Samasuk Thammachantha¹, Courtney Duong¹, Ann Chan¹, Lynn Gordon¹, William Yong¹, Madhuri Wadehra¹, Isaac Yang¹

¹UCLA, Los Angeles, California, United States

Background: Intracranial meningiomas have been associated with a heterogeneous set of genetic and molecular alterations. Despite these genetic associations, targeted therapies have been unable to increase progression free survival in recurrent or residual meningiomas. There is a need for identification of therapeutic molecular targets in meningioma.

Materials and Methods: Nonpathologic brain tissue from autopsy and tumor specimens from patients undergoing surgical resection for meningioma were collected. Microscopic pathologic analysis, immunohistochemistry and western blot analysis were performed to evaluate EMP2

expression. The NCBI GEO Database was used to evaluate EMP2 mRNA expression data.

Results: EMP2 expression was not identified in normal brain tissue samples from different locations including gray matter, white matter, and meninges in three patients. In comparison, 16 patients with meningioma, there was strong EMP2 staining in 100% of samples ($p < 0.001$). EMP2 expression was confirmed with western blot in a portion of these samples with 100% positive expressivity and correlated with histologic staining. EMP2 mRNA expression levels were higher in meningioma relative to nonpathologic meninges ($p = 0.0013$) and brain ($p = 0.0011$; **Fig. 1**). There was no association between EMP2 levels and WHO grade ($p = 0.299$) or markers of proliferation ($p = 0.797$; **Fig. 2**). However, specimens with increased EMP2 were associated with increased angiogenesis on microscopic evaluation ($p = 0.059$), increased VEGF-A mRNA expression ($p < 0.001$) and increased clinical markers of tumor vascularity, such as surgical blood loss ($p = 0.037$; **Fig. 3**).

Conclusion: EMP2 is a protein previously associated with cell migration, invasion, and angiogenesis not identified in normal brain tissue but found in meningioma. It is associated with increased angiogenesis but not tumor proliferation. EMP2 may serve as molecular target for meningioma therapy.

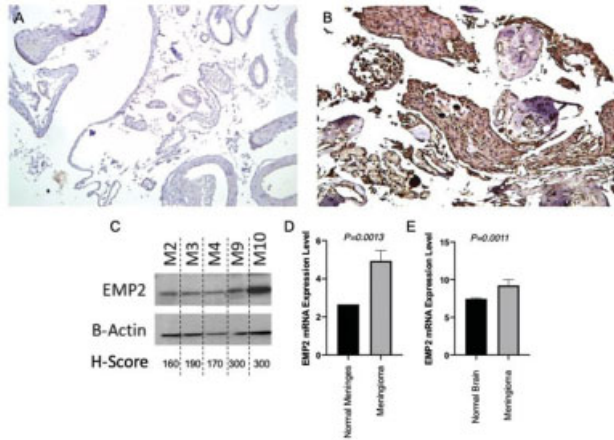


Fig. 1

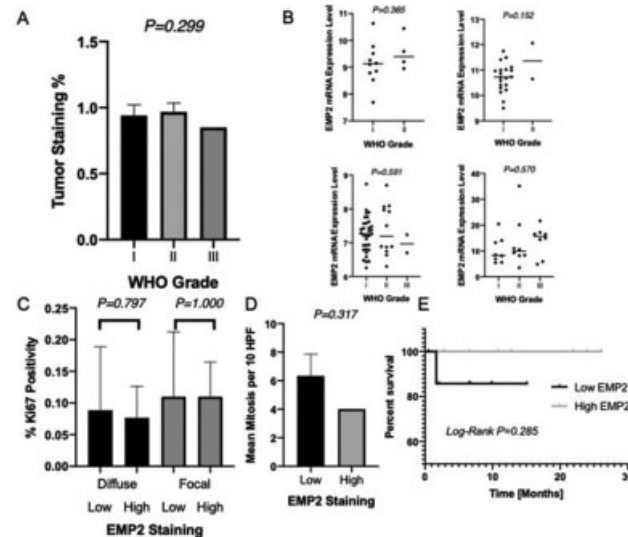


Fig. 2

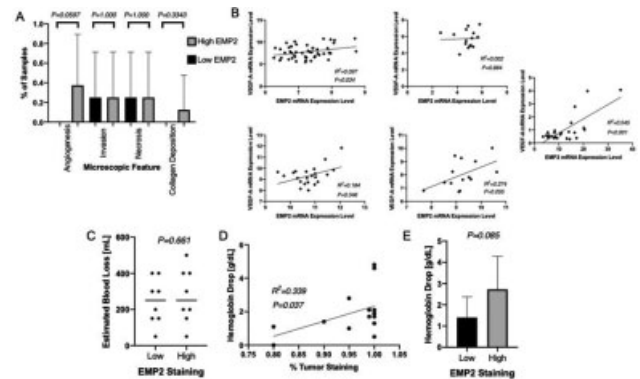


Fig. 3

A053. Impact of Age on the Treatment and Survival in Sinonasal Malignancies

Chandala Chitguppi¹, Tawfiq Khoury¹, Pascal Lavergne², Prachi Patel¹, Kira Murphy¹, Mindy Rabinowitz¹, Gurston Nyquist¹, James Evans², Marc Rosen¹

¹Department of Otolaryngology and Head and Neck Surgery, Thomas Jefferson University Hospital, Philadelphia, Pennsylvania, United States

²Department of Neurological Surgery, Thomas Jefferson University Hospital, Philadelphia, Pennsylvania, United States

Introduction: Proportion and duration of survival of sinonasal malignancy (SNM) patients has consistently increased in the past decade. However, the disease characteristics and survival outcomes in the elderly patients are not well defined. This study was performed to analyze the survival outcomes in elderly SNM patients.

Methods: Retrospective chart review of SNM treated at a tertiary care center. Patients were divided into three groups based on age at presentation: ≤ 65 years (younger; group Y; 56%), 66 to 80 years (elderly; group E; 35%) and >80 years (very elderly; group VE; 10%). Group Y has been considered as the reference group. Pretreatment comorbidity levels, treatment, and survival outcomes were analyzed (Chi-square and *t*-tests).

Results: A total of 230 patients were included. 58% were males, 59% smokers, 42% squamous cell carcinoma, 42% TNM stage III/IV, and 90% underwent surgical treatment.

Operative Characteristics: Group E had higher Charlson's comorbidity index score ($p = 0.001$; 2.99 vs. 2.39), nine times higher incidence of myocardial infarction and three times higher incidence of Diabetes mellitus ($p = 0.005$) in comparison to the Y group. Group VE in comparison to group Y had, 14 times higher incidence of myocardial infarction ($p = 0.004$). Demographics including smoking were comparable.

Tumor Characteristics: Group VE had 3.3 times higher proportion of pterygopalatine fossa involvement ($p = 0.03$) and five times higher proportion of nodal disease at presentation ($p = 0.04$). TNM staging, skull base, and orbital extension was comparable.

Treatment Characteristics: Groups Y and E underwent comparable treatment, namely, modality, surgical approach, extent of resection, and intent of treatment (curative vs. palliative). Mean radiation dose used to treat group Y was higher than that used for group E ($p = 0.01$; 62.41 vs. 56.60). Exenteration was thrice more commonly used in group E than group Y ($p = 0.04$). Debulking procedures ($p = 0.02$) were 3.4

times and palliative treatment 12 times more commonly used in VE group. Chemotherapy was thrice ($p = 0.04$) and radiotherapy 3.8 times ($p = 0.004$) less likely to be used in VE groups.

Posttreatment Complications: Sinusitis was 2.5 times ($p = 0.006$), adhesions 2.3 times ($p = 0.01$), and nasal stenosis 2.7 times ($p = 0.03$) less likely in group E. Group VE also showed 14 times lower incidence of sinusitis ($p = 0.002$). Other complications including epistaxis, crusting, septal perforation, dysphagia, wound infections, thromboembolism, airway issues, and intra- and postoperative CSF leak rates were comparable.

Survival Outcomes: Group E had two times lower recurrence rates ($p = 0.04$) while VE had recurrence rate comparable to group Y. A 30-day readmission rates, number of recurrences, and number of reoperations were comparable. Kaplan–Meier survival curves (log rank test) were comparable ($p = 0.75$ and $p = 0.1$ for group E and VE, respectively). Mean duration of follow-up was significantly different (group Y: 37.41 months vs. group E: 24.23 months vs. group VE: 15.31 months).

Conclusion: Although, elderly and very elderly patients report worse pretreatment comorbidities than their younger counterparts, they had a lower incidence of sinonasal complications and recurrence. For patients who do undergo curative treatment, survival curves are comparable with that in younger population. Therefore, age, in itself, should not be the main deterrent for SNM treatment.

A054. Posttreatment Surveillance for Recurrence in Sinonasal Malignancies

Gurston Nyquist¹, Prachi N. Patel¹, Chandala Chitguppi¹, Swar Vimawala¹, Tawfiq Khoury¹, Mindy Rabinowitz¹, Pascal Lavergne², James Evans², Marc Rosen¹

¹Department of Otolaryngology - Head and Neck Surgery, Thomas Jefferson University, Philadelphia, Pennsylvania, United States

²Department of Neurosurgery, Thomas Jefferson University, Philadelphia, Pennsylvania, United States

Background: Sinonasal malignancy (SNM) represents a variety of aggressive tumors with a high rate of local recurrence. Surgery is a mainstay of treatment and when combined with chemotherapy and radiation, this often leads to the best overall prognosis. Nasal endoscopy is essential for posttreatment surveillance along with physical exam and radiologic evaluation. The ability to directly visualize the sinus cavities after surgery may also improve early detection of tumor recurrence and is another reason to potentially advocate for surgery in these patients.

Purpose: The objective of this study was to assess tumor surveillance modalities and how surgically patent sinus cavities effect the ability of nasal endoscopy to identify tumor recurrence.

Methods: A single-center, retrospective review from 2005 to 2019 of 231 patients with pathology proven primary SNM was conducted. Patients were divided into three subgroups based on treatment: surgery, surgery with adjuvant radiotherapy, and definitive radiotherapy.

Results: The nasal cavity and maxillary sinus were the two most common primary tumor sub-sites. The average follow-up was 42 ± 35 months. The median time to recurrence was 9.8 months. Recurrence was initially detected endoscopically in 23 (34.3%) patients, by imaging in 42 (62.7%) patients, and by physical exam in 2 (3.0%) patients. There was a total of 46 patients (68.7%) with local recurrences, the majority of which (24) were identified via nasal endoscopy as opposed to imaging. Thirteen recurrences were identified via endoscopic surveillance within the surgically

patent paranasal sinuses, while 13 were identified of the nasal cavity; 2 patients had multiple sites of recurrence. With the exception of the sphenoid sinus, recurrences following surgical treatment that were detected endoscopically were more likely to be found in the original site of the primary tumor ($p < 0.05$). Twenty (87.0%) of these cases had confirmation of the location of recurrence in the subsequent imaging. Seven recurrences were identified in the XRT only group, and only two were identified via endoscopy which were within the nasal cavity. Both cases had follow-up imaging that identified additional tumor involvement of the paranasal sinuses. Two local recurrences were identified on MRI surveillance of the paranasal sinuses which were not surgically opened for endoscopic inspection. Overall recurrence including local, regional and metastatic disease was most likely to be detected by routine surveillance with imaging (62.7%).

Conclusion: More than two-thirds of SNM recurrences were local in location, a majority of which were identified by nasal endoscopy. Half of the recurrences identified endoscopically were within the paranasal sinuses. These would not have been easily identified in a clinical examination if the sinuses were not open for inspection. Thus, open sinus cavities aid in the detection of tumor recurrence and are another advantage of surgery for primary SNM. In addition, follow-up radiographic findings have shown to improve the accuracy of clinical exam findings and therefore should be used in compliance with physical examination including nasal endoscopy.

A055. Pattern of Regional and Distant Metastasis in Sinonasal Malignant Tumors

Neelesh Tiwari¹

¹Tata Memorial Hospital, Mumbai, Maharashtra, India

Background: Malignant tumors of paranasal sinus tumors belong to a wide variety of histology and present with different biological behavior. Incidence of nodal metastasis is low. Elective neck dissection is not routinely practiced. There is no clear guideline available for management of neck in such tumors

Aims and Objectives

- To study incidence of nodal and distant metastases in common sinonasal malignant histologies at presentation in primary and recurrent cases.
- To assess the need of dedicated imaging for metastatic workup.
- To assess the nodal recurrence in different types of sinonasal malignant tumors.
- To assess the need of elective neck dissection in histology specific manner.

Materials and Methods: This is a retrospective observational study. Study included patients with sinonasal malignant tumors registered in the skull base clinic at Tata Memorial Hospital and treated subsequently till Dec 2017. Data collection was done from the hospital database and electronic medical records. Patients with recurrent tumor at presentation were excluded.

Results: A total of 397 patients were included in the study. Squamous cell carcinoma was the most common histology (22.4%) followed by sinonasal adenocarcinoma (17%). A total of 80% of the tumor were of nasoethmoid origin. Most of the patients had only local disease, regional metastasis was present in 33(8%) patients and distant metastasis was present in eight cases (2%). Lung was the most common site of distant metastasis. Five patients had both regional and distant metastasis at the time of presentation. Retropharyngeal node was seen in 10 cases.

Esthesioneuroblastoma (ENB) and sinonasal neuroendocrine (SNEC) carcinoma patients had highest proportion of regional metastasis (12% incidence in each). Among them, 346 patients who completed treatment were analyzed for disease control and recurrence. Local failure was the most common pattern of recurrence. Nodal metastasis was seen in 5% of the initial cases. Esthesioneuroblastoma had highest nodal recurrences.

Conclusion: Nodal metastasis has low incidence in sinonasal malignancy. Clinically, patients may not need dedicated imaging for the neck nodes. Retropharyngeal node at presentation is also rare. However, some histological varieties like ENB, SNEC, sinonasal undifferentiated carcinoma need active metastatic workup. No neck should be addressed in these cases either at the time of surgery or during adjuvant radiation therapy

A056. The Influence of Hospital Volume on the Outcomes of Nasopharyngeal, Sinonasal and Skull-base Tumors: A Systematic Review of the Literature

Rahul K. Sharma¹, Stephanie Flukes², Marc A. Cohen²

¹Columbia University Vagelos College of Physicians and Surgeons, New York, New York, United States

²Head and Neck Service, Department of Surgery, Memorial Sloan Kettering Cancer Center, New York, New York, United States

Background: Health care researchers are pursuing strategies focusing on providing quality care for the lowest possible cost. The center of excellence model hypothesizes that increased volume in a specialized center will lead to better and more affordable care. A focus in outcome research studies, including those in skull base, is volume-outcome associations. In this systematic review, we sought to characterize the volume-outcome data for primary surgically treated sinonasal and skull base (anterior and lateral) tumors and (chemo) radiation treated nasopharyngeal malignancy.

Methods: PubMed was searched for relevant National Database and Multi-institutional studies published between 1990 and 2019. Key words included “hospital volume,” “surgeon volume,” “surgeon experience,” and outcomes for “nasopharyngeal carcinoma,” “sinonasal carcinomas,” “pituitary tumors,” “acoustic neuromas,” “chordomas,” and “skull base tumors.” Single-institution studies and self-reported surveys were excluded.

Results: A total of 18 studies addressed volume-outcome associations. These studies focused on the impact of volume on either survival or treatment related complications depending on whether the pathology was benign or malignant. Two studies were excluded for being either single-institution or survey-based. Five studies utilized the National Cancer Database (NCDB), four used the National Inpatient Sample (NIS), and one used the U.S. Surveillance, Epidemiology, and End Results (SEER) database. All others used either state-specific databases or large multi-institution retrospective databases. With malignant pathology, interest was focused on survival outcomes. Five studies showed improved survival with treatment in high volume centers and two showed no association with survival. One showed an increased risk of complications. For those treated with definitive radiation for nasopharyngeal carcinoma (NPC), three studies identified a statistically significant positive association between hospital volume and overall survival (OS). In studies of patients treated surgically for sinonasal malignancy, two studies demonstrated no relationship between volume and survival and one study noted improvement between middle-tertile volume centers and low-tertile centers only. One study of the NIS found an increased risk of complications at high-volume centers. In one study of the SEER database, greater hospital volume was

associated with improved survival for patients with skull base chordomas. For benign pathologies, interest was focused on perioperative complications. One study showed reduced risk of perioperative mortality in high-volume centers and three showed no association. Seven showed a reduced risk of complications and one showed no association. On assessment of three pituitary adenoma surgery NIS studies, one showed a correlation between high-volume centers and lower perioperative morbidity and mortality, and two demonstrated equal morbidity and mortality. Four studies of volume outcomes for acoustic neuroma demonstrated reduced perioperative morbidity in high-volume centers, while one found no association with complications.

Conclusion: Systematic review of the literature does not demonstrate consistent findings among the subsites assessed. Survival outcomes following primary radiation treatment for NPC do appear related to hospital volume but surgically treated sinonasal cancer does not. Most of the literature, evaluating surgery for benign conditions of the skull base demonstrates lower perioperative morbidity in high-volume centers. This suggests that further studies must be conducted to understand the effect of treatment centralization on outcomes.

A057. Hybrid Robotics in Endoscopic Transnasal Skull Base Surgery: Report of an Initial, Single-Centre Clinical Experience

Francesca Zappa¹, Alba Madoglio¹, Davide Mattavelli², Alberto Schreiber², Stefano Taboni², Marco M. Fontanella¹, Piero Nicolai¹, Francesco Doglietto¹

¹Division of Neurosurgery, Department of Medical and Surgical Specialties, Radiological Sciences and Public Health, University of Brescia, Brescia, Italy

²Division of Otorhinolaryngology, Department of Medical and Surgical Specialties, Radiological Sciences and Public Health, University of Brescia, Brescia, Italy

Background and Objective: Robotics has been widely developed in various surgical specialties, but its role for skull base surgery remains debated, except for transoral robotic surgery (TORS). Different prototypes have been developed for endoscopic transnasal surgery. Only recently a dedicated robotic system has become available for clinical practice for endoscopic skull base surgery (Endoscope Robot, Medineering Surgical Robotics). Aim of the study is to describe the first clinical experience with this robotic hybrid solution.

Methods: Patients, who underwent endoscopic transnasal transsphenoidal surgery with the aid of this robotic endoscope-holder at the University of Brescia in Italy, were prospectively included in the study. After preparation of the transnasal surgical corridor, Endoscope Robot was used to hold the endoscope during the opening of the sphenoid, tumor removal and skull base reconstruction (when needed); the endoscope movements were controlled robotically with a foot-pedal, used by the primary surgeon. Demographic data, pathology, type of procedure, operating time, intra- and postoperative complications were prospectively recorded.

Results: Twenty-one patients underwent robot-assisted endoscopic transsphenoidal surgery for different pathologies (17 pituitary adenomas, 3 clival chordomas, and 1 craniopharyngioma) for a total of 23 procedures. Mean robot set-up time was 7 minutes. Surgical complications included: diabetes insipidus (one persistent in craniopharyngioma and one transient); two transient VI cranial nerve palsies; a recurrent CSF leak in a clival chordoma, successfully treated with a temporoparietal fascia flap. None of the recorded complications could be related to the robot nor differences in mean surgical timing between ordinary and robot-assisted procedures were observed (a

matched-paired analysis with a nonrobotic group is ongoing). Subjective advantages that were perceived by the whole team included having a steady image during tumor removal and an increased ease of maneuvering with angled endoscopes, especially in narrow corridors or long procedures.

Conclusion: To our knowledge, this is the first clinical series described in literature of robotic-assisted transnasal skull base surgery. Though these preliminary data have to be confirmed by larger studies, Endoscope Robot proved to be a safe and effective tool, especially advantageous in long interventions through deep and narrow corridors.

A058. Contralateral Transmaxillary Corridor to the Cavernous Sinus: A Useful Adjunct to the Endoscopic Endonasal Approach to the Parasellar Region

Yury Anania¹, Sheng Han¹, Zenonos Georgios², Eric W. Wang³, Carl H. Snyderman³, Paul A. Gardner²

¹Center for Cranial Base Surgery, University of Pittsburgh, Pittsburgh, Pennsylvania, United States

²Department of Neurosurgery, University of Pittsburgh Medical Center, Pittsburgh, Pennsylvania, United States

³Department of Otolaryngology, University of Pittsburgh Medical Center, Pittsburgh, Pennsylvania, United States

Background: Cavernous sinus (CS) invasion influences the extent of resection and is a prognostic factor for recurrence for many sellar/parasellar tumors. The internal carotid artery (ICA) limits access to the parasellar region with a standard endoscopic endonasal approach (EEA), and is at increased risk for injury. The contralateral transmaxillary approach (CTM) has been shown to improve access to the petrous apex deep to the petrous and paraclival ICA. The aim of this study was to investigate the utility of the CTM approach for CS compartments deep to the parasellar ICA.

Methods: With the aid of image guidance, EE and CTM approaches were performed by two right-handed surgeons on six colored silicone-injected human head specimens (12 CS). Qualitative and quantitative analysis of EE and CTM approaches to CS were conducted using 0-degree lens endoscope only. A comparative subanalysis of EEA and CTM to the oculomotor triangle and parapeduncular space was conducted by evaluating the area of exposure of the oculomotor triangle, and the angle of surgical trajectory to the oculomotor triangle and the lateral limit of the parapeduncular space (mesial temporal lobe, and MTL).

Results: The angle of the surgical trajectory relative to the parasellar ICA was significantly greater ($p < 0.001$) for the CTM approach (left CS, 51.6 ± 9.2 degree; right CS, 56.9 ± 9.6 degree) compared with EEA (left CS, 31.9 ± 7.8 degree; right CS, 34.6 ± 7.7 degree). Improved visualization of superior and posterior CS compartments was provided by CTM without the need for ICA manipulation. Overall mean area of exposure of the oculomotor triangle was significantly wider ($p = 0.012$) with the CTM ($23.1 \pm 13 \text{ mm}^2$) compared with EE ($13.4 \pm 9 \text{ mm}^2$) approach. The angle of the surgical trajectory to the oculomotor triangle was significantly greater ($p < 0.001$) for the CTM (left CS, 48 ± 10.1 degree; right CS, 56.1 ± 12.3 degree) compared with EE (left CS, 29 ± 6.8 degree; right CS, 34 ± 9.5 degree) approach. Moreover, the angle of surgical trajectory to the MTL was significantly greater ($p < 0.001$) for CTM (left MTL, 52 ± 9.8 degree; right MTL, 60 ± 9.6 degree) than for EE (left MTL, 33.3 ± 5.3 degree; right CS, 38.2 ± 10 degree) approach. Right-handedness of both surgeons likely accounts for the slight difference in CTM and EEA's angle of attack to left and right CS. Direct access to the lateral and inferior CS compartments did not benefit from the CTM approach (Fig. 1).

Conclusion: In combination with an EEA, the CTM approach provides a more direct working angle into the superior and posterior CS compartments, with enhanced access to the oculomotor triangle and parapeduncular space. This may improve resection of CS tumors and decrease risk to the ICA, while avoiding a combined transcranial approach. The utility and efficacy of a CTM approach still needs to be evaluated in a clinical setting (Figs. 2 and 3).

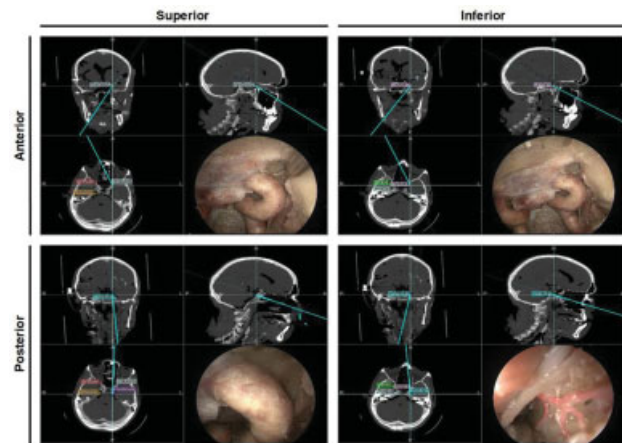


Fig. 1 Superior and inferior compartments.

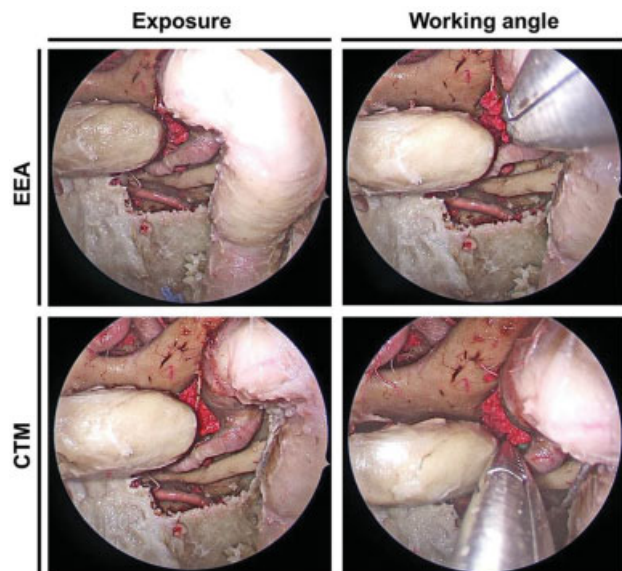


Fig. 2 EEA and CTM exposures and working angles.

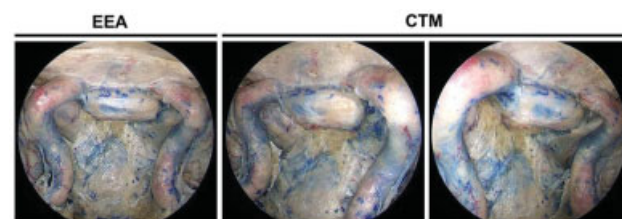


Fig. 3 EEA and CTM compartments.

This document was downloaded for personal use only. Unauthorized distribution is strictly prohibited.

A059. Three-Dimensional Exoscopic Temporal Bone Resections for Advanced Head and Neck Cancer

Mallory J. Raymond¹, Roberto M. Soriano¹, Ryan Belcher², C. Arturo Solares¹

¹Emory University, Atlanta, Georgia, United States

²Vanderbilt University, Nashville, Tennessee, United States

Background: The three-dimensional (3D) exoscope has several advantages over the operative microscope including improved ergonomics, reduced space occupancy and broadened teaching ability. Small series have described its successful use in lateral skull base surgery for temporal bone encephaloceles, vestibular schwannomas, cochlear implants, and more, but none have described its use for lateral skull base resections in the context of malignancy.

Objectives: We sought to investigate the surgical characteristics and outcomes of temporal bone resections (TBR), both lateral (LTBR) and subtotal (STBR), with sole visualization via the three-dimensional exoscope for complex head and neck cancers.

Methods: A retrospective chart review of all patients undergoing LTBR or STBR with the Karl Storz VITOMÖ 3D exoscope from the start of its availability at our tertiary care center in August 2016 until August 2019 was performed. Demographic information was collected. Tumor type, staging, margin status, recurrence rate and survival were descriptively analyzed.

Results: Fifty-five patients underwent exoscopic temporal bone resections from 2016 through 2019, of which 18% ($n = 10$) underwent STBR. The mean age was 67 ± 14 years, and the majority (89%, $n = 49$) of patients were male. Most tumors were of cutaneous origin (62%, $n = 34$), followed by primary parotid gland tumors (27%, $n = 15$). Preoperatively, 64% ($n = 35$) of patients had a cranial nerve VII deficit. Based on the histologic type and AJCC 8th Edition staging guidelines, 51% ($n = 28$) were considered to be at least a size T4, and 42% ($n = 42$) were considered to be at least a size T3. These TBR were often a part of a larger oncologic resection which included most commonly infratemporal fossa resections (87%, $n = 48$), auriclectomies (47%, $n = 26$), mandibulectomies (53%, $n = 29$), parotidectomies (96%, $n = 53$), and other procedures. On final pathology, 24% ($n = 13$) had microscopically positive margins, 49% ($n = 27$) had lymphovascular invasion and 80% ($n = 44$) had perineural invasion. Twenty-six patients required adjuvant therapy, of which 65% ($n = 17$) underwent radiation alone, and 35% ($n = 9$) underwent combined chemotherapy and radiation. Over the study period, 20% ($n = 11$) of patients had recurrences, with a median recurrence time of 5 months (range, 2–30 months).

Conclusion: The 3D exoscope is an oncologically sound alternative to the operative microscope for LTBR and STBR in the context of advanced head and neck cancer. Its ergonomic and spatial properties are particularly advantageous during these cases, which require larger surgical set-ups, necessitate prolonged operative time, and include more learners and operative team members.

A060. Endoscopic Endonasal Skull Base Surgery using Indocyanine Green and Relationship to Preoperative Radiological Imaging

Mostafa Shahein^{1,2}, Thomas L. Beaumont³, Luciano M. Prevedello⁴, Khaled Ismail², Radwan Nouby², Marilly Palettas⁵, Ricardo L. Carrau⁶, Bradley A. Otto⁶, Daniel M. Prevedello¹

¹Department of Neurological Surgery, The Ohio State University, Wexner Medical Center, Columbus, Ohio, United States

²Department of Neurosurgery, Aswan University, Aswan, Egypt

³Department of Neurological Surgery, University of California, San Diego, California, United States

⁴Department of Radiology, The Ohio State University, Wexner Medical Center, Columbus, Ohio, United States

⁵Department of Biomedical Informatics—Center for Biostatistics, The Ohio State University, Wexner Medical Center Columbus, Ohio, United States

⁶Department of Otolaryngology—Head and Neck Surgery, The Ohio State University, Wexner Medical Center Columbus, Ohio, United States

Background: Endoscope integrated Indocyanine green (E-ICG) has been recently introduced to skull base surgery. Quantitative correlation between ICG fluorescence and T1-weighted gadolinium (T1wGd) that enhanced images for skull base tumors has never been assessed.

Objective: Propose indications, limitations of E-ICG, and correlate the endoscopic fluorescence pattern with MRI contrast enhancement.

Methods: Following IRB approval, 20 patients undergoing endoscopic endonasal skull base surgery between June 2017 and August 2018 were enrolled in the study. Tumor fluorescence was measured using a blue color value and blood fluorescence as a control. Signal intensity (SI) of tumor T1-wGd images was measured and the internal carotid artery (ICA) SI was used as control. For pituitary adenoma, the pituitary gland fluorescence was also measured. The relationship between ICG fluorescence and MRI enhancement measures were analyzed (**Fig. 1**).

Results: Data showed that in pituitary adenoma, there was a strong correlation between the gland/blood fluorescence to gland/ICA SI ratios ($n = 8$; $r = 0.92$; $p = 0.001$) and tumor/blood fluorescence to tumor/ICA SI ratios ($n = 9$; $r = 0.82$; $p = 0.006$). In other pathologies there was a strong correlation between the tumor/blood fluorescence and tumor/ICA SI ratios ($n = 9$; $r = 0.74$; $p = 0.022$). The ICG fluorescence allowed assessment of the pituitary gland perfusion as well as that of the nasoseptal flaps. Visualization of the surrounding vasculature was also feasible (**Fig. 2**).

Conclusion: Defining the indications and understanding the limitations are critical for the effective use of E-ICG. Tumor fluorescence seems to correlate with preoperative MRI contrast enhancement.

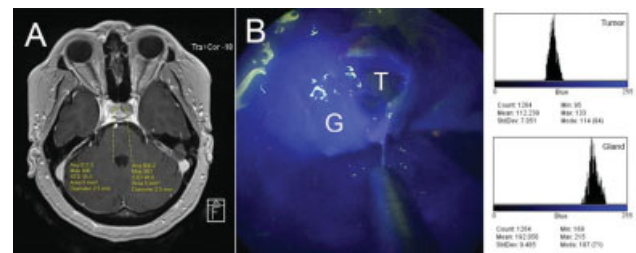


Fig. 1 (A): Axial post contrast MRI showing the measurement of signal intensity of the pituitary gland and the adenoma. **(B)** Intraoperative endoscopic ICG scene showing the measurement of the blue color value of both the pituitary gland and the adenoma.

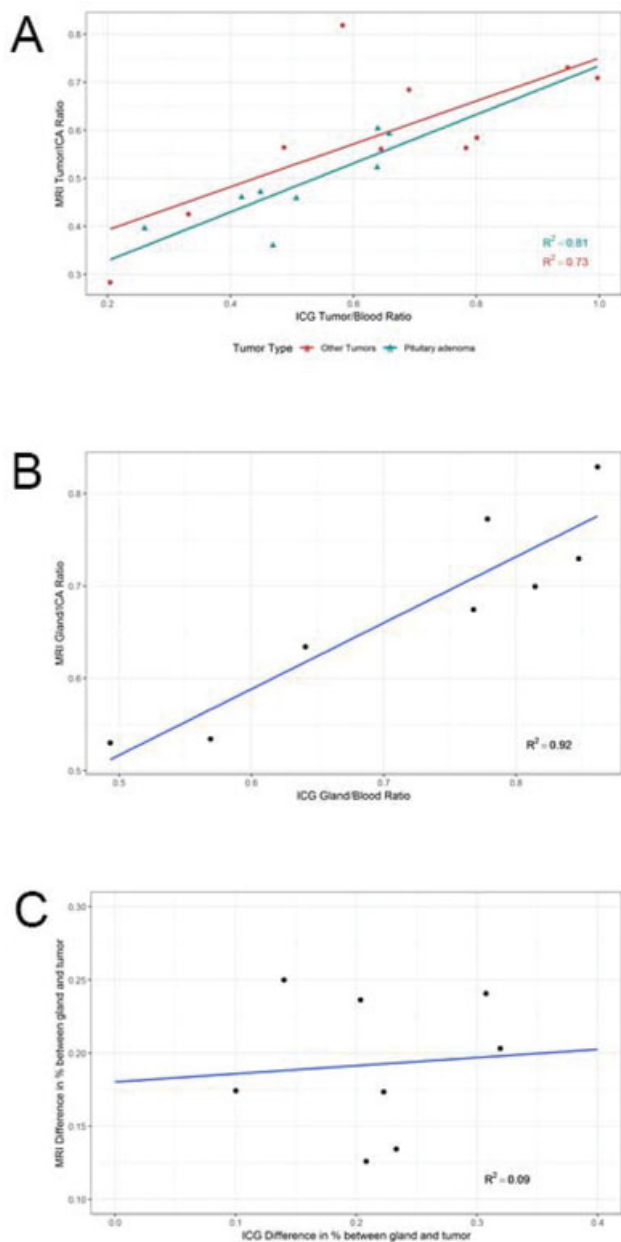


Fig. 2 Scatter plots showing the relationship between the ICG fluorescence and the MRI T1WGD SI in pituitary adenoma and other pathologies subgroup. **(A)** represents the relationship between MRI tumor/ICA SI ratio on the vertical axis to the tumor/blood ICG fluorescence ratio on the horizontal axis in both subgroups. **(B)** represents the relationship between the pituitary gland/ICA MRI SI ratio on the vertical axis to the pituitary gland/blood ICG fluorescence ratio on the horizontal axis in pituitary adenoma subgroup. **(C)** represents the relationship between the difference between the ratio of MRI gland/ICA and tumor/ICA SI on the vertical axis to the difference between the ratio of ICG gland/blood and tumor/blood fluorescence on the horizontal axis in pituitary adenoma subgroup.

A061. Neurosurgical Applications of a Novel Tough Adhesive Biomaterial

Kyle C. Wu¹, Benjamin R. Freedman², David J. Mooney², Wenya L. Bi¹

¹Center for Skull Base and Pituitary Surgery, Brigham and Women's Hospital, Boston, Massachusetts, United States

²Harvard John A. Paulson School of Engineering and Applied Sciences, Cambridge, Massachusetts, United States

Introduction: Cerebrospinal fluid (CSF) leaks complicate up to 30% of skull base operations. Current surgical adhesives for CSF leak repair are limited by poor adhesion in dynamic and aqueous environments and an inability to reconstruct large cranial defects that span multiple types of tissue. In contrast, tough adhesives are a novel hydrogel coated with an adhesive bridging polymer that provides high performance as a sealant within biological fluids. This novel technology demonstrates extraordinary mechanical toughness, capacity to repeatedly withstand significant strain, and the ability to bind strongly to wet surfaces. However, their application to dural tissue has not been investigated. The purpose of this study was to investigate the use of this novel biomaterial for dural reconstruction and CSF leak prevention. We hypothesized that tough adhesives will exhibit a greater burst pressure compared with existing commercial sealants.

Methods: We evaluated the effectiveness of the tough adhesives to withstand high pressures using a porcine cadaveric model with a dural defect (3-mm diameter, $n = 6$). Testing was conducted with an established burst pressure test setup. We recorded the maximum burst pressure achieved prior to the loss of integrity of the biomaterial graft or its detachment from the underlying dura (**Fig. 1**). We further investigated its effectiveness after 5 days of bathing within an artificial CSF environment of variable physiologic (37°C, $n = 5$) and supraphysiologic (45°C, $n = 5$) temperatures.

Results: The tough adhesive provided strong adhesion to cadaveric porcine dura (burst pressure: 140.2 ± 23.7 mm Hg), with several-fold higher strength than existing commercial sealants (**Fig. 2**). The tough adhesive also maintained its integrity under variable thermochemical conditions after prolonged exposure to an aqueous CSF environment. Burst pressures demonstrated similar burst points at 37°C and 45°C (37°C burst pressure: 71.59 ± 44.70 mm Hg; 45°C burst pressure: 78.30 ± 57.92 mm Hg, $p = 0.843$; **Fig. 3**).

Conclusion: We present a novel biomaterial with unique mechanical properties suited to complex neurosurgical reconstruction applications. In vitro testing demonstrates its ability to maintain integrity under supraphysiologic temperatures and with higher performance than existing commercial solutions. Ongoing work will focus on assessing the long-term durability and biocompatibility of this material within the central nervous system. Additional potential applications include wound closure, hemostasis, and scaffolding for drug delivery and brachytherapy.



Fig. 1 Tough adhesive demonstrating strong adherence to porcine dura during peel-testing.

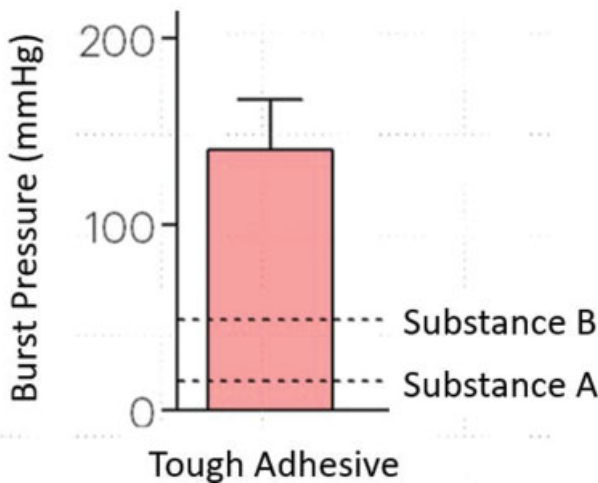


Fig. 2 Burst pressure performance of tough adhesives compared with two commonly used industry sealants.

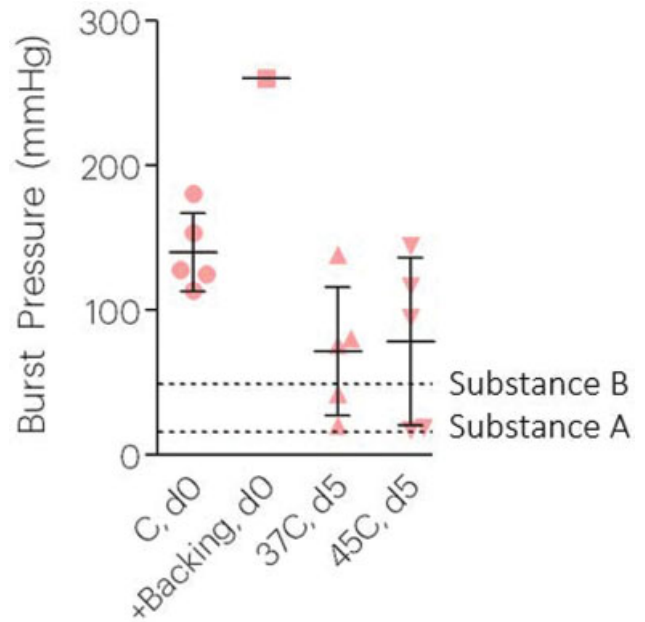


Fig. 3 Burst pressure performance of tough adhesive control and control with 1-mm plastic backing run on day 0, as well as following a 5-day bath in artificial CSF at 37°C and 45°C.

A062. Single Institutional Experience with Bioabsorbable Steroid Eluting Stent Treatment of Recurrent Rathke's Cleft Cyst

Matthew Z. Sun¹, Marvin Bergsneider¹, Marilene B. Wang¹
¹UCLA, Los Angeles, California, United States

Introduction: Rathke's cleft cysts (RCC) can recur after surgical drainage or resection, at a rate of approximately 8% after an endoscopic transnasal transsphenoidal (TNTS) approach. One common method to prevent cyst recurrence involves making a permanent marsupialization of the RCC to minimize cyst wall closure and subsequent cyst reaccumulation. Despite this method, RCC can still recur with scar formation leading to cyst wall closure. Therefore, we aimed to optimize the creation of a permanent stoma between recurrent RCCs and the sphenoid sinus by placing bioabsorbable steroid eluting stents during revision TNTS surgery. We present here the largest single institutional series of bioabsorbable steroid eluting stenting for the treatment of recurrent RCC that were previously marsupialized.

Methods: We performed a retrospective chart review of all patients who underwent endoscopic TNTS for marsupialization with subsequent stent placement for a recurrent RCC, diagnosed based on histopathologic analysis from prior surgeries or from the most recent procedure. The stents (Propel Mini, Intersect ENT, Palo Alto, California) consisted of a bioabsorbable, sustained drug release platform of poly-(DL-lactide-co-glycolide) and polyethylene glycol embedded with 370 micrograms of mometasone furoate which was gradually released over time. The revision TNTS surgeries consisted of marsupialization, followed by stent placement. In some instances, an additional nasoseptal flap was created.

Results: Six patients underwent drainage of recurrent RCC via marsupialization followed by stent placement (**Table 1**). All patients underwent surgeries via an endoscopic TNTS approach both during the revision and the previous surgeries. The median age was 40.5, and the number of prior drainage procedures ranged from 1 to 3. The stents were placed directly into the cyst cavity through the wall opening

(Fig. 1). The stents were bioabsorbable and were not removed after surgery, but were evaluated endoscopically at 2 and 6 weeks after surgery. The patients were followed for a mean of 19 months after revision surgery with no evidence of recurrence on endoscopic exam or imaging. While only one patient had transient diabetes insipidus that self-resolved, no patient had cerebrospinal fluid leak during or after the operation or permanent endocrinopathy.

Conclusion: In all six patients, the use of a bioabsorbable steroid eluting stent had no unanticipated consequences. All drainage pathways of all the recurrent RCCs remained patent and there has been no evidence of recurrence in all patients. The use of this technology may decrease recurrence rates in revision or complex cases where patients have extensive scarring operative field from prior drainage procedures. Longer follow-up of the current cases and further study in an even larger cohort are warranted.

Table 1 Patients' demographics of recurrent RCC via marsupialization

Gender	Age	Months since last surgery	Presenting symptoms	Number of Prior Surgeries	Prior Reconstruction	Previous Cyst size	Recurrent Cyst size	Reconstruction	Months till recurrence	Postop Follow up (Months)	Postop Complications	Recurrence at most recent follow up
M	55	11	Headache, fatigue, diplopia	1	Free mucosal septal graft	17	18	steroid eluting stent	6	25	None	no
F	60	59		0	none	20	14	steroid eluting stent	59	37	diabetes insipidus, resolved without treatment	no
F	55	98	Headache, weight gain, polyuria	2	nasoseptal flap	11	11	steroid eluting stent + nasoseptal flap inferior to marsupialized cyst	98	21	None	no
F	70	79	visual changes, headache, diplopia	1	fully packed with bone, get septal, intact	16	21	steroid eluting stent	79	21	none	no
F	23	78	headache, diplopia	1	none	13	9	steroid eluting stent	78	2	none	no
F	48	17	headaches	1	Free septal mucosal graft	15	14	steroid eluting stent	15	1	none	no

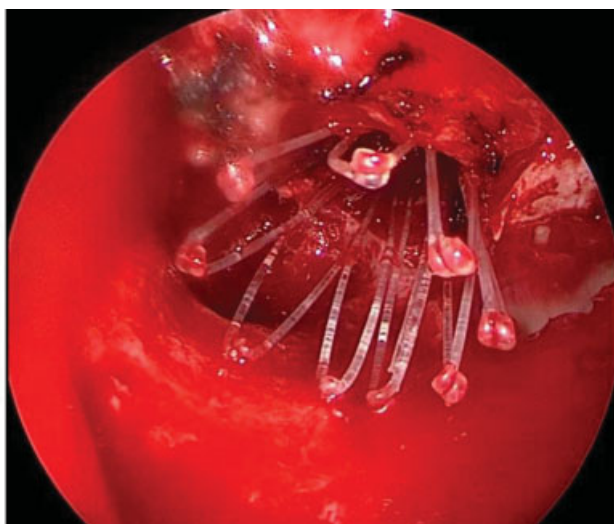


Fig. 1 The cyst cavity through the wall opening.

A063. Endoscopic Transnasal Eustachian Tube Closure using the V-LOC Wound Closure Device

Andrew J. Thomas¹, Sachin Gupta², Aclan Dogan², Timothy L. Smith², Justin Cetas², Jeremy N. Ciporen², Mathew Geltzeiler²
¹Oregon Health and Science University, Ochsner Clinic Foundation, Portland, Oregon, United States
²Oregon Health and Science University, Portland, Oregon, United States

Background: Closure of the Eustachian tube (ET) is a valuable procedure for addressing cerebrospinal fluid (CSF) rhinorrhea from lateral skull base defects (otorhinorrhea). Open approaches to these CSF leaks are more invasive and may require addressing multiple sources, relative to endoscopic endonasal ET obliteration (EEETO) targeting the final common pathway of otorhinorrhea in the nasopharynx. However, anecdotally, EEETO using previously described methods can be technically challenging and prone to failure.

Methods: The V-Loc wound closure device (Covidien, New Haven, Connecticut, United States) was used endoscopically and endonasally to close the torus tubarius, obliterating the medial ET orifice, and resolving CSF otorhinorrhea in three cases. The surgical methodology of V-Loc EEETO and representative case examples are described, along with illustrative images and supplemental video.

Results: V-Loc EEETO involved four key procedural steps (Fig. 1A-D, illustrated steps): (1) endoscopic obliteration of the medial ET mucosa with cautery (Fig. 1A), (2) straightening of the distal half of the V-Loc needle to a "J" and passing anterior to posterior through the superior torus tubarius (Fig. 1B), (3) passing the needle back through the anchor loop on the distal end of the suture (Fig. 1C), and (4) additional anterior to posterior passes through the torus tubarius to close the ET orifice (Fig. 2, V-Loc suture passes; Fig. 3, complete ET closure). The device remainder is cut and removed, and V-Loc suture barbs hold tissue closure with no need for knot tying (Fig. 1D). This method of V-Loc EEETO increased subjective procedural ease and speed, which was attributed primarily to avoiding endoscopic knot tying in the confined location of the nasopharynx or passing multiple knots to this site. V-Loc EEETO was utilized successfully (cessation of CSF otorhinorrhea) in three cases; all cases remained successful, without recurrence of CSF otorhinorrhea, at their most recent respective follow-up evaluations 4, 6, and 12 months postoperatively (Fig. 4, postoperative endoscopy at 3 weeks).

Conclusion: This study describes a novel method of EEETO utilizing the V-Loc closure device to successfully resolve CSF otorhinorrhea in three cases. EEETO with V-Loc has greater simplicity and ease compared with previously reported methods involving knot tying and/or various packing; this may reduce time and frustration associated with EEETO which can be deceptively challenging.

This document was downloaded for personal use only. Unauthorized distribution is strictly prohibited.

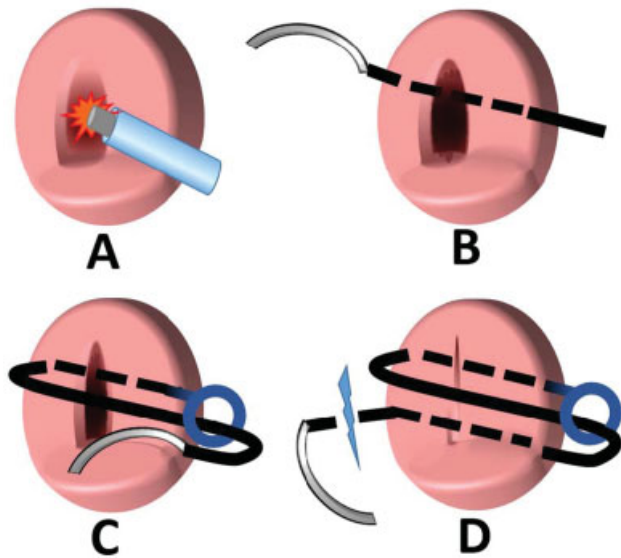


Fig. 1 Illustrated key steps (A–D) of the V-Loc EEETO procedure, as described in results.

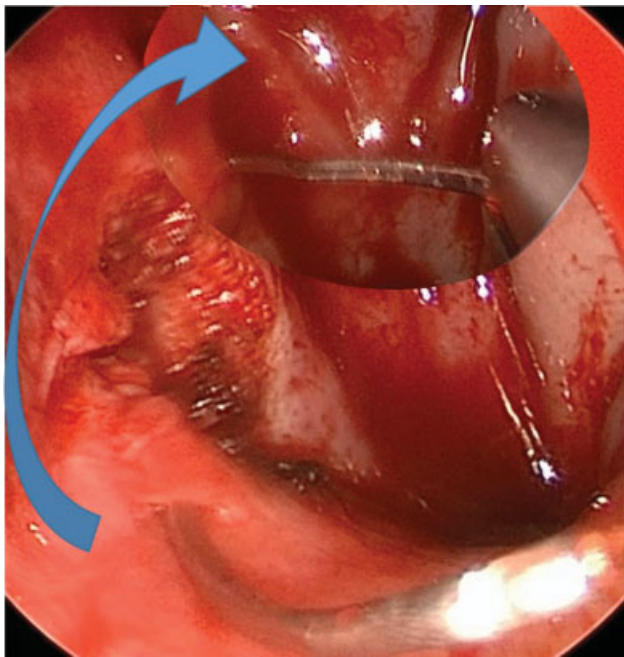


Fig. 2 Intraoperative endoscopic images of right sided V-Loc EEETO demonstrating the anterior to posterior passes of the V-Loc needle through the torus tubarius.

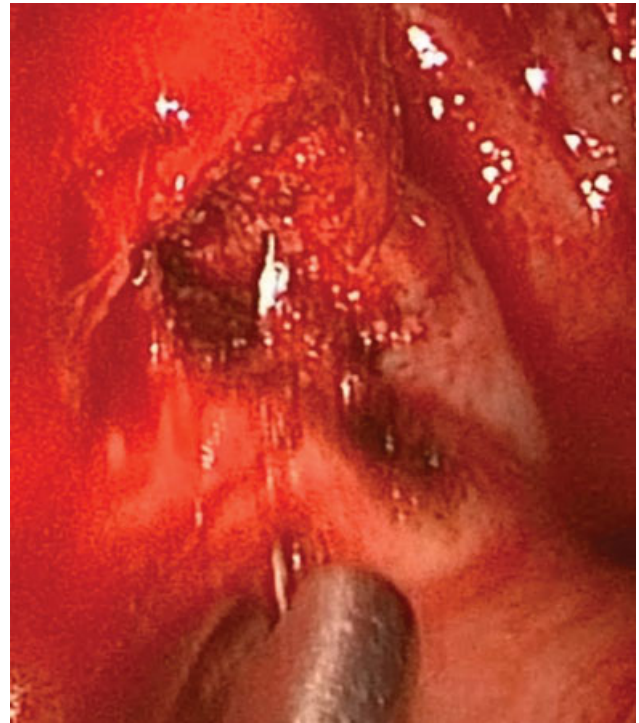


Fig. 3 Intraoperative endoscopic image of right sided V-Loc EEETO at completion of ET closure.



Fig. 4 Endoscopic image of 3 week postoperative result after successful right sided V-Loc EEETO with cessation of otorrhea. Left side is normal unoperated ET.

A064. Anatomical Analysis and Proposed Design of an Angled Drill for Endoscopic Endonasal Petrosectomy
 Huy Q. Truong¹, Hamid Borghei-Razavi², Pinar Celtikci³, Emrah Celtikci³, David T. Fernandes Cabral⁴, Aldo Equiluz-Meléndez⁴, Paul A. Gardner⁴, Juan C. Fernandez-Miranda⁵
¹Medical College of Wisconsin, Milwaukee, Wisconsin, United States
²Cleveland Clinic Florida, Weston, Florida, United States
³Gazi University Faculty of Medicine, Ankara, Turkey
⁴University of Pittsburgh Medical Center, Pittsburgh, Pennsylvania, United States
⁵Stanford University Medical Center, Stanford, California, United States

Background: Endonasal endoscopic surgery actively and continuously evolves with the trend to expand the

targeted anatomical areas laterally, dragging along with it is the development of finer and more specialized instruments. One of the major obstacles for the lateral expansion of endonasal endoscopic approach (EEA) is the internal carotid artery. Although detailed techniques for endoscopic anterior petrosectomy have been described by several authors, including our group, the extent of the surgery is limited mainly by the degree of ICA mobilization and its configuration. As angled visualization is available, a well-fit designed angled drill may be the game-changer in targeting petrous apex lesions. In this abstract, we present our anatomical analysis and propose a dimension-wise concept design of such drill.

Materials and Methods: This study was performed at the Surgical Neuroanatomy Laboratory of the Department of Neurological Surgery, University of Pittsburgh School of Medicine on 68 anatomical specimens. All specimens were injected with colored latex in neurovascular system and scanned with thin sliced CT, ranging from 0.625 to 1.2 mm for navigation purpose. We defined three key anatomical landmarks for petrosectomy: (A) most anterior part of the nasal septum, (B) posteromedial border of lacerum ICA, and (C) the projection of medial rim of internal acoustic meatus on the axis of petrous apex. The AB, BC distances, and ABC angle were measured radiographically (**Fig. 1**). Means, standard deviations, and box-plot graphs were performed in SPSS Statistics Base 22.0 (SPSS, Inc., Chicago, Illinois).

Results: Detailed findings are presented on **Table 1**. From the results, we propose the dimensions for the angled drill to be at 135 degree and the distal arm of hand piece to be 20 mm long, the nasal portion of proximal arm to be 90-mm long. Concept was tested and demonstrated on two dissected anatomical specimens (**Fig. 1**).

Conclusion: We present our anatomical analysis and proposed dimension for an ideal angled drill for the purpose of endoscopic petrosectomy. We strongly believe the availability of such drill will improve the safety and extent of tumor resection during endoscopic surgery to the petrous apex.

Table 1 Detailed findings of this study

	Right side (mean ± SD)	Left side (mean ± SD)	Both side (mean ± SD)
AB distance (mm)	81.1 ± 5.7	81.8 ± 5.9	81.1 ± 5.7
BC distance (mm)	20.4 ± 2.8	19.2 ± 2.4	19.8 ± 2.7
ABC angle	137.4 ± 4.5	136.1 ± 5.5	136.7 ± 4.5

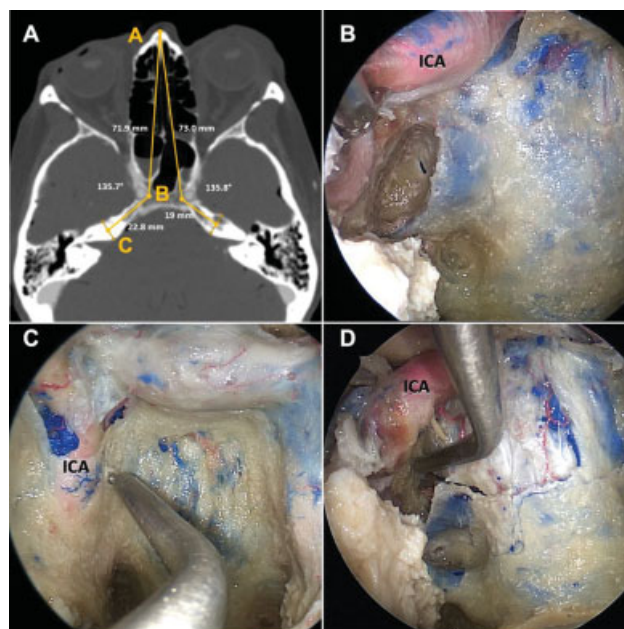


Fig. 1 (A): Screenshot of CT scan image demonstrating landmarks and methods for measurements; (B) Endoscopic view of an anterior petrosectomy performed on an anatomical specimen with straight drill and mobilization of ICA. (C and D) Illustration of angled drill in surgical perspective using bent instrument with proposed dimensions.

A065. Glycerol Rhizotomy for the Management of Tumor-Associated Trigeminal Neuralgia

Christina Jackson¹, Jennifer Franke¹, Michael Lim¹

¹Johns Hopkins School of Medicine, Baltimore, Maryland, United States

Background: Gross total resection of the adjacent tumor is often the most effective option for pain control in tumor-associated trigeminal neuralgia (TN). However, these tumors are often located near critical neurovascular structures or in difficult to access locations, and therefore gross total surgical resection may not always be feasible. One alternative to surgical resection in patients at high surgical risk or with unfavorable medical comorbidities is glycerol rhizotomy. However, there is currently limited evidence for the efficacy of glycerol rhizotomy in the management of tumor-associated TN, and a better understanding of this treatment option may optimize preoperative patient counseling and postoperative management.

Methods: To characterize the efficacy of glycerol rhizotomy in tumor-associated TN, we conducted a retrospective review of patients who underwent glycerol rhizotomy for TN at a tertiary care center between 2008 and 2019. Tumor association was identified by confirmation of adjacent mass to the trigeminal complex on MRI (**Fig. 1**). We evaluated baseline clinical and radiographic characteristics of patients who underwent glycerol rhizotomy for tumor-associated TN. We further assessed clinical outcomes including pain improvement, pain recurrence, and complications after glycerol rhizotomy. Neuralgic pain was measured based on the Barrow Neurological Institute (BNI) pain score.

Results: We identified 837 patients who underwent glycerol rhizotomy for TN, of which 23 (2.7%) patients had tumor-associated TN (**Table 1**). Five (21.7%) patients had previous surgical resection and 10 (43.5%) patients had prior radiation to the associated tumor. A total of 22 (95.7%)

patients presented with typical trigeminal pain with 20 (87%) patients having an initial BNI pain score of IV or higher. Three patients were lost to follow-up at the time of study analysis. The mean follow-up time for the remainder patients was 21.7 months. Of the 20 remaining patients, neuralgic pain improvement was achieved in 17 (85%) patients (Table 2). The mean preoperative BNI score was 4.1 (SD 0.89) and mean postoperative BNI score at best response was 2.55 (SD 1.20, Fig. 2). Seven patients (35%) achieved complete resolution of pain, defined as having no facial pain and not taking any pain medications. In the three patients who had persistent pain postoperatively, two had reduction in either the dose or regimen of pain medications. During the follow-up period, pain recurred in eight (40%) patients. Seven (35%) patients experienced new postoperative facial numbness and no patients experienced hemorrhage, infection, CSF leak, hearing deficit, or mortality related to the procedure.

Conclusion: Tumor-associated TN can pose a challenging management problem as these tumors' locations often prohibit safe gross total resection for alleviation of trigeminal pain. In the largest series to our knowledge, we demonstrate that glycerol rhizotomy for tumor-associated TN led to improvement in pain level or decrease in pain medication requirement in the majority of patients without significant complications. Therefore, glycerol rhizotomy can be an effective and safe minimally invasive tool in the management of tumor-associated TN patients who may not be amenable to gross total surgical resection.

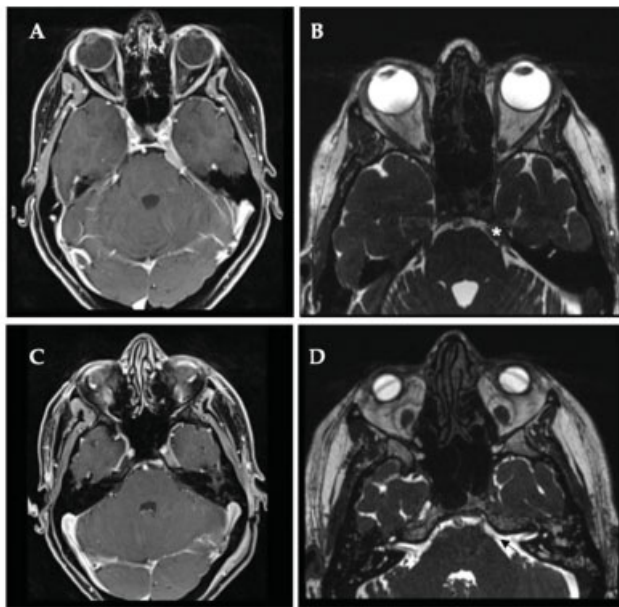


Figure 1. Middle aged patient who presents with left facial pain in the setting of an extra-axial long the left anterior tentorial surface causing compression (*) of the left trigeminal nerve (A,B). Patient underwent subtotal resection of the tumor with decompression of the trigeminal nerve and CSF cleft (arrow) evident around the trigeminal nerve at its nerve root entry zone and mid to distal cisternal segments (C,D). The patient had persistent trigeminal pain post surgery and subsequently underwent left glycerol rhizotomy with resolution of neuralgic pain (BNI I).

Table 1. Baseline characteristics of 23 patients who underwent glycerol rhizotomy for tumor-related TN.

	No. of Patients	Percent or Range
Total	23	
Sex		
Male	4	17.4%
Female	19	82.6%
Mean age at rhizotomy (yrs)	61.3	43 - 82
No. of CN V divisions involved		
1 division	6	26.1%
2 divisions	7	30.4%
3 divisions	8	34.8%
Undetermined	2	8.7%
Mean preoperative symptom duration (yrs)	5	0.4 - 18
Tumor type		
Meningioma	16	69.6%
Vestibular Schwannoma	1	4.3%
Trigeminal Schwannoma	5	21.7%
Undetermined radiographically	1	4.3%
Presenting Symptoms		
Typical TN	22	95.7%
Atypical TN	1	4.3%
Previous tumor resection		
Gross total resection	1	4.3%
Subtotal resection	3	13.0%
Unknown	1	4.3%
Previous ipsilateral interventions for TN		
Microvascular decompression	4	17.4%
Rhizotomy	13	56.5%
Radiation to tumor	10	43.5%
Any radiation history	12	52.2%
Comorbidities		
Alcohol	9	39.1%
Smoking	6	26.1%
Diabetes	1	4.3%
Multiple Sclerosis	0	0%
Lupus	1	4.3%
Rheumatoid arthritis	0	0%
Other autoimmune disorders	0	0%
Other pain syndromes	1	4.3%

Table 2. Summary of clinical outcomes in 20 patients following glycerol rhizotomy.

	No. of Patients	Percent or Range
Cases with follow up	20	
Mean length of follow up (mos)	21.7	2 - 92
Procedure (all patients)		
Rhizotomy	12	52.2%
Rhizotomy + Radiofrequency	11	47.8%
Preoperative mean BNI score (1-5)	4.10 ± 0.89	2 - 5
Postoperative mean BNI score at best response (1-5)	2.55 ± 1.20	1 - 4
Improvement in pain postoperatively	17	85%
Persistent pain	3	15%
Pain recurrence	8	40%
BNI pain score at best response		
I	7	35%
II	0	0%
III	8	40%
IV	5	25%
V	0	0%
Complications		
Hemorrhage	0	0%
Infection	0	0%
Facial palsy	0	0%
CSF leak	0	0%
Hearing deficit	0	0%
Mortality	0	0%
Facial numbness	7	40%

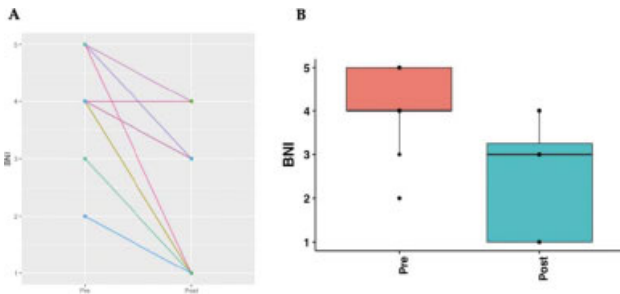


Figure 2. Change in pre- and post-glycerol rhizotomy BNI pain scores. A. 17 (85%) of patients achieved improvement in neuralgic pain after glycerol rhizotomy and decrease in BNI pain score. B. There is substantial decrease in the mean BNI score post-operatively compared to mean pre-operative score (mean 4.2 vs. 2.55).

A066. Adjuvant Radiotherapy in Skull Base–Located Grade II, Atypical Meningioma

David P. Bray¹, Bryan Buster¹, Joseph W. Quillin¹, Robert H. Press², Bree R. Eaton², Jeffrey J. Olson¹

¹Department of Neurosurgery, Emory University Medical Center, Atlanta, Georgia, United States

²Department of Radiation Oncology, Emory University Medical Center, Atlanta, Georgia, United States

Introduction: World Health Organization (WHO) grade II meningioma, known as atypical meningioma (AM), are meningiomas that are more aggressive than their grade I counterparts and have a resultant higher rate of recurrence. AM were thought to represent only 5% of all meningiomas, however, due to changes in WHO grading, they now comprise up to 20 to 35% of newly diagnosed meningiomas. Adjuvant radiotherapy (ART) after resection of AM, regardless of Simpson's grade, has been employed to combat the higher rate of recurrence observed in this population. Use of ART has been controversial; some retrospective studies suggest that ART reduces the risk of recurrence and increases time to recurrence after primary resection. New research suggests that meningiomas of skull-base may have a lower overall rate of recurrence when compared with meningiomas arising from other locations. The effect of ART on skull base meningiomas or AMs is not defined. At our institution, some neurosurgeons employ ART on all newly resected AMs, while some prefer watchful-waiting with serial imaging. This dichotomy allows for retrospective studying of the effect of ART on skull-base located AM.

Methods: A retrospective review of all skull-base located AMs primarily resected at our institution from 1996 to 2015 was completed. Patient demographics, radiographic findings, use of ART, time of follow-up, and recurrence were collected. ART was defined as radiotherapy (RT) that occurred within 6 months of initial resection, regardless of Simpson's grade. Patients with ART received fractionated external-beam RT with minimum 50.4 gray dose (only three patients in this cohort received less than 59.4 gray). Minimum time length of follow-up after resection was 2 years. Recurrence was defined as any progression of previously resected AM noted on follow-up imaging. Statistical analysis was performed using SAS.

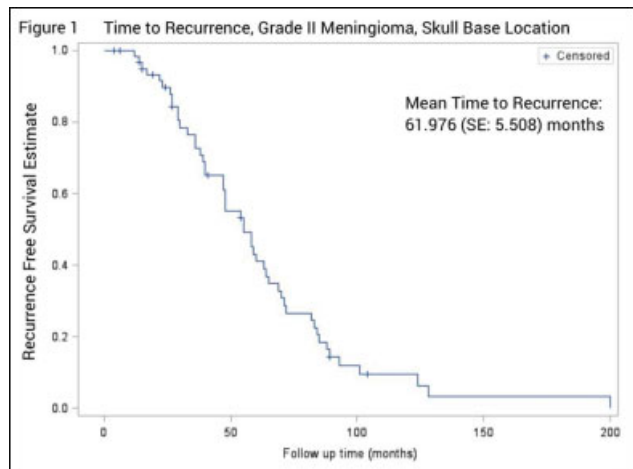
Results: There were a total of 300 AMs resected at our institution from 1996 to 2015. Sixty-three total skull-base located AMs were resected at our institution and met the inclusion criteria for our cohort (Table 1). The average age of our cohort was 53.4 years. Females comprised 73%. Average AM size on preoperative imaging was 4.74 cm, measured in greatest dimension. Gross-total resection, defined as Simpson's grade I-III resection, was achieved in 39 (62%) of cases.

38 of 63 (60%) patients received ART. Recurrence was observed in 14 patients (22%), and mean time to recurrence was 62 months (Fig. 1). Patients that received ART had a lower observed rate of recurrence, however, time to recurrence was not significantly different between the two populations (Fig. 2). There was no significant difference in mean follow-up time.

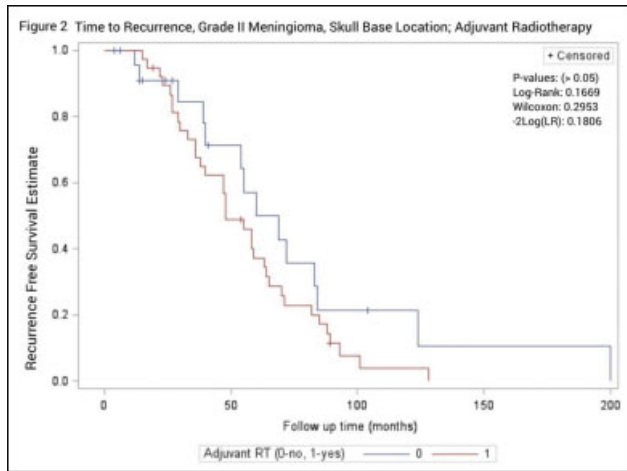
Conclusion: We observe that AM in the skull-base location have higher recurrence rates than we would expect from grade I meningioma. These data suggest that ART may offer benefit to the overall observed recurrence of skull-base located AM, however, the time to recurrence between patients who received ART and those who did not was not statistically significant in survival analysis. More prospective studies will be needed to further elucidate the role of ART in skull-base located AM.

Table: Summary statistics for population

	Adjuvant RT	No Adjuvant RT	Total/Combined
Average Age at Surgery (years)	51.9	56.4	53.4
Received Adjuvant RT?	38	25	63
Sex	M: 11 (29%) F: 27 (71%)	M: 6 (24%) F: 19 (76%)	M: 17 (27%) F: 46 (73%)
Location of Meningioma:	Sphenoid wing: 17 Cavernous sinus: 1 Planum/olfactory groove: 12 Tuberculum sellae: 1 Petroclival: 0 Cerebellopontine angle: 3 Posterior fossa: 1 Orbital: 3	Sphenoid wing: 7 Cavernous sinus: 1 Planum/olfactory groove: 13 Tuberculum sellae: 0 Petroclival: 1 Cerebellopontine angle: 2 Posterior fossa: 0 Orbital: 1	Sphenoid wing: 24 Cavernous sinus: 2 Planum/olfactory groove: 25 Tuberculum sellae: 1 Petroclival: 1 Cerebellopontine angle: 5 Posterior fossa: 1 Orbital: 4
Simpson Grade Resection:	I: 8 II: 9 III: 2 IV: 19 V: 0	I: 7 II: 10 III: 3 IV: 5 V: 0	I: 15 II: 19 III: 5 IV: 24 V: 0
Average Tumor Size (cm; in greatest dimension, preoperative imaging):	4.93	4.5	4.74
Osseous involvement (intraoperatively)?	Yes: 27 (71%) No: 11 (29%)	Yes: 16 (64%) No: 9 (36%)	Yes: 43 (68%) No: 20 (32%)
Brain involvement (preop imaging)?	Yes: 23 (61%) No: 15 (39%)	Yes: 15 (60%) No: 10 (40%)	Yes: 38 (60%) No: 25 (40%)
Recurrence?:	Yes: 3 (8%) No: 35 (92%)	Yes: 11 (44%) No: 14 (56%)	Yes: 14 (22%) No: 49 (78%) P = < 0.05



This document was downloaded for personal use only. Unauthorized distribution is strictly prohibited.



A067. Imaging-Based Score for Predicting Higher-Grade Meningiomas

Yaroslav Gelfand¹, Abigail Funari¹, Michael Longo¹, Samuel Ahmad¹, Sadiq Rahman¹, Vijay Agarwal¹

¹Albert Einstein College of Medicine, Montefiore Medical Center, Bronx, New York, United States

Introduction: Predicting whether an intracranial meningioma will be higher grade based on preoperative imaging studies remains challenging. While various imaging characteristics have been previously found in the literature to correlate with higher grade lesions, such as presence of edema, heterogeneous enhancement, and shape irregularity, no single finding has been shown to have a high positive predictive value for higher grade meningiomas.

Materials and Methods: After IRB approval we retrospectively reviewed all patients operated on at a single academic institution for intracranial meningiomas between 2014 and 2018. Patient demographics, preoperative laboratories, and imaging were reviewed. One point was assigned for each of the following imaging characteristics: presence of parenchymal edema, heterogeneous enhancement, irregular borders, presence of calcifications, and volume over 40 mL. The Imaging Score (IS) was calculated by adding up the points, with the total score ranging from 0 to 5. Predictive ability of the score to identify meningiomas with grade higher versus WHO grade 1 lesions was evaluated.

Results: Eighty-seven patients who underwent surgery for intracranial meningiomas from 2014 to 2018 who had appropriate imaging, demographic information, and pathological results available were included in the analysis. Nine lesions were infratentorial and 78 were supratentorial. Fifty-two percent were WHO grade 1 tumors and 48% were WHO grade 2 tumors. A total of 70% of the patients were male and 30% were female. There was no significant difference in age between patients with WHO grade 1 and tumors. Individual imaging characteristics of the tumor were analyzed and compared between WHO grades 1 and 2. WHO grade 2 meningiomas were more likely to be larger in size and more likely to demonstrate inhomogeneous enhancement and irregular contours. Interestingly, calcifications were more likely in grade 2 tumors, although the difference was not statistically significant. Using the Imaging Score, the probability of having a WHO Grade 2 meningioma was 0% with the

score of 0, 33.3% for those with the score of 1, 35.7% with score of 2, 66.7% with score of 3, 76.2% with score of 4, and 100% with score of 5 (Table 1).

Conclusion: The current population of patients studied has a significantly higher rate of WHO grade 2 meningiomas than that which has been previously reported. The Imaging Score presented combines various imaging characteristics and shows a good positive predictive value in this patient cohort for identifying a WHO grade 2 or higher lesion. Further studies to validate this scoring system on a wider cohort of patients are necessary (Table 2).

Table 1: Demographics and imaging characteristics

	WHO Grade 1	WHO Grade 2	P value
Age	59.6	59.7	0.950
Male (%)	22.2	38.1	0.106
Volume (ml)	30.2	74.3	<0.001
Edema (%)	48.9	88.1	<0.001
Nonhomogeneous Enhancement (%)	20.5	61.9	<0.001
Irregular Contours (%)	31.8	85.7	<0.001
Calcifications (%)	17.8	28.6	0.232

A068. Inhibition of PDGFR May Be a Viable Treatment Option for Meningiomas

Tadeusz Wroblewski¹, Philip D. Tatman¹, Anthony Fringuello¹, William Foreman¹, Sameul Scherer¹, Denise Damek¹, Kevin Lillehei¹, Randy Jensen², David Ormond¹, Michael Graner¹

¹University of Colorado, Boulder, Colorado, United States

²University of Utah, Salt Lake City, Utah, United States

Background: Meningiomas are the most common primary tumor in the central nervous system. Aside from surgery, no consensus on the benefit of adjuvant therapy exists for these tumors. One possible avenue to address the need for additional therapies for meningiomas is high-throughput drug screening. Through our screening efforts, we identified platelet-derived growth factor receptor (PDGFR) inhibitors as potential treatments for patients with meningiomas.

Methods: We utilized our high-throughput drug screening system, developed for central nervous system (CNS) tumors, to screen meningiomas shortly after resection. We also included previously established meningiomas cell lines in our screening efforts. We screened an expanded version of the National Cancer Institute's Anti-Cancer Library at a 1- μ m dose, in triplicate, for each tumor. After 72 hours of treatment, we evaluated tumor viability by MTS assay. Any compound that significantly reduced viability compared with an untreated control was considered a positive hit for further validation.

Results: Thus far, 12 meningiomas have been tested with our expanded screen. Ponatinib was identified as the most effective tyrosine kinase inhibitor in this cohort of compounds. Ponatinib can inhibit the Abelson murine leukemia viral oncogene homolog 1 (ABL), PDGFR α , vascular endothelial growth factor receptor (VEGFR), and fibroblast growth factor receptor (FGFR). Comparing the targets of Ponatinib to targets of compounds that did not significantly reduce meningioma cell viability, we were able to identify PDGFR as the receptor responsible for Ponatinib's activity. Using dose curves, we calculate the IC50 of Ponatinib in a cell-based assay to be between 900 nm and 1 μ m. To fully elucidate the efficacy of targeting the PDGFR family of tyrosine kinase inhibitors, we are in the process of screening PDGFR β inhibitors, as well as pan-PDFGR inhibitors in meningiomas. While meningiomas are not known to have activating PDGFR mutations,

activation of PDGFR signaling has been shown to drive NF2 deleted arachnoid cap cells into meningiomas, making PDGFR a potential target for meningioma therapy.

Conclusion: Additional therapies are needed for the treatment of meningiomas. Using our novel cell culturing technique and high-throughput drug screening capabilities, we identified Ponatinib as a compound that significantly reduced meningioma cell viability. Additional work is needed to fully investigate the potential of targeting PDGFR signaling in meningiomas as well as in vivo experiments to validate our findings.

A069. The Impact of Clinical Frailty on Overall Survival following Surgical Resection in Patients with High-Grade Meningiomas

Jianning Shao¹, Pranay Soni², Arbaz Momin¹, Diana Lopez¹, Konrad K. Knusel³, Patrick J. Elsworth³, Varun Kshetry², Pablo F. Recinos⁴

¹Cleveland Clinic Lerner College of Medicine at Case Western Reserve University, Cleveland, Ohio, United States

²Department of Neurosurgery, Cleveland Clinic, Cleveland, Ohio, United States

³Case Western Reserve University School of Medicine, Cleveland, Ohio, United States

⁴Section Head—Skull Base Surgery, Department of Neurosurgery, Cleveland Clinic, Cleveland, Ohio, United States

Introduction: World Health Organization (WHO) grade II and III meningiomas, though relatively uncommon, represent an important subset of meningiomas that are characterized by increased recurrence and decreased survival. The standard treatment paradigm for these high-grade meningiomas generally consists of maximum safe resection, often in combination with adjuvant radiotherapy. As the general population ages, older patients are presenting with meningiomas more often, and the impact of patient frailty on postoperative outcomes emerges as an especially important question. “Patient frailty,” however, has been loosely defined, and prior studies on this topic have only examined patient populations with predominantly WHO I meningiomas. Thus, an adequate understanding of the impact of frailty on overall survival (OS) in patients undergoing surgical resection of high-grade meningiomas remains unclear. This study provides a comprehensive assessment of the impact of patient frailty on postsurgical survival in patients with high-grade meningiomas in the largest patient cohort of its kind to date.

Methods: A retrospective review was performed to identify all patients who underwent surgical resection for WHO grade II and III meningiomas at our institution between 1995 and 2019. Measures of frailty, including patient age, clinical frailty index (CFI), and Charlson’s comorbidity index (CCI) were recorded. Patients for whom adequate demographic or clinical information was unavailable were excluded from the study. Univariate and stepwise multivariate cox proportional hazards models were used to determine the best fit predictive model for overall survival based on a variety of patient- and tumor-specific variables. Correlations between frailty measures were controlled for via a collinearity analysis.

Results: A total of 253 patients were included in the final analysis. Mean follow-up was 5.5 years. A total of 141 patients (55.7%) were female, and 112 patients (44.3%) were male. The mean CFI and CCI were 3.68 ± 1.21 , 4.52 ± 1.98 , respectively. A total 144 patients (57.4%) received either adjuvant or salvage radiation therapy, and 7 patients (2.8%) received chemotherapy. Tumor location was as follows: skull base—75 (29.6%), convexity—63 (24.9%), parasagittal/falcine—92 (36.4%), and other—23 (9.1%). Univariate cox regression

analysis revealed that higher values of age, CFI, and CCI were all significantly correlated with increased risk for mortality (adjusted hazard ratios of 1.82, 1.67, and 1.34, respectively; p -value < 0.001 for all measures). The final cox proportional hazards model found CFI to be associated with increased risk for mortality (HR = 1.72, $p < 0.001$). Other, nonfrailty, parameters independently associated with increased risk for adverse OS included male gender (HR = 1.94, $p = 0.029$), WHO grade III (vs. grade II; HR = 4.45, $p = 0.0055$), and recurrent tumor (HR = 2.49, $p = 0.012$). Protective factors included bilaterality of tumor location (HR = 0.462, $p = 0.027$).

Conclusion: Higher degrees of patient frailty using the CFI was correlated with decreased OS in patients who underwent surgical resection for high-grade meningiomas. Frailty appears to be an important element in understanding overall survival in patients with high-grade meningiomas. Further study is needed to determine if functional optimization preoperatively in frailer patients may have a positive impact on OS in patients with high-grade meningiomas.

A070. Clinical Frailty Is an Important Predictor of Functional Outcome following Surgical Resection in Patients with High-Grade Meningiomas

Jianning Shao¹, Arbaz Momin¹, Pranay Soni², Diana Lopez¹, Konrad K. Knusel³, Patrick J. Elsworth³, Varun R. Kshetry², Pablo Recinos⁴

¹Cleveland Clinic Lerner College of Medicine at Case Western Reserve University, Cleveland, Ohio, United States

²Department of Neurosurgery, Cleveland Clinic, Cleveland, Ohio, United States

³Case Western Reserve University School of Medicine, Cleveland, Ohio, United States

⁴Section Head—Skull Base Surgery, Department of Neurosurgery, Cleveland Clinic, Cleveland, Ohio, United States

Introduction: High-grade meningiomas (WHO grades II and III), represent approximately 20% of all meningiomas but are characterized by markedly increased recurrence and aggression. As meningioma incidence increases progressively with age, the impact of patient frailty on postoperative quality of life becomes an increasingly relevant question. While several scales for quantifying frailty exist, they are inconsistently utilized and have not been studied in relation to postoperative outcomes in a large patient cohort of high-grade meningiomas. This study presents a thorough evaluation of the impact of preoperative frailty on postsurgical quality of life in patients with high-grade meningiomas in the largest such cohort of its kind to date.

Methods: A retrospective review was performed to identify all patients who underwent surgical resection for WHO grade II and III meningiomas at our institution between 1995 and 2019. Extensive data on patient demographics, frailty measures, surgical parameters, and quality of life were collected. In particular, frailty measures include Clinical Frailty Index (CFI), Charlson’s comorbidity index (CCI), and age. Postoperative Karnofsky’s performance scores (KPS) at the 3-month and 12-month follow-up appointments were utilized as a proxy for quality of life after surgical resection. Patients with inadequate documentation were excluded from the study. Multivariate analysis was performed to determine the best-fit model for postoperative KPS scores based on a variety of patient and tumor-specific variables. The model that yielded the lowest Akaike’s information criteria (AIC) was selected as the final model.

Results: A total of 253 patients were included in the final analysis. A total of 141 patients (55.7%) were female, and 112 patients (44.3%) were male. The mean CFI and CCI were

3.68 ± 1.21 and 4.52 ± 1.98 , respectively. Tumor location was as follows: skull base—75 (29.6%); convexity—63 (24.9%); parasagittal/falcine—92 (36.4%); and other—23 (9.1%). On multivariate analysis, three independent factors were significantly associated with lower KPS scores both the 3-month and 12-month postoperative time points: (1) black race (3 months: $p = 0.0012$, 12 months: $p < 0.001$), (2) CFI (3 months: $p = 0.045$, 12 months: $p = 0.039$), and (3) laterality of tumor location (3 months: $p = 0.047$, 12 months: $p = 0.014$). Two factors associated with higher postoperative KPS scores were higher values of preoperative KPS (3 months: $p < 0.001$, 12 months: $p = 0.023$) and grade III tumor (3 months: $p = 0.0022$, 12 months: $p = 0.0058$). CCI was not selected to be in the final model as it did not minimize AIC.

Conclusion: Frailty using CFI and preoperative KPS were significantly correlated with postoperative quality of life following surgical resection in patients with high-grade meningiomas. Patients with lower preoperative CFI tend to have worse postoperative functional outcomes, while patients with higher preoperative KPS scores tend to have significantly higher functional outcomes after surgery. Our results underlie the importance of appropriate patient selection and preoperative optimization to minimize frailty in patients undergoing surgical resection for high-grade meningiomas. Further are needed to evaluate if functional optimization preoperatively in frailer patients may have a positive impact on postoperative quality of life in patients with high-grade meningiomas.

A071. Extent of Resection and Survival Outcomes in World Health Organization Grade II and III Meningiomas

Pranay Soni¹, Jianning Shao¹, Arbaz Momin¹, Diana Lopez¹, Varun R. Kshetry¹, Pablo F. Recinos¹

¹Cleveland Clinic, Cleveland, Ohio, United States

Background: Meningiomas account for 13 to 26% of all intracranial tumors, and while most are benign, a substantial portion of them can be more aggressive. These high-grade meningiomas can be classified as World Health Organization (WHO) grade II or III. While complete resection in low-grade meningiomas is associated with a relatively low recurrence rate, high-grade meningiomas are more aggressive, with recurrence rates reported between 29 and 94%. The purpose of this study is to describe the association of extent of resection with progression-free and overall survival in patients with WHO grade II and III meningiomas (Fig. 1).

Methods: A retrospective database review was performed to identify all patients who underwent surgical resection for WHO grade II and III meningiomas at our institution between 1995 and 2019. Patients undergoing surgery for recurrent tumors, or for whom adequate demographic or surgical information was unavailable, were excluded from the study. Patients were divided into two cohorts based on the extent of surgical resection. Patients undergoing Simpson's grade I or II resection were classified as gross total resection (GTR), and patients undergoing Simpson's grade III or IV resection were classified as subtotal resection (STR). Two-sided unpaired *t*-tests and Fisher's exact tests were used as appropriate to compare demographic and tumor-specific factors between the cohorts. Kaplan–Meier curves and log-rank analyses were used to plot and assess overall and progression-free survival. A *p*-value of <0.05 was considered to be statistically significant (Fig. 2).

Results: A total of 216 patients who underwent surgical resection for WHO grade II or III meningiomas were included in this study. Median follow-up in this study was 45.0 months. Of these patients, 159 had gross total resection and 57 had subtotal resection. There were no significant

differences between the two cohorts with respect to age, gender, race, preoperative Karnofsky's performance status (KPS), proportion of WHO grade II/III tumors, or patients receiving chemotherapy. Radiation was significantly more common in the STR cohort than in the GTR cohort ($p = 0.012$). Additionally, tumors within the STR cohort were more likely to be located in the sphenoid wing and other skull base locations and less likely to be convexity tumors ($p = 0.008$). Kaplan–Meier curves showed a significant difference in overall survival between GTR and STR cohorts ($p = 0.042$), but there was no statistically significant difference in progression-free survival between the cohorts ($p = 0.71$).

Conclusion: Despite an increased proportion of patients within the STR cohort undergoing radiation therapy postoperatively, greater extent of resection significantly correlated with prolonged overall survival. In an era of increasing support for adjuvant treatment modalities in the management of meningiomas, our data reinforce the belief that the goal of surgery for these tumors should remain maximal safe resection.

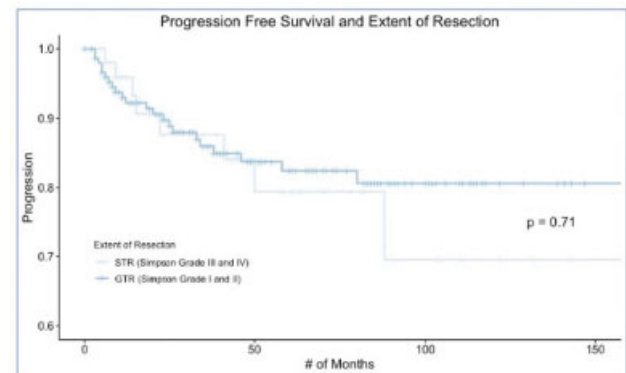


Figure 1 - Kaplan Meier curves showing progression-free survival based on extent of resection. Log rank analysis showed no statistically significant difference in progression-free survival between GTR and STR (*p*-value 0.71).

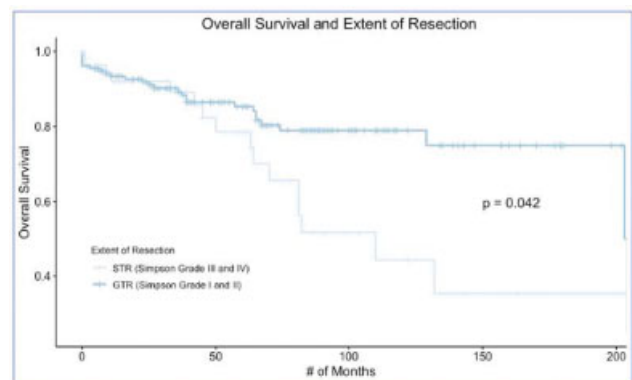


Figure 2 - Kaplan Meier curves showing overall survival based on extent of resection. Log rank analysis showed a statistically significant difference in overall survival between GTR and STR (*p*-value 0.042).

A072. Delayed Otologic Complications Following the Translabyrinthine Approach for Acoustic Neuroma Resection

John P. Leonetti¹, Michael Hutz¹, Sam Marzo¹, Matthew Kircher¹, Dennis Moore¹, Douglas Anderson¹
¹Loyola

Introduction: The translabyrinthine approach has long been a safe and effective technique used in the extirpation of tumors of the internal auditory canal and cerebello-pontine angle. Most otologic complications, such as CSF leak, dizziness, or wound issues occur in the early postoperative period. This presentation will focus on delayed otologic complications following translabyrinthine surgery.

Materials and Methods: This was a retrospective medical records review of all patients treated at our tertiary care academic medical center for a variety of delayed otologic complications following a TLC approach for acoustic neuroma resection. The review period was between July 1988 and July 2018.

Results: A delayed complication was defined as any untoward otologic event occurring 1 year or more after the initial translabyrinthine approach. Twenty-seven delayed complications were identified with a range of time to presentation from 1 year to 21 years. These complications included CSF leak (10), ear canal erosion (5), bone cement granulation fistula (4), tympanic membrane perforation (3), cholesteatoma (3), and fat graft liquefaction necrosis (2).

Conclusion: Tumor recurrence or progressive growth is the main reason for following surgically managed acoustic neuroma patients. We presented six types of otologic complications which can occur several years following the translabyrinthine approach for acoustic neuroma resection.

A073. Incidence of Iatrogenic Inner Ear Breaches from Vestibular Schwannoma Surgery: A Review of 1,153 Hearing Preservation Approaches

Nir Ben-Shlomo¹, A. Rahimi², A.M. Abunimer¹, J.P. Guenette¹, A. Juliano³, J. Jayender¹, C.E. Corrales¹

¹Brigham and Women's Hospital, Boston, Massachusetts, United States

²Harvard Medical School, Boston, Massachusetts, United States

³Massachusetts Eye and Ear Infirmary, Boston, Massachusetts, United States

Background: Vestibular schwannoma (VS) surgery is a common procedure which often requires precise drilling close to the inner ear labyrinth. A breach of the vestibulocochlear system from drilling is correlated with hearing loss and third window symptoms such as vertigo, nystagmus, autophony, and Tullio's phenomenon (sound induced vertigo), among others.¹ Inner ear breaches (IEB) have been reported as high as 30% in the patients undergoing retrosigmoid approaches to the internal auditory canal,² but these figures were reported in the early 1990s with small cohorts. Studies describing VS surgical complications commonly report CSF leak, hydrocephalus, wound infection, and hematoma, among others, all with incidences below 10%;^{3,4} but there remains a paucity of data regarding IEB from VS surgery in the recent literature.

Objective: The aim of the study is to assess the rate of iatrogenic injury to the inner ear labyrinth in VS resections via hearing preservation (retrosigmoid [RS] and middle cranial fossa [MCF]) approaches.

Methods: We performed a multi-institutional chart review of all operative cases of VS performed between 1993 and 2015 across three tertiary care centers. Only surgeries undergoing hearing preservation approaches were consid-

ered for analysis. Preoperative imaging, operative notes, and postoperative imaging were reviewed for each case. IEBs were confirmed by report in operative note or consensus opinion of two neuroradiologists reviewing the postoperative CT.

Results: A total of 1,153 patients underwent hearing preservation approaches for VS resection. One thousand seventy-five (93.2%) patients underwent RS, and 78 (6.8%) underwent MCF approaches. IEB was confirmed in 248 (21.5%) of all cases reviewed: operative notes reported IEB in 102 cases, of which 50 had no postoperative CT for review; postoperative CT confirmed an additional 146 cases of IEB. Postoperative CT was available in 378 patients (32.8% of total cases reviewed), of which 198 (52.4% of postoperative CTs) showed areas of inner ear dehiscence attributable to drilling. Of the patients with confirmed IEB on postoperative CT, 96 patients (38.7%) did not have a record of IEB mentioned in the operative note.

Conclusion: IEB was confirmed in 21.5% of VS surgeries utilizing hearing preservation approaches. IEB is correlated with hearing loss and its occurrence negates the intention of selecting a hearing preservation approach for tumor resection. Due to low rates of postoperative CT available and the lack of reporting IEB in operative notes, we postulate that our confirmed cases likely underestimate the true incidence of IEB sustained in VS surgery undergoing RS and MCF approaches.

References

1. Bartholomew RA, Poe D, Dunn IF, Smith TR, Corrales CE. Iatrogenic inner ear dehiscence after lateral skull base surgery: therapeutic dilemma and treatment options. *Otol Neurotol* 2019;40(4):e399–e404
2. Tatagiba M, Samii M, Matthies C, el Azm M, Schönmayr R. The significance for postoperative hearing of preserving the labyrinth in acoustic neurinoma surgery. *J Neurosurg* 1992;77(5):677–684
3. Samii M, Matthies C. Management of 1000 vestibular schwannomas (acoustic neuromas): surgical management and results with an emphasis on complications and how to avoid them. *Neurosurgery* 1997;40(1):11–21, discussion 21–23
4. Nuño M, Ugiliweneza B, Boakye M, Monfared A. Morbidity of vestibular schwannomas as documented by treating providers. *Otol Neurotol* 2019;40(2):e142–e149

A074. Facial Nerve Function and Risk Factors in Resection of Large Cystic Vestibular Schwannomas

Daniela Stastna¹, Richard Mannion¹, Patrick Axon¹, Neil Donnelly¹, James Tysome¹, Mahonar Bance¹, David Moffat¹, David Hardy¹, Robert Macfarlane¹

¹Addenbrooke's Hospital, Cambridge University NHS Foundation Trust, Cambridge, United Kingdom

The incidence of cystic change in vestibular schwannomas (VS) ranges from 4 to 23%. Cystic VS tend to have different characteristics to solid VS namely larger initial volume, accelerated growth, atypical presentation, and a lobulated/adherent capsule. In general, cystic VS are more challenging, with worse surgical outcomes and higher rates of subtotal resection (STR).

From a total of 655 consecutive VS patients undergoing surgery in Cambridge between 2005 and 2019, 125 were cystic (19.1%). This retrospective study analyzed demographic, clinical, radiological, and intraoperative characteristics

and postoperative outcomes, with particular reference to facial nerve outcome (House-Brackmann [HB] scale). Median age was 56 years (range, 17–85 years; 65 M, 60 F). The atypical presentation was common, including facial numbness (42%), headache (30%), diplopia (5%), facial palsy/hemifacial spasm (5.8%), and lower cranial nerve impairment (2.5%).

Median tumor volume was 9,048 mm³ (range: 715–48,950 mm³). Tumor growth was documented in 27.1%. In two, cyst formation occurred postradiotherapy. VS growth was caused by cyst enlargement in 73.5% and both the solid/cystic part in 14.7%. Cysts were peripheral/thin-walled in 74.4% and central in 34.6%. Seventy-nine percent of peripheral cysts were located on the brainstem surface. Translabyrinthine surgery was the preferred approach (97.6%). Gross total resection (GTR) was achieved in 78 (62.4%), near-total resection (NTR) with capsular remnant (<5%) in 43 (34.4%), and STR in 4 (3.2%). NTR/STR were significantly associated with tumor volume >4,000 mm³, high jugular bulb, intraoperative tumor adherence to the brainstem and/or facial nerve ($p = 0.017$; $p = 0.012$; $p = 0.0006$; $p < 0.0001$, respectively).

The facial nerve was preserved anatomically in all cases. Facial nerve outcome was available at 1 year in 100 cases; 76% were HB 1 to 2, 16% were HB 3 to 4, and 8% were HB 5 to 6. Worse outcomes (HB, 3–6) were associated with tumor volume >19,000 mm³, tumor cyst adjacent to the brainstem, inferior/posterior course of facial nerve, preoperative facial palsy ($p = 0.039$; $p = 0.048$; $p = 0.3$; $p = 0.79$).

Nonfacial morbidity included CSF leak (7.3%), meningitis (0.8%), facial numbness (6.5%), trigeminal neuralgia (1.6%), lower cranial nerve palsy (5.7%), VI nerve palsy (4.8%). There was no mortality. Tumor control was achieved in 99.1%. Regrowth was observed in one patient after STR, requiring radiotherapy. HB 1 to 2 rates when comparing solid VS operated in our unit were significantly higher than in cystic VS; 94 versus 76%, $p = 0.03$.

Our results compare favorably with the Thakur et al literature review of 428 cases from nine studies. Although our GTR rate was lower (62.4% vs. review rate of 81.2%), good facial function (HB, 1–2) was significantly higher in our cohort (76 vs. 39%; $p = 0.0001$), with comparable nonfacial morbidity (19.5 vs. 24.5%; $p = 0.3$).

Conclusion: Surgery for cystic VS has significantly worse outcome for facial nerve preservation compared with solid VS. This can be mitigated by performing less than total excision, with low risk of recurrence.

A075. Surgery versus Radiosurgery for Facial Nerve Schwannoma: Systematic Review and Meta-analysis of Facial Nerve Function

Juliana Rotter¹, Victor M. Lu¹, Avital Perry¹, Christopher S. Graffeo¹, Matthew L. Carlson¹, Colin L. Driscoll¹, Michael J. Link¹
¹Mayo Clinic, Rochester, Minnesota, United States

Introduction: Facial nerve schwannomas (FNS) are uncommon, slow-growing tumors that may cause facial weakness. Although management algorithms continue to evolve, long-term facial function remains a key treatment priority. Historically, patients underwent surgical resection with nerve graft following confirmation of FNS; by contrast, contemporary management typically proceeds from a period of conservative management, until facial nerve weakness or other symptoms referable to tumor compression prompts consideration for treatment. The aim of this study was to compare facial nerve function after resection or stereotactic radiosurgery (SRS) for FNS.

Methods: A search of seven electronic databases from inception to July 2019 was conducted following PRISMA guidelines. Systematically-identified articles were screened against prespecified criteria. Facial nerve function outcomes were classified as improved, stabilized, or worsened, from last preintervention exam until last follow-up. Incidence was then pooled by random-effects meta-analyses of proportions.

Results: Forty-three articles with a pooled cohort of 576 FNS satisfied criteria. Thirty-three and 10 articles described outcomes following surgery in 464 (81%) and SRS in 112 (19%) patients, respectively. In the surgery cohort, facial nerve function improved in 20% (95% CI, 12–29%), stabilized in 41% (95% CI, 34–49%), and worsened in 34% (95% CI, 25–43%). In the SRS cohort, facial nerve function was improved in 20% (95% CI, 9–34%), stable in 66% (95% CI, 54–78%), and worse in 9% (95% CI, 3–16%). As compared with SRS, surgery was significantly associated with a lower incidence of stable facial nerve function, and a higher incidence of worsened facial nerve function ($p < 0.01$). These significant differences were preserved after adjusting for preoperative House-Brackmann grade (≤ 2 vs. > 2).

Conclusion: Although the incidences of improved facial nerve function after FNS treatment are comparable following surgery or SRS, surgery is significantly associated with lower rates of stable facial nerve function, and higher rates of worsened facial nerve function. Further study is required to address potentially confounding sources of clinical heterogeneity.

A076. Safety and Efficacy of Postoperative Anticoagulation for Deep Vein Thrombosis Prophylaxis in Vestibular Schwannoma Microsurgical Resection

Malika Bhargava¹, Komal Naeem¹, Randall W. Porter¹

¹Barrow Neurological Institute, Phoenix, Arizona, United States

Introduction: This institute experienced multiple devastating consequences of chemical anticoagulation-induced intracranial hemorrhages (ICH) after successful posterior fossa (PF) vestibular schwannoma (VS) resection surgeries, prompting the implementation of an anticoagulation protocol in May 2015: Stop Treating with Enoxaparin Postoperatively for Posterior fossa Surgery (STEPPS). The STEPPS Protocol calls for patients who have undergone PF craniotomies not to receive any chemical venous thromboembolism (VTE) chemical anticoagulation for 3 days postoperatively. All patients were to use mechanical anticoagulation while in bed and have lower extremity Doppler ultrasounds performed every other day to monitor for deep vein thromboses (DVT). Unfractionated heparin (UFH) could be used in a twice-daily dosage after 3 days and/or an inferior vena cava (IVC) filter could be placed. Enoxaparin would not be used prophylactically or therapeutically for 1 month postoperatively. This study sought to determine the efficacy of this protocol, and whether the reduction in enoxaparin use had a significant impact on reducing the incidence of ICH in this patient population.

Methods: Demographic, clinical, surgical, and postoperative treatment-related information on patients who underwent a VS microsurgical resection by a single neurosurgeon in one institution from 2011 through May 2019 was retrospectively recorded. The postoperative outcomes were followed with regard to the STEPPS protocol. A p -value of less than 0.05 was considered statistically significant.

Results: A total of 132 VS microsurgical resections were included in the analysis from 2011 through May 2019. Sixty-seven (50.8%) surgeries were performed before the STEPPS protocol was implemented from 2011 through April 2015. Of these, information regarding chemical

anticoagulation use could be obtained for 33 patients. Twenty-nine (87.9%) of these patients received chemical anticoagulation (UFH or enoxaparin), including 63.6% (21/33) who received enoxaparin. Twenty (95.2%) of these patients received enoxaparin within 72 hours postoperatively, including three of the four patients who developed a postoperative, anticoagulation-related ICH. The incidence of postoperative anticoagulation-related ICH prior to the STEPPS protocol implementation is 5.97% (4/67) compared with 0% (0/65) after its start ($p = 0.0457$). Of the four ICH patients, one succumbed to the complexities of his care within 2 years and one is bedridden at a functional Glasgow Outcome Scale of 2. Of the 65 (49.2%) operations performed after May 2015, 12 (18.5%) patients received prophylactic or therapeutic chemical anticoagulation, including only 4.6% (3/65) who received enoxaparin. The difference between the proportion of patients receiving enoxaparin before and after the STEPPS protocol was statistically significant ($p < 0.0001$). Three (4.6%) patients developed a DVT (two in lower extremities, one in upper extremity) and two (3.1%) patients developed a PE, at which point, they received UFH and one received an IVC filter. Both patients recovered well.

Conclusion: Chemical VTE prophylaxis can increase the susceptibility of PF neurosurgical patients to ICH. The STEPPS protocol results indicate that there is a statistical significance between the rates of ICH and enoxaparin use before and after implementation. Relying more strongly on mechanical prophylaxis and vigilant surveillance in the population of neurosurgical patients undergoing posterior fossa craniotomies can help prevent devastating ICHs from occurring.

A077. Evidence for a Biological Shift behind the Increasing Incidence of Sporadic Vestibular Schwannoma

John P. Marinelli¹, Matthew L. Carlson²

¹Department of Otolaryngology—Head and Neck Surgery, San Antonio Military Medical Center, San Antonio, Texas, United States

²Departments of Otolaryngology—Head and Neck Surgery and Neurologic Surgery, Mayo Clinic, Rochester, Minnesota, United States

Background: The incidence of sporadic vestibular schwannoma (VS) has significantly increased over the last several decades. Most often, this increase is attributed to the increasingly widespread use of magnetic resonance imaging (MRI) and screening protocols for asymmetrical hearing loss. However, apart from the recognition that incidence rates have risen in the post-MRI era, no study to date has directly investigated this supposed etiology.

Objective: The objective of the current work was to characterize the incidence of head MRIs over the previous two decades in Olmsted County, Minnesota and compare this trend to the incidence of asymptomatic, incidentally diagnosed VS over the same time period.

Methods: Procedure codes for head MRIs among residents of Olmsted County, Minnesota between January 1, 1995 and December 31, 2016 were retrieved using the Rochester Epidemiology Project—a unique medical records-linkage system covering the complete population of Olmsted County supported by the National Institute on Aging. Incidence rates of VS were obtained following review of each resident of Olmsted County who was diagnosed with VS over the same time interval. Incidence rates of head MRI and VS were calculated on a per-year basis and directly standardized to the total United States population from the 2000 United States Decennial Census. Trends in tumor size over time were evaluated using Spearman rank correlation coefficients.

Results: A total of 43,561 head MRIs among 30,002 residents of Olmsted County were identified from 1995

through 2016. The incidence of head MRI significantly increased between 1995 and 2003 ($p < 0.001$), but remained stable between 2004 and 2016 ($p = 0.14$). Over the same time interval, 25 cases of incidentally diagnosed VS were identified. The incidence of asymptomatic VS increased over time from 0.72 per 100,000 person-years between 1995 and 1999 to 1.29 between 2012 and 2016 ($p = 0.058$). No plateauing of incidence rates was observed in incidental tumors over the study period. The size of incidentally diagnosed tumors did not change over the study period ($p = 0.93$), suggesting that the increasing incidence of asymptomatic tumors is not explained by improved diagnostic capability of more recent MRI studies.

Conclusion: Despite the plateauing of head MRI incidence rates after 2004, the incidence of asymptomatic, incidentally diagnosed VS continued to increase. Therefore, these data provide evidence that there may exist a true biological shift behind the rising incidence of VS beyond simply greater detection alone.

Acknowledgments: This study was made possible using the resources of the Rochester Epidemiology Project, which is supported by the National Institute on Aging of the National Institutes of Health under Award Number R01AG034676. The content is solely the responsibility of the authors and does not necessarily represent the official views of the National Institutes of Health.

A078. Local Control and Radiographic Response as a Function of Isodose Adjustment in Stereotactic Radiosurgery Treatment for Sporadic Vestibular Schwannoma

Avital Perry¹, Achiraya Teyateeti¹, Christopher S. Graffeo¹, Paul D. Brown¹, Bruce E. Pollock¹, Michael J. Link¹

¹Mayo Clinic, Rochester, Minnesota, United States

Background: Stereotactic radiosurgery (SRS) is a common, safe, and effective treatment for vestibular schwannoma (VS), which is typically prescribed at the 50% isodose line (IDL). Decreasing the IDL for a fixed prescription dose increases both the maximum dose and the fraction of tumor receiving a higher physical dose; however, the impact on clinical outcomes of such an approach to treatment planning has not been studied.

Methods: Propensity score-matched analysis of patients with sporadic VS treated with SRS planned at IDL = 40% vs. IDL = 50%, with prescription dose of 12 to 14 Gy, treatment volume ≤ 10 mL, and follow-up ≥ 2 years. Cohorts were matched on age, volume, and prescription dose.

Results: After matching 40% IDL and 50% IDL groups, mean ages were 55 versus 54 years ($p = 0.891$), mean volumes were 2.15 versus 2.03 cm³ ($p = 0.844$), and median prescription doses were 12 Gy ($p = 1$). Median total follow-up times were 111 versus 72 month. Tumor control was assessed actuarially at 2, 5, and 10 years, observed rates of 100, 96.4, and 96.4% for 40% IDL and 96.4, 86.7, and 86.7% for 50% IDL ($p = 0.243$). Follow-up MRI studies were volumetrically analyzed for 19 patients treated at 40% IDL and 21 patients treated at 50% IDL; overall volume reduction was significantly greater in the 40% IDL cohort (48.1 vs. 38.3%, $p = 0.05$), but annual rates-of-reduction were comparable (5.5 vs. 6%, $p = 0.749$). Serviceable hearing was documented at time of SRS in eight patients treated at 40% IDL and 13 patients treated at 50% IDL. Hearing preservation was significantly greater among 40% IDL patients, with 2-, 5-, and 10-year rates of 100, 83.3, and 62.5%, as compared with 76.2, 57.1, and 11.4% ($p = 0.017$). Differences in rare complications including facial paresthesia, facial palsy, ataxia/gait

disturbance, and new shunt-dependent hydrocephalus were not significantly difference between the IDL groups.

Conclusion: Based on a small, retrospective sample, SRS treatments for VS planned at 40% IDL may achieve improved tumor control and hearing outcomes, as compared with treatments planned at 50% IDL.

A079. Anticoagulation for Cerebral Venous Sinus Thrombosis after Posterior Fossa Schwannoma Surgery: Worth the Risk?

Christina Jackson¹, Pavan Shah¹, Laura Saleh¹, Gary Gallia¹, Chetan Bettegowda¹, Jon Weingart¹, Henry Brem¹, Rafael Tamargo¹, Michael Lim¹

¹Johns Hopkins School of Medicine, Baltimore, Maryland, United States

Background: Cerebral venous sinus thrombosis (CVST) is a rare complication after posterior fossa schwannoma surgeries. Previous reports on the development and management of postoperative CVST after posterior fossa schwannoma surgery are limited to case reports or by small sample sizes. Moreover, there is limited evidence that therapeutic anticoagulation (tAC) improves outcomes in this patient population. Therefore, we sought to characterize the risk of postoperative CVST in the largest series to date, and to compare post-thrombosis symptoms and radiographic improvement in patients who were treated with tAC and those who were not.

Methods: We conducted a retrospective review of patients who underwent resection for posterior fossa schwannomas at a tertiary care center between 2009 and 2019. MRIs were routinely obtained within 48-hours postoperatively, 3-months postoperatively, or as clinically indicated. We defined CTSV as radiographic evidence of filling defects within the sinus (Fig. 1). We compared clinical, radiographic, and intraoperative characteristics between patients who developed postoperative CVST and those who did not. We used logistic regression to identify risk factors associated with the development of postoperative CVST. Among patients who developed postoperative CVST, we further compared post-thrombosis symptoms, radiographic improvement, and bleeding complications between patients who received tAC and those who did not.

Results: We identified 646 patients who underwent resection for posterior fossa schwannomas, of which 44 (6.8%) patients developed postoperative CVST. There were no significant differences in clinical, radiographic, and intraoperative characteristics between patients who developed postoperative CVST and those who did not (Table 1). For example, mean tumor size (2.16 vs. 2.28 cm, $p = 0.48$), mean operating time (9.9 versus 9.5 hours, $p = 0.21$), surgical fluid balance (2.2L vs. 1.9, $p = 0.14$), and surgical approach (81.8% retrosigmoid vs. 88.2%, $p = 0.13$) were similar between groups. Among patients who developed postoperative CVST, 21 (47.7%) patients had medical risk factors for thrombosis (e.g. smoking, malignancies), and 37 (84.1%) patients were asymptomatic (Table 2). Patients who received tAC ($n = 9$) were largely similar to patients who did not ($n = 35$), with the exception that median time to diagnosis was significantly longer in those who received tAC (median 11 vs. 2 days, $p < 0.001$). Despite this, there were no significant differences in thrombosis-related complications and radiographic improvement of thrombosis at 6 months between the two groups. However, one patient (11.1%) who received tAC developed a clinically significant bleeding complication (epidural hematoma), which required a prolonged ICU stay.

Conclusion: In the largest series of CVST after posterior fossa schwannoma resection to date, postoperative CVST remains an uncommon complication (6.8%). However, we did not identify any predictors of postoperative CVST, making the identification of high-risk patients challenging. Nevertheless, we found that patients who did not receive tAC did not have lower rates of radiographic resolution of CVST nor were they more symptomatic from the CVST. In light of collateral drainage from the contralateral sinus system, the risk of clinically significant bleeding complications with tAC in the immediate postoperative setting, and the equivalent outcomes between patients who received tAC and those who did not, avoidance of tAC may be a reasonable management strategy for these patients.

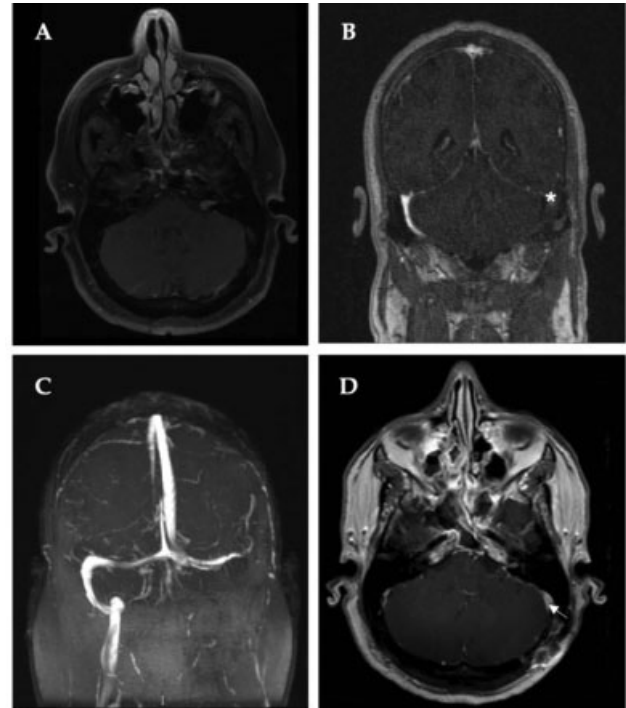


Figure 1. Middle aged patient who underwent uneventful retrosigmoid resection of left vestibular schwannoma (A) who was found to have filling defect (*) of the left transverse and sigmoid sinuses on routine postoperative imaging (B). (C) MRV demonstrated incidental left sigmoid and transverse sinus thrombosis. The patient was managed conservatively without anti-coagulation and (D) MRI at 6 months post-operatively demonstrated recanalization of the transverse and sigmoid sinuses with no neurological sequela (arrow).

Table 1. Characteristics of 646 patients who underwent surgical resection of posterior fossa schwannomas

Number of patients	No Thrombosis		Thrombosis		p Value
	n(%)		n(%)		
Sex					0.96
M	271 (45.1%)		20 (45.5%)		
F	330 (54.9%)		24 (54.5%)		
Age (yrs), mean (SD)	50.1 (12.9)		49.6 (10.7)		0.81
Preop KPS					0.49
50	4 (0.7%)		0 (0%)		
60	3 (0.5%)		0 (0%)		
70	21 (3.5%)		1 (2.3%)		
80	62 (10.3%)		1 (2.3%)		
90	506 (84.1%)		41 (93.2%)		
100	6 (1.0%)		1 (2.3%)		
Symptomatic	592 (96.7%)		43 (97.7%)		0.61
# of prior resection					0.49
0	583 (96.8%)		44 (100%)		
1	13 (2.2%)		0 (0%)		
2	6 (1.00%)		0 (0%)		
Dominant sinus					0.88
Right	123 (20.4%)		7 (15.9%)		
Left	31 (5.1%)		2 (4.5%)		
Side of Tumor					0.5
Right	292 (48.5%)		19 (43.2%)		
Left	310 (51.5%)		25 (56.8%)		
Tumor on the same side of non-dominant sinus	43 (27.9%)		3 (33.3%)		0.73
Petrosal sinus sacrificed	151 (63.7%)		7 (43.8%)		0.11
Surgical approach					0.13
Retrosigmoid	531 (88.2%)		36 (81.8%)		
Translabyrinthine	58 (9.6%)		8 (17.4%)		
Middle fossa	13 (2.2%)		-		
Steroid use preoperatively	74 (12.3%)		6 (13.6%)		0.8
Extent of resection					0.57
Gross total	485 (80.6%)		38 (84.1%)		
Subtotal	117 (19.4%)		7 (15.9%)		
Tumor size (cm), mean (SD)	2.28 (1.08)		2.16 (1.12)		0.48
Koos Grade					0.66
I	95 (15.8%)		9 (20.5%)		
II	155 (25.7%)		14 (31.8%)		
III	137 (22.8%)		9 (20.5%)		
IV	207 (34.4%)		12 (27.3%)		
BMI, mean (SD)	28.31 (6.04)		28.23 (7.87)		0.94
Surgical fluid balance (L), mean (SD)	1.9 (1.2)		2.2 (0.9)		0.14
Intraoperative mannitol use	402 (85.9%)		30 (93.8%)		0.71
Operative time (hr), mean (SD)	9.5 (2.1)		9.9 (1.4)		0.21
Pathology					0.98
Trigeminal	14 (2.3%)		0 (0%)		
Facial	4 (0.7%)		0 (0%)		
Vestibular	576 (95.7%)		44 (100%)		
Glossopharyngeal	2 (0.3%)		0 (0%)		
Vagus	5 (0.8%)		0 (0%)		
Hypoglossal	1 (0.2%)		0 (0%)		

Table 2. Characteristics of 44 patients who developed cerebral venous thrombosis post resection of posterior fossa schwannomas

Number of patients*	Anti-coagulated*		Not Anti-coagulated	
	n (%)		n (%)	
Age, mean (SD)	55.0 (7.7)		49.5 (11.4)	
Medical risk factors for thrombosis				
Smoking	3 (33.3%)		8 (22.9%)	
Hypercoagulable state	1 (11.1%)		0 (0%)	
Prior history of thrombosis	0 (0%)		0 (0%)	
Malignancy	0 (0%)		3 (8.5%)	
Hormonal therapy	1 (11.1%)		5 (14.3%)	
Post op day of thrombosis diagnosis, median (IQR)	11 (4-17)		2 (1-2)	
Location of thrombosis				
Transverse Sinus	0 (0%)		2 (5.7%)	
Sigmoid Sinus	1 (11.1%)		9 (25.7%)	
>1 Sinus				
T+S	3 (33.3%)		16 (45.7%)	
S+IJ	2 (22.2%)		2 (5.7%)	
T+S+IJ	2 (22.2%)		6 (17.1%)	
SSS+T*	1 (11.1%)		0 (0%)	
Thrombosis Symptom				
Symptomatic (headaches)	3 (33.3%)		3 (8.5%)	
Asymptomatic	6 (66.7%)		31 (88.6%)	
Treatment				
Unfractionated Heparin to Coumadin	5			
LMWH to Coumadin	1			
Aspirin	2			
Complications from treatment				
Hemorrhage	1 (11.1%)			
Thrombosis related complications at 6 months	0 (0%)		0 (0%)	
Thrombus status at 6 months				
Persistent	5 (55.6%)		5 (14.3%)	
Partially recanalized	2 (22.2%)		10 (28.5%)	
Resolved	2 (22.2%)		4 (11.4%)	

* 3 patients treated for concurrent PE/DVT/history of aortic valve replacement
 * 1 patient with previously coiled dural AVF, 1 patient with intra-operative injury to sigmoid sinus
 † 1 patient presented with multi-sinus thrombosis 2 years post-operatively, found to be hypercoagulable
 IQR=interquartile range; LMWH=low molecular weight heparin; T=transverse Sinus; S=sigmoid sinus; IJ=internal jugular vein; SSS=superior sagittal sinus

A080. Comprehensive Approach to Treatment of Pediatric Skull Base Lesions: A Case Series

Craig Miller¹, Alizabeth Weber¹, Kate Carroll¹, Neeraja Konuthula¹, Abdullah Feroze¹, Jacob Ruzevick¹, Manuel Ferreira¹, Kris S. Moe¹, Randall A. Bly¹

¹University of Washington, Seattle, Washington, United States

Objective: The use of endoscopic or combined endoscopic and open approaches to pediatric skull base tumors and CSF leaks is a relatively recent advancement. An endoscopic approach, either alone or in conjunction with traditional craniotomy, can provide less disruptive and more efficacious treatment than craniotomy alone, especially in children. Additionally, current advances in endoscopic approaches have allowed for increased access through additional anatomical portals including transorbital neuroendoscopic surgery, paramaxillary, and other described pathways. The authors present their institutional experience with all noninflammatory skull base pathology, including trauma, treated endoscopically, or via combined endoscopic and open approach in a pediatric population.

Methods: The authors retrospectively reviewed pediatric patients (age ≤18 years) who had undergone treatment of skull base pathology via an endoscopic or combined endoscopic and open approach, including transorbital, between 2006 and 2019.

Results: This series included 57 unique patients who underwent 67 operations between the age of 1 and 18 years old (average age 12.1 years). Patients were treated for a variety of pathology including trauma/CSF leak (n = 27, 38.5%), followed by skull base tumor, including juvenile angiofibroma and chordoma (n = 21, 29.6%), craniopharyngioma (n = 10, 14.1%), pituitary adenoma (n = 9, 12.7%), and encephalocele (n = 4, 5.6%). Of the cases that employed an

endoscopic approach, 23 (34%) utilized a transorbital approach for access, whereas 57 (85%) used either an endonasal alone or an endonasal combined with nontransorbital approach. Nasoseptal flaps were used in 27% ($n = 18$) of cases, fat grafts in 13% ($n = 9$), and lumbar drains in 24% ($n = 16$). For patients with nontraumatic pathology, median length of hospital stay was 3 days (range, 1–43 days). Patients were followed for a median of 23 months (range, 0–1,091 months), with mean radiological follow-up of 18 months (range, 0–108 months). Postoperative CSF leak occurred in eight patients (14%). Favorable outcomes of surgery were sustained during the follow-up period with low rate of revision surgery (7%). Complication rate beyond CSF leaks was low with four patients (7%) suffering some other complication including bitemporal hemianopsia due to packing from leak closure impinging on the optic chiasm ($n = 1$), hardware infection ($n = 1$), and meningitis ($n = 2$).

Conclusion: In this single-institution report of endoscopic or combined endoscopic and open approach to pediatric skull base pathology, we demonstrate safety and effectiveness of treatment. Broad conclusions are challenging to make from this heterogeneous patient population. Of note, this is the first major review of pediatric transorbital series in the literature. Overall favorable effects of surgery were sustained during the follow-up period. Further refinement of technology and training will allow for more widespread use of these techniques in the pediatric population. Long-term craniofacial and radiologic outcomes are needed to further validate this method of approach.

A081. Reconstruction of Pediatric Skull Base Defects: A Retrospective Analysis Emphasizing the Very Young

Nyall London¹, Gustavo G. Rangel², Amanda Onwuka³, Ricardo L. Carrau², Daniel Prevedello², Jeffrey Leonard², Patrick Walz³

¹Johns Hopkins University/NIDCD, Baltimore, Maryland, United States

²The Ohio State University, Columbus, Ohio, United States

³Nationwide Children's, Columbus, Ohio, United States

Background: Pathology of the pediatric skull base is rare and ranges from congenital defects to malignancy and traumatic defects. Pediatric patients, particularly those ≤ 6 years of age, present a unique set of anatomical challenges for the skull base surgeon. The goal of this study was to retrospectively review our experience with reconstruction of pediatric skull base defects with particular emphasis on those ≤ 6 years of age.

Methods: A retrospective chart review was conducted of patients ≤ 20 years of age who underwent endoscopic endonasal and combined endoscopic and open approaches to address cranial base pathology from 2007 to 2018. Fifty-five patients were identified and charts were reviewed with particular attention paid to reconstructive techniques utilized, postoperative outcomes, and complications.

Results: Intraoperative CSF leak was noted in 50% (3/6) of the patients ≤ 6 years of age compared with 32.7% (16/49) in patients > 6 years of age and ≤ 20 years of age ($p < 0.40$). A vascularized flap was utilized for reconstruction in 66.7% (4/6) of the patients ≤ 6 years of age and most commonly included a nasoseptal flap in 33.3% (2/6). A vascularized flap was utilized for reconstruction in 38.8% (19/49) of the patients > 6 years of age and ≤ 20 years of age and most commonly included a nasoseptal flap (22.4%, 11/49; $p < 0.50$). Absorbable packing was utilized to support the reconstruction in 83.3% (five of six) patients ≤ 6 years of age and 79.6% (39/49) patients > 6 years of age and ≤ 20 years of age. Merocele nonabsorbable packing was used in 50% (three of six) of the patients ≤ 6 years of age. Nonabsorbable packing was utilized in 44.9% (22/49) of the patients > 6 and ≤ 20 years

of age and included merocele (30.6%, 15/49) or Foley's catheter (12.2%, 6/49; $p < 0.68$). A lumbar drain was utilized in 50% (three of six) of the patients ≤ 6 years of age compared with 18.4% (9/49) in patients > 6 and ≤ 20 years of age ($p < 0.08$). Postoperative CSF leak was found in 16.7% (one of six) of patients ≤ 6 years of age compared with 10.2% (5/49) in patients > 6 and ≤ 20 years of age ($p < 0.63$). Behavioral issues were noted to contribute to failed skull base reconstruction in patients < 6 years of age. There were no cases of new cranial nerve injury in patients ≤ 6 years of age and two instances in patients > 6 years of age and ≤ 20 years of age ($p < 0.65$). A similar rate of persistent or recurrent disease was noted between both groups ($p < 0.39$ and 0.98 , respectively). The median length of stay was 7.5 days in patients ≤ 6 years of age and 4.0 days in patients > 6 and ≤ 20 years of age ($p < 0.44$).

Conclusion: Pediatric patients, particularly those ≤ 6 years of age, present a unique set of anatomical and behavioral challenges for the skull base surgeon as highlighted in this study.

A082. Effects of Preoperative Vascular Embolization on Juvenile Nasopharyngeal Angiofibroma Surgical Outcomes: A Study of the Kids' Inpatient Database

Jonathan Choi¹, Justin Yu¹, Benjamin Lovin¹, K. Kelly Gallagher¹

¹Baylor College of Medicine, Houston, Texas, United States

Objectives: The aim is to evaluate the effect of preoperative vascular embolization (PVE) on juvenile nasopharyngeal angiofibroma (JNA) surgical outcomes using a national pediatric hospitalization database.

Methods: The Healthcare Cost and Utilization Project (HCUP) Kids' Inpatient Database was queried for all cases of JNA operative management between the years of 1997 and 2016. Cases were stratified based on whether the patient received preoperative vascular embolization. A multiple linear regression (MLR) was used to predict the effect of embolization on hospital length of stay (LOS) and total cost while controlling for patient demographic factors and comorbidities. The odds ratio (OR) of receiving a perioperative blood transfusion was computed using a binary logistic regression (BLR) for PVE patients.

Results: A total of 473 patients were identified who underwent JNA surgical resection in this time period. The use of PVE has increased from 0% in 1997 and 2000 to 66% of all cases by 2016. PVE was found to decrease LOS by 1 day ($p = 0.036$) and decrease the odds of needing a perioperative blood transfusion (OR = 0.511, $p = 0.041$). Patients receiving vascular embolization were charged an additional \$35,600 ($p < 0.001$), but recent data in 2016 indicate that hospital costs for PVE are decreasing.

Conclusion: PVE is becoming increasingly prevalent in JNA surgical management. Embolization results in decreased hospital LOS and a lower odds of needing blood transfusions. While embolization increases the cost of admission, this trend should be re-evaluated as this procedure become more widespread.

A083. Pediatric Trauma Patients with Temporal Bone Fractures Are at Risk for Multiple Cranial CT Scans

Joshua Ewy¹, Martin Piazza¹, Brian Thorp¹, Michael Phillips¹, Carolyn Quinsey¹

¹UNC School of Medicine, Chapel Hill, North Carolina, United States

Background: High energy traumatic brain injury (TBI) patients suspected of having a fracture often receive a significant amount of radiation in diagnostic imaging studies. Computed tomography of the head (CT-H) is a widely

accepted tool for initial radiographic evaluation of traumatic brain injury (TBI); however, patients with suspected temporal bone fracture (TBF) often undergo additional scans of the maxillofacial bones (CT-MF) and of the temporal bones (CT-TB) to better characterize skull base injuries that may put the patient at risk for cranial nerve injuries and hearing loss. CT-TB is commonly performed on adult TBF patients; however, it has been found that this scan is largely unnecessary for adequate injury evaluation and treatment. No such studies have been performed in the pediatric population. With the well-documented increase risk of malignancy linked to excess CT usage amongst pediatric patients, we aim to characterize temporal bone injuries and imaging in children and identify over-use of ionizing imaging in this population.

Methods: After institutional IRB approval a retrospective review of all pediatric trauma patients (<18 y) with diagnosed skull fracture from a 10-year period, data on patient demographics, mechanism of injury, initial physical exam, imaging, and complications, were compiled into a database.

Results: A total of 412 patients were identified who met inclusion criteria for the study. TBFs accounted for 108 (26.21%) patients while the remaining 304 (73.79%) patients were diagnosed with a non-TBF skull fractures. The most common mechanism of injury for TBF was motor vehicle collision (27.78%) followed by fall (25.00%) and bike/scooter/skateboard accident (19.44%). Presenting signs of TBF included hemotympanum (41.67%), blood otorrhea (25.00%), and hearing loss (25.00%). In association with TBF, complications included facial nerve injury (FNI) (6.48%), CSF leak (8.33%), permanent hearing loss (15.74%), and arterial dissection (0.93%). Imaging performed on all skull fracture patients yielded 31 (28.70%) patients with a TBF received CT-H, CT-MF, and CT-TB while only 3 (0.99%) patients with a nontemporal skull fracture received similar scanning. Of patients with TBF, CT imaging changed clinical management in 34 (31.48%) patients, of which 7 (6.48%) received treatment for FNI and 29 (26.85%) received vascular imaging of the head/neck. Dedicated CT-TB changed clinical management in 11 (10.19%) patients, of which 1 (0.93%) patient received treatment for FNI and 10 (9.26%) patients received vascular imaging of the head/neck.

Conclusion: These data demonstrate nearly 30% of children with temporal bone fracture, underwent three complete separate cranial CT scans including high resolution imaging. Additionally, most temporal bone fractures in children do not result in hearing loss, facial nerve injury, vascular injury, nor CSF leak. This suggests that, for children whose fracture is well characterized on CT-H or CT-MF, additional ionizing high resolution imaging such as CT-TB does not significantly change clinical management and should be obtained thoughtfully as to minimize radiation exposure in diagnostic work-up.

A084. Simulation of Pediatric Anterior Skull Base Anatomy Using a 3D Printed Model

Nyall London¹, Gustavo G. Rangel², Kyle VanKoeveering³, Ashley Zhang³, Allison Powell³, Daniel Prevedello², Ricardo L. Carrau², Patrick Walz⁴

¹Johns Hopkins University/NIDCD, Baltimore, Maryland, United States

²The Ohio State University, Columbus, Ohio, United States

³University of Michigan, Ann Arbor, Michigan, United States

⁴Nationwide Children's, Columbus, Ohio, United States

Background: The pediatric skull base may present anatomical challenges to the skull base surgeon including limited sphenoid pneumatization and a narrow nasal corri-

dor. The rare nature of pediatric skull base pathology makes it difficult to gain experience with these anatomical challenges.

Objective: The objective of this study was to create a 3D printed model of the pediatric skull base and assess its potential as a training tool.

Methods: Twenty one participants at various stages of training and practice were included in our study. They were asked to complete a predissection questionnaire assessing anticipated challenges followed by endoscopic endonasal skeletonization of the carotid arteries and sella face using the 3D printed model (Figs. 1, 2). Each participant was given a new, identical 3D printed model for individual drilling. After completion, participants completed a postdissection questionnaire assessing challenges faced.

Results: The majority of participants had completed a skull base surgery fellowship (71.4%), were <5 years into practice (61.9%), and had <10 cases of pediatric skull base experience (80.1%) (Table 1). Frequent challenges anticipated by the participants included limitation of maneuverability of instruments (76.2%), narrow nasal corridor (66.7%), and non-pneumatized bone (61.9%). On a scale of 0 to 10, 10 being very difficult, the average participant expected level of difficulty with visualization was 7.1 ± 1.73 (range, 5–10) and expected level of difficulty with instrumentation was 7.5 ± 1.94 (range, 5–10). On postdissection assessment, there was a nonstatistically significant increase to 7.3 ± 2.1 (range, 3–10) with experienced level of difficulty with visualization and 8.0 ± 2.06 (range, 3–10) with experienced level of difficulty with instrumentation, respectively. Participants endorsed on a scale of 0 to 10, 10 being very realistic, an overall model realism of 7.0 ± 1.86 (range, 3–10) and haptic realism of 7.1 ± 1.96 (range, 3–10).

Conclusion: A 3D printed model of the pediatric skull base may provide a realistic model to help participants gain experience with anatomical limitations characteristic of the pediatric anterior skull base.

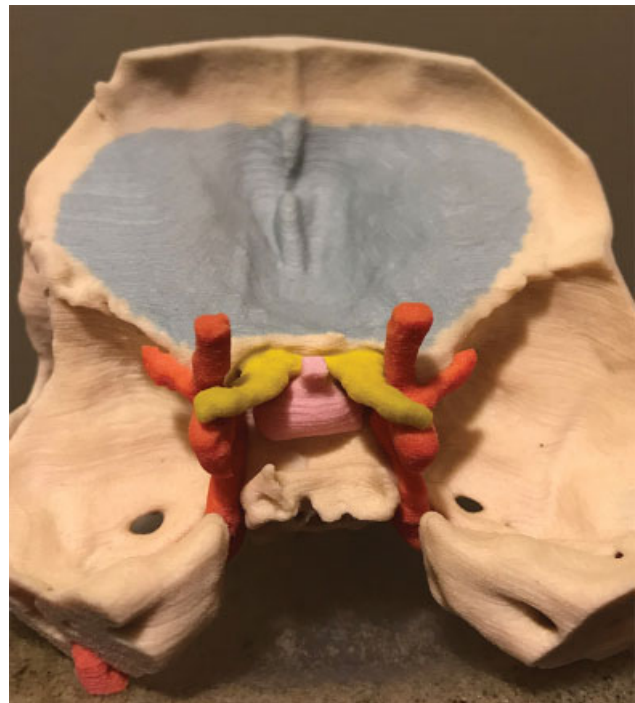


Fig. 1 Posterior view of 3D printed pediatric skull base model. Red, carotid arteries; yellow, optic nerves; pink, pituitary gland; gray, anterior skull base.

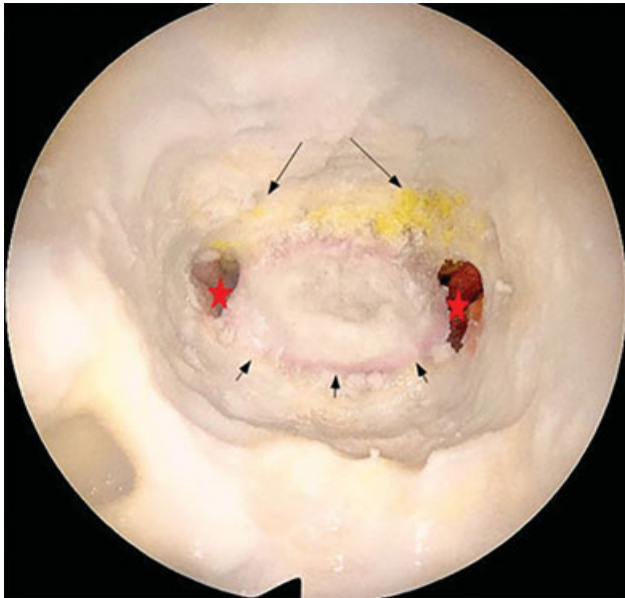


Fig. 2 Endonasal view after drilling. Red stars, carotid arteries; long arrows, optic nerves; short arrows, pituitary gland.

Table 1. Study participant demographics

Participant age	
18-35	10 (47.6%)
36-45	7 (33.3%)
46-55	2 (9.5%)
>56	2 (9.5%)
Specialty	
Otolaryngology	7 (33.3%)
Neurosurgery	13 (61.9%)
Not specified	1 (4.8%)
Highest level of training completed	
Medical school	1 (4.8%)
Residency	5 (23.8%)
Fellowship	15 (71.4%)
Completion of a skull base fellowship	
Yes	15 (71.4%)
No	6 (28.6%)
Years in practice	
<5	13 (61.9%)
5-10	4 (19.0%)
10-15	2 (9.5%)
>15	2 (9.5%)
% of skull base surgery in your practice	
<10%	12 (57.1%)
10-50%	7 (33.3%)
51-75%	1 (4.8%)
>75%	1 (4.8%)
% of pediatric patients in your practice	
<10%	15 (71.4%)
10-50%	4 (19.0%)
51-75%	0 (0%)
>75%	2 (9.5%)
Experience with pediatric skull base surgery	
<10 cases	17 (80.1%)
11-50	4 (19.0%)
51-100	0 (0%)
>100	0 (0%)

A085. Multi-institutional Experience with Pediatric Olfactory Neuroblastoma

Nadeem R. Kolia¹, Shirley Y. Su², Ehab Y. Hanna², Uma S. Ramaswamy³, Eric W. Wang¹, Paul A. Gardner¹, Carl H. Snyderman¹

¹University of Pittsburgh Medical Center, Pittsburgh, Pennsylvania, United States

²The University of Texas MD Anderson Cancer Center, Houston, Texas, United States

³Texas Children's Hospital, Houston, Texas, United States

Background: Olfactory neuroblastoma is a rare malignancy arising from the olfactory epithelium. In adults, surgical resection followed by adjuvant radiation therapy is considered the standard of care. However, there is no established standard of care for pediatric olfactory neuroblastoma.

Objectives: The aim of the study is to review the current literature on pediatric olfactory neuroblastoma and report on the combined experience of treating this disease entity at three different institutions.

Methods: A retrospective multi-institutional review of patients diagnosed with olfactory neuroblastoma between 1995 and 2018 with an age at diagnosis less than 21 years old.

Results: Fifteen patients were identified with a mean age at diagnosis of 14.2 years old. Nine of the patients had dual modality treatment, while five had triple modality therapy. Of the patients treated with dual modality therapy, seven had surgery plus either chemotherapy or radiation therapy, while two patients were treated with chemoradiation therapy. Average follow-up duration was approximately 31 months. Thirteen patients were alive at last follow-up, 10 of whom were with no evidence of disease. Review of the medical literature suggests that pediatric olfactory neuroblastoma may be more advanced at presentation and responds well to neoadjuvant chemotherapy.

Conclusion: Our findings suggest that multimodality therapy is effective in the treatment of pediatric olfactory neuroblastoma. These results are encouraging, but further investigation is needed to determine the optimum treatment strategy.

A086. Pediatric Pituitary Surgery: Claims-Based Analysis of Practice Patterns and Clinical Outcomes

Vijay A. Patel¹, Eric W. Schaefer¹, Brad E. Zacharia¹, Neerav Goyal¹, Chan Shen¹, Meghan N. Wilson¹

¹Penn State Health Milton S. Hershey Medical Center, Hershey, Pennsylvania, United States

Objectives: The aim of the study is to investigate variations in practice patterns and clinical outcomes for pediatric pituitary surgery from a national perspective.

Study Design: Retrospective analysis of the Truven Health Analytics MarketScan Research Database.

Subjects and Methods: The MarketScan Research Database in years 2005 to 2016 was queried to identify children <18 years of age who had pituitary surgery. Operative intervention was identified using Current Procedural Terminology (CPT) code 61546 (craniotomy for hypophysectomy or excision or pituitary tumor, intracranial approach), 61548 (hypophysectomy or excision of pituitary tumor, transnasal or transseptal approach, no stereotactic), and 62165 (neuroendoscopy, intracranial; with excision of pituitary tumor, trans nasal or transphenoidal approach) via inpatient and outpatient claims. Pediatric patients were required to be continuously enrolled in a private insurance plan from 3 months prior to definitive surgery to 6 months after discharge from surgery and have an International Classification of Diseases Ninth Revision (ICD-9) or Tenth Revision (ICD-10) diagnosis code of 227.3 (ICD-9) or D35.2 (ICD-10), indicating "benign neoplasm of pituitary gland." Statistical analysis focused on patient characteristics, procedure type, practice setting, and clinical outcomes.

Results: A total of 268 patients were identified, with a mean age of 15.2 years (median, 16 years; range, 3–18 years) at time of surgery and female predominance (63.1%). Most pediatric pituitary surgeries occurred in the inpatient setting (95.1%). For the time frame examined, pediatric pituitary surgeries occurred with microscopic assistance (59.0%), followed by endoscopic approaches (35.1%), combined endoscopic and microscopic assistance (4.5%) and open (1.5%) techniques. The majority of procedures were performed without the use of intraoperative image guidance (72.8%). The median length of stay was 3 days (interquartile range, 2–5 days), with the vast majority of children (97.9%) discharged to home or self-care.

Conclusion: This nationwide database study is the largest to-date demonstrating practice patterns and clinical outcomes in the area of pediatric pituitary surgery. Pediatric

pituitary resection through microscopic and endoscopic approaches in the inpatient setting continues to remain the predominant surgical technique employed in the United States.

A087. Applications of the Endoscopic Endonasal Approach in Early Childhood

Michael M. McDowell¹, Georgios Zenonos¹, Eric Wang¹, Carl Snyderman¹, Elizabeth Tyler-Kabara¹, Paul A. Gardner¹

¹Neurosurgery Institute Dr. Alfonso Asenjo

Introduction: Endoscopic endonasal surgery (EES) has been slower to gain popularity in early childhood due to multiple concerns such as a smaller nasal aperture, poor sinus pneumatization, tighter anatomical intracranial corridors, and reconstructive challenges.

Methods: All patients up to age six who underwent EES at a large Cranial Base Center from 2002 to 2019 were retrospectively reviewed. Demographic information, pathology, operative characteristics, complications, radiographic outcomes, and long-term outcomes were assessed.

Results: Thirty-six patients underwent EES before age seven. Four patients had two-stage EES. Two patients required combined cranial and endonasal approaches. Mean age at the time of initial surgery was 4 years (range: 1–6). Twenty patients were male and 16 were female. There were ten different pathologies, of which encephaloceles/traumatic CSF leak (12), craniopharyngioma (11), dermoid tumor (3), chordoma (3), and rhabdomyosarcoma (2) were most common. Of 21 tumors intended for resection, 11 patients had gross total resections and 10 had near total (>95%) resections. Nine patients had recurrences, of which six were craniopharyngiomas ($p = 0.01$). One chordoma patient and one rhabdomyosarcoma patient died from tumor recurrence during follow-up. There was no difference in recurrence rates based on degree of resection ($p = 0.67$). For craniopharyngiomas, two of five gross total resections recurred and four of six near total resections recurred ($p = 0.57$). Five patients underwent repeat EES for tumor recurrences; two craniopharyngiomas, one chordoma, and one rhabdomyosarcoma. Four craniopharyngiomas and one rhabdomyosarcoma had gamma knife radiosurgery for recurrence. Sixteen patients had unilateral nasoseptal flaps raised. Two patients had vascularized flaps elevated from other sources (one temporalis and one rhinopharyngeal). Eight patients had free mucosal grafts. Ten patients had lumbar drains placed, one had an external ventricular drain, and four patients had shunts placed prior to EES. Three cerebrospinal fluid (CSF) leaks occurred following primary EES (8% rate) and one occurred following surgery for recurrence. All CSF leaks were managed with revision surgery. Following an increase in nasoseptal flap usage (31–52%) and CSF diversion (15–39%) in 2008, there was only one CSF leak out of 23 patients (4 vs. 15%; $p = 0.54$). There was only one permanent new cranial neuropathy (rhabdomyosarcoma developed a partial third nerve palsy after a second surgery for recurrence). One craniopharyngioma patient developed a permanent field cut postoperatively. Six patients developed permanent postoperative panhypopituitarism, of which all were craniopharyngiomas ($p < 0.001$). The other craniopharyngioma patients had preoperative panhypopituitarism. One patient required an emergent craniotomy for an epidural hematoma due to a pin site skull fracture. No major vascular injuries occurred. There were no operative mortalities. Mean follow-up was 64 months.

Conclusion: EES can be performed safely under the age of 7 for a variety of skull base pathologies. Nasoseptal flaps are technically feasible and may reduce CSF leak rates. Craniopharyngioma remains a challenging subgroup frequently

requiring multiple interventions for tumor control, but patients in this group have competitive outcomes in comparison to adults and superior rates of >95% resection compared with adult data previously published from our center.

A088. Risk of Internal Carotid Artery Stenosis or Occlusion after Single-Fraction Radiosurgery of Benign Parasellar Tumors

Christopher S. Graffeo¹, Michael J. Link¹, Scott L. Stafford¹, Ian F. Parney¹, Robert L. Foote¹, Bruce E. Pollock¹

¹Mayo Clinic, Rochester, Minnesota, United States

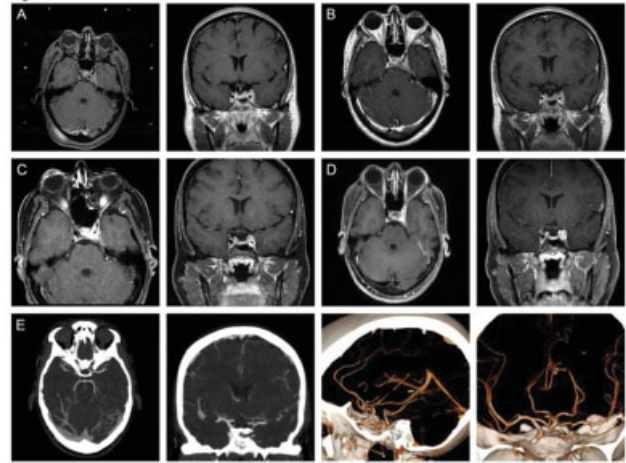
Introduction: Stereotactic radiosurgery (SRS) is an accepted treatment option for patients with benign parasellar tumors. Our objective was to determine the risk of developing new or progressive internal carotid artery (ICA) stenosis/occlusion after single-fraction SRS of cavernous sinus meningiomas (CSM) or growth-hormone secreting pituitary adenomas (GHA).

Methods: Retrospective review of 283 patients (155 CSM/128 GHA) treated with single-fraction SRS, 1990 to 2015. Study criteria included no prior irradiation and ≥ 12 months of post-SRS radiologic follow-up. Pre-SRS grading of ICA involvement was as described by Hirsch (1993) for CSM or Knosp's (1993) for GHA. Ninety-three (60%) CSM had Hirsch's grade II and III tumors; 97 (76%) GHA had Knosp's grade II to IV tumors.

Results: Median follow-up after SRS was 6.6 years (range, 1–24.9). No GHA or grade I CSM developed ICA stenosis/occlusion. Three grade II CSMs (5.2%) had asymptomatic ICA stenosis ($n = 2$) or occlusion ($n = 1$); 1 (1.1%) had transient ischemic symptoms. Five grade III CSM (14.3%) progressed to ICA occlusion (4 asymptomatic, 1 symptomatic). Median time to stenosis/occlusion was 4.8 years (range, 1.8–7.6). Five- and 10-year risks of ICA stenosis/occlusion in grade II/III CSM were 7.5 and 12.4%. Five- and 10-year risk of ischemic stroke from ICA stenosis/occlusion in grade II/III CSM was 1.2%. Multivariable analysis found patient age (HR = 0.92; 95% CI 0.86–0.98; $p = 0.01$), meningioma pathology (HR, 95% CI not defined; $p = 0.03$), and carotid grade (HR = 4.51; 95% CI = 1.77–14.61; $p = 0.004$) to be associated with ICA stenosis/occlusion. ICA stenosis/occlusion was not related to post-SRS tumor growth (HR, 95% CI not defined; $p = 0.41$).

Conclusion: New or progressive ICA stenosis/occlusion was common after SRS for CSM but was not observed after SRS for GHA, suggesting a tumor-specific mechanism not related to radiation dose. Pre-SRS ICA encasement/constriction increases the risk of ICA stenosis/occlusion, however, the risk of ischemic complications is very low.

Figure 1



A089. Biological Effective Dose as a Predictor of Hypopituitarism after Single-Fraction Pituitary Adenoma Radiosurgery: Dosimetric Analysis Cohort Study of Patients Treated Using Contemporary Techniques

Christopher S. Graffeo¹, Avital Perry¹, Michael J. Link¹, Paul D. Brown¹, William F. Young¹, Bruce E. Pollock¹

¹Mayo Clinic, Rochester, Minnesota, United States

Background: Stereotactic radiosurgery (SRS) is a safe and effective adjuvant treatment for pituitary adenoma. Hypopituitarism is the most frequent complication after pituitary adenoma SRS, yet clinical and dosimetric factors predicting post-treatment hypopituitarism remain incompletely understood. Biological effective dose (BED) is a dosimetric parameter that incorporates a time component, to adjust for mechanisms of DNA repair activated by neoplasms during the treatment itself, potentially resulting in differential efficacy between patients treated at the same prescription dose over varying treatment times.

Methods: Cohort study of 97 patients having single-fraction SRS from 2007 until 2017. Eligible patients had no history of prior radiation, normal age- and gender-specific pituitary function before SRS, and at least 24 months of endocrine follow-up. Forty patients (41%) had hormone secreting tumors; 57 patients had nonsecreting tumors (59%). The median prescription isodose volume was 2.8 cm³ (IQR, 1.3–4.7); the median tumor margin dose was 20 Gy (IQR, 15–25). BED was assessed as a predictor of new post-SRS hypopituitarism using Cox proportional hazards.

Results: Median post-SRS follow-up was 48 months (IQR, 34–68), during which time 27 patients (28%) developed new hypopituitarism at a median 22 months (IQR, 12–36). Actuarial rates of new endocrinopathy were 17% at 2 years (95% CI: 10–25%) and 31% at 5 years (95% CI: 20–42%). On univariate analysis, sex ($p = 0.01$), gland volume ($p = 0.03$), mean gland dose ($p < 0.0001$), and BED significantly predicted new hypopituitarism ($p < 0.0001$). Receiver operating characteristic (ROC) curve analysis identified optimal cut-points for BED and mean gland dose of 45Gy2.75 and 10 Gy, respectively. After adjusting for sex and gland volume, BED > 45Gy2.75 was associated with a 16-fold increase in risk of hypopituitarism, as compared with glands exposed to BED $\leq 45Gy2.75$. ($p = 0.0002$, AICc = 196.06). Similarly, mean gland dose > 10 Gy was associated with a 14-fold increase in risk of hypopituitarism, as compared with glands exposed

to ≤ 10 Gy, adjusting for sex and gland volume ($p < 0.0003$, AICc = 199.67).

Conclusion: Hypopituitarism following pituitary adenoma SRS is a function of dose, time, sex, and gland-specific parameters. BED appears to predict new post-SRS hypopituitarism more reliably than radiation dose, but confirmatory study is needed. Reduction of gland BED is anticipated to decrease the incidence of post-SRS hypopituitarism.

A091. A Phase I/II Clinical Trial of Proton Therapy for Chordomas and Chondrosarcomas

Alexandra D. Dreyfuss¹, Michael J. LaRiviere¹, Jahan J. Mohiuddin¹, Brian C. Baumann², David M. Miller¹, Susan Mazzone¹, Robert A. Lustig¹, Jay F. Dorsey¹, Alexander Lin¹, Sean M. Grady³, Bert W. O'Malley⁴, John Y. Lee³, Jason G. Newman⁴, James M. Schuster³, Michelle Alonso-Basanta¹

¹Department of Radiation Oncology, Perelman School of Medicine, University of Pennsylvania, Philadelphia, Pennsylvania, United States

²Department of Radiation Oncology, Washington University School of Medicine, St. Louis, Missouri, United States

³Department of Neurosurgery, Perelman School of Medicine, University of Pennsylvania, Philadelphia, Pennsylvania, United States

⁴Department of Otorhinolaryngology—Head and Neck Surgery, Perelman School of Medicine, University of Pennsylvania, Philadelphia, Pennsylvania, United States

Background/Objectives: Radiation therapy (RT) for chordomas and chondrosarcomas typically requires doses >70 Gy for optimal local tumor control. Proton therapy may afford safer dose escalation to the tumor; however, prospective data on outcomes and toxicity are lacking. Here we report results from a prospective clinical trial of proton beam radiation for the treatment of chordomas and chondrosarcomas.

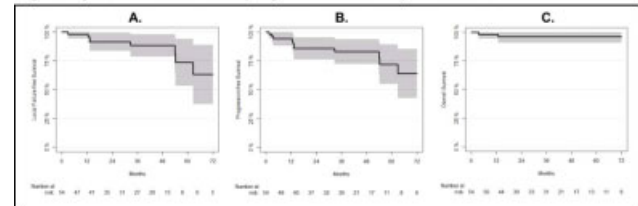
Materials/Methods: Fifty-five adult patients with pathologically confirmed, nonmetastatic chordoma or chondrosarcoma with an ECOG score ≤ 2 were enrolled in a single-institution prospective trial of proton therapy from 2010 to 2018. Forty-seven patients received adjuvant RT, five received definitive RT, one received neoadjuvant RT, and one received RT for recurrence; one patient enrolled did not receive RT and was excluded from toxicity and survival analyses. Median dose was 78.3 Gy (cobalt Gray equivalent [CGE]; range, 50.4–79.2 Gy [CGE]) using protons only ($n = 21$), combination protons/IMRT ($n = 33$) with double-scatter or pencil beam scanning techniques, or IMRT only ($n = 2$). Patients were followed with MRI or CT at 3-month intervals. The primary end points were feasibility and $\leq 20\%$ rate of unexpected acute grade ≥ 3 toxicity. Secondary end points included cancer-specific outcomes and other toxicities which were scored using CTCAEv4.0. Kaplan–Meier analysis was used to estimate local control, progression-free survival, and overall survival with respect to the date of RT completion. Local control was defined by most recent imaging; progression-free and overall survival were defined by most recent follow-up (Fig. 1).

Results: Of the 55 patients (22, male; 33, female) with a median age of 54, 26 had skull base chordomas, 11 had sacral chordomas, 6 had spinal chordomas, 9 had base of skull chondrosarcomas, 1 had sacral chondrosarcoma, and 2 had sinonasal chondrosarcomas. Positive margins or gross disease was noted in 67% of the patients at the time of RT. Median follow-up was 41.2 months, with 51/54 (96%) patients alive at last follow-up. Feasibility end points were met, with only 3/55 (5.5%) patient RT plans failing to meet dosimetric constraints with protons and 4/54 (7.4%) experiencing a delay or treatment break >5 days. Two patients developed distant disease, one with a metastasis

in the craniospinal axis, and one with a biopsy-confirmed inguinal lymph node metastasis. Three-year local recurrence-free, progression-free, and overall survival were 88.4% (95% confidence intervals 78.6–98.2%), 83.2% (72.4–94.0%), and 96.0% (90.6–100%), respectively. Among the 3/54 patients who died, one died 3.5 months after completing RT; however, her death was not definitively attributed to treatment. No grade 4 to 5 toxicities were reported. One grade 3 acute toxicity (sensory neuropathy) was recorded. The only two grade 3 late toxicities recorded, osteoradionecrosis and intranasal carotid blowout, occurred in a single patient.

Conclusion: We report favorable feasibility, local tumor control, survival, and toxicity following high-dose proton therapy for chordomas and chondrosarcomas.

Figure 1. A) Local Failure-free Survival. B) Progression-free Survival. C) Overall Survival



A092. Outcomes with IMRT versus SRS Salvage Radiotherapy for Recurrent High-Grade Meningioma

Arbaz Momin¹, Pranay Soni², Jianning Shao¹, Diana Lopez¹, Patrick Elsworth³, Konrad Knusel³, Pablo F. Recinos⁴, Varun R. Kshetry⁴

¹Lerner College of Medicine, Cleveland Clinic, Cleveland, Ohio, United States

²Department of Neurosurgery, Cleveland Clinic, Cleveland, Ohio, United States

³Case Western Reserve School of Medicine, Cleveland, Ohio, United States

⁴Rose Ella Burkhardt Brain Tumor and Neuro-Oncology Center, Cleveland Clinic, Cleveland, Ohio, United States

Introduction: The standard treatment for accessible World Health Organization (WHO) grade II and III meningiomas is surgical resection. Unfortunately, even after gross-total resection, recurrence rates in high-grade (HG) meningiomas can range from 9 to 32%. Intensity-modulated radiotherapy (IMRT) and stereotactic radiosurgery (SRS) are mainstay therapeutic modalities used to treat recurrent high-grade meningioma after surgical resection. The role of radiotherapy (RT) modality, in particular IMRT versus SRS, on survival outcomes in patients with recurrent high-grade meningiomas is not well-established. In the present study, we compare progression-free survival in patients undergoing salvage IMRT and SRS for recurrent HG meningiomas.

Methods: A retrospective review was performed to identify all patients undergoing radiotherapy for recurrent WHO grade II and III meningiomas between 1996 and 2019 at our institution. Patients for whom adequate treatment data was unavailable or who had not previously undergone surgical resection were excluded. Predictors of survival were analyzed using multivariate Cox proportional hazards model. Kaplan–Meier survival analysis was used to assess progression-free survival in IMRT and SRS treatment groups. A p -value of <0.05 was considered statistically significant (Tables 1 and 2).

Results: A total of 67 cases were identified and included in the study. The median radiation doses for IMRT and SRS were 59.4 Gy (range, 16–60 Gy) and 15 Gy (range, 12–30 Gy),

respectively. Two patients received fractionated SRS (25 Gy/5 fx and 30 Gy/5 fx). Median IMRT fractions were 30.5 fractions (26–33 fractions). There was no significant difference in tumor location and previous brain radiation therapy between SRS and IMRT ($p = 0.44$, $p = 1$). In a multivariate Cox's regression model, age at radiation (HR = 1.19, $p < .001$) and male sex (HR = 20.32, $p = 0.008$) were found to be independent predictors of mortality. Kaplan–Meier survival analysis and Cox's proportional hazards model found no significant difference in progression-free survival between patients treated with SRS versus IMRT for recurrent HG meningiomas (HR = 1.06; 0.47–2.41; **Fig. 1**).

Conclusion: Our study suggests that irrespective of tumor location, there is no significant difference in progression-free survival between SRS and IMRT in patients undergoing salvage radiotherapy for recurrent high-grade meningiomas.

Table 1 Demographic of IMRT and SRS treatment groups

Baseline demographics			
	IMRT	SRS	<i>p</i> -Value
<i>n</i>	19	48	
Age (SD)	62.6 (15.65)	60.1 (10.43)	0.446
Baseline KPS (SD)	85.00 (9.72)	87.18 (8.87)	0.5
Male (%)	10 (52.6)	19 (39.6)	0.485
Caucasian (%)	16 (84.2)	35 (72.9)	0.51
African American (%)	3 (15.8)	13 (27.1)	0.51

Table 2 Parameters of IMRT and SRS treatment groups

Tumor and treatment parameters			
	IMRT	SRS	<i>p</i> -Value
WHO grade II	19 (100)	43 (89.6)	0.344
WHO grade III	0 (0)	5 (10.4)	0.344
Chemotherapy received (%)	3 (15.8)	8 (17.8)	1
Previous radiation therapy (%)	5 (26.3)	14 (29.2)	1

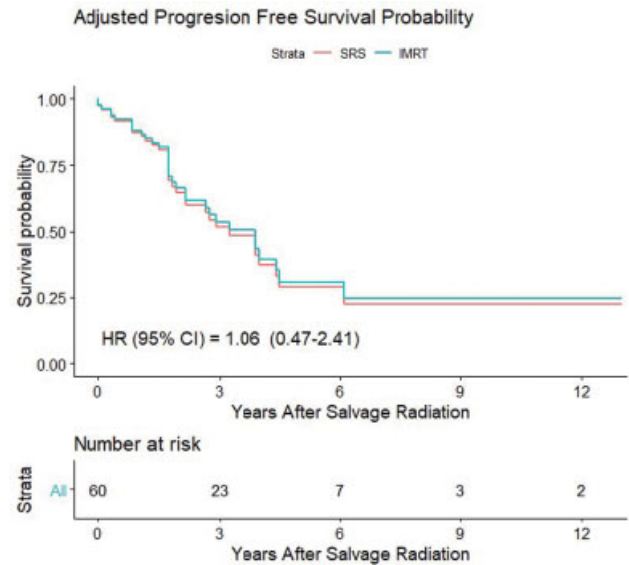


Fig. 1 (A, B): Progression-free survival between patients treated with SRS versus IMRT.

A093. A Multidisciplinary Central Nervous System Clinic Model for Radiation Oncology and Neurosurgery (Radians): Three-Year Experience with Brain and Skull Base Lesions in a Community Hospital Setting

Wencesley Paez¹, Rohi Gheewala², Shearwood McClelland III³, Jerry J. Jaboin¹, Jr. Charles R. Thomas¹, Timur Mitin¹, Jeremy N. Ciporen²

¹Department of Radiation Medicine, Oregon Health and Science University, Portland, Oregon, United States

²Department of Neurosurgery, Oregon Health and Science University, Portland, Oregon, United States

³Department of Radiation Oncology, Indiana University School of Medicine, Indianapolis, Indiana, United States

Background: Outpatient collaboration between Radiation Oncology and Neurosurgery for central nervous system (CNS) disease via the RADIANS (RADIation oncology And NeuroSurgery) clinic has been previously reported. Although novel and early in its multidisciplinary clinic design, patients found the tandem visit with the radiation oncologist and neurosurgeon highly favorable. Investigators hypothesized the clinic model would optimize patient and physician time by reducing clinic visits, improve quality of care, deliver evidence-based treatment modalities, while providing access for on-going clinical trials. The present study reports on the 3-year experience with patients evaluated for brain and skull base CNS lesions in a community hospital setting.

Methods: Clinical and demographic data were prospectively collected and maintained in a secure database for patients seen in the RADIANS clinic. Patient surveys were administered (0–5 scale, 0 = not satisfied; 5 = very satisfied), and data were reviewed over 3 years. Descriptive statistics are reported as mean and percentages for patient characteristics, diagnosis, treatment, and outcomes.

Results: Sixty-seven patients were evaluated between August 2016 and August 2019 in RADIANS with histologic confirmation of CNS brain or skull base lesions. Mean age was 61.0 years. Females represented 58.2% ($n = 39$) and males 41.8% ($n = 28$) of patients. Mean distance traveled to RADIANS was 66.5 miles (median = 16.9; range = 0.6–340). The most common referral source was medical oncology (28.4%). Mean overall satisfaction score was 4.77 ($n = 26$ respondents). Forty-three patients had malignant CNS disease; 24

had benign disease. Of those with malignant CNS disease, 28 patients had metastatic brain disease and 6 had both metastatic brain and spine disease (lung = 19; breast = 5; other = 4). Nine had malignant primary brain lesions (glioblastoma = 7; astrocytoma = 2) and 24 had benign primary brain lesions (meningioma = 15; glioma = 2; cavernoma = 1; pineal cyst = 1; pituitary adenoma = 1; other = 4). Forty-three patients had at least one comorbidity of which chronic obstructive pulmonary disease (34.3%) and hypertension (28.4%) were the two most common. Thirty-six percent of patients had a BMI ≥ 30 kg/m² (n = 24). Thirty-eight patients had stage IV disease (deceased = 12; hospice = 6, and active treatment = 20). Fifty-two percent (35/67) of patients with brain and skull base CNS lesions received radiation therapy (RT)—the majority (69%, 24/35) of which was stereotactic radiosurgery/stereotactic body RT. Fifteen percent (10/67) received neurosurgical intervention only in the form of craniotomy with tumor resection. Twenty-five percent (17/67) had both RT and neurosurgery. One-third of patients with benign CNS disease received surgical intervention, the remaining two-thirds were observed and followed-up with repeat surveillance imaging.

Conclusion: The RADIANS multidisciplinary clinic is the first of its kind to be reported, and continues to be viewed favorably by patients at extended follow-up. These results demonstrate the RADIANS clinic model is suitable in a community setting and can serve as an adequate regional referral center for CNS brain and skull base disease. Patients with varying degrees of comorbidities, systemic disease status, and cancer staging were appropriately treated. Continued data collection and treatment analysis will be of priority for future investigation regarding cost-benefit, clinical long-term outcomes, and possible mechanisms for early detection by means of vigilant follow-up and imaging surveillance.

A095. Fundal Fluid CAP is Associated with Short-Term Hearing Preservation in the Radiosurgical Treatment of Vestibular Schwannoma

Dennis Bojrab II¹

¹Michigan Ear Institute, Michigan, United States

Objective: The aim is to study the association between the fluid fundal cap and hearing preservation after gamma knife radiosurgical (GKRS) treatment of vestibular schwannoma (VS).

Study Design: Retrospective chart review.

Setting: Tertiary referral center.

Patients: Patients treated with GKRS for VS between March 2007 and March 2017. The diagnosis of VS was based on the clinical presentation and the typical radiological tumor appearance. Exclusion criteria included pretreatment PTA above 90 dB, neurofibromatosis type II, and follow-up less than 1 year.

Intervention(s): Therapeutic.

Main Outcome Measure(s): AAO-HNS guidelines for reporting hearing results in patients pre-GKRS and post-GKRS for VS were followed, including patient stratification into AAO-HNS Classes A-D. Pure-tone average (PTA) was calculated using thresholds at 0.5, 1, 2, and 3 kHz.

Results: Of the 137 patients included in the study, 47 had class A hearing, 37 had class B hearing, 19 had class C hearing, and 34 had class D hearing. Within each class the 1-, 2-, and 3-year hearing preservation rates were as follows: 75, 58, and 52% among class A; 75, 61, and 30% among class B; 89, 75, and 60% among class C; and 82, 66, and 61% among class D. Analysis revealed the presence of a fundal cap is associated with short-term hearing preservation according to Kaplan-

Meier method with log-rank testing. However, **Fig. 1** reveals the long-term mean change in PTA did not differ between patients with and without a fundal fluid cap on pretreatment MRI.

Conclusion: The presence of a fundal fluid cap on pretreatment MRI is predictive of short-term hearing preservation in patients undergoing Gamma Knife radiosurgery for vestibular schwannoma.

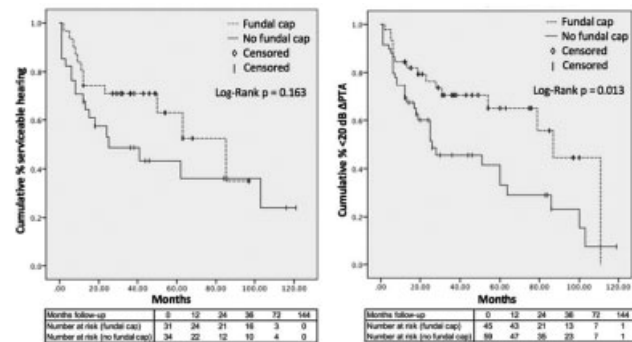


Fig. 1 Kaplan–Meier actuarial curves showing maintenance of serviceable hearing (n = 65) (A) and hearing preservation (n = 104) (B) according to fundal cap presence.

A096. Biometric Analysis of Simulation of Sylvian Fissure Dissection and Cerebrovascular Bypass under Subarachnoid Hemorrhage Conditions

Avital Perry¹, Christopher Graffeo¹, Lucas P. Carlstrom¹, William J. Anding¹, Kenton Kaufman¹, Michael J. Link¹

¹Mayo Clinic, Rochester, Minnesota, United States

Introduction: Sylvian fissure dissection and microvascular anastomosis/repair of intraoperative vascular injury are core skills in skull base, cerebrovascular, and other areas of complex cranial surgery. Additionally, the technique is frequently required under subarachnoid hemorrhage (SAH) conditions, which are more technically demanding, unpredictable, and potentially stress-inducing. We previously described and validated a rodent model for simulation of Sylvian fissure dissection and cerebrovascular bypass (e.g., microvascular anastomosis), which was demonstrated by subject self-reporting and blinded video assessment to be a realistic, challenging, and high-fidelity model system. In the present study, we sought to expand our validation of the model to formal biometric analyses, to confirm that the experimental condition constitutes a meaningful physiologic stressor for the subject.

Methods: Rat femoral artery and vein end-to-end microvascular anastomoses were used for control model and experimental framework. In the experimental protocol, following vessel exposure, we completed an extensive, 1- to 2-mm soft tissue debridement, and hematoma initiation, followed by wound closure and delayed re-exploration at intervals of 7 to 14 days. Three resident subjects dissected one rat each under control and experimental conditions (total n = 6 rats), during which heart rate (HR), hand tremor, and axial EMG were monitored.

Results: All dissections and anastomoses were successfully completed, with an overall patency rate of 100%. HR monitoring demonstrated a significant mean difference, with an increase of 10 to 20 bpm in the experimental condition, as compared with the control condition, for each subject (p = 0.01). Hand tremor demonstrated an inconsistent but statistically significant increase in incidence of 5 to 15 Hz during the experimental condition, as compared with control

(2/36 vs. 14/36, $p = 0.001$). Axial EMG did not show a significant difference between the conditions.

Conclusion: To our knowledge, ours is the unique and novel model of SAH simulation for microsurgical training, particularly in a live animal system. The current study provides objective, biometric data in support of the experimental condition in our simulation system as a significant physiologic stressor that appears to reproduce the impact of SAH conditions, with respect to technical, physiologic, and potentially psychological difficulty-of-dissection. These data have motivated a randomized, controlled study, which is presently underway at our institution; pending those results, the simulation system may have broad utility in skull base training programs.

A097. Network Analysis of NASBS Membership

John Luebs¹, Carl Snyderman²

¹SUNY Downstate Health Sciences University, Brooklyn, New York, United States

²University of Pittsburgh, Pittsburgh, Pennsylvania, United States

Background: The membership of the NASBS has grown considerably in recent years with diversity in subspecialty training, gender, and geography. The academic relationships and contributions of its membership have not been studied.

Objectives: The primary objectives of the study are: (1) Measure academic contributions of NASBS membership; (2) Identify influential nodes of academic collaboration; (3) Identify opportunities for future collaboration and mentorship.

Methods: Peer-reviewed publications of members of NASBS (2019 NASBS Web site) were identified using Scopus API author name search. Author and abstract records were collected in an SQL database for offline processing. Duplicate author profiles and alternate spellings were merged via automated similarity matching followed by manual review using institution affiliation and publication history. A commercial gender labeling database with scoring was applied to first names with manual intervention for lower confidence (<0.95) labels. Network structures were constructed and analyzed using the graph-tool python library to produce a weighted co-authorship network and compute centrality measures. Network maps were then produced using Gephi's network visualization software.

Results: The coauthor network contained 952 members with found publications and 4,996 connections. A total of 846 (88.9%) members were contained in a single connected giant component, whereas, 102 members were unconnected and 64 members had a single connection. The maximum shortest-path distance between nodes was 8 with an average path length of 3.3. The mean number of connections without respect to weighting was 10.5 (SD = 12.2), median 7. The mean weighted number of connections was 9.7 (SD = 21.1), median 3.3. Member unweighted connection count range from 0 to 102 and weighted connections ranged from 0 to 260. A total of 333 members (35.0%) had unweighted connection above mean and 221 members (23.2%) had weighted connection count above mean. There were 578 (60.7%) members that were part of the shortest path (nonzero betweenness centrality). Girvan–Newman clustering identified 267 communities, where 13 contained at least 1% of the total membership each. The 3 largest communities contained 23.3, 8.4, and 6.9% of members. Weighted degree was correlated with publication count ($r^2 = 0.44$) and weighted betweenness centrality was correlated with publication count ($r^2 = 0.40$). There were 111 published members identified as women. 5.4% of women were unconnected versus 11.4% of

men. Mean unweighted connection count for women was 8.42 (SD = 7.6), median 6 versus 10.7 (SD = 12.6), median 7 for men weighted connection count for women was 4.9 (6.1), median 2.5 versus 10.3 (22.3), median 3.4 for men. Mean betweenness centrality for women was 1.9×10^{-3} (3.7×10^{-3}) versus 4.2×10^{-3} (0.0156) for men. Mean closeness centrality for women was 1.91 (0.53) versus 1.96 (0.59) for men. Average publication count for women was 32.3 (38.5) versus 70.5 (106) for men. Average citation count for women was 543 (1,012) versus 1,389 (2,893) for men.

Conclusion: Network mapping of membership of the NASBS helps to visualize the academic activities and relationships of the NASBS and reveals areas of concentration and influence within the specialty. Network analysis can help better understand demographic disparities and trends within the membership. These findings can be used to mentor and foster increased collaboration among the membership.

A098. Endoscopic Skull Base and Advanced Rhinology Training in Neurosinology Fellowships: Standardization and Case Classification of Operative Volume

Satyan B. Sreenath¹, Mark Gelpi¹, Brian D. Thorp¹, Adam J. Kimple¹, Adam M. Zanation¹

¹University of North Carolina, North Carolina, United States

Background: Continued advancement in the field of endoscopic skull base (ESB) surgery has allowed for progressive use of endoscopic techniques in the management of complex skull base pathology. Fellowship-training programs have had to adapt their training paradigm to account for the evolution in surgical management. For this reason, the Rhinology Training Council (RTC) was created as an oversight committee for the goal of establishing uniform training. However, there remains limited transparency regarding the specific endoscopic and open skull base volume that exists within the neurosinology training fellowships. Despite this evolution in ESB surgery, fellowship level skull base training remains fairly nonstandardized, and the diversity of operative cases within each fellowship has not been well studied.

Objective: The goal of this study is to survey published information across the North American Skull Base Society (NASBS) and American Rhinologic Society (ARS) Web sites with regard to skull base training paradigm and characteristics of the operative volume. We sought to assess how fellowship programs delineate their training experience with respect to unique operative volume. This study will provide a better understanding of how fellowship training has potentially changed to accommodate evolving surgical treatments, and where opportunities for improved transparency can be achieved.

Methods: Online information in the NASBS and ARS Web sites was studied with a specific focus on open versus endoscopic skull base, advanced rhinologic, and standard sinonasal surgery volume for each program. Emphasis was placed on understanding what proportion of rhinology fellowships incorporated skull base and advanced rhinology training and how these cases were classified. Additionally, the RTC's guidelines for neurosinology accreditation were assessed in the scope of published case numbers for each program.

Results: Of 32 published rhinology fellowships in the ARS database, 28 (88%) fellowships report anterior and middle skull base training over a yearlong training program. Of these 28, 11 (39%) programs have published case numbers to demonstrate the level of skull base experience to be expected during the training period. Overall, the experience in anterior and middle skull base surgery range from 20 to 65% of the overall operative volume. With respect to the RTC's

guidelines including skull base approaches, resection of sinonasal tumors, skull base reconstruction, and advanced rhinologic procedures, there is minimal transparency in operative volume with respect to these categories. There are no uniform descriptive parameters for characterizing the nature of skull base and advanced rhinologic experience in a single fellowship to allow for comparative evaluation

Conclusion: With evolving surgical corridors and widespread advancements in endoscopic technology, rhinologists have become a vital component of the skull base surgery team. However, the advanced rhinology-training paradigm remains poorly characterized. The establishment of the RTC within the ARS has been a pivotal first step in better establishing standardization. However, improved knowledge of how operative cases are classified per institution will help understand the diversity in surgical experience. Improvements in classification of fellowship training and case characteristics will not only allow potential fellows to better understand what unique experiences each fellowship offers but also globally improve fellowship education in advanced rhinologic surgery.

A099. Network Analysis of Past NASBS Presidents

John Luebs¹, Carl Snyderman²

¹SUNY Downstate Health Sciences University, Brooklyn, New York, United States

²University of Pittsburgh, Pittsburgh, Pennsylvania, United States

Background: Past presidents of the NASBS include pioneers and leaders across multiple disciplines in skull base surgery. Since the inception of the NASBS, there have been major paradigm shifts in the management of skull base pathology. Little is known about the relative contributions and interactions of the past presidents and skull base centers.

Objectives: The primary objectives of this study are: (1) Measure academic contributions of past presidents; (2) Identify influential nodes of academic collaboration; (3) Identify opportunities for future collaboration.

Methods: Peer-reviewed publications of past presidents of NASBS from 1964 to July 2019 were identified using the Scopus author name search. Author and abstract records were collected in an SQL database for offline processing. Duplicate author profiles and alternate spellings were merged via automated similarity matching followed by manual review using institution affiliation and publication history. Network structures were constructed and analyzed using the graph-tool python library to produce a weighted co-authorship network base and compute centrality measures. Girvan–Newman clustering was applied to identify community structure. Network maps were then produced using Gephi's network visualization software with force-directed layout algorithms.

Results: The coauthor network of 29 presidents was fully connected, with a maximum shortest-path distance between presidents of 5. The mean number of connections from each node without respect to weighting was 5.31 (SD 3.53), and the mean number of connections with weighting was 8.40 (SD 7.28). The number of unweighted connections ranged from 1 to 14 and weighted connections ranged from 0.25 to 24.7. A total of 12 members (41.4%) had weighted connections above the mean. Girvan–Newman clustering identified three communities with two that covered 93% of the network. The largest communities contained 14 and 13 presidents and had mean unweighted connections of 5.79 and 5.31 and mean weighted connections of 10.10 and 7.45, respectively. The largest community had seven presidents with magnitude of weighted connections above the mean and the next largest community had five members with weighted

connections above the mean. The number of connections was correlated with *h*-index, both unweighted ($r^2 = 0.34$) and weighted ($r^2 = 0.26$).

Conclusion: Network mapping of past presidents of the NASBS helps to capture the history of the NASBS and reveals areas of concentration and influence within the specialty.

A100. Intraoperative Protocol for the Management of Carotid Artery Injury during Endoscopic Endonasal Surgery **Zachary Kassir¹, Carl H. Snyderman², Paul A. Gardner², Eric W. Wang², Georgios A. Zenonos²**

¹University of Pittsburgh School of Medicine, Pittsburgh, Pennsylvania, United States

²UPMC Center for Cranial Base Surgery, Pittsburgh, Pennsylvania, United States

Background: Intraoperative injury to a major vessel, most commonly the internal carotid artery (ICA), during endoscopic endonasal surgery, is a serious adverse event that is associated with significant morbidity and risk of mortality. At least 20% of surveyed surgeons have experienced ICA injury.

Objectives: The primary objectives of the study are to: (1) Assess knowledge of management of intraoperative ICA injury; (2) Develop intraoperative protocol for surgical team.

Methods: A 14-question survey of skull base surgeons (course participants and Web site) was performed to assess knowledge of management of intraoperative carotid artery injury. Responses were then used to develop a teaching curriculum for skull base surgeons. Members of the surgical team were interviewed to determine roles and responsibilities intraoperatively. Prior experiences with ICA injury were reviewed using root-cause analysis to identify contributing factors and errors in management.

Results: There were 71 respondents for the knowledge survey. Correct responses to individual questions ranged from 6 to 87%. Areas identified for education included risk factors for injury, neurological monitoring, surgical management, angiographic management, equipment, and functions of surgical team members. Review of prior ICA injuries revealed inconsistent practices and poor communication regarding roles of team members. An educational curriculum was constructed based on responses. An intraoperative protocol that is inclusive of all team members was developed based on interviews and past experiences with ICA injury as well as a review of the literature. A surgical simulation training activity is proposed that incorporates all of these elements.

Conclusion: There is a need for education and enhanced training of skull base surgeons and the operative team to improve management of intraoperative ICA injury. We believe that our educational curriculum can help to meet this need.

A102. A Model Is Worth 1,000 Pictures: Applications of 3D-Modeling in Skull Base Surgery Neuroanatomy Education

Christopher S. Graffeo¹, Avital Perry¹, Lucas P. Carlstrom¹, Michael J. Link¹, Jonathan Morris¹

¹Mayo Clinic, Rochester, Minnesota, United States

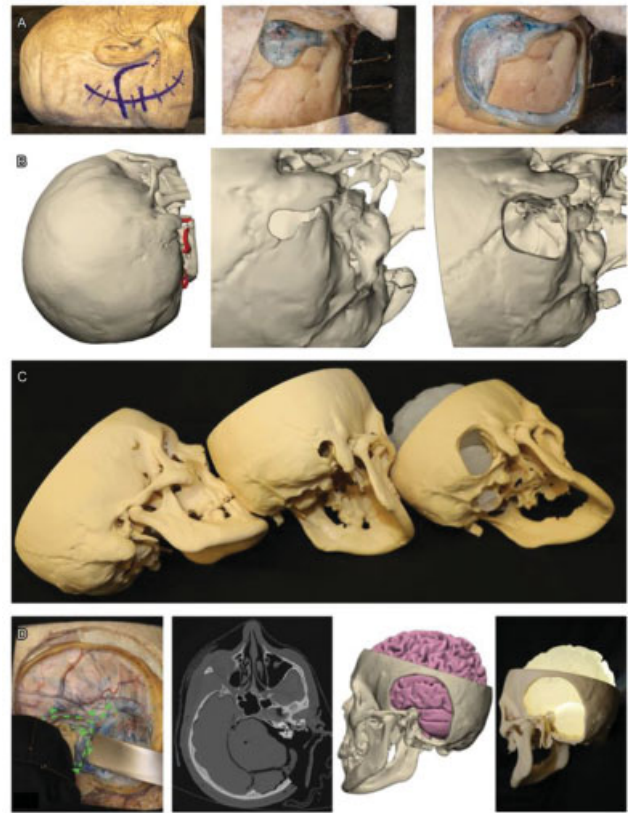
Introduction: Complex skull base surgery is a technically challenging niche that requires not only sound operative skills, but also nuanced consideration of various operative approaches, and an intimate appreciation for neuroanatomy and its pathologic variations. Successful training models have been consistent over many years, and include the mainstay of

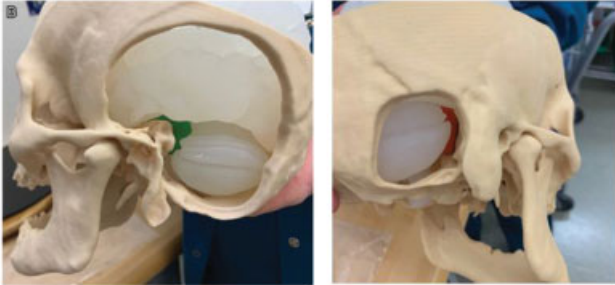
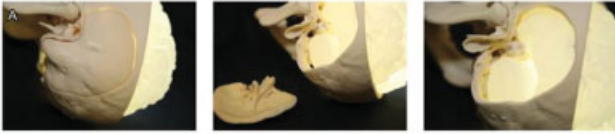
traditional apprenticeships (e.g., residency, fellowship), supplemented by cadaver-based laboratories and dissection courses, as well as surgical atlases, textbooks, and other 2D resources. However, mentored experiences and cadaver dissection are resource-intensive, and while it can provide insight regarding normal anatomy, the considerations of complex skull base pathology are not always made clear by the combination of normal cadaveric specimens combined with 2D images. Our goal was to use new 3D modeling technologies including 3D printing, and virtual/augmented/mixed realities, spaces to develop neurosurgical education resources that are approach-based, resident-oriented, and derived from advanced neuroanatomic dissections.

Methods: We manufactured anatomically accurate 3D models obtained through high-resolution head CTs that included actual patient skull base pathology neoplastic and cerebrovascular lesions. Neurologic surgery and ENT residents and fellows at all training levels, were asked to describe the surgical approach and intraoperative considerations after reviewing one of the following: (1) Patient imaging along; (2) Patient imaging, supplemented by pertinent neuroanatomy print resources; (3) Patient imaging supplemented by 3D-printed models; or (4) Immersive AR/MR models derived from the patient imaging and pathology. Subjects were then tested on their neuroanatomical knowledge, and asked to complete a self-reported survey based on a validated Likert's agreement scale (e.g., strongly agree, agree, neutral, disagree, strongly disagree), which assessed their perception of the utility of the resources provided with respect to parameters such as understanding of anatomical relationships, knowledge of approach indications and relative risks/benefits, and appropriately anticipated operative complications.

Results: Survey and neuroanatomy test results indicated a significant improvement in understanding of 3D neuroanatomic relationships and principles of approach selection after having seen the printed models, as compared with 2D imaging alone. Residents across all training levels survey reported significantly enhanced appreciation for surgical approach considerations, better understanding of nuanced pathology involvement with surrounding neuroanatomy, and increased rates of confidence in their ability to perform various aspects of the surgical case. Subjects participating in the dissection and/or 3D modeling phases of development performed at a higher level than those provided access to study resources, who in turn outperformed residents using traditional resources.

Conclusion 3D printing and related modeling techniques have a very high potential to positively impact neuroanatomy education for skull base trainees, with particular attention to the nuances of individualizing approach selection across a wide range of pathologies. Applied appropriately, 3D modeling is anticipated to improve the educational yield of almost all aspects of skull base education, ranging from understanding of basic neuroanatomic relationships, to augmented laboratory dissections, preparation for cases, intraoperative augmentation for positioning or approach planning, and studying operative results and complications.





A103. 3D Tractography in Skull Base Surgery: Technological Advances and Feasibility-Initial Experience

Srikant S. Chakravarthi¹, Melanie B. Fukui¹, Alejandro Monroy-Sosa¹, Jonathan E. Jennings¹, Austin Epping¹, Sammy Khalili¹, Lior Gonen¹, Juanita M. Celix¹, Bhavani Kura¹, Nathaniel Kojis¹, Richard A. Rovin¹, Amin B. Kassam¹

Aurora Neuroscience Innovation Institute, Milwaukee, Wisconsin, United States

Background: Despite neural anatomy being one of the primary drivers of corridor selection in skull base surgery, 3D tractography has not previously been incorporated into routine image guidance for skull base surgery due to numerous obstacles.

Objective: The aim of the study is to determine the feasibility of incorporating automated generation of 3D white matter tractography into the routine skull base surgery planning and corridor selection using an integrated planning and navigation solution.

Methods 100 skull base endonasal and transcranial procedures were planned in 94 patients and retrospectively reviewed. The main outcome measures were the following: (1) Ability to automate generation of 3D tractography; (2) Ability to co-register 3D tractography with CT and CTA in addition to structural MRI; (3) Accuracy of co-registration of 3D tractography to structural imaging (CT, CTA, and MRI); and (4) Ability to demonstrate real-time manipulation of 3D tractography intraoperatively for sequential reassessment of depth of resection and proximity to critical neural structures.

Results: The integrated planning software produced automated 3D tractography in all cases. In all cases, multiple imaging sequences were accurately merged to permit visualization of tractography overlaid on MRI, CT, and CTA during surgical planning and navigation. The registration of MRI, CT bone algorithm, and CTA images using an overlay tool was judged to be accurate in all cases. The geometric fit of 3D tractography was judged to be within 0.25 mm in all cases. In all cases, the full 3D tractography dataset was available for use during intraoperative navigation.

Conclusion: This initial series of 100 cases has established the feasibility of incorporating 3D tractography into the skull base surgical armamentarium.

A104. WHO Grade III Meningiomas: De Novo Tumors Show Improved Progression-Free Survival Compared to Secondary Progressive Tumors

Jacob Ruzevick¹, Sam Emerson¹, Kate Carroll¹, Jr. Manuel Ferreira¹

¹University of Washington, Seattle, Washington, United States

Background: Emerging evidence suggests de novo versus secondary progressive intracranial grade III meningiomas may harbor differing prognoses.

Objective: The aim of the study is to better understand the prognosis of patients treated for grade III meningioma.

Methods: A single institution, retrospective analysis of prospectively acquired patients between 1999 and 2018 was performed. Clinical data and radiographic parameters were reviewed to calculate progression-free survival and overall survival in patients undergoing microsurgical resection. Next generation targeted sequencing of meningioma associated genes was performed on 11 tumors.

Results: Between 1999 and 2018, 18 patients met the inclusion criteria for this study. Nine patients (50%) had de novo arising tumors and nine patients had secondary progressive tumors. There was an improvement in median progression-free survival for de novo resected tumors as compared with secondary progressive tumors (27 months vs. 5 months, $p = 0.02$). There was a trend toward improvement in overall survival for patients with de novo tumors (91 months vs. 22 months, $p = 0.17$). Similar trends were seen when stratifying based on the extent of resection and tumor location. Next generation sequencing of targeted genes (NF2, BAP1, TRAF7, KLF4, SMO, and AKT) revealed 5/11 tumors containing mutations in the NF2 gene, 2/11 containing BAP1 mutations, and a single tumor containing mutations in both NF2 and TRAF7. More mutations in NF2 and BAP1 were seen in the secondary progressive tumors.

Conclusion: Patients undergoing treatment for de novo arising grade III meningiomas showed improved progression-free survival compared with those patients with secondary progressive tumors. Further studies are needed to improve risk-stratification and development of therapeutics.

A105. Romidepsin Is a Possible Treatment for Meningiomas through Dual Inhibition of Classes 1 and 2 HDACs

Philip D. Tatman¹, Anthony Fringuello¹, William Foreman¹, Samuel Scherer¹, Tadeusz Wroblewski¹, Randy Jensen², Denise Damek¹, Kevin Lillehei¹, David Ormond¹, Michael Graner¹

¹University of Colorado, Boulder, Colorado, United States

²University of Utah, Salt Lake City, Utah, United States

Background: Meningiomas are common central nervous system tumors with few treatment options aside from surgery. Approximately 20 to 35% of these tumors are diagnosed as a WHO grade 2 or 3, necessitating a great need for additional therapies. To address this need, we previously reported our results on high-throughput screening of 30 meningiomas against a panel of FDA approved drugs as well as epigenetic inhibitors. Both panels indicated several Histone Deacetylase (HDAC) inhibitors as possible targets, the most efficacious of which was romidepsin. Romidepsin works by inhibiting zinc-dependent classes of HDACs, which include classes 1 and 2 HDACs. In this study, we performed an expanded screen of HDAC inhibitors to understand if romidepsin's activity is due to inhibition of class 1, class 2, or both classes of HDACs; as well as validation of romidepsin using two in vivo mouse model.

Methods: Using our brain-matrix culturing system, we screened meningiomas against a panel of classes 1, 2a, 2b, and pan-HDAC inhibitors. Dose curves were performed six times

and IC50 values were calculated for each drug in relation to each tumor. Two separate intracranial in vivo meningioma mouse models were used to validate romidepsin. The cells used for both in vivo experiments express luciferase, allowing for frequent monitoring of tumor volume. Romidepsin was injected intraperitoneal, at 2 mg/kg, every 3 days for the duration of the experiment.

Results: No single-class HDAC inhibitor produced IC50 values below 1 μm ; however, sub 1 μm IC50 values were achievable using pan HDAC inhibitors. The least efficacious class of inhibitors was class 2a, followed by class 2b, class 1, and pan-HDAC inhibitors, respectively. Romidepsin consistently inhibited cell viability at a lower IC50 than other HDAC inhibitors in our screen. Romidepsin does significantly inhibit meningioma growth after 2 weeks in vivo, making this a promising potential therapy for the treatment of meningiomas.

Conclusion: Romidepsin is a promising therapy for the treatment of meningiomas. This drug's benefit appears to stem from pan inhibition of class 1 and 2 HDACs.

A106. The Simpson's Grading Scale Continues to Hold Strong Prognostic Value in Modern Meningioma Surgery: 10-Year Single-Institution Experience

Colin J. Przybylowski¹, Benjamin Hendricks¹, Xiaochun Zhao¹, Claudio Cavallo¹, Leandro Borba Moreira¹, Sirin Gandhi¹, Nader Sanai¹, Kaith K. Almefty¹, Andrew S. Little¹

¹Barrow Neurological Institute, Phoenix, Arizona, United States

Background: Over the past 10 years, the relevance of the Simpson's resection grading scale has been called into question in modern meningioma surgery. We have continued to pursue Simpson's grade I resection when safe and possible over this time period. Considering this surgical strategy, we aimed to analyze the relationship between Simpson's resection grade and meningioma recurrence in our institutional experience.

Methods: This is a retrospective review of all patients who underwent surgical resection of a WHO grade I intracranial meningioma at our institution from 2008 to 2017. Tumor recurrence was defined by radiographic growth on serial MRI in comparison to the immediate postoperative MRI. Logistic regression analysis was utilized to assess predictors of Simpson's grade IV resection. Kaplan–Meier analysis and Log-Rank tests were utilized to assess and compare progression-free survival (PFS) of Simpson's resection grades, respectively.

Results: A total of 498 patients with evaluable data were included for analysis, including 398 females (79.9%) and 100 males (20.1%) with a mean age of 58.7 ± 12.9 years. The tumors were most commonly located at the skull base ($n = 307$; 61.6%) or the convexity ($n = 132$; 26.5%), and the mean tumor volume was $13.8 \pm 19.5 \text{ cm}^3$. Ninety-seven tumors (19.5%) invaded into a major dural sinus, and 50 tumors (10%) encased the internal cerebral, middle cerebral, or basilar artery. Simpson's grade I, II, III, or IV resections was achieved in 106 (21.3%), 154 (30.9%), 50 (10%), and 188 (37.8%) patients, respectively. In multivariate analysis, larger tumor volume ($p = 0.04$), sinus invasion ($p < 0.01$), and higher preoperative mRS score ($p = 0.01$) predicted Simpson's grade IV resection. Tumor recurrence occurred in 60 patients (12%) at a mean duration of 41.4 ± 33 months from surgery. Simpson's grade I resection resulted in superior PFS compared with both Simpson's grade II ($p = 0.02$) and grade III resections ($p < 0.01$). Simpson's grade I to III resections resulted in superior PFS compared with Simpson's grade IV resection ($p < 0.01$).

Conclusion: In this large, single-institution experience of WHO grade I intracranial meningioma resection, there was

a strong correlation between Simpson's resection grade and tumor recurrence. Simpson's grade I resection resulted in superior PFS to both Simpson's grade II and III resection, and, when safe, should remain the goal of intracranial meningioma surgery. The Simpson's resection grading scale continues to hold strong prognostic value in the modern neurosurgical era.

A107. Incidence of Surgery after Gamma Knife Radiosurgery for Parasagittal Meningiomas Is Higher than Meningiomas in Other Locations: A 10-Year Review

Andrew J. Montoure¹, Jennifer Connelly¹, Joseph Bovi¹, Nathan Zwagerman¹

¹Medical College of Wisconsin, Milwaukee, Wisconsin, United States

Background: Gamma Knife radiosurgery (GKRS) and surgical resection are a well-established and accepted potential first line treatment modalities for meningiomas. Many factors play a role in the decision making for treatment. There are certain cases which necessitate surgical intervention even after GK treatment due to continued tumor growth or patient symptoms. Evaluating the tumor characteristics in such cases can lead to improved decision making for which primary treatment is preferred, and how to better guide the patients on the options they have.

Methods: A retrospective review evaluating each meningioma receiving GKRS treatment at the Medical College of Wisconsin between 2009 and 2019. The patient's charts and relevant imaging were reviewed.

Results: There were 132 total treatments for meningiomas on 124 different patients, 39 (31.5%) of these were parasagittal meningiomas. The female to male ratio for this group was 2.25:1 and the average age was 61 (range, 28–86). We found a 17.9% incidence of parasagittal meningiomas requiring surgical intervention after treatment with GKRS, compared with a 3.5% incidence of tumors in other locations. The average tumor size (maximum diameter) for the parasagittal meningiomas was 21.8 mm with a range of 10 to 31 mm. The average radiation treatment dose prescribed for these tumors was 14 Gy at the 50% isodose line with a range of 12 to 15 gray. The time from GKRS to open surgery ranged from 6 to 67 months with 4 patients (57%) occurring within 9 months of GKRS treatment, and the most common reason leading to surgery was increased brain edema with worsening symptoms in all seven patients. In addition, one tumor exhibited tumor growth and two patients had a new onset seizure.

Conclusion: Surgery after GKRS for parasagittal meningiomas may be more common than previously thought. This is likely a result of peritumor edema from the treatment. This information can help guide patient and physician discussion in regard to preferred first line treatment for these parasagittal meningiomas.

A108. Brachytherapy with Surgical Resection as Salvage Treatment for Recurrent High-Grade Meningiomas: A Matched Cohort Study

Michael A. Mooney¹, Wenya L. Bi², Jonathan Cantalino², Kyle Wu², Thomas Harris², Lucas Possatti², Parikshit Juvekar², Liangge Hsu², Ian F. Dunn², Ossama Al-Mefty², Phillip M. Devlin²

¹Barrow Neurological Institute, Phoenix, Arizona, United States

²Brigham and Women's Hospital, Boston, Massachusetts, United States

Background: Outcomes of recurrent high-grade meningiomas are poor with high rates of re-recurrence,

increased risk of subsequent intervention, and increased disease-related mortality.

Objective: The aim of this study is to evaluate brachytherapy after surgical resection as a salvage treatment strategy in patients with recurrent high-grade meningioma who exhausted prior external beam treatment options.

Methods: Single-center retrospective review of our institutional experience of brachytherapy implantation from 2012 to 2018. The primary outcome of the study was progression-free survival (PFS). Secondary outcomes included overall survival (OS) and complications. A matched cohort of patients not treated with brachytherapy over the same time period was evaluated as a control group. All patients had received prior radiation treatment and underwent planned gross total resection (GTR) surgery.

Results: A total of 27 cases were evaluated. Compared with prior treatment, brachytherapy implantation demonstrated a statistically significant improvement in tumor control [HR 0.316, 0.101–0.991, $p = 0.034$]. PFS-6 and PFS-12 were 92.3 and 84.6%, respectively. Compared with the matched control cohort, brachytherapy treatment demonstrated improved PFS [HR 0.310 (0.103–0.933, $p = 0.030$). Overall survival was not statistically significantly different between groups [HR 0.381 (0.073–1.982, $p = 0.227$). Overall postoperative complications were comparable between groups, although there was a higher incidence of radiation necrosis in the brachytherapy cohort.

Conclusion: Brachytherapy with planned GTR improved PFS in recurrent high-grade meningioma patients who exhausted prior external beam radiation treatment options. Future improvement of brachytherapy dose delivery methods and techniques may continue to prolong control rates and improve outcomes for this challenging group of patients.

A109. The Impact of Patient Frailty on Hospital Stay and Discharge Disposition following Surgical Resection in Patients with High-Grade Meningiomas

Jianning Shao¹, Arbaz Momin¹, Pranay Soni², Diana Lopez¹, Konrad K. Knusel³, Patrick J. Elsworth³, Varun R. Kshetry², Pablo F. Recinos⁴

¹Cleveland Clinic Lerner College of Medicine at Case Western Reserve University, Cleveland, Ohio, United States

²Department of Neurosurgery, Cleveland Clinic, Cleveland, Ohio, United States

³Case Western Reserve University School of Medicine, Cleveland, Ohio, United States

⁴Section Head—Skull Base Surgery, Department of Neurosurgery, Cleveland Clinic, Cleveland, Ohio, United States

Introduction: The current treatment paradigm for World Health Organization (WHO) grade II and III meningioma is maximum safe surgical resection, often with postsurgical adjunctive radiotherapy. Important postoperative considerations in these patients include length of stay (LOS) and discharge disposition. Since the association between prolonged LOS and hospital-associated complications, such as infection and patient falls, is well documented, timely discharge is important to minimize the risks associated with protracted hospitalization. The level of continued care required at discharge determines the disposition and has been used as a proxy for postoperative patient clinical status. In older patients with meningiomas, the impact of frailty on LOS and discharge disposition becomes an especially important question. In this study, we assessed the impact of frailty measures on LOS and discharge disposition in patients with high-grade meningiomas.

Methods: A retrospective review was performed of patients with WHO II and III meningiomas who underwent surgical resection at our institution between 1995 and 2019. Data collected included patient demographics, Clinical Frailty Index (CFI), Charlson's comorbidity index (CCI), surgical parameters, postoperative hospital course, and discharge disposition. Univariate and multivariate analyses were performed to determine parameters significantly associated with LOS and discharge disposition. The best-fit model for predicting discharge disposition based on patient and tumor-specific parameters was determined via a logistic regression analysis informed by Akaike information criteria (AIC), with the outcome designated as discharge to home versus facility, which included SNF, acute rehab, and LTAC.

Results: A total of 235 patients were included in the final analysis. One-hundred thirty-one patients (55.7%) were female and 104 patients (44.3%) were male. Black race and age were identified on multivariate analysis to be significantly correlated with increased LOS ($p < 0.001$ for both). With respect to disposition, 166 patients (70.6%) were discharged to home, and 69 patients (29.4%) were discharged to facility. Three parameters were significantly associated on multivariate analysis with discharge to a facility: (1) age at time of surgery (66.5 ± 15.9 years for AOH vs. 59.6 ± 13.4 years for home, $p < 0.001$), (2) CFI (4.16 ± 1.53 for facility vs. 3.46 ± 0.98 for home, $p < 0.001$), and (3) CCI (5.34 ± 1.76 for AOH vs. 4.12 ± 1.80 for home, $p < 0.001$). The logistic regression model that yielded the minimum AIC was selected as the final model and included age (OR = 1.59, $p = 0.0012$), black race (OR = 0.26, $p = 0.029$), and CFI (OR = 1.39, $p = 0.032$) as the most significant predictors of discharge to facility.

Conclusion: Clinical frailty (as assessed by CFI), CCI, and age, were significantly correlated with discharge to facility after surgical resection in patients with high-grade meningiomas in this study. CFI and age were selected as significant predictors of discharge to facility and age was the only significant predictor for increased LOS in best-fit logistic regression models. Clinical frailty parameters may help guide preoperative optimization and counseling in patients with high-grade meningiomas.

A110. Adjuvant Radiation Does Not Decrease the Risk of Short-Term Tumor Recurrence in Patients with Atypical Meningioma

Jacob Ruzevick¹, Timothy Woodiwiss¹, Sam Emerson¹, Kate Carroll¹, Jason Rockhill¹, Patrick Cimino¹, Luis Gonzalez-Cuyar¹, Laligam Sekhar¹, Jr. Manuel Ferreira¹

¹University of Washington, Seattle, Washington, United States

Purpose: Intracranial atypical meningiomas (WHO grade II) represent a significant challenge for the treating surgeon. While not histologically benign, the ability to risk-stratify patients into high and low risk for recurrence, and thus who may benefit from adjuvant therapies, remains elusive.

Methods: A single institution, retrospective analysis of prospectively acquired patients between 2000 and 2018 was performed. Clinical data and radiographic parameters were reviewed to calculate progression-free survival and overall survival in patients undergoing microsurgical resection and those undergoing microsurgical resection with adjuvant radiation.

Results: Between 2000 and 2018 a total of 143 patients met the inclusion criteria for this study. A total of 85 patients underwent microsurgical resection only and 58 underwent microsurgical resection with adjuvant radiation. A greater percentage of patients achieved gross total resection in the

microsurgery only group ($p < 0.001$); however, there was no difference in progression-free survival or overall survival as compared with those patients who received adjuvant radiation. There was an improvement in progression-free survival in those patients undergoing microsurgical resection ($p = 0.047$) and a trend toward improved progression-free survival in the microsurgery and adjuvant radiation cohorts ($p = 0.18$) in tumors in skull base as compared with nonskull base locations, though adjuvant radiation did not improve the outcomes of either subset of patients compared with microsurgery alone. Of those patients who failed initial treatment, a majority were in nonskull base locations, were associated with a more aggressive histological phenotype, were male, and were more likely to succumb to disease during the study period.

Conclusion: Adjuvant radiation does not improve short-term progression-free survival in patients who undergo gross total resection of atypical meningiomas over a follow-up of approximately 4 years. In addition to extent of resection, sex, histological characteristics, and tumor location should be included in the algorithm for determining the utility of adjuvant radiotherapy.

A111. Preoperative Cranial Nerve Deficits as Crucial Outcome Predictor for Skull Base Meningiomas

Sebastian Liao¹, Shao-Ching Chen², Sanford Hsu²

¹Taichung Veterans General Hospital, Taichung, Taiwan

²Taipei Veterans General Hospital, Taipei, Taiwan

Objective: Meningiomas have various clinical presentations, and skull base meningioma harbors the most diversified symptoms of them. Many outcome-predicting factors for skull base meningiomas were profoundly discussed. However, we have yet to see a single predicting factor, which was easy to be evaluated preoperatively and was able to predict both functional and clinical outcomes. Our objective of this study was to examine the correlation between a single category of preoperative symptoms and outcomes of skull base meningiomas after multimodality treatments.

Material and Methods: The authors retrospectively reviewed the medical records and radiological data to obtain outcomes of patients who underwent treatments at our institute for their skull base meningiomas during 2010–2018. The analyses were designed to address the association among the preoperative cranial nerve deficits (CNDs), functional outcomes, and survival prognosis.

Results: A total of 143 patients were included with the median follow-up time of 27.3 months. Mostly mentioned chief complaints were eye symptoms (32.2%), unsteady gait (29%), headache (15.4%), and dizziness (7.7%). Eighty-one patients (56.6%) presented with preoperative CNDs, of which were smelling dysfunctions (CN1, 2.5%), eye symptoms (CN2–4, 54.8%), facial pain (CN5, 9.5%), facial palsy and tinnitus or hearing loss (CN7–8, 22.6%), and swallowing difficulties (CN9–12, 3.6%). The presentation of preoperative CNDs was associated with new onset or worsen postoperative CNDs ($p < 0.001$), tumor recurrence ($p = 0.019$), and requirements of adjuvant therapies (e.g., gamma knife surgeries or endoscopic endonasal surgeries, $p = 0.006$). The mean resection rate of patients with and without preoperative CNDs were 90 and 97%, respectively, ($p < 0.0001$). It may also correlate to a longer progression-free survival ($p = 0.03$), independent to the pathological grading ($p = 0.25$).

Conclusion: The presentation of preoperative CNDs may be considered as an outcome predictor for skull base meningiomas.

A112. The Sound of Happiness: Hearing-Related Quality of Life and Patient Satisfaction with Management Decision-Making in Vestibular Schwannoma

Lucas P. Carlstrom¹, Maria Peris Celda², Avital Perry¹, Christopher S. Graffeo¹, Geffen Kleinstern¹, Matthew L. Carlson¹, Michael J. Link¹

¹Mayo Clinic, Rochester, Minnesota, United States

²Albany Med, Albany, New York, United States

Introduction: Patient satisfaction is increasingly emphasized in all aspects of neurosurgical care; however, strategies for identifying patients at highest risk for treatment dissatisfaction remain sophomoric. The goal of the present study was to assess in a large sample of vestibular schwannoma (VS) patients the relationship between hearing loss, patient satisfaction with shared decision-making for initial management strategy, and associated impacts on hearing-related quality-of-life (QOL).

Methods: Prospective, observational, multicenter, multinational, cross-sectional study, analyzed via multivariable linear and logistic regression.

Results a total of 422 VS patients with formal audiometry within 1 year of survey date were identified. Median age was 54 (range, 12–82); 223 (53%) were female. At the time of survey, 386 individuals responded to the question “Are you happy with the treatment type (surgery, radiation, or observation)?,” of whom 26 (7%) indicated dissatisfaction with the elected management strategy. Hearing loss domains significantly associated with dissatisfaction, included word recognition score (WRS; $p < 0.0001$), pure tone average (PTA; $p = 0.0003$), AAO-HNSF Hearing Class ($p = 0.003$), subjective hearing loss severity ($p = 0.0005$), and loss of ipsilateral telephone. Subjective hearing loss and telephone use were co-linear with WRS, PTA, and derived parameters. Neither tinnitus nor regular hearing air use was not significantly associated with treatment dissatisfaction. Adjusting for age and sex, the odds ratio for treatment dissatisfaction with Class B or worse hearing, as compared with Class A, was 4.1 (95% CI = 1.3–17.6, $p = 0.01$). Unhappiness with initial management strategy was significantly associated with other unfavorable QOL outcomes, including adverse impacts on personal relationships or conversations due to hearing loss ($p = 0.01$, $p = 0.005$).

Conclusion: Patient dissatisfaction with initial management strategy is uncommon, occurring in 5 to 10% of all VS patients. Hearing loss, even at a modest degree of disability, appears to be the predominant driver of dissatisfaction, particularly when associated with adverse impacts on personal relationships or conversations.

A113. Internal Auditory Canal Variability and Facial Nerve Outcome after Translabrynthine Resection of Vestibular Schwannomas

Michael A. Cohen¹, Forrest Hamrick¹, Austin S. Gamblin¹, Michael Karsy¹, Richard Gurgel¹, Clough Shelton¹, William T. Couldwell¹

¹University of Utah, Salt Lake City, Utah, United States

Background: The internal auditory canal (IAC) contains the vestibulocochlear and facial nerves and serves as an important landmark during resection of vestibular schwannomas (VSs). We have observed anatomical variability of the IAC and differences in surgical exposure depending on individual anatomy. Based on these observations, we analyzed whether facial nerve outcome after a translabrynthine approach for resection of a VS is correlated with IAC anatomic variability.

Methods: We retrospectively identified patients with pathologically confirmed VSs treated using the translabyrinthine approach between May 2014 and March 2019. Patients <18 years, with tumors found intraoperatively to be arising from the facial nerve, or who underwent nonelective procedures were excluded. To determine the size and variability of the IAC, we assessed preoperative axial thin-slice T2-weighted MRI sequences. We measured the anterior (APD) and posterior (PPD) petrous distances, the porus dilation, and the internal auditory angle (IAA). We also estimated tumor volume. Facial nerve outcomes were quantified using the House-Brackman (HB) score recorded in the medical record on postoperative day (POD) 1, at discharge, and at 1-month follow-up.

Results: The study population included 65 consecutive patients (33 female) with a mean age of 50.5 years (18–85 years). All patients presented with moderate to severe sensorineural hearing loss. Tumor volume ranged from 0.03 to 52.8 cm³ (mean, 8.3 cm³). APD ranged from 7.3 to 34.9 mm (mean, 13.29 mm). PPD ranged from 7.8 to 33.3 mm (mean, 25.19 mm). IAA ranged from 0 to 28 degrees (mean 12.8 degrees). PD ranged from 0 to 11.3 mm (mean 3.17 mm). On univariate and multivariate linear regression, there was weak correlation between tumor volume and facial nerve outcomes at POD 1 ($p = 0.03$), discharge ($p = 0.01$), and follow-up ($p = 0.1$). IAA was an independent predictor of facial nerve outcomes at POD 1 ($p = 0.0001$), discharge ($p = 0.0001$), and follow-up ($p = 0.0001$). Using an ROC curve, an IAA cutoff value of 14.5 degrees predicting poor HB grade (≤ 2) was identified. This cutoff yielded a sensitivity and specificity, respectively, of 0.72 and 0.66 at POD1, 0.76 and 0.64 at discharge, and 0.76 and 0.64 at follow-up.

Conclusion: We have shown that the IAA is an independent predictor of short-term facial nerve outcome in patients being treated via a translabyrinthine approach for VSs. We hypothesize that the angle of the facial nerve toward the IAC affects its visualization during the translabyrinthine approach and that a smaller IAA (anteriorly angled IAC) is likely to direct tumor growth anteriorly. Therefore, the IAA is a critical measurement that can be used to determine the relative risk of facial nerve palsy using the TL approach. Our results here indicate that the translabyrinthine approach will likely provide suboptimal facial nerve visualization with an IAA <14.5 degree and a retrosigmoid approach should be considered because of the better visualization of the facial nerve and worse facial nerve outcome in the group using a translabyrinthine approach.

A114. Cochlear Fiesta Signal Intensity Predicts Hearing Outcomes after Middle Fossa Resection of Acoustic Neuroma

Kareem O. Tawfik¹, Marin McDonald¹, Yin Ren¹, Omid Moshtaghi¹, Marc S. Schwartz¹, Rick A. Friedman¹

¹University of California San Diego, San Diego, California, United States

Background: In select patients with small acoustic neuromas (AN) and serviceable hearing, microsurgical resection via the middle fossa approach allows for complete tumor removal and preservation of hearing. Published rates of hearing preservation vary widely, and accurate prediction of hearing preservation based on preoperative factors remains elusive. Previous literature has shown that ANs can produce proteins that may contribute to cochlear cell damage. Cochlear protein concentration may increase in the setting of AN, potentially portending a higher risk of hearing loss after AN resection. Given that FIESTA magnetic resonance (MR) signal intensity declines as protein concentrations increase, cochlear FIESTA signal intensity may serve as a pragmatic, readily

available clinical predictor of postoperative hearing decline in AN patients undergoing hearing preservation surgery.

Objectives: In the present study, we aimed to determine the relationship of preoperative cochlear FIESTA signal intensity to postoperative hearing decline after middle fossa AN resection.

Design: We performed a retrospective analysis of adult AN patients who underwent middle fossa resection for hearing preservation at a quaternary care AN program between November 2017 and May 2019. All patients underwent preoperative MR imaging with FIESTA sequence and had preoperative four-frequency pure tone average (PTA) <50 dB and word recognition score (WRS) $\geq 50\%$. Postoperative hearing preservation was defined as WRS $\geq 50\%$. Patients with neurofibromatosis 2, a history of previous surgical resection or radiosurgery were excluded. FIESTA cochlear signal intensity ratio was defined as the ratio of ipsilateral to contralateral cochlear FIESTA signal intensity, such that a lower numerical value was associated with lower FIESTA signal in the ipsilateral cochlea. FIESTA cochlear signal intensity was determined by a fellowship-trained neuroradiologist blinded to patients' preoperative and postoperative audiometry. Cochlear signal intensity was gathered from hand-drawn regions of interest that included the basal and middle turns of each cochlea.

Results: Forty-two patients met criteria for analysis. Mean age was 47.5 years (± 10.5) and mean tumor size 8.9 mm (± 3.9). Hearing was preserved in 52.4% ($n = 22$) of the cases. Demographic variables, tumor size, preoperative PTA, and WRS did not significantly differ between patients with and without postoperative hearing preservation. On univariate and multivariate analysis of demographic variables, tumor characteristics, and audiometric measures, none was statistically predictive of hearing preservation. However, low preoperative FIESTA signal ratio was positively correlated with degree of postoperative decline in hearing as measured by PTA ($r = 0.304$, $p = 0.05$) and WRS ($r = 0.394$, $p = 0.01$).

Conclusion: In patients undergoing middle fossa resection of AN for hearing preservation, low preoperative cochlear FIESTA signal ratio is associated with a greater postoperative hearing decline. This finding has not been previously reported, to our knowledge. Owing to the widespread use of FIESTA imaging in patients with retrocochlear pathology, cochlear FIESTA signal ratio is a practical predictor of hearing outcome and should be taken into consideration when counseling patients about their risk of hearing decline after surgery. These findings support the notion that increased cochlear fluid protein concentration portends worse hearing outcomes in patients with AN undergoing hearing preservation surgery.

A115. Evolution in Management Trends of Sporadic Vestibular Schwannoma from 1970 through 2019 Using the Acoustic Neuroma Association Patient Registry

Stephen A. Chan¹, John P. Marinelli¹, Debbie L. Hahs-Vaughn², Michael J. Link³, Allison Feldman⁴, Chad Nye⁴, Matthew L. Carlson³

¹Department of Otolaryngology—Head and Neck Surgery, Mayo Clinic, Minnesota, United States

²Department of Learning Sciences and Educational Research, University of Central Florida, Orlando, Florida, United States

³Department of Neurologic Surgery and Otolaryngology—Head and Neck Surgery, Mayo Clinic, Rochester, Minnesota, United States

⁴Acoustic Neuroma Association, Cumming, Georgia, United States

Background: Limited data currently characterize management trends of sporadic vestibular schwannoma (VS) in the United States over recent decades. Serving as the primary patient support organization in the United

States, the Acoustic Neuroma Association (ANA) facilitates amalgamation of patient data from patients treated in 1970 through January, 2019.

Objectives: The aim of the study is to characterize the evolution in the management of sporadic VS among ANA survey respondents from 1970 to 2019.

Study Design: Cross-sectional survey.

Patients: ANA survey respondents diagnosed with sporadic VS.

Main Outcome Measures: Trends in rates of microsurgery, radiosurgery, and observation from 1970 to 2019.

Results: Among 878 patients with sporadic VS that reported data over the study period, 633 (70%) patients underwent definitive management with either microsurgery or radiosurgery/radiotherapy between 1970 and 2019. The proportion of patients treated with microsurgery gradually increased from 80% (4) in the 1970s to a peak of 95% (58/63) by 1989. The proportion of cases treated with microsurgery declined into the 2000s, with approximately 66% (234/356) of patients treated from 2010 to 2019 undergoing microsurgery. Only 56 (6%) patients underwent radiosurgery/radiotherapy over the study period. The proportion of patients treated with radiosurgery/radiotherapy increased from 1970 through the turn of the century, with approximately 17% (22/126) of the patients treated with radiosurgery/radiotherapy from 2000 to 2009. This proportion decreased over the following decade from 2010 to 2019 to 11% (28/249). In total, only 30% of the respondents underwent observation over the study period (245/878).

Conclusion: Overall, these data support a progression toward a greater proportion of patients treated with observation over recent decades. However, when compared with population-based data within the United States from the Surveillance, Epidemiology, and End Results database,¹ it is evident that far more ANA patients are aggressively managed with microsurgery for initial treatment of their tumor. This observation likely stems from the tendency of patients who participate in the ANA to present with more severe disease at time of diagnosis.^{2,3}

References

- Carlson ML, Habermann EB, Wagie AE, et al. The changing landscape of vestibular schwannoma management in the United States—a shift toward conservatism. *Otolaryngol Head Neck Surg* 2015;153(3):440–446
- Marinelli JP, Prummer CM, Link MJ, Carlson ML. Differentiating the general vestibular schwannoma patient population, tertiary referral center cohorts, and the acoustic neuroma association survey respondents: a response to the benefits and drawbacks of survey-based studies. *Otol Neurotol* 2019;40(7):980–982
- Prummer CM, Kerezoudis P, Tombers NM, Peris-Celda M, Link MJ, Carlson ML. Influence of selection bias in survey studies derived from a patient-focused organization: a comparison of response data from a single tertiary care center and the acoustic neuroma association. *Otol Neurotol* 2019;40(4):504–510

A116. Set Your Phasers to Kill: Outcomes after High-Rose Stereotactic Radiosurgery for Vestibular Schwannoma

Lucas P. Carlstrom¹, Avital Perry¹, Christopher S. Graffeo¹, Bruce E. Pollock¹, Michael J. Link¹

¹Mayo Clinic, Rochester, Minnesota, United States

Introduction: Contemporary treatment guidelines for stereotactic radiosurgery (SRS) of vestibular schwannoma

(VS) recommend limiting the margin dose to 12.5 Gy in patients with useful hearing, and 14 Gy in those without. The long-term efficacy and safety profile associated with higher doses is incompletely understood.

Methods: Prospectively maintained cohort study of VS treated with SRS marginal doses of 15 to 16 Gy at a single institution from 1993 to 2018.

Results: Of 818 VS treated with SRS at our institution, 4 received marginal doses of 15 Gy (0.5%) and 35 received 16 Gy (4.3%). The median maximum dose was 32 Gy (range, 26.7–32), and the median treatment volume was 1700 mm³ (range, 90–8,667). A total of 34 patients had follow-up of at least 12 months (median, 106 months; range, 15–233), with 0 deaths attributable to VS sequelae or SRS complications. SRS was the primary treatment in 22 patients (64.7%); 33 out of 34 patients with routine radiographic surveillance demonstrated stable or smaller tumor size at last follow-up (97.1%). One patient demonstrated cystic changes after chronically stable surveillance, and the patient did not undergo further treatment. There were no instances of new, permanent, post-SRS facial weakness. One patient had transient facial weakness at 2 days after primary SRS; this was effectively treated with a short steroids course. Of the 18 patients with pre- and posttreatment audiometric outcome assessments, only one patient had serviceable hearing (AAO-HNS class A or B) at last follow-up (139 months). Other post-SRS complications included new facial pain in two (5.9%), altered gustation, olfaction, and trigeminal sensation in one (2.9%), and one new cavernous malformation (2.9%)—first observed on MRI approximately 3 years following primary SRS.

Conclusion: High-dose SRS for VS appears to demonstrate a favorable risk-benefit profile, with no patients in this small cohort study requiring additional treatments for tumor progression. Although the risk of hearing loss is likely accelerated accordingly with the disease natural history, there is no evidence of additional apparent risk to the facial nerve. Correspondingly, margin doses of 15 to 16 Gy may be considered in patients thought to be at highest risk of treatment failure, although patient counseling regarding possible sensory toxicity is advisable.

A117. Cerebrospinal Fluid Leak following Vestibular Schwannoma Surgery—Factors that Impact Outcomes

Anne M. Selleck¹, Sarah Hodge¹, Kevin Brown¹

¹UNC, Chapel Hill, North Carolina, United States

Cerebrospinal fluid leaks are associated with significant morbidity following acoustic neuroma surgery. The incidence of cerebrospinal fluid leak varies greatly in the literature and the best method for prevention is still debated. Our objective in this study was to evaluate the incidence of cerebrospinal fluid leak following vestibular schwannoma surgery for retrosigmoid approaches, translabyrinthine approach with mesh cranioplasty, or translabyrinthine approach with water-tight periosteum closure. Our secondary objective was to determine the association of nonsurgical variables with higher rates of cerebrospinal fluid leak following acoustic neuroma surgery. This is a retrospective chart review of 219 patients who underwent sporadic vestibular schwannoma resection via a translabyrinthine or retrosigmoid approach between 2000 and 2019. These surgeries were performed at a tertiary academic referral center. Patient variables that were analyzed included patient's age at time of surgery, sex, body mass index, and the largest dimension of the tumor based on preoperative magnetic resonance imaging. Surgical variables that were analyzed included length of surgery, from incision to the end of closure, and surgical approach as well as method of closure in the

translabyrinthine approach group (watertight periosteal closure vs. titanium mesh plate closure). Postsurgical variables that were analyzed included total number of hospital days (including total hospital days during the initial stay as well as hospital days during any re-admission within 30 days), number of days spent in the intensive care unit, cerebrospinal fluid leak, the site of the cerebrospinal fluid leak, the need for a second operation and pseudomeningocele occurrence. Our overall cerebrospinal fluid leak rate was 12.3% with a leak rate of 17.2% in our retrosigmoid group, 12.8% in our translabyrinthine titanium mesh closure group, and 0% in our translabyrinthine periosteal closure. A significant difference was found in the cerebrospinal fluid leak rate between the two translabyrinthine groups ($p = 0.019$) and between the watertight periosteal closure translabyrinthine and retrosigmoid groups ($p = 0.005$). There was no difference in cerebrospinal fluid leak rate between the titanium mesh translabyrinthine and retrosigmoid groups ($p = 0.413$). There was no statistically significant effect of age, body mass index, and size of tumor on the incidence of cerebrospinal fluid leak in these postsurgical patients. There was also no statistically significant difference between the three groups on length of operative time or number of days spent in the ICU. Total hospital days demonstrated a trend parallel to cerebrospinal fluid leak rates, with the shortest amount of hospital days in the watertight periosteal translabyrinthine group (average of 5.2), 6.4 days in the mesh translabyrinthine group, and 7.4 days in the mesh retrosigmoid group; however, this did not reach statistical significance ($p = 0.119$). Watertight periosteal closure of a translabyrinthine approach is an effective means of closing the temporal bone defect that allows for lower cerebrospinal fluid leak rates in comparison to closure with titanium mesh.

A118. Dysregulated Genes and Biologic Pathway Analysis in Early versus Late Recurrences of Sporadic Vestibular Schwannomas

Moran Amit¹, Diana Bell¹, Greg Fuller¹, Mohamed Aashiq¹, Gautam Mehta¹, Patrick J. Hunt¹, Paul W. Gidley¹, Shaan M. Raza¹, Franco DeMonte¹

¹The University of Texas MD Anderson Cancer Center, Houston, Texas, United States

Background: Vestibular Schwannomas (VS) are slow-growing, benign tumors that arise from the myelin-producing Schwann cells of the vestibular branch of CN VIII. Though benign, these tumors carry significant morbidity, primarily due to their close association with important nerves. They are usually sporadic and unilateral and comprise 8% of all intracranial tumors. The role of genetic and epigenetic alterations in sporadic VS is not well established. The current gold standard of treatment for these tumors is total surgical resection, though radiotherapy is also efficacious. Recurrence in patients undergoing subtotal resection (STR) approaches 90%, while recurrence with gross total resection (GTR) is >15% on follow-up >10 years. Previous surgical series examining sporadic VS have discussed recurrence risks through surgical, histological, and immunohistochemical perspectives. However, there is a paucity of literature focusing on the genetic mechanisms involved in the recurrence of schwannomas.

Objective: In this study, we use RNA-sequencing data to identify gene expression differences in early and late recurrences of VS and further identify the pathways associated with tumor recurrence. We aim to identify genes and their biologic pathways associated with recurrences in vestibular schwannomas.

Methods: We reviewed 20 patients surgically treated for CN VIII schwannomas in the 10-year period between 2005 and 2015 at our institution. Biopsies of their tumors were sequenced using an RNA-sequencing platform. Patient demographics, tumor characteristics, treatment modalities, pathologic data, and patient performance data were collected. Differential expression analysis of RNA-sequencing data was performed using EdgeR and DeSeq2 programs to determine the significant gene expression changes in our cohort of early versus late recurrences. The significant upregulated and downregulated genes were then matched for biologic pathways involved using REACTOME pathway analyzer.

Results: Our patients were predominantly females (60%), with a median age of 50 years (range, 29–71 years). Disease-free survival (DSS) ranged from 8 to 132 months of follow-up, with 65% of the patients developing recurrence in the allotted follow-up time. Gross total resection was accomplished in 15% of the patients, and we report a 100% disease-specific survival in our cohort. Gene expression analysis of these tumors uncovered 56 genes that were significantly upregulated or downregulated in our cohort. Thirty-one genes were involved in cellular signal transduction pathways, 21 genes in immune system function, 14 genes involved in transcription regulation, 9 genes involved in cell development, 6 genes involved in cellular metabolism, and 3 genes were involved in axonal guidance pathways (overlapping occurring).

Conclusion: These findings provide a framework to evaluate tumor recurrence risk in patients with schwannoma based on RNA-sequencing results. Our results implicate immune system dysregulation as an associated factor in early schwannoma recurrence, suggesting the potential for immunotherapy as a treatment for schwannomas. As sequencing technology becomes increasingly available, these findings can guide future treatment decisions regarding the extent of therapy, including both surgical resection and radiotherapy.

A119. Blood-Labyrinthine Barrier Permeability Assessed Using Postcontrast Delayed 3D-FLAIR MRI Imaging in Vestibular Schwannoma

Andrew J. Bowen¹, Michael L. Carlson¹, John I. Lane¹

¹Department of Otorhinolaryngology, Mayo Clinic, Rochester, Minnesota, United States

Background: The primary mechanism(s) driving hearing loss in untreated vestibular schwannoma (VS) remain controversial. Leading hypotheses include cochlear nerve or labyrinthine artery compression, cochlear nerve invasion, or compromise of fluid circulation in the fundus or cochlea. Delayed gadolinium enhanced three-dimensional fluid-attenuated inversion recovery (3D-FLAIR). MRI is a novel imaging technique that previously showed promise in evaluating the integrity of the blood-labyrinthine barrier (BLB). While delayed 3D-FLAIR imaging was previously used to investigate multiple pathologies of the inner ear, to date no current study has evaluated the technique in VS patients. This is the first study examining whether this imaging modality can provide valuable insight into the underlying pathophysiology driving audiovestibular injury in VS patients.

Methods: Patients under surveillance for small to medium-sized radiographically diagnosed VS were recruited. Consented patients received a standard dose of intravenous gadolinium and underwent MR imaging on a 3T MRI scanner, followed by repeat imaging 4 to 8 hours later. During each session, 3D-FLAIR imaging was performed generating pre-contrast, immediate (10 minute) postcontrast, and delayed (4–8 hours) images. Using image software, a region of interest

(ROI) was drawn around the cochlea and vestibule in both the ipsilateral and contralateral ears through its greatest diameter on 3D-FLAIR axial slices. From the ROI, signal intensity ratios (SIRs) were generated comparing inner ear structures on the tumor-affected side versus the nonaffected side. The difference in SIR from immediate to delayed images was compared through Wilcoxon ranked sum testing. Simple linear regression was used to assess any relationship between SIRs and pure tone averages (PTAs) of the tumor-affected ear and the degree of hearing asymmetry across ears through PTAs and word recognition score difference (Figs. 1 and 2).

Results: Five males and three females with a mean tumor size of 7.5 mm were included. Nearly all delayed 3D-FLAIR imaging demonstrated asymmetric enhancement of inner ear structures only occasionally seen on the tumor-affected side of immediate postcontrast scans. Mean cochlear SIRs for delayed imaging were significantly greater than the SIRs on immediate scans (1.91 vs. 1.21; $p < 0.05$). The mean vestibular SIR for delayed imaging was also significantly greater than the SIRs on immediate scans (1.74 vs. 1.15; $p < 0.05$). While linear regression showed increasing differences in PTAs from tumor-affected ear to nonaffected ear with greater SIRs, there was only a significant association with SIRs at the vestibule ($p < 0.05$). No significant correlations were found between immediate postcontrast image SIRs or SIRs and tumor characteristics or audiometric data ($p > 0.05$).

Conclusion: This is the first study to utilize delayed gadolinium MRI to assess BLB permeability in patients under observation for VS. Our study demonstrates that BLB permeability appears enhanced in the presence of VS. More investigations into the significance of these findings, as well as their potential clinical relevance are warranted.

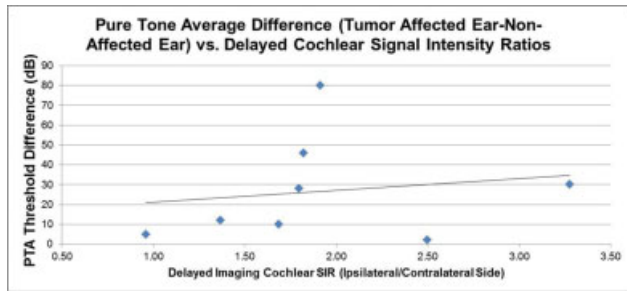


Fig. 1. PTA difference versus delayed cochlear SIR.

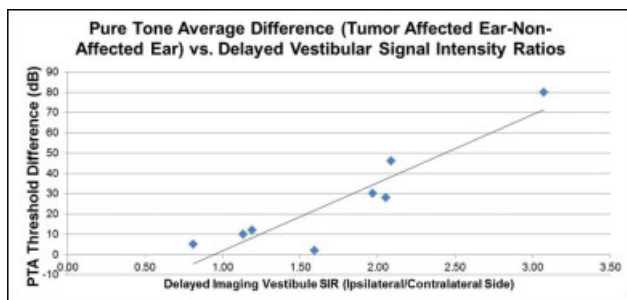


Fig. 2. PTA difference versus vestibular SIR.

A120. Emotional Lability as a Symptom of Extra-axial Posterior Fossa Tumors: A Case-Control Review of Neuroanatomy and Patient-Reported Quality of Life
 Swetha Prakash¹, Ryojo Akagami¹

¹University of British Columbia, Vancouver, Canada

Introduction: Emotional lability (EL), the uncontrollable and unmotivated expression of emotion, is a rare and distressing symptom of brainstem compression from extra-axial posterior fossa tumors. In all published case reports, EL is alleviated by surgical resection of the tumor. The primary goal of this study was to radiographically compare the degree of compression from mass lesions onto brainstem structures between EL cases and matched controls. We hypothesized that distortion of brainstem nuclei by mass lesions specifically in the basis pontis region causes EL. Because EL can be a significant social and professional burden, the secondary goal of the study was to compare acute changes in quality of life (QOL) survey scores pre- and postoperatively. We hypothesized that postoperative QOL improvements for patients with EL would be greater than those of matched non-EL control patients.

Methods: In a retrospective review of 673 patients treated for posterior fossa tumors with brainstem compression between 2002 and 2018 at Vancouver General Hospital, 11 patients with confirmed EL were identified. Each case was matched to three controls for tumor pathology, general tumor location, and time of surgical treatment (± 2 years). Cases and controls were homogeneously treated by the same fellowship-trained skull base neurosurgeon.

Neuroanatomy: Preoperative axial T2-weighted MRI scans were reviewed and a lateral brainstem compression scale (Fig. 1) was used to characterize the degree of mass effect at the level of the medulla, pons, and midbrain. Compression scale scores were compared between EL patients and control patients to identify which brainstem regions are implicated in the EL pathway. Variables including gender, age, handedness, tumor laterality, and tumor size were also compared.

QOL: Patients complete SF-36v1 surveys at clinic visits as standard of care. Preoperative and postoperative surveys were retrospectively obtained from patient charts. Gender, age, total survey scores, and survey subscores were compared.

Results: EL symptoms ceased postoperatively for all patients. A binomial logistic regression found that compared with the control group, EL-causing tumors occurred in younger patients (EL mean age = 38.1 years, control mean age = 51.3 years, two-tailed $p = 0.04$) and EL tumors exert greater compression onto the pons (EL mean compression score = 2.91, control mean compression score = 1.91, one-tailed $p = 0.03$). A linear mixed-effects model found that patients with EL-causing tumors experience greater improvement postoperatively in the “Role Limitations Due to Physical Health” (two-tailed $p = 0.02$) and “Overall Health Change” (two-tailed $p = 0.04$) sub-scores. Other tested variables remained consistent between groups.

Conclusion: This is the largest case series to date on adult extra-axial posterior fossa tumors that cause EL. The neuroanatomy results suggest that compression onto the pons inhibits control over involuntary, stereotyped expression of emotion. This study adds to the body of evidence that EL may be attributed to deafferentation of the cerebellum from cortical and limbic structures through the basis pontis, leading to impaired modulation of emotional response. The QOL results suggest that increased improvement for EL patients in the “Role Limitations Due to Physical Health” and “Overall Health Change” QOL subcategories augments the benefits of obtaining EL-alleviating surgery.

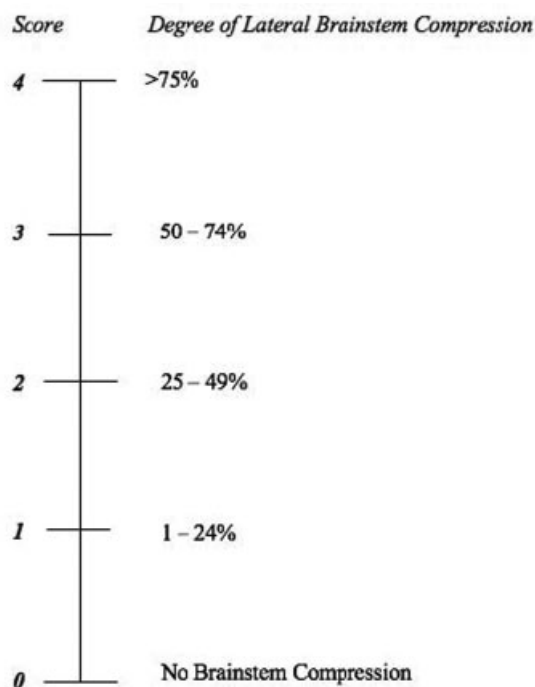


Figure 1. Lateral brainstem compression scale.

A121. Validation of the Skull Base Inventory Quality of Life Questionnaire in a Multi-institutional Prospective Cohort Study of Patients Undergoing Open and Endoscopic Skull Base Surgery

David Forner¹, Katrina Hueniken¹, Tom Yoannidis¹, Ian Witterick¹, Eric Monteiro², Allan Vescan¹, Gelareh Zadeh³, Patrick Gullane¹, Carl Snyderman⁴, Eric Wang⁴, Paul Gardner⁴, Benita Valappil⁵, Dan Fliss⁶, Barak Ringel⁶, Ziv Gil⁷, Shorook Na'ara⁷, Nidal Muhanna⁶, Eng Ooi⁸, David Goldstein¹, Fred Gentili¹, John de Almeida¹

¹Department of Otolaryngology—Head & Neck Surgery, University Health Network, Toronto, Ontario, Canada

²Department of Otolaryngology—Head & Neck Surgery, Sinai Health System, Chicago, Illinois, United States

³Department of Neurosurgery, University Health Network, Toronto, Ontario, Canada

⁴Department of Neurosurgery, University of Pittsburgh Medical Center, Pittsburgh, Pennsylvania, United States

⁵University of Pittsburgh Medical Center, Pittsburgh, Pennsylvania, United States

⁶Department of Otolaryngology—Head & Neck Surgery, Tel-Aviv Sourasky Medical Center, Tel-Aviv-Yafo, Israel

⁷Department of Otolaryngology—Head & Neck Surgery, Rambam Medical Center, Haifa, Israel

⁸Department of Otolaryngology—Head & Neck Surgery, Flinders Medical Centre, Bedford Park, Australia

Background: Surgical treatment for skull base neoplasms has seen much advancement over the past two decades. Oncological outcomes have steadily improved and are well understood. However, sound knowledge of the quality of life (QOL) in patients treated for these neoplasms is lacking. The Skull Base Inventory (SBI) was developed as a

means to better assess QOL in patients with anterior and central skull base neoplasms treated by both endoscopic and open approaches. Previous studies have shown satisfactory psychometric properties of the SBI in cross-sectional analysis, but none have yet reported gold-standard prospective reliability and validity measures.

Methods: The current study is part of a multicenter, prospective cohort study examining endoscopic and open procedures from 2012 to 2018. The SBI is a 11-domain questionnaire with 41 items, previously generated through chart review, systematic review, expert opinion, and patient focus groups, with item reduction through an impact score method. The SBI was administered at several time points, including preoperatively, 2-weeks postoperatively, and 3, 6, and 12-months postoperatively. Reliability of the SBI was assessed through test-retest and internal consistency. Concurrent validity was assessed through comparison with the Anterior Skull Base (ASB) questionnaire and the Sinonasal Outcome Test (SNOT-22). Convergent validity was assessed through comparison of five global QOL ratings (ranging from “much worse” to “much better”). Discriminative validity was assessed by comparing SBI score between the preoperative time period and the acute postsurgical period (2-weeks). The minimally important clinical difference was determined as the mean change in SBI score in patients who rated their symptoms as “a little better” or “a little worse.”

Results: One-hundred eighty-seven patients were included across five centers, with 121 having an endoscopic procedure. The mean age was 53.5 years, and the majority of patients were female (60%). Internal consistency was excellent (Cronbach's $\alpha = 0.95$). Test-retest at 12-months and 12-months plus 2 weeks was also excellent (intraclass correlation > 0.90) in all SBI domains except two. Concurrent validity was demonstrated by the presence of a very strong correlation, at all-time points, between total SBI scores and ASB scores (range of $r = 0.810-0.869$, $p < 0.001$), and moderate correlation of the nasal domain SBI scores with SNOT-22 scores (range of $r = -0.616$ to -0.738 , $p < 0.001$). Convergent validity was demonstrated by the presence of a moderate correlation of the mean change in SBI scores with the global QOL ratings from preoperative to 1-year postoperative ($r_s = 0.4942$, $p < 0.001$). The SBI demonstrates discriminative validity, showing significant mean differences between the preoperative and 2-week periods, for total scores and seven of the domains (emotional, family, financial, social, nasal, neurologic, and other). Lastly, the minimally important clinical difference was determined to be 6.0 out of a possible 100.

Conclusion: The SBI questionnaire is reliable and valid for patients treated with endoscopic and open approaches for anterior skull base neoplasms, and can be used for assessment of QOL in this setting.

A122. Assessment of Psychological Well-Being in Nasopharyngeal Carcinoma Survivors

Kira A. Murphy¹, Chandala Chitguppi¹, Alexander Graf², Tawfiq Khoury¹, James J. Evans³, Marc R. Rosen¹, Gurston G. Nyquist¹, Mindy Rabinowitz¹

¹Department of Otolaryngology—Head and Neck Surgery, Thomas Jefferson University Hospital, Philadelphia, Pennsylvania, United States

²Thomas Jefferson University, Philadelphia, Pennsylvania, United States

³Thomas Jefferson University Hospital, Philadelphia, Pennsylvania, United States

Background: Nasopharyngeal cancer patients have high levels of psychological morbidity after treatment due

to factors including the sequelae of chemoradiation. Our objective is to assess self-reported psychological symptoms, quality of life, and social support in patients treated for nasopharyngeal carcinoma, and to identify correlates within patient histories.

Methods: We conducted a cross-sectional cohort study, collecting patient-reported inventories of emotional distress (Hospital Anxiety and Depression Scale, HADS), cancer-related quality of life (Functional Assessment of Cancer Therapy-Nasopharyngeal Cancer, FACT-NP), and social support (Medical Outcomes Study Social Support Scale, MOS-SS scale). We conducted a retrospective chart review of patient demographics, pathology, and treatment data. HADS (scored on a scale from 0 to 28) scores of 7 or more prompted referral for psychiatric care. Spearman's rho was used to assess correlation between scales. Patients belonging to two groups—those who did and those that did not require psychiatric referral—were compared.

Results: A total of 14 patients were included. Median age at treatment was 58 years (range, 35–72), and median time from treatment completion to survey was 3.8 years (1.1–14.1). Ten patients (71%) had advanced stage (III/IV) disease. Thirteen patients (93%) were treated with definitive chemoradiation. Mean total HADS score was 10.36 ± 6.7 , depression (D) component mean was 5.21 ± 3.3 , and anxiety (A) component mean was 5.14 ± 4.2 . 5 patients (36%) were referred for psychiatric care due to elevated HADS scores, of whom one patient declined with no plans for treatment, two were receiving treatment already, and two accepted referral. Age, gender, race, smoking hx, skull base invasion, tumor histology (squamous vs. non squamous cell carcinoma), TNM stage, and recurrence were comparable between the groups. Total HADS score inversely correlated with both the emotional ($r_s = -0.687$, $p = 0.028$) and tumor site-specific concern ($r_s = -0.667$, $p = 0.035$) subscales of FACT-NP. MOS-SS also negatively correlated with HADS ($r_s = -0.738$, $p = 0.023$). None of the functional, physical, or social subscales showed a strong correlation to HADS score. There was no strong association between any of the FACT-NP subscales with the MOS social support scale, or between any two of the FACT-NP subscales.

Conclusion: Quality of life and social support play key roles in psychological outcomes of nasopharyngeal cancer patients. There were no identifiable differences in psychological well-being in any specific patient demographic, highlighting the importance of continued monitoring in the surveillance period of all NPC patients. Notably, time from treatment did not show an association, indicating that psychological sequelae tend to be persistent.

A123. Sinonasal Outcomes after Pituitary Surgery in Patient's with Cushing's Disease

Nadeem R. Kolia¹, Paul A. Gardner¹, Carl H. Snyderman¹, Eric W. Wang¹

¹University of Pittsburgh Medical Center, Pittsburgh, Pennsylvania, United States

Background: Endoscopic endonasal skull base surgery is a common treatment intervention for pituitary tumors, with minimal sinonasal morbidity after the initial postoperative healing period. However, patients with Cushing's disease may represent a subgroup of these patients who may demonstrate poor healing due to their endocrinopathy.

Objectives: The aim of the study is to investigate if patients with Cushing's disease have worse sinonasal outcomes after endoscopic endonasal skull base surgery compared with patients without Cushing's disease.

Methods: We identified patients with Cushing's disease who had undergone endonasal endoscopic skull base surgery at our institution between December 1, 2016 and April 31, 2019. Case-controls patients with pituitary tumors were matched by age, gender, and the extent of endoscopic approach. Patients with prior surgical or radiation treatment were excluded, as were patients with chronic rhinosinusitis. A retrospective chart review was conducted for all included patients. The primary outcome was the 22-item Sino-Nasal Outcome Test (SNOT-22) scores collected at 1, 3, and 6 months postoperatively. Statistical analysis of data was performed using a two-tailed *t*-tests. *p*-Values less than 0.05 were considered significant.

Results: Ten patients with Cushing's disease met the selection criteria and were included in the study. Seventeen case controls were selected for comparison. Comparing patients with Cushing's to the controls, there was no difference in postoperative SNOT-22 score at 1 month (30.8 ± 28.5 vs. 25.9 ± 18 , $p = 0.71$) and at 3 months (26.4 ± 24.6 vs. 17.7 ± 12.9 , $p = 0.21$). However, at 6-months postoperatively, SNOT-22 scores were significantly higher in patients with Cushing's disease (28.8 ± 23.2 vs. 3.0 ± 2.2 , $p = 0.04$). **Fig. 1** shows SNOT-22 scores over time. While SNOT-22 scores improved from 1 month to 6-months postoperatively in patient's without Cushing's ($p < 0.01$), in patients with Cushing's disease scores were not significantly different at 1 and 6 months postoperatively ($p = 0.71$).



Fig. 1 SNOT-22 scores of patients with Cushing's disease.

Conclusion: Patients with and without Cushing's disease have similar initial postoperative SNOT-22 scores after endoscopic endonasal skull base surgery. Control patients show a return to baseline SNOT-22 scores after 6 months while in patients with Cushing's disease, these scores remain fairly stagnant and do not improve over time. This suggests that the endocrinopathies associated with Cushing's disease impair postoperative wound healing with resulting sinonasal morbidities.

A124. Quality from the Patient's Perspective: Implementation of an Established Patient-Reported Outcome Platform in a Multidisciplinary Skull Base Tumor Clinic

Stephanie Flukes¹, Jennifer Cracchiolo¹, Eliza Geer¹, David Goldstein², John De Almeida², Vivian Tabar¹, Marc A. Cohen¹

¹Multidisciplinary Pituitary and Skull Base Program, Memorial Sloan Kettering Cancer Center, New York, New York, United States

²Department of Otolaryngology Head & Neck Surgery, Princess Margaret Cancer Centre, Toronto, Ontario, Canada

Background: Utilization of patient-reported outcomes (PROs) in clinical care for skull base tumor patients treated in a multidisciplinary management team has been proposed to focus on outcomes most important to patients and to enhance shared decision making. Specific options for treatment, including endoscopic and open surgery as well as chemoradiation have both acute and long-term sequelae. Identification of how these treatments impact the individual patient has implications for both quality of care and the value of the treatment provided.

Objective: The aim of the study is to assess the ability to implement real time PROs on an electronic platform within a multidisciplinary skull base clinic.

Methods: Descriptive analysis of implementation of PROs for the skull base tumor program at a cancer center is given. Two validated instruments, the Skull Base Inventory (SBI), developed at the Princess Margaret Cancer Center, Toronto, CA and/or Head and Neck Patient Reported Outcomes (HNPROs) developed at Memorial Sloan Kettering Cancer Center, NY, NY were administered at baseline, after intervention, and at follow-up visits. All patients treated for sinonasal, pituitary, or anterior skull base pathology are eligible for electronic PROs assessment as a part of standard of care within a larger initiative of the Head and Neck Service at MSKCC.

Results: Since July 2018, patients with pituitary, nasal cavity, and ethmoid pathology have received the SBI and those with malignancies of the maxillary sinus (or other head and neck malignancy) received the HNPROs. Automatic "time out" information technology settings prevent delivery of duplicate surveys. ICD-10 diagnosis codes were used to allow for domain-specific questionnaires based on the specific subsites. For example, a patient with a diagnosis of maxillary sinus cancer will receive questions that include inquiry about numbness, rhinorrhea, epiphora, vision, facial appearance, and cancer worry. Graphical reports provide representation of domains over time. From July 1, 2018 to July 1, 2019, 91 of 124 possible patients with anterior skull base pathology have submitted surveys within a broader context of 2,723 of 3,758 head and neck cancer (nonthyroid) patients having submitted surveys. A total of 76% completed the module on the institutional patient portal and 24% completed on a tablet at the time of physician visit. Median time to completion was 5 minutes.

Conclusion: Integration of electronic sinonasal, pituitary, and skull base PROs as part of a multidisciplinary management team is feasible. This has the potential to provide important patient-specific data that can educate patient and clinician alike and assist in decision making. Over time, normative data can be gleaned to demonstrate what a large population of patients have experienced at different time points when pursuing specific treatment options. This can ultimately improve the quality of care and value provided per intervention.

A125. Comparing Sinonasal Outcomes between Functional and Nonfunctional Pituitary Lesions after Endoscopic Sellar and Parasellar Surgery

Yossawee Wangworawut¹, Kawinyarat Jitaroon¹, Peter H. Hwang¹, Jayakar Y. Nayak¹, Juan Fernandez-Miranda¹, Robert Dodd¹, Zara M. Patel¹

¹Stanford University, Stanford, California, United States

Background: Pituitary tumors can be divided into functional and nonfunctional lesions. The systemic effects of pituitary hormones are well-known but local effects in the sinonasal region are not well characterized. We aimed to examine the difference in sinonasal outcomes between functional and nonfunctional pituitary lesions after endoscopic surgical resection.

Methods: We performed a retrospective review of 304 patients presenting to a tertiary skull base center between 2014 and 2019, with a pituitary lesion who received endoscopic sellar or parasellar surgical resection. This population was then divided into nonfunctional and functional groups. We examined both surgical outcomes, as well as pre- and postoperative quality of life scores between the two groups.

Results: High cortisol and GH levels were associated with significant preoperative nasal findings ($p < 0.05$). Preoperative total SNOT 22 scores were not different between the two groups, but the rhinologic and extrarhinologic subdomain scores in the functional group was higher than in the nonfunctional group (3.57 ± 3.95 vs. 2.58 ± 3.64 , and 1.48 ± 2.2 vs. 0.92 ± 1.75 , respectively; $p = 0.038$ and 0.017). Postoperative SNOT 22 score improvement was significantly greater in the functional group at 6-weeks post-operation (6.75 ± 17.51 vs. 1.4 ± 16.83 , respectively; $p = 0.011$). This was true in both rhinologic and extrarhinologic subdomain scores (4.79 ± 5.93 vs. 2.83 ± 5.98 , and 1.74 ± 2.72 vs. 0.91 ± 2.87 , respectively; $p = 0.008$ and 0.018). Time to complete normalization on nasal endoscopy was longer in the functional group compared with the nonfunctional group ($p = 0.018$).

Conclusion: Functional pituitary tumors are associated with preoperative sinonasal changes, particularly corticotrophic and somatotrophic tumors. These changes affect quality of life both pre- and postoperation, in both rhinologic and extrarhinologic subdomains of the SNOT-22. Patients with functional tumors took longer to reach full healing and normalization of the sinus cavity postoperatively.

A126. Internal Neurolysis for the Treatment of Trigeminal Neuralgia: Systematic Review

Victor Sabourin¹, Jacob Mazza¹, Jeffery Head¹, Pascal Lavergne¹, Tomas Garzon¹, Anthony Stefanelli¹, Fadi Al-Saiegh¹, James Evans¹

¹Thomas Jefferson University Hospital, Philadelphia, Pennsylvania, United States

Introduction: Trigeminal neuralgia (TN) is a pain syndrome commonly treated with microvascular decompression when an offending vessel is identified. However, internal neurolysis (IN) has become increasingly utilized as an adjunct or standalone therapy when no neurovascular compression (NVC) is identified, or as a salvage procedure for TN unresponsive to other treatment modalities.

Methods: A literature search was performed using the search terms: "Trigeminal Neuralgia, Neurolysis," "Trigeminal Neuralgia, Internal Neurolysis," and "Trigeminal Neuralgia, Microvascular Decompression, Neurolysis" resulting in 57 articles. After accounting for duplicates, eliminating non-English articles, and screening by title to remove alternative methods of treatment, a total of 17 articles remained. Articles

without a case series or that did not differentiate the results of IN from other treatments were excluded. Nine articles were considered for final analysis in the systematic review (Table 1). PRISMA guidelines were followed for the systematic review (Fig. 1).

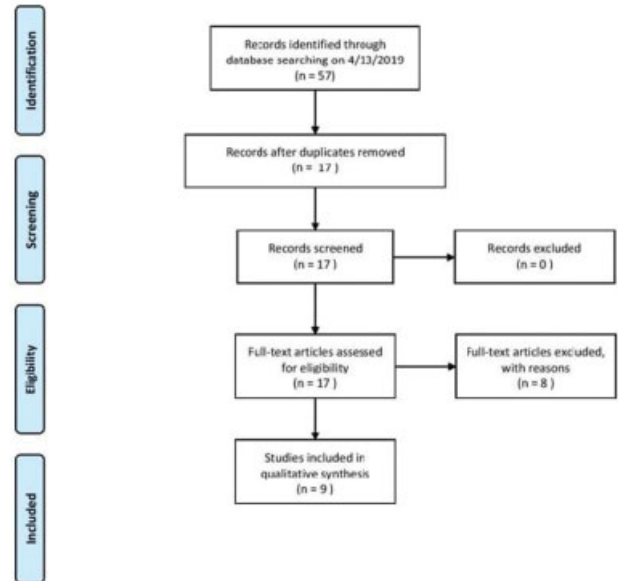
Results: A total of 459 patients were included in the 9 studies, 323 (70.4%) of whom underwent an IN. With a mean/median range of follow-up of 12 to 90 months, results for Barrow Neurological Institute–Pain Score (BNI-PS): I: immediate postoperative rates ranged: 85 to 94.6%, 1-year rates ranged: 58 to 78.4%, and overall rates ranged: 47 to 82.1%. Results for BNI-PS: I/II showed: immediate postoperative rates ranged: 96 to 100%, 1-year rates ranged: 77 to 93.75%, and overall rates ranged from: 62.5 to 87.1%. Results for BNI-PS: I-III showed: immediate postoperative rates ranged: 96 to 100%, 1-year rates ranged: 80 to 93.75%, and overall rates ranged from: 80 to 100% (Fig. 2). The recurrence of any pain at 1-year ranged from: 3.92 to 42%, and overall rates ranged from: 3.6 to 50%. When considering significant recurrence of pain as BNI-PS: I/II → III–V the 1-year recurrence rates ranged from: 3.92 to 17%, and overall recurrence rates ranged from: 3.6 to 25% (Fig. 3).

Conclusion: IN represents a reasonable primary or secondary treatment option for TN with low grade or no NVC. Pain control rates seem comparable to standard MVD, but more data on long-term outcomes are needed to assess the durability of the intervention.

Author/Year	Article
Wu et al./2018	Outcome of Internal Neurolysis for Trigeminal Neuralgia without Neurovascular Compression and Its Relationship with Intraoperative Trigemino-cardiac Reflex.
Hussain et al./2018	Re-Exploration of Microvascular Decompression in Recurrent Trigeminal Neuralgia and Intraoperative Management Options.
Liang et al./2017	A retrospective study of neurocombing for the treatment of trigeminal neuralgia without neurovascular compression.
Zhao et al./2017	Nerve Combing for Trigeminal Neuralgia Without Vascular Compression.
Zhang et al./2017	Long-Term Efficacy of Nerve Combing for Patients with Trigeminal Neuralgia and Failed Prior Microvascular Decompression.
Zhou et al./2016	Comparison of nerve combing and percutaneous radiofrequency thermocoagulation in the treatment for idiopathic trigeminal neuralgia.
Ko et al./2015	Long-term efficacy and safety of internal neurolysis for trigeminal neuralgia without neurovascular compression.
Jie et al./2013	The long-term outcome of nerve combing for trigeminal neuralgia.
Ma et al./2009	"Nerve combing" for trigeminal neuralgia without vascular compression: report of 10 cases.

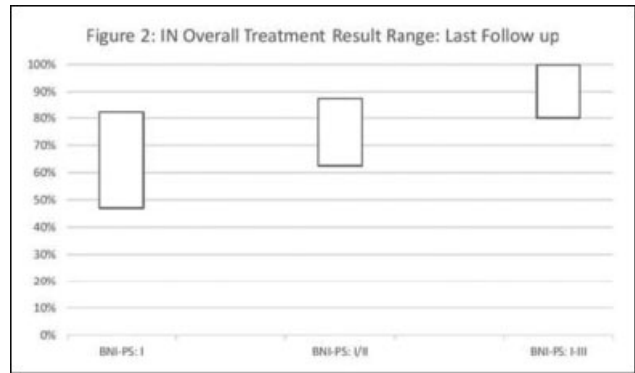


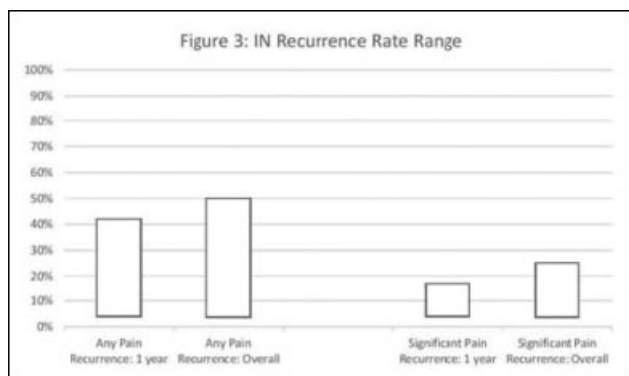
PRISMA Flow Diagram



From: Moher D, Liberati A, Tetzlaff J, Altman DG, The PRISMA Group (2009). Preferred Reporting Items for Systematic Reviews and Meta-Analyses: The PRISMA Statement. *PLoS Med* 6(7): e1000097. doi:10.1371/journal.pmed.1000097

For more information, visit www.prisma-statement.org.





A127. Ergonomics in Endoscopic Transsphenoidal Surgery: A Survey of the North American Skull Base Society

Pier Paolo Mattogno¹, Davide Mattavelli², Filippo Marciano³, Michael P. Catalino⁴, Alberto Schreiber², Paola Cocca³, Piero Nicolai², Jr. Edward R. Laws⁴, Ian Witterick⁵, Shaan M. Raza⁶, Anand K. Devaiah⁷, Liverana Lauretti¹, Alessandro Olivi¹, Marco M. Fontanella⁸, Fred Gentili⁹, Francesco Doglietto⁸

¹Department of Neurosurgery, Agostino Gemelli Foundation, Rome, Italy

²Division of Otorhinolaryngology, Department of Medical and Surgical Specialties, Radiological Sciences and Public Health, University of Brescia, Brescia, Italy

³Department of Mechanical and Industrial Engineering, University of Brescia, Brescia, Italy

⁴Pituitary and Neuroendocrine Center, Department of Neurosurgery, Brigham and Women's Hospital, Harvard Medical School, Boston, Massachusetts, United States

⁵Department of Otolaryngology-Head and Neck Surgery, University of Toronto, Toronto, Ontario, Canada

⁶Department of Neurosurgery, The University of Texas MD Anderson Cancer Center, Houston, Texas, United States

⁷Department of Otolaryngology-Head and Neck Surgery, Boston University School of Medicine, Boston Medical Center, Boston, Massachusetts, United States

⁸Division of Neurosurgery, Department of Medical and Surgical Specialties, Radiological Sciences and Public Health, University of Brescia, Brescia, Italy

⁹Department of Neurosurgery, Toronto Western Hospital, University of Toronto, Toronto, Ontario, Canada

Background and Objective: Different surgical set-ups have been described for endoscopic transsphenoidal surgery (ETS), but studies on their ergonomics are limited. The aim of this paper is to describe present trends in surgical positioning and other ergonomics aspects of ETS.

Methods: A 33-question, web-based survey was administered to North American Skull Base Society members from January to April 2018.

Results: Out of 116 respondents, 107 reported being involved in ETS (92%) and 93 completed the survey (response rate: 87%). Most respondents were from North America (76%) in academic practice (87%), not in training (91%) and neurosurgeons (65%). Most (73%) had more than 5-year experience in ETS, received specific training (66%), and performed at least five procedures/month (55%). Mean reported time for standard and complex procedures were 3.7 and 6.3 hours, respectively. Most use image guidance (84%), use a binostri technique and work with a partner (95%). The most frequent position of the first surgeon during tumor removal is: standing (94%), holding suction (89%), and dissector (83%) or

grasping forceps (38%). In some set-ups the endoscope is held by the primary surgeon (22–24%). Usually, the second surgeon holds the endoscope (72%) and irrigation (42%) or suction (37%). Most respondents position the patient in a supine position, with the head in neutral position (46%) or rotated to the side (38%). During tumor removal surgeons stand on the same side (65–66%). Most (81%) tailor surgery for ergonomic considerations and select instruments accordingly (92%). Surgical factors that are considered important for maximizing ergonomics in addition to surgical access and visualization include: sphenoidotomy (71%), septectomy (69%), removal of sphenoid septa, and sellar opening (67%) and dural opening (51%). Patient-specific factors include: modification of middle turbinate (53%) and need of septoplasty (31%). The most looked-at ergonomic attendances are: height of table/bed head (86%), monitor placement (80%), attention to posture (60%), and patient position adjustments during surgery (50%). Many respondents report strain at the dorso-lumbar (50%) or cervical (26%) level. Almost one-third incorporates a pause during surgery to stretch and move. Half of the respondents engage in physical activity to be fit for surgery and 16% sought medical attention for ergonomic-related symptoms.

Conclusion: Most responders value ergonomics as an element to be taken into consideration for ETS. The variability in surgical set-ups and the relatively high report of complaints underline the need of studies to optimize ergonomics in endoscopic transnasal skull base surgery.

A128. Stenting for Prevention of Carotid Blowout Syndrome in High-Risk Head and Neck Cancer Patients

Bradley Kolb¹, Andre Beer-Furlan¹, Bledi Brahimaj¹, Hormuzdiyar Dasenbrock¹, Samer Al-Khudari¹, Demetrius Lopes², Michael Chen¹, R. Webster Crowley¹

¹Rush University Medical Center, Chicago, Illinois, United States

²Advocate Aurora Health, Aurora, United States

Background: Carotid blowout syndrome is a surgical emergency caused by structural compromise of the extracranial carotid artery either due to local invasion from head and neck malignancies or to secondary effects from radiotherapy, resulting in uncontrolled hemorrhage. Patients with newly diagnosed nonresectable head and neck cancers with involvement of the carotid artery may benefit from prophylactic stenting to prevent carotid blowout. Prophylactic carotid stenting may also benefit patients already treated for advanced head and neck cancer presenting with newly observed disease progression or threatened carotid blowout.

Objective: The study aims to report outcomes from a single institution experience with prophylactic endovascular stent-reconstruction of the extracranial carotid artery in head and neck cancer patients with at high risk for carotid blowout syndrome.

Methods: A retrospective review of the electronic medical record was conducted to identify patient characteristics, laboratory findings, devices used, complications, imaging, and clinical follow-up data for patients with head and neck cancers undergoing prophylactic stenting of the extracranial carotid artery at Rush University Medical Center between 2012 and 2019.

Results: Twelve patients underwent prophylactic carotid artery stent placement, with average age 59 (range = 32–71). All twelve patients (100%) had invasive squamous cell carcinoma of the head or neck judged to be advanced based on clinical staging. Eight patients (66%) had locally advanced stage II or III disease, while four (33%) had metastatic stage IV disease. Two (17%) patients received prophylactic stenting prior to any other treatment, while two (17%)

patients received radiation therapy, but no surgery prior to stenting. The remaining eight (66%) patients all received surgical resection and radiotherapy prior to stenting. One patient was unable to receive proper stent placement due to anatomic tortuosity. This patient was also the only of the twelve to experience intraoperative complications. One patient died 4 days following stent placement from nonprocedure-related causes. One was lost to follow-up. Of the remaining nine patients, mean length of follow-up was 11.6 months (range = 1–43 months). All nine received postoperative imaging that demonstrated patent stents. Three patients (25%) received radiation postprocedure. One patient experienced hemorrhage from the stented artery 31 months after placement and 30 months after radiation therapy, which was treated with the placement of additional covered stents.

Conclusion: Endovascular stent reconstruction of the extracranial carotid artery represents a safe and effective method for preventing carotid artery blowout in patients with advanced head and neck cancers.

A129. Surgical Outcomes with Midline versus Lateral Approaches for Skull Base Chordomas: A Systematic Review and Meta-Analysis

Devi P. Patra¹, Ryan Hess¹, Evelyn Turcotte¹, Matthew Welz¹, Rudy Rahme¹, Tanmoy Maiti¹, Karl Abi-Aad¹, Ahmed AlMekawi¹, Sameer Keole¹, Devyani Lal¹, Michael Marino¹, Maciej Mrugala¹, Alyx Porter¹, Sujoy Vora¹, Bernard R. Bendok¹
¹Mayo Clinic, Phoenix, Arizona, United States

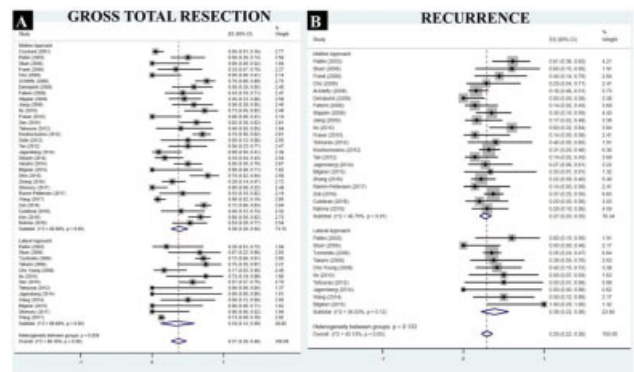
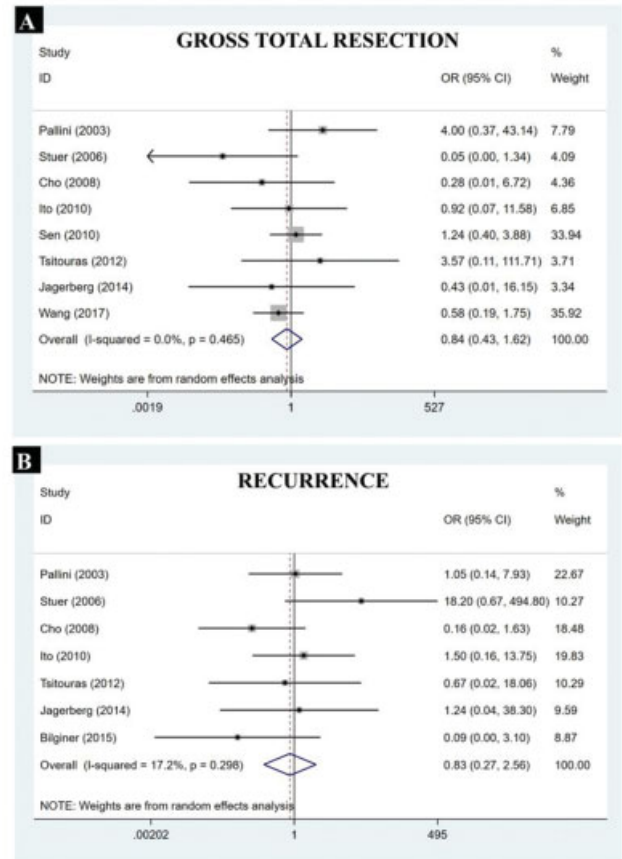
Objective: Skull base chordomas are complex lesions centered on the clivus with or without multicompartmental extension, and surgically can be approached both from a midline or lateral corridor. The present study aimed to compare the surgical outcomes of skull base chordomas from midline versus lateral approaches by conducting a systematic review of the literature and meta-analysis.

Methods: A systematic review and meta-analysis was conducted using the PRISMA protocol. Electronic database search was performed to identify studies between the years 2000 and 2018. The primary outcome was gross total resection rate (GTR). The secondary outcomes were recurrence rate at last follow-up, rate of cerebrospinal fluid (CSF) leak, and new cranial nerve palsy. Odds Ratios (ORs) were calculated using Mantel-Haenszel random effect model for each outcome using studies describing both approaches. An indirect (proportion) meta-analysis was performed pooling all studies describing either of the approaches. Individual patient data were analyzed to see difference in GTR or recurrence rate with different tumor extensions.

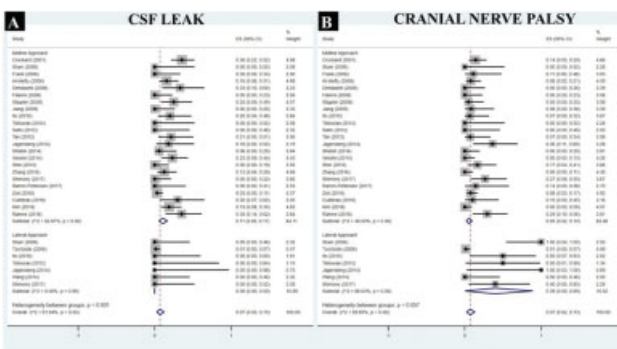
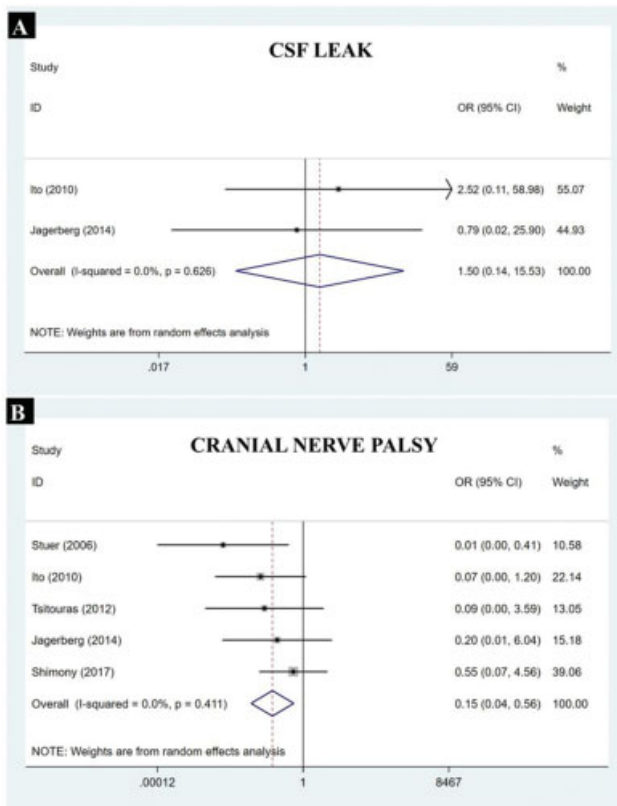
Results: Total 33 and 10 studies comprising a total of 951 and 406 patients were found suitable for indirect and direct meta-analysis, respectively. Various midline approaches included endonasal, transoral, transmaxillary and approaches, and lateral approaches included pterional, orbitozygomatic, retrosigmoid, transpetrosal approaches, etc. The overall odds of having GTR with midline approach as compared with lateral approach was found to be 0.83 (95% CI: -0.43 to 1.62; Fig. 1). The pooled estimates for GTR in midline and lateral approaches were 38 and 34%, respectively ($p = 0.84$; Fig. 2). The ORs for recurrence, CSF leak, and new cranial nerve palsy were 0.82 (95% CI: 0.26–2.56), 1.49 (95% CI: 0.14–15.5), and 0.14 (95% CI: 0.04–0.56), respectively (Figs. 1 and 3). The pooled estimates with midline versus lateral approaches for recurrence was 27 versus 38% ($p = 0.13$); for CSF leak was 11% versus 0% ($p \leq 0.001$) and for cranial nerve palsy was 5 versus 39% ($p = 0.06$; Figs. 2 and 4). With individual patient data analysis, the difference in GTR or recurrence rates between the two approaches did not

reach to significance with different tumor extensions, although the GTR rate was double with lateral approaches (51 vs. 25%) in patients with significant lateral extension.

Conclusion: The current meta-analysis failed to show any significant difference in overall GTR or recurrence rates between the midline versus lateral approaches for skull base chordomas. Tumor extension to different compartments did not affect the GTR or recurrence rates, although lateral approaches showed a slight nonsignificant better resection rate in tumors with significant lateral extension. In terms of complications, CSF leak rate was higher in midline approaches in contrast to the postoperative cranial nerve palsy which was higher in lateral approaches.



This document was downloaded for personal use only. Unauthorized distribution is strictly prohibited.



A130. Computed Tomography Findings of Bony Anterior Cranial Base Erosion as a Predictor of Pathologic Cranial Base Invasion in Sinonasal Malignancies

Tawfiq Khoury¹, Aarti Agarwal¹, Pascal Lavergne¹, Chandala Chitguppi¹, James J. Evans¹, Mindy Rabinowitz¹, Gurston Nyquist¹, Marc Rosen¹

¹Thomas Jefferson University, Philadelphia, Pennsylvania, United States

Introduction: Sinonasal malignancies are a group of tumors which tend to be diagnosed late in their disease course and can invade the surrounding cranial base and orbit.

With ever-improving imaging and endoscopic techniques, detailed information about the extent of sinonasal tumor involvement is increasingly available prior to treatment planning. This study evaluates bony erosion of the anterior cranial base (ACB) seen on high resolution computed tomography (CT) in predicting tumor involvement of the bone of the ACB on final histopathology.

Methods: Patients with sinonasal malignancies were identified from 2006 to 2019. Patients were included if they underwent endoscopic surgery and radiographic, pathological, and operative data were available for review in the medical record. Operative reports, CT images, CT reports, and histopathology reports of each patient were reviewed. Binary test classification functions were then calculated to evaluate ACB erosion on CT as a predictor of histopathologic ACB involvement.

Results: Forty-nine patients were identified who met inclusion criteria. On CT, 37 of those patients were noted to have bony erosion of the ACB, and 12 patients were noted to have tumors abutting, but not eroding the ACB. Of the patients with bony erosion on CT, 13 patients were noted to have evidence of intracranial tumor. One patient without bony erosion of the ACB on CT was found to have ACB involvement on histopathology. All 13 patients with intracranial tumor on CT were noted to have positive bone or dura on final histopathology. Of the patients with bony erosion, but no intracranial tumor noted on CT 13 (54.1%) had positive ACB bone or dura on final histopathology, while 11 did not. On CT, bony erosion of the ACB without intracranial extension was found to be 92.7% (95% CI: 66.1–99.8%) sensitive for the involvement of bone or dura on final histopathology, but only 47.6% specific (95% CI: 25.7–70.2%). Surgical intraoperative assessment of the ACB was both more sensitive and specific at predicting final histopathology than CT findings, but differences were not statically significant. (Sensitivity 100% CI: 80.49–100% and specificity: 59.09% CI: 36.35–79.29%).

Conclusion: About half of the patients in our cohort with bony erosion, but no evidence of intracranial tumor on CT, did not ultimately have tumor involving the ACB or dura on final histopathology. Despite this, surgeons should be prepared to resect bone, dura, and intracranial structures if necessary for complete oncologic resection. Patients without erosion but tumor abutment of the ACB on CT scan are unlikely to have tumor involvement of the bone and dura on final histopathology. Advances in endoscopic ACB surgery allow detailed intraoperative assessment of tumor margins and attachment points, and may provide surgeons with an opportunity to achieve a more complete oncologic resection while preserving intracranial structures.

A131. Sinonasal Malignant Melanoma and the Orbit
Justin N. Karlin¹, Mark Jameson², Steven A. Newman²

¹UCLA, Los Angeles, California, United States

²UVA, Charlottesville, Virginia, United States

Introduction: Primary sinonasal melanoma (PSM) is thought to arise from mucosal melanocytes, which in turn are of neural crest origin. Mucosal melanoma is rare, comprising less than 1% of all melanomas; and Ff all nasal cavity and sinus malignancies, melanoma comprises 6%. Mutations in NRAS, KIT, and BRAF are commonly seen in this disease. Survival is poor and case series in the literature report 5-year survival between 14 and 33%. We review here 19 cases of PSM and examine whether direct extension to the orbit is a poor prognostic factor.

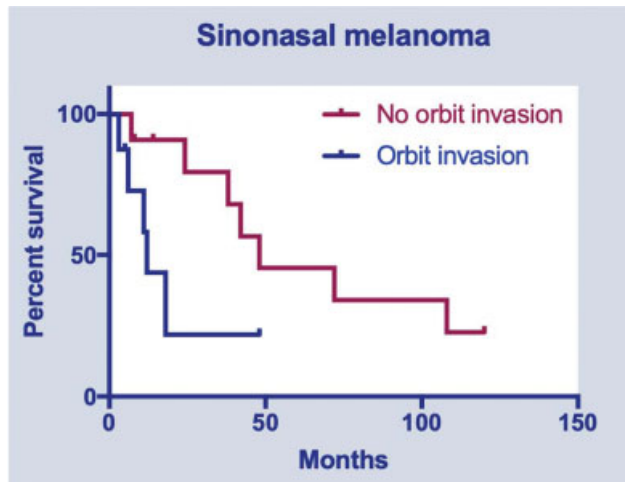
Methods: In this retrospective case series, we examined 19 patients (13 women and 6 men) with nasal cavity or sinus melanoma. We excluded patients with oral or

This document was downloaded for personal use only. Unauthorized distribution is strictly prohibited.

pharyngeal melanoma. We review demographics, clinical features, and Kaplan–Meier survival data comparing patients with direct orbit extension versus those without evidence of orbital disease.

Results: In this series, PSM arose from the paranasal sinuses in 8/19 (42%) and in the nasal cavity in 11/19 (58%). Median age at diagnosis was 71 years. All patients presented with nasal congestion or epistaxis or both. The most common orbital signs were diplopia, proptosis, tearing, and pain. Local extension of tumor into the orbit was noted in nine patients. Sinus melanoma (6/8, 75%) invaded the orbit more frequently than nasal cavity melanoma (3/11, 27%). Seven patients were lost to follow-up. For patients with complete follow-up, the median survival for patients without orbital extension ($n = 7$) was 48 months, and for those with orbit extension ($n = 5$), it was 12 months. This difference trended toward statistical significance ($p = 0.06$, logrank; $p = 0.03$, Gehan–Breslow–Wilcoxon). Overall 5-year survival in this series was 27%. All patients with complete follow-up died of disseminated disease.

Discussion: The overall survival rates reported in this study agree well with those reported in other series. Likewise, the lower median survival seen in patients with orbit involvement agrees well with American Joint Committee on Cancer staging guidelines, which state that invasion of sinonasal malignant melanoma into the orbit or skull base is classified as “very advanced” disease.



References

1. Manolidis S, Donald PJ. Malignant mucosal melanoma of the head and neck: review of the literature and report of 14 patients. *Cancer* 1997;80(8):1373–1386
2. Cheng YF, Lai CC, Ho CY, Shu CH, Lin CZ. Toward a better understanding of sinonasal mucosal melanoma: clinical review of 23 cases. *J Chin Med Assoc* 2007;70(1):24–29
3. Yii NW, Eisen T, Nicolson M, et al. Mucosal malignant melanoma of the head and neck: the Marsden experience over half a century. *Clin Oncol (R Coll Radiol)* 2003;15(4):199–204
4. American Joint Committee on Cancer. *AJCC Cancer Staging Manual*. 8th ed. New York, NY: Springer;2016

A132. Survival and Patterns of Relapse of Head and Neck Malignancies with Large Nerve Perineural Spread after Skull Base Surgery and Postoperative Radiation Therapy

Ryan Sommerville¹, Charles Lin¹, Papacostas Jason¹
¹Royal Brisbane and Women's Hospital, Herston, Australia

Purpose: Cutaneous head and neck malignancies can undergo perineural spread (PNS) due to the rich innervation. Patients with large nerve PNS of the head and neck region commonly had cranial nerves five and seven affected. Our aim study was to evaluate the survival and pattern of relapse for patients with PNS of cutaneous head and neck malignancies, predominantly squamous cell carcinoma (SCC), staged with a high-resolution MRI neurogram, who have undergone curative intent skull base surgery and/or radiation therapy.

Method and Materials: A review of a prospective database identified 47 patients diagnosed with PNS of head and neck cancer between the years 2013 and 2018. Kaplan–Meier methods were used to estimate relapse free survival (RFS) and overall survival (OS). Multivariate analysis of patient age, sex, histological subtype, zone of spread, and margin status was performed to identify patients with a higher propensity for relapse and death.

Results: Forty-seven patients with a median follow-up of 17 months (range = 3–59) from the time of diagnosis were identified with head and neck malignant PNS from our institutions database. The overall 2-year RFS from time of diagnosis was 54% and overall survival 88%. The most common histological type was SCC (SCC: 38 patients; basal cell carcinoma: 1; adenoid cystic carcinoma: 6; mucosal SCC: 1; and mucoepidermoid carcinoma: 1). Patients aged 65 years or older at time of diagnosis had a statically significant worse relapse free survival. The most commonly affected nerve was V2. Out of these 46 patients, 21 had zone I (PNS to but not involving the skull base foramen: 46%), 12 had zone IIa (PNS to the foramen but not the ganglion: 26%), 11 had zone IIb (PNS to the ganglion: 24%), and 2 had zone III (PNS to the preganglionic segment: 4%) involvement. Patients with central PNS to zones IIb and/or III did not appear to have worse outcomes compared with the more peripheral PNS (zones I and IIa; HR: 1.1; $p = 0.9$). Those with involved surgical margins demonstrated higher trend of relapse (HR: 2.5; $p = 0.08$). Patients with >1 involved nerve also showed a trend of higher relapse (HR: 2.5; $p = 0.08$). A total of 14 patients developed recurrence (1 dermal metastasis, 2 at the in-field primary tumor sites, 1 at the lymph node in-field, 1 at both in-field primary site and nodal site, 1 at the primary site and distal PNS, 6 had distant metastasis, 1 at central PNS out-field, and 1 had distal PNS out-field).

Conclusion: Failure at primary tumor site and peripheral PNS represent a common mode of relapse. Treatment to the peripheral nerve track and the primary tumor should be optimized by improving the surgical margins and more extensive peripheral nerve coverage by postoperative radiotherapy.

A133. High-Throughput Screening of Epigenetic Inhibitors in Chordoma and Chondrosarcoma

William Foreman¹, Philip D. Tatman¹, Anthony Fringuello¹, Tadeusz Wroblewski¹, Samuel Scherer¹, Randy Jensen², Kevin Lillehei¹, Denise Damek¹, Michael Graner¹, David Ormond¹
¹University of Colorado, Boulder, Colorado, United States
²University of Utah, Salt Lake City, Utah, United States

Background: Chordoma and chondrosarcoma are rare tumors of the central nervous system. Once thought of as related tumors, genetic and molecular profiling has resulted in their independent classification. Chordomas have a 5-year

survival rate of 61%, while chondrosarcoma have 5-year survival rates of 29 to 90% depending on grade. Adjuvant therapy for chordomas and CNS chondrosarcoma are highly debated. The poor patient outcomes and lack of therapeutic options for these patients require additional research to identify novel therapies to treat these tumors. Some genetic studies have found a high incidence of mutations in epigenetic and cell cycle genes, suggesting epigenetic dysregulation may play a role in these diseases and offer a therapeutic target. We sought to address the need for additional therapies for these tumors by profiling their sensitivity to epigenetic inhibition.

Methods: One chondrosarcoma and two chordomas were resected and collected via our neural tissue bank. Four chordoma cell lines were provided by the Chordoma Foundation. We screened the tumors using the Caymen Chemical Epigenetic Inhibitor Library. Drugs were dosed at a concentration of 5 μ m in triplicate, and cell viability was assayed 72 hours later via MTS. Any compound that significantly reduced cell viability compared with an untreated control was considered for further evaluation.

Results: One chondrosarcoma and six chordomas were screened in this study. Notably, we are actively screening additional chordoma cell lines from the Chordoma Foundation. Chordoma and chondrosarcoma have nonoverlapping drug sensitivity profiles, further marking the differences between these tumors. The chondrosarcoma was sensitive to inhibition of bromodomain (BET) proteins, Jumonji domains, and DNA methyltransferase activity by OTX015, JIB-04, and SGI102, respectively. No single agent was able to significantly reduce chordoma viability across all tumors; however, four of the six tumors were sensitive to histone deacetylase (HDAC) inhibition by HC toxin or panobinostat, and three tumors were sensitive to G9a inhibition by UNC0631 or BIX01294. G9a regulates Histone-Three-Lysine-residue-9 (H3K9) methylation. One of the chordomas was sensitive to both HDAC and G9a inhibition. Collectively, inhibition of HDAC activity and G9a has potential as a treatment for patients with chordoma.

Conclusion: Chordoma and chondrosarcoma have unrelated sensitivity profiles to epigenetic inhibition, although both tumors have the potential to be treated via inhibition of epigenetic mechanisms. Chordoma are sensitive to HDAC and G9a inhibition, suggesting a combinatorial treatment may be beneficial to patients with chordoma.

A134. Clinicopathologic Associations of Partial-EMT in Sinonasal Squamous Cell Carcinoma

Anuraag S. Parikh¹, Shekhar K. Gadkaree¹, Eric Barbarite¹, Stacey T. Gray¹, William C. Faquin¹, Sidharth V. Puram², Derrick T. Lin¹

¹Massachusetts Eye and Ear, Boston, Massachusetts, United States

²Department of Otolaryngology, Washington University, St. Louis, Missouri, United States

Objectives: This study aims to quantify by immunohistochemistry (IHC), a partial epithelial-to-mesenchymal transition (p-EMT) population in sinonasal squamous cell carcinoma (SCC) and determine its associations with adverse clinicopathologic features.

Methods: All patients treated surgically for sinonasal SCC between January 2006 and December 2013 at our tertiary care institution were identified. IHC staining was performed for each of three p-EMT markers and one marker of anticorrelated well-differentiated epithelial cells. Staining was quantified as 1+, 2+, or 3+ in a blinded manner. A simple average of p-EMT markers was taken as the p-EMT score and used to quantify the p-EMT population. Clinical and patho-

logic data for these patients were also collected retrospectively from patient charts.

Results: Forty-eight patients were identified. Thirty patients (63%) had advanced T4 disease, and four patients (8.3%) had nodal disease at presentation. Twenty-five patients (52%) had positive margins, 24 (50%) had high grade tumors, 18 (38%) had PNI, and 15 (31%) had LVI. Associations of p-EMT scores with adverse pathologic features were determined by ANOVA and chi-squared analyses. Kaplan-Meier curves and multivariate Cox-proportional hazards models were used to determine the association of p-EMT and adverse pathologic features on overall survival (OS) and disease free survival (DFS).

Conclusion: In our single-institution experience of 48 sinonasal SCC patients, we determine the clinicopathologic associations of p-EMT, a program previously demonstrated to be associated with adverse pathologic features such as perineural invasion and high grade in oral cavity SCC.

A135. En Bloc Modified Subtotal Temporal Bone Resection for Advanced Squamous Cell Carcinoma of the Temporal Bone

Noritaka Komune¹, Satoshi Matsuo², Takashi Nakagawa¹

¹Kyushu University Hospital, Fukuoka, Japan

²Clinical Research Institute, National Hospital Organization, Kyushu Medical Center, Fukuoka, Japan

Objective: The temporal bone's complex, intricate structure is a product of its close association with vital organs; anatomical structures it houses, in whole or in part, include the internal carotid artery, otic capsule, jugular bulb, superior and inferior petrosal sinuses, and facial, trigeminal, and lower cranial nerves. The malignancies of the temporal bone are rare. Squamous cell carcinoma (SCC) is the most common form. The rarity of the temporal bone squamous cell carcinoma (TB-SCC) has delayed the establishment of the standard treatment strategy. There is little consensus about how best to treat TB-SCC. Margin-negative surgical resection seems to offer the best prognosis, which has cemented its status as the first-choice treatment for the disease. However, en bloc resection of the temporal bone is challenging due to the anatomical complexity of the temporal bone. In this study, we summarize the outcomes for surgical cases of advanced (T3-T4) TB-SCC in our department, with an accompanying description of the surgical procedure utilized: modified STBR.

Study Design: Retrospective chart review.

Method: Chart information was collected for all patients who underwent initial treatment includes surgical resection for TB-SCC at our Hospital between September 1998 and February 2019. Tumor staging followed the modified Pittsburgh classification. Local control rate was the primary outcome of interest, calculated according to the Kaplan-Meier's method.

Results: Thirty-two patients with advanced TB-SCC underwent surgery during the review period. En bloc lateral temporal bone resection (LTBR) was employed in a total of 21 cases (5-year local control rate: 77.43%). En bloc STBR was utilized in seven cases (control: 75%). TB-SCC was recurrent in three, and fresh in the other four. Three cases were T3, and four were T4. Negative medial resection margins were achieved in six of the seven cases.

Conclusion: En bloc margin-negative resection is a good treatment strategy for advanced TB-SCC, and affords excellent local control. Our hospital's procedure, modified subtotal bone resection, can be an effective option for the TB-SCC without posterior fossa dura invasion.

A136. Tailoring the Surgical Corridor to the Basilar Apex in the Pretemporal Transcavernous Approach: Morphometric Analysis of Different Neurovascular Mobilization Maneuvers

Mohamed Labib¹, X. Zhao¹, Komal Naeem¹, M. Preul¹, M. Lawton¹

¹Barrow Neurological Institute, Phoenix, Arizona, United States

Objective: The pretemporal transcavernous approach (PTA) provides optimal exposure and access to the basilar artery; however, a full PTA can be relatively invasive when several vital neurovascular structures are mobilized. The goal of this study is to evaluate the feasibility of different mobilization strategies to plan-tailored approaches to the basilar apex.

Methods: After a full orbitozygomatic craniotomy, ten sides of five cadaveric heads were used to assess the surgical access to the basilar artery via the optico-carotid triangle (OCT), carotid-oculomotor triangle (COT), and oculomotor-tentorial triangle (OTT). Measurements and morphometric analysis were taken for natural neurovascular positions and after each stepwise addition of several expansion maneuvers. A line connecting the midpoints of the limbus sphenoidale and dorsum sellae was used as a reference to normalize measurements of basilar artery exposure and to facilitate the clinical applicability of this technique. Similarly, an imaginary vertical line, the basillometer, along the actual basilar artery and extending up to the mammillary bodies was used to indicate the different segments that could be exposed along the extent of the vessel.

Results: In the OCT, the natural width and maximum width with the ICA lateral mobilization were 4.1 ± 1.62 and 6.3 ± 1.66 mm. The distance from the exposed BA segment to the reference line in a natural position ranged from -1.3 ± 3.94 to $+5.7 \pm 2.03$ mm. In the COT, the natural width, maximum width with the ICA medial mobilization before, after the carotid collar (CC) dissection, and oculomotor nerve lateral mobilization were 6.7 ± 1.81 , 8.6 ± 1.79 , 9.9 ± 1.84 , and 13.1 ± 1.94 mm, respectively. The accessible BA segment ranged from -4.5 ± 2.30 to -1.7 ± 2.95 mm at the natural position. Via the OTT, the natural width and maximum width with the oculomotor nerve medial mobilization were 5.1 ± 1.69 and 8.2 ± 1.60 mm, respectively. The accessible BA segment ranged from -7.1 ± 2.57 to -5.1 ± 2.81 mm at the natural position. In the OCT, COT, and OTT, a posterior clinoidectomy extended the exposure down to -6.2 ± 2.66 , -8.2 ± 2.48 , and -9.3 ± 2.94 mm, respectively.

Conclusion: This study provides a method to quantitatively evaluate the need for the expansion maneuvers in the PTA to basilar artery aneurysms according to individual anatomical characteristics.

A137. Endoscopic Sinus Approaches versus Transcranial Anterior Petrosectomy: A Volumetric Comparative Study of Access to the Petrous Bone and the Petrous Apex

Vanessa Hernandez-Hernandez¹, Aldo Eguiluz-Melendez¹, Belen Vega¹, Eric W. Wang¹, Carl H. Snyderman¹, Paul A. Gardner¹

¹University of Pittsburgh Medical Center, Pittsburgh, Pennsylvania, United States

Objective: The petrous portion of the temporal bone (PB) and the petrous apex (PA) are complex regions in the skull base that are affected by many pathologies. Surgical approaches to access these structures all have limitations for achieving maximal tumor resection with minimal comorbidity.

The purpose of this study is to evaluate petrous access by examining volume of removed bone via five different approaches: anterior petrosectomy “Hakuba–Kawase–Dolenc” (HKD) approach, endoscopic endonasal pure transclival approach (EEAT), endoscopic endonasal approach with internal carotid artery lateralization (EEA+ICA), contralateral transmaxillary approach (CTM), and CTM with internal carotid artery lateralization (CTM+ICA).

Methods: Ten cadaveric specimens were dissected using image guidance. Endoscopic endonasal techniques with or without contralateral Caldwell-Luc approaches in selected cases were performed to be compared with a classic open technique (HKD). Pre- and postdissection CT scans were obtained with 3D reconstructions of the volume resected on each specimen. Analyses of the resection and surgical aspects of the endoscopic techniques and HKD are discussed with the addition of two illustrative cases.

Results: For the PA alone, the greatest quantities of bone were resected via the HKD, CTM, and CTM + ICA. The HKD showed 71.2% of the PA (± 1.87) resected; CTM alone 58.1% (± 6.8); and CTM + ICA 67.2% (± 3.86). There was no significant difference between HKD and CTM + ICA ($p = 0.741$). The percent resected on the PA varied between the use of CTM ($58.12\% \pm 6.83$) and CTM + ICA ($67.19\% \pm 3.86$) although there were no statistically significant differences between them ($p = 0.104$). For the PB, the CTM + ICA provided the greatest quantity of bone resected ($81.0\% \pm 1.1$) followed by CTM ($69.6\% \pm 10.9$), with no significant difference between both techniques ($p = 0.125$). The volume resected with HKD was $46.8\% \pm 5.2$; CTM and CTM + ICA showed significantly greater resection of the PB compared with the HKD ($p = 0.001$ and $p < 0.0001$, respectively).

Conclusion: The CTM approach offers a new corridor to reach the petroclival region. The CTM provides access to resect paramedian tumors with significant lateral and inferior extension into the petrous bone while minimizing complex maneuvers like carotid mobilization or manipulation of the eustachian tube diminishing the morbidity of the endoscopic. For PA lesions, the CTM + ICA provides similar access as the classic open techniques and superior access to the PB.

A139. The Upper Petroclival Region as Seen Through Different Surgical Windows: An Extensive Anatomical Study

Michael G. Kim¹, Filippo Veneziani Santonio¹, Lara Mastino¹, Lukasz Przepiórka¹, Philip E. Stieg¹, Alexander I. Evins¹, Antonio Bernardo¹

¹Neurological Surgery, Weill Cornell Medicine, New York, United States

Background: Lesions involving the upper petroclival region—including meningiomas, vascular malformation, chordomas, chondrosarcomas, and plasmacytomas—can be approached through several different operative windows. Given the complex anatomy of the upper petroclival region, including retrosellar area and interpeduncular fossa, it is essential to understand the conventional and topographic anatomy of this region from different surgical perspectives as well as the complex surrounding neurovasculature. We describe the surgical anatomy of the upper petroclival region and present an analytical evaluation of the degree of exposure provided by several different surgical approaches.

Methods: Using 12 cadaveric specimens (24 sides), subfrontal, pterional, fronto-orbitozygomatic, middle fossa anterior transpetrosal, subtemporal, translabyrinthine, and retrosigmoid approaches were performed. The anterior and antero-lateral approaches were extended by anterior and posterior clinoidectomies and unroofing of the optic canal,

in addition to other periclinoid and pericavernous maneuvers. The subtemporal and middle fossa approaches were extended by incising the tentorium. To quantify exposure, the upper petroclival region was divided into four compartments by an axial plane passing along the petrous ridges and a sagittal plane passing through the lateral border of the posterior clinoid process, including the lateral and medial supra- and infratentorial compartments. The neurovascular structures occupying each compartment were described and evaluated analyzing degree of exposure and surgical accessibility and maneuverability throughout the different approaches.

Results: The anterior approaches provided wide exposure of the upper petroclival region, but the deep trajectory and number of neurovascular structures encountered limited maneuverability, whereas the anterolateral approaches offered adequate visualization and maneuverability of the surgical targets. Though, the narrow surgical corridors provided by the pterional and fronto-orbitozygomatic approaches without pericavernous maneuvers did not offer the same surgical maneuverability. The lateral approaches required significant cerebral retraction, but the subtemporal approach provided the most direct corridor to the basilar apex. The retrosigmoid approach did not provide visualization of the interpeduncular fossa but allowed for good visualization of the region lateral to CN III, although it involved deep corridors, significant cerebellar retraction, and limited surgical maneuverability.

Conclusion: Surgical approach selection to the upper petroclival region depends upon the size, nature, and general location of the lesion, as well as on the capability of the particular approach to better expose the area of interest. Adequate preparation and dissection of the surgical corridors whether extradural as initial preparation for a combined intraextradural approach or as the main avenue of surgical exposure, widens the available working space, and facilitates access to the upper petroclival region. While the subtemporal approach provides the most direct access to the upper clivus, the limitations and pitfalls of temporal lobe retraction should be carefully considered.

A140. Foundations of Advanced Neuroanatomy: Technical Guidelines for Specimen Preparation, Dissection, and Three-Dimensional Photodocumentation in a Surgical Anatomy Laboratory

Luciano César P.C. Leone¹, Lucas P. Carlstrom², Christopher S. Graffe², Avital Perry², Carlos Diogenes Pinheiro-Neto¹, Jeffrey Sorenson³, Michael J. Link², Maria Peris-Celda¹

¹Northeast Professor Rhoton Skull Base Dissection Laboratory, Department of Neuroscience and Experimental Therapeutics, Albany Medical Center, Albany, New York, United States

²Department of Neurologic Surgery, Mayo Clinic, Rochester, Minnesota, United States

³Department of Neurological Surgery, University of Tennessee and Semmes-Murphy Clinic, Memphis, Tennessee, United States

Introduction: Professor Albert L. Rhoton Jr., MD, was a pioneer in neurosurgical anatomy study, and his methodology regarding dissections and photodocumentation remains a standard and reference in surgical anatomy research. The objective of this work is to provide a key update to the seminal methodology works of Professor Albert L. Rhoton Jr, MD, with particular attention to previously unpublished insights from the oral tradition of his fellows, recent technological advances including endoscopy and high dynamic range (HDR) photodocumentation, and local improvements in technique, we have developed to optimize efficient neuroanatomic study.

Materials and Methods: Ten formaldehyde-fixed cadaveric heads were injected with colored latex to demonstrate step-by-step specimen preparation for microscopic or endoscopic dissection. One formaldehyde-fixed brain was utilized to demonstrate optimal 3D photodocumentation techniques.

Results: Key steps of specimen preparation include vessel cannulation and securing of carotid arteries, vertebral arteries, internal jugular veins, serial tap water flushing, specimen drainage, vessel injection with optimized and color-augmented latex material, and storage in 70% ethanol (Fig. 1). Optimizations for photodocumentation included the incorporation of dry black drop cloth and covering materials, an imaging-oriented approach to specimen positioning and illumination, and single-camera stereoscopic capture techniques, emphasizing the 3 exposure times per eye approach to generating images for HDR postprocessing (Figs. 2–4). Recommended tools, materials, and technical nuances were emphasized throughout. Relative advantages and limitations of major 3D projection systems were comparatively assessed, with sensitivity to audience size and purpose specific recommendations.

Conclusion: We describe the first consolidated, step-by-step approach to advanced neuroanatomy, including specimen preparation, dissection, and 3D photodocumentation, supplemented by previously unpublished insights from the Rhoton fellowship experience and lessons learned in our laboratories in the past years such that Professor Rhoton's model can be realized, reproduced, and expanded upon in surgical neuroanatomy laboratories worldwide.

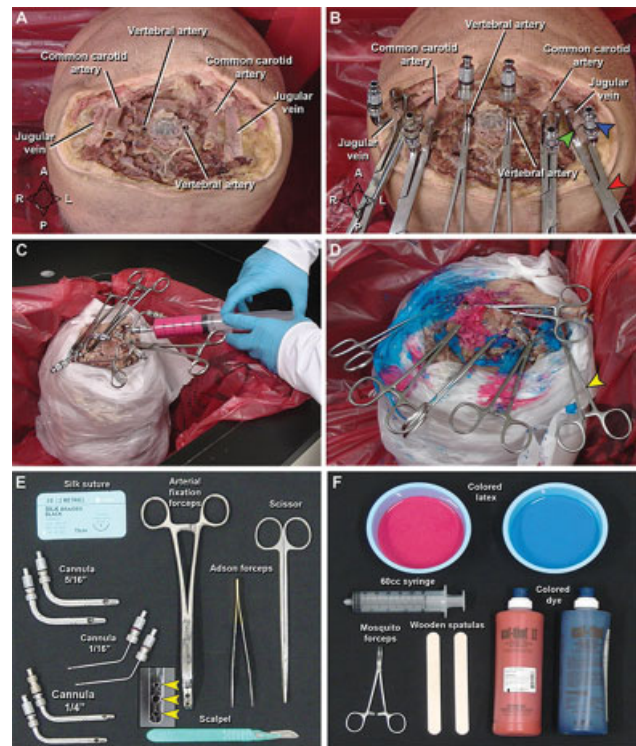


Figure 1. Cannulation, flushing and latex injection of the specimen. A. Vessels isolated before cannulation (vertebral and carotid arteries, internal jugular veins). B. The same vessels with stainless-steel cannulas (blue arrowhead), supported by a suture (green arrowhead), and an arterial fixation forceps (red arrowhead) for latex perfusion (C). D. Final view after injection. In order to avoid overflowing of latex during perfusion, mosquito forceps (yellow arrowhead) were used to clamp the leaking soft tissue neck vessels and the perfused vessels. E, F. Materials necessary for cannulation, flushing (E) and latex perfusion (F) of the specimen. Note the arterial fixation forceps with three holes (yellow arrowheads) to hold the cannulas.

A – anterior, P – posterior, L – left, R – right.

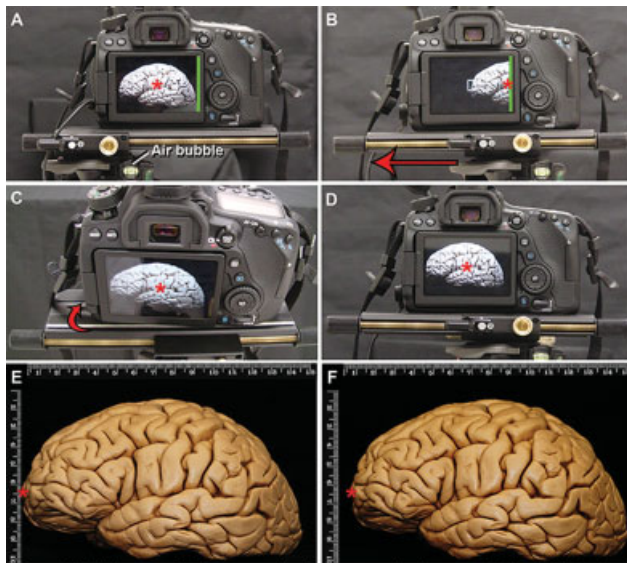


Figure 2. Technique for 3D documentation for macroscopic pictures of a formaldehyde-fixed brain, lateral view. The basic principle is to take one picture for each eye focused on the same center. All the pictures are taken with the 100 mm lenses modifying the distance to the object to achieve far away or closer views. **A.** The sliding plate has to be parallel to the floor, in order to ensure this, the air bubble (which must be located in the middle square of the 3-way tripod head) needs to be in the middle, and the sliding plate completely positioned towards the right side. The center of the screen is the reference to take the picture (red asterisk). The edge of the camera screen is marked with a green line. The first picture to be taken represents the right eye view. **B.** After taking the picture, the sliding plate has to be moved to the left (red arrow) until the right border of the photography camera screen (green line) is located in the previous center of the right picture (red asterisk) or half-way through that distance. Complex calculations have been described to know the exact horizontal displacement needed between the two pictures to achieve a perfect stereoscopic pair of images taking into account the distance of the camera to the object, but the method described here has been proven very efficient in obtaining 3D for anatomical dissections. **C.** In order to take the second picture (left eye view), the camera must be slightly rotated to the right (red arrow) until the previously chosen center of the right eye picture is also the center of the left eye image (red asterisk). Having both right and left images with the same focus center achieves stereoscopic images. **D.** View of the left eye image. **E.** Observe in this picture that the red point is closer to the vertical rule than observed in **F** (right eye view), both images are slightly different.

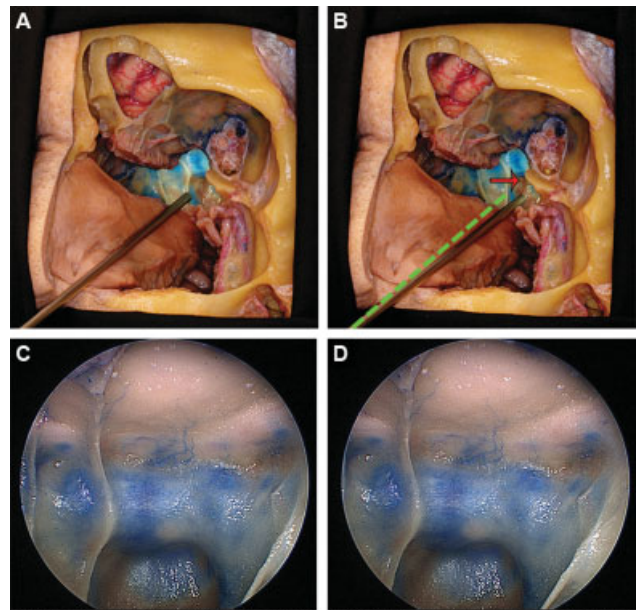


Figure 3. Endoscopic technique to take 3D images, oblique section of the nasal cavity and cranial base. The endoscope has been introduced through the left nostril. **A** represents the endoscope positioned in order to take the picture of the left eye view and in **B** the endoscope was slightly moved to the right (red arrow) to take the picture representing the right eye view. The green dotted line represents the initial position of the endoscope, which is rotated at the nostril level. For any other endoscopic pictures, which are not endonasal, another fixed axis of rotation has to be chosen. **C** and **D** represent endoscopic pictures of the sphenoid sinus taken with the endoscope when placed in **A** and **B**.

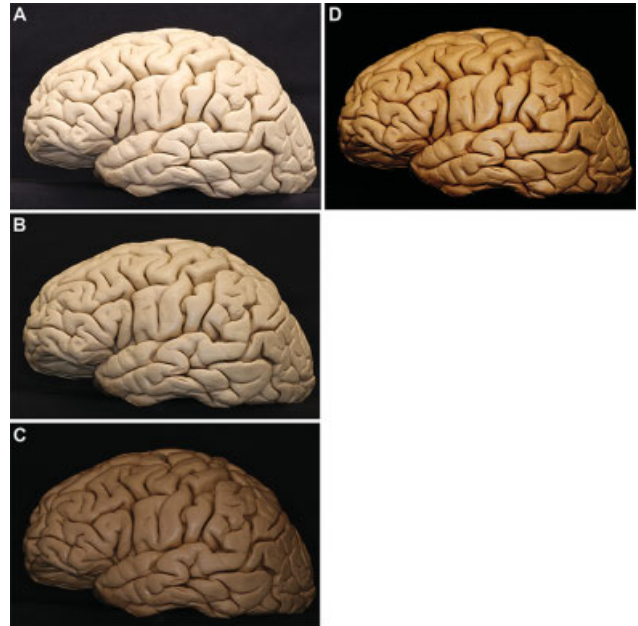


Figure 4. HDR technique. Three pictures are uploaded in Photomatix Pro 6.1.1, one considered overexposed (**A**), one presenting medium time of exposure (**B**) and the last one underexposed (**C**) the software fuses all images and provides a *final image* with improved contrast and brightness as observed in **D**. The final images can be used in 2D or 3D projection. HDR techniques are recommended although not mandatory for stereoscopic presentations.

A141. Endoscopic Transoral Evaluation of Hypoglossal Nerve and Its Relation to Surrounding Structures

Roberto M. Soriano¹, Gustavo Pradilla¹, C. Arturo Solares¹
¹Emory University (SSO), Atlanta, Georgia, United States

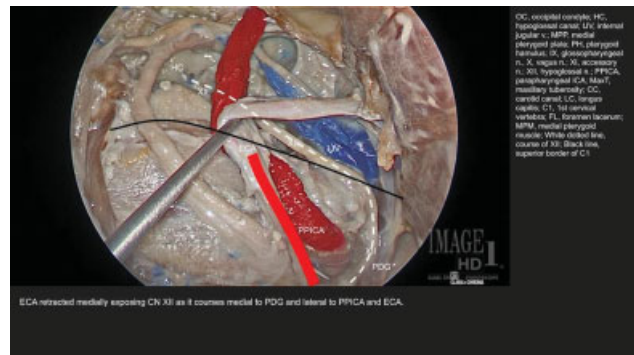
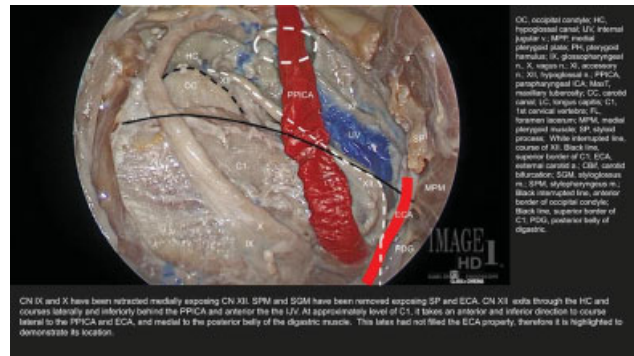
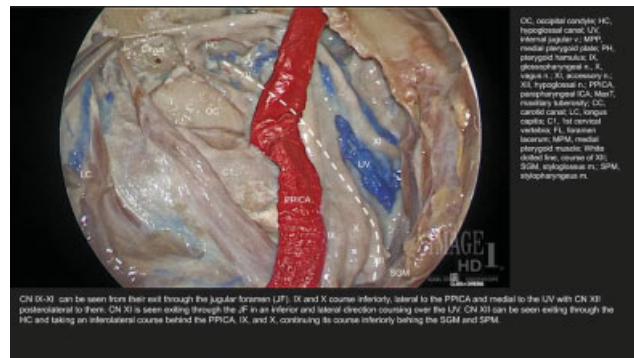
Background: Previous anatomical studies have described the relationship of the hypoglossal nerve (XII) to surrounding structures through open approaches; however, no studies have clarified this relation from an endoscopic transoral perspective. This study aims to describe XII in relation to surrounding structures through a transoral endoscopic approach.

Study Design: Cadaveric study.

Methods: Endoscopically assisted transoral dissection was performed bilaterally on three latex-injected cadaveric specimens. Following parapharyngeal space dissection, eustachian tube removal, and exposure of skull base, the parapharyngeal internal carotid artery (PPICA), internal jugular vein (IJV), glossopharyngeal nerve (IX), vagus nerve (X), accessory nerve (XI), and hypoglossal nerve (XII) were exposed and skeletonized from their corresponding foramina to the point where XII intersects with the PPICA and external carotid artery (ECA) inferiorly.

Results: XII exits from the skull base through the hypoglossal canal (HC) and courses laterally and inferiorly, running posterior to the PPICA, IX, and X, and anterior to the IJV. It then runs parallel and inferomedial, but not adjacent to XI and posterolaterally adjacent to IX and X. Subsequently, XII continues its course in a caudal direction, lateral and inferior to the stylopharyngeus muscle (SPM) and styloglossus muscle (SGM). It then courses anteriorly, running lateral to the ECA, and medial to the posterior belly of the digastric (PDG) where it continues its course anteriorly to the lingual musculature.

Summary: This study demonstrates the course of XII and its relation to important neurovascular structures in its descending portion from its exit through the HC to its intersection with the ECA. XII travels posterior to the PPICA, IX, X, and lateral to the ECA. It must be taken into consideration when dissection extends past these structures to avoid inadvertent injury. Detailed anatomical knowledge of XII and its trajectory is essential to perform safe and effective transoral endoscopic surgery.



This document was downloaded for personal use only. Unauthorized distribution is strictly prohibited.

A142. The Lateral Craniopharyngeal Canal (Sternberg's Canal) in Pediatric and Adult Populations

Adedamola Adepoju¹, Christopher S. Graffeo², Lucas P. Carlstrom², Avital Perry², Carlos D. Pinheiro-Neto³, Michael J. Link², Maria Peris-Celda¹

¹Department of Neurologic Surgery, Albany Medical Center, Albany, New York, United States

²Department of Neurologic Surgery, Mayo Clinic, Rochester, Minnesota, United States

³Division of Otolaryngology and Head and Neck Surgery, Department of Surgery, Albany Medical Center, Albany, New York, United States

Introduction: The location of lateral craniopharyngeal canal (LPC) aka Sternberg canal has been a source of controversy in the literature over the years, and there are more studies suggesting that the canal could be a possible source of spontaneous cerebrospinal fluid (CSF) leak in adults. There is controversy regarding the location and even existence of the Sternberg canal. Studies have indicated based on radiographic images of patients with CSF leak that the canal is located lateral to the foramen rotundum¹. Others have questioned this suggestion and claimed the canal to be medial to the foramen rotundum. In the original publication by Maximilian Sternberg in 1888, the canal was described to be located at the medial angle of the superior orbital fissure, directly at the base of the outer root of lesser wing of the sphenoid. In addition, he mentioned the canal was constant in the skull of 3 to 4 years old, but only persisted in 4% of adult skulls. The objective of the study is to provide clarification on the existence, prevalence, and surgical anatomy of the lateral craniopharyngeal canal.

Methods: Total 50 contrasted computer tomography (CT) images of 3-year-old patients and 125 adult patients (>18 years), who presented to Albany Medical Center, were studied. The exclusion criteria included were poor quality images (>1.3 mm slices), disorders of anterior skull base including trauma, prior surgery, and congenital brain and skull disease.

Results: A tract was found to be originating at the medial angle of superior orbital fissure below the root of the lesser wing of the sphenoid (Fig. 1). The tract was present in 61.4% of the pediatric group. The tract originates above and slightly medial to the foramen rotundum and it projects posteriomediaally and connects with processus vaginalis (Fig. 2). The tract is at the junction of the presphenoid, basisphenoid, and alisphenoid similar to the description by Sternberg. However, this tract is usually obliterated in adult population by the development and pneumatization of the sphenoid sinus (Fig. 3). Only two (1.6%) patients showed a bone defect (Fig. 4) at the same location of the canal with the same trajectory, which is consistent with a remnant of LPC. In the adult population when present, the canal had reduced diameter as compared with the pediatric population (Figs. 1 and 2).

Conclusion: This study showed that LPC, as described by Sternberg, originates medial to the foramen rotundum. The canal projects posteriorly and medially toward the processus vaginalis. LPC is a common occurrence in the 3-year-old age group. Pneumatization and development of the sphenoid bone obliterates the canal in adult population and reduces it to less than 2%.

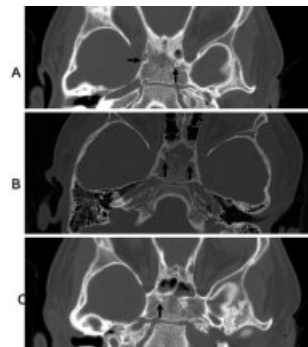


Figure 1: Axial views (1.3mm CT scan slice) of representative images (a,b, and c) of a lateral craniopharyngeal canal in pediatric group. The canal is highlighted by the black arrow

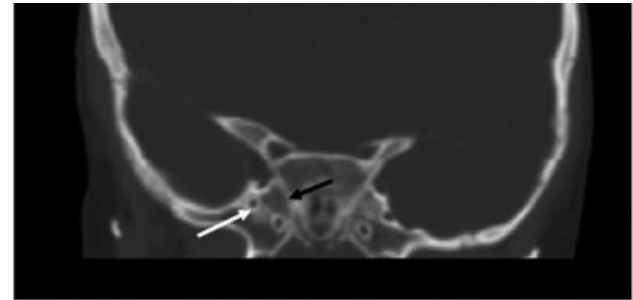


Figure 2: Coronal view (1.3 mm CT scan) of a representative image of a lateral craniopharyngeal canal in a 3 year old. The black arrow highlights the canal and the white arrow highlights the location of foramen rotundum

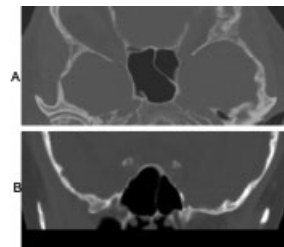


Figure 3A: An axial view of a CT scan showing a pneumatized sphenoid sinus, which shows the obliteration of the lateral craniopharyngeal canal. This was a common image in adult population. Figure 3B showing the coronal view of the scan in 3A

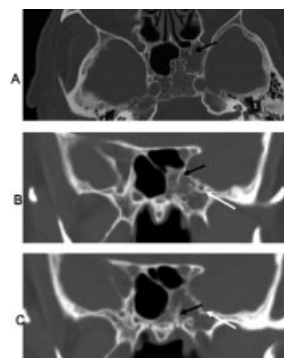


Figure 4A: An axial view of a defect on the left sphenoid bone corresponding to the trajectory of the lateral craniopharyngeal canal in an adult patient. Figure 4A and 4B showing similar defect mentioned in 4A on the same patient. The possible canal is highlighted by the black arrow and foramen rotundum is highlighted by the white arrow

A143. Comparing the Pterional, Supraorbital, Supraorbital with Orbital Osteotomy, and Extended Endoscopic Transplanum Approaches for Reaching the Anterior Communicating Artery Complex: An Anatomical Study

Hongwei Zhu^{1,2}, Amandeep S. Ahluwalia³, Adib A. Abila^{2,4}, Ivan El-Sayed^{2,5}, Roberto Rodriguez Rubio^{2,4,5}

¹Department of Neurological Surgery, The First Affiliated Hospital of Xiamen University, Xiamen, China

²Skull Base and Cerebrovascular Laboratory, University of California, San Francisco, California, United States

³University of Chicago, Chicago, Illinois, United States

⁴Department of Neurological Surgery, University of California, San Francisco, California, United States

⁵Department of Otolaryngology –Head and Neck Surgery, University of California, San Francisco, California, United States

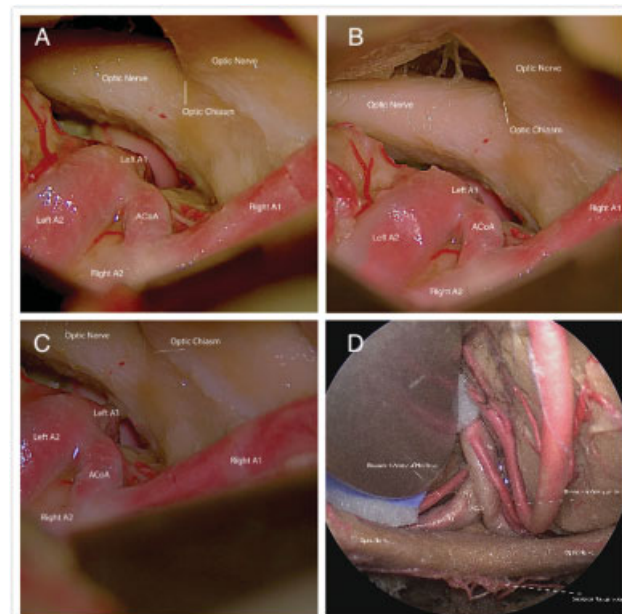
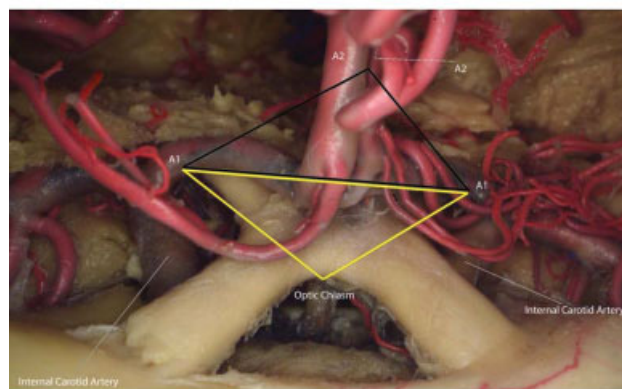
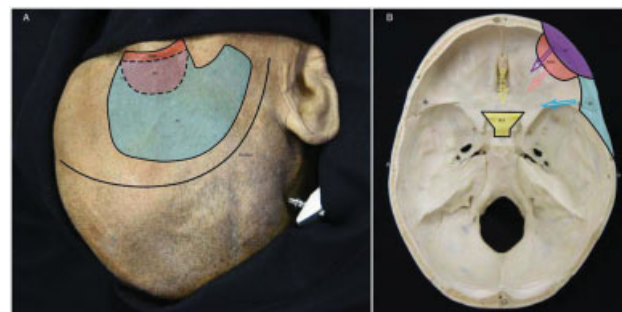
Background:: About 30 to 37% of intracranial aneurysms occur at the anterior communicating artery (ACoA) complex, making it one of the most common locations for cerebral aneurysms. Frequent anatomical variations, deep interhemispheric location, and the perforators that supply important structures are several factors that contribute to the complexity of ACoA aneurysms. Recently, several minimally invasive approaches have been implemented to treat these aneurysms while simultaneously reducing brain exposure and retraction, including microscopic and endoscopic approaches. However, no anatomical studies analyzing the efficacy of reaching the ACoA complex between microsurgical and endoscopic approaches have been conducted.

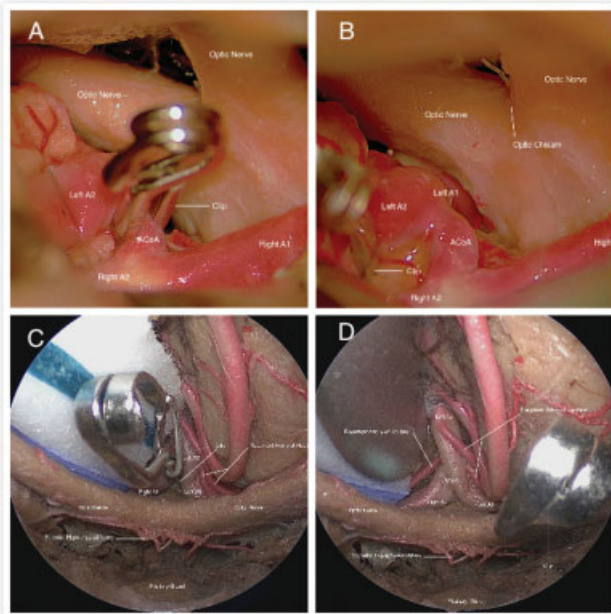
Methods:: Right-sided the pterional (PT), supraorbital (SO), supraorbital with orbital osteotomy (SOO) approaches, and endoscopic endonasal transplanum approach (EEA) were performed on 10 embalmed heads. The navigation system was used to measure the surgical exposure and freedom, including distance exposure of A1, A2, surgical area, horizontal, and vertical attack angles. The superior exposure of ACoA complex was calculated using the surrounding 3 points—the coordinate of the furthest right A1, the coordinate of the furthest left A1, and the midpoint between the left and right A2s. Inferior exposure also involved 3 points—again, the coordinate of the furthest right A1, the coordinate of the furthest left A1, and the anterior portion of the optic chiasm. The possibility of clipping the right and left A1 and A2 was assessed in all approaches; in each approach, the greatest distance of clipping (from the A1-ACoA-A2 junction to the aneurysm clip) was measured whenever it was feasible. A one-way ANOVA test was used to compare the means of the various parametric variables. Additionally, with this data, we considered a *p*-value of less than or equal to 0.05 as statistically significant.

Result:: There was a significantly longer distance in right A1 exposure in the PT (12.20 ± 2.48 mm) approaches when compared to the EEA (9.52 ± 2.09 mm, $p = 0.029$). The EEA has the shortest distance for right A1 clipping (6.56 ± 1.33 mm, $p = 0.001$) in four approaches. Additionally, EEA had the longest clipping distance in the right A2 (4.94 ± 0.90 mm) when compared to the other three microscopic approaches ($p = 0.03$). The EEA (50.90 ± 17.45 mm²) had more exposure area in superior part of ACoA complex than SO (29.37 ± 17.27 mm², $p = 0.05$). The PT (36.88 ± 5.85 degrees) provided the greatest horizontal angle of attack, while SOO (19.37 ± 4.7 degrees) achieved the greatest vertical angle of attack.

Conclusion:: The SO, SOO, and PT approaches provided parasagittal exposure of the ACoA complex, while EEA provided direct axial exposure of the complex. EEA can better expose the upper part of ACoA complex with relative limit

surgical freedom. EEA appears to be a feasible alternative to treating select aneurysms with anterior and superior project of the ACoA complex.





A144. Cerebral Revascularization for Aneurysm Treatment in the Era of Endovascular Flow Diversion

Mohsen Nouri¹, Julia R. Schneider¹, Kevin Shah¹, David J. Bonda¹, Amir R. Dehdashti¹

¹Department of Neurosurgery, North Shore University Hospital, Northwell Health, Manhasset, New York, United States

Background: With the advances in endovascular armamentarium, majority of giant, wide neck, or fusiform aneurysms are being treated with flow diversion rather than cerebral revascularization. The purpose of this study was to evaluate the indication and outcomes of cerebral revascularization for brain aneurysms in recent years when flow diversion is widely available as an option.

Methods: Among 132 patients who had undergone 148 cerebral revascularizations in our center over the past 10 years, 30 patients had the procedure for aneurysm treatment with at least 1 year follow-up. Indications for surgery were large aneurysms in 16, blister aneurysms in 3, fusiform aneurysms in 10, and a complex basilar tip aneurysm in 1 patient. Eight patients underwent combined endovascular treatment and surgical revascularization.

Results: Immediate aneurysm occlusion was achieved in 26 patients, and 4 were treated with retrograde flow strategy. Postoperative new deficit was observed in four patients (13.3%). Twenty-six patients were available for 1 year clinical and radiological follow-up. Bypass patency was confirmed in 24 cases (92.3%) in 1 year follow-up. The two patients with occluded bypass did not have new stroke. Two of the aneurysms needed additional treatment at follow-up. Clinical evaluations at 1 year showed that 21 patients were living independently (mRS 2 or less), while four patients had mRS 4 or higher. Eighteen patients had follow-up studies

beyond 3 years with no evidence of stroke or aneurysm recurrence.

Conclusion: Despite advances in endovascular flow diverting technologies, there is still a small subset of patients with brain aneurysms who benefit from cerebral revascularization. Our results suggest that cerebral revascularization can be regarded as a viable and durable treatment option for these challenging aneurysms with acceptable morbidity.

A145. Clinical Outcomes of the Superior Ophthalmic Vein Approach for Closure of Carotid Cavernous Fistulas

Jurij R. Bilyk¹, Archana Srinivasan¹, Ann P. Murchison¹, Stavropoula I. Tjoumakaris², Pascal M. Jabbour²

¹Wills Eye Hospital, Philadelphia, Pennsylvania, United States

²Thomas Jefferson University Hospital, Philadelphia, Pennsylvania, United States

Precis: The transorbital superior ophthalmic vein (SOV) approach is a viable alternative for the management of carotid cavernous fistulas (CCFs) when conventional approaches through the femoral artery/vein, facial vein, or inferior petrosal sinus are unsuccessful. A review of 25 consecutive patients treated by this technique revealed successful clinical and angiographic outcomes with minimal orbital and no intracranial complications.

Background Statement: Transvenous embolization of CCFs via the SOV was first described in the 1980s. To date, the only published report evaluating outcomes of this technique included 10 patients. Herein, we study the largest cohort of 25 patients over two decades.

Purpose: This study aims to report outcomes of CCF closure through SOV cannulation.

Methods: Retrospective chart review of 25 consecutive patients.

Results: The median patient age was 67 years (range = 41–84) and majority were females (68%). The most common CCF type by arteriogram was Barrow type D (72%) and posterior cortical venous outflow was noted in 20%. The 22/25 (88%) fistulas were completely obliterated in one attempt. Ptosis was the most common postoperative complication (69%). Visual acuity worsened from light perception to no light perception in one patient. Another patient developed an orbital compartment syndrome, requiring canthotomy and cantholysis with full visual recovery. There were no cases of iatrogenic stroke, intracranial hemorrhage, or other intracranial complications.

Conclusion: The SOV approach is an excellent alternative for CCFs that have failed conventional approaches.

A146. Endoscopic Endonasal Aneurysm Clipping

Matthew E. Welz¹, Rudy J. Rahme¹, Ahmad Kareem Almekkawi¹, Karl R. Abi-Aad¹, Devi P. Patra¹

¹Mayo Clinic, Rochester, Minnesota, United States

Introduction: Modern innovations in vascular neurosurgery have allowed for safer and less invasive approaches to treat a wide range of pathologies. Intracranial aneurysms are formidable lesions with high morbidity and mortality rates associated with rupture. While endovascular approaches have significantly improved in the past decade, there are still indications for aneurysm clipping. The endoscopic endonasal approach (EEA) gives access to the skull base and its cisterns. In this paper, we review the use of the EEA for aneurysm clipping.

Methods: A systematic review was conducted in accordance to the Preferred Reporting Items for Systematic Reviews and Meta-analysis (PRISMA) guidelines. Specific

terms such as “endoscopic endonasal” and “aneurysm” were used to search three independent databases. Inclusion and exclusion criteria were set, and the extracted literature was reviewed in two phases by two independent reviewers to include only papers that discussed the use of EEA for aneurysmal clipping. Extracted data included age, gender, history, location of the aneurysm, approach, and reason for approach with preoperative and postoperative assessments.

Results: A total of 930 papers were reviewed. Fifteen papers met the inclusion criteria with a total of 31 patients reported. Mean age was 51.61 years (range = 28–74 years). Presenting symptoms included headaches (35.5%), gait disturbances (12.9%), loss of consciousness (12.9%), and cranial nerve palsy (12.9%). The total number of clipped aneurysms clipped was 42. The most common location of these aneurysms was the anterior communicating artery ($n = 8$), the carotid ophthalmic segment ($n = 8$), and the basilar artery ($n = 7$), paraclinoid carotid segment ($n = 6$). Seven were ruptured aneurysms. Various approaches were used depending on aneurysm location. These include extended endonasal, transclival, transsphenoidal, transplanum, transplanum–trans-tuberculum, and transsellar–transplanum. The mean follow-up was 8.6 months. Thirty aneurysms did not have occlusion outcomes reported. Eleven aneurysms were completely occluded and one had a residual neck. Postoperatively, complications included ischemic strokes ($n = 5$), CSF leak ($n = 4$), cranial nerve palsies ($n = 2$), weakness ($n = 2$), pneumonia pulmonary embolism ($n = 2$), and four patients had CSF leak.

Conclusion: The literature on EEA for aneurysm clipping is scarce. CSF leaks and proximal control remain the main limitations. The development of 3D endoscopes, better dural closure techniques, and increase in experience and familiarity with the endoscope are the next necessary steps before the adoption of EEA as an approach for aneurysm clipping. However, at this time, treatment recommendations based on this approach is premature.

A147. Analysis of the Safety and Advantage of Ligation/Transection of the Superior Sagittal Sinus at the Level of Crista Galli: Basal Interhemispheric Approach for Anterior Communicating Artery Aneurysms

Junichi Yamamoto¹

¹Department of Neurosurgery, Albany Medical Center, Albany, New York, United States

Introduction: Anterior communicating artery (A com) aneurysms are most frequently clipped by pterional approach or trans-sylvian approach with or without some modifications, and they are much less frequently clipped by anterior/basal interhemispheric approach because of unfamiliarity to these approaches. The basal interhemispheric approach includes a ligation/transection of the superior sagittal sinus (SSS) and exposure/cranialization of the frontal air sinus, which allows wider working space for safe clipping without significant brain retraction. Thus, this approach is safer and better for high-positioned or large/giant A com aneurysms. There is a concern for venous infarction by the occlusion of the SSS. We retrospectively reviewed 42 consecutive cases and evaluated the safety of the SSS ligation at the skull base.

Methods: After a bifrontal craniotomy and cranialization of the frontal air sinus, the SSS was ligated and transected at the most proximal part at the level of the crista galli in all the 42 cases. Then the falx was also cut all the way down to the interhemispheric fissure. The interhemispheric fissure was dissected and split by using the usual sharp dissection technique and brain holding with minimum retraction under microscope and clipped aneurysms.

Results: Forty-two cases (20 males and 22 females with a mean age of 55.26 years) were reviewed. Total 25 aneurysms were ruptured and 17 were unruptured. Total 27 aneurysms were less than 10 mm, 12 were 10 to 20 mm, and 3 were greater than 20 mm. Twenty-three aneurysms were located higher than 10 mm from the anterior skull base. The A1–Acom–A2 complex was well exposed in all cases. Bilateral A2 and A3 segments were exposed well. All the aneurysms were dissected and exposed for safe and complete clipping. By cutting the falx and SSS, a wider working space was obtained without brain holding but not retraction compared with the conventional anterior interhemispheric approach. The hypothalamic arteries were easily identified through this approach even with large/giant or posterior projecting aneurysms. In four ruptured cases, the bilateral A1 and A2 segments were temporarily occluded without difficulty. No patient had venous congestion or infarction associated with the ligation/transection of the SSS at the base of the skull adjacent to the crista galli in all cases.

Conclusion: Ligation and transection of the SSS is safe and provides wider enough for safe clipping of A com aneurysms. Basal interhemispheric approach is unfamiliar to many vascular neurosurgeons, but once surgeons have knowledge about the required microsurgical anatomy and technique, this approach can be very useful for A com aneurysms which are challenging by the conventional pterional/trans-sylvian approach, such as large/giant, superiorly/posterior projecting, and high-positioned ones.

A148. Transethmoidal Endoscopic Endonasal Treatment of Ethmoidal Artery Dural Arteriovenous Fistulas

Nathan Quig¹, Michael Cools¹, Darshan Shastri¹, Michael Catalino¹, Adam Zanation¹, Deanna Sasaki-Adams¹

¹University of North Carolina, Chapel Hill, North Carolina, United States

Intracranial dural arteriovenous fistulas (dAVF) supplied by the ethmoidal arteries present a challenging surgical problem if not amenable to endovascular treatment. These dAVFs historically require larger open approaches via pterional or bifrontal craniotomies. We present a series of two cases via novel endonasal and transorbital approaches sparing the need for craniotomy.

Patient 1: A 64-year-old male presented with an intraparenchymal hemorrhage of the right gyrus rectus and diffuse subarachnoid hemorrhage. A cerebral angiogram demonstrated an ethmoidal dAVF (Fig. 1) with frontal basal vein venous drainage (Fig. 2). The dAVF was unable to be embolized due to difficulty penetrating the main draining vein.

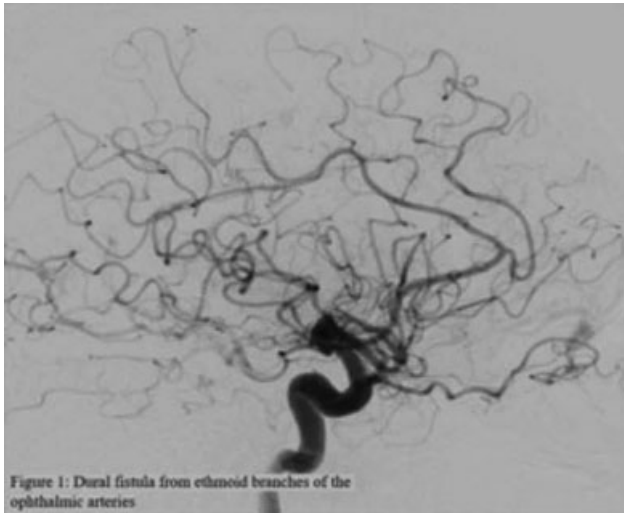


Figure 1: Dural fistula from ethmoid branches of the ophthalmic arteries

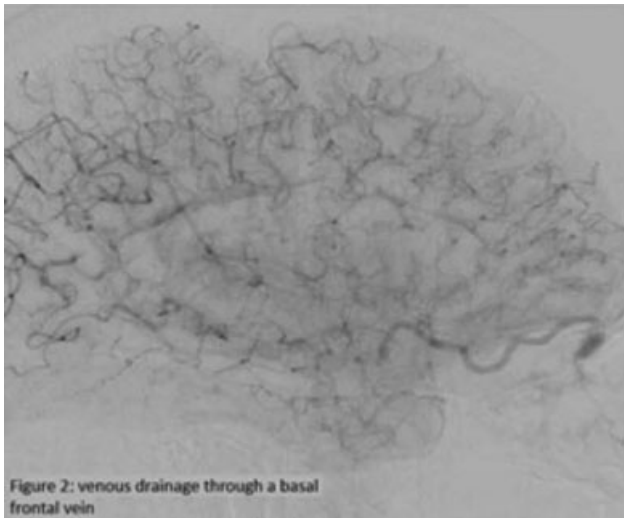


Figure 2: venous drainage through a basal frontal vein

Patient 2: A 60-year-old female presented with a diffuse subarachnoid hemorrhage secondary to a basilar tip aneurysm which was treated endovascularly. An incidental ethmoidal dAVF was found with drainage through a small frontal vein to the superior sagittal sinus. Follow-up angiogram showed a basilar tip aneurysm neck remnant requiring pipeline flow diversion and dual antiplatelet therapy (DAPT). Given the risk of hemorrhage on DAPT, it was decided to treat the dAVF first. Small lateral feeders prevented embolization of the dAVF. An endoscopic endonasal and transorbital approach was planned.

A right superior eye lid incision was carried deep to the orbital rim periosteum and the periosteum was elevated (Fig. 3). Care was taken to avoid significant depression of the orbit. The anterior ethmoidal artery was identified with a zero degree endoscope, ligated with hemoclips, and subsequently cauterized. A pedicled nasoseptal flap was harvested endonasally. The natural ostium of the sphenoid was opened and to gain access to the anterior skull base the ethmoid and maxillary sinuses were opened widely. High speed drill was

used to perform a transcribiform craniotomy. The dura was opened and reflected away revealing several dural-based, arterialized venous structures originating from the ethmoid arteries. These venous structures were coagulated and cut. One large draining vein along the falx and several smaller draining veins were also coagulated (Fig. 4). Closure was performed with a dura repair inlay, dural flap, and the previously harvested nasoseptal flap. A follow-up angiogram demonstrated complete obliteration of the dAVF.

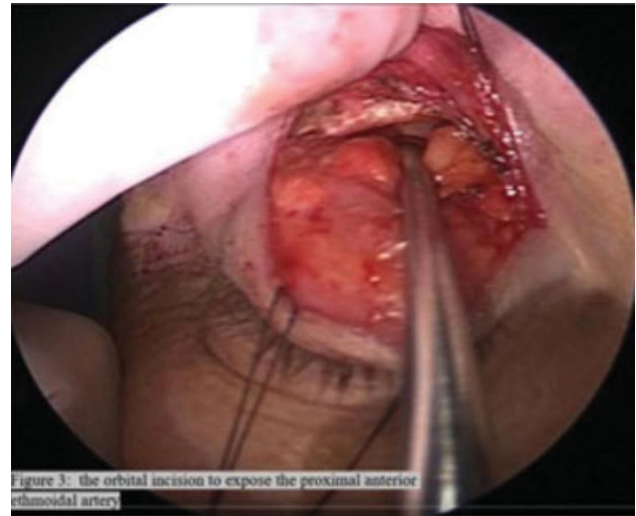


Figure 3: the orbital incision to expose the proximal anterior ethmoidal artery

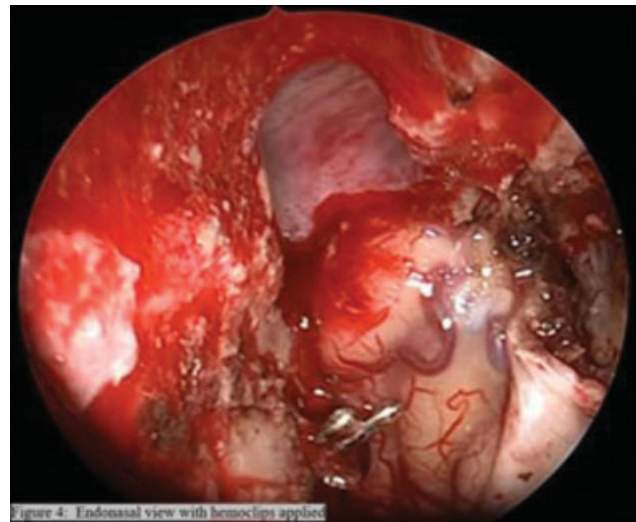


Figure 4: Endonasal view with hemoclips applied

Conclusion: dAVFs with arterial supply from the ethmoidal arteries present a challenging problem that can be successfully and safely treated through endonasal and transorbital approaches sparing the need for pterional or bifrontal craniotomy.

A149. Giant Fusiform and Dolichoectatic Aneurysms of the Basilar Trunk and Vertebrobasilar Junction:

Clinicopathological and Long-Term Follow-Up Study

Satoshi Kiyofuji¹, Hirofumi Nakatomi¹, Hideaki Ono¹, Minoru Tanaka¹, Kazuo Tsutsumi², Hiroyasu Kamiyama³, Nobuhito Saito¹, Yoshiaki Shiokawa⁴, Akio Morita⁵, Kelly Flemming⁶, Michael J. Link⁷

¹Department of Neurosurgery, The University of Tokyo Hospital, Tokyo, Japan

²Department of Neurosurgery, Showa General Hospital, Kodaira, Japan

³Department of Neurosurgery and Stroke, Teishinkai Hospital, Sapporo, Japan

⁴Department of Neurosurgery, Kyorin University, Mitaka, Japan

⁵Department of Neurosurgery, Nippon Medical University, Tokyo, Japan

⁶Department of Neurology, Mayo Clinic, Rochester, Minnesota, United States

⁷Department of Neurologic Surgery, Mayo Clinic, Rochester, Minnesota, United States

Background: Giant fusiform and dolichoectatic aneurysms of the basilar trunk and vertebrobasilar junction (BTVBJ-GFDA) are extremely difficult to treat.

Objective: We retrospectively analyzed our two-institution series to elucidate the factors affecting long-term survival.

Methods: Thirty-two patients with BTVBJ-GFDA treated at our hospitals were included in this study. Clinicopathological characteristics, treatment measures, and outcomes were based on the medical records and all available imaging studies. Autopsy and histological findings of the aneurysm and adjacent brain tissue were obtained in nine cases.

Results: Eleven patients did not undergo surgery, of whom 10 died (mortality 90.9%); three from progressive brainstem compression, four from subarachnoid hemorrhage, two from brainstem infarction, and one from associated atherosclerotic disease. Four types of surgical treatments were performed in 21 patients, consisting of immediate proximal parent artery occlusion, remote proximal parent artery occlusion, reconstructive clipping, and distal bypass, and these patients had significantly longer overall survival compared with those who received conservative therapy (adjusted hazard ratio: 1.508, 95% confidence interval: 1.058–2.148; $p = 0.02$). Histological examination of the aneurysms demonstrated staged clots, open lumen, and intrathrombotic channels with endothelial lining. A subgroup analysis demonstrated patients younger than 45 years of age had longer survival in Kaplan–Meier plots and the log rank test ($p = 0.03$). Those younger patient group had less atherosclerosis risk factors/diseases ($p = 0.004$), and tended to have favorable Pcom collaterals ($p = 0.073$). These differences could potentially guide treatments.

Conclusion: Parent artery occlusion should be performed at remote sites from the aneurysm, and ideal hemodynamic conditions within the aneurysm to maintain sufficient but not excess blood supply should be targeted based on the hemodynamics of both the posterior communicating arteries and perforating vessel collaterals.

A150. Predictors of Functional Outcome in Patients with Poor-Grade Aneurysmal Subarachnoid Hemorrhage

Sami Khairy¹, Munzir Abbas¹, Ahmed Aloraidi¹, Ahmed Alkhami¹
¹King Abdulaziz Medical City- Riyadh, Saudi Arabia

Background: Aneurysmal subarachnoid hemorrhage carries a high mortality and morbidity. The last few years the mortality rate improving due to improving in the diagnostic and treatment modalities. However, the patients with poor-grade aneurysmal subarachnoid hemorrhage receive a less aggressive management, and there is little known about the factors predicting the functional outcome for these patients.

Study Design and Methods: This is a retrospective study conducted in large medical city. A total of 822 consecutive patients admitted with aneurysmal subarachnoid hemorrhage during a period of 10 years (2007–2017). We retrospectively reviewed the patient's demographic features (age, sex, and BMI), severity of SAH at admission (Hunt and Hess grade, Glasgow Coma Scale score, Fisher grade, and the World Federation of Neurosurgeons Scale score), as well as functional outcome. Multivariable logistic regression was used to identify predictors of functional outcome.

Results: Total 181 out of 822 patient were classified as poor-grade aneurysmal subarachnoid hemorrhage based on Hunt and Hess Grades IV and V. Multivariable analysis identified aneurysmal size above 15 mm ($p < 0.001$), size of bleeding upon presentation ($p < 0.001$), age above 65 years ($p < 0.001$) as significant predictive factor of poor functional outcome. Also, we found hyperglycemia ($p < 0.04$) and leukocytosis ($p < 0.002$) predictor of poor functional outcome. On multivariate analysis, there was no significant association observed between presence of intraventricular bleeding ($p = 0.09$) seizure ($p = 0.10$) and long-term functional outcome.

Conclusion: We are reporting the largest study on functional outcome predictors in patients with poor-grade aneurysmal subarachnoid hemorrhage. The functional outcome was strongly predicted by unmodifiable factor like patient age on presentation and aneurysm size and modifiable factor like hyperglycemia. The new predictive scale based on our parameter appears to strongly predict the functional outcome in patients with poor-grade aneurysmal subarachnoid hemorrhage, which make it a strong tool in preoperative planning and management of these patients.

A151. Initial Experience with Exoscopic-Based Intraoperative Indocyanine Green Fluorescence Video Angiography in Cerebrovascular Surgery: Assessment of Feasibility, Safety, and Next Generation Form-Factor

William Smithee¹, Srikant Chakravarthi¹, Austin Epping¹, Mikael Kassam¹, Alejandro Monroy-Sosa¹, Bhavani Kura¹, Richard A. Rovin¹, Melanie B. Fukui¹, Amin B. Kassam¹

¹Aurora Neuroscience Innovation Institute, Milwaukee, Wisconsin, United States

Background: Technological evolutions in cerebrovascular surgery (CVS) have greatly reduced morbidity, especially with real-time visualization of two primary sources: (1) native vessel patency and (2) residual lesion. Microdoppler and indocyanine green fluorescence-microscopy (ICG-M) have emerged as potential replacements of intraoperative angiography (IA), while digital subtraction angiography (DSA) remains the gold standard. Recent studies have shown a potential benefit of exoscopic visualization in microsurgery, with more recent applications to CVS. The feasibility of ICG in conjunction with exoscopic visualization (ICG-E), to our knowledge, has not yet been reported for CVS.

Objective: This study aims to provide initial experience with an exoscopic-based ICG video angiography in CVS.

Methods: Retrospective cohort study with two inclusion criteria: (1) ICG-E was the primary method of determining patency and residual lesion; and (2) confirmatory postoperative DSA was performed. ICG-E consisted of two form factors: (1) exoscopic-coupled or (2) self-contained handheld imager. Chart review was undertaken to analyze ICG dosage, perioperative complications, work flow/setup time, and the concordance of ICG-E with IA and postoperative DSA. Stratification was based on form factor used, pathology, location, size, grade, and rupture status.

Results: Eleven patients met the inclusion criteria, eight aneurysms (two ruptured and six unruptured), and three

arteriovenous malformations (AVMs; 1 previously ruptured). ICG-E was feasible in all cases. There were two residual aneurysmal necks noted on the ICG-E (middle cerebral artery [MCA]) that were intentional to avoid flow-obstructive stenosis. There was an additional remnant posterior communicating artery (PCoA) infundibulum, which was not clipped to preserve the fetal posterior cerebral artery (PCA). No clinical sequelae were noted. IA was used if there was a question of stenosis, residual, or complex geometry, yielding seven aneurysm cases with a concordance of 88% with ICG-E and 88% with postoperative DSA. Case 4 (MCA) demonstrated discordance between ICG-E and DSA, with DSA revealing stenosis of the MCA superior division. All AVM cases were fully obliterated, with 100% concordance between ICG-E, IA, and DSA. ICG dosage "per run" averaged 4.2 mg per dose and ranged from 1 to 4 doses per case. Total ICG received per patient averaged 10.2 mg. There were no intra- or perioperative complications noted. The last four cases (two aneurysms and two AVMs) utilized the handheld system, whereas the previous cases utilized an exoscopically coupled ICG detection unit.

Conclusion: In this preliminary, hypothesis-generating study, ICG-E was a safe and feasible means of providing real-time cerebrovascular visualization. We noted a preferential transition into the more readily accessible handheld form factor, a more portable, less resource-dependent and readily accessible real-time imaging modality. Larger studies will be needed to assess broader safety, dose escalation, and efficacy data to validate the hypothesis.

A152. Epidemiology, Natural History, and Optimal Management of Neurohypophyseal Germ Cell Tumors

Avital Perry¹, Hirokazu Takami¹, Christopher S Graffeo¹, Caterina Giannini¹, David J Daniels¹

¹Mayo Clinic, Rochester, Minnesota, United States

Background: Intracranial germ cell tumors (iGCT) preferentially arise at the neurohypophysis—their second most common origination, following the pineal region. Neurohypophyseal iGCT present with stereotypic symptoms due to their suprasellar location, including pituitary dysfunction or visual field deficit.

Methods: This is a retrospective, single-institution cohort study of neurohypophyseal iGCT focused on the epidemiology, presentation, natural history, and treatment outcomes, 1988 to 2017.

Results: Thirty-five neurosurgically managed patients met inclusion criteria; median age was 18 years (3 months to 49 years), and 74% were males ($n = 26$). Thirty-one were germinomas and four were nongerminomatous GCTs. Presenting symptoms included pituitary insufficiency in 76% ($n = 25$), visual deficit in 40% ($n = 14$), and diabetes insipidus (DI) in 61% ($n = 20$). Index symptoms included isolated diabetes insipidus (DI) in 10 (36%), isolated hormonal deficiency in 14 (50%), and concomitant DI and hormonal deficiency symptoms in 4 (14%). Radiographic diagnostic latency was common, occurring at a median 363 days (range = 9–2,626) onset of first symptoms, and significantly associated with both DI and hormonal deficiency as the index symptom (360 vs. 1,083 days, $p = 0.009$; 245 vs. 953 days, $p = 0.004$). Biochemical abnormalities were heterogeneous: each pituitary-axis was dysfunctional in at least 1 patient, with most patients demonstrating ≥ 2 abnormalities, and pretreatment dysfunction demonstrating a non-significant trend toward association with long-term posttreatment hormonal supplementation. Among germinomas, whole-brain and whole-ventricle radiation demonstrated significantly improved progression-free and overall survival, as compared with local therapy ($p = 0.009$, $p = 0.004$).

Conclusion: Neurohypophyseal iGCT are insidious tumors that may pose a diagnostic dilemma, evidenced by the prototypically prolonged latency before radiographic confirmation. Serial imaging and close endocrine follow-up is recommended in patients with a characteristic clinical syndrome and negative imaging due to the propensity for radiographic latency. Pretreatment biochemical abnormalities may indicate higher risk of posttreatment pituitary insufficiency, and all patients should receive careful endocrine follow-up. Local radiotherapy is prone to treatment failure, while whole-ventricle treatment is associated with improved survival in germinomas.

A153. Endoscopic Endonasal Surgery as an Alternative to Radiotherapy for Recurrent or Residual Pituitary Adenomas

Eugenio Cardenas¹, Ariel Kaen¹, Edinson Najera¹, Pablo Remon², Ignacio Martin Schrader¹, Alfonso Soto²

¹Department of Neurological Surgery, Hospital Universitario Virgen del Rocío, Sevilla, Spain

²Department of Endocrinology and Nutrition, Hospital Universitario Virgen del Rocío, Sevilla, Spain

Background: Recurrent or residual tumors are often treated with nonsurgical therapies such as observation, medical therapy, radiotherapy, or radiosurgery, all of which have low procedure-related morbidity. However, there are limited reports on the role of endoscopic endonasal surgery for recurrent or residual pituitary adenomas. In this study, we analyze a series of endoscopically resected recurrent and residual pituitary adenomas that had been previously operated on with a transsphenoidal microscopic or endoscopic approach. Clinical outcomes and complications are reported.

Objective: The aim of this study is to demonstrate that endoscopic endonasal surgery is a valid and safe alternative to radiotherapy in patients with recurrent or residual pituitary adenomas.

Methods: Retrospective analysis was conducted on a series of consecutive patients at a single tertiary referral institution who underwent endoscopic endonasal surgeries for residual or recurrent pituitary adenomas after original transsphenoidal microscopic or endoscopic surgeries. Thirty-three patients met the inclusion criteria. Patient complications, resection, and remission rates were assessed.

Results: Out of 33 patients, 19 had nonfunctional adenomas and 14 had functional adenomas, including five growth hormone-secreting tumors and nine adrenocorticotrophic hormone-secreting tumors. Of the five growth hormone-secreting adenomas, all were macroadenomas; three also had a cavernous sinus invasion (Knosp Grade 3 or 4). A cure (IGF-1 < 100) was obtained in 100% of the tumors that invaded the cavernous sinus. The overall cure rate was 60%. Of the nine adrenocorticotrophic hormone-producing adenomas, six were microadenomas, and three were macroadenomas; one also had a cavernous sinus invasion (Knosp Grade 3 or 4). A cure (salivary and free urine cortisol) was obtained in 50% of the microadenomas and 50% of the macroadenomas. The overall cure rate was 66.7%. Out of 19 cases with nonfunctional adenomas, all had macroadenomas and 11 presented visual impairment. Radiographically, 10 of the cases were Knosp Grades 3 and 4. Gross total resection was achieved in six (31.5%) cases. Total or partial improvement of vision was obtained in 90% of the patients. The mean follow-up was 20 months for patients with functional adenomas and 15 months for those with nonfunctional adenomas. No postoperative CSF leaks, postsurgical visual disorders, or cranial nerve palsies were detected.

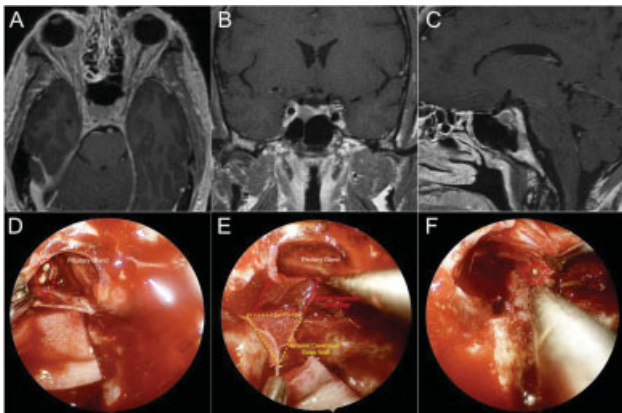
Conclusion: Endoscopic endonasal surgery can achieve similar cure rates in reoperations as radiotherapy without exposing patients to the long-term side effects of this therapy.

A154. Intraoperative, Histological, and Stimulated Raman Scatter Microscopy Evaluation of Cavernous Sinus Medial Wall Disease in Functional Pituitary Tumors

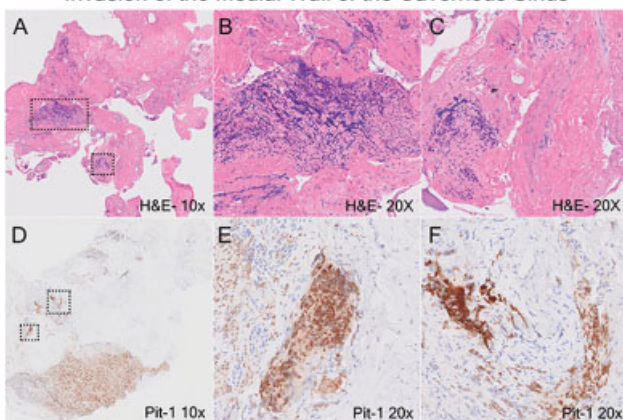
Ahmed Mohyeldin¹, Ayoze Doniz-Gonzalez¹, Pedro Augusto Sousa Rodrigues¹, Guillermo Blasco Garcia de Andoain¹, Kumar Abhinav¹, Juan C. Fernandez-Miranda¹

¹Stanford University, Stanford, California, United States

Recurrence of functional pituitary tumors remains a surgical and medical challenge to manage due to local invasion of tumor cells into surrounding sellar structures that were previously thought to be unresectable. Surgical resection of the medial wall of the cavernous sinus has recently been proposed as a strategy to reduce tumor burden and in some cases complete resection of microscopic disease rendering patients disease free. In this study, we provide direct intraoperative and histological correlative evidence of microscopic disease invasion of the medial cavernous sinus wall. Furthermore, we propose the application of a novel and rapid intraoperative evaluation of the medial wall using Raman Scatter Microscopy to prove disease involvement and allow for intraoperative decision-making for its resection. In this case series of only functional pituitary tumors, we demonstrate that intraoperative specimens from unilateral and bilateral medial wall resections demonstrate Pit-1 and CK CAM5.2 positive cells diffusely invading the cavernous sinus. In addition, we provide correlative images from the same specimens using Raman Scatter Microscopy demonstrating infiltrating tumor cells. Finally, we show early and mid-term biochemical control rates in this patient population.



Invasion of the Medial Wall of the Cavernous Sinus



A156. Outcomes of Intraoperative Ultrasound for Endoscopic Endonasal Transsphenoidal Pituitary Surgery

Joseph Domino¹, Domenico Gattozzi¹, Megan Jack¹, Charoo Iyer², Nick Harn¹, David Beahm¹, Roukoz Chamoun¹

¹University of Kansas Medical Center, Kansas City, Kansas, United States

²Medical College, Maharaja Sayajirao University of Baroda, Vadodra, Gujarat, India

Introduction: Pituitary tumors with parasellar extension into the cavernous sinus present a technical challenge for adequate visualization and gross total resection (GTR). The introduction of endoscopes into common use for transsphenoidal pituitary surgery has augmented the ability for intraoperative identification of parasellar extension with wider views and an enhanced ability to inspect the medial wall of the cavernous sinus. GTR and endocrinological remission in the case of pituitary adenomas are impacted by parasellar extension, significantly decreasing reported cure rates. Intraoperative MRI has been shown in some studies to increase the likelihood of GTR, guiding further tumor removal in a variable number of cases depending on the strength of magnet utilized. However, this comes with a significant increase in operative time and implementation costs secondary to the required infrastructure and equipment. Therefore, there remains interest in the development and validation of more time- and cost-effective intraoperative imaging techniques to aid in tumor resection. Intraoperative ultrasound may provide an effective and inexpensive solution.

Methods: A series of 20 consecutive patients, who underwent endoscopic endonasal transsphenoidal surgery for pituitary tumors with the assistance of intraoperative ultrasound, were prospectively collected. The intraoperative ultrasound findings were prospectively recorded at the time of each case. The 3-month postoperative MRI studies were obtained and independently reviewed to assess for residual tumor. The findings from the postoperative MRI were then compared with the intraoperative findings based on ultrasound.

Results: Median preoperative Knosp grade was 2. Cavernous sinus invasion was encountered intraoperatively in three patients, all of whom were Knosp grade 3 preoperatively. Three patients had undergone previous resection. Median operative time was 152 minutes. Based on intraoperative ultrasound findings, 17 patients (85%) were expected to have a GTR while three patients (15%) underwent subtotal resection and residual tumor was expected. Eighteen patients completed a 3-month postoperative MRI. The intraoperative ultrasound and MRI findings were concordant in 17 cases (94.4%) with only one instance of discordance where GTR was expected, but a small amount of residual tumor was noted on the postoperative MRI. No intraoperative complications were observed.

Conclusion: Intraoperative ultrasound can reliably predict tumor resection as assessed by 3-month postoperative MRI in pituitary adenomas with parasellar extension. Image capture and interpretation may vary based on operator experience with a learning curve likely present. However, once proficiency is gained, ultrasound provides immediate assessment of extent of resection and can assist in identification of tumor remnant, normal pituitary gland, and other important structures in the sellar region without significantly increasing operative time.

A157. Modeling Postoperative Cortisol Using Normalized Decay Rates in Cushing's Disease

Michael P. Catalino¹, Alexander Munoz¹, Le Min¹, Jr. Edward R. Laws¹

¹Brigham and Women's Hospital, Boston, Massachusetts, United States

Background: Cushing's disease is caused by an ACTH-hypersecreting adenoma of the pituitary gland and is associated with a five-time increased mortality compared with the general population. Only two-thirds of tumors are visible on MRI. Despite an 86% initial postoperative biochemical remission rate, one-quarter of patients recur at 5 years. For other benign brain tumors, extent of resection on imaging predicts survival, but it is the biochemical response that determines surgically induced remission in Cushing's disease. ACTH and cortisol levels drop immediately after successful surgery, which is due to both removal of ACTH producing adenoma cells and residual normal gland suppression. The considerable temporal variation in nadir cortisol levels after surgery makes single point cortisol level measurements a suboptimal metric for predicting truly definitive remission. In this study, postoperative cortisol levels were modeled using a serum cortisol decay function.

Methods: Cushing's disease patients from a single institution between 2010 and 2019 were included in the study. Criteria for diagnosis included two of these tests: an elevated 24-hour UFC, elevated midnight salivary cortisol, or a failed 1-mg dexamethasone suppression test. Patients were excluded from the study if they did not have histopathologic confirmation of a corticotroph adenoma. Serum cortisol was sampled every 6 hours after surgery, and steroids were not administered perioperatively unless serum cortisol dropped to <2 µg/dL or <5 µg/dL with symptoms of adrenal insufficiency. Cortisol levels were modeled using the decay function $y = Ae^{(-Bx)}$, where y is the cortisol level and x is the postoperative time. Single patient fitting algorithms were created. Data were normalized by first postoperative cortisol levels and crude data visualized using scatter plots and individual decay rate violin plots to identify potential bimodal conditions for the decay rate.

Results: Patient characteristics for the rapid and gradual decay groups are shown in Table 1. Median follow-up time was 47.4 weeks (interquartile range = 13.5–126). Three patients had persistently elevated cortisol levels after surgery and were excluded. Violin plots of decay rates for the initial remission group (Fig. 1) were bimodal at 0.15, and thus rapid decay was defined as a rate ≥ 0.15 , and gradual decay defined as a rate < 0.15 . A decay rate of 0.15 means that cortisol will decrease to 36.8% (1/e) of the original value over 6.7 hours. Gender, age, duration of symptoms, revision surgery, tumor size, EGFR, remission status (i.e., steroid dependency), and immunohistochemical staining correlated with decay rate. Crude decay rates were significantly higher in the remission group compared with the recurrence group at last follow-up (Fig. 1; $p < 0.05$).

Conclusion: Cortisol decay rate is bimodal after removal of corticotroph adenomas in patients with initial remission. Proper decay rate cutoffs and their association with recurrence probability are still unclear, but rapid decay may predict definitive remission after complete resection of the tumor. Further investigation into cortisol decay rates in Cushing's disease is needed.

Table 1: Patient characteristics (N=44) by rapid (≥ 0.15) and gradual (< 0.15) decay rate. Data are presented as means with standard deviations or medians and interquartile ranges for continuous normally distributed data or skewed data, respectively. Proportions shown using n (%). Groups compared with chi-square, Fisher-exact, or t-test if appropriate.

Variable		Rapid decay (N=10)	Gradual decay (N=34)	p-value
Gender	Male (%)	6 (60%)	3 (9%)	<0.001
	Female (%)	4 (40%)	31 (91%)	
Age (SD)		35.0 (16.9)	44.0 (13.1)	0.09
Duration of symptoms (SD)		4.0 (3.1)	2.6 (2.1)	0.053
Revision surgery	Yes (%)	3 (30%)	11 (32%)	<0.001
	No (%)	7 (70%)	23 (68%)	
Tumor size	<1cm (%)	9 (90%)	18 (53%)	<0.001
	≥ 1 cm (%)	0 (0%)	12 (35%)	
	No tumor (%)	1 (10%)	4 (12%)	
BMI, kg/m ² (SD)		30.6 (4.3)	36.4 (9.6)	0.07
EGFR, mL/min/m ² (SD)		65.8 (12.9)	59.4 (6.3)	0.04
AST, U/L (SD)		19.4 (3.9)	24.7 (15.1)	0.31
ALT, U/L (SD)		26.0 (17.1)	46.3 (64.3)	0.36
Albumin, g/dL (SD)		4.3 (0.3)	5.5 (6.7)	0.61
Remission status	Hypocortisolemic (%)	9 (90%)	13 (52%)	<0.001
	Normal (%)	1 (10%)	12 (48%)	
Follow-up weeks, median (IQR)		17 (1-58)	53 (18-133)	
Immunohistochemical staining	ACTH (%)	10 (100%)	34 (100%)	0.01
	PRL (%)	2 (20%)	10 (29%)	
	HGH (%)	3 (30%)	5 (15%)	
	LH (%)	1 (10%)	0 (0%)	
	FSH (%)	1 (10%)	1 (3%)	
	TSH (%)	1 (10%)	1 (3%)	
MIB-1 index mean (SD)		1.7% (2.0)	2.2% (5.6)	0.58

SD = standard deviation; BMI = body mass index; EGFR = estimated glomerular filtration rate; AST = Aspartate transaminase; ALT = Alanine transaminase; IQR = interquartile range; ACTH = adrenocorticotropic hormone; PRL = prolactin; HGH = human growth hormone; LH = luteinizing hormone; FSH = follicle stimulating hormone; TSH = thyroid stimulating hormone.

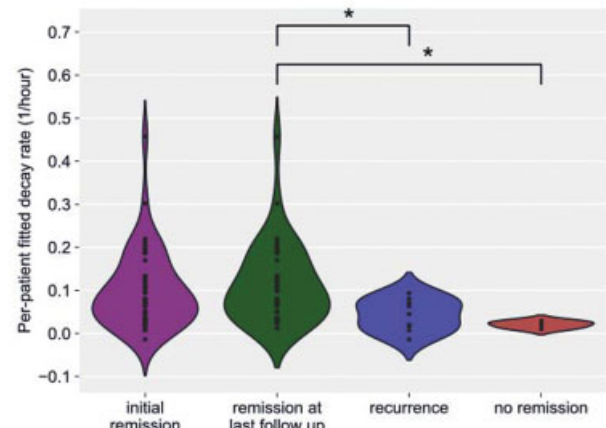


Figure 1: Violin plots showing crude data on decay rate by remission status. The decay function is $y = Ae^{(-Bx)}$ where y is cortisol level and x is days after surgery. A is a scaling parameter and B is the decay rate. The individual decay lines were fit with square root y least-squares weights and normalized by first post-operative cortisol level. Asterisks indicate $p < 0.05$.

A158. Unexpected Residual after Endoscopic Transphenoidal Surgery for Large and Giant Pituitary Adenomas

Ivo Peto¹, Timothy G. White², Abdullah M. Abunimer³, Hussam Abou-Al-Shaar⁴, Kevin Kwan², Katherine Wagner², Mark B. Eisenberg², Margherita Bruni², Amir R. Dehdashti²

¹University of South Florida, Tampa, Florida, United States

²Hofstra Northwell School of Medicine, Hempstead, New York, United States

³Harvard Medical School, Boston, Massachusetts, United States

⁴University of Pittsburgh Medical Center, Pittsburgh, Pennsylvania

Introduction: Pituitary adenomas constitute approximately 5 to 15% of all intracranial tumors. Most commonly,

giant and large pituitary adenomas are defined by their largest diameter >4 cm and >3 cm, respectively. Gross total resection after transsphenoidal pituitary surgery for giant pituitary adenomas is reported to be from 40 to 50%. To our best knowledge, there is no data on unexpected residual tumor after TSPS for large and giant adenomas, meaning residual tumor which felt to have been completely resected.

Methods: Medical records and imaging were queried for all patients who underwent transsphenoidal pituitary surgery between January 2015 and December 2018 at our institution. Only patients operated on by two experienced high volume pituitary were included (134 patients).

Results: Forty patients (13 females and 27 males) were included, comprising 30 large and 10 giant pituitary adenomas, respectively. The mean age was 57.85 ± 14.75 years (range = 25–80 years). The mean MRI follow-up time was 5.9 ± 6.54 months (range = 0–24) postresection. Intraoperative CSF leak occurred in 14 patients (35%): in seven (23.3%) with large and seven (70%) with giant PA ($p = 0.007$). Postoperative CSF leak occurred in three patients (7.5%).

In patients with large PAs, gross total resection (GTR) was achieved in 25 patients (83.3%), subtotal resection (STR) in four (13.3%), and inconclusive in one (3.3%). In patients with giant PAs, GTR was achieved in four patients (40%), STR in five (50%), and inconclusive in one (10%). Residual tumors were identified in nine (22.5%) patients, of which seven (77.7%) were unexpected. Increased longest working distance (LMax) was significantly associated with all residual tumors ($p = 0.049$). LMax was measured from the most anterior point of the sellar floor to the furthest tumor margin. Suprasellar width, height, and AP of the tumor were not associated with residual tumor ($p = 0.599$, $p = 0.651$, and $p = 0.171$, respectively). A statically significant association between unexpected residual tumor and larger retrosellar extension as well as increased LMax were observed ($p = 0.003$ and $p = 0.018$, respectively). No association was observed with suprasellar height, width, AP dimension, and unexpected tumor residual ($p > 0.05$). Analysis of intraoperative factors associated with presence of unexpected residual tumors revealed one case in which suspicious tissue was not removed due to uncertainty of its nature (tumor vs. gland). In one case, angled endoscope visualized suspicious tissue which was subsequently removed; however, follow-up MRI revealed residual tumor in the same location. Premature herniation of diaphragm was identified as contributing factor in one case. No factors were identified in remaining four cases.

Conclusion: Complete tumor resection in giant pituitary adenomas is achieved in minority of cases. Intraoperative visualization and assessment seem to be unreliable. Supplemental means of identifying residual tumor in transsphenoidal pituitary surgery for giant and large pituitary adenoma might increase the resection rate in patients with unexpected residual adenoma, in whom GTR is anatomically possible.

A159. Recurrence of Rathke's Cleft Cysts Based on Gross Total Resection of Cyst Wall: A Meta-analysis

Victor Lu¹, Avital Perry¹, Christopher Graffeo¹, Krishnan Ravindran², Jamie Van Gompel¹

¹Mayo Clinic, Rochester, Minnesota, United States

²University of Florida, Gainesville, Florida, United States

Background: Rathke's cleft cysts (RCCs) are benign growths of the embryological Rathke's pouch. Surgical decompression provides effective symptomatic relief in most cases; however, the effect of gross total resection (GTR) of the cyst wall on recurrence as well as pituitary function is unclear. The aim of this meta-analysis was to pool the current

literature and ascertain the recurrence control afforded by GTR of the cyst wall compared with subtotal resection (STR).

Methods: Searches of seven electronic databases from inception to January 2019 were conducted following PRISMA guidelines, resulting in 476 articles to be screened. Outcomes were analyzed using meta-analysis of proportions.

Results: A total of 10 retrospective cohort studies satisfied selection criteria, describing 655 surgically managed RCC cases, with 254 (39%) and 401 (61%) achieving GTR and STR of the cyst wall, respectively. GTR was associated with significantly reduced overall RCC recurrence by fixed-effects (FE) modeling (RR: 0.66; 95% CI: 0.45–0.96), but not by random effects (RE) modeling (RR: 0.75; 95% CI: 0.51–1.12). Based on both models, GTR was associated with significantly reduced symptomatic recurrence (RE model; RR: 0.37; 95% CI: 0.14–0.95) and significantly increased postoperative diabetes insipidus (RE model, RR, 2.60; 95% CI: 1.34–5.03). There was insufficient data to evaluate other pituitary axes in this context.

Conclusion: The current evidence indicates that GTR of the RCC cyst wall has the potential to affect the incidence of overall and symptomatic RCC recurrences, as well as drive postoperative DI incidence. However, expectations of clinical and pragmatic benefit following cyst wall resection should be titrated carefully against the potential for postoperative and pituitary morbidities, which currently remain poorly defined. Greater granularity is required to understand all factors that can influence recurrence and quality of life when evaluating a GTR approach to RCC.

A160. Predictors of Postoperative Visual Outcomes following Surgical Operation for Craniopharyngiomas

Srujan Koppurapu¹, Adham M. Khalafallah¹, Masaru Ishii¹, Gary L. Gallia¹, Nicholas Rowan¹, Debraj Mukherjee¹

¹Johns Hopkins University School of Medicine, Baltimore, Maryland, United States

Background: Craniopharyngiomas frequently present with visual deterioration due to involvement of the optic apparatus. Although visual improvement is a primary goal of surgical intervention, the predictors of postoperative visual change are not well characterized in the current literature.

Objective: This study intends to investigate and characterize preoperative, intraoperative, and postoperative variables related to surgical intervention of craniopharyngiomas to identify predictors of postoperative visual change. Such findings aim to improve shared decision-making between surgeons and patients by facilitating a better understanding of the visual outcomes to expect following surgical intervention.

Methods: A retrospective chart review was conducted of 97 total craniopharyngioma operations, corresponding to 67 patients undergoing at least one craniopharyngioma surgery at one of two medical centers (a tertiary care academic medical center and a related teaching hospital) between 2014 and 2019. Information was collected regarding demographics, comorbidities, radiological characteristics, laboratory studies, operative details, radiation therapy, hormone replacement, length of hospitalization, and vision. Visual acuity (VA) and visual fields (VF) were scored and combined quantitatively into visual impairment (VI) scores, according to guidelines defined by the German Ophthalmological Society. The difference between postoperative and preoperative VI scores served as the primary measure for visual change.

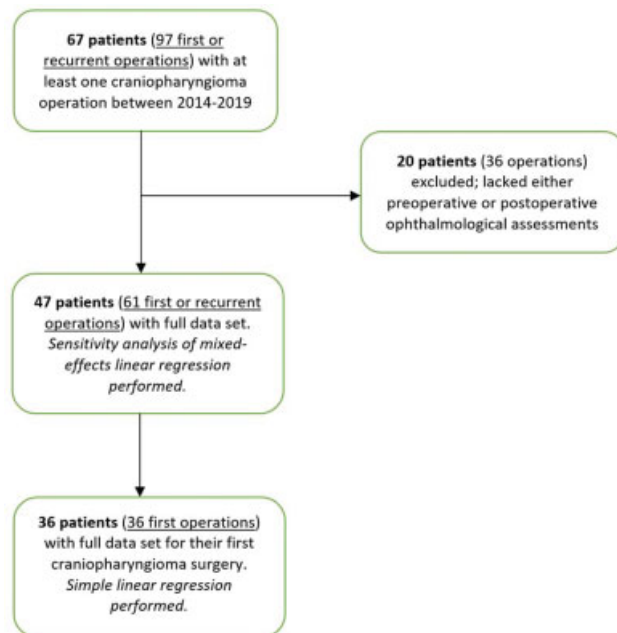
Results: Among the 67 total patients reviewed, preoperative and postoperative ophthalmological assessments were available for 47 patients, corresponding to 61 total

operations. The age range was 4 to 73 years and 27 (57%) patients were female. Visual improvement followed 36 (59%) of those operations, while vision remained stable after 15 (25%) operations and deteriorated after 10 (16%) operations. For these 61 operations, the mean estimated preoperative cyst volume was $26.5 \pm 47.3 \text{ cm}^3$, mean maximum cyst dimension was $3.01 \pm 1.16 \text{ cm}$, mean length of ICU stay was $3.65 \pm 3.96 \text{ days}$, and mean length of total hospitalization was $8.20 \pm 9.62 \text{ days}$. Radiologic involvement of the anterior cerebral arteries (ACAs) occurred in 27 (44%) of the operations.

First, a simple linear regression analyzed a subset of 36 of these operations that corresponded to a patient's first craniopharyngioma surgery. Significant predictors for visual deterioration were increased preoperative cyst volume and maximum dimension ($p = 0.017$ and $p = 0.041$), radiologic involvement of the ACAs ($p = 0.018$), increased length of ICU and total hospitalization days ($p = 0.004$ and $p = 0.014$), and worse preoperative VA and VI scores ($p < 0.001$ each).

A sensitivity analysis performed a mixed-effects linear regression involving all 61 operations to account for repeat surgeries. This analysis also found that all the above variables were significant predictors of postoperative visual worsening, except for preoperative cyst volume and dimension ($p \leq 0.02$ each). Newly identified predictors of worsening VI score included preoperative desmopressin replacement ($p = 0.027$) as well as worse preoperative and postoperative VA, VF, and VI scores ($p < 0.05$ each). Length of visual symptoms experienced preoperatively was not a significant predictor.

Conclusion: Vision improved in a majority of the operations reviewed in this study. Significant predictors of worsened VI score included greater preoperative cyst size, radiologic involvement of the ACAs, increased length of ICU and total hospitalization days, preoperative desmopressin replacement, and preoperative/postoperative VA, VF, and VI measurements.



A161. The Application of an “In Situ Bone Flap” in Skull Base Reconstruction after Extended Endoscopic Endonasal Approaches for Craniopharyngioma

Gang Yang¹

¹Department of Neurosurgery, The First Affiliated Hospital of Chongqing Medical University, P.R. China

Objective: This study aims to describe and evaluate a rigid skull base reconstruction method of using an “in situ bone flap (ISBF)” after extended endoscopic endonasal approaches (EEAs) for craniopharyngioma.

Background: EEAs for craniopharyngioma cause large skull base bone defects with an open cistern/ventricle, resulting in high-flow cerebrospinal fluid (CSF) leaks intraoperatively. The vascularized pedicled nasoseptal flap (PNSF) is the best method for reconstruction of skull base soft tissue at present. However, no reliable method exists for repairing bone defects repair after EEAs.

Methods: We describe the ISBF for cranial base repairs in EEAs. In all 116 cases of craniopharyngioma patients who underwent EEA at the First Affiliated Hospital of Chongqing Medical University between January 2017 and June 2019. The skull base repair was performed using an ISBF in comparison to repairs in the initial period without an ISBF. The clinical outcomes of these methods were compared.

Results: Among the latter repairs with an ISBF, the postoperative CSF leak rate was 1.82% (1/55), reflecting a significant improvement compared with those (7/61, 11.5%) repairs without ISBF ($p < 0.05$). The follow-up CT images revealed good bone healing in the surgical region, and no neurovascular complications were observed.

Conclusion: A craniotomy-harvested ISBF for skull base reconstruction is feasible and safe in EEAs. The ISBF combined with PNSF may further decrease postoperative CSF leaks and restore skull base anatomical structures postoperatively.

A162. The Benefits of Progressive Occipital Condylectomy in Enhancing the Far Lateral Approach to the Foramen Magnum

Alexander X. Tai¹, Aalap Herur-Raman², Walter C. Jean³

¹Medstar Georgetown University Hospital, Washington, District of Columbia, United States

²Surgical Theater,

³George Washington University, Washington, District of Columbia, United States

Background: The portion of the occipital condyle that is “safe” to remove remains controversial in the transcondylar approach. We aimed to correlate the gain in exposure with incremental removal of the occipital condyle to determine if there is a point where further drilling yields diminishing gains.

Methods: Virtual reality (VR) rendering of the skull was generated from 25 subjects with no pathology in the posterior fossa. A suboccipital far lateral craniotomy was done in VR space, stopping at the posterior edge of the occipital condyle. Angular measurements in the surgical corridor were taken at this point, as well as after removal of 25 and 50% of the condyle. Two surgical targets were used in this study: at the anterior midline of the foramen magnum (MFM) and the vertebrobasilar junction (VBJ).

Results: Progressive removal of the occipital condyle increased the angular exposure to both targets in a linear fashion. For the MFM, the working angle increased from 12 to 18 degrees for quarter condylectomy and then to 25 degrees for half condylectomy. The corridor to VBJ was much tighter, and the angle increased from 5.5 to 9 degrees for quarter

condylectomy and then to 12 degrees for half condylectomy. The gain in exposure for low target was greater than for the high target ($p < 0.001$).

Conclusion: Progressive removal of the occipital condyle yielded a linear increase in exposure, and there was no “sweet spot” beyond which the drilling was futile. However, the impact of condylectomy was greater for the low target at the level of the foramen magnum. For the high target at VBJ, the gain may be clinically irrelevant.

A163. Comparison of the Impact on Simulated Airflow and Heat Transport between the Superior Ethmoidal Approach for Endoscopic Endonasal Anterior Cranial Base Resection and the Traditional Endoscopic Anterior Cranial Base Approach

Varun Patel¹, Rohan Viswanathan², Maria Peris-Celda³, Tyler Kenning³, Carlos Pinheiro-Neto¹

¹Division of Otolaryngology/Head and Neck Surgery, Department of Surgery, Albany Medical Center, Albany, New York, United States

²Albany Medical College, Albany, New York, United States

³Department of Neurosurgery, Albany Medical Center, Albany, New York, United States

Background: The traditional endoscopic endonasal anterior cranial base approach (TA) involves total removal of intranasal structures. The endoscopic endonasal superior ethmoidal approach (SEA) is a more conservative technique to access the anterior cranial base with preservation of middle turbinates, osteomeatal complex, part of the ethmoid cells, and most of the septum (Fig. 1). It has been designed as an alternative method to resect anterior cranial base lesions that have minimal or no extension intranasally. Previous studies have noted altered nasal airflow and heat transport following TA. The severity of postoperative changes in airflow and mucosal wall interactions may correlate with the amount of nasal tissue removed.

Objective: This study aims to compare the impact on simulated airflow and heat transport between TA and SEA using computational fluid dynamics.

Methods: Nine patients were included in the study: three control patients with normal sinus anatomy and no intracranial pathology, and six patients with intracranial pathology: three patients who underwent SEA and three patients who underwent TA. Computed tomographies (CT) from control patients and postoperative CT of SEA and TA patients were studied. Three-dimensional sinonasal models were constructed from CT scans, and hybrid computational meshes were created from these models. Nasal Advanced Systems of Airflow Laboratory (NASAL) was used to analyze changes in airflow, temperature, pressure distribution, and wall shear stress in coronal equidistant slices of the CT images. Nasal cavity volume calculations were completed using Osirix MD.

Results: In the SEA group, nasal preservation did not limit tumor resection as complete resection was achieved in all cases despite large tumor sizes (mean tumor size $3.4 \times 3.0 \times 1.8$ cm). Comparing patient controls with the SEA group, total nasal cavity volume did not change significantly after SEA approach ($p = 0.91$), and the average flow rate increased 1.37 l/min ($p = 0.25$). The average nasal cavity temperature did not change significantly ($p = 0.23$), reaching a maximum of 36.5°C in the nasopharynx. Average wall shear stress (WSS) increased by 0.01 Pa in the SEA group ($p = 0.12$). Comparing patient controls with the TA group, total nasal cavity volume increased significantly after TA approach ($p = 0.03$), and the average flow rate increased 7.20 L/min ($p = 0.03$; Fig. 2). The average nasal cavity temperature reduced 3.47°C ($p = 0.02$). Average WSS increased by 0.02

Pa ($p = 0.08$). In both groups, average airflow velocity peaked at 1.0 to 2.0 cm from the nostril, corresponding to the area of surgical resection. Furthermore, changes in average velocity throughout the nasal cavity correlated with changes in average WSS.

Conclusion: The TA demonstrated significant increase in nasal cavity volume and average flow rate and reduced nasal cavity temperatures, whereas the SEA did not result in significant changes in these parameters when compared with patient controls. The SEA preserves not only the majority of anatomical structures of the nasal cavity in the anterior cranial base resection, but also maintains the physiologic airflow and heat transport mechanisms postoperatively. Due to the impact in nasal physiology, SEA is indicated in patients with anterior cranial base pathology with minimal or no intranasal involvement.

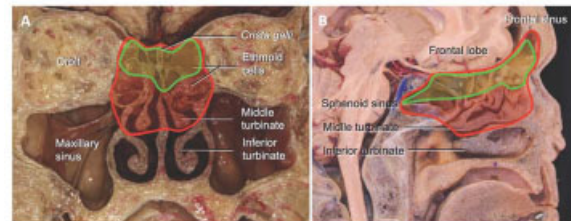


Figure 1: Cadaver anatomical sections outlining the intranasal structures removed during the traditional endoscopic endonasal anterior cranial base approach (red) and the more conservative endoscopic endonasal superior ethmoidal approach (green) in coronal (A) and sagittal (B) planes.

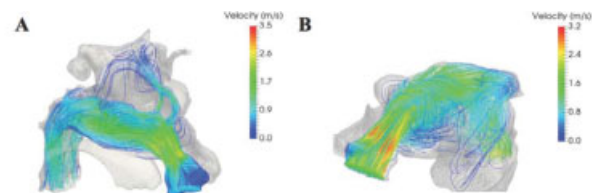


Figure 2: Three-dimensional nasal cavity airflow distribution and velocity profile following (A) endoscopic endonasal superior ethmoidal approach and (B) traditional endoscopic endonasal anterior cranial base approach. The traditional approach demonstrated wider airflow distributions and increased nasal cavity volumes postoperatively compared to superior ethmoidal approach.

A164. Endoscopic Endonasal Orbital Surgery

Jeffrey Glicksman¹, Maria Peris-Celda^{2,3}, Tyler Kenning², Edward Wladis⁴, Carlos Pinheiro-Neto^{1,2}

¹Division of Otolaryngology/Head and Neck Surgery, Department of Surgery, Albany Medical Center, Albany, New York, United States

²Department of Neurosurgery, Albany Medical Center, Albany, New York, United States

³Adjunct Assistant Professor, Department of Neurosurgery, Mayo Clinic, Rochester, Minnesota, United States

⁴Department of Ophthalmology, Albany Medical Center, Albany, New York, United States

Background: Through an endoscopic endonasal route, it is possible to access the medial orbital structures as well as the orbital apex without a facial skin incision or the need for brain retraction. There is documented use of the endoscopic endonasal approach for several orbital pathologies. The purpose of this study is to evaluate outcomes of the use of the

endoscopic endonasal approach in the treatment of a variety of orbital pathologies.

Methods: Medical records were reviewed and data were collected on patients who underwent endoscopic endonasal orbital surgery by a single surgical team at a tertiary care medical center between March 1, 2013 and July 1, 2019. Data were analyzed using simple statistical techniques including sums, ratios, and averages.

Results: From March 2013 to July 2019, 59 patients underwent endoscopic endonasal orbital surgery. This approach was performed for indications including: infection ($n = 19$, 32.2%), trauma ($n = 13$, 22.0%), neoplasm ($n = 13$, 22.0%), Grave's ophthalmopathy ($n = 8$, 13.6%), epistaxis ($n = 3$, 5.1%), and cranial nerve V2 neuralgia ($n = 2$, 3.3%). Seventeen patients underwent endoscopic endonasal drainage of an orbital subperiosteal abscess. This was performed in conjunction with external orbitotomy in 13 (76.4%) of cases. Of these cases 94.1% of patients went on to complete resolution, one required reoperation prior to full resolution. Neoplasms were either identified by biopsy, debulked, or radically resected. Pathology identified includes: lymphoma (3), adenoidcystic carcinoma (2), cavernous hemangioma (2), meningioma (2), sinonasal adenocarcinoma, metastatic melanoma, plasmocytoma, and dacrocystocele. Orbital trauma was addressed by this approach for reduction and rigid fixation of the orbital floor fracture (6) or medial orbital wall fracture (4), and removal of infected retained orbital implants (3). Endoscopic endonasal orbital decompression for Grave's ophthalmopathy was performed unilateral in 4 (50%) and bilateral in 4 (50%) of cases. In two of the bilateral procedures, the patient developed persistent diplopia that was corrected with subsequent medial rectus muscle surgery. One patient required reoperation for revision of a displaced medial orbital wall implant. In two patients, V2 nerve decompression was performed for neuralgia; in one case, this leads to resolution of symptoms. The endoscopic endonasal approach was also used to perform an intraorbital anterior ethmoid artery ligation in three patients with persistent episodes of epistaxis despite prior ligation of both sphenopalatine arteries.

Conclusion: The endoscopic endonasal orbital approach provides unique access and is an effective method of addressing multiple different pathologies involving the orbit, allowing increased clarity and avoiding morbidity associated with open approaches. No irreversible complications were noted in our dataset.

A165. Gains Realized in Pituitary Carcinoma Survival: A Contemporary Evaluation Using the Seer Database

Nathan J. Wallace¹, Anand K. Devaiah¹

¹Boston University School of Medicine, Boston, Massachusetts, United States

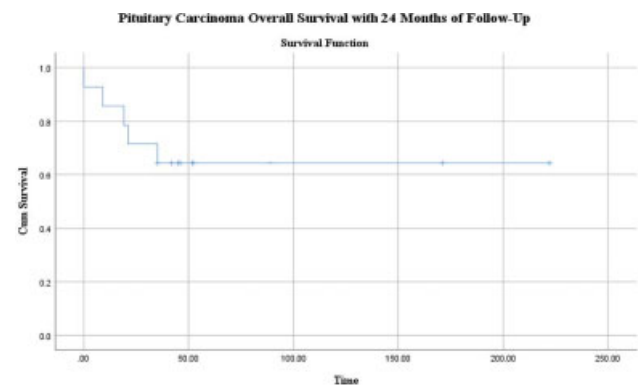
Background: Pituitary carcinomas are rare tumors accounting for 0.1% of all pituitary tumors. They are defined as having noncontiguous metastases from their primary sellar origin and can be difficult to diagnose due to a lack of histological differentiation. The difficulty of diagnosis can result in delay of critical treatment in these patients, and treatment is best managed by a multidisciplinary team. Treatment delay combined with presence of metastases and complexity of treatment regimens results in poor prognoses for patients. During the last several decades, our understanding of pituitary carcinomas has dramatically increased, and there have been recent initiatives to improve patient access to healthcare, specifically the 2010 Affordable Care Act (ACA). We investigated whether there were any changes in incidence and treatment outcomes of pituitary

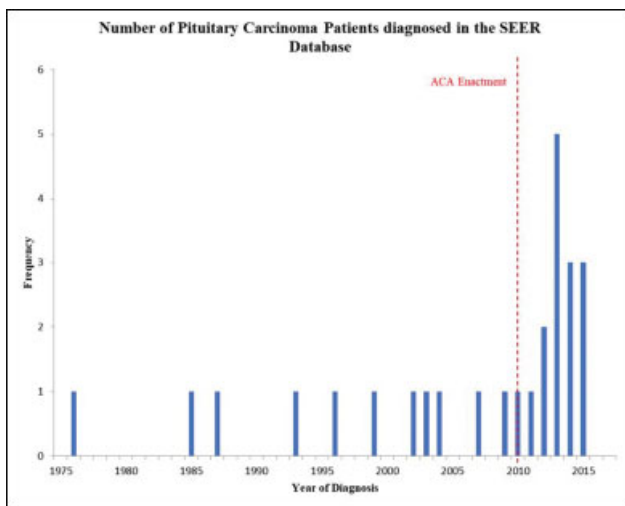
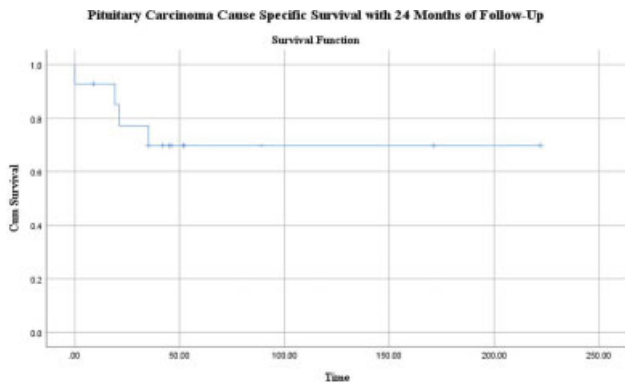
carcinoma that correlated with these legislative and informational advances.

Methods: The Surveillance, Epidemiology, and End Results Program (SEER) (November 2018 data submission) was used to identify study participants. Patients with primary site pituitary tumors (ICD-0-3 Code C75.1) classified as having malignant behavior and diagnosed between January 1, 1975 and December 31, 2016 were identified. Those patients younger than 18 years of age at the time of diagnosis, without a known age, or exhibiting histology other than adenoma or adenocarcinoma (8,140–8,389) were excluded. Total 175 participants were identified from these parameters. As the SEER malignant classification encompasses both invasive adenomas and carcinomas, additional stratification based on presence of noncontiguous metastases narrowed our analysis to 26 pituitary carcinomas. We sought to examine whether there was an increase in the number of pituitary carcinoma patients since the enactment of the ACA.

Results: Overall survival of pituitary carcinoma patients after 1, 2, and 5 years was 86, 71, and 64%, respectively after controlling for adequate follow-up. Cause-specific survival of these participants was similar with findings of 94, 77, and 68%, respectively. These findings offer a marked improvement in prognosis, with previous studies noting worse survival (20% after 8 years postdiagnosis with 66% mortality within the first year) (Oh [2012], Scheithauer [2005], and Pernicone [1997]). The present study shows greater incidence and better prognosis compared with the most recent SEER data (Hansen [2014]). Furthermore, there has been a 116.7% increase in pituitary carcinoma diagnosis since 2010, coinciding with the ACA.

Conclusion: Pituitary carcinomas in the United States are rare but have shown an increased incidence in the SEER database over time. Given that these are rare, revisiting this diagnosis and its prognosis is important to gain a contemporary perspective. Our data show a marked improvement in prognosis for pituitary carcinoma and significantly increased numbers from prior studies, changing our understanding of this disease. While the exact cause of these trends is unclear, it is most likely due to a combination of many factors. These may include better powered studies, improved diagnostic capability, expanded treatment options, physician awareness, and improved access to healthcare. Our data showing a significant increase in pituitary carcinoma diagnosis since the enactment of the ACA support the inclusion of improved healthcare access as a factor improving patient prognosis.





A166. Endoscopic Transnasal Odontoidectomy: A Single-Center's Experience and Approach to Pathology of the Craniocervical Junction

Rocco M. Dabecco¹, Raj Nangunoori¹, Alexander Yu¹

¹Allegheny General Hospital, Pittsburgh, Pennsylvania, United States

Introduction: The craniocervical junction is an important anatomical compartment with unique structural and functional relationships that present challenges to surgeons. Historically, transoral microscopic approaches with additional posterior stabilization have been accepted as the standard of care when treating pathology in this area. However, with the advancement of newer technology, endoscopic transnasal clivus and odontoid surgeries are gaining interest as alternative approaches. We reviewed our experience of using endoscopic transnasal odontoidectomy in the treatment of pathology at the craniocervical junction. Our objective is to further validate the effectiveness of this approach in selected cases and describe several operative nuances and pearls based on experiences at our institution.

Methods: We retrospectively evaluated nine patients (two males and seven females; age range = 28–81 years) who underwent endoscopic transnasal odontoidectomy between 2013 and 2019.

Results: Among the nine patients, seven had basilar invagination with focal neurologic deficits and two had

metastatic osseous lesions invading the odontoid. Seven of the patients underwent posterior stabilization with occiput to cervical fusions of varying construct lengths. Mean modified Rankin scale average demonstrated improvement from 3 to 2, respectively. The follow-up period ranged from 3 to 52 months. Our series demonstrated moderately less overall surgical and medical complications as compared with other retrospective studies.

Conclusion: The endoscopic transnasal modality represents an attractive minimally invasive surgical approach to the craniocervical junction. With proper patient selection and continued development of technique and experience, this approach is a safe and effective tool for a surgeon's armamentarium.

A167. Discontinuation of Postoperative Prophylactic Antibiotics for Endoscopic Endonasal Surgery

Carolina G. Benjamin¹, Yosef Dastagirzada², Julia Bevilacqua², Jason Gurewitz², Chandra Sen², John G. Golfinos², Dimitris Placantonakis², Jafar J. Jafar², Rich Lebowitz², Seth Lieberman², Ariane Lewis², Donato Pacione²

¹University of Miami, Miami-Dade County, Florida, United States

²NYU Langone Medical Center, New York City, New York, United States

Direct access through the sinuses and nasopharyngeal mucosa in the endoscopic endonasal approach (EEA) raises concern for a contaminated operative environment and subsequent infection. The reported rate of meningitis in endoscopic endonasal skull base surgery in the literature ranges from 0.7 to 3.0% [1, 2]. The only factor identified as being independently associated with meningitis in a statistically significant manner is cerebrospinal fluid (CSF) leak [1–5]. However, many centers performing high volume of EEAs use postoperative antibiotic coverage independent of the presence intraoperative or postoperative CSF leak. Furthermore, while meningitis remains a severe concern, most centers use postoperative gram-positive coverage to prevent toxic shock syndrome caused by *Staphylococcus aureus* infection in the setting of prolonged nasal packing. There are currently a multitude of approaches regarding perioperative antibiotic coverage in EEAs [1–4]. Given the lack of consensus in the literature and our experience regarding the benefit of discontinuation of prolonged prophylactic antibiotics throughout the breadth of neurosurgical procedures, we sought to analyze the need for postoperative antibiotics in EEAs further. As such, we performed a prospective analysis compared with a retrospective cohort to delineate whether discontinuation of postoperative antibiotics leads to a change in the rate of postoperative infections.

The retrospective cohort consisted of patients who underwent an EEA from January 1, 2013 to May 31, 2019. These patients all received postoperative antibiotics while nasal packing was in place (median 7 days). Starting on April 1, 2019 until August 1, 2019, we discontinued postoperative antibiotic use. Patients from this group made up the prospective cohort. The retrospective cohort had 315 patients (66% pituitary macroadenomas vs. 7% microadenomas, 4% meningiomas, 4% craniopharyngiomas, 4% chordomas, and 15% others) while the prospective group had 23 patients (57% pituitary macroadenomas, 30% craniopharyngiomas, 8% meningiomas/chordomas, and 5% others). The primary endpoint was rate of postoperative infections and specifically, meningitis and multidrug resistant organism (MDRO) infections.

There was no statistically significant difference in the use of nasal packing ($p = 0.085$), intraoperative CSF leak ($p = 0.133$), and postoperative CSF leak ($p = 0.507$) between the two groups. There was also no significant difference in the number of patients with positive preoperative MSSA and

MRSA nasal swabs ($p = 0.622$). There was a significant decrease in the number of patients discharged with antibiotics (55.1% in the retrospective and 4.5% in the prospective group, $p = 0.000$). The number of patients with positive blood cultures ($p = 0.701$) and positive urine cultures ($p = 0.691$) did not differ significantly between the two groups. Finally, there was no statistically significant difference in postoperative CSF infections ($p = 0.34$) or MDRO infections (0.786) between the two groups.

We describe promising preliminary results that demonstrate that discontinuation of postoperative antibiotics in EEAs do not lead to a statistically significant increase in the rate of postoperative CSF or MDRO infections. The previous algorithm for postoperative antibiotic coverage in our center, like many centers, called for gram-positive coverage, which may have contributed to the overall preponderance of gram-negative meningitis cases in this cohort.

A168. Automated Meningioma Detection and Segmentation Using Deep Neural Networks

Maya Harary¹, Alessandro Boaro², Vasilios Kavouridis², Jakub Kaczmarzyk², Marco Mammi², Hassan Dawood², Satrajit Ghosh³, Omar Arnaout²

¹Department of Neurosurgery, David Geffen School of Medicine, University of California Los Angeles, Los Angeles, California, United States

²Computational Neuroscience Outcomes Center, Department of Neurosurgery, Brigham and Women's Hospital, Boston, Massachusetts, United States

³McGovern Institute, Massachusetts Institute of Technology, Cambridge, Massachusetts, United States

Introduction: Though tumor volume and growth rate assessment are a central part of surgical planning and surveillance in meningioma patients, these can be time consuming and potentially inaccurate task when done using the presently available manual or semiautomatic tumor segmentation methods. Machine learning approaches have the potential to allow for automated meningioma detection and segmentation on magnetic resonance imaging (MRI).

Methods: Using a dataset of 812 brain MRIs of meningioma patients, with a total of 940 tumors represented, we designed a deep learning (DL) algorithm based on a three-dimensional convolutional neural network (3D CNN) architecture with the goal of automatically detecting and accurately segmenting meningiomas. Accuracy compared with expert labels of the same MRIs was assessed using a Dice's score. The algorithm's potential impact on clinical workflow was assessed in a simulated clinical scenario, measuring time needed for accurate segmentation and volume estimation accuracy.

Results: The automated segmentation performed with a Dice's score reaching a median of 91% and a mean of 85% for single and multiple tumors with volume $>3\text{cc}$ (Fig. 1). Automated segmentation reduced time to create clinically usable segmentations by experts by an average of 65%. The predicted volumes generated by the algorithm showed a stronger correlation (0.98, $p < 0.001$) to real tumor volume values compared with traditional two- and three-dimensional estimation techniques (Fig. 2).

Conclusion: We developed a high-performing DL algorithm for meningioma segmentation with the potential of significantly impacting current clinical workflow. Further prospective investigation can assess both the accuracy of this tool and its utility in meningioma surveillance over time.

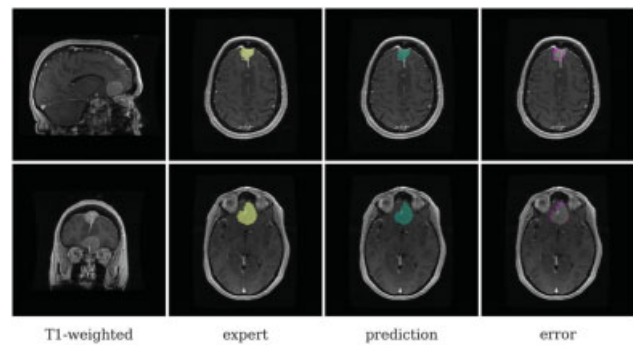


Fig. 1 Meningioma segmentation by expert and algorithm in a patient with two lesions.

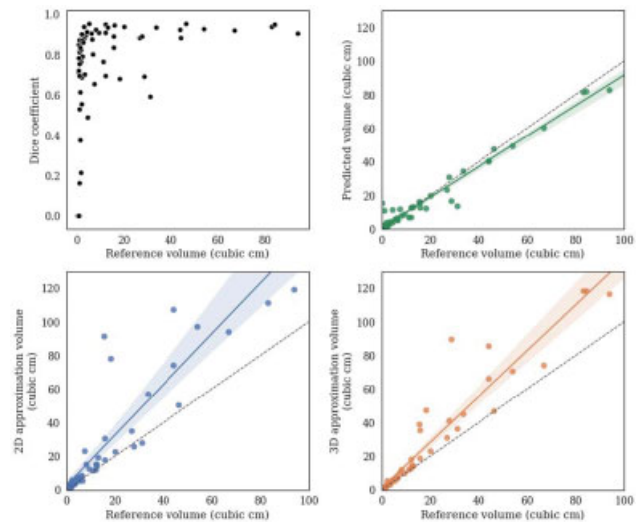


Fig. 2 Performance of deep learning algorithm at different tumor volumes (top) compared with traditional two- and three-dimensional volumetric estimation methods (bottom).

A169. Molecular Taxonomy of Meningioma

Wenya Linda Bi¹, Samantha Hoffman¹, Eleanor Woodward¹, Joseph Driver¹, Sherwin Tavakol¹, Ayal A. Aizer¹, Malak Abdalthagafi², Ossama Al-Mefty¹, Ian F. Dunn³, Sandro Santagata¹

¹Brigham and Women's Hospital, Boston, Massachusetts, United States

²Saudi Human Genome Laboratory, King Fahad Medical City and King Abdulaziz City for Science and Technology, Riyadh, Saudi Arabia

³Oklahoma University Health Science Center, Oklahoma City, Oklahoma, United States

Background: Meningiomas, as the most common primary brain tumor in adults, are undergoing a reawakening in biological understanding. An increasing array of genomic and epigenetic studies has unveiled a cascading array of molecular signatures for meningiomas, with prognostic and phenotypic implications. Among these, aggregates of chromosomal alterations and methylation profiles may portend meningioma recurrence beyond the scope of current histopathologic criteria. However, a rigorous molecular scheme for determination of meningioma behavior, with long-term clinical annotation and outcomes and which is widely accessible to clinicians, is still lacking.

Methods: We analyzed 530 meningiomas from patients who underwent surgical resection between 1999 and 2017 (350 women and 180 men; mean age = 72.5 years) and whose tumors were analyzed by high-resolution array comparative genomic hybridization (aCGH). Clinical data, histopathology, anatomic location, volumetric quantification of preoperative and postoperative MRIs, and radiographic recurrence were evaluated. We devised a molecular classification of meningiomas based on the copy number profile of chromosomes lost or gained and compared the association of progression-free survival with this molecular classification versus standard histopathology.

Results: Meningiomas harbor recurrent chromosomal copy number alterations that significantly associate with classic histopathology but not in all cases. In cases where the molecular classification scheme differed from WHO histopathology grade, the molecular classification augmented prediction of tumor recurrence. We further inferred the chromosomal copy number profile from 150 meningiomas that underwent sequencing for a panel of cancer-associated genes, and demonstrate strong correlation between this profile and that obtained from aCGH, suggesting that copy number analysis may be broadly accessible to clinicians.

Conclusion: We propose a molecular classification for meningioma based on its chromosomal copy number signature, with implication for clinical management and prognostication.

A170. Gamma Knife Radiosurgery for Patients with Foramen Magnum Meningiomas: Cohort Study

Salomon Cohen-Cohen¹, Avital Perry¹, Christopher S. Graffeo¹, Lucas P. Carlstrom¹, Bruce E. Pollock¹, Link J. Michael¹
¹Department of Neurologic Surgery, Mayo Clinic, Rochester, Minnesota, United States

Background: Meningiomas are the most common tumors of the foramen magnum, but represent only 2 to 3% of all intracranial meningiomas. Standard management strategies include observation, resection, or stereotactic radiosurgery (SRS), with consideration for each depending on factors including size, anatomic configuration, patient age, medical comorbidities, and individual preferences. Surgical resection is typical challenging due to the intimate relationship between these tumors and surrounding neurovascular structures; correspondingly, SRS presents an attractive, safe, and effective strategy for appropriately selected patients including those without brainstem compression, or with recurrent/progressive tumors following resection. Given the relative rarity of these lesions, long-term clinical outcomes data after SRS are limited. We report our experience with a single-center cohort study of patients with foramen magnum meningiomas treated with primary SRS.

Methods: Cohort study of all foramen magnum meningiomas treated with SRS at our institution during the study period, 1990 to 2018. Histology- and imaging-based diagnoses were included, provided that they were the basis for treatment. Patients without 6 months of post-SRS imaging follow-up were excluded. Data abstraction included demographics, clinical presentation, treatment history, and dosimetry. The primary outcome was treatment failure (defined as radiographic progression after SRS based on post-SRS MRI), the secondary outcome was radiation-induced complications, and statistics were reported descriptively as counts with frequencies for categorical data, or medians with ranges for continuous data.

Results: Twenty-two patients were included, 16 of whom were female, with an overall median age at SRS of 59 years (range = 39–81). Incidental diagnoses accounted for 6

patients (27%), while the remaining 16 presented with cranial neuropathy (75%), imbalance (50%), craniocervical pain (43%), paresthesias (25%), or hydrocephalus (12%). Fourteen tumors were ventral (64%). A total of 12 patients underwent primary SRS (55%), while 10 were treated after subtotal resection (45%). Median pre-SRS volume was 6.3 cm³ (range = 0.8–19.9). Median SRS margin dose was 14.8 Gy (13–18); median maximal dose was 29.8 Gy (26–36). One individual was treated with volume-staged SRS for a larger tumor (16 Gy to 9 cm³ followed by 16 Gy to 10.4 cm³) in the setting of postoperative deficits. Median radiologic follow-up was 80 months (range = 6–178 months); median clinical follow-up was 80.7 months (range = 6–128 months). As of last follow-up, 7 tumors had regressed (32%), 14 were stable (64%), and 1 demonstrated evidence of progression after SRS (4%)—an event that occurred in the only patient with a known grade II meningioma and which was treated with two courses of repeat SRS. RIC were limited to one instance of extremity numbness and hemifacial pain (4%) associated with medullary T2 changes on MRI; the patient improved clinically and radiographically in follow-up.

Conclusion: Foramen magnum meningiomas are rare, typically benign posterior fossa tumors. The current cohort study is small but extensively followed, and demonstrates that these lesions respond favorably to SRS in both the primary and adjuvant/salvage settings. Modest margin doses (13–18 Gy) appear to confer excellent tumor control, while also effectively minimizing the toxicity profile. Atypical lesions are predisposed to treatment failure and may require aggressive, multimodality treatment for achieve durable growth arrest.

A171. Surgical Implication of the Supralabyrinthine Aircell Tract in Combined Petrosal Approach

Je Beom Hong¹, Chang Ki Hong², Hankyu Kim³

¹Kangbuk Samsung Hospital, Seoul, South Korea

²Gangnam Severance Hospital, Gangnam-gu, Seoul, South Korea

³Cha Bundang Medical Center, Seongnam, South Korea

Purpose: The aim is to safely perform the combined petrosal approach, a comprehensive understanding of the anatomy of the petrous pneumatization is required. The purpose of this study is to clarify the supralabyrinthine air cell tract and its surgical implication in combined petrosal approach.

Methods: From 2010 to 2019, we analyzed total 45 patients who underwent a combined petrosal approach for the petroclival meningioma removal. Medical records including operative findings and imaging studies were reviewed. We performed the 3D volumetric analysis of the supralabyrinthine air cell tract and analyzed the relationship between surgical corridor and exposed area of the lesion.

Results: Mean volume of supralabyrinthine air cell tract was 0.331 mm³ (SD = 0.542, range = 1.91) from internal acoustic canal to posterior semicircular canal. In cases with small supralabyrinthine air cell tract, we had to perform the additional petrosectomy including transcrural petrosectomy, translabyrinthine petrosectomy, exposure of the jugular bulb, or exposure of the retrosigmoid space more widely. Large supralabyrinthine aircell tracts required less retraction of the sigmoid sinus. We found preoperative consideration of supralabyrinthine aircell tract, as well as lesion location, size, patient's hearing condition and neurological abnormalities, was an important factor in the successful treatment of petroclival meningioma.

Conclusion: Before performing the combined petrosal approach, analysis of the supralabyrinthine aircell tract can help in more accurate surgical planning.

A172. Access Corridor for Intentionally Target Devascularization of Feeding Arteries of the Petroclival Meningioma

Kentaro Watanabe¹

¹Jikei Medical University, Tokyo, Japan

Background: Surgeries of petroclival meningioma is one of the most difficult and challenging operations in skull base cases. Devascularization of the tumor is basic step of the meningioma resection. Even complex petroclival meningioma surgery, surgical steps should be constructive and rational as same as the normal meningioma surgery. Devascularization, debulking, decompression, and dissection are basic steps but imperative technique. We consider again from the point of view of microdissection and use surgical procedures as rational steps and are used for surgery.

Objects: Considering the microanatomical location of the feeding arteries of the petroclival meningiomas, we performed target devascularization of feeding arteries through the surgical corridor to achieve early coagulation when the feeding arteries are able to embolize by endovascular devascularization. Based on a microanatomical understanding of the location of feeding arteries, constructive operative strategy for devascularization and removal of the tumor compartment through individual access corridor and showing a concept of the compartment tumor removal of each artery.

Methods: The preoperative angiographical examination was performed and analyzed the vascularization in the petroclival meningioma (PCM) recent 10 cases. The feeding arteries were embolized by the endovascular team as much as possible. Surgery was performed following the target devascularization steps. Each artery was approached through the individual access corridors based on the anatomical location. The surgical results of patients operated per this strategy were compared with a historic series of patients who underwent conventional surgery.

Results: The surgical duration was reduced and the surgical result was improved. Endovascular embolization was effective for feeders from APA. MHT is difficult to embolize in most cases.

A173. Phosphoproteomic and Kinomic Signature of Clinically Aggressive Grade I (1.5) Meningiomas Reveals RB1 Signaling as a Novel Mediator and Biomarker

Jacob Ruzevik¹, Sam Emerson¹, Kate Carroll¹, Jr. Manuel Ferreira¹

¹University of Washington, Tacoma, Washington, United States

Purpose: Most WHO Grade I meningiomas carry a favorable prognosis. Some become clinically aggressive with recurrence, invasion, and resistance to conventional therapies (grade 1.5; recurrent/progressive WHO grade I tumors requiring further treatment within 10 years). We aimed to identify biomarker signatures in grade 1.5 meningiomas where histopathology and genetic evaluation has fallen short.

Experimental Design: The MS-based phosphoproteomics and peptide chip array kinomics were used to compare grade I and 1.5 tumors. Ingenuity Pathway Analysis (IPA) identified alterations in signaling pathways with validation by western blot. The selected biomarker was evaluated in an independent cohort of 140 samples (79/140 genotyped for meningioma mutations) by tissue microarray and correlated with clinical variables.

Results: The MS-based phosphoproteomics revealed differential Ser/Thr phosphorylation in 32 phosphopeptides. The kinomic profiling by peptide chip array identified 10 phosphopeptides, including a 360% increase in phosphoryla-

tion of RB1, in the 1.5 group. IPA of the combined datasets and western blot validation revealed regulation of AKT and cell cycle checkpoint cascades. Rb1 hyperphosphorylation at the S780 site distinguished grade 1.5 meningiomas in an independent cohort of 140 samples and was associated with decreased progression/recurrence-free survival. Mutations in NF2, TRAF7, SMO, KLF4, and AKT1 E17K did not predict RB1 S780 staining or progression in grade 1.5 meningiomas.

Conclusion: Rb1 S780 staining distinguishes grade 1.5 meningiomas, independent of histology, subtype, WHO grade, or genotype. This promising biomarker for risk stratification of histologically bland WHO grade I meningiomas provides insight into the pathways of oncogenesis driving these outlying clinically aggressive tumors.

A174. Predicting Discharge Disposition Following Meningioma Resection Using a Multiinstitutional Natural Language Processing Model

Meredith A. Monsour¹, Whitney E. Muhlestein², Gabriel Friedman³, Aniket Zinzuwadia⁴, Marcus Zachariah³, Jean-Valery Coumans³, Bob Carter³, Lola B. Chambless⁵

¹Vanderbilt University School of Medicine, Nashville, Tennessee, United States

²Department of Neurosurgery, University of Michigan Medical Center, Ann Arbor, Michigan, United States

³Department of Neurosurgery, Massachusetts General Hospital, Boston, Massachusetts, United States

⁴Harvard Medical School, Boston, Massachusetts, United States

⁵Department of Neurological Surgery, Vanderbilt University Medical Center, Nashville, Tennessee, United States

Introduction: Machine learning (ML)-based predictive models are increasingly prevalent in neurosurgery, though most require resource-intensive discrete variable collection. Natural language processing (NLP) allows one to extract meaningful information from large quantities of unstructured free text in a relatively simple manner. Here, we create an NLP-based model that utilizes preoperative notes and radiology reports to predict nonhome discharge. We then present a web-based, point-of-care implementation that can be used to make real-time predictions.

Methods: We retrospectively reviewed 1,291 adults treated for intracranial meningioma at two academic centers from 1995 to 2015. Age and text from preoperative notes and radiology reports were collected. Text was represented via term frequency-inverse document frequency (TF-IDF). Thirty-two ML algorithms were trained to predict nonhome discharge from the database. Top performing algorithms were combined to form an ensemble model, which was then validated on data excluded from initial training.

Area under the curve (AUC) was calculated for internal and holdout validation. Permutation importance was used to determine the relative impact of each input on predictions. Word clouds were generated to visualize which words best predict nonhome discharge. Nonnegative matrix factorization (NMF) was used to model topics, or related collections of words that occur within the notes of patients with nonhome discharge. Finally, a public website was built to house the completed model.

Results: Among 1,291 patients, 987 (76.5%) were discharged to home and 394 (23.5%) were discharged elsewhere. Mean age was 56.9 years, though patients with nonhome disposition were significantly older (63.6 vs. 54.8 years, $p \leq 0.001$). A model comprising a regularized logistic regression, support vector machine, and gradient boosted machine best predicted nonhome discharge, with an AUC = 0.78 (95% CI = 0.74–0.81) on internal validation and 0.76 on holdout validation (Fig. 1). Preoperative notes most influenced

predictions, followed by imaging reports, then age. Words including “large,” “ventricle,” and “extremity” were predictive of nonhome discharge (Fig. 2). Topics identified using NMF are illustrated in Table 1. The public web address housing the model is <http://nlp-home.insds.org>. Patient age and text from the preoperative note and radiology report are entered, and the model returns odds of nonhome discharge.

Conclusion: The ML is an expanding but still underutilized analytic resource in neurosurgery. Here, we use NLP to construct a multiinstitutional model that predicts nonhome discharge. To our knowledge, this represents the first NLP-based predictive model and point-of-care ML application in the field.

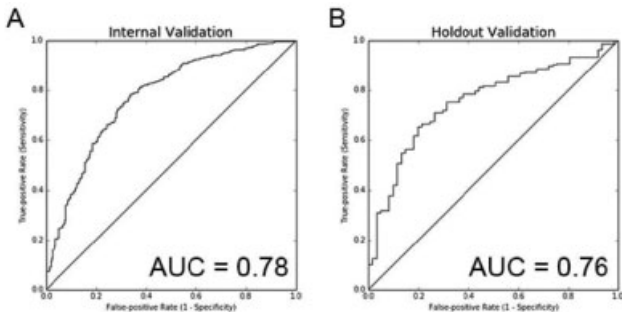


Fig. 1 Area under the curve for internal (A) and holdout (B) validation of the natural language processing model.

AUC = 0.78 (95% CI = 0.74–0.81).



Fig. 2 Word clouds.

Word clouds demonstrating the importance of words to the model from the (A) preoperative note and (B) radiology report. Red denotes association with nonhome discharge; blue denotes association with home discharge. Size is proportional to how influential the word is in either direction.

Table 1 Topic modeling

Clinic Note
base skull left mass today approach vision time excellent vanderbilt
00 patient right frontal surgery history meningioma tumor discussed radiation
feel think visual headaches following optic does half surgery involve
cardiac perform seizure 00 like history patency disorder proceeding pleasant
Imaging Report
right left unchanged cm frontal lesion superior brain normal sinus
cavernous left optic m1 projecting sinus extends possibly segment nerve
residual craniotomy resection pneumocephalus enhancing lobes similar interval gliosis chronic
meningiomas auditory multiple canal parafalcine internal acoustic extends falx schwannoma

A175. Exploring Whether Statins or Metformin Influence the Growth of Vestibular Schwannomas

Shafeen Qazi¹, Sophia Tran¹, Sanjana Balachandra¹
Daniel E. Killeen¹, Jacob B. Hunter¹

¹University of Texas Southwestern Medical Center, Dallas, Texas, United States

Objective: This study aims to assess whether statins and or metformin impact the growth of vestibular schwannomas (VS).

Study Design: Retrospective case series.

Setting: Single, tertiary care academic hospital.

Patients: Patients diagnosed with a sporadic VS, with at least two MRI studies at least 6 months apart prior to any intervention.

Intervention: Serial MRI studies. Using Brainlab cranial planning software, a combination of three reviewers measured the greatest linear diameter on axial imaging, in addition to manually segmenting each tumor to calculate volumes in serial MRI studies.

Main Outcome Measure: The VS tumor growth, defined as either ≥ 2 mm increase in tumor size when measuring the greatest axial diameter, or a 20% increase in tumor volume, between consecutive MRI studies, or between the first and last available MRI study. Growth rates in patients, who had evidence per their electronic medical record (EMR) of having been prescribed either a statin or metformin, were compared with growth rates in patients on neither medication.

Results: A total of 426 patients met inclusion criteria, 53.4% of which were women. For all patients, the median age was 61.5 years (IQR: 53.5–68.2 years), the median linear tumor diameter at diagnosis was 11.3 mm (IQR: 6.5–16.4 mm), and the median tumor volume was 0.31 cm³ (IQR: 0.12–0.79 cm³). Reviewing the EMR, 48 patients (11.3%) were taking metformin; 146 patients (34.3%) were taking a statin; and the remainder 232 patients were considered controls. Comparing tumor measurements between raters, the intra-class correlation coefficient (ICC) for linear measurements was 0.934 (95% CI: 0.865–0.967) while for volumetric measurements, it was 0.902 (95% CI: 0.802–0.952). In assessing metformin, utilizing linear measurements, 17.0% of patients demonstrated growth compared with 19.1% of controls ($p = 0.844$). Utilizing volumetric measurements, 48.9% of patients demonstrated growth as compared with 61.9% of controls ($p = 0.112$). With regard to statin use, utilizing linear measurements, 13.1% of patients demonstrated growth, which was significantly fewer than the control group in which 22.2% of controls demonstrated growth. ($p = 0.032$). When utilizing volumetric analysis, 57.2% of statin users demonstrated volumetric growth compared with 62.1% of controls ($p = 0.393$).

Conclusion: Utilizing linear measurements, VS patients taking a statin demonstrated significantly less VS growth as compared with controls. However, when assessing tumor volumes, there was no significant growth rate between statin users and controls. In regard to metformin usage, neither linear nor volumetric measurements demonstrate any difference in VS growth between patients and controls.

A176. Vestibular Schwannomas Guidelines

Roberto Leal Da Silveira¹, Eder Rocha¹
¹Madre Teresa Institute

Introduction: The publication of the Congress of Neurological Surgeons (CNS) Vestibular Schwannomas guidelines last year was remarkable.

This document was downloaded for personal use only. Unauthorized distribution is strictly prohibited.

With the wonderful help from the CNS, they granted me permission to use the VS guidelines to teach others and encourage them to visit the CNS website. Vestibular schwannomas (VSs) lesions remain challenging. As outcomes remain imperfect, improvements in therapy are necessary. An important point is to use evidence-based techniques for future scientific and clinical research. The CNS objective was to study the best evidence-based management of VS, including initial audiologic evaluation, imaging diagnosis, use of surgical techniques, hearing preservation, and the administration of radiation therapy.

Methods: The Guideline Committee of the Joint Tumor Section of the CNS recruited experts from a multidisciplinary task force. Literature search strategy was undertaken. The inclusion/exclusion criteria to screen the citations for each of the questions were determined ahead of time for each section by the respective writing group. Evidence tables, reporting the extracted study information and evidence classification, were generated for the included studies for each of the questions.

Results: This guideline yielded some level 2 recommendations and a greater number of level 3 recommendations. In some case there was information that justified the recommendations.

The list of these recommendations can be reviewed at: <https://www.cns.org/guidelines/guidelines-management-patients-vestibular-schwannoma>.

Conclusion: This series of guidelines was constructed to assess the most current and clinically relevant evidence for the management of VS and future clinical research for which no recommendations could be formulated.

A177. Superior Semicircular Canal Dehiscence Revisional Surgery Outcomes

Kevin Ding¹, Prasanth Romiyo¹, Edwin Ng¹, Dillon Dejam¹, Roan N. Anderson¹, Adam Enomoto¹, Courtney Duong¹, John P. Sheppard¹, Matthew Z. Sun¹, H. Westley Phillips¹, Quinton Gopen², Isaac Yang²

¹Department of Neurosurgery, University of California, Los Angeles, Los Angeles, California, United States

²Department of Head and Neck Surgery, University of California, Los Angeles, Los Angeles, California, United States

Background: Revisional repair of superior semicircular canal dehiscence due to a failed primary surgery poses additional risks to patients, such as the formation of scar tissue that may worsen preoperative symptoms. Though the middle cranial fossa (MCF) approach offers better intraoperative visualization of the dehiscence and greater postoperative symptom resolution, the current literature lacks evaluation of surgical approaches for revisional SSCD surgery.

Methods: We retrospectively identified a cohort of 25 patients who had undergone revisional surgery at our institution. Patient demographics, primary and secondary surgical approach, dates of consultation, and most recent follow-up were noted. Preoperative and postoperative symptoms of autophony, amplification, aural fullness, tinnitus, hyperacusis, hearing loss, vertigo, dizziness, imbalance, oscillopsia, and headache were recorded.

Results: Mean age was 52.2 ± 11.2 years with 8 (32%) males and 17 females (68%). Twelve of these patients had a primary surgery using the middle cranial fossa approach, and seven patients had a primary surgery using the transmastoid approach. Six had a primary combined MCF-TM approach. All secondary revisions for SSCD were performed through a middle cranial fossa approach. Seventeen(68%) of the revisions were performed on left-sided lesions. Three (12%) of the original surgeries were complicated by CSF leakage. Total 17

patients (68%) reported previous ear anomalies, and 14 (56%) had bilateral SSCD. No mentions of preoperative ear trauma, autophony, amplification, aural fullness, tinnitus, hyperacusis, hearing loss, vertigo, dizziness, imbalance, oscillopsia, or headache were made in the medical documents

Conclusion: The MCF approach for SSCD surgery is comparable to TM and combined MCF-TM outcomes for patients undergoing revisional surgery. However, given the advantages of the MCF approach intraoperatively, it should still be a primary consideration when planning revisional cases.

Table 1 Demographics

Variable	Value
Patients, <i>n</i>	25
Age (y)	
Mean ± SD	54 ± 11.2
Range	32–74
Sex, <i>n</i> (%)	
Female	17 (68)
Male	8 (32)
Characteristics, <i>n</i> (%)	
Bilateral	14 (56)
Previous ear anomaly	17 (68)
Primary approach	
MCF	12 (48)
TM	7 (28)
Combined	3 (12)
MCF then TM	2 (8)

Abbreviations: MCF, middle cranial fossa; *n*, population; SD, standard deviation; TM, transmastoid.

A178. Transtemporal Venous Decompression for Pulsatile Tinnitus

Patrick Slater¹

¹Austin Ear Clinic, Austin, Texas, United States



Objective: This study aims to evaluate the clinical characteristics and present surgical outcomes of transtemporal venous decompression technique in the treatment of pulsatile tinnitus.

Study Design: Prospective cohort study.

Setting: Tertiary private neurologic skull base clinic.

Patients: The primary author, between March 2012 and February 2013, evaluated 55 patients with the complaint of pulsatile tinnitus. Total 7 out of the 55 patients were diagnosed with severe, unrelenting idiopathic pulsatile tinnitus, and were placed into the study.

Intervention: These seven patients had temporal bone computed tomography, magnetic resonance imaging, arteriogram, videonystagmography, electrocochleography, and lumbar puncture based on the symptoms. All seven patients underwent transtemporal venous decompression surgery.

Main Outcome Measure: Resolution of pulsatile tinnitus was determined as the primary outcome measure.

Results: Six out of seven patients had complete resolution of their pulsatile tinnitus immediately after surgery and at 3- to 6-year follow-up. One patient developed intracranial hypertension after 3 months requiring ventriculoperitoneal shunt, which resolved pulsatile tinnitus as well. No complications occurred.

Conclusion: A significant subset of the pulsatile tinnitus patient population has known reversible causes. The more common include conductive hearing loss, superior canal dehiscence, benign intracranial hypertension, jugulo-sigmoid venous anomalies and stapedial myoclonus, etc. There exists a subset of patients that have idiopathic pulsatile tinnitus. Transtemporal venous decompression is a surgical technique that can be employed to give patients with idiopathic pulsatile tinnitus long-term relief.

IRB Number: CR-10-059.

A179. Cochlear Implantation after Radiosurgery for Vestibular Schwannoma

Neil S. Patel¹, Michael J. Link¹, Brian A. Neff¹, Matthew L. Carlson¹, Colin L. Driscoll¹

¹Mayo Clinic, Rochester, Minnesota, United States

Objective: The optimal strategy for hearing rehabilitation in neurofibromatosis type 2 (NF2) and sporadic vestibular schwannoma (VS) remains undefined. Unfortunately, audiologic outcomes of auditory brainstem implantation are generally limited. In contrast, cochlear implantation (CI) typically yields open-set speech understanding and access to sound by pure tone audiometry in the near-normal range, both of which exhibit durability over time. This has led many to adopt treatment strategies for patients with bilateral sensorineural hearing loss (SNHL) and unilateral or bilateral VS that emphasize preservation of an anatomic cochlear nerve. At our institution, radiosurgical treatment of VS with subsequent ipsilateral cochlear implantation has been utilized for a series of patients with sporadic and NF2-related VS. In this report, audiologic outcomes of CI following radiosurgery are presented.

Setting: Tertiary academic referral center.

Methods: A retrospective review of adult patients with VS treated with stereotactic radiosurgery (SRS), followed by cochlear implantation, between 1990 and 2019 was performed. Patient demographics, tumor features, treatment parameters, and pre- and postimplantation audiometric outcomes (including pure tone average [PTA] and word and sentence test scores) are presented.

Results: Sixteen patients (17 ears) underwent SRS and ipsilateral CI during the study period. Thirteen patients (81%) had NF2. Median age at SRS and CI were 44 and 48 years,

respectively. Median time from SRS to CI was 38 days, but notably, five patients underwent SRS and CI within 1 day and four patients underwent CI greater than 7 years following SRS. Median tumor volume at the time of SRS was 1,400 mm³ (range = 83.6–6080 cubic mm, $n = 15$). Fifteen patients underwent primary Gamma Knife SRS at our institution with a median marginal dose of 13 Gy delivered to the 50% isodose line. Median post-CI PTA was 29 dB HL, improved from 110 dB HL preoperatively ($p = 0.004$). Overall, 11 patients exhibit speech understanding without visual cues. All underwent sentence testing at a median 7 months (range = 1–143 months) post-CI. The median AzBio sentence score was 85% (range = 46–95%, $n = 8$). Two ears exhibited HINT sentence scores of 49 and 95%, respectively. The remaining five patients achieved environmental sound awareness without open-set speech recognition.

Conclusion: Patients who undergo CI following SRS for VS enjoy access to sound at near normal levels, with the majority achieving open-set speech understanding. Implantation can be performed immediately following SRS or in a delayed fashion, depending upon hearing status among other factors. This strategy may be applied to cases of sporadic or NF2-associated VS.

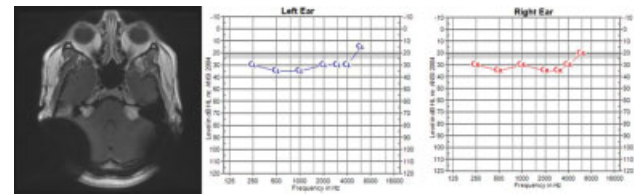


Fig. 1 Axial T1 postcontrast MRI with artifact suppression and cochlear implant only audiometry for a patient with neurofibromatosis type 2 who underwent bilateral sequential cochlear implantation after L sided SRS and R sided surgery and SRS. The patient enjoys open-set speech understanding with both implants. MRI, magnetic resonance imaging; SRS, stereotactic radiosurgery.

A180. Cannot Stop, Will Not Stop: Assessing the Impact of Tinnitus on Patient-Reported Hearing-Related Quality-of-Life Outcomes in Vestibular Schwannoma

Avital Perry¹, Christopher S. Graffeo¹, Maria Peris-Celda², Lucas P. Carlstrom¹, Geffen Kleinstern¹, Matthew L. Carlson¹, Michael J. Link¹

¹Mayo Clinic, Rochester, Minnesota, United States

²Albany Med, Albany, New York, United States

Introduction: Tinnitus is the third most common presenting vestibular schwannoma (VS) symptom after hearing loss and headache. Although recognized as a prevalent contributor to lost quality-of-life (QOL) in VS, the relationship between tinnitus, hearing loss, and other hearing-related QOL outcomes remains incompletely characterized.

Methods: Prospective, observational, multicenter, multinational, and cross-sectional study, analyzed via multivariable linear and logistic regression.

Results: Total 422 VS patients with formal audiometry within 1 year of survey date were identified. Median age was 54 (range = 12–82) and 223 (53%) were females. Tinnitus was the primary presenting symptom in 34 of the 354 who recalled initial symptomatology (10%) and time-of-survey prevalence was 319 of 422 (76%). Among 34 patients presenting with tinnitus, it persisted in 32 at time of survey (OR: 6.5, 95% CI: 1.5–27.5).

After adjusting for age and sex, patients reporting tinnitus were significantly more likely to report subjective

hearing loss (OR: 3.2; 95% CI: 1.8–5.9; $p = 0.0001$), as well as that concentration was affected by ringing, hissing, or other noises in their ears (OR: 7.2; 95% CI: 3.7–17.2; $p < 0.0001$). However, no significant differences were noted in subjective hearing loss severity, word recognition score, AAO-HNSF hearing class, ability to use the telephone in either ear, frequent hearing aid use in either ear, happiness with initial management strategy elected, or adverse impact on either personal relationships or conversations attributable to hearing loss. When patients with presenting, persistent tinnitus were compared with all patients without tinnitus at time-of-survey, none of the above-listed variables was significant.

Conclusion: Tinnitus may confer a subjective impression of hearing loss that is neither captured by audiometric assessments nor associated with the same dramatic decline in quality-of-life associated with moderate-to-severe hearing loss. The QOL impact of tinnitus is predominantly limited to cognitive domains such as concentration, and appears to be significantly more pronounced in patients without tinnitus at presentation.

A181. Keyhole Middle Fossa Approach with Titanium Mesh “Gull Wing” Repair for Tegmen Defects

Andrew K. Wong¹, Michael Shinnars², Ricky H. Wong²

¹Rush University, Chicago, Illinois, United States

²Northshore University, Skokie, Illinois, United States

Objective: The optimal surgical strategy for tegmen defect repair remains controversial. Transmastoid approaches theoretically provide a simple approach with a quicker recovery, though more anterior defects may be inaccessible. Higher flow leaks may also be more challenging to manage.¹ The middle fossa craniotomy provides wide access to the entire tegmen. This approach often requires temporal lobe manipulation, lumbar drain placement, and longer recovery.² We describe the use of a keyhole middle fossa approach with a simple titanium skull base repair that allows for wide access with no temporal lobe manipulation and does not require lumbar drain placement.

Methods: A retrospective review was performed on 14 consecutive patients with spontaneous CSF otorrhea. Each patient underwent a keyhole (~1 × 2 cm craniectomy) middle fossa approach, with complete visualization of the posterior middle fossa tegmen region, followed by multilayer dural repair with titanium mesh “gull wing” skull base reconstruction (Figs. 1 and 2).³ If there was a prior myringotomy, a myringoplasty then performed. Demographic information, including BMI and defect laterality, was recorded. Postoperative measures included operative time, length-of-hospital stay, CSF leak recurrence, and surgical complications (seizures, hemorrhage, aphasia, and infection).

Results: Preoperative patient demographics are seen in Table 1A, operative times and hospital length of stay (LOS) are seen in Table 1B, and postoperative complications are seen in Table 1C. Lumbar drain was placed postoperatively for 1 day in three patients due to fluid egress from myringoplasty site to aid in myringoplasty healing. There were no recurrences over a mean follow-up of 20.3 months (range = 5–48 months).

Conclusion: A minimally invasive keyhole middle fossa approach with a multilayer dural reconstruction including titanium mesh “gull wing” skull base repair provides a quick and effective treatment for a broad spectrum of tegmen defects and meningoencephaloceles. This exposure and reconstruction technique does not require the use of a lumbar drain and results in minimal hospitalization.

Table 1A. Patient Characteristics		
Gender	Male	5 (35.7%)
	Female	9 (64.3%)
Body Mass Index (kg/m ²)		32.8 ± 7.9
Age (years)		60.7 ± 12.7
Laterality	Left	4 (28.6%)
	Right	10 (71.4%)

Table 1B. Surgical and Postoperative Metrics	
Operative time (minutes)	103.8 ± 32.8
Myringoplasty (n=8)	122.8 ± 30.5 ^a
No myringoplasty (n=6)	77.2 ± 8.5 ^a
Hospital LOS (days)	1.4 ± 0.6
LD placed (n=3)	2.3 ± 0.6 ^b
No LD placed (n=11)	1.1 ± 0.3 ^b

^a statistically different operative time ($p=0.0022$)
^b statistically different hospital LOS ($p=0.0002$)

Table 1C. Postoperative Complications	
Recurrent CSF leak	0
Seizures	0
Aphasia	0
Meningitis	0
Death	0
Hematoma	0

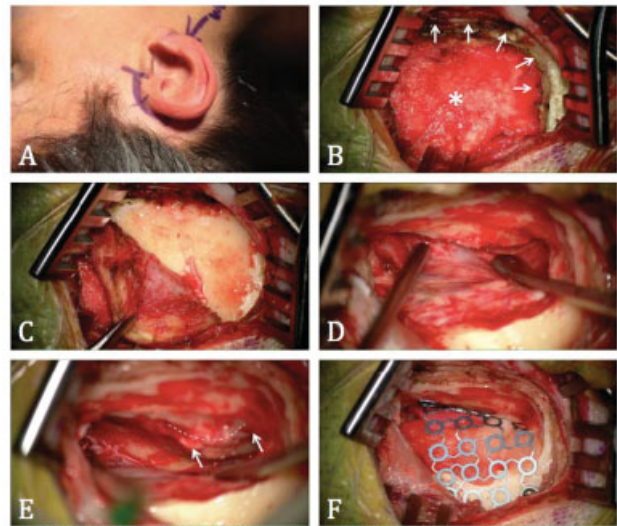


Figure 1 (A) Peri-auricular incision (B) Incision made along the periphery of the temporalis muscle (asterisk) from the zygomatic root to the supramastoid crest (white arrows) (C) Temporalis elevation (D) Temporalis elevation (E) Complete exposure with the arcuate eminence (dotted line) and petrous ridge (white arrows) (F) Reconstruction demonstrating “gull wing” titanium mesh secured laterally at the squamous temporal bone.

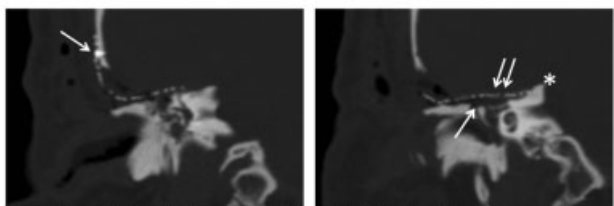


Figure 2 Coronal CT of the right temporal bone (left image) "Gull wing" technique with lateral fixation (white arrow) (right image) Complete titanium mesh (double arrows) reconstruction of the large defect (single arrow) to the petrous ridge (asterisk)

References

1. Marchioni D, Bonali M, Alicandri-Ciuffelli M, Rubini A, Pavesi G, Presutti L. Combined approach for tegmen defects repair in patients with cerebrospinal fluid otorrhea or herniations: our experience. *J Neurol Surg B Skull Base* 2014;75(4):279–287
2. Perez E, Carlton D, Alfarano M, Smouha E. Transmastoid repair of spontaneous cerebrospinal fluid leaks. *J Neurol Surg B Skull Base* 2018;79(5):451–457
3. Wong RH, Agazzi S, van Loveren H. "Inverted gull wing" dural closure and middle fossa floor reconstruction after transzygomatic infratemporal fossa approach. *World Neurosurg* 2016;89:280–284

A182. Vestibular Schwannoma Clinical Phenotypes Are Associated with Differential Methylation Patterns

Avital Perry¹, Christopher S. Graffeo¹, Lucas P. Carlstrom¹, Amanda Munoz Casabella¹, Matthew L. Carlson¹, Colin L. Driscoll¹, Michael J. Link¹

¹Mayo Clinic, Rochester, Minnesota, United States

Background: Vestibular schwannoma (VS) is a benign nerve sheath tumor, with an incompletely characterized genomic and epigenomic profile. Beyond the assumption of progressive growth, phenotypic behavior of VS is unpredictable, with some tumors rapidly growing and precipitating symptoms, while others are essentially indolent; similarly, following resection, some tumor remnants involute or remain stable over many years, while others recur quickly. Based on preceding clinical research at our institution and elsewhere, VS genomic profiling has provided some preliminary insights into predicting tumor behavior; however, there have been no definitive investigations of VS epigenetics, such as methylation status.

Methods: Forty-five sporadic VS treated with primary resection and with at least 24 months of clinical and radiographic posttreatment follow-up were included. VS phenotypes were characterized both pre- and postresection, which were tested for associations with methylation abnormalities. Tumor tissue specimens underwent DNA extraction followed by reduced representation bisulfite sequencing (RRBS), for high-throughput genome-wide single-nucleotide-level methylation profiling. The primary statistical technique was differential analysis, using a negative binomial logistic regression.

Results: VS that demonstrated robust growth (>2 mm/y) prior to resection, or that experienced postoperative recurrence/progression, was associated with characteristic patterns of increased CpG density. Areas of methylation enrichment included immune regions, neural crest regions, and others. Hypomethylation was inconsistently noted in a variety of gene promoter regions, including those associated

with growth factor receptors. No significant abnormality was consistently noted in the MERLIN gene in correlation with rapid preoperative growth and/or postoperative recurrence/progression. Cross-referencing with whole-exome sequencing is under active investigation, with additional results anticipated for presentation in tandem with these data.

Conclusion: VS methylation patterns are associated with characteristic behavioral phenotypes. These relationships are preserved in both the preoperative and postoperative settings. Correlation with whole-exome sequencing is pending at the time of submission, but may provide additional insights into critical gene loci for future targeted therapies in VS, with particular consideration for adjuvant treatments in the setting of recurrent/refractory disease, or timing of postoperative stereotactic radiosurgery following subtotal resection.

A183. The Rhinopharyngeal (RP) Flap as an Adjunct to Endoscopic Endonasal Reconstruction of Lower Clival and Craniovertebral Junction Defects

Pierre-Olivier Champagne¹, Georgios Zenonos¹, Eric E. Wang¹, Carl H. Snyderman¹, Paul A. Gardner¹

¹University of Pittsburgh Medical Center, Pittsburgh, Pennsylvania, United States

Context: Endoscopic endonasal approach (EEA) to the lower clivus and craniovertebral junction (CVJ) has been traditionally performed via resection of the nasopharyngeal soft tissues. Alternatively, an inferiorly based rhinopharyngeal (RP) flap can be dissected to help cover the postoperative defect and separate it from the oropharynx. To date, there is no evidence on the viability and potential clinical impact of the RP flap.

Methods: A retrospective cohort of 60 patients who underwent EEA to the lower clivus and craniovertebral junction was studied. The RP flap was used in 30 patients (RP group) and the nasopharyngeal soft tissues were resected in 30 patients (control group).

Results: Chordoma was the most common surgical indication in both groups (47 vs. 63% in RP and control group, respectively, $p = 0.313$), followed by odontoid pannus (20 vs. 10% in RP and control group, respectively, $p = 0.313$). No complications occurred during the RP flap harvesting. The two groups did not differ in terms of extent and size of tumor ($p = 0.271$), intraoperative CSF leak ($p = 0.438$), and skull base reconstruction techniques other than RP flap (nasoseptal flap: $p = 0.301$, fascia lata: $p = 0.791$, inlay graft: $p = 0.793$, and prophylactic lumbar drain: $p = 0.781$). Postoperative soft-tissue enhancement (MRI) covering the lower clivus and CVJ was significantly higher in the RPF group (70 vs. 23%, $p < 0.001$). The control group had a significantly higher rate of nasoseptal flap necrosis (20 vs. 3%, $p = 0.044$) and surgical site infection (27 vs. 3%, $p = 0.026$) while having similar rates of postoperative CSF leak (17 vs. 20% in RP and control groups, respectively, $p = 0.739$) and meningitis (7 vs. 17% in RP and control groups, respectively, $p = 0.424$).

Conclusion: The RP flap provides vascularized tissue coverage in anterior and inferior to the lower clivus and CVJ. Its use was associated with decreased rates of nasoseptal flap necrosis and local infection.

A184. Petrous Apex Cephaloceles: Radiology Features and Surgical Management of a Rare Entity

Madeline Epstein¹, Mehmet Kocak¹, Andre Beer Furlan¹, Bledi C. Brahimaj¹, Richard W. Byrne¹, R. Mark Wiet¹

¹Rush University Medical Center, Chicago, Illinois, United States

Introduction: Petrous apex cephalocele (PAC) is an uncommon condition resulting from the herniation of the posterolateral wall of Meckel's cave into the petrous apex. These lesions are usually asymptomatic and diagnosed as an incidental finding on adult brain imaging. However, PAC may be a cause of spontaneous CSF leak. In the present study, we outline radiologic features of this rare lesion and describe the surgical management of three spontaneous CSF leak cases secondary to PAC.

Methods: A retrospective review of all cranial imaging archived at an academic center between 2008 and 2019 identified 32 patients with PAC (27 females and 5 males; age range: 7–87; mean: 57 years). All imaging was reviewed by a neuroradiologist to characterize the identified lesions including associated radiographic anomalies. Patients who were radiographically diagnosed with a PAC were further characterized by demographics, further workup, and surgical intervention. In addition, three patients were clinically identified as having been treated for CSF leak in the presence of PAC.

Results: Radiological assessment showed the following characteristics of PAC: 9 (25.7%) bilateral and 26 (74.2%) unilateral. There was an association with a partially or expanded empty sella in 29 (82.8%) of the cases and arachnoid pits in 5 (14.2%). Enlarged CSF spaces of the optic nerve sheath were seen in 7 (20.0%) with a decreased interpeduncular distance in 3 patients (8.6%). Coexisting pathology included temporal, sphenoid, and bilateral jugular foramen meningocele; as well as cribriform, middle crania fossa, and right temporal defect. Initial presentation, radiographic data, intraoperative findings, significant surgical anatomy, and follow-up will be reviewed of three spontaneous CSF leak cases secondary to PAC that were managed with the middle cranial fossa approach.

Conclusion: The authors provide a comprehensive analysis of the incidence of PAC and associated radiographic abnormalities. PAC is an uncommon condition; furthermore, PAC is an exceedingly unusual cause for CSF leak in the adult and pediatric population. A middle fossa approach may be used to treat CSF as a result of PAC. Both radiologically and clinically diagnosed PAC cases display features of IIH that require vigilance and may warrant future treatment. Typically CSF otorrhea originates from an encephalocele that extends via a bony defect in the tegmen tympani or tegmen mastoideum. However, on occasion the source of the CSF otorrhea is not via the tegmen; in these cases defects in the middle fossa floor medial to the ridge for the gasserian ganglion need to be considered.

A185. Evaluating Sellar Healing following Various Reconstruction Techniques in Transsphenoidal Surgery: An Imaging and Endoscopic Review

Mark B. Chaskes¹, Joshua Mccambridge¹, Chandala Chitguppi¹, Tawfiq Khoury¹, Pascal Lavergne¹, Mindy R. Rabinowitz¹, Gurston G. Nyquist¹, Marc Rosen¹, Adam E. Flanders¹, James J. Evans¹

¹Thomas Jefferson University Hospital, Philadelphia, Pennsylvania, United States

Background: Many institutions utilize a graded algorithm to dictate sellar reconstruction following transsphenoidal pituitary surgery based on the defect encountered. At

our institution, one of three repair techniques are commonly used for pituitary surgery: a regenerated oxidized cellulose onlay, a synthetic dural substitute inlay with dural sealant glue, or synthetic dural substitute inlay with nasoseptal flap (NSF) onlay and dural sealant glue. The objective of this study is to assess postoperative healing of the sphenoid and sella following reconstruction with these three techniques based on magnetic resonance imaging (MRI) and endoscopic features, and to compare these modalities.

Methods: Twenty consecutive patients who underwent sellar reconstruction with each of the above-mentioned techniques were included (regenerated oxidized cellulose onlay = group ROC, synthetic dural substitute inlay/dural sealant glue = group DS, and synthetic dural substitute inlay/NSF onlay = group F). Three-month postoperative MRIs were reviewed and compared with preoperative MRIs and 3-month postoperative nasal endoscopy when available. Each MRI was reviewed by a neuroradiologist and graded on a binary scale based on the presence of imaging features of sinusitis and mucosal health including an air-fluid level, the uniformity of mucosal thickness, the presence of enhancing soft tissue, and the presence of layering of the sella. Likewise, each endoscopy video was reviewed by two otolaryngologists and evaluated for the presence of crusting, sinusitis, and degree of remucosalization. Postoperative morbidity was evaluated. Data were analyzed using Chi-squared and ANOVA; a result was considered significant when $p < 0.05$. Imaging and endoscopic assessments were compared.

Results: There were three exclusions from group F due to incomplete imaging records. MRI evaluation showed that all patients appeared to have complete sphenoid remucosalization, including the sella. Sphenoid mucosal thickening, asymmetric soft-tissue thickening, and sphenoid air-fluid levels were all most frequently identified in group F; however, these features were not statistically significant (70% in group F vs. 45 and 45% in groups ROC and DS, $p = 0.25$; 100 vs. 5% and 5%, $p < 0.001$; 12 vs. 10% and 5%; $p = 0.34$). Soft-tissue enhancement was identified in one patient in each group ($p = 0.99$). Layering of the sella was seen frequently in groups DS and F (100 and 71%, respectively) but was not observed in group ROC ($p < 0.001$). On nasal endoscopy, the sella and sphenoid were predominantly remucosalized in 100% of cases in all groups. Group F patients were more likely to have crusting, although this was not statistically significant (50 vs. 20% and 14%, $p = 0.22$). Group F patients were more likely to require postoperative antibiotics for a clinical sinusitis (OR = 6.0). There were no complications of cerebrospinal fluid leak in any group. There was no correlation between positive endoscopic findings and positive imaging features ($\chi^2 = 2.32$, $p = 0.99$).

Conclusion: Imaging features of sinusitis and asymmetric sphenoid mucosal healing are more frequently identified on postoperative MRI than on nasal endoscopy. All techniques heal equally well both radiographically and via direct visualization, although the use of a NSF increases morbidity. More conservative reconstruction methods when safe may reduce the postoperative morbidity while not sacrificing remucosalization and sinonasal health.

A186. Inferior Meatus Mucosal Flap Based on the Incisive Foramen Artery for Septal Reconstruction and Resurfacing of Septum Donor Site after Nasoseptal Flap Harvest

Randall S. Ruffner¹, Marcelo Charles¹, Tyler Kenning¹, Maria Peris-Celda¹, Carlos Pinheiro-Neto¹

¹Albany Medical Center, Albany, New York, United States

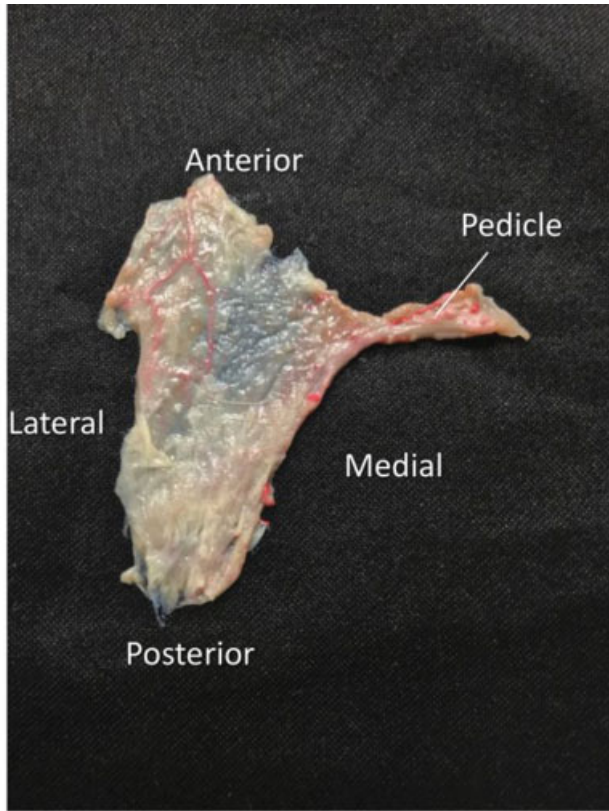


Figure 1: Specimen obtained from the anatomical dissection for measurements. Observe the pedicle of the inferior meatus mucosal flap.

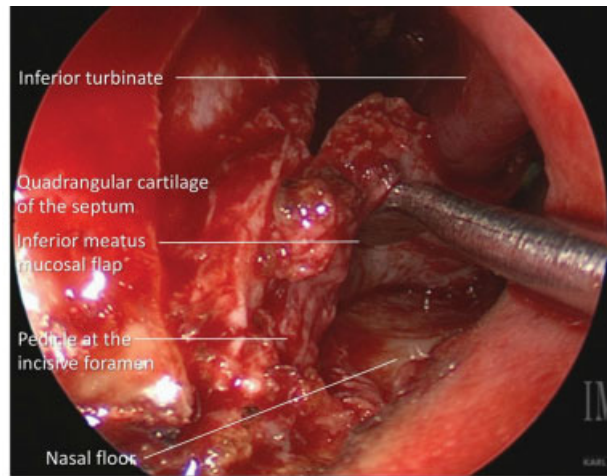


Figure 2: Intraoperative picture obtained with a 0 degree endoscope from the left nasal cavity during the harvest of the inferior meatus mucosal flap. Observe the robust pedicle based on the incisive foramen artery.

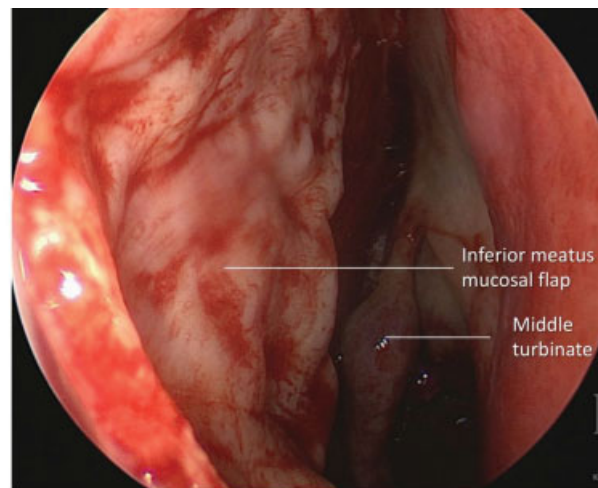


Figure 3: Picture obtained with a 0 degree endoscope from the left nasal cavity after the rotation of the inferior meatus mucosal flap to cover the quadrangular cartilage of the septum (nasoseptal flap donor site).

Introduction: Postoperative nasal morbidity related to the nasoseptal flap (NSF) harvest is well described. The exposed septal cartilage predisposes to crusting formation for several months after surgery with impact on patient's quality of life. Few studies have described reliable methods for addressing NSF donor site morbidity. This study describes of a novel rotational flap using inferior meatus mucosa pedicled from the incisive foramen artery to resurface the septum donor site. Additionally, this flap can be utilized to repair septal perforations.

Methods: An anatomical study was done analyzing the dimensions of inferior meatal flap pedicled from the incisive foramen (IMF; Fig. 1). Four incisions are made to harvest the IMF. Posterior incision is performed from the septum to the tail of the inferior turbinate at the transition between the nasal surface of the soft palate and the nasal floor. Lateral

incision is carried along the attachment of the turbinate. Anterior incision is made along the inferior edge of the nostril at the mucocutaneous junction toward the anterior nasal spine. Medial incision is performed along the transition between the septum and nasal floor. This corresponds to the inferior incision of the NSF harvest. Then the flap is elevated leaving it attached to the incisive foramen (Fig. 2). After harvest, the IMF is rotated anteriorly to cover the cartilage of the septum or repair a septal perforation (Fig. 3). From the anatomical study, total flap area and max radial reach from the pedicle were compared for each specimen. A CT scan study using sagittal images of the septum was done to estimate the area of the quadrangular cartilage that is exposed after NSF harvest. A case series of patients who underwent this technique is presented.

Results: Twelve IMF were harvested from male anatomical specimens. The average total flap area is 6.9 cm² (6.5–7.4 cm²). The maximal radial length from the incisive foramen pedicle was 3.3 cm (2.9–3.6 cm; Fig. 2). Ten CT scans (5 males and 5 females) were studied and the average area of the quadrangular cartilage of the septum was 9.6 cm² (8.7–10.4). Comparing the anatomical study with the CT scans, potentially the IMF can cover 72% of the quadrangular cartilage. A total of four patients had IMF technique: three patients for resurface of the quadrangular cartilage after NSF harvest (Fig. 3) and one patient for closure of septal perforation. The repair of the perforation was successful. Transient numbness of the maxillary incisors was present in two of four patients. There was no flap necrosis or other complications observed.

Conclusion: The NSF continues to be the standard of care for skull base reconstruction but comes with significant morbidity. We describe a novel, robust, pedicled rotational flap based on the incisive foramen using nasal floor mucosa which can be utilized to reduce donor site morbidity and crusting along the cartilaginous septum. This flap also showed applicability for repair of septal perforation. Future work is needed to better characterize the improvement in donor site morbidity following the use of this graft.

A187. Comparative Analysis of Autograft- and Xenograft-Based Spinal Fluid Leak Prevention after Translabyrinthine Resection of Cerebellopontine Angle Tumors

Douglas J. Totten¹, Nauman F. Manzoor², Alexander D. Sherry¹, Robert J. Yawn³, Reid C. Thompson⁴, David S. Haynes², Alejandro Rivas²

¹Vanderbilt University School of Medicine, Nashville, Tennessee, United States

²Department of Otolaryngology, Vanderbilt University Medical Center, Nashville, Tennessee, United States

³Department of Otolaryngology, University of Tennessee Health Science Center, Memphis, Tennessee, United States

⁴Department of Neurologic Surgery, Vanderbilt University Medical Center, Nashville, Tennessee, United States

Objective: To compare the use of porcine small intestine submucosal grafts (PSISG, Biodesign) and standard autologous material (fascia) for the prevention of cerebrospinal fluid (CSF) leak after surgical resection of cerebellopontine (CPA) angle tumors.

Setting: Tertiary skull base center.

Methods: Retrospective chart review. After IRB approval, we performed a retrospective cohort study evaluating cerebrospinal fluid (CSF) leak in patients who underwent translabyrinthine (TL) surgical resection for CPA tumors using either fascia autograft or porcine small intestinal submucosal grafts (PSISG, Biodesign). Demographics were summarized with descriptive statistics. The Kruskal–Wallis test compared

the cohorts. Single-predictor binary logistic regressions evaluated the association of covariates with outcomes.

Results: Seventy-seven patients (mean age: 49 years; range: 17–73; female = 51 [66%]) underwent TL surgical resection of CPA tumors. Composite repair consisting of dural substitute, adipose tissue, and either fascia autograft (56 patients; 73%) or PSISG (Biodesign) (21 patients; 27%) from 2016 to 2018 were evaluated. Patients were followed up for a minimum of 6 months after surgery. The mean tumor size was 2.3 cm (range: 0.4–6.1) and there was no significant size difference between the cohorts ($p = 0.2028$). The most common pathologic diagnosis was vestibular schwannoma ($n = 71$, 92%), followed by epidermoid ($n = 2$, 2.6%), meningioma ($n = 2$, 2.6%), and facial nerve schwannoma ($n = 2$, 2.6%). All tumors were excised via TL approach. There were seven overall postoperative leaks (9.1%) of which 3 (5.4%) required operative repair. One leak (4.8%) occurred in the Biodesign cohort while six leaks (10.7%) occurred in the autograft cohort (OR: 0.417, 95% CI: 0.047–3.684, $p = 0.4312$). Size was not associated with postoperative leak (OR: 0.782, 95% CI: 0.310–1.975, $p = 0.634$). One pseudomeningocele (4.8%) was identified in the Biodesign cohort, while five pseudomeningoceles (8.9%) were identified in the autograft cohort (OR: 0.510, 95% CI: 0.056–4.642, $p = 0.5501$). No operative repairs occurred in the Biodesign cohort, while three operative repairs (5.4%) occurred in the fascia autograft cohort.

Conclusion: Porcine small intestinal submucosal grafts (Biodesign) appear to provide an effective barrier as a component of complex skull base reconstruction after surgical extirpation of CPA tumors. Biodesign performs well in preventing CSF leaks and appears noninferior to autologous tissue in skull base reconstruction.

A188. Operative Strategy in Lateral Skull Base Reconstruction: Comparative of Rigid and Nonrigid Techniques

Kristen Yancey¹, Nauman F. Manzoor¹, Douglas J. Totten², Alexander D. Sherry², Alejandro Rivas¹, David S. Haynes¹

¹Department of Otolaryngology, Vanderbilt University Medical Center, Nashville, Tennessee, United States

²Vanderbilt University School of Medicine, Nashville, Tennessee, United States

Objective: To evaluate the use of rigid and soft-tissue reconstruction in lateral skull base (LSB) repair to prevent cerebrospinal fluid (CSF) leak after resection of spontaneous encephalocele or chronic middle ear disease–related middle fossa defect.

Setting: Tertiary skull base center.

Methods: Retrospective chart review. After IRB approval, a retrospective cohort study evaluating patients who underwent repair of LSB from spontaneous or chronic ear disease–related defects using either rigid or soft-tissue repair. Demographics were summarized with descriptive statistics. The Kruskal–Wallis and Fisher's exact tests compared the cohorts. Single-predictor binary logistic regressions evaluated the association of covariates with outcomes.

Results: Forty-five patients (mean age = 56 years; range: 26–73; and female = 30 [67%]) who underwent LSB defect repair using multilayer rigid repair involving bone (32 patients; 71%) or soft-tissue repair (13 patients; 29%) from 2016 to 2019 were evaluated. Patients were followed up for a minimum of 6 months after surgery. The mean BMI across all cohorts was 36 (range: 22–57). BMI did not differ significantly between the rigid and soft-tissue cohorts ($p = 0.7830$). The most common location of defect was the tegmen mastoidium (39, 87%) followed by the tegmen tympani (19, 42%) and

posterior fossa plate (2, 4%). Intraoperatively, 21 patients (47%) were noted to have dural defects, 41 patients (91%) were noted to have encephalocele, and 34 (76%) were noted to have an active CSF leak. There was no significant difference in defect location or intraoperative findings between the rigid and soft-tissue repair groups. There were no postoperative leaks in either cohort (0.0%). Lumbar drains were used in 10 (31%) rigid repair cases and 8 (62%) soft-tissue repair cases (rigid vs. soft tissue: OR, 0.284; 95% CI, 0.0874–1.090, $p = 0.0666$).

Conclusion: Both rigid and soft-tissue repair strategies provide an effective LSB reconstruction done for spontaneous as well as chronic ear disease–related defects. Choice of repair (rigid vs. nonrigid) is based on intraoperative determination of defect size and surgeon preference.

A189. Spontaneous Cerebrospinal Fluid Leaks from Multiple Anterior and Lateral Skull Base Defects

Nofrat Schwartz¹, Deanna Sasaki-Adams¹, Kevin D. Brown¹, Adam M. Zanation¹, Brian D. Thorp¹, Brendan P. O’Connell¹
¹University of North Carolina School of Medicine, Chapel Hill, North Carolina, United States

Introduction: Spontaneous cerebrospinal fluid (CSF) leaks are frequently idiopathic and appear to develop in part from elevated intracranial pressure (ICP). As this pressure is diffused throughout the cranial cavity, it is possible to develop CSF leaks in multiple locations. There are a limited number of studies on this particular situation, in which multiple defects and sites of CSF leak are present. We intend to evaluate the characteristics of this population and assess outcomes after surgical repair.

Methods: A retrospective chart review from 2014 to 2019 was performed at a tertiary medical center. Patients 18 years or older with a diagnosis of spontaneous CSF leak were eligible for study inclusion. History of skull base trauma, diagnosis of a neoplasm, chronic inflammatory disease, or iatrogenic CSF leaks were excluded. From this cohort, patients with multiple skull base defects, defined as more than one skull base defect separated by intervening bone occupying different anatomical areas in either the lateral skull base, anterior skull base, or both, were included for further analysis. Anterior and lateral skull base thickness was measured on computed tomography scans using previously defined methodologies; these values were compared with those from a cohort of single-site CSF leak patients matched for BMI.

Results: Review of our institutional experience in the past 5 years revealed a total of 292 patients with a diagnosis of spontaneous CSF leak, from which 11 (3.8%) had multifocal CSF leaks. Age did not differ between the single site and multiple site CSF groups ($p = 0.36$). Body mass index, however, was significantly higher (31.5 ± 0.5 vs. 46.2 ± 2.9 , $p < 0.0001$) in the multifocal leak cohort. Furthermore, there was a higher prevalence of women ($p = 0.012$) and African Americans ($p = 0.003$). The average anterior and lateral skull base thickness in the multifocal leak cohort measured 3.5 ± 0.47 and 4.1 ± 0.43 , respectively; this was not found to differ significantly from BMI-matched patients who had only one site of skull base defect and CSF leak ($p = 0.56$). Of the 11 patients, 4 had multiple distinct anterior skull base defects, 4 had multiple distinct lateral skull base defects, and 3 presented with a combination of anterior and lateral skull base defects. The overall success rate of repair of CSF leak was 95%; one patient experienced a recurrent leak after initial surgery. Three patients required placement of a ventriculoperitoneal shunt due to the onset of severe headaches or blurry vision after surgery. Interestingly, 50% of patients endorsed the onset of nonsevere headaches or blurry vision

after surgical repair. No association between the risk of headache after repair and BMI was noted ($p = 0.39$).

Discussion: The data support an increased incidence of multiple skull base defects with distinct site of CSF leak in more obese subjects. African American women also had a higher risk. Surgical repair in patients with multifocal CSF leaks remains highly successful (95%) with low recurrence rates similar to that observed in the single-site CSF leak cohort. Patients with multifocal leaks are at high risk of developing symptoms such as headaches or blurry vision, suggestive of elevated ICP postoperatively.

A190. The Role of Diamox and High-Volume Lumbar Puncture for Treatment of Iatrogenic Postoperative Cerebrospinal Fluid Leak

Aria Jamshidi¹, Aashish Shah¹, Rick Komotar¹, Michael Ivan¹
¹Jackson Memorial Hospital, Miami, Florida, United States

Case #	Age	Gender	Pathology	Initial Surgery	Time to CSF Leak	Treatment for CSF leak	Follow-Up	Complications
1	61	F	Falcotentorial Meningioma	Left Occipital Craniotomy	30 days, Leak from EVD site	Overseen EVD site, Diamox	No CSF leak at 2 and 4 weeks post-op	None
2	26	F	Pituitary Macroadenoma	Trans-sphenoidal	4 days, rhinorrhea	High Volume LP, Diamox	No CSF leak at 2 and 4 weeks post-op	None
3	37	M	Pituitary Macroadenoma	Trans-sphenoidal	30 days, rhinorrhea	Diamox, High volume LP	No CSF leak at 2 and 4 weeks post-op	None
4	45	F	Spheno-orbital Meningioma	Left Periorbital Craniotomy	7 days, CSF leak from wound	Diamox, High Volume LP, Oversewn	No CSF leak at 2 and 4 weeks post-op	None
5	34	F	Planum Meningioma	Left Periorbital Craniotomy	14 days, rhinorrhea	Diamox, High Volume LP	No CSF leak at 2 and 4 weeks post-op	None
6	42	F	Pituitary Macroadenoma	Trans-sphenoidal	8 days, rhinorrhea	Diamox, High Volume LP	No CSF leak at 2 and 4 weeks post-op	None

Introduction: Iatrogenic cranial cerebrospinal fluid (CSF) leaks after skull base surgery remain a challenging, albeit common, management issue for both neurosurgeons and otolaryngologists. Unlike traumatic CSF leaks which typically resolve with conservative measures, iatrogenic CSF leaks tend to be refractory to these techniques. This study is focused on the safety and proof of concept of a strategy employing acetazolamide with high-volume lumbar puncture as a treatment option for postoperative CSF leak.

Methods: We conducted an exploratory study of six patients who were given acetazolamide therapy after developing iatrogenic cerebrospinal fluid leak following craniotomy or transsphenoidal approach for tumor resection from July 2018 to July 2019. Patients who presented with CSF leaks on clinical exam were started on acetazolamide 250 mg three times a day for 10 days and underwent a high-volume lumbar puncture (30–40 mL of CSF). These patients were given strict instructions to avoid the Valsalva maneuvers/strenuous activity and maintain head of bed elevated for 2 weeks. These patients were followed up in clinic postoperatively by otolaryngology and neurosurgery to assess for the presence of CSF leak at 10 and 30 days postoperatively.

Results: At our institution, six patients were randomly assigned to acetazolamide therapy after they developed iatrogenic cerebrospinal fluid leak secondary to after craniotomy or transsphenoidal surgery for tumor resection. Table 1 shows a summary of patient demographics. The average age

This document was downloaded for personal use only. Unauthorized distribution is strictly prohibited.

of patients was 40.8 years. Five patients were female, and one was male.

Four patients, three of who had previously undergone transsphenoidal surgery and the fourth a pterional craniotomy for a planum meningioma, presented postoperatively with CSF leak from the nares. They were admitted for an average of 3 days after undergoing high-volume lumbar puncture and adhering to strict CSF leak precautions. The remaining two patients had previously undergone craniotomy for skull-base tumor resection and presented with CSF leak from the EVD site in one instance and from the incision in the second patient. The patient leaking CSF from the EVD site had their incision oversewn and was started on acetazolamide, and the latter was managed similarly but also additionally underwent a high-volume lumbar puncture. They were both discharged from clinic without complication. CSF profiles, gram stains, and cultures were monitored and followed up for 5 days to rule out meningitis. All six patients had resolution of their CSF leak on clinical exam at their interval follow-up appointments. No patients experienced serious complications or permanent neurological deficits.

Conclusion: The use of acetazolamide with concomitant high-volume lumbar puncture is a safe and effective management strategy for treating iatrogenic postoperative CSF leak in skull-base neurosurgery. It is a novel approach to managing these complex patients who helps avoid prolonged hospital stays associated with lumbar drainage and can obviate the need for additional surgery.

A191. The Importance of Long-Term Follow-up after Endoscopic Pituitary Surgery: Durability of Results and Tumor Recurrence

Joao Paulo Almeida¹, Hirokazu Takami¹, Raha Tabasinejad¹, Miguel Marigil Sanchez¹, Carlos Velasquez¹, Gelareh Zadeh¹, Fred Gentili¹

¹University of Toronto, Toronto, Ontario, Canada

Introduction: Endoscopic transsphenoidal surgery (ETS) has become the preferred surgical approach for resection of pituitary adenomas in most centers. This technique has a series of advantages such as improved visualization and maneuverability when compared with microscopic transsphenoidal approach. However, long-term results are still scarce. Ten years ago, we published our initial series with short-term results. This project aims to revisit the results of that series, assessing now the long-term results regarding radiological recurrence of pituitary adenomas.

Methods: Retrospective analysis of consecutive, endoscopically managed pituitary adenomas in a single center from 2004 to 2007. Only patients with >5 years of follow-up (FU) were included in this study.

Results: A total of 98 patients matched the inclusion criteria for this study. The median follow-up period was 144 months. Nonfunctioning adenoma was the most common subtype ($n = 66$, 67.3%), followed by GH-secreting tumors ($n = 19$, 19.4%), ACTH-secreting tumors ($n = 7$, 7.1%), prolactinomas ($n = 4$, 4.1%), and TSH-secreting adenomas ($n = 2$, 2%). Age ranges from 23 to 82 years, with median age of 53 years. Preoperative visual deficits were observed in 46 patients (46.9%) and hormonal deficits were identified in 31% of cases. 22.4% of patients had undergone a previous pituitary adenomas resection prior to treatment in our center. Surgery achieved gross total resection (GTR) and near-total resection in 86 cases (85%; 50 and 35%, respectively). A total of 37 cases had recurrences during FU (mean recurrence free survival: 80 months). Recurrences were observed in 32% of patients who had had GTR, with mean RFS of 87.25 months, while recurrences were observed in

41.9% of patients who underwent near-total or partial resection (mean RFS = 69.22 months). Most recurrences occurred after 5 years of FU (23 cases <63% of all recurrences) and only four cases had recurrences in the first 2 years after surgery. Surgery and/or radiation were done for management of recurrences in 29/37 cases. Cavernous sinus invasion and cases that had undergone previous surgery were significantly associated with shorter RFS, among which recurrent case was most significantly associated in multivariate analysis ($p = 0.05$).

Conclusion: Long-term FU analysis demonstrates that progression/recurrence of previously resected adenomas is observed in a significant number of patients, especially in those in whom GTR was not achieved. Short-term FU may shadow real tumor control rates achieved after ETS and therefore, long-term FU should be pursued in all cases.

A192. Long-Term Outcomes of Transsphenoidal Surgery for Management of Growth Hormone-Secreting Adenomas: Single-Center Results

Mohammed Asha¹, Hirokazu Takami¹, Carlos Velasquez¹, Selfy Oswari¹, Joao Paulo Almeida¹, Gelareh Zadeh¹, Fred Gentili¹

¹University of Toronto, Toronto, Ontario, Canada

Introduction: Transsphenoidal surgery is advocated as the first-line management of growth hormone (GH)-secreting adenomas. While disease control is defined by strict criteria for biochemical remission, the length of follow-up needed is not well defined in literature. In this report, the authors present their long-term remission rate and identify various predictive factors that might influence the clinical outcome.

Materials and Methods: The authors conducted a single-institute retrospective analysis of all transsphenoidal procedures for GH-secreting adenomas from January 2000 to June 2016. The primary outcome was defined as biochemical remission according to the 2010 consensus criteria and measured at the 1-year mark postoperatively as well as on the last recorded follow-up appointment. Secondary variables included recurrence rate, patterns of clinical presentation, and outcome of adjuvant therapy including repeat surgery, and subgroup analysis for patients who have “biochemical or radiological discordance”—patients who achieved biochemical remission but with incongruent IGF1/GH or residual tumor on MRI. Recurrence-free survival analysis was conducted for patients who achieved remission at 1-year postop.

Results: Eighty-one cases (45 females and 36 males) with confirmed acromegaly treated with transsphenoidal surgery were included (62 pure endoscopic cases and 19 microscopic endoscopic-assisted cases). Primary biochemical remission after surgery was achieved in 59 cases (73%) at 1-year mark postoperatively. However, only 41 patients (51%) remained in primary surgical remission (without any adjuvant treatment) at their last follow-up appointment indicating a recurrence rate of 31% (18/59 patients) over the duration of follow-up (average: 100 ± 61 months). Long-term remission rates for pure endoscopic and endoscopic-assisted cases appeared similar (48 vs. 52%, $p = 0.6$). Similarly, no significant difference in long-term remission was detected between primary surgery and repeat surgery (54 vs. 33%, $p = 0.22$). Long-term remission was significantly influenced by extent of surgical resection, cavernous sinus invasion (radiologically as well as surgically reported), preoperative IGF-1 levels, and early postoperative GH and IGF-1 levels (within 24–48 hours postoperative) as well as by the clinical grade with lower remission rates in patients with dysmorphic features and/or medical comorbidities (grades

2–3) compared with minimally symptomatic/silent cases (grade 1).

Conclusion: Long-term surgical remission rate appears to be significantly less than “early” remission rates and is highly dependent on the extent of tumor resection. The authors advocate a long-term follow-up regimen and propose a clinical grading system that may aid in predicting long-term outcome in addition to the previously reported anatomical factors. The role of repeat surgery is highlighted.

A193. Pituitary Incidentaloma and Nonincidentaloma: A Comparison of Pretreatment and Postoperative Characteristics

Kurren S. Gill¹, Chandala Chitguppi¹, Rahul Alapati¹, Sarah Collopy¹, Prachi Patel¹, Tawfiq Khoury¹, Pascal Lavergne¹, Mindy Rabinowitz¹, Gurston Nyquist¹, Marc Rosen¹, Christopher Farrell¹, James Evans¹

¹Thomas Jefferson University Hospital, Philadelphia, Pennsylvania, United States

Background: With the advent of more advanced imaging modalities and its widespread use, pituitary incidentalomas (PI) are increasingly being detected at a higher rate than before when patients are worked up for nonpituitary-related conditions. Criteria for surgical and nonsurgical management of this clinical entity are now more clearly delineated than previously. This study analyzes our institution's robust experience in the operative management of PIs over a 14-year period, making it the largest cohort of surgical PIs in the literature.

Methods: Retrospective chart review of pituitary adenoma patients who underwent a transsphenoidal hypophysectomy from 2005 to 2019 performed at a single tertiary care facility. Patients were subdivided into those whose tumors were detected incidentally (PI) versus those who presented with a disease-specific complaint such as vision changes or hormone-related symptoms (non-PI). Primary outcome measures included reason for PI detection, indication for surgery, and length of time from detection to surgery. Secondary outcome measures included comorbidities, tumor size, length of stay (LOS), complications, readmission, and resurgery.

Results: Pituitary incidentaloma detection: 684 patients were included in the study, of which 159 (23%) patients had PI. The most common modality for detection was CT (43%, $n = 69$) followed by MRI (17%, $n = 27$). Headache and/or migraine (14%, $n = 23$) was the most common reason for the initial imaging workup that detected PI. Increase in size during follow-up (27%, $n = 43$) was the most common indication for surgery. Median time of detection to date of surgery was 5.3 months.

Demographics: Gender, age, BMI, smoking, preoperative comorbidities—hypertension, congestive heart failure, atrial fibrillation, thromboembolism, and COPD were comparable between both groups ($p > 0.05$).

Tumor and Treatment Characteristics: Smaller tumor size ($p < 0.0001$) and lower tumor volume ($p < 0.0001$) were seen in PI. The PI group was more likely to have optic nerve involvement ($p < 0.001$), more likely to be secretory type ($p = 0.04$), and acromegaly comprised 67% of PI. PIs were more likely to undergo complete resection ($p < 0.001$), therefore less likely to require reoperation ($p = 0.005$). Cavernous sinus involvement, invasiveness, apoplexy at presentation, and rate of intraoperative CSF leak were comparable.

Postoperative Outcomes: Synechiae ($p = 0.001$) as a postoperative complication was significantly less in the PI group, while rates of sinusitis, septal perforation, thromboembolism, epistaxis, sellar hemorrhage, and crusting were

comparable. LOS ($p = 0.025$) was lower for PI, while 30-day readmission rate was comparable.

Conclusion: This study serves as the largest single institution analysis of surgically managed PIs currently in the literature. Based on our data, workup of headaches/migraines is the most common reason for detection of PI, and an increase in tumor size is the most common indication for surgery. On average, patients had surgery approximately 5 months after diagnosis with shorter LOS. PIs have a similar rate of complications as compared with non-PIs. As our cohort continues to expand, we will be able to draw more meaningful conclusions regarding our experience with pituitary incidentalomas.

A194. Do We Need Intraoperative Magnetic Resonance Imaging in all Endoscopic Endonasal Pituitary Adenoma Surgery Cases? A Retrospective Study

Emrah Celtikci¹, Hakan Emmez¹

¹Department of Neurosurgery, Gazi University Faculty of Medicine, Ankara, Turkey

Introduction: Advances in the field of intraoperative imaging, especially intraoperative magnetic resonance imaging (IOMRI), have led to its increasing usage during endoscopic endonasal pituitary surgery (EEPS). Recent studies advocated the usage of this expensive technology. But is it worth to use this technology in every single case?

Methods: Patients with functional or nonfunctional pituitary tumors that were operated via endoscopic endonasal approach (EEA) between June 2017 and May 2019 in the Department of Neurosurgery, Faculty of Medicine, Gazi University, were enrolled. The Institutional Review Board and Ethics Committee approved this retrospective study; oral and written consents of the patients were obtained prior to the study. Also, all patients were informed about the technique and gave their signed consent to IO-MRI during surgery and to the data being used for research purpose. Patients younger than 18 years and patients who did not undergo IO-MRI procedure or not operated via EEA were excluded from the study.

Analysis of the retrospective data was performed using SPSS 21.0 (IBM Corp., Armonk, New York, USA). To compare predictions and to compare residual mass ratios between two Knosp's grade groups, Fisher's exact test was used. Variables were preoperative, largest diameter of tumor (< 4 cm or ≥ 4 cm), Knosp's grade, age, gender, and recurrent surgery.

Results: A total of 200 patients enrolled in the study. In Knosp's grade 0–2 group, primary surgeon's opinion and IO-MRI findings were compatible in 150 patients (98.6%). In Knosp's grade 3–4, correct prediction was performed in 32 (66.6%) patients. When incorrectly predicted, Knosp's grade 3–4 patients ($n = 16$) was investigated, in 13 patients, there were still residual tumor in cavernous sinus and in 3 patients there was no residual tumor. Fisher's exact test showed there is a statistically significant difference of correct prediction between two different Knosp's grade groups (two-tailed $p < 0.0001$).

Conclusion: Our results demonstrated IO-MRI is significantly useful in higher Knosp's grade patients. On the other hand, we do not recommend IO-MRI usage in patients with lower Knosp's grade adenomas because of increased treatment costs.

A195. Association of Preoperative Hemorrhage with Postoperative Hormonal Dysfunction in Surgically Resected Pituitary Adenomas

Reyanne Strong¹, Nathan Quig², Avinash Chandran³, Carlos Zamora⁴, Carolyn Quinsey²

¹University of North Carolina School of Medicine, Chapel Hill, North Carolina, United States

²Department of Neurosurgery, University of North Carolina School of Medicine, Chapel Hill, North Carolina, United States

³Matthew Gfeller Sport-Related TBI Research Center, Department of Exercise and Sport Science, University of North Carolina, Chapel Hill, North Carolina, United States

⁴Division of Neuroradiology, Department of Radiology, University of North Carolina School of Medicine, Chapel Hill, North Carolina, United States

Background: Of all brain tumors, adenomas have the highest proportions of preoperative hemorrhage with occurrence in 10 to 27% of all cases. Hemorrhage may present with apoplexy, an urgent clinical syndrome characterized by rapid onset of severe headache, nausea, vision changes, or changes in consciousness; however, hemorrhage may also remain clinically silent. Apoplexy has been well studied and identified as a risk factor for worse postsurgical outcomes. The presence of a clinically silent hemorrhage is not well understood as an individual factor and debate remains. Previous studies of pituitary adenoma at large found a 46 and 49% improvement, respectively, in pituitary function postoperatively. We aim to characterize and compare the postoperative outcomes in patients with clinically silent hemorrhages and apoplectic hemorrhage to patients without radiographic evidence of hemorrhage.

Methods: We conducted a retrospective analysis of all patients who were treated with an endoscopic endonasal transsphenoidal approach to pituitary adenomas. MRI and operative reports were reviewed for evidence of preoperative hemorrhage. All potential hemorrhage cases were reviewed by attending neuroradiologist and neurosurgeon to classify and characterize the tumor and hemorrhage. Medical records were reviewed for demographic information, preoperative symptoms, histology, extent of resection, and postoperative outcomes including pituitary function (**Figs. 1 and 2**).

Results: Of 180 patients, 36 were found to have preoperative hemorrhage. Of the 36 patients, 25 (69.4%) presented with apoplectic events while 11 (30.6%) presented silently. Postoperatively, 24 patients (66.7%) had gross total resection, while 12 (33.3%) were subtotal. Recurrent tumor growth occurred in four patients with two of them undergoing a second surgical resection. The vast majority of patients with cranial neuropathies experienced improvements post-surgically. Transient SIADH occurred in five patients (13.9%), transient DI in three patients (8.3%), and nontransient DI in three patients (8.3%). Preoperative hypopituitarism was present in 16 patients (44.4%), 22 patients (61.1%) remained on medications for pituitary dysfunction at last known follow-up, 6 patients (16.7%) were on medications temporarily postoperatively, and 1 patient (2.8%) had continued dysfunction but was not on medication. No postoperative medications for pituitary dysfunction were necessary in seven patients (19.4%). The mean follow-up was 19 months.

Conclusion: Our data suggest that patients with hemorrhage, both apoplectic and silent, are more likely to experience endocrinopathies. These data will be helpful in the preoperative counseling and perioperative management.

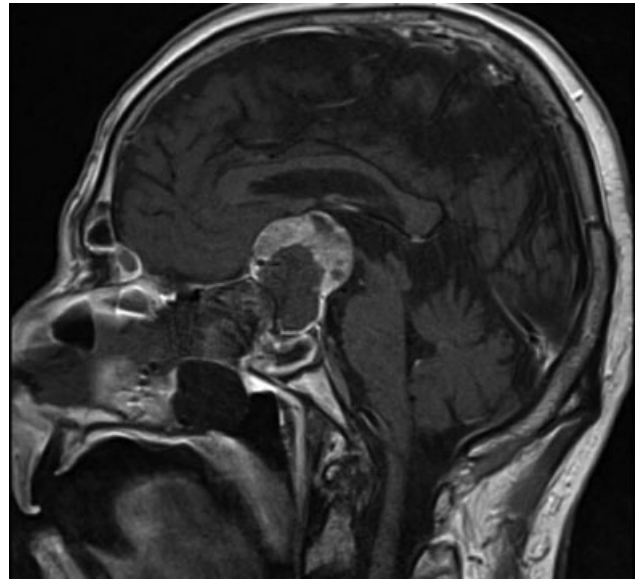


Fig. 1 Macroadenoma with silent hemorrhage measuring 3.8 × 3.2 × 4.5 cm.

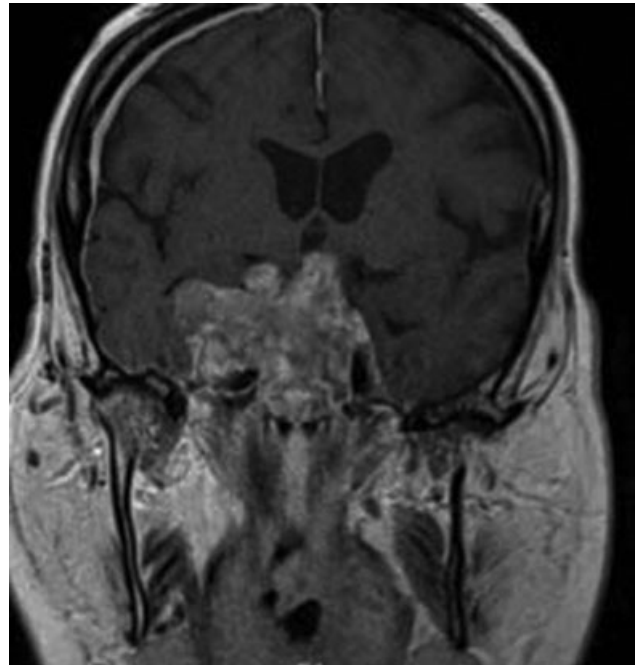


Fig. 2 Macroadenoma with pituitary apoplexy measuring 3.5 × 4.8 × 5.6 cm.

A196. Pituitary Apoplexy: Management and Outcomes at a Single-Center Over 15-Year Experience

Scott C. Seaman¹, Mark C. Dougherty¹, Mario Zanaty¹, Leslie A. Bruch¹, Scott M. Graham¹, Jeremy D. Greenlee¹

¹University of Iowa Hospitals and Clinics, Iowa City, Iowa, United States

Introduction: Pituitary apoplexy commonly presents with visual and hormonal deficits. While traditionally regarded as an emergency, there have been increasing trends toward conservative management. We present our

institutional series in regard to vision outcomes, hormone function, and complications.

Methods: We retrospectively reviewed our series of apoplexy patients identified by review of pathological studies and confirmed by chart review. We recorded basic demographic features, radiographic and operative features, and preoperative and postoperative vision and hormone status. Univariate and multivariate statistical analyses were performed. We then pooled our data with the available literature for Bayesian inference.

Results: Forty-nine patients were identified and confirmed to have pituitary apoplexy and underwent transnasal transsphenoidal decompression with >70% within 24 hours of presentation. Mean BMI was 34.8; 65% of patients had a visual deficit, of which 40.8% had a cranial nerve palsy, 34% had anopsia, and 18% had a visual acuity deficit. Hypothyroidism (36.7%) and low testosterone (26%) were common. Postoperatively, 100% of CN palsies improved, 82% of anopsias improved, and 60% of visual acuity deficits improved. Most hormone abnormalities improved after surgery, but long-lasting panhypopituitarism (26%) and diabetes insipidus (20%) were common. Other than preoperative anticoagulation use associated with long-term adrenal insufficiency ($p = 0.007$), there were no independent predictors of long-term hormone dysfunction. Cavernous sinus involvement predicted residual tumor ($p = 0.006$). Mean length of stay was 4 days, and independent predictors were anticoagulation use (OR: 6.434, $p = 0.011$), postoperative diabetes insipidus (OR: 3.8204, $p = 0.041$), and postoperative visual acuity deficits (OR: 8.6759, $p = 0.008$). There were eight medical and two surgical complications with one CSF leak. Bayesian inference demonstrated an absolute risk reduction for persistent visual deficit of 0.303 with surgery compared with conservative management. This represents a number needed to treat (NNT) of 3.3 for improved visual outcomes with surgery.

Conclusion: Early surgery for pituitary apoplexy is associated with excellent long-term visual deficits, although visual acuity was more resistant to improvement than anopsia or cranial nerve palsies. The need for long-term hormone replacement is common and there are no preoperative features to predict which hormones will be altered other than general incidence measures. Cavernous sinus involvement is an independent predictor of residual tumor. Despite a high mean BMI, our CSF leak rate was nominal. Our data in addition to the pooled data across publications show long-term visual benefit with surgery.

A197. Endoscopic Endonasal Approach to Giant Pituitary Adenomas in Low-Income Country: Single Surgeon's Experience from Azerbaijan

Tural Rahimli¹

¹Baku Medical Plaza, Baku, Azerbaijan

Background: Giant pituitary adenomas represent a surgical challenge. Lack of certain equipments, such as navigation system, intraoperative MRI, and others, makes the challenge more difficult to achieve.

Methods: We retrospectively reviewed medical records of 235 patients and identified 32 (22 males, 10 females) with giant pituitary adenoma who underwent an endoscopic endonasal approach from 2014 to 2019 years. The follow-up period ranged from 7 to 64 months (mean: 36).

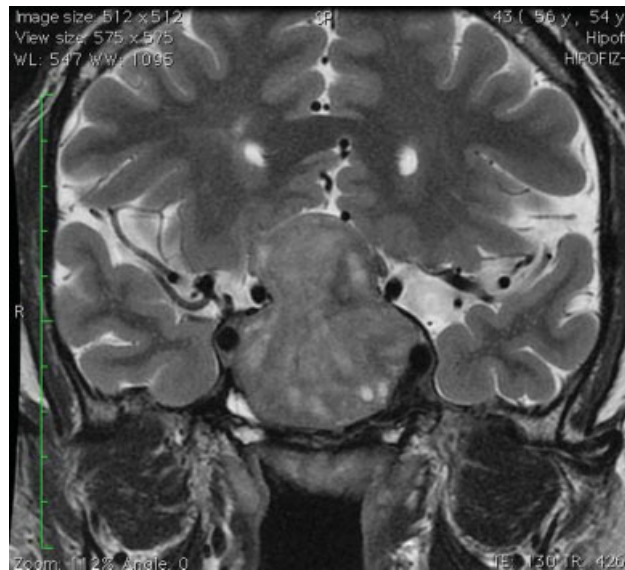
Results: A transsphenoidal approach was used in the treatment of 32 patients. Mean age of patients was 45 years old. Nonfunctioning tumors were present in 18 (56.25%); among functioning adenomas, 6 patients (18.75%) had GH-secreting tumors and 8 (25%) had prolactinomas. Cavernous

sinus invasion has seen in 12 (37.5%) and sphenoid sinus invasion in 7 (22%). Tumor extension to the third ventricle was 5 (16%) and tumor filled third ventricle totally. Tumor extension to the anterior fossa was 4 (12.5%) and to the posterior fossa it was 2 (6.25%). Eighteen tumors (56.25%) demonstrated round shape, 5 (16%) were dumbbell shape, and 9 (28%) were multilobulated.

Gross total and near-total resection was achieved in 28 (87.5%); partial resection was achieved in 4 patients (12.5%). Intraoperative ICA bleeding happened in three (9%) patients, two cases were controlled and carried on and surgical mortality was 3%.

Postoperative improvement in visual acuity was achieved in 23 (72%). Transient diabetes insipidus following surgery occurred in 9 (28%). A total of eight patients (25%) underwent adjuvant medical and/or radiotherapy. CSF leak occurred in four patients managed by lumbar drain (12.5%).

Conclusion: Endoscopic endonasal transsphenoidal surgery is an effective treatment method for patients with giant pituitary adenomas, which results in high rates of resection and improvement in visual function. It is not associated with high rates of major complications and is safe when performed by experienced surgeons.





A198. Predicting Pituitary Adenomas Consistency with Preoperative Magnetic Resonance Elastography

Salomon Cohen-Cohen¹, Joshua D. Hughes¹, Ziyang Yin², Matthew K. Ball³, John Huston III², Jamie J. Van Gompel¹

¹Department of Neurologic Surgery, Mayo Clinic, Rochester, Minnesota, United States

²Department of Radiology, Mayo Clinic, Rochester, Minnesota, United States

³Department of Pathology, Mayo Clinic, Rochester, Minnesota, United States

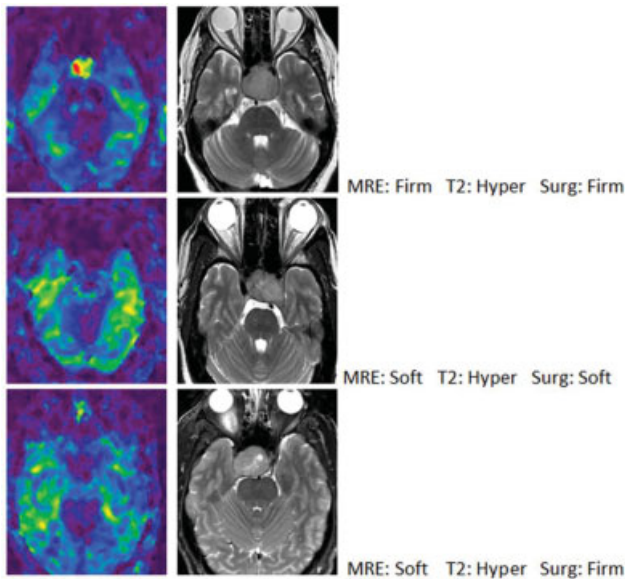
Background: Pituitary adenomas account for 15% of all primary intracranial neoplasms, which makes them the third most common primary intracranial tumor. Pituitary adenomas

are usually soft but up to 15% have a firm consistency. Tumor consistency is a common characteristic associated with surgical outcome and extent of tumor resection, as well as time spent in the operative theater. Knowledge of consistency preoperatively may improve preoperative counseling of the risks to the patient. Multiple studies have tried to predict pituitary tumor consistency with conventional MR imaging techniques. Magnetic resonance elastography (MRE) is a noninvasive, dynamic imaging technique that characterizes the viscoelastic properties of tissue. The purpose of this study is to evaluate the efficacy of preoperative MRE and MRI in 40 patients undergoing surgical treatment for pituitary adenomas to determine tumor consistency. This is an update of our previously published experience.

Methods: With institutional review board approval and written informed consent, 40 patients with pituitary adenomas were prospectively evaluated with MRI and MRE before surgery from September 2013 to July 2019. Tumors were classified into three groups: soft consistency (easily removable through aspiration), intermediate consistency (parts easily removed with suction but other portions difficult to remove with suction requiring mechanical techniques such as a sharp dissection), and firm consistency (not removable through aspiration and requiring piecemeal resection). MRE classifications were determined prospectively by radiologists unaware of the surgical findings. A Chi-squared test was performed to compare surgical grading and MRE classification. *p*-Values < 0.05 were considered significant.

Results: Forty patients (22 males; median age at surgery: 53 years; range: 22–74) with pituitary adenomas were prospectively imaged with MRI and MRE prior to resection. Thirty-nine patients underwent endoscopic endonasal approach (EEA) and only one patient had a frontotemporal craniotomy. Thirty-four patients had a nonfunctional adenoma (85%), five patients had a GH-secreting adenoma (12.5%), and one patient had an ACTH-secreting adenoma (2.5%). The mean tumor size in maximal diameter was 3.6 cm (range: 2–6 cm). By intraoperative findings, two tumors had a firm consistency (5%), six had an intermediate consistency (15%), and 32 were soft tumors (80%). MRE measurements and intraoperative findings correlated in 35 (87.5%) of 40 patients. One patient had an MRE predicting a soft tumor and the intraoperative finding was a firm tumor.

Conclusion: In our study, MRE predicted soft tumors well, but only one of the two firm tumors was correctly identified. Further study is needed and development of this technology, particularly in patients with firm tumors, is necessary to determine the usefulness of MRE for pituitary tumor surgery.



A199. Adenoid Cystic Carcinoma of the Skull Base: Retrospective National Cohort Analysis of Treatment Paradigms and Outcomes

Shekhar K. Gadkaree¹, Anuraag S. Parikh¹, Eric Barbarite¹, Andrew Holcomb¹, Justin McCarty², Stacey T. Gray¹, Derrick T. Lin¹

¹Massachusetts Eye and Ear, Harvard Medical School, Boston, Massachusetts, United States
²Department of Surgery, St. Elizabeth's Medical Center, Tufts University School of Medicine, Boston, Massachusetts, United States

Objectives: To examine a national cohort of patients with nasopharyngeal adenoid cystic carcinoma (ACC) for incidence, skull base invasion, overall survival, and treatment paradigms.

Design, Setting, and Participants: Retrospective national population-based study using Surveillance, Epidemiology, and End Results (SEER) program data of patients with ACC of the nasopharynx and skull base (NACC) between 2004 and 2016.

Main Outcomes and Measures: Primary outcomes included 5-year overall survival and locoregional control. Statistical analysis was performed using STATA 15.0 (STATA-Corp, College Station, Texas, United States). Spearman's rank order correlation was used for ordinal, monotonic variables with *p*-values <0.05 considered statistically significant. Survival analysis was performed by Kaplan–Meier method, and comparison between groups was performed using log-rank test.

Results: Of the 2,385 cases of adenoid cystic carcinoma, 70 cases were classified as NACC. Twenty-one percent (15) involved invasion of the skull base or posterior pharyngeal wall, and 42% (30) were either stage 3 or stage 4. The 3- and 5-year overall survival rates were 73 and 61%, respectively. Zero percent had metastasis to the neck and 6 percent had metastasis to the lungs in the study population. Eighty percent of patients with advanced stage NACC received radiation therapy, while 35% of patients underwent surgery, and 35% received chemotherapy. Five-year survival was not significantly affected between the radiation and nonradiation treatment groups (*p* = 0.18). Histologic subtypes of adenoid cystic carcinoma were not assessed in this study.

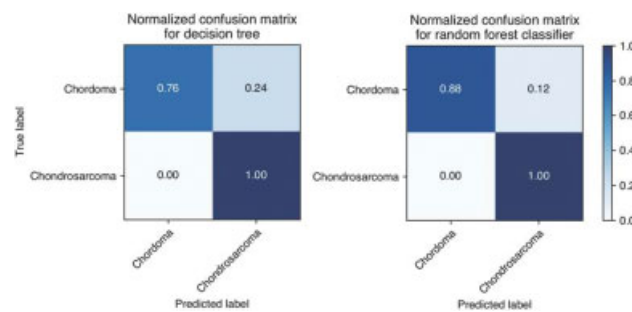
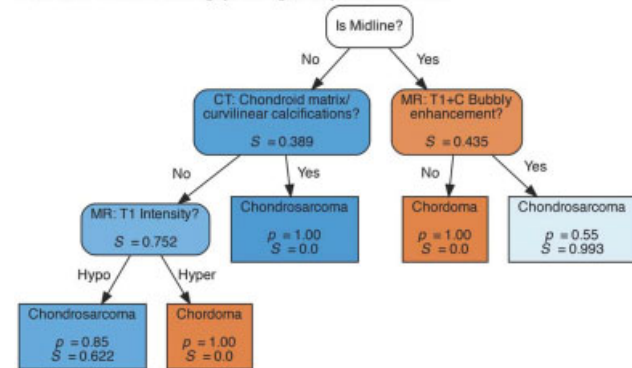
Conclusion: NACC is rare in incidence and was most commonly treated with radiation therapy when advanced in stage, despite its general reputation as a radio-resistant tumor. Type of radiation therapy was not assessed in this study. Surgery can be useful in appropriately selected tumors. These results raise the possibility that nasopharyngeal ACC is a unique entity from ACC in other subsites and it may arise in a different genetic background. Long-term survival for NACC patients requires further study with the need for pathologic and genetic characterization to better stratify high- and low-risk subtypes of NACC.

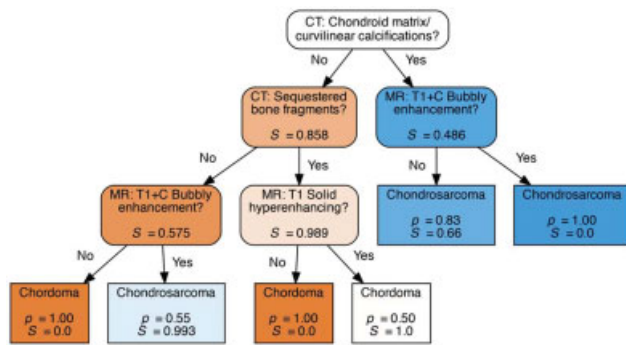
A200. Decision-Tree Classification of Chordomas and Chondrosarcomas

John Luebs¹, Tyson Tragon², Katie Traylor², Carl H. Snyderman³

¹SUNY Downstate Health Sciences University, Brooklyn, New York, United States
²Department of Radiology, University of Pittsburgh Medical Center, Pittsburgh, Pennsylvania, United States
³UPMC Center for Cranial Base Surgery, Pittsburgh, Pennsylvania, United States

UPMC Center for Cranial Base Surgery, Pittsburgh, Pennsylvania, United States





Background: Primary neoplasms of the clivus are uncommon and can be difficult to diagnose radiographically. Differentiation of chordomas and chondrosarcomas has clinical relevance for treatment and prognosis.

Objectives (1) Develop a decision-tree model for radiographic differentiation of chordomas and chondrosarcomas; (2) determine most predictive diagnostic criteria; (3) validate the model.

Methods: Patients with pathologic confirmation of chordoma or chondrosarcoma of the skull base were identified in our tumor registry. Retrospective review of preoperative CT and MRI was performed by neuroradiologists using possible diagnostic criteria posed as yes/no questions. A stratified sample of 70% of records was used as a training set with the remaining records used as a test set. Decision tree classifiers were fit using the CART algorithm. Search of hyperparameters with k-fold cross-validation on the training set was used to guide model selection. A random forest classifier was trained on the same data for comparison. Area under ROC curve was computed against the test set.

Results: There were 57 chordomas and 16 chondrosarcomas with complete imaging for review. Of nine yes/no features labeled, nine were discriminatory in the single-tree model trained with all features. Important features: midline location—0.719; MRI T1 + C bubbly enhancement—0.169; chondroid matrix/calcifications on CT—0.074; MRI T1 hypo vs. hyperintense—0.037. Area under ROC curve was 0.86. A random forest classifier composed of 500 trees used 7 features with area under the ROC curve of 0.97 when applied to the test set.

Conclusion: This decision-tree model for radiographic differentiation of chordomas and chondrosarcomas may be useful for inexperienced physicians to establish a diagnosis and guide clinical decisions. A random forest classifier may overcome weakness due to over-fitting; however, interpretability is limited.

A201. The Role of Cervical and Parotid Lymph Nodes in Surgical Management of Malignant Tumors of the Lacrimal Sac

Brian Swendseid¹, Joseph Godovchik¹, Swar Vimawala¹, Samuel Garrett¹, Michael Topf², Adam Luginbuhl¹, David Cognetti¹, Joseph Curry¹

¹Thomas Jefferson University Hospitals, Philadelphia, Pennsylvania, United States

²Stanford University, Stanford, California, United States

Introduction: Treatment of lacrimal sac malignancies can entail numerous challenging decisions, including the need for orbital exenteration, skull base resection, adequate

neck dissection, appropriate adjuvant therapy, and ideal reconstruction. Given the rarity and diversity of these tumors, treatment recommendations are based on small patient series. Lymph node positivity has been predictive of decreased recurrence free and overall survival in one of the lone large series of lacrimal sac tumors. Despite the likely importance of cervical and parotid lymph node status for these tumors, the optimal nodal management has not been described.

Methods: Thirty-one patients with malignant tumors of the lacrimal sac that were treated surgically were identified for retrospective review. Preoperative imaging, surgical treatment, pathology, adjuvant treatment, and recurrence data were collected and univariate analysis was performed.

Results: Forty percent of patients have nodal positivity on preoperative imaging; however, only 60% of these patients had pathologically involved lymph nodes. When pathologically positive nodes were identified, the intraparotid nodes were nearly always involved (6/6 patients in whom parotidectomy was performed, 6/7 patients overall). A majority of recurrences occurred in the neck or parotid lymph nodes (88%), including in 31% of patients with negative preoperative imaging (mean 11 months to regional recurrence). If T1N0 tumors are excluded, failure to perform neck dissection or sentinel lymph node biopsy is associated with regional recurrence (OR: 7.1, 95% CI: 1.02–49.5, $p = 0.047$).

Discussion: Optimal management of lacrimal sac malignancies remains unclear due to their rarity. Lymph node status appears to play an important role in lacrimal sac tumor spread and recurrence. The intraparotid lymph bed is often involved when lymph node spread is present, and parotidectomy should be considered for high-risk tumors or when there is evidence of cervical lymph node spread. Performing sentinel lymph node biopsy or neck dissection at the time of surgery for tumors larger than T2 decreases regional recurrence rates.

A202. New Classification of Endoscopic Transnasal Nasopharyngectomy for Recurrent Nasopharyngeal Carcinoma: Shanghai EENT Hospital's Experience

Hongmeng Yu¹, Quan Liu¹, Xicai Sun¹, Yurong Gu¹, Houyong Li¹, Dehui Wang¹

¹Department of Otolaryngology; Eye, Ear, Nose and Throat Hospital; Shanghai Medical College of Fudan University, Shanghai, China

Objective: Transnasal endoscopic nasopharyngectomy (TEN) has been an alternative treatment for recurrent nasopharyngeal carcinoma (rNPC). Current classification of the TEN needs updating. This study aims to establish new classification system of endoscopic endonasal nasopharyngectomy for rNPC.

Methods: A retrospective analysis was performed in 98 patients who underwent TEN for rNPC from January 2016 to November 2018 in our institution. Based on the stepwise exposed anatomic structures, the TEN was categorized into four types, which included type I ($n = 41$) with resection of the nasopharynx and sinus; type II ($n = 12$) with lateral extension to the parapharyngeal space; type III ($n = 40$) with lateral extension to the floor of the middle cranial fossa and infratemporal fossa, superior extension to orbital apex and cavernous, back to the prevertebral region; type IV ($n = 5$) with the resection of the involved internal carotid artery.

Results: The mean age was 51 years. There was no major complication. The median time of follow-up was 23 months. Ten patients were lost. Twenty-two patients recurred after surgery. Seventeen patients died. Among these patients, six patients died of massive bleeding, and four

patients died of distant metastasis. The 2-year overall survival rate (OS) was 80.8%. The 2-year OS rates for rT1, rT2, rT3, and rT4 were 92.4, 100, 75.5, and 66.3%, respectively. The 3-year OS was 66.7%. The 2-year and 3-year local relapse-free survival (LRFS) rates were 56.2 and 43.2%, respectively. Two-year LRFS rates for rT1, rT2, rT3, and rT4 were 84.9, 38.9, 49.8, and 41.9%, respectively.

Conclusion: The four types of endoscopic endonasal nasopharyngectomy are effective in the surgical treatment of the rNPC. The preoperative evaluation and staged exposure of the ICA are reliable method, which will be an effective guideline for surgical treatment of the rNPC.

A203. Endoscopic Endonasal Nasopharyngectomy and Its Use in Rt3 and Rt4 Recurrent Nasopharyngeal Carcinoma

Roberto M. Soriano¹, Rima S. Rindler¹, Gustavo Pradilla¹, C. Arturo Solares¹

¹Emory University (SSO), Atlanta, Georgia, United States

Background: Endoscopic endonasal nasopharyngectomy (EEN) has been extensively used for rT1 and rT2 recurrent nasopharyngeal carcinoma (rNPC); however, limited literature exists about its use in recurrent T3 (rT3) and T4 (rT4) rNPC. We have performed a systematic review of the literature and reported preliminary data regarding the efficacy and safety of its use in rT3 and rT4 rNPC.

Study Design: Systematic review.

Methods: A systematic PubMed search adherent to PRISMA guidelines included relevant clinical studies reporting the use of the endoscopic endonasal nasopharyngectomy (EEN) for salvage surgery of rT3 and rT4 nasopharyngeal carcinoma (rNPC) in adult humans from 1974 onward. Available data regarding clinical outcomes were abstracted and preliminary results are reported.

Results: Sixteen of 400 articles were eligible for a detailed review of which the majority ($n = 11$) were retrospective studies. They report on a total of 238 rT3 and rT4 rNPC patients undergoing salvage EEN. Only one study included patients with only rT3 and rT4 disease. A total of 193 rT3 patients were reported in all studies. Six of the 9 studies specifying the extension of rT3 disease included only patients with rT3 disease confined to the sphenoid sinus; 11 studies included individual rT3 survival data. OS is most frequently reported as 2-year OS resulting in a combined 74.1% 2-year OS. DFS was most frequently reported as a 2-year DFS resulting in a combined 2-year DFS of 67.9%. As for rT4, a total of 45 patients were reported in five studies. Four studies included individual rT4 survival data. OS was most frequently reported as 2-year OS by three studies, resulting in a combined 48.5% 2-year OS. DFS was most frequently reported by two studies, as a 2-year DFS resulting in a combined 2-year DFS of 42.9%. No studies specified the extension of rT4 disease. The mean follow-up for all studies was 26.1 (SD: 9.9) months. Of the nine studies reporting complications, the most common was secretory otitis media. Apart from the presence of distant metastasis, and comorbidities contraindicating anesthesia, the most common reasons for exclusion from surgical management were ICA involvement, intracranial intradural extension of disease, and neck metastasis.

Summary: Among these two groups of patients, EEN was mostly used for rT3 rNPC. OS and DFS are higher in rT3 than in rT4 rNPC; however, it must be taken into account that the majority of rT3 patients included have exclusive involvement of the sphenoid sinus as this might greatly improve outcomes given the extent of resection necessary. Overall, limitations of the literature reviewed include lack of rT3 and rT4 subgroup analysis of survival, recurrence and complica-

tions, and limited individual patient data. Although the majority of these studies include the use of EEN on rT3 and rT4 rNPC, there is still a need to evaluate its use uniquely on rT3 and rT4 patients.

A204. Radiological Findings of Medial Orbital Wall Bony and Periorbital Dehiscence in Sinonasal Malignancies as a Predictor of Final Histopathologic Orbital Invasion

Prachi N. Patel¹, Tawfiq Khoury¹, Chandala Chitguppi¹, Kurren Gill¹, Gurston Nyquist¹, Marc Rosen¹, Pascal Lavergne², James Evans², Mindy Rabinowitz¹

¹Department of Otolaryngology - Head and Neck Surgery, Thomas Jefferson University, Philadelphia, Pennsylvania, United States

²Department of Neurosurgery, Thomas Jefferson University, Philadelphia, Pennsylvania, United States

Background: Malignant tumors of the nasal cavity and paranasal sinuses have the potential to invade into surrounding structures including the orbit and skull base. The orbital periosteum has long been considered a barrier to the spread of such tumors into the orbital cavity and can be regarded as the decisive layer when determining extent of tumor resection. However, interpretation of orbital invasion can become extremely challenging as the periosteum can be difficult to visualize separately from the orbital bony wall on imaging.

Purpose: This study aims to determine the impact of computed tomography findings and operative assessment of orbital bony and periosteal tumor involvement as an accurate predictor of final microscopic invasion.

Methods: A single-center, retrospective review of 188 patients undergoing surgical resection of sinonasal malignancy between 2008 and 2019 was performed. Patients were included if they had a sinonasal malignancy involving the orbit with the appropriate radiographic, operative, and final pathologic reports available.

Results: A total of 82 cases met inclusion criteria. All patients underwent either endoscopic or open resection for invasive sinonasal malignancy. Treatment was by orbital exenteration in 27 patients (33%) and orbital preservation in 55 patients (67%).

A total of 26 patients (31.7%) were found to have medial orbital bony wall dehiscence on preoperative CT imaging. Of these patients, 14 were noted to have bone involvement on operative assessment and 7 patients had positive orbital wall bone on final pathology. Forty-nine (59.7%) patients had periorbital involvement on imaging, 19 of who were noted on operative assessment and 13 with final positive pathology. Periorbital involvement was defined as gross tumor extension into the orbit, suggesting breach.

Erosion of the orbital bony wall and periorbital involvement on preoperative CT was found to be 70% [95% CI 35.4%, 91.9%] and 28% [95% CI 12.9%, 50%] sensitive and 69.8% [95% CI 56.8%, 80.4%] and 62% [95% CI 46.4%, 75.1%] specific respectively for involvement on final pathology. The positive predictive values (PPV) were 26.92 and 33.3% and the negative predictive values (NPV) were 93.62 and 63.4%, respectively.

Operative assessment of bony erosion and periorbital involvement was found to be 60% [95% CI 27.4%, 86.3%] and 45.8% [95% CI 26.2%, 66.8%] sensitive and 68.7% [95% CI 56.0%, 79.1%] and 59.6% [95% CI 45.1%, 72.7%] specific, respectively, for invasion on final pathology. The PPVs were 22 and 34.4% and NPVs were 92 and 70.45%, respectively.

Overall, it is more likely that a patient with pathologic evidence of bony involvement had bony erosion on operative assessment (OR: 3.28, $p < 0.05$).

Conclusion: Radiologic findings and intraoperative assessment for bony and periorbital erosion are valuable

tools when assessing orbital margins, but neither are perfect. This re-enforces the need for intraoperative pathological consultation when attempting to preserve critical structures. Additionally, surgeons should therefore be aware of the potential need for aggressive tumor resection within the orbit in cases with low preoperative probability of invasion.

A205. Surgical Management of Skull Base Chordomas: Single-Center Results in the Last 10 Years

Joao Paulo Almeida¹, Randy Van Ommeren¹, Jeffrey Zuccato¹, Allan Vescan¹, John de Almeida¹, Eric Monteiro¹, Ian Witterick¹, Fred Gentili¹, Gelareh Zadeh¹

¹University of Toronto, Toronto, Canada

Introduction: Skull base chordomas are aggressive tumors arising from the clivus that pose a significant surgical challenge due to their location, invasiveness, and relationship with surrounding neurovascular structures. Endoscopic endonasal approaches (EEA) have been successfully applied as a strategy to manage those tumors in the last decade. In the current abstract, we report the results of our center in the surgical management of clivus chordomas in the past 10 years.

Methods: The authors conducted a retrospective analysis of all skull base chordomas operated on our institution from January 2007 to December 2017. Clinical and radiological characteristics of patients and tumors were extracted. The primary outcome was defined as recurrence-free survival. Secondary outcome included extent of resection, adjuvant therapy, and complications and impact of the Sekhar's Grading System for Cranial Chordomas on the outcome of patients. Patients with less than 12 months of follow-up (FU) were excluded from the analysis.

Results: A total of 37 patients matched the inclusion criteria. Mean age of patients was 52.03 (\pm 15.1); range: 19–79 years old. 10 patients (27%) had had previous surgery and radiotherapy. Tumors were located at upper clivus: 23 (62.1%), middle clivus: 22 (59.4%), and lower clivus in 14 (37.8%) cases. Tumor extension into the cavernous sinus, vascular encasement, and dura invasion were observed in 40.5, 43.2, and 43.2%, respectively. The mean Sekhar Grading System score was 8.1 \pm 4.3. Most cases underwent EEA for tumor resection (n = 33, 89.2%). Gross total and partial resection were achieved in 8 cases (21.6%) and 29 cases (78.4%), followed by adjuvant IMRT in 32 cases (86.4%). Most common complications were postoperative CSF leak and meningitis (5.4 and 8.1%). Recurrences were observed in 18 cases (48.6%), mean follow-up of 46.5 \pm 36.4 months. Progression-free survival was 66 months (95% CI: 21.7–110.2) in the entire cohort. Improved PFS was associated with lower Sekhar scores (p = 0.01), first-time surgery (no prior treatment) (p = 0.006), adjuvant radiation (p = 0.01), and gross total resection (p = 0.04).

Conclusion: Our results demonstrate the important role of EEA for the management of chordomas. The invasiveness of chordoma, however, impacts its extent of resection. A low rate of complications has been achieved in our series, but gross total resection was observed in only one out of five patients. Factors such as Shekhar's grading score, adjuvant radiation, and extent of resection impacted PFS of skull base chordoma.

A206. The Impact of Induction Chemotherapy and Socioeconomic Factors on Survival in Sinonasal Undifferentiated Carcinoma

Khodayar Goshtasbi¹, Brandon M. Lechrich², Arash Abiri¹, Tyler Yasaka², Frank P. Hsu³, Gilbert Cadena³, Edward C. Kuan¹

¹Department of Otolaryngology - Head and Neck Surgery, University of California Irvine, Irvine, California, United States

²University of California Irvine, Irvine, California, United States

³Department of Neurological Surgery, University of California Irvine, Irvine, California, United States

Introduction: Sinonasal undifferentiated carcinoma (SNUC) is a rare and aggressive malignancy of the sinonasal cavity. The role of induction chemotherapy (IC) and demographic or socioeconomic factors on overall survival (OS) of patients with SNUC is yet to be determined.

Methods: The National Cancer Database (NCDB) was queried for all patients diagnosed with histologically confirmed SNUC from 2004 to 2015. IC was defined as chemotherapy administered 6 months to 2 weeks before surgery or \geq 45 days prior to radiotherapy.

Results: Of 440 patients with a diagnosis of SNUC, 70 (16%) underwent treatments involving IC. This consisted of 52 (12%) patients receiving IC before definitive radiation therapy without surgery, 15 (3%) receiving IC before surgery and adjuvant radiotherapy, and 3 (1%) receiving IC before surgery only. On univariate analysis, patients with primary site location in the paranasal sinuses (HR: 1.37; 95% CI: 1.04–1.79; p = 0.02), having government insurance (HR: 1.79; 95% CI: 1.37–2.34; p < 0.001), and living in regions with \geq 13% of the population without a high school diploma (HR: 1.38; 95% CI: 1.06–1.79; p = 0.02) were associated with worse OS. On log-rank test, patients with advanced stage had similar OS regardless of receiving IC or not (p = 0.96). Patients who received IC lived closer to their treatment site (p = 0.02). Additionally, on logistic regression, patients with a lower Charlson–Deyo comorbidity score, a measure of overall health and existence of comorbidities, were more likely to receive IC (p = 0.04). The timing of IC prior to definitive surgery or radiation did not affect OS (p = 0.69).

Conclusion: IC did not seem to provide additional survival benefit to patients with SNUC regardless of disease stage or timing prior to definitive treatment. Having government insurance and residing in less educated regions may impact OS for patients with SNUC.

A207. Thirty-Day Complications following Intradural Versus Extradural Excision of the Skull Base

Khodayar Goshtasbi¹, Arash Abiri¹, Mehdi Abouzari¹, Harrison W. Lin¹, Hamid R. Djalilian¹, Edward C. Kuan¹

¹Department of Otolaryngology - Head and Neck Surgery, University of California Irvine, Irvine, California, United States

Background: Inherent disparities between surgical approaches for intradural and extradural excisions of skull base lesions may engender varying risks for acute complications. This study aims to elucidate such differences by comparing rates of 30-day morbidity and mortality between intradural and extradural resection of the skull base.

Methods: The 2005 to 2017 American College of Surgeons National Surgical Quality Improvement Program database was queried for surgical cases with primary current procedural terminology codes designating intradural and extradural excision of lesions in anterior, middle, or posterior cranial fossae. All noted complications occurred within 30 days of the operation. Total complications included any surgical or medical complications, readmission, reoperation, and mortality.

Results: A total of 1,168 cases were extracted for analysis, consisting of 701 (60.0%) intradural and 467 (40.0%) extradural resection of skull base lesions. The two cohorts had similar age ($p = 0.133$), body mass index ($p = 0.254$), race ($p = 0.656$), functional status ($p = 0.986$), and ASA scores ($p = 0.911$). However, the intradural excision cohort had more females (59 vs. 49%; $p = 0.001$), more nonelective surgeries (16 vs. 10%; $p = 0.013$), and fewer surgeries by otolaryngologists (11 vs. 71%; $p < 0.001$). Compared with extradural excision, intradural excision of anterior cranial fossa lesions had higher rates of medical complications (15 vs. 7%; $p = 0.031$), readmission (18 vs. 8%; $p = 0.040$), and longer hospital stay (7.1 ± 9.4 vs. 4.1 ± 6.5 days; $p = 0.004$). Regarding lesions of the infratemporal fossa, parapharyngeal space, and petrous apex, only medical complication rate was higher in intradural compared with extradural excision (22 vs. 9%, $p = 0.012$). Intradural excision of lesions in the parasellar region, cavernous sinus, clivus, or midline skull base led to higher rates of reoperation (10 vs. 1.5%; $p = 0.029$), total complications (29 vs. 15%; $p = 0.016$), and longer hospital stay (6.1 ± 10.3 vs. 3.7 ± 4.3 days; $p = 0.004$). Furthermore, length of hospital stay was the only significantly different factor between intradural (7.1 ± 8.2 days) and extradural (5.2 ± 4.9 days) excision of lesions in the posterior cranial fossa, jugular foramen, foramen magnum, or C1–C3 vertebral bodies ($p = 0.016$). When combining all cases of resecting skull base lesions, there were similar rates of mortality ($p = 0.910$), surgical complications ($p = 0.332$), and total complications ($p = 0.205$). However, compared with extradural excision, intradural excision of skull base lesions had higher rates of medical complications (14 vs. 8%; $p = 0.002$), readmission (12 vs. 8%; $p = 0.032$), reoperation (10 vs. 6%; $p = 0.033$), and higher length of hospital stay (6.9 ± 8.1 vs. 4.5 ± 5.7 days; $p < 0.001$).

Conclusion: Resection of skull base lesions, especially in the anterior cranial fossa and parasellar or midline skull base region, can carry different risks for postoperative complications depending on extent of dural dissection. Intradural resection of skull base lesions is associated with higher rates of medical complications, readmissions, reoperations, and lengthier hospital stays.

A208. Case Series of Skull Base Meningioma Resections in the Octogenarian Population

Dorian M. Kusyk¹, Gordon Mao¹, Alexander Yu¹

¹Allegheny General Hospital, Pittsburgh, Pennsylvania, United States

Introduction/Hypothesis: With an aging population, the octogenarian patients are increasingly seen by neurosurgeons for consultation. Although these patients present with a variety of cranial and spinal pathologies, meningiomas are a comparatively common pathology, given that the prevalence of incidentally found tumors in elderly patients is 1.6%.¹

Unfortunately, though octogenarian patients with meningiomas are increasing seen in neurosurgical clinics, providers do not have clear data to help guide their decision making. In particular, the data for skull base lesions are scarce. Current research in the elderly looks at a wide range of age groups, classifying anyone above 65 as “elderly.” In the studies looking at patients in their seventh or eighth decade of life, mortality for skull base procedures ranged from 0 to 29%.² However, these studies were inconsistent in their capture of comorbidities and morbidities. This article strives to clarify the experiences and outcomes of patients in their eighth decade of life.

Methods: This retrospective series reviews all octogenarian skull base tumor surgeries performed at a single

academic institution over the past 15 years. Records are reviewed for surgical indications, preoperative neurologic deficits; perioperative wound healing and neurologic recovery. Specific attention is focused on requirement of tracheostomy or gastrostomy after surgery, sepsis, respiratory infections, and withdrawal of care or early death within 30 days of the operation. Multivariate logistic regression is performed to identify relevant perioperative and medical characteristics that increases the risk of these adverse events.

Results: Fourteen patients underwent craniotomies for skull base procedures in our series with an average age of 84.5. Of the patients, 79% had serious comorbidities and the same number was either on antiplatelet agents or systemic anticoagulation. Though two of the patients expired before 30 days postop, only one patient required a tracheostomy on discharge and approximately half were able to either go home or inpatient rehab after their procedure. On statistical analysis, there were no noted patient characteristics that predisposed any of our patients to a poorer outcome.

Conclusion: In our series, extremely elderly patients were able to tolerate the surgeries for resection of skull base meningioma. However, the decision to pursue surgery was often forced by acute neurologic decline refractory to medical therapy. In spite of often being in extremis, the patients did not seem to be at higher risk for a tracheostomy or a feeding tube postoperative. Ultimately, the decision making regarding octogenarian surgeries is complex, and this series shows that the patients in their eighth decade of life can still be valid surgical candidates.

References

1. Vernooij MW, Ikram MA, Tanghe HL, et al. Incidental findings on brain MRI in the general population. *N Engl J Med* 2007;357(18):1821–1828
2. Meling TR, Da Broi M, Scheie D, Helseth E. Skull base versus non-skull base meningioma surgery in the elderly. *Neurosurg Rev* 2019 42(4):961–972

A209. Identification of the Aggressive Atypical Meningioma: Histopathology, Proteomic Signatures, and Genotyping

Kate Carroll¹, Jake Ruzevick¹, Sam Emerson¹, Jr. Manuel Ferreira¹

¹University of Washington, Washington, District of Columbia, United States

Purpose: After a gross total resection, some atypical, WHO Grade II, meningiomas carry a favorable prognosis without further therapy. However, ~40% follow a clinically aggressive course with recurrence, invasion, and resistance to conventional therapies. Histopathology is unable to identify these “bad acting” tumors. We aimed to identify biomarker signatures in atypical meningiomas where histopathology has fallen short.

Experimental Design: Targeted next-generation sequencing for mutations in NF2, TRAF7, SMO, KLF4, and AKT1 E17K, MS-based phosphoproteomics and peptide chip array kinomics were used to explore atypical meningiomas. Ingenuity Pathway Analysis (IPA) identified atypical meningioma signatures. The selected biomarkers were evaluated in an independent cohort of 320 meningioma samples and correlated with clinical variables.

Results: The MS-based phosphoproteomics and kinomic profiling revealed unique Ser/Thr phosphorylation signatures. While mutations in NF2, TRAF7, SMO, KLF4, and AKT1 E17K or histological criteria (e.g., sheeting, mitoses,

brain invasion, necrosis, macronucleoli) did not identify aggressive atypical meningiomas, the unique proteomic signature was associated with decreased progression/recurrence-free survival.

Conclusion: A unique aggressive atypical meningioma signature was identified using MS-based phosphoproteomics and peptide chip array kinomics. The signature was independent of histology, subtype, WHO grade or genotype. This may provide promising biomarkers for risk stratification of histologically unidentifiable aggressive WHO grade II atypical meningiomas.

A210. Management of Petroclival Tumors

Diego Mendez Rosito¹

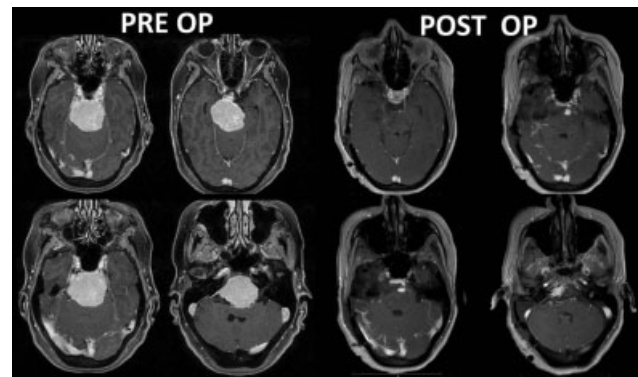
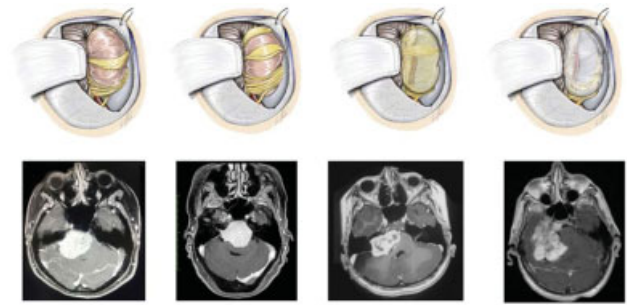
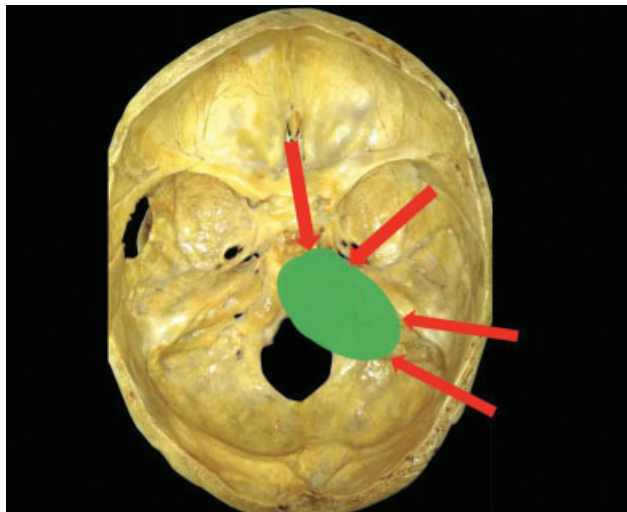
¹Centro Medico Nacional 20 de Noviembre, ISSSTE

Objective: Management of petroclival tumors is challenging. Tumors in the petroclival region may have different origins resulting in distinct positions and displacement of normal neurovascular structures. The objective of this project is to do a thorough preoperative analysis to decide which surgical approach is appropriately tailored to each case.

Methods: A series of 20 petroclival tumors was analyzed. Each case was prospectively reviewed to decide the surgical approach. Postoperatively, each case was reanalyzed evaluating several preoperative factors including tumor type, tumor origin, consistency, and nerve and arterial involvement.

Results: The series included nine petroclival meningiomas, one clival meningioma, three trigeminal schwannomas, three epidermoid, two petrous apex meningiomas, two glomus jugulare tumor, and two tentorial meningioma. In each case, the preoperative factors were analyzed and the surgical approach was decided based on it. The selected approaches were anterior petrosal (eight cases), posterior petrosal (five), combined anterior and posterior petrosal (two), and retrosigmoid (two). The postoperative deficit was analyzed.

Conclusion: Each case should be preoperatively analyzed to tailor the approach to each case. The skull base surgeon is required to have a full armamentarium of surgical approaches according to the need of each case. The origin and the displacement of the cranial nerves are the most important preoperative risk factors to consider when deciding the surgical approach to avoid postoperative cranial nerve deficit.



A211. Evaluating the Safety of Ligating the Anterior Superior Sagittal Sinus

Racheal Peterson¹, Jennifer Kosty¹, Bharat Guthikonda¹

¹LSUHSC Shreveport, Shreveport, Louisiana, United States

Background: It is a common belief within neurosurgery that ligation of the anterior third of the superior sagittal sinus (SSS) is safe. This principle can be traced back to Cushing's meningiomas text, wherein he states that ligation of the sinus anterior to the Rolandic vein has little comorbidity and allows for aggressive resection of tumors involving the sinus. There are few publications in modern literature examining the outcomes following ligation of the sinus. The goal of this study is to outline the complications seen following SSS ligation.

Methods: A retrospective review was performed utilizing our institution's electronic medical records system. Patients who underwent bifrontal craniotomy between 2010 and 2019 were screened to identify those with operative ligation of the sinus. A total of 38 patient records were reviewed for the presence of postoperative infarct, edema, or new neurological deficit.

Results: Of the 40 bifrontal craniotomies performed among 38 patients, 15 included ligation of the SSS. This group comprised 11 parafalcine meningiomas, 3 olfactory groove meningiomas, and 2 other anterior skull base lesions. Ten of these patients had imaging demonstrating preoperative occlusion of the sinus. After ligation, 2 patients developed worsening of preoperative deficits and 4 developed new deficits. Four patients had new anterior cerebral artery

infarcts and 5 demonstrated worsening edema on postoperative MRI. Tumor recurrence occurred in one patient.

Authors	Year Published	No. of cases with SSS ligation	Pathology	Venous infarct/edema (%)	Death (%)
Dilmeço, et al.	2004	30	PSM	6 (20)	0
Colli, et al.	2007	17	OGM	1 (5.9)	2 (11.8)
Nakamura, et al.	2007	46	OGM	10 (21.7)	4 (8.7)
Nowak and Marchel	2007	9	PSM	0	2 (22.2)
Salunke, et al.	2013	62	OGM, PSM, DACA Aneurysm, and ASBM	5 (8.1)	2 (3.2)
Nowak, et al.	2014	13	PSM	7 (53.8)	0
Pallini, et al.	2015	70	OGM	13 (18.6)	4 (5.7)
Nanda, et al.	2016	16	OGM	0	0
Farooq, et al.	2018	19	OGM	5 (26.3)	1 (5.3)
Cho, et al.	2019	61	DACA Aneurysm	0	0
Xu, et al.	2019	54	ASBM	0	0

Conclusion: Our evaluation identified patients with poor neurological outcomes following ligation of the anterior superior sagittal sinus, particularly venous infarct and edema. While this has typically been regarded as a safe surgical technique, this does not hold true in all cases. Review of the literature shows morbidity relating to venous edema ranging from 0 to 54% and mortality ranging from 0 to 22% for bifrontal craniotomy with sinus ligation. The incidence of venous infarct following SSS ligation may be related to disruption of collateral veins associated with the tumor in an already-compromised venous system. Recent anatomical studies suggest that there are varying degrees of vascularity in the frontal lobes ranging from minimal to dominant drainage into the SSS, making certain individuals more sensitive to disruption of the sinus. Anterior SSS ligation is not a universally safe maneuver and should be considered carefully before it is performed.

A212. Short-Term Olfactory Changes after Endoscopic Transsphenoidal Pituitary Surgeries: Identification, Discrimination, and Threshold Results

Hazan Basak¹, Deniz Uluc¹, Suha Beton¹, Gokmen Kahilogullari¹, Cem Meco¹

¹Ankara University, Ankara, Turkey

Background: It has been shown that endoscopic transsphenoidal pituitary surgery (ETPS) preserves olfaction better than microscopic techniques. Nevertheless, even if ETPS is utilized, olfaction can be affected. The aim of this study is to assess short-term changes in olfactory functions and the quality of life in the postoperative second month in patients having ETPS.

Materials and Methods: Patients who underwent ETPS between June 2017 and December 2018 were evaluated with preoperative and postoperative 2nd month olfaction tests including identification, discrimination, and threshold scores as well as SNOT-22 questionnaire.

Results: From 73 patients included, 48 (65.8%) were female and 25 (34.2%) were male; the mean age was 44.8 (8 – 76 ± 16.4). 29 patients (39.7%) were asymptomatic and 20 patients (27.4%) described headaches as their primary symptoms. There were intraoperative cerebrospinal fluid (CSF) leakage during surgery in 41 (56.2%) patients, and nasoseptal pedicled flaps were used in 47 (64.4%) patients for watertight closure. The mean score for SNOT-22 was 23.46 preoperatively and 27.86 postoperatively. The preoperative and postoperative mean scores for odor identification, discrimination, and threshold tests were 7.29 to 5.43, 6.99 to 5.00, and 6.58 to

3.70, respectively, showing worsening of scores in all components of olfactory tests postoperatively at second month.

Conclusion: Even though previous studies showed that olfactory functions are better preserved in ETPS, our data indicate that a worsening in olfaction is to be expected at postoperative second month. Patients should be informed on this fact preoperatively. Larger series with longer follow-up periods are needed to better assess olfactory function in the long run.

A213. Free Flap Reconstruction of Skull Base Defects: A Retrospective Review

Sen J. Ninan¹, Katherine Liu¹, Todd Spock¹, Eric Lee¹, Andrey Filimonov¹, Brett Miles¹, Alfred M. Illoreta¹

¹Icahn School of Medicine at Mount Sinai, New York City, New York, United States

Due to the anatomic challenges of surgery of the anterior and lateral skull base, defects in these regions pose complex reconstructive challenges, given the need to anatomically isolate the intracranial cavity to prevent CSF leak and infection. While microvascular free tissue transfer is an increasingly used reconstructive technique for large or complex skull base defects following oncologic ablative surgery, the risk of perioperative morbidity is not well described. A retrospective chart review was conducted in an effort to better understand the risk factors, complications, and outcomes of free tissue transfer for skull base reconstruction. 28 patients were identified with tumors requiring anterior and/or lateral skull base resection and reconstruction using microvascular free flaps at a tertiary care hospital from 2009 to 2015. Of these patients, 22 were male and 6 were female. The most common initial diagnosis was squamous cell carcinoma (60.71%). The majority of tumors invading the skull base had a sinonasal origin (71.43%). Of the 19 skull base tumors that had staging data available, 7 were classified as stage 4a, 5 as stage 3, 4 as stage 4b, and 2 as stage 2. The most common flaps used were anterolateral thigh free flaps (57.14%), followed by scapular (14.28%), and rectus abdominis (10.71%) flaps. There were 8 relevant complications, which included a CSF leak, airway edema after neck dissection, a serious incident of postoperative bleeding from a donor site that required an emergent surgical evacuation of a hematoma, and acute blood loss anemia requiring multiple blood transfusions. There were a total of three free-flap-specific complications. The first complication was flap ischemia caused by an arterial thrombus in a known smoker that required debridement, removal, and replacement of the flap. The second complication involved pneumocephalus and removal of the free flap secondary to swelling and compression of the brain at the surgical site. The third complication involved venous congestion that required revision surgery. In this preliminary study, we found that in this high-risk patient population, skull base defects can be repaired utilizing free flap reconstruction with a similar morbidity profile to other head and neck subsites. By adding to the fund of knowledge for free tissue transfer for skull base reconstruction, we hope to decrease complication rates and improve surgical outcomes while reducing hospital length of stay and costs.

A214. Predictive Value of the ACS-NSQIP Surgical Risk Calculator in Patients Undergoing Transsphenoidal Hypophysectomy

Ashlee N. Seldomridge¹, Meghan T. Turner²

¹West Virginia University School of Medicine, Morgantown, West Virginia, United States

²Department of Otolaryngology/Head and Neck Surgery, West Virginia University School of Medicine, Morgantown, West Virginia, United States

Background: Transsphenoidal hypophysectomy (TSSH) is the preferred treatment approach for pituitary tumors. Given the potential for serious complications, we aimed to assess the utility of the ACS-NSQIP calculator for accurately predicting which patients are at increased risk for complications. We hypothesized that the ACS-NSQIP would accurately predict length of stay (LOS) and hospital readmission and postsurgical complications following TSSH.

Methods: A retrospective chart review of all patients who underwent transsphenoidal hypophysectomy for pituitary tumors at West Virginia University School of Medicine from August 2017 to present was performed.

Results: ACS-NSQIP predicted average LOS at 4.0 days compared with observed 4.9 days LOS ($p = 0.2$). Of the patients we reviewed, only 5.6% were readmitted to the hospital. For patients who were readmitted, the average predicted risk of readmission was 9.6% compared with 8.5% risk for those who were not actually readmitted. Of the patients with a high predictive rate of complication, 15% had an increased length of stay due to those complications.

Conclusion: No significant difference was found between predicted LOS and observed LOS, indicating that the ACS-NSQIP calculator provides an accurate estimate for hospital LOS. The predicted risk of hospital readmission was lower for the patients who were not actually readmitted, although the data were limited via too few numbers of hospital readmission. Future directions include expanding data collection and evaluating ACS NS-QIP predictive value for serious complications and return to operating room.

A215. Efficacy and Safety of Bevacizumab for Vestibular Schwannoma in Neurofibromatosis Type 2: A Systematic Review and Meta-analysis of Treatment Outcomes

Victor Lu¹, Ravindran Krishnan², Christopher Graffeo¹, Avital Perry¹, Jamie Van Gompel¹, David Daniels¹, Michael Link¹

¹Mayo Clinic, Rochester, Minnesota, United States

²University of Florida, Gainesville, Florida, United States

Background: Individual evidence suggests that the antiangiogenic agent bevacizumab may control vestibular schwannoma (VS) growth and promote hearing preservation in patients with neurofibromatosis type 2 (NF2). However, such metadata has yet to be consolidated, as well as its side-effect profile yet to be fully understood. Our aim was to pool systematically identified metadata in the literature and substantiate the clinical efficacy and safety of bevacizumab with respect to radiographic tumor response, hearing, and treatment outcomes.

Methods: Searches of 7 electronic databases from inception to March 2019 were conducted following PRISMA guidelines. Articles were screened against prespecified criteria. The incidence of outcomes was then extracted and pooled by random-effects meta-analysis of proportions.

Results: Eight articles reporting 161 NF2 patients with 196 assessable VS met all criteria. Radiographic response to bevacizumab was partial regression in 41% (95% CI, 31–51%), no change in 47% (95% CI, 39–55%), and tumor progression in 7% (95% CI, 1–15%). In patients with assessable audiometric

data, bevacizumab treatment resulted in hearing improvement in 20% (95% CI, 9–33%), stability in 69% (95% CI, 51–85%), and additional loss in 6% (95% CI, 1–15%). Serious bevacizumab toxicity was observed in 17% (95% CI, 10–26%). Subsequent surgical intervention was required in 11% (95% CI, 2–20%).

Conclusion: Bevacizumab may arrest both tumor progression and hearing loss in select NF2 patients presenting with VS lesions. However, a considerable proportion of patients are anticipated to experience serious adverse events; correspondingly, judicious use of bevacizumab for symptomatic management of VS in NF2 is recommended.

A216. Novel Grading System of Sigmoid Sinus Dehiscence for Radiologic Evaluation of Pulsatile Tinnitus

Shelby Willis¹, Courtney Duong², Isaac Yang², Quinton Gopen¹

¹Department of Head and Neck Surgery, University of California Los Angeles, Los Angeles, California, United States

²Department of Neurosurgery, University of California Los Angeles, Los Angeles, California, United States

Background: There is no consensus on the prevalence of sigmoid sinus dehiscence, with each study offering various definitions and mechanisms of symptoms. Patients who undergo resurfacing surgery for sigmoid sinus dehiscence do so for the defining symptom of pulsatile tinnitus that they experience. Few studies have considered the prevalence of this bony abnormality in asymptomatic populations and those that have find disparate results ranging from 1 to 18%. Understanding a nonpulsatile tinnitus population's prevalence of sigmoid sinus dehiscence will clarify how distinct this abnormality is to pulsatile tinnitus patients and which types of sigmoid sinus dehiscence are less prevalent in nonsymptomatic patients and more likely to be contributing to symptoms. This study analyzes a cohort of patients without pulsatile tinnitus to characterize the prevalence and types of sigmoid sinus wall anomalies in a non-symptomatic cohort. In this analysis, a grading system is developed to standardize sigmoid sinus dehiscence.

Methods: In this retrospective study, temporal bone CT scans of 91 patients without pulsatile tinnitus at a single institution were analyzed for sigmoid sinus dehiscence. The dehiscence was divided into three grades: grade 1 indicating a micro dehiscence of <3.5 mm with an opening to the mastoid air cells, grade 2 indicating a major dehiscence of >3.5 mm with an opening to the mastoid air cells, and grade 3 indicating a sigmoid sinus wall dehiscence that significantly opens directly to the underlying tissue rather than into the mastoid air cells. Dehiscences were measured for their greatest distances.

Results: In nonsymptomatic patients, sigmoid sinus dehiscence occurred in 34% of the cohort. Of these dehiscences, 75% were grade 1 and 25% were grade 2. The range of dehiscence measurements for grade 1 dehiscences was 0.9 to 3.4 mm. The range of dehiscence measurements for grade 2 was 4 to 7.5 mm. There were no cases of grade 3 dehiscence among this cohort.

Conclusion: Sigmoid sinus dehiscence occurred in over a third of our nonsymptomatic cohort. While all grades of sigmoid sinus dehiscence may currently be treated surgically, it is important to consider that a large portion of nonpulsatile tinnitus patients may have these sigmoid sinus anomalies asymptotically. This grading system allows for the standardization of sigmoid sinus dehiscence definition and severity in future studies. Grade 3 dehiscences were completely absent in this cohort of nonpulsatile tinnitus patients. This type of significant dehiscence through the temporal bone leaving the underlying tissue exposed with no bony covering

over the sinus is rare and less likely an incidental finding. Larger cohort studies are necessary and should consider which grades of dehiscence are most common in patients with pulsatile tinnitus, particularly in patients undergoing sigmoid sinus wall reconstruction to clarify which grades of sigmoid sinus wall anomaly are most responsive to surgical repair.

A217. The Clinical Implications of Spontaneous Hemorrhage in Vestibular Schwannomas

Christopher S. Hong¹, Lan Jin¹, Yawaei Zhang¹, Wyatt B. David¹, Brian Shear¹, E. Z. Erson-Omay¹, Robert K. Fulbright¹, Anita Huttner¹, John Kveton¹, Jennifer Moliterno¹

¹Yale University School of Medicine, New Haven, Connecticut, United States

Background: Spontaneous hemorrhage into vestibular schwannomas (VS) is a rare phenomenon that can render more rapid symptom onset and a seemingly poorer prognosis for an otherwise benign pathology. We describe our series of hemorrhagic vestibular schwannomas (HVS) and systematically reviewed the literature to better understand relevant clinical factors and outcomes.

Methods: A retrospective case review series and systematic review of the literature using PRISMA guidelines was performed. Data collected included patient demographics, blood thinning medication use, pre- and postoperative symptoms, tumor size, and extent of resection (EOR). Statistical methods analyzing clinical outcomes with perioperative variables including Fisher's exact test, student's *t*-test, and linear regression modeling were performed. In addition, all of our tumor samples underwent whole-exome sequencing (WES), and we conducted a histopathologic comparison of our HVS patients to matched nonhemorrhagic VS (NHVS) patients.

Results: Fifty-three patients with HVS met inclusion criteria. Compared with historical data for all VS, patients with HVS had astonishingly higher rates of perioperative mortality (9.7%), significant preoperative facial weakness (58.5%; defined as House–Brackmann grade 3) and harbored relatively larger tumors (mean tumor size 3.1 cm ± 0.9). Regardless of EOR, among patients with HVS, surgery resulted in significant improvement of facial weakness ($p = 0.041$), facial numbness ($p < 0.001$), vertigo ($p < 0.001$), headache ($p < 0.001$), and hearing loss ($p < 0.001$). Upon further analysis, patients who presented with facial weakness, in particular, tended to have larger tumors ($p = 0.058$) on average and demonstrated significant improvement after surgery, irrespective of EOR ($p < 0.01$). The use of blood thinning medications (17% of patients) did not affect outcome. While WES was unrevealing as all tumors were NF2 mutated, histopathologic assessment of our cohort, when compared with a matched NHVS cohort, showed an increased number of dilated/ectatic thin-walled vascular channels, which tended to form focal clusters but were also distributed throughout the tumor. The vessels were immunoreactive for CD31. Taken together, these findings were reflective of potentially increased vascular permeability and hypervascularity.

Conclusion: Our findings identify HVS to be an aggressive subgroup of VS as they are associated with a surprisingly high mortality rate (9.4 vs. 1% for all VS). When the features of HVS are identified on imaging studies, these patients should be treated expeditiously, especially given the fact that the facial nerve dysfunction, which is identified in more than half of patients presenting with HVS, appears to be reversible. We postulate EOR does not seem to affect clinical outcomes in these patients, presumably because the blood clot may comprise the bulk of the relatively larger tumor and as

such, evacuation of mass effect from the clot may be considered the primary goal of surgery in HVS patients who are particularly ill. Overall, this study has significant implications in the management of VS, raising awareness of a small, but highly morbid subgroup. Given our histopathologic findings, further studies evaluating the underlying mechanisms of spontaneous hemorrhage in VS are needed to better elucidate risk factors, improved prognostication, and optimal management of these rare tumors.

A218. Preliminary Results of Semi-Sitting Retrosigmoid Surgery for Vestibular Schwannomas from a North American Skull Base Practice

Domenico A. Gattozzi¹, Mairaj T. Sami¹, Casey Rosso¹, Roukoz B. Chamoun¹, Kushal J. Shah¹, Hinrich Staecker¹, James Lin¹, Helena Wichova¹, Paul J. Camarata¹

¹University of Kansas Medical Center, Kansas City, Kansas, United States

Background/Rationale: The semisitting position for surgical treatment of vestibular schwannomas is under-represented in North America. We changed the practice at our institution from supine to semisitting position for retrosigmoid approaches. We hypothesized semisitting position demonstrates shorter operative time and better facial nerve function when accounting for tumor size.

Methods: This is a retrospective review after a prospective change in practice. In 2018, all fellowship-trained skull base neurosurgeons at our institution changed to using only semi-sitting positioning for retrosigmoid approaches for vestibular schwannomas. We compared results with supine retrosigmoid and translabyrinthine surgeries regarding operative time, postoperative House–Brackmann (HB) scale, cerebrospinal fluid leaks, and other surgical complications.

Results: From January 2014 to March 2019, a total of 71 patients underwent first-time resection for vestibular schwannoma. Thirty-seven patients underwent surgery via translabyrinthine approach, 14 had supine retrosigmoid approach, and 20 had semisitting retrosigmoid approach. Mean operative time for tumors under 2.5 cm was 247 minutes for semisitting retrosigmoid, 399 minutes for supine retrosigmoid approach, and 383 minutes for translabyrinthine approaches ($p = 0.009$). Mean operative time for tumors over 2.5 cm was 420 minutes for semisitting approach, 502 minutes for supine retrosigmoid approach, and 513 minutes for translabyrinthine approaches ($p = 0.024$). For tumors under 2.5 cm, immediate postoperative HB scale was 1 to 2 in 71.4% of patients in the semisitting group, compared with 60% in the supine group and 69.6% in the translabyrinthine group, while at 6 months 85.7% of semisitting patients had HB 1 to 2 facial nerve function, compared with 80% in the supine group and 82.6% in the translabyrinthine group. For tumors over 2.5 cm, immediate postoperative HB scale was 1 to 2 in 53.8% of patients in the semisitting group, compared with 66.7% in the supine group and 71.4% in the translabyrinthine group, while at 6 months 69.2% of semisitting patients had HB 1 to 2 facial nerve function, compared with 77.8% in the supine group and 71.4% in the translabyrinthine group. For tumors less than 2.5 cm, 14.3% of semisitting patients had a postoperative cerebrospinal fluid leak compared with 20% for supine patients and 17.4% for translabyrinthine patients. For tumors over 2.5 cm, 30.8% of semisitting patients had a postoperative cerebrospinal fluid leak compared with 11.1% for supine patients and 21.4% for translabyrinthine patients. There were no significant intraoperative venous air embolus events in any of the groups.

Conclusion: Our data demonstrate statistically significantly shorter operative time using semisitting approach.

Semisitting position demonstrates an equivalent percentage of patients with HB grade 1 and 2 facial nerve functions at 6 months for tumors under 2.5 cm, but not for tumors over 2.5 cm. Cerebrospinal fluid leak rate was lower in the semi-sitting group for tumors under 2.5 cm, but higher for tumors over 2.5 cm. The shorter operative time is likely due to ability of the surgeon to perform bimanual dissection while removing tumor, rather than holding a suction in one of their hands at all times. The advantage of our study is that the surgeons serve as their own controls when comparing the results of semi-sitting and supine retrosigmoid approaches.

A219. Surgery after Surgery for Vestibular Schwannoma
 Lukasz Przepiorka¹, Przemyslaw Kunert¹, Tomasz Dzedzic¹,
 Wiktoria Rutkowska², Andrzej Marchel¹

¹Department of Neurosurgery, Medical University of Warsaw, Warsaw, Poland

²Medical University of Warsaw, Warsaw, Poland

Introduction: Management options of vestibular schwannoma (VS) include surgery, radiosurgery, and observation. Although benign in character, failure to remove it completely may result in a regrowth. Management of tumor recurrence after gross total resection (GTR) or progression after non-GTR is much more difficult to treat than initial VS and remains controversial as well as challenging, both for the surgeon and the patient.

Aim of the Study: The aim of the study was to evaluate the oncological and functional effectiveness of revision surgery for recurrent VS (rVS).

Materials and Methods: Twenty-nine consecutive patients operated for rVS were analyzed. Analyzed group included 16 women and 13 men with the mean age of 42.1 years old. Eleven of them were previously operated at our department and GTR using retrosigmoid approach (RSA) was initially performed. The mean time to recurrence in this group was 9.45 years.

Eighteen patients were referred from other centers with tumor progression after subtotal resection (RSA in all), including 4 patients with the additional radiosurgery treatment and 3 patients who have had multiple previous surgeries. The mean time for revision surgery was 5.1 years.

All patients presented with unilateral hearing loss (AAO-HNS class D) and with a different grade of facial nerve (FN) weakness [House-Brackmann (HB) grades: II-VI], including deep long-lasting FN paresis (HB grades: IV-VI) in 22 cases (75.86%). The size of recurrent tumor ranged from 6 to 51 mm (mean: 23.3 mm). Seven patients had neurofibromatosis type 2.

Results: GTR has been accomplished during revision surgery in all cases. Translabyrinthine approach (TLA) was the most common (14 small to medium tumors arising from IAC bottom) followed by RSA (12 large tumors as well as smaller ones located predominantly in CPA) and by the combination of TLA and RSA in 2 cases. Middle fossa approach was employed for 1 tumor progressing to the petrous apex.

In 15 patients, facial neuroorrhaphy was performed, 11 of them had hemihypoglossal-facial neuroorrhaphy (HHFN), of which 9 simultaneously with the revision surgery. In follow-up, 10 patients (34.48%) still had deep FN paresis (HB grades IV-VI). All patients after HHFN improved from HB grade VI to HB grade III, except for one who improved to grade IV. No subsequent tumor recurrence was noted during the mean follow-up of 3.46 years.

Conclusion: Complete tumor removal via tailored approaches together with modern FN reconstruction techniques yield durable oncological effect and may restore satisfactory FN function.

A220. Quality of Life Assessment among Vestibular Schwannoma Patients Treated with Microsurgery versus Stereotactic Radiosurgery versus Observation
 Komal Naem¹, Mohamed Labib¹, Malika Bhargava¹, Michele Wang¹, Randall Porter¹

¹Barrow Neurological Institute, Phoenix, Arizona, United States

Table: Demographic characteristics and PANQOL score details.

S. No.	Parameter (N=28)	Mean (SD)/ Frequency(%)
1	Age at the time of survey	56.79 (15.89)
2	Male: Female	11:16 (1:1.45)
3	Difference between diagnosis and survey (months)	39.23 (66.28)
4	Presenting complains	
	Hearing loss	21 (77.78)
	Dizziness/balance difficulty	17 (58.62)
	Tinnitus	12 (44.44)
	Facial symptoms	8 (29.63)
	Headache	6 (22.22)
	Others (dysgeusia, ear fullness, NF2 screening, eye ex)	7 (25.92)
5	Co-morbidities >2	10 (37.04)
6	Body mass index (kg/m ²)	26.84 (5.42)
7	Pre-treatment AAO-HNS score (n= 9)	
	A	4 (44.44)
	B	3 (33.33)
	C	1 (11.11)
	D	1 (11.11)
8	Treatment modality	
	Microsurgery	10 (35.71)
	Radiosurgery	3 (10.71)
	Observation	15 (53.57)
9	Clinic follow-up duration (months)	
	Microsurgery	34.45
	Stereotactic radiosurgery	6.04
	Observation	16.46
10	PANQOL score(all modalities, n=28)	53.5 (23.72)
	Microsurgery (n=10)	54.52 (17.85)
	Stereotactic radiosurgery (n=3)	60 (12.53)
	Observation (n=15)	53.54 (28.48)

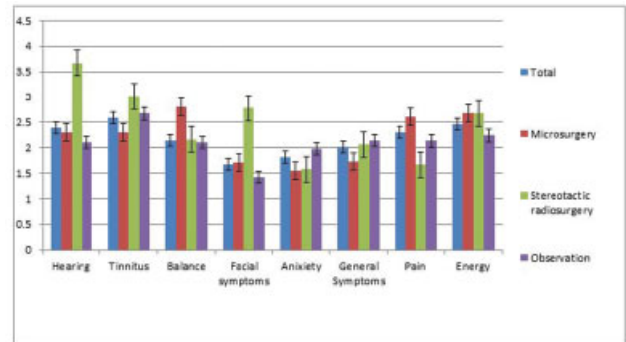


Fig 1: Bar graph showing the average PANQOL score and comparison of each modality including microsurgery, stereotactic radiosurgery and observation.

Introduction: Vestibular schwannoma (VS) is a benign and slow-growing tumor of cranial nerve VIII. Patients usually present with hearing loss, balance difficulty, tinnitus, and facial nerve dysfunction. There are multiple treatment options available including surgical resection, stereotactic radiosurgery, and observation. In spite of benign nature of the tumor, VS is associated with high rate of morbidity due to its anatomical location, in close proximity of the brainstem. Therefore, it is important to choose a modality with significant favorable benefit to risk ratio, which makes the decision for the management particularly difficult. Assessment of

quality of life among VS patients is critical for functional outcome analysis of each treatment modality.

Objectives: We aim to assess the quality of life among VS patients who underwent microsurgical resection, stereotactic radiosurgery, or observation.

Methods: We prospectively collected data by asking the VS patients to fill out disease-specific quality of life (Penn Acoustic Neuroma Quality of Life—PANQOL) survey who visited the clinic between January 2019 and August 2019, treated by the senior author. We only included patients who had undergone the treatment/or had follow-up visit in case of observation. For the patients who underwent multiple treatment modalities, the recent treatment was considered. PANQOL was divided into eight domains including hearing, tinnitus, balance, facial symptoms, anxiety, general symptoms, pain, and energy and analysis was performed accordingly. While comparing the parameters for each modality, the total mean of the cohort was considered as reference.

Results: We enrolled 28 patients through survey. Mean age was 57 years (SD: 15.89 years) with male:female ratio of 1:1.45. The mean difference of duration between the time of diagnosis and survey was reported to be 39 months and mean clinical follow-up was calculated as 22 months (SD: 55.29 months). Around one-half of the patients were being observed, whereas 10 (35.71%) and 3 (10.71) patients underwent microsurgery and radiosurgery, respectively.

The mean PANQOL score for our cohort was 53.5 and no significant difference between all the three modalities was found, p -value > 0.05 (details in the Table). An in-depth analysis of all 8 domains of the PANQOL revealed better scores for the patients undergoing observation. Patients who underwent microsurgery reported poor scores for balance and pain. Patients who underwent radiosurgery reported poor scores in hearing, tinnitus, and facial symptoms (Fig. 1).

Conclusion: An in-depth analysis of the quality of life provides useful insight to the functional outcomes following vestibular schwannoma treatment. It helps choose the treatment modality to ensure better functional outcomes.

A221. Surgical Resection after Radiosurgery for the Management of Vestibular Schwannomas: A Systematic Review

Max Whitmeyer¹, Bledi C. Brahimaj², Andre Beer Furlan², Sameer Alvi³, Richard W. Byrne², Madeline Epstein², R. Mark Wiet²

¹Ohio State University, Columbus, Ohio, United States

²Rush University Medical Center, Chicago, Illinois, United States

³Northwestern Medicine Regional Medical Group, Winfield, Illinois, United States

Introduction: Multiple short series have evaluated the efficacy of salvage microsurgery after radiosurgery for the treatment of vestibular schwannomas; however, there is a lack of large patient data available for interpretation and clinical adaptation.

Methods: The MEDLINE/PubMed, Web of Science, Cochrane Reviews, and EMBASE databases were queried. All English language and translated publications were included. Case studies of malignant transformation were excluded as were studies lacking adequate study characteristics and outcomes.

Results: Twenty studies containing 319 cases met inclusion criteria. Three additional cases from Rush University were added for 322 total cases. Tumor growth with or without symptoms was the primary indication for salvage surgery (91% of cases), followed by worsening of symptoms without growth (5%) and cystic enlargement (4%). The aver-

age time to microsurgery after radiosurgery was 38.6 months. The average size and volume of tumor at surgery was 2.49 cm and 8.50 cm³, respectively. The surgical approach was retrosigmoid (44%) and translabyrinthine (56%). 60% of patients had a House-Brackman (HB) score of 1 or 2. The facial nerve was not preserved in 8.4% of cases. Facial nerve severance and HB scores were lower for retrosigmoid versus translabyrinthine approach ($p = 0.46$, $p = 0.18$, respectively); however, fewer complications were noted in the translabyrinthine approach ($p = 0.09$). Gross total resection (GTR) was completed in 56% of surgeries. Studies which used predominately STR were associated with a lower rate of facial nerve lesioning (5.7 vs. 11.2%, $p = 0.09$) and higher rate of HB 1 to 2 (67.6 vs. 51.1%, $p = 0.005$) versus majority of GTR. However, majority of STR was associated with a recurrence rate of 5.6% as compared with 1.4% for majority of GTR ($p = 0.07$).

Conclusion: Microsurgery following radiosurgery was universally considered more difficult than primary resection due to loss of surgical planes and greater adherence between tumor and cranial nerves. Concurrence among studies was to avoid surgery for the first 2 to 3 years following radiosurgery. There is disagreement among authors over whether to attempt GTR or use primarily STR for recurrent tumors. STR shows better facial nerve outcomes at the possible expense of tumor control. Longer follow-up times with more patients will be required to determine the true rate of tumor recurrence following STR. The trade-offs of each should be considered in patient counseling and treatment.

A222. Sigmoid Sinus Patency following Vestibular Schwannoma Resection via Retrosigmoid versus Translabyrinthine Resection

Andrea M. Ziegler¹, Nadeem El-Kouri², Zaneta Dymon¹, David Serrano¹, Mariah Bashir¹, Douglas Anderson¹, John Leonetti¹

¹Loyola University Medical Center, Maywood, Illinois, United States

²Loyola University Stritch School of Medicine, Maywood, Illinois, United States

The treatment options for acoustic neuromas are observation with serial imaging, stereotactic radiation, or surgical resection. The most common surgical approaches are the translabyrinthine (TL), the retrosigmoid (RS), and the middle cranial fossa (MCF). During the translabyrinthine approach, the sigmoid sinus is decompressed with bipolar cautery to allow greater medial exposure. It is unknown if this causes any long-term narrowing or thrombus of the sigmoid sinus. We performed a retrospective review of patients who underwent acoustic neuroma resection to determine if patients undergoing a translabyrinthine approach for acoustic neuroma resection develop radiographic evidence of sigmoid sinus stenosis or thrombosis compared with patients undergoing a retrosigmoid approach. A total of 128 patients were included in this study; 56 patients underwent a translabyrinthine approach and 72 patients underwent a retrosigmoid approach. We compared the preoperative and postoperative diameter of the ipsilateral and contralateral sigmoid sinus at proximal, midpoint, and distal locations. There was no significant difference between the preoperative and postoperative diameter of the ipsilateral or contralateral sigmoid sinus based on surgical approach. Decompression of the sigmoid sinus during the TL approach does not have a significant postoperative effect on the dural venous sinus patency.

A223. Minimizing Postoperative CSF Leaks: An Algorithm for Sellar Reconstruction following Transsphenoidal Pituitary Surgery

Stephanie Flukes¹, Lily Mclaughlin¹, Marc A. Cohen¹, Vivian Tabar¹

¹Multidisciplinary Pituitary and Skull Base Tumor Program, Memorial Sloan Kettering Cancer Center, New York City, New York, United States

Introduction: One of the common and troublesome complications of endoscopic pituitary surgery is postoperative cerebrospinal fluid (CSF) leak. Options for repair of the skull base include synthetic materials, autografts such as fat or fascia, and pedicled flaps. The vascularized nasoseptal flap has been popularized as the preferred option for most surgeons for complex defects. Our group typically reconstructs with a nasoseptal flap for tumor larger than 1.5 cm in size and performs a rescue flap intervention for smaller defects. Our primary objective was to retrospectively evaluate the rate of postoperative CSF leak with our reconstructive approach. Our secondary objective was to identify factors predictive of postoperative CSF leak.

Methods: A retrospective review was conducted of all transnasal endoscopic pituitary cases performed at a single institution over a 6-year period. Patient demographic, diagnostic, and postoperative management details were collected from the electronic health record and confirmed using pathology reports. Details of intraoperative CSF leak and skull base reconstructive techniques were obtained from the operative report. Categorical data were compared using Pearson's chi square test.

Results: A total of 167 cases were identified, 19 of which were revision procedures. Median age was 53 years (range: 18–82) and the male to female ratio was 1:1.6. Repair techniques ranged from a simple closure using absorbable products to complex multilayer repair with a combination of underlay and overlay grafts and a vascularized flap. Seventy-four patients (44.3%) had CSF leaks detected intraoperatively, 15 of which were of high volume (11.1%). Intraoperative leak was associated with patients undergoing revision procedures ($p = 0.02$). It was not associated with age, gender, or tumor histopathology (including secreting tumors). Most patients underwent reconstruction with a vascularized pedicled nasoseptal flap (62.7% of low-volume and 100% of high-volume leaks), combined with allograft underlay. Of those who did not, the majority had an underlay with either synthetic material or fat graft.

Three patients (1.8%) had postoperative CSF leaks. Two of the three had large tumors (4.4 and 4.7 cm), one resolved with lumbar drain insertion and one required return to the operating room. The final patient had an ACTH-secreting microadenoma and required surgical repair. None of these patients had high-volume leaks, and all had undergone nasoseptal flap reconstruction. Due to the low number of postoperative CSF leaks, it was not possible to draw any conclusions regarding predictive factors. There was no significant difference between the incidence of leaks in patients who had nasoseptal flaps compared with those who did not ($p = 0.30$).

Conclusion: Our data demonstrate there is a low rate of postoperative CSF leaks in endoscopic pituitary surgery. Our reconstruction approach consists of a nasoseptal flap for tumors larger than 1.5 cm and a rescue flap for those with smaller tumors that require intervention. For those with a small defect and low-flow CSF leak, we favor allograft underlay with sealant. Determining optimal reconstructive techniques remains a challenge and is impacted by individual surgeon preferences. A more comprehensive evaluation of larger patient numbers should be undertaken, including quality of life and patient-reported outcome parameters.

A224. Surgical Outcomes of the Endonasal Endoscopic Approach within a Standardized Management Protocol for Repair of Spontaneous CSF Leaks: A Retrospective Review of 46 Patients

Daniel Kreatsoulas¹, Varun Shah², Douglas Hardesty¹

¹The Ohio State University Wexner Medical Center, Columbus, Ohio, United States

²The Ohio State University College of Medicine, Columbus, Ohio, United States

Background: Spontaneous cerebrospinal fluid (CSF) leaks are rare, often delayed in diagnosis, and can precipitate meningitis. Craniotomy is the historical “gold standard” repair. An endonasal endoscopic approach (EEA) offers potentially less invasiveness and lower surgical morbidity than a traditional craniotomy but must yield the same surgical success. A paucity of data exists studying EEA as the primary management for spontaneous CSF leaks.

Methods: We retrospectively reviewed patients undergoing spontaneous CSF leak repairs between July 2010 and August 2018. Standardized management at the authors' institution is surgical repair with EEA as first-line treatment after radiological diagnosis. Lumbar puncture is performed 24 to 48 hours postoperatively. If opening pressure is >20 cm H₂O, the patient is evaluated for CSF diversion or a trial of acetazolamide, at the provider's discretion.

Results: Of 46 patients identified, the most common leak etiology was encephalocele (28/46, 60.9%), and the most common location was cribriform/ethmoid (26/46, 55.9%). Forty-three patients underwent EEA alone, and three patients underwent simultaneous EEA/craniotomy. The most common repair strategy was nasoseptal or other pedicled flaps (18/46, 39.1%). Postoperatively, 15 patients received CSF diversion (32.6%), with BMI > 40 kg/m² being the only significant risk factor (OR = 4.35, $p = 0.033$) for postrepair shunt placement. Two patients underwent repair revision—one because of progressive fungal sinusitis, the other because of recurrent CSF leak. Mean follow-up duration was 15 months.

Discussion: Here we demonstrate a paradigm of EEA repair of spontaneous CSF leaks with postoperative lumbar puncture to identify undiagnosed idiopathic intracranial hypotension and effectively manage the disease without undue recurrence rates. In our cohort, the single significant risk factor predicting postoperative shunt placement was morbid obesity. This has implications for future surgical treatment as obesity levels continue to rise worldwide.

A225. Institutional Insight on Fatless Reconstruction of the Skull Base for CSF Leak Repair following Endoscopic Transnasal Transsphenoidal Surgery: 44 Case Series

Sophie M. Peeters¹, Marvin Bergsneider¹, Marilene Wang¹, Jivianne Lee¹, Jeffrey Suh¹, Won Kim¹

¹University of California, Los Angeles, Los Angeles, California, United States

Introduction: Reconstruction of the anterior skull base for a CSF leak following endonasal transsphenoidal surgery has commonly employed fat or fascia lata grafts. Institutionally, we have transitioned to a combination of more modern allografts, dural sealants, and free and vascularized mucosal grafts. We find that this closure is comparable to traditional fat-based CSF leak repair methods, while saving patients from a separate incision and the associated 1 to 3.7% donor-site complication rate.

Methods: Single-institution retrospective review of all CSF leaks after an eTNTS repaired without a fat graft, from two neurosurgeons, from May 2014 to present. Primary

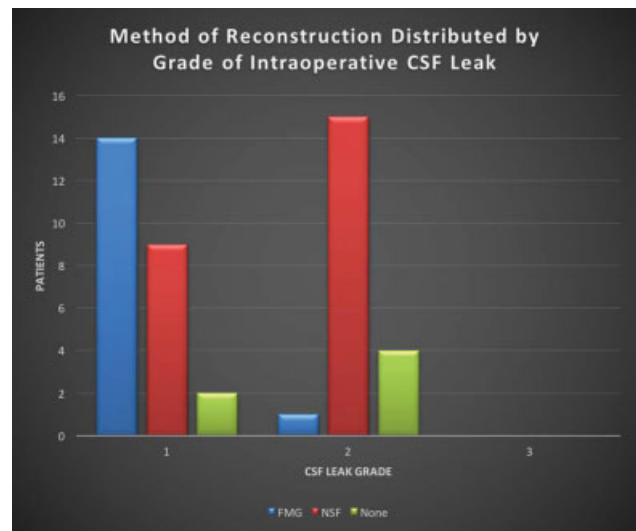
outcome measures are postoperative CSF leak, return to OR, and lumbar drain placement.

Results: We performed this fatless reconstruction on a wide variety of patients (Table 1). Similar to our previously published principles, we used nasoseptal flaps (NSFs) for higher grade leaks (2 and 3) and mucosal free flaps for low-grade ones (Fig. 1). In line with multilayer closure techniques previously described, multiple layers of repair were addressed to a variable degree in each case, including arachnoid closure with Anastoclips, sellar space obliteration with Helistat or Gelfoam, sellar floor reconstruction with bone or absorbable plates, and episellar buttressing (coude catheter, NasoPore packing, or Merocel-filled gloves). Dural sealants (Adherus, DuraSeal, and Tisseel) were used in 48% of cases. Dural substitutes (DuraMatrix, DuraGen, and DuraGen Plus) were used 55% of the time. Two patients had prophylactic lumbar drains placed intraoperatively, and eight patients were placed on acetazolamide postoperatively. Only one patient had a CSF leak postoperatively requiring surgical repair, despite lumbar drain trial. The leak was grade 2, repaired with a nasoseptal flap, a dural substitute, Anastoclips, NasoPore packing, and no dural sealant. The tumor measured 25 mm, was soft, nonadherent, without cavernous sinus involvement, and there was no history of prior TNTs. Complete pseudocapsular dissection was achieved.

Conclusion: Similar CSF leak repair rates can be achieved without using a fat graft for intrasellar reconstruction. There is unlikely one ideal alternative and we demonstrate multiple permutations within our series; however, the principles of multilayer reconstruction remain the same. Successful repair relies on reducing the rate of CSF flow (arachnoid closure or sellar obliteration), more permanent dural and mucosal reconstruction (allograft, free or pedicled mucosa), and for higher flow leaks, a pedicled NSF with or without buttressing the repair. Further studies are required to determine the most effective and cost conscientious fat graft free methods that achieve the optimal degree of repair while continuing to minimize patient morbidity.

Table 1. Patient characteristics

Gender	Male	18
	Female	30
BMI	<18.5 (underweight)	1
	18.5-24.9 (normal weight)	15
	25.0-29.9 (overweight)	14
	30.0-34.9 (class I obesity)	8
	35.0-39.9 (class II obesity)	6
	≥ 40 (class III obesity)	4
Diagnoses	Pituitary adenoma	20
	Non-functional	5
	Functional	15
	Acromegaly	3
	Cushing's disease	3
	Prolactinoma	1
	Gonadotrophic	3
	Rathke's Cleft Cyst	2
	Chordoma	1
	Chondrosarcoma	1
Meningioma	2	
Esthesioneuroblastoma	1	
Squamous Cell Carcinoma	1	
Other	6	
Tumor size	<10mm	6
	≥10mm	36



A226. Outcomes for Repair of Middle Cranial Fossa Encephaloceles Using Pedicled Temporalis Myofascial Flaps with Bone Grafts

Matthew R. Bartindale¹, Douglas D. Backous¹
¹Puget Sound ENT, Edmonds, Washington, United States

Objectives: To determine whether our repair technique using pedicled temporalis myofascial flaps with bone grafts renders an advantage in outcomes in comparison to more frequently described techniques.

Design: Retrospective, single-center case series.

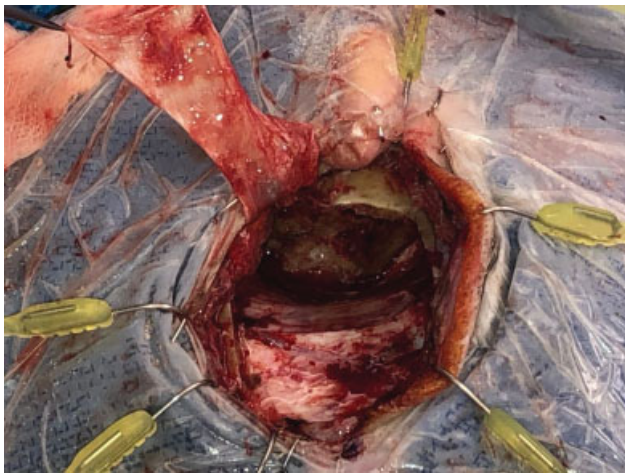
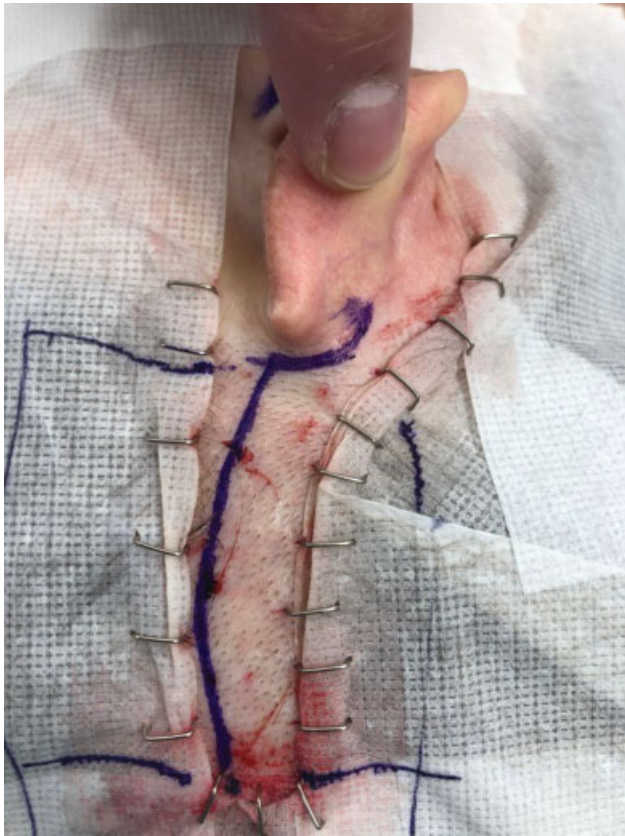
Participants: Patients who underwent surgical repair of middle fossa encephaloceles using a middle cranial fossa approach with pedicled temporalis myofascial flaps and bone grafts between 2017 and 2019.

Main Outcome Measures: Resolution of cerebrospinal fluid otorrhea, facial nerve outcomes, audiologic outcomes, postoperative temporomandibular joint and temporal pain, and complications.

Results: Thirty-eight patients were included in the study. All patients had middle cranial fossa approaches using anteriorly based pedicled temporalis myofascial flaps with split calvarial bone grafts to create a vascularized, multilayer dural closure. This is shown in the attached images. This has led to decreased temporomandibular joint and temporal pain compared with previous techniques used with an excellent success rate. There have been minimal complications to date.

Conclusion: The use of a pedicled temporalis flap creates a more durable repair while minimizing donor-site morbidity. We recommend this technique as an effective, efficient method to manage this pathology.

This document was downloaded for personal use only. Unauthorized distribution is strictly prohibited.



A227. Straws Don't Suck

Erin K. Reilly¹, Mindy R. Rabinowitz¹, Colin T. Huntley¹, Maurits S. Boon¹, Judd Fastenberg¹, Gregory A. Epps¹, Swar Vimawala¹, Chandala Chitguppi¹, Jena Patel¹, Gurston G. Nyquist¹, Marc R. Rosen¹, James J. Evans¹

¹Thomas Jefferson University Hospital, Philadelphia, Pennsylvania, United States

Educational Objective: There exists a belief that straws should not be used after endoscopic cranial base surgery. The

warning against straws has made its way into discharge instructions for sinus precautions despite a lack of evidence and literature. It has been hypothesized that the negative pressure created within the nasal cavity while drinking from a straw has a potential unfavorable effect on the operative site, especially in patients who have undergone dural repair. The goal of this study is to show that straws do not actually alter the pressure within the nose compared with normal deglutition.

Methods: A previously validated cadaveric model using intracranial sensor catheters has proved to be a reliable technique for measuring sinonasal pressures. Sensors were placed in the midnasal cavity of 20 healthy individuals. Pressures within the nose were recorded while participants drank water and a milkshake from a cup and from a straw. Measurements were taken both with and without the soft part of the nose pinched closed to simulate postoperative nasal obstruction.

Results: The average pressure in the nasal cavity while drinking water from a cup was -0.86 cm H₂O, while drinking water from a straw was -1.09 cm H₂O, and while pinching the nose and using a straw was -0.81 cm H₂O. The average pressure in the nasal cavity while drinking a milkshake from a cup was -0.98 cm H₂O, while drinking a milkshake from a straw was -1.88 cm H₂O, and while pinching the nose and using a straw was -1.37 cm H₂O. There was no statistically significant difference in pressure when comparing any of these tasks and consistencies ($p > 0.05$).

Conclusion: The pressure within the nasal cavity while drinking from a straw is not statistically different from the pressure generated while drinking from a cup. We propose that it is likely safe for patients to use straws after sinus and skull base surgery.

A229. Relationship between Recurrence Rates of Rathke's Cleft Cysts and Surgical Approaches to Sellar Reconstruction

Rebecca Limb¹, James King¹

¹Royal Melbourne Hospital, Melbourne, Australia

Introduction: Rathke's cleft cysts are rare, benign lesions that can present due to local compression upon the pituitary gland, stalk, and optic chiasm. Following initial surgical management, recurrence rates can be high; reportedly up to 40% in some studies. The modern era of endoscopic transsphenoidal surgery has afforded the skull base surgeon improved methods of reconstructing the pituitary fossa floor (or sellar face) following cyst drainage. However, an issue not fully resolved in the literature is whether specific surgical techniques are associated with higher rates of cyst recurrence, and/or iatrogenic complications.

Study Aim: To specifically address the question of whether reconstructing the pituitary fossa floor following cyst drainage or excision results in increased rates of recurrence.

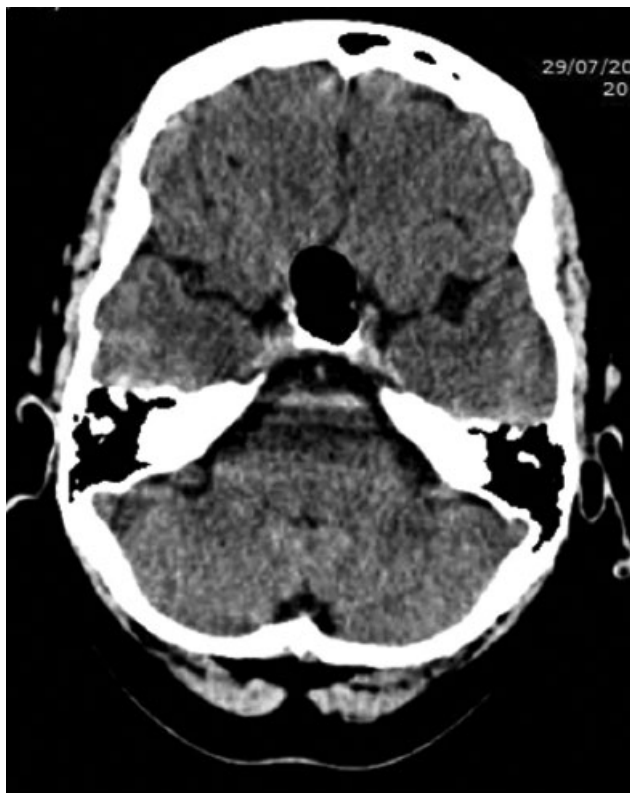
Methods: A retrospective case series was compiled from examination of medical records and radiological investigations at a single institution (The Royal Melbourne Hospital, Melbourne, Australia) over a time period spanning 25 years. The presence and timing of cyst recurrence was determined from previous MRI scans and outpatient encounters. Details regarding type of surgical procedure, and absence or presence of fossa floor reconstruction (and technique) were obtained from operation notes. The other outcome measure was morbidity (specifically pertaining to CSF leak and meningitis rates).

Results: A total of 23 patients were treated surgically for a Rathke's cleft cyst at the study institution between 1992

and 2017. The overall cyst recurrence rate was 48%, with 39% of all patients requiring redo surgery within the timeframe of the study. The mean time to redo surgery for recurrence was 4 years (range: 2 months–20 years). The total number of procedures performed among this group of patients was 38 (5 transcranial, 14 microscopic transsphenoidal, and 19 endoscopic transsphenoidal). Among the transsphenoidal procedures, 6 (18%) involved no reconstruction, and 27 (82%) involved fossa floor reconstruction using variations of fat graft, bone or plastic sellar implant, and vascularized nasoseptal flap.

Cyst recurrence rates were 0% post transcranial procedures, 57% post microscopic procedures, and 26% post endoscopic procedures. In the nonreconstructed group, there was a recurrence rate of 17%, whereas in the reconstructed group the recurrence rate was 41%. Notable surgical morbidity included prolapse of the optic chiasm into the pituitary fossa with deterioration in vision requiring multiple endoscopic “Chiasmopexy” procedures to correct. Complications specifically arising after non-reconstructive procedures were as follows: development of CSF rhinorrhea 3 weeks postoperatively, spontaneous pneumocephaly 2 months postoperatively after sneezing, and multiple episodes of meningitis. All of these patients required return to theater for secondary reconstruction of the pituitary fossa floor.

Conclusion: Although the small and skewed numbers of this study preclude reliable statistical analysis, the results suggest that reconstruction of the pituitary fossa floor, and microscopic rather than endoscopic techniques, may be associated with a higher rate of Rathke’s cleft cyst recurrence. However, complication rates among patients undergoing the alternative procedure of nonreconstruction may be higher, and such patients may be more likely to require repeat surgery to address this. Further studies involving greater numbers of patients are still required to answer this question.



A230. Soft Gasket Seal: Refining the Closure Technique following EEA: Case Series and Review of Literature

Thiago Albonette Felício¹, Gustavo Guimarães Rangel², Mostafa Shahein^{1,3}, Giuliano Schmidt Bertazzo Silveira¹, Rafael Martinez-Perez¹, Marcus Zachariah¹, Luis C. Requena-Requena¹, Douglas Hardesty¹, Bradley A. Otto², Ricardo L. Carrau², Daniel M. Prevedello¹

¹Department of Neurological Surgery, The Ohio State University Wexner Medical Center, Columbus, Ohio, United States

²Department of Otolaryngology and Head and Neck, The Ohio State University Wexner Medical Center, Columbus, Ohio, United States

³Department of Neurological Surgery, Aswan University, Aswan, Egypt

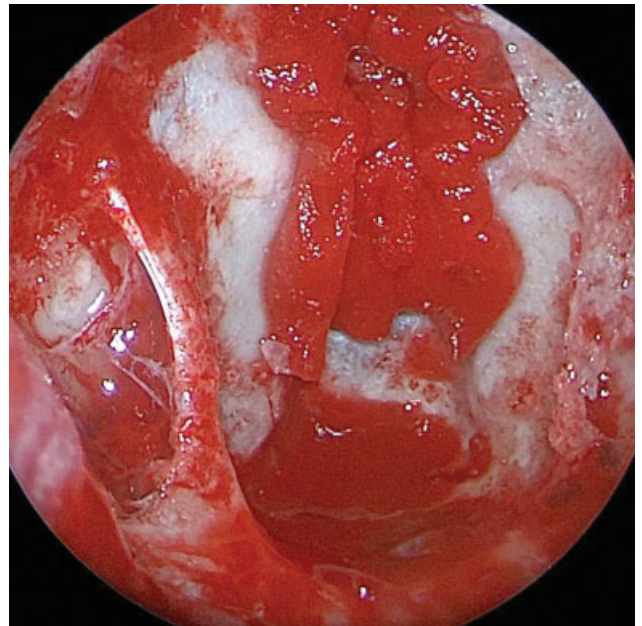
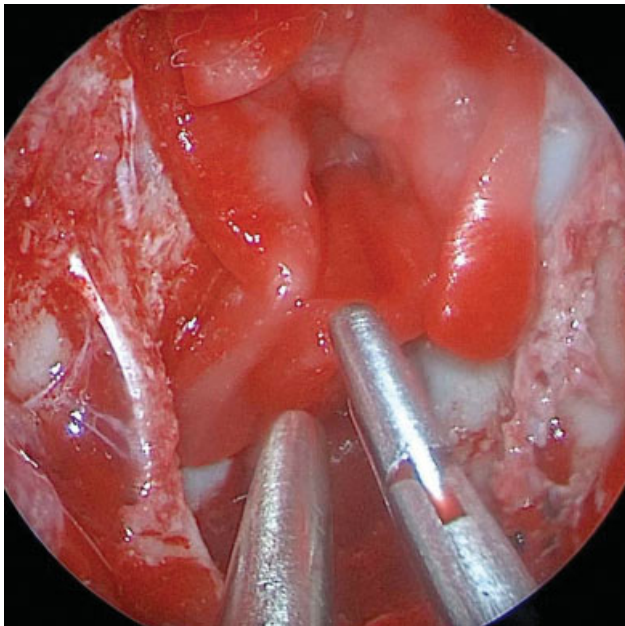
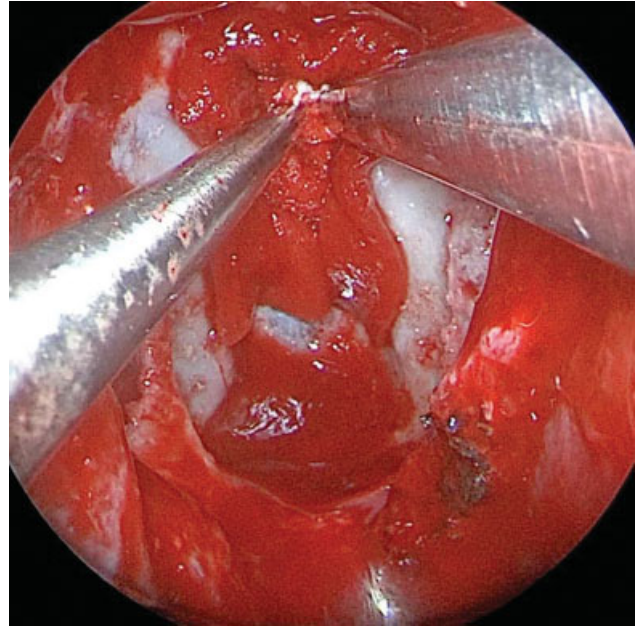
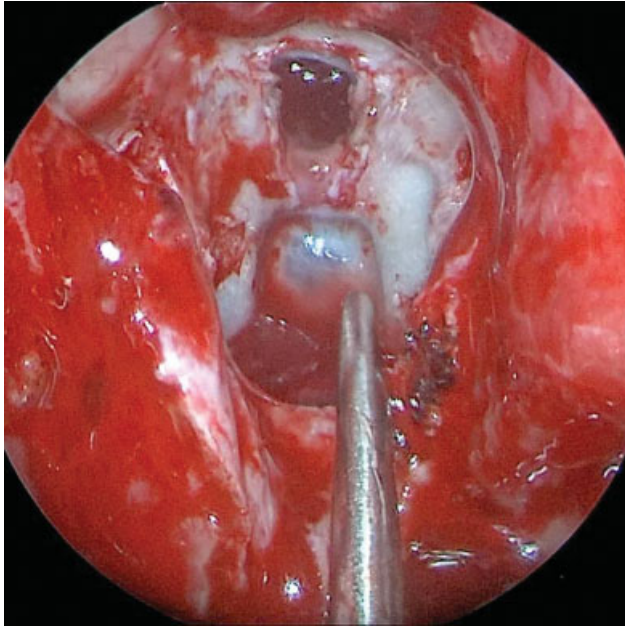
Introduction: Endoscopic endonasal approaches (EEA) have become the standard for various skull base pathologies, but cerebrospinal fluid (CSF) fistula has been a main concern. After the introduction of the nasoseptal flap by Hadad et al in 2006, the rates of CSF fistula have dramatically decreased. Since then, several authors attempted to improve the technique, with some proposing a multilayered closure. In such a closure, a rigid buttress (autologous bone or cartilage or some synthetic absorbable material) is employed in addition to the nasal septal flap to keep the construct in place. Herein, we propose a refinement of this technique, not requiring the use of rigid materials known as “Soft Gasket Seal (SGS).” This is distinct from the already described “Gasket Seal.” In addition, we present a series of craniopharyngioma to illustrate such concept.

Materials and Methods: Data for patients undergoing EEA for craniopharyngioma were retrospectively reviewed. These included demographic, clinical, operative, radiographic, and pathological information. Incidence of postoperative complications and CSF leaks were recorded. Descriptive statistical analysis was performed. The patients were categorized in one of two groups of closure technique, SGS and non-SGS, and compared. The SGS technique is described as follows: a piece of Duragen, at least 10 mm larger than the dural defect, is placed over the defect. Then, its central portion is gently pushed in, producing a small central depression, which is filled in with small pieces of Gelfoam. Next, the Duragen borders are checked for any gaps. If any breach is identified, more pieces of Gelfoam are added until there are no gaps. Subsequently, for both techniques the nasoseptal flap is placed over the construct, followed by Gelfoam, Merocel, and/or Nasopore, as usual.

Results: There were 31 patients operated between 2010 and 2018, and the SGS was used in 13. The mean age was 42.9 years (range: 12–78), the mean follow-up was 36 months (range: 3–91), and the mean hospital length of stay was 5.4 days (range: 2–22). Sixty-four percent were female. There were three CSF leak cases (9.6%), one in the SGS (7.6%) and two in the non-SGS (11.1%), $p > 0.05$.

Discussion: EEA has revolutionized the skull base surgery and the nasoseptal flap has dramatically reduced the CSF fistula rates. Previous authors described the use of rigid materials and/or fat graft as an adjuvant technique for closure, sometimes requiring dural sealants and lumbar drains. Our SGS technique, which is really simple to apply, showed to be feasible with acceptable results and no need for adjuvants.

Conclusion: The Soft Gasket Seal technique is a simple, safe, and feasible technique, associated with CSF leak rates comparable to previous techniques. This could impact on hospital length of stay and complication rates overall.



A231. Visual and Endocrine Recovery following Conservative and Surgical Treatment of Pituitary Apoplexy: A Meta-analysis

Khodayar Goshtasbi¹, Arash Abiri¹, Ronald Sahyouni¹, Hossein Mahboubi¹, Sophia Raefsky¹, Edward C. Kuan¹, Frank P. Hsu¹, Gilbert Cadena¹

¹University of California Irvine, Irvine, California, United States

Introduction: Pituitary apoplexy (PA) can present with visual and endocrine defects. The literature lacks strong support for either surgical or conservative management with respect to symptomatic improvement of these deficits.

This meta-analysis compares the visual and endocrine outcomes in conservative and surgical treatment of PA.

Methods: A systematic literature search was performed in PubMed, Cochrane, and Ovid MEDLINE for articles published between 1988 and 2018. Recovery outcomes were binarized, such that complete and partial improvements were combined as “improvement.” The primary outcome variables evaluated via a binary random-effects model were improvements in endocrine dysfunction, visual field and acuity deficits, and ophthalmoplegia or ocular nerve palsy (O/ONP).

Results: Of 483 published articles, 14 studies of a collective 457 cases (259 surgical and 198 conservative) were included. On initial examination, 58% of patients had endocrine dysfunction, 37% had visual acuity or field deficit, and 47% had O/ONP. Evaluation of outcomes for surgically and conservatively managed patients yielded odds ratios of 0.609 (95% CI: 0.199–1.859; $p = 0.383$), 0.763 (95% CI: 0.307–2.374; $p = 0.763$), 1.167 (95% CI: 0.433–3.146; $p = 0.760$), and 0.801 (95% CI: 0.305–2.105; $p = 0.653$) for improvements in endocrine dysfunction, visual acuity dysfunction, visual field dysfunction, and ONP/O, respectively.

Conclusion: Both surgical intervention and conservative management of PA can lead to visual and endocrine recovery, though the management decision may heavily rely on the severity of initial deficits. Treatment of PA can be multifaceted and tailored to the individual case and clinical judgment. Further investigation into the appropriate intervention based on longitudinal outcome data is warranted.

A233. Pituitary Adenoma Recurrence: Modeling Using a New Modification of the SIPAP Classification

Mohammed S. Alahmari¹, Fahad Alkherayf², Andrea Lasso¹, Fatmahalzahra Banaz¹, Sepideh Mohajeri¹, Pourya Masoudian¹, Andre Lamothe¹, Charles Agbi², Lisa Caulley¹, Mohammad Alshardan², Shaun Kilty¹

¹Department of Otolaryngology-Head and Neck Surgery, University of Ottawa, Ottawa, Canada

²Division of Neurosurgery, Department of Surgery, University of Ottawa, Ottawa, Canada

Introduction: Pituitary adenomas are a common skull base tumor that varies in size, often classified based on function and size, either micro- or macroadenoma. Patient clinical presentation depends on multiple factors, including excessive hormone secretion, the mass effect of large tumors, and tumor invasion to surrounding structures. With the advancement of diagnostic modalities, MRI is considered being the modality of choice to evaluate pituitary tumor features including parasellar extension. Endoscopic endonasal transsphenoidal (EETS) resection is the surgical standard of care for pituitary adenoma resection due to its superior visualization of the sella and surrounding anatomy. However, recurrence of the pituitary tumor following surgery has been reported widely. Yet, intuitively, adenoma size and involvement of parasellar structures should impact gross tumor resection (GTR) and recurrence. We evaluated a modified score using the SIPAP classification system, combining the suprasellar and parasellar extension scores of the pituitary tumor to determine its impact on adenoma recurrence.

Study Design: Retrospective cohort, single institutional study.

Methods: Institutional REB approval was attained for a retrospective review of all EETS cases for pituitary tumor resection between November 2009 and October 2018. Queries of the hospital database were completed by medical records personnel to identify cases of pituitary tumor treated using the EETS approach. Patient characteristics, tumor type,

endocrine data, and operation characteristics were then extracted from medical records pertaining to patient baseline characteristics. Preoperative MRI images were reviewed and the SIPAP classification applied to the pituitary tumors. Postoperative results were extracted for the duration of the follow-up period available for each patient. Within the SIPAP score, the suprasellar (S) and parasellar (P) scores are the most variable and believed to be the main drivers of surgical GTR. The suprasellar score and the highest parasellar score from both sides were numerically summed a bilateral suprasellar and parasellar (SaP) score and combined to make four grades.

Results: A total of 276 patients were identified, 56.5% of the cohort was male. The mean age of the cohort was 54 years old. During the study period, five different neurosurgeons performed EETS for patients with pituitary tumors. The mean of the length of follow-up was 32 months. Patient perioperative tumor grade according to SaP classification and recurrence rate in each grade were as follows: grade 1: 11%; grade 2: 10%; grade 3: 15%; and grade 4: 22%. The results followed a pattern of logarithmic curve.

Conclusion: The SaP classification was demonstrated to be useful for determining the expected recurrence of pituitary tumor following EETS, with the most advanced tumors demonstrating the highest rates of recurrence. Use of the SaP score will allow for more accurate preoperative counseling of patients with pituitary adenoma when considering recurrence requiring further surgery.

A234. Marsupialization of Rathke's Cleft Cysts Does Not Increase the Risk of Postoperative Intracranial Infection

Thad W. Vickery¹, Sophie Peeters², Alina Chen³, Sahyouni Ronald⁴, Edward C. Kuan⁴, Marvin Bergsneider², Wang Marilene¹

¹Department of Head and Neck Surgery, David Geffen School of Medicine at UCLA, Los Angeles, California, United States

²Department of Neurosurgery, David Geffen School of Medicine at UCLA, Los Angeles, California, United States

³David Geffen School of Medicine at UCLA, Los Angeles, California, United States

⁴Department of Head and Neck Surgery, University of California Irvine School of Medicine, Irvine, California, United States

Objectives: Marsupialization of Rathke's cleft cysts into the sphenoid sinus is a safe and effective technique which avoids the extracapsular dissection required for complete removal, with subsequent increased risk of endocrinopathies and CSF leak. However, the marsupialized cyst results in exposure of dura covered with only a single layer of epithelium directly into the nasal cavity. The objective of this study was to determine whether the risk of postoperative intracranial infection is increased in marsupialized Rathke's cleft cysts, compared with patients undergoing skull base reconstruction after transnasal resection of pituitary adenomas.

Design: Retrospective chart review.

Setting: Two tertiary academic medical centers.

Participants: Patients undergoing endonasal endoscopic surgery for resection of pituitary lesions including Rathke's cleft cysts ($n = 72$) and pituitary adenomas ($n = 77$) were identified between 2008 and 2019. Demographic data were collected including age (mean: 45 years), gender (35% male), BMI (mean: 28.7), type II diabetes mellitus (12.7%), active smoking (3.4%), presence of perioperative antibiotics (99.3%), method of skull base reconstruction, and prior skull base surgery (8.1%). Patients with Rathke's cleft cysts who experienced intraoperative CSF leaks (19.4%) were excluded from the analysis.

Primary Outcome Measures: Development of postoperative intracranial infections including meningitis, abscess, or hypophysitis.

Results: The final study cohort included 58 patients undergoing endonasal endoscopic marsupialization of a Rathke's cleft cyst in which the cyst wall was exposed to the sinonasal cavity at the completion of the case. There were 77 patients in the control group with pituitary adenomas who all underwent free mucosal graft reconstruction of the skull base defect. The mean follow-up period was 29 months for pituitary adenoma patients and 66 months for Rathke's cleft cyst patients. There were no documented cases of intracranial infections, including meningitis, abscess, or hypophysitis. Nearly all patients (99.3%) received perioperative antibiotics including cefazolin ($n = 142$), clindamycin ($n = 4$), or vancomycin ($n = 2$). Within the pituitary adenoma cohort, 2.6% (2/77) of patients were readmitted for hyponatremia but were not found to have an intracranial infection.

Conclusion: Marsupialization of Rathke's cleft cysts does not increase the risk of postoperative intracranial infections such as meningitis, brain abscess, or hypophysitis even though dura covered by a single layer of epithelium is exposed to the nasal cavity. Perioperative CSF penetrating antibiotic prophylaxis may not be indicated for routine transnasal marsupialization of Rathke's cleft cysts given the low overall incidence of postoperative intracranial infection in this population.

A235. Surgical Outcome of Endoscopic Transsphenoidal Pituitary Adenoma Resection in Elderly Patients Compared to Younger Patients

Kira A. Murphy¹, Chandala Chitguppi¹, Pascal Lavergne², Prachi Patel¹, Tawfiq Khoury¹, Mindy Rabinowitz¹, Gurston G. Nyquist¹, Marc R. Rosen¹, Christopher J. Farrell², James J. Evans²

¹Department of Otolaryngology – Head and Neck Surgery, Thomas Jefferson University Hospital, Philadelphia, Pennsylvania, United States

²Thomas Jefferson University Hospital, Philadelphia, Pennsylvania, United States

Introduction: Increases in life expectancy, as well as the increase in pituitary adenoma incidence with age, will lead to large numbers of elderly patients presenting for treatment. Endoscopic transsphenoidal surgical resection has become the standard of practice in many centers for the treatment of symptomatic pituitary adenomas. Taken together, these trends lead to a larger number of elderly patients being considered for surgery. Although they are considered high risk for surgery, surgical outcomes in patients aged 80 years and older remain poorly characterized.

Methods: We conducted a retrospective chart review of all patients treated with endoscopic transsphenoidal surgery for pituitary adenoma between 2005 and 2019 at a single institution. A total of 686 patients met inclusion criteria, and were stratified into three age groups: a control group of <65 years (493 patients), comparison groups of 65 to 79 years (170 patients), and ≥ 80 years (23 patients). Tumor characteristics and outcomes were analyzed using Fisher's exact test for categorical data, and student's t -test for continuous data.

Results: Compared with the <65-year-old group, patients 65 to 79 years old were less likely to have a functional tumor (OR: 0.176, $p < 0.001$, 95% CI: 1.079–7.092), had a higher rate of macroadenoma versus microadenoma (OR: 2.771, $p = 0.028$, 95% CI: 0.141–0.927), and had higher rate of optic nerve compression/involvement (OR: 1.798, $p = 0.004$, 95% CI: 1.206–2.679). However, we observed no corresponding significant difference between the <65 age group and the

≥ 80 age group in the rate of functional tumors, macroadenoma, or optic nerve compression. There were no trends between <65-year-old patients and either the 65 to 79 years group or the ≥ 80 group with regard to gender, incidental tumor detection, primary versus recurrent tumor, cavernous sinus invasion, or pituitary apoplexy.

Intraoperatively, the 65 to 79 years age group had a lower CSF leak rate compared with the <65 group (OR: 0.617, $p = 0.029$, 95% CI: 0.398–0.955), although the ≥ 80 group showed no significant trend. There were no correlations between any groups in rate of nasoseptal flap reconstruction, patulous sellar diaphragm, extent of resection, postoperative length of stay, or 30-day readmission rate postoperatively. There was one perioperative mortality in the 65–79-year age group.

From an endocrinologic standpoint, the rate of new-onset postoperative thyroid insufficiency was higher in both the 65–79 age group (OR: 1.651, $p = 0.043$, 95% CI: 1.012–2.694) and the ≥ 80 age group (OR: 3.375, $p = 0.024$, 95% CI: 1.237–9.207) than in the <65 group. Interestingly, the rate of postoperative diabetes insipidus was lower in the 65–79 group (OR: 0.415, $p = 0.042$, 95% CI: 0.174–0.992) than in the <65 group, although there was no significant trend in the ≥ 80 . There were no differences in postoperative rates of hypocortisolism, hypogonadism, or SIADH between groups. Diabetes insipidus and SIADH were no more likely to be permanent versus transient in any age group.

Conclusion: Transsphenoidal pituitary adenoma resection is a safe and effective intervention for elderly patients, including the growing cohort of patients over 80 years old. With comparable surgical outcomes and complications, advance age should not disqualify a patient as a surgical candidate.

A236. Racial and Ethnic Differences in Presenting Characteristics of Pituitary Adenoma Patients and Outcomes

Angela M. Richardson¹, Taylor Hartlein¹, G. D. Brusko¹, Ricardo J. Komotar¹, Jacques J. Morcos¹, Corinna G. Levine¹

¹University of Miami/Jackson Memorial Hospital, Miami, Florida, United States

Introduction: Although socioeconomic status and race have been associated with higher odds of undergoing surgery for pituitary adenoma, the impacts of race and ethnicity on preoperative patient/tumor variables and surgical outcomes have not been elucidated.

Methods: Retrospective review was performed for patients undergoing pituitary adenoma surgery by two high-volume neurosurgeons (R.J.K. and J.J.M.) at a single academic center from 2012 to 2018. Self-reported race and ethnicity (distinct variables), patient/tumor variables, and postoperative outcome data were collected. Tumor size was assessed using largest diameter.

Results: A total of 422 patients were included in this study. 90 self-identified as black with 251 Caucasians; 132 identified as Hispanic and 209 non-Hispanic. Rates of functional adenomas did not differ with race or ethnicity. Apoplexy rates were also similar across all populations examined. Caucasian patients presented with smaller tumors (2.27 vs. 2.51 cm in blacks; $p = 0.0437$); however, the duration of symptoms was similar in these two cohorts (18.7 months Caucasians, 13.0 months blacks). Rates of intraoperative cerebrospinal fluid (CSF) leak in nonfunctional adenomas were higher in Caucasians (36.8%) than in blacks (22.7%, $p = 0.0445$), while 30-day readmission rates were comparable. Hispanic and non-Hispanic patients were compared and assessed the impact of ethnicity in our cohort. Hispanic

patients presented at a younger age (51.9 vs. 56.5 years, $p = 0.0136$) with smaller tumors (2.2 vs. 2.4 cm, $p = 0.0325$). Hispanic patients also had a longer preoperative duration of symptoms (23.8 vs. 13.5 months, $p = 0.0063$). Following surgery, 30-day readmissions were more frequent in Hispanic patients (16.2 vs. 7.7%, $p = 0.0334$). The most common reasons for readmission were epistaxis and CSF leak.

Conclusion: This is the first report detailing racial and ethnic differences in patients undergoing surgery for pituitary adenoma. Hispanic patients have smaller tumors at presentation but longer duration of preoperative symptoms. Importantly they have higher rates of 30-day readmissions. Identifying these differences may allow the development of targeted interventions to bring these patients to care earlier and prevent readmissions. Results of a survey assessing understanding of discharge instructions comparing the different groups are being conducted.

A237. Cavernous Sinus Exploration in Cushing's Disease: Indications and Outcomes

Elizabeth Hogan¹, Gretchen Scott², Charlampos Lysikatos-Lyssikatos³, Raven McGlotten⁴, Constantine Stratakis⁵, Lynnette Nieman³, Prashant Chittiboia²

¹Department of Neurosurgery and Surgical Neurology Branch, National Institute of Neurological Disorders and Stroke, George Washington University, Washington, District of Columbia, United States

²Surgical Neurology Branch, National Institute of Neurological Disorders and Stroke, Bethesda, Maryland, United States

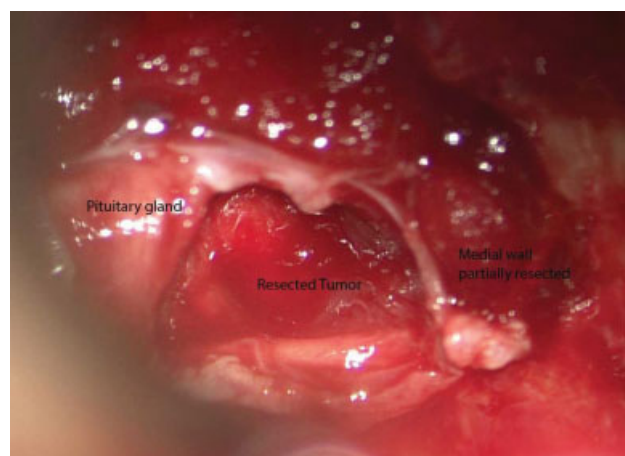
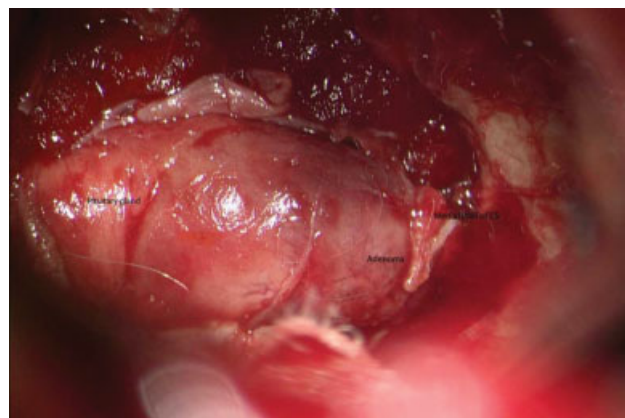
³Eunice Kennedy Shriver National Institute of Diabetes and Kidney Disease, National Institutes of Health, Bethesda, Maryland, United States

⁴National Institute of Diabetes and Digestive and Kidney Diseases, Bethesda, Maryland, United States

⁵Section on Endocrinology and Genetics, Eunice Kennedy Shriver National Institute of Child Health and Human Development, National Institutes of Health, Bethesda, Maryland, United States

Introduction: Microscopic and macroscopic cavernous sinus invasion by adrenocorticotropic hormone (ACTH) secreting adenomas is associated with surgical failures and recurrence of Cushing's disease (CD). The adenoma will often invade the medial wall of the sinus without extending further into the cavernous sinus compartments, allowing gross total resection of the involved medial wall. It is crucial to identify the extent of cavernous sinus invasion during transsphenoidal surgery (TSS) to attempt potential gross total resection of the ACTH secreting adenomas in CD. Additionally, it is necessary to identify when gross total resection is not feasible to initiate early adjuvant sellar/parasellar radiation. Here, we present our experience with the indications, intraoperative findings, and outcomes of cavernous sinus exploration during TSS for CD.

Methods: Between September 2012 and 2019, a total of 255 patients underwent transsphenoidal surgery (TSS) performed by author P.C. for suspected CD under a current clinical trial (NCT00060541). The patients underwent sublabial TSS with wide sellar and parasellar exposure, pseudo-capsule-based adenectomy, exploration of the cavernous sinus, and resection of the medial wall of the cavernous sinus as described by Edward H. Oldfield (Figs.1 and 2).



Results: The cavernous sinus was explored in 34 patients (22 females) with a median age of 27 years. Preoperative MRI demonstrated distinct cavernous sinus invasion in 10 (29%) patients. In the remainder, the cavernous sinus was explored as a result of intraoperative findings. The adenoma was found to be adherent to the medial wall in 7 (21%) with frank invasion of the medial wall discovered in the rest ($n = 27$). In 15 surgeries, a gross total resection including the involved medial wall of the cavernous sinus was noted by the surgeon and the patients were in endocrinologic remission postoperatively. No further adjuvant radiation was recommended based on intraoperative findings. However, two of these patients recurred at 3 and 4 years postoperatively, respectively. In 19 (56%) patients, adjuvant radiation therapy was recommended as a result of these intraoperative findings—free tumor within the cavernous sinus or incomplete circumferential tumor resection. Of these 19 patients, 6 were in remission in the immediate postoperative period despite of intraoperative findings. So far, adjuvant sellar/parasellar radiation (administered to 10/19) has resulted in remission in eight patients. One has undergone bilateral adrenalectomy. The median length of follow-up for the entire cohort was 32 months. Postoperative complications include delayed central sinus thrombosis and transient cranial nerve 6th palsy in one patient each.

Conclusion: Our study suggests that preoperative MRI underestimates cavernous sinus invasion in CD. The indications for cavernous sinus exploration include adenoma adherence to or invasion of the medial wall of the cavernous sinus. We find that the medial wall of the cavernous sinus can be removed safely and effectively leading to durable remission from CD in many instances. Additionally, we illustrate the necessity for adjuvant radiation therapy when it is evident intraoperatively that gross total resection cannot be achieved (even if hormone values suggest endocrinologic remission).

A238. Analysis of Preoperative Imaging as a Predictive Marker for Intraoperative and Postoperative Surgical Management in the Endoscopic Endonasal Resection of Pituitary Macroadenomas

Laila Perez de San Roman Mena¹, Srikant Chakravarthi¹, Melanie B. Fukui¹, Austin Epping¹, Alejandro Monroy-Sosa¹, Sammy Khalili¹, Juanita M. Celix¹, Bhavani Kura¹, Richard A. Rovin¹, Amin B. Kassam¹

¹Aurora Neuroscience Innovation Institute, Milwaukee, Wisconsin, United States

Background: Macroadenomas are one of the most common pathologies encountered in skull base surgery. The primary surgical management goals are maximizing cytoreduction and achieving optic nerve decompression. Devastating intraoperative complications, such as carotid laceration or optic nerve damage, have been significantly reduced over the years through skull base anatomy and advances in imaging, optics, and instrumentation. However, postoperative hypothalamo-hypophyseal axis injuries and cerebrospinal fluid (CSF) leaks remain issues.

Objective: The objective of this study is to utilize preoperative MRI to predict the relative location of critical neuroanatomic structures, including the pituitary gland and diaphragm, to create a preoperative plan and an intraoperative map to enable a safer surgical resection.

Methods: Thirty surgical cases of pituitary macroadenomas (>2 cm) were prospectively analyzed. Three main elements were analyzed by a neuroradiologist on the preoperative MRI: gland location, diaphragm integrity, and sellar diaphragm ascent. The criterion for diaphragm disruption was irregularity or loss of enhancement along its perimeter. Diaphragm ascent was measured on sagittal MRI and was predicted to descend to the same degree after total resection. Pseudocapsular tumor dissection was also performed to preserve PG.

Results: Mean tumor diameter was 27.8 mm (20–62 mm). Partial or complete preoperative pituitary insufficiency was present in 15 patients (50%). After surgery, 2 (13%) completely recovered pituitary function, 12 (80%) remained unchanged, and 1 (3.3%) presented a new hormonal deficit. Among preoperative hormonally intact patients, one (7%) experienced a transient diabetes insipidus (DI). Among the 15 (50%) patients who were hormonally intact before surgery, 1 (7%) experienced a new hormonal deficit (adrenal insufficiency) and 1 (7%) developed transient DI that resolved within weeks. The diaphragm was predicted to be preserved in 24 (80%) cases, in 5 (17%) to be disrupted, and in 1 (3%) case it was unclear. Intraoperatively, the 24 intact-predicted diaphragms were confirmed. Among the five violated diaphragms, three (60%) were confirmed, one (20%) was preserved, and one (20%) was not evaluated because goal of surgery was ON decompression. The unclear case was found to be violated intraoperatively. The ascent of the diaphragm was an average of 11.61 mm (3–25 mm). Intraoperatively, an equivalent degree of descent was observed in all cases, except

for the previous case. Three patients (10%) presented a postoperative CSF leak. Among them, only one was found to have a violated diaphragm preoperatively. Of the patients who presented with visual impairment, 16 (100%) experienced some degree of visual improvement after surgery with 6 (37.5%) regaining normal vision, 8 (50%) experiencing a significant improvement, and 2 (12.5%) having a slight improvement. Twenty-seven patients (90%) underwent gross total resection (GTR). Two (7%) patients had subtotal resection (STR) and one (3%) patient underwent partial resection of a giant macroprolactinoma.

Conclusion: Systematic preoperative radiological analysis using MRI and integration has the potential to assist and provide a guide for the surgeon in addressing pituitary tumors. Detailed preoperative MRI analysis, combined with a pseudocapsular dissection technique, offers a positive result in terms of postoperative preservation of pituitary function, diaphragm preservation, and reducing residual tumor.

A239. Transsphenoidal Approach for Pituitary Adenomas in the Elderly: Meta-analysis of Safety and Surgical Efficacy

Angela M. Richardson¹, Sumedh S. Shah¹, Justin Cheng¹, Ricardo J. Komotar¹, Michael E. Ivan¹, Jacques J. Morcos¹

¹University of Miami/Jackson Memorial Hospital, Miami, Florida, United States

Objective: Pituitary adenomas (PA) in the elderly (≥ 65 years old) represent 5% of all adenomas, and due to an aging population, this proportion is likely to increase. Transsphenoidal surgery (TSS) is a treatment mainstay for these lesions; however, safety and efficacy of TSS in the elderly is controversial. Here, we perform a safety and efficacy meta-analysis of TSS for PAs in the elderly.

Methods: A literature search of PubMed and Google Scholars databases was performed to capture pertinent English-language studies from 1995 to 2019 discussing efficacy (extent of resection; recurrence) and safety (complication; mortality) of TSS in patients ≥ 65 years. Search terms included combinations of “transsphenoidal” and “elderly” (e.g., [“transsphenoidal surgery” AND “elderly”], so forth). Data extraction was performed by two authors (S.S.S. and J.C.).

Results: Twenty-six papers describing 1,264 elderly patients undergoing TSS for PAs were identified, six of which included 1,610 non-elderly (<65 years) control patients undergoing similar treatment. Average age (72.7 ± 4.2 vs. 39.5 ± 9.9 years, $p < 0.0001$), male gender (62 vs. 41%, $p < 0.0001$), and American Society of Anesthesiology preoperative scores ($p < 0.001$) were significantly higher in the elderly group versus control group. Nonfunctional PAs were the most common tumor type in both groups (63 and 55%). Average length of stay was similar between elderly and non-elderly cohorts (6.2 vs. 6.0 days). Comparison between surgically treated elderly and non-elderly patients revealed no difference in rates of gross total resection (59 vs. 71%, $p = 0.22$), recurrence (8.4 vs. 20.1%, $p = 0.054$), intraoperative complications (1.1 vs. 1.3%, $p = 0.35$; mainly intraoperative CSF leak), serious postoperative complication (4.5 vs. 6.0%, $p = 0.62$), or disease-related mortality at follow-up (0.4 vs. 0.2%, $p = 0.64$). However, the rates of intraoperative CSF leak were lower in the elderly cohort (OR: 0.4, 95% CI: 0.26–0.67, $p < 0.01$). As expected, all-cause mortality was higher in the elderly group (OR: 4.22, 95% CI: 1.28–13.9, $p = 0.01$).

Conclusion: Elderly patients are not subject to higher rates of overall complications than the non-elderly cohort. Lower rates of intraoperative CSF leak were seen in the elderly population; we hypothesize that this decreased risk of intraoperative CSF leak in the elderly is related to more

conservative resection strategies in an attempt to avoid complications. The results of this meta-analysis indicate that age should not be a sole contraindication to TSS.

A240. First-in-Human Intraoperative MRI Coil for High-Resolution Imaging during Transsphenoidal Surgery

Elizabeth Hogan¹, Lalith Talagala², Joelle Sarlls², Hellmut Merkle³, Alan Koretsky³, Gretchen Scott⁴, John Butman⁵, Prashant Chittiboina⁴

¹ Department of Neurosurgery and Surgical Neurology Branch, National Institute of Neurological Disorders and Stroke, George Washington University, Washington, District of Columbia, United States

² MRI Research Facility, National Institutes of Health, Bethesda, Maryland, United States

³ Laboratory of Functional and Molecular Imaging, National Institute of Neurological Disorders and Stroke, Bethesda, Maryland, United States

⁴ Surgical Neurology Branch, National Institute of Neurological Disorders and Stroke, Bethesda, Maryland, United States

⁵ Radiology and Imaging Sciences, the National Institutes of Health, Bethesda, Maryland, United States

Introduction: For pituitary adenomas, including non-functioning pituitary adenomas and hormone secreting adenomas causing Cushing's disease (CD) or acromegaly, transsphenoidal surgery (TSS) remains the therapy of first choice. In modern series, failure rates following TSS range from 20 to 80% with recurrences in up to 7 to 35% cases. Surgical failures and recurrences are particularly challenging for hormone-secreting adenomas. The causes of surgical failures include inability to visualize small adenomas, the true extent of large adenomas, or invasion of parasellar structures. Surgeons have historically utilized ultrasonography, intraoperative MRI (iMRI), or Doppler ultrasound as surgical adjuncts with limited success. iMRI potentially allows significant improvements in visualization during surgery with visualization proportional to magnetic field strength of the iMRI magnet. However, increasing the magnetic field strength over 3 Tesla is expensive and is currently impractical for iMRI studies. To improve on the imaging resolution of the pituitary gland and the parasellar structures, we developed an intraoperative coil that can be placed within the sphenoid sinus (the endosphenoidal coil [ESC]) during sublabial TSS. Here, we assessed the feasibility of using the ESC as a surgical adjunct during TSS.

Methods: We designed a first-in-human interventional trial (NCT03678389) to evaluate the feasibility of ESC use during TSS at the NIH Clinical Center in Bethesda. Patients >18 years of age with a known or suspected pituitary tumor that requires surgical resection through a transsphenoidal approach are included. Children and patients with unfavorable anatomy are excluded. Primary outcome is to test the feasibility of using ESC as a surgical adjunct. Feasibility criterion is met if ESC use adds less than 90 minutes to the standard-of-care procedure. A hard stop for all research procedures occurs at 120 minutes after which only clinical standard-of-care procedures are allowed. The safety outcome measure is to evaluate whether ESC (images 1 and 2 below) causes local trauma, bleeding, burns, or other unanticipated safety issues.



Results: Since initiating recruitment in June 2019, we have enrolled two patients. For both patients, ESC insertion and imaging were performed under sterile conditions following initial approach to the sphenoid sinus. For patient 1, we successfully inserted the ESC and obtained clinically useful images in 110 minutes (failed to meet primary outcome criterion). For patient 2, we completed all research procedures including ESC insertion and imaging within 90 minutes (primary outcome measure met). In both cases, safety outcomes were met. We observed a significant improvement in the workflow during this period. The patients tolerated the procedures well and sustained no unanticipated adverse events.

Conclusion: So far, we find that it is safe and feasible to use ESC for intraoperative MRI imaging during sublabial TSS. The future use of this coil could allow visualizations of microadenomas, microscopic cavernous sinus invasion, or residual macroadenomas currently not visualized with standard techniques. (Images below are intraoperative MRI images obtained using the ESC, coronal slices through the sella.)



A241. A Single-Center Experience in Brachytherapy for Treatment-Refractory Nonsecreting Pituitary Adenomas

Aaron R. Plitt¹, Ashleigh Halderman¹, Robert Timmerman¹, Bruce Mickey¹, Samuel L. Barnett¹

¹University of Texas Southwestern, Dallas, Texas, United States

Introduction: Recurrent pituitary adenomas are challenging lesions. The typical second-line treatment is radiotherapy. Stereotactic radiosurgery and fractionated external beam radiotherapy are the modalities of choice. Pituitary adenomas refractory to photon radiation present a challenging clinical dilemma. There is no strong evidence to support a standard third-line therapy. At our institution, in select cases, we utilize brachytherapy as the third-line treatment option. We present our experience with the use of brachytherapy with I-125 seeds for multiple recurrent pituitary adenomas.

Methods: Eight patients with surgery- and radiation-refractory nonsecreting pituitary adenomas were treated with I-125 brachytherapy at our institution from April 2010 to June 2019. The primary end point was tumor control. The secondary point was vision preservation.

Results: All patients underwent endoscopic, endonasal implantation of I-125 seeds, with four patients having additional seeds implanted via craniotomy. The median number of seeds implanted was 2 per patient. In seven patients, the seeds were placed with frame-based stereotactic navigation to a preplanned target. In one patient, the seeds were placed using frameless stereotactic navigation via an endoscopic, endonasal approach. The median number of prior surgeries per patient was 2 (range: 1–3). The median number of prior radiotherapy treatments per patient was 1 (range: 0–2). Four patients were treated to a dose of 100 Gy early in the experience (2010–2012), and four patients were treated to a dose of 50 Gy thereafter (2013–2019). Overall, tumor control rate was 100% at a mean follow-up of 47.2 months (range: 3–124 months). All patients treated to 100 Gy demonstrated imaging evidence of radiation necrosis in the brainstem or mesial temporal lobe at a mean of 23 months after treatment. Two patients treated to 100 Gy experienced visual decline. No patients treated to 50 Gy demonstrated imaging evidence of radiation necrosis or visual decline.

Conclusion: Brachytherapy with I-125 seeds is a viable third-line treatment option for multiply recurrent pituitary adenomas. A dose equivalent of 50 Gy appears to have the optimal balance of tumor control while minimizing side effects.

A242. A Patient-Driven Quality Improvement Initiative for Pituitary Adenoma Care

Irene Druce¹, Mary-Anne Doyle¹, Amel Arnaut¹, Dora Liu¹, Fahad Alkherayf¹, Charles Agbi¹, Erin Keely¹, Janine Malcolm¹

¹University of Ottawa, Ottawa, Canada

Pituitary adenomas are common and often require complex multidisciplinary care with multiple specialists. This

may result in a health care system that is challenging for patients to navigate. Audits of care at our institution revealed opportunities for improvement to better align care with patients' needs. A quality improvement initiative that incorporated a patient advisory committee of patients who had received treatment for pituitary adenoma at our center and their family members was used to help identify opportunities for improvement. The patient-identified gaps in care included the need to coordinate and minimize appointments and the desire for better communication and education. Based on this information, changes were implemented to the pituitary program, including increasing access to the multidisciplinary clinic and developing a standardized and centralized triage process. A pre- and postintervention analysis consisting of retrospective chart reviews revealed that these changes had an impact on wait times for first assessment, and a significant shift in location of this first visit—with a larger proportion of patients being seen in the multidisciplinary clinic after intervention. We demonstrate that patient involvement, beyond individual patient–physician interactions, can lead to meaningful and observable changes, and can improve the quality of care for pituitary adenoma.

A243. Morphometric Changes in the Skull in Acromegalic Patients: Anatomical Perspective and Surgical Implications

Danielle de Lara¹, Joao G. Valim¹, Louise B. Willrich¹, Thiago B. Sonogo²

¹Universidade Regional de Blumenau, Blumenau, Brazil

²Hospital Santa Isabel, São Paulo, Brazil

Introduction: Acromegaly is a chronic endocrinopathy resulting from excessive growth hormone (GH) secretion leading to several body alterations, including morphological changes in skull and face. These modifications are of remarkable surgical interest, especially the increase of the working corridor length and the extensive paranasal sinus pneumatization.

Objective: The objective of this study was to describe and analyze morphometric changes of the skull and paranasal sinuses resulting from GH hypersecretion and describe findings that may be useful to skull base surgery planning and complication prediction.

Methods: Craniometric measurements were performed on 30 patients with acromegaly (Group A) and 30 control patients, with nonfunctional pituitary adenomas (Group B). Preoperative CT scans were used to evaluate cranial vault thickness; diameter of the skull and of the frontal, sphenoid, and maxillary sinuses; sphenoid sinus pneumatization patterns; and distance from vomer anterior limit to the dorsum sellae. Both groups were compared, and results were also correlated with hormonal and clinical data.

Results: Cranial vault thickness, diameter of the skull, and distance from vomer anterior limit to the dorsum sellae differed significantly ($p < 0.005$) between groups A and B. These findings also correlated considerably with preoperative growth hormone and insulin-like growth factor I serum levels. A correlation of the craniometric changes with the extent of clinical history in acromegalic patients could not be established.

Conclusion: Skull and paranasal sinuses alterations in acromegalic patients are of paramount importance when planning a skull base approach. The reported data may help surgeons to select the best working corridor, choose appropriate instruments, and anticipate complications for a safe and successful surgery.

A244. Surgical Outcome of Endoscopic Endonasal versus Microsurgical Transsphenoidal Approach for Pituitary Adenomas: An Institutional Experience

Ovanes Akobyan¹, Yury Shulev², Marat Yusupov¹

¹City Hospital 2

²North-Western State Medical University Named After I.I. Mechnikov, St. Petersburg, Russia

Objective: The aim of this study was to compare the efficacy of endoscopic versus microscopic resection of pituitary adenomas, and to evaluate the surgical possibilities of each approach.

Methods: Retrospective data were collected on patients who were operated for a pituitary lesion in our department between 2008 and 2018. Age, sex, presenting symptoms, length of stay (LOS), surgical approach, duration of surgery, tumor pathological features, grade of tumor resection (GTR), recurrence rate, and intraoperative and postoperative complications were noted. All procedures were performed by the same senior neurosurgeons.

Results: A total of 247 patients with pituitary adenoma were operated. One hundred seventeen patients were operated by endonasal endoscopic approach (EEA) and 130 patients were operated by microscopic transsphenoidal approach. Age and gender distribution did not differ between groups. The mean age was 52.3 ± 11.64 years (range: 21–72 years). The number of men was 150 (60.7%) and the number of women was 97 (39.3%). Nonfunctioning pituitary adenoma had 163 (66%) patients and 84 (34%) patients had a functioning pituitary adenoma. Among functioning pituitary adenoma, 60 (71.4%) patients had acromegaly and 24 (28.6%) patients had Cushing's syndrome. Mean follow-up was 51 months (range: 5–112). In an endoscopic group (EG), complete tumor excision was achieved in 83 (70.9%) patients, and in microscopic group (MG), it was achieved in 72 (55.4%) patients. Postoperative sinusitis was present in 1 (0.85%) patient in EG and in 2 (1.54%) patients in MG. In our material we have no vascular complication in both groups. Slightly higher percentage of cerebrospinal fluid (CSF) leak (6.9 vs. 3.4%) was observed in MG as compared with EG. Postoperative anterior pituitary dysfunction rate in formerly intact patients was higher in the MG (11.5 vs. 6.8%). However, there was no significant difference between the groups regarding the rate of permanent diabetic insipidus. For the long-term outcomes, the rate of visual improvement was significantly higher in the EG than that in MG (77 vs. 50%, $p < 0.001$).

Conclusion: EEA for pituitary adenomas is a safe and effective procedure. It had minimal invasiveness; wider and direct control of the operative fields allows a greater and safer potential of tumor resection with respect to the critical neurovascular structures.

A245. Recovery of Cranial Nerve Deficits in Patients Presenting with Pituitary Apoplexy: A Case Series

Mohammed Alahmari¹, Fahad Alkherayf², Andrea Lasso¹, Fatmahalzahra Banaz¹, Sepideh Mohajeri¹, Pourya Masoudian¹, Andre Lamothe¹, Charles Agbi², Lisa Caulley¹, Mohammad Alshardan², Shaun Kilty¹

¹Department of Otolaryngology-Head and Neck Surgery, University of Ottawa, Ottawa, Canada

²Division of Neurosurgery, Department of Surgery, University of Ottawa, Ottawa, Canada

Background: Pituitary tumors account for up to 15% of all intracranial tumors, 90% of which are adenomas.

One of the rare but urgent presentations of a pituitary tumor is pituitary apoplexy (PA). Typically, patients with PA present emergently with a symptom cluster that may include

sudden severe headache, nausea, vomiting, and new-onset impairment of the visual acuity with or without visual field defect. Occasionally, these patients may exhibit other cranial nerve palsies. These manifestations are due to the sudden increase of the tumor size due to intratumor hemorrhage and/or infarction. Usually, hypopituitarism develops as a result of gland ischemia. After patient stabilization and hormonal replacement, surgical decompression is often recommended with controversy on the timing of intervention. In this case series, we describe our experience regarding the cranial nerve recovery in patients with pituitary apoplexy following the endoscopic endonasal transsphenoidal (EETS).

Study Design: Retrospective cohort, single institutional study.

Methods: Institutional REB approval was attained for a retrospective review of all EETS cases for pituitary tumor resection between November 2009 and August 2018. Queries of the hospital database were completed by medical records personnel to identify cases of pituitary tumor apoplexy treated using the EETS approach. Patient characteristics, tumor type, endocrine data, and operation characteristics were then extracted from medical records pertaining to patient baseline characteristics. Postoperative results were extracted for the duration of the follow-up period available for each patient.

Results: A total of 15 cases of pituitary apoplexy were identified. Several cranial nerve deficits were present at admission. 33% of patients had a visual deficit; 47% had unilateral 3rd nerve palsy; and 27% had a unilateral 6th nerve palsy. No patients had 4th nerve palsy. Following EETS, there was significant recovery for all cranial nerve deficits. Postoperatively, 60% of patients with preoperative visual deficit had normal visual fields postoperatively and the other 40% showed improvement. For those with oculomotor nerve dysfunction preoperatively, 43% had returned to normal cranial nerve function, 57% had improvement and abducens nerve palsy resolved in 75% postoperatively, and 25% demonstrated improvement.

A246. Endoscopic versus Nonendoscopic Surgery for Resection of Pituitary Adenomas: A National Cancer Database Study

Khodayar Goshtasbi¹, Brandon M. Lehigh², Arash Abiri¹, Tyler Yasaka², Frank P. Hsu³, Gilbert Cadena³, Edward C. Kuan¹

¹Department of Otolaryngology-Head and Neck Surgery, University of California Irvine, Irvine, California, United States

²University of California Irvine, Irvine, California, United States

³Department of Neurological Surgery, University of California Irvine, Irvine, California, United States

Background: For symptomatic nonsecreting pituitary adenomas, surgical resection remains a critical option for treatment. In this study, we utilize a large-population national database to compare endoscopic surgery (ES) to nonendoscopic surgery (NES) for surgical management of pituitary adenomas.

Methods: The National Cancer Database (NCDB) was queried for all patients diagnosed with histologically confirmed pituitary adenoma from 2010 to 2015 with specified surgical approach. Due to limitations of NCDB, transsphenoidal microsurgery and craniotomy were both categorized as NES.

Results: Of 30,488 identified patients undergoing surgical resection of pituitary adenomas with specified approach, 16,373 (53.7%) underwent ES and 14,115 (46.3%) underwent NES. There was a significant increase in ES utilization over time ($R^2 = 0.903$; $p = 0.013$). Compared with NES, ES patients were younger ($p = 0.006$), had smaller

tumors ($p < 0.001$), were Caucasian ($p < 0.001$), had greater medical comorbidity burden ($p = 0.043$), had private insurance ($p < 0.001$), were treated at an academic center ($p < 0.001$), had higher household income ($p < 0.001$), and lived a greater distance from their treatment site ($p < 0.001$). Additionally, compared with NES, ES had lower rates of gross total resection (73.4 vs. 77.2%; $p < 0.001$), lower rates for adjuvant radiotherapy (3.5 vs. 4.5%; $p < 0.001$), and shorter postoperative length of stay (3.7 ± 4.6 days vs. 4.3 ± 6.1 days; $p < 0.001$). Though rates of 30-day readmission were similar ($p = 0.085$), ES had lower rates of both 30- ($p = 0.002$) and 90-day mortality ($p < 0.001$). On multivariate logistic regression, African American race (OR: 0.852; 95% CI: 0.783–0.927, $p < 0.001$) and tumor size above 2 cm (OR: 0.885; 95% CI: 0.825–0.950, $p = 0.001$) were less likely to be associated with receiving ES, while diagnosis at a more recent year (OR: 1.162; 95% CI: 1.141–1.185, $p = 0.001$), Charlson/Deyo score ≥ 1 (OR: 1.101; 95% CI: 1.025–1.184, $p = 0.009$), receiving treatment at an academic institution (OR: 1.673; 95% CI: 1.564–1.789, $p < 0.001$), having private insurance (OR: 1.094; 95% CI: 1.002–1.170, $p = 0.009$), higher household income (OR: 1.112; 95% CI: 1.028–1.203, $p = 0.008$), and living greater than 20 miles distance from treatment site (OR: 1.167; 95% CI: 1.091–1.249, $p < 0.001$) were associated with receiving ES.

Conclusion: There is an increasing trend toward ES for pituitary adenoma resection. Factors such as tumor size, insurance, facility type, income, race, and existing comorbidities may predict receiving ES. Rates of gross total resection and the need for adjuvant therapy may differ between ES and NES approaches.

A247. CSF Flow Improvement after Chiari Malformation Type I Surgery as a Prognostic Indicator for Clinical Improvement

Luke Mugge¹, Camila Dassi², Thiago Albonette Felicio², Rafael Martínez-Perez², Giuliano Schmidt Bertazzo Silveira², Mostafa Shahein^{2,3}, Gustavo Guimarães Rangel⁴, Marcus Zachariah², Douglas Hardesty², Daniel M. Prevedello²

¹Department of Neurosurgery, The University of Toledo Medical Center, Toledo, Ohio, United States

²Department of Neurological Surgery, The Ohio State University Wexner Medical Center, Columbus, Ohio, United States

³Department of Neurological Surgery, Aswan University, Aswan, Egypt

⁴Department of Otolaryngology and Head and Neck, The Ohio State Wexner Medical Center, Columbus, Ohio, United States

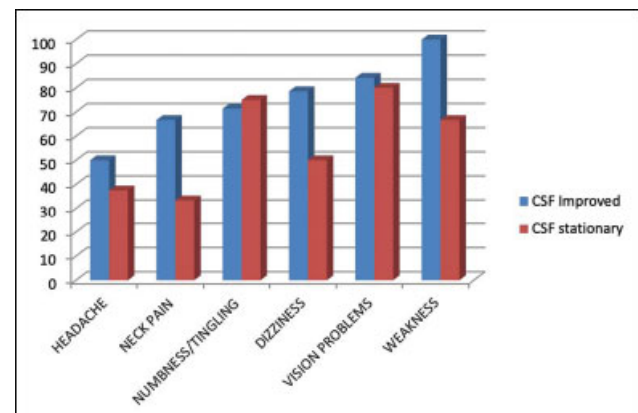
Objective: Chiari malformation type I (CMI) is a common neurological condition for which surgical decompression is the standard treatment. We aim to establish that cerebral spinal fluid (CSF) flow as a potential objective indicator of surgical efficacy in symptom alleviation after decompression.

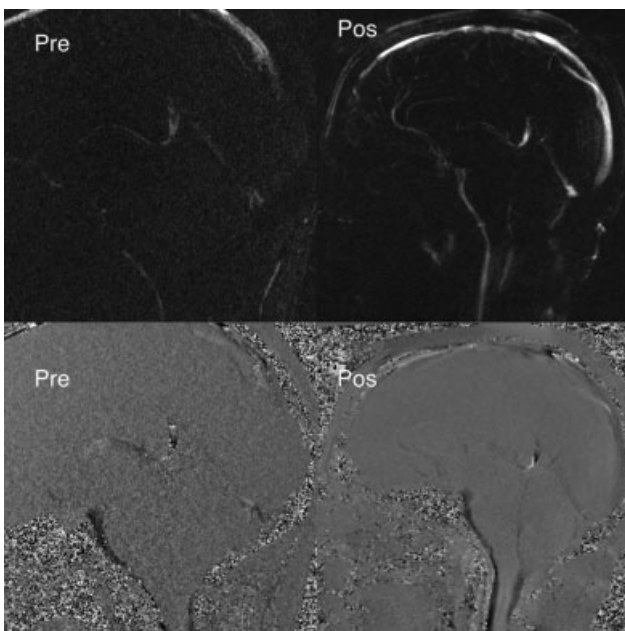
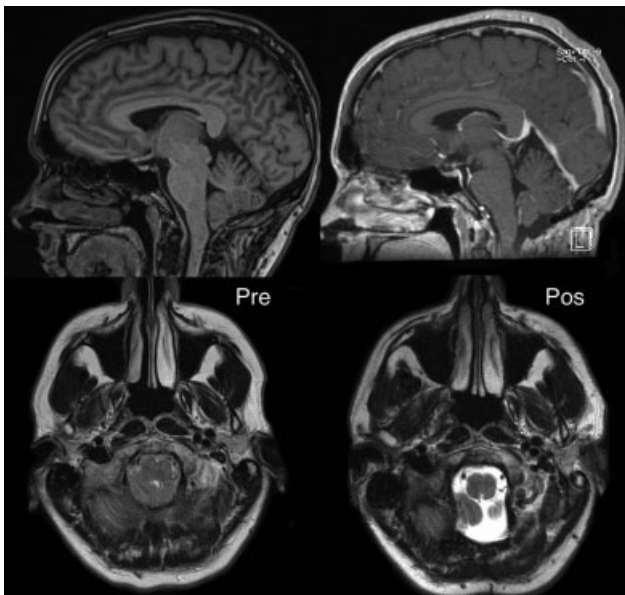
Methods: We performed a retrospective, two-center analysis of patients who underwent a suboccipital craniotomy due to symptomatic CMI. Qualitative CSF flow studies pre- and postoperative were analyzed to determine if any improvement in CSF flow was achieved. Finally, symptoms including headache, dizziness, weakness, and others were recorded, observing if improvement, worsening, or unchanging status was present.

Results: Forty-nine patients were identified who met inclusion criteria among four different surgeons at two institutions between 2010 and 2017. The average age was 36.06 years with 47 females and 2 males. Post decompression, 41 patients demonstrated improved CSF flow via flow studies. Regarding clinical outcomes, 38 patients were reported to

be improved symptomatically by the attending physician on follow-up, 10 were unchanged, and 1 was worse. Subsequently, patients were divided into two groups: Group A, composed of patients with improved CSF flow, and Group B, with those with no improved CSF flow. Group A had a mean age of 34.82 years and an average tonsillar herniation distance of 8.30 mm vs Group B, which had a mean age of 42.25 years and an average tonsillar herniation of 8.56 mm ($p < 0.05$ and $p = 0.40$, respectively). Postoperatively, improved CSF flow (Group A) was associated with improved clinical outcomes, whereas a non-improved CSF flow (Group B) was associated with poorer outcomes ($p = 0.024$). More specifically, Group A demonstrated superior improvement of symptoms compared with Group B among the total patient population including headache (50 vs. 37.5% improvement), neck pain (66.67 vs. 33.33%), dizziness (78.5 vs. 50%), vision (84.2 vs. 80%), and weakness (100 vs. 66.67%). Group B had the only patient who did worse on clinical follow-up and had the worst headaches postoperatively.

Conclusion: Patients with CMI often present with a constellation of symptoms. We demonstrated a significant association between improved CSF flow post-decompression and symptom improvement. Further, our study suggests that improved CSF flow, post-decompression, could represent an objective indicator for positive patient outcomes and symptoms betterment.





A248. Giant Solitary Fibrous Tumor: Case Series and Effective Management

Mostafa Shahein^{1,2}, Thomas L. Beaumont³, Bradley A. Otto⁴, Ricardo L. Carrau⁴, Oliver Adunka⁴, Daniel M. Prevedello¹

¹Department of Neurological Surgery, The Ohio State University, Wexner Medical Center, Columbus, Ohio, United States

²Department of Neurosurgery, Aswan University, Egypt

³Department of Neurological Surgery, University of California, San Diego, United States

⁴Department of Otolaryngology–Head and Neck Surgery, The Ohio State University, Wexner Medical Center Columbus, Ohio, United States

Background: Solitary fibrous tumors are rare tumors. The first reported case series of solitary fibrous tumors documented only 6 cases among 6,348 cases underwent pathological examination at Mayo Clinic tissue registry in 65 years. Subsequent published reports showed the rarity of the disease. These tumors have variable radiological appearance intermixes with many other tumors. Multidisciplinary team is needed to achieve maximum control of the disease.

Cases Description: We present four cases of giant solitary fibrous tumor:

Case 1: A 35-year-old male (Fig. 1) presented with left side hearing loss and swallowing disorder. He was found to have a mass of 4.4, 5.7, and 5.7 cm in the three dimensions originated from the sigmoid sinus with projection to the posterior fossa and middle fossa. He underwent two-staged surgeries. The first surgery was achieved through a trans-mastoid and translabyrinthine approach. Though the patient underwent preoperative embolization, the tumor was bloody. In the second stage, retrosigmoid approach was added achieving near-total resection. This was followed by 60-Gy radiation in 30 fractions. Swallowing disorder improved. No recurrence with 2-year follow-up period.

Case 2: A 44-year-old male presented with a headache and papilledema. He was found to have a mass of 5.9, 5.0, and 7.8 cm in the three dimensions based on the tentorium and transverse sinus with supra and infratentorium projections. He underwent a right occipital and suboccipital craniotomy with complete excision of the right transverse sinus. The patient is stable and neurologically intact for 4 years of follow-up period.

Case 3: A 54-year-old male presented with headache and loss of vision in the left eye and diminution of vision in the right eye that necessitated urgent surgery. He was found to have 7.2, 7.3, and 8.0 cm in all three dimensions originated from the inferior sagittal sinus. The patient underwent right frontal orbitozygomatic approach followed by second stage surgery of combined endoscopic endonasal and open craniotomy through the same previous approach. The surgery was followed by 50.4 Gy of radiation. The patient improved vision on the right eye and is blind on the left, stable for 3 years of follow-up period with no recurrence.

Case 4: A 60-year-old male presented to the emergency department with headache and syncope; the patient was found to have a mass in the Pineal region originating from the straight sinus causing hydrocephalus. He underwent emergent V-P shunting. He underwent two-staged supracerebellar infratentorial followed by interhemispheric approach. The patient is stable for 3 months of follow-up period. The patient received 60 Gy in 33 fractions of radiation.

All pathological examination revealed STAT6 positive staining. None of the patients had distant metastasis.

Conclusion: Solitary fibrous tumors are rare diseases that seem to be related to a venous sinus as origin. Understanding of these diseases is important as they carry similar radiological appearance with other common pathologies. Some of these tumors are highly vascular. Aggressive approach followed by radiation helped in the control of the disease knowing that 20% carry the risk of distant metastases.

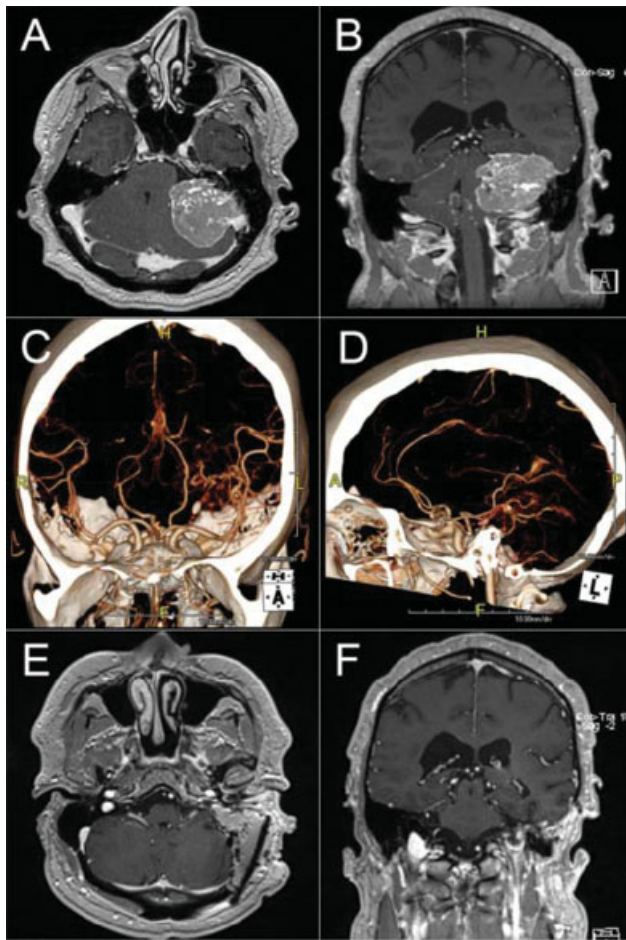


Figure 1: MRI T1 weighted Post contrast imaging showing Left CPA hyperintense lesion on axial (A) and Coronal (B) sections. CT angiogram (C and D) showed hyper-vascular lesion on the left side. MRI T1 weighted Post contrast imaging axial (E) and coronal (F) sections after two staged operation and completion of radiotherapy.

A249. Cochlear Implantation in Patients with Neurofibromatosis Type 2 and Other Retrocochlear Pathology: A Review of 32 Cases over 25 Years

Nicholas L. Deep¹, Evan Patel¹, William H. Shapiro¹, Susan B. Waltzman¹, Daniel Jethanamest¹, Sean O. McMenemy¹, Jr., Thomas Roland¹, David R. Friedmann¹

¹NYU Langone, New York City, New York, United States

Objective: To describe cochlear implantation (CI) outcomes for rehabilitation of hearing loss due to retrocochlear pathology and/or its treatment.

Methods: Retrospective review between 1995 and 2019 from a single tertiary care center of all patients with retrocochlear pathology who underwent CI. Demographics, clinical history, and audiometric data were reviewed. Study endpoints include (1) logged device use, (2) ability to achieve auditory perception, and (3) word recognition score (WRS) in the CI-only condition.

Results: Thirty-two patients (63% of females) with retrocochlear pathology were implanted at our center. The average age at implantation was 46.9 years (SD: 19, range: 13–80). Mean duration of deafness was 4.5 years (SD: 5.0, range: 0.4–19.0). Etiology of hearing loss included VS in 24

(75%), CNS malignancy treated with radiation in 4 (13%), intralabyrinthine schwannoma in 2 (6%), head and neck malignancy treated with radiation in 1 (3%), and superficial siderosis in 1 (3%). The mean preoperative PTA was 95.8 dBHL (SD 24.7) and WRS was 7.2% (SD 13.1).

Of the 24 VSs, 21 were NF2-associated and 3 were sporadic. The mean tumor size was 1.64 cm (SD: 0.6, range: 0.5–2.6 cm). At the time of CI, 11 patients had prior microsurgery, 6 patients had prior radiation to the ipsilateral tumor, and 7 patients had stable tumors without prior surgery or radiation.

Device use was classified as regular (>7 hours/day) in 15 (47%), limited (<7 hours/day) in 12 (38%), and nonuse in 5 (16%). The audiometric outcomes of 26 patients are reported, as the other 6 patients have been implanted too recently for review. Auditory perception was achieved in 24/26 patients. The two patients who failed to achieve auditory perception underwent prior surgery. Open-set speech recognition (WRS > 20%) was achieved in 18 patients. Meaningful sound perception but without significant open-set speech (WRS < 20%) was seen in six patients. Altogether, the mean WRS at most recent follow-up (mean: 3.4 years, SD: 1.8) for the observation, microsurgery, and radiation cohorts was 51% (SD: 15), 36% (SD: 28), and 39% (SD: 26), respectively.

Over long-term follow-up, two patients experienced decline in CI performance associated with tumor regrowth and necessitated additional surgery; both underwent explantation of the CI and successful auditory brainstem implantation. The remaining patients have demonstrated durable benefit.

A multivariate analysis is presented to evaluate the effects of the following variables: duration of deafness, time interval between treatment and CI, diagnosis of NF2, treatment cohort, pathology, and status of hearing in the contralateral ear.

Conclusion: In appropriately selected patients, cochlear implantation is feasible for the rehabilitation of hearing loss due to retrocochlear pathology and/or its treatment. Given the heterogeneity inherent to this population, outcomes are variable. In most cases, auditory percept was achieved and over half of the patients obtained open-set speech perception, irrespective of prior management and treatment.

A251. Clinical Characterization of Thin Bone Overlying the Superior Semicircular Canal

Michelle K. Hong¹, Courtney Duong², Isaac Yang², Quinton Gopen³

¹David Geffen School of Medicine at UCLA, Los Angeles, California, United States

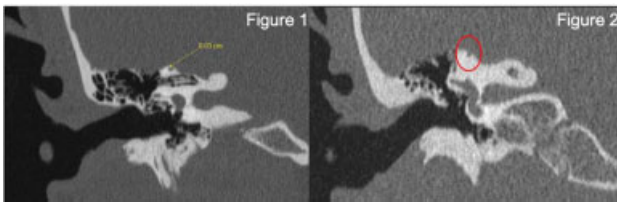
²Department of Neurosurgery, UCLA, Los Angeles, California, United States

³Department of Head and Neck Surgery, UCLA, Los Angeles, California, United States

Superior semicircular canal dehiscence (SSCD) is a rare disorder that causes vestibular and auditory symptoms resulting from a dehiscence in the middle cranial fossa floor overlying the superior semicircular canal (SSC). The symptoms that result from this include vertigo, autophony, hearing loss, hearing distortion, ear fullness, and tinnitus. It has been found that patients with thinning of the bone overlying the canal without true dehiscence can also experience these symptoms, but there has not been much work done yet to characterize thin bone patients' presentation. It is therefore important to establish diagnostic criteria for classifying thin bone patients and study what symptoms these patients present with.

Currently, many institutions do not perform surgeries on symptomatic patients with thin bone and will only consider surgical intervention with a true dehiscence. Our aim is to provide more data on thin bone patients to characterize their symptoms and explore possible surgical intervention to alleviate these symptoms.

This retrospective study involves examining coronal CT scans of temporal bones from 256 SSCD patients and determining whether they had a true dehiscence or thin bone overlying the SSC. A threshold of 0.5 mm perpendicular distance was used for thin bone classification. An example of a thin bone patient (Fig. 1) compared with a dehiscence patient (Fig. 2) is shown. There were 37 patients with bilateral thin bone (bilat-thin), 33 patients with unilateral thin bone and normal bone (thin-normal), and 73 patients with unilateral thin bone and dehiscence (thin-dehisc). We then examined the thin bone patients' consult notes pre- and postoperatively to better characterize the clinical presentation of these patients.



In bilat-thin patients, recovery of pulsatile tinnitus in postsurgical thin bone patients is affected by the thinness of the bone presurgery ($p = 0.02$). Additionally, the sex of bilat-thin patients affects whether they present with hearing loss presurgery ($p = 0.03$) and postsurgery ($p = 0.001$). The age of bilat-thin patients has a role in presenting with dizziness ($p = 0.05$) and headache ($p = 0.05$) presurgically. In thin-normal patients, autophony is more likely to present on the left ear presurgically ($p = 0.04$). Bone thinness also affects the presentation of autophony ($p = 0.02$) and vertigo ($p = 0.07$) in thin-normal patients.

In this study, bilat-thin and thin-normal patients were highlighted under the assumption that their symptoms were caused by the thin bone itself without confounding by the presence of a true dehiscence. These results show that there are a variety of different symptoms that are present in thin bone patients. Pulsatile tinnitus, autophony, and vertigo are directly affected by how thin the bone is compared with normal patients. Thus, the thinness of the bone can be used as a relative indication of symptom severity. The results also show that there are other factors such as age and sex that could affect thin bone patient presentation. This could be taken into account when assessing whether a patient would benefit from surgical correction of their thin bone. Future studies will include a comparison of symptoms and patient vestibular testing between true dehiscence and thin bone patients.

A252. A Model of Success: Incorporating 3D-Printed Models of Skull Base Pathology for Surgical Approach Planning

Lucas P. Carlstrom¹, Avital Perry¹, Christopher S. Graffeo¹, Colin L. Driscoll¹, Michael J. Link¹, Jonathan M. Morris¹

¹Mayo Clinic, Rochester, Minnesota, United States

Introduction: Skull base pathologies are uniquely demanding with respect to surgical approach planning, given

the competing demands of optimizing exposure and potential for treatment success, while minimizing brain retraction and reducing risk to adjacent neurovascular structures. Conventional 2D modalities including a variety of imaging studies are critical to preoperative assessment; however, they require significant skill and experience to integrate and synthesize mentally during approach planning. 3D modeling technology—which includes 3D printing, and virtual/augmented/mixed reality spaces—provides a powerful tool for enhancing preoperative approach planning, with potential advantages for optimizing patient safety and surgical outcomes alike.

Methods: We prospectively created 3D models of diverse, patient-specific skull base pathologies, to generate an extensive print and digital space models. Prototypical example cases were then selected for explicit study, including three cases of extra-axial, intracranial skull base neoplasms (vestibular schwannoma, trigeminal schwannoma, foramen magnum meningioma), three intracranial cerebrovascular lesions (anterior circulation aneurysm, hypoglossal dural arteriovenous fistula, brainstem cavernoma), and three pediatric complex cranial cases (MCA aneurysm, Vein-of-Galen malformation, immature teratoma of the parasellar and orbital regions). Multicolor additive printing was then used to generate physical models, which were printed within both skulls that had prespecified standard skull base craniotomy exposures completed, and complete skulls. Study subjects from both neurosurgery and ENT then participated in two-phase model assessment. In Phase 1, the first cohort of subjects were provided skulls with planned craniotomies removed which were used to determine an optimal approach, after which subjects were surveyed regarding their subjective impression of the models' utility in approach planning. In Phase 2, subjects were asked to preselect an approached using standard 2D imaging modalities alone, after which they were provided identical pathologic lesions contained within complete skulls, on which they performed the selected approach. Following the procedure, they were provided models, and surveyed regarding whether they felt that their decision making would have been altered had the models been available prior to approach selection. Surveys were administered via a 5-point Likert agreement scale.

Results: Phase 1 subjects universally endorsed "Agreement" or "Strong agreement" that their decision making was assisted by the 3D-printed model. Phase 2 subjects reported a more diverse range of responses, with "Agreement" and "Neutral" predominating. When stratified by level-of-training, trainees and more junior staff were more likely to agree that 3D models significantly enhanced their ability to select and plan a surgical approach. These findings were preserved across pathologic categories (e.g., tumor, cerebrovascular, pediatrics), and lesion location (e.g., posterior/lateral, anterior).

Conclusion: Surgical approach planning via traditional 2D imaging modalities for complex skull base pathology depends on surgeon's skill and, perhaps most importantly, experience. The expansion of approach planning technologies to incorporate 3D modeling for patient-specific pathologies appears to provide a significant degree of benefit, particularly among less experienced skull base surgeons. Future applications may include not just surgical planning, but simulation systems for trainees, patient education modules, and applications within neuropathology sphere.

A253. MRI T2-Weighted Cochlear Intensity as a Predictor of Hearing Loss with Vestibular Schwannoma Patients

Peter Q. Luong¹, Claudia I. Cabrera², Nirav Patil³, Hammad A. Khan¹, Carlito Lagman⁴, Thomas A. Ostergard⁴, Gary Huang², Nicholas C. Bambikidas⁴, Sarah E. Mowry²

¹Case Western Reserve University School of Medicine, Cleveland, Ohio, United States

²Department of Otolaryngology, University Hospitals Cleveland Medical Center, Cleveland, Ohio, United States

³University Hospitals Cleveland Medical Center/Case Western Reserve University, Cleveland, Ohio, United States

⁴Department of Neurological Surgery, University Hospitals Cleveland Medical Center, Cleveland, Ohio, United States

Introduction: Vestibular schwannomas are benign tumors found in the internal auditory canal and cerebello-pontine angle that can present with hearing loss, tinnitus, and vertigo. Advances in MRI technology and screening protocols have led to an increased incidence. While a large proportion of these tumors can undergo conservative observation, it is important to know if and when to intervene to preserve a patient's hearing. To date, there is no single best predictor for a vestibular schwannoma patient's audiologic outcomes. This study examines the association between cochlear intensity on T2 MR imaging and audiologic outcomes in patients.

Methods: A retrospective analysis was conducted with adult patients diagnosed with vestibular schwannoma at a single academic medical center. MRI and audiologic data were reviewed at two different time points. MRI data included tumor side, size, and location. Region of interests were placed on T2-weighted images, and cochlear and pontine intensity were used to calculate a relative signal intensity (RSI)—a ratio of cochlear-to-pontine intensity. Audiologic data included air conduction hearing values used to calculate a pure-tone average (PTA); speech recognition threshold and word recognition score were also noted; *t*-test and linear regressions were used to compare groups; significance was defined at $\alpha < 0.05$.

Results: Forty-four patients (mean age: 65; 57% female) with unilateral vestibular schwannoma were included in the final analysis. Tumors were predominately left sided (57%). 43% of tumors were confined in the IAC and 2% in the CPA; 55% had portions in both areas. Baseline MRIs mean RSI values were 2.03 for the ipsilateral and 1.98 for the contralateral ears. Baseline audiology found mean PTA values for the ipsilateral (44.24 dB) and contralateral ears (19.01 dB). Follow-up MRIs found mean RSI values for ipsilateral (1.87) and contralateral ears (1.82). Follow-up audiology found mean PTA values for the ipsilateral (61.42 dB) and contralateral ears (22.78 dB).

Overall, RSI decreased from baseline to follow-up, while PTA increased for both ipsilateral and contralateral ears. Both ears also showed a negative correlation between initial RSI and initial PTA. A statistically significant negative correlation was found between initial ipsilateral RSI and ipsilateral PTA for patients with PTA under 40 dB (Pearson's $= -0.063$; $p \leq 0.001$); there was no significance between these variables in the PTA over 40-dB group. Additionally, for either ear, there was a negative albeit nonsignificant correlation between the difference in initial and follow-up PTA, and the initial and follow-up RSI.

Conclusion: This study revealed a general trend between baseline testing and follow-up testing. Overall, our study found that as RSI decreases PTA increases; however, ipsilateral and contralateral ears have different trends. This conflicted with some previous literature showing increased cochlear intensity can be used as an indicator of worse hearing. In addition, when trying to associate T2 imaging with hearing status, there may be better utility for patients still with a degree of preserved hearing, as compared with those who initially have worse hearing (evidenced by the PTA

under 40-dB group finding). Further research is needed to further elucidate the relationship between these variables.

A254. Retrosigmoid Intradural Suprameatal Approach (RISA): A Single-Center Experience with 19 Cases

Minsoo Kim¹

¹Samsung Medical Center, Seoul, Korea

Background: Several surgical approaches were introduced to overcome the risk of complication for the management of tumors involving the posterior fossa and adjacent part of middle fossa.

Objective: The retrosigmoid intradural suprameatal approach (RISA) was introduced in 1983; modification and variation have been suggested. We introduce the variable indications and surgical outcomes of patients treated with RISA in a single center.

Methods: Nineteen patients (9 men and 10 women) were treated with RISA between July 2014 and June 2019. Their diagnoses were meningiomas (petroclival, petrous apex, sphenopetroclival, and cerebellopontine angle) and schwannomas (trochlear, trigeminal, and vestibular). Surgical outcomes and related complications were analyzed.

Results: Extent of tumor removal was variable; 5 in 19 had achieved gross total resection (26.3%), 6 achieved near total (31.6%), 7 achieved subtotal (36.8%), and 1 achieved partial (5.3%) resection. Three patients had a change in brainstem auditory evoked potential intraoperatively, which resulted in persistent hearing loss in two patients. Two patients had a temporal ipsilateral third nerve palsy. Preoperative hypesthesia in five patients was not improved postoperatively. Postoperative facial nerve palsy in four patients was recovered in three patients. One patient with neurofibromatosis type 2 died with a complication not related to the surgery.

Conclusion: RISA is a useful approach that results with acceptable treatment-related complications for the treatment of various posterior fossa tumors having a lesion reaching a part of middle fossa.

A255. Assessment of Vascular Configurations of the Suprachiasmatic Region Using Endoscopic Endonasal Corridors: A Cadaveric Anatomical Study

Hongwei Zhu^{1,2}, Amandeep S. Ahluwalia³, Ivan El-Sayed^{2,4}, Adib A. Abl^{2,5}, Roberto Rodriguez Rubio^{2,4,5}

¹Department of Neurological Surgery, The First Affiliated Hospital of Xiamen University, Xiamen, China

²Skull Base and Cerebrovascular Laboratory, University of California, San Francisco, California, United States

³University of Chicago, Chicago, Illinois, United States

⁴Department of Otolaryngology – Head and Neck Surgery, University of California, San Francisco, California, United States

⁵Department of Neurological Surgery, University of California, San Francisco, California, United States

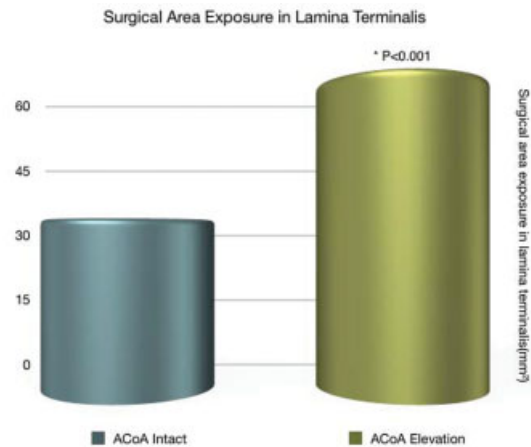
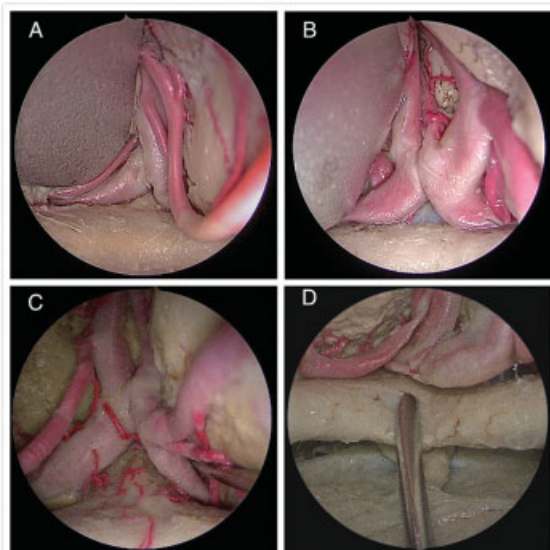
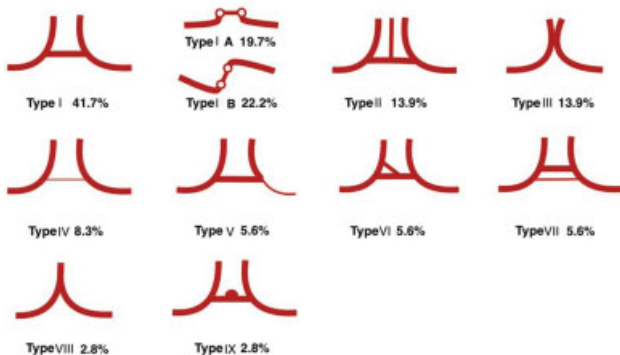
Background: Endoscopic endonasal surgery has been an effective approach to treat suprasellar lesions, including tumor and vascular pathology. Understanding the anatomical variations of anterior cerebral communicating artery (ACoA) complex is relevant to guarantee a safe surgery and reducing complications through endoscopic endonasal surgery.

Methods: An endoscopic transplanum–transtubercular approach was performed on 36 cadaveric heads (72 sides). We studied and classified the anatomical variations of ACoA complex. The feasibility of reaching ACoA and its adjacent structure relationship was assessed. We also qualified surgical exposure of lamina terminalis influenced by the variation of ACoA complex. Surgical exposure was measured using three coordinates obtained by a neuronavigation system. A

Student's *t*-test was used to compare the means of the various parametric variables, and a *p*-value of less than 0.05 was considered statistically significant.

Result: The ACoA complex was observed in all 36 specimens. The regular ACoA complex configuration was found in 15 (41.7%) of specimens: 8 cases (22.2%) with twisted ACoA and 7 cases (19.4%) without twisted ACoA. The ACoA complex anatomical variations encountered were the following: accessory A2 (5, 13.9%), common trunk of ACA with absence of ACoA (5, 13.9%), hypoplasia ACoA (3, 8.3%), asymmetry A1 (2, 5.6%), fenestrated ACoA (2, 5.6%), accessory ACoA (2, 5.6%), azygos ACA (1, 2.8%), and aneurysm (1, 2.8%). The mean length of ACoA was 2.63 ± 1.39 mm (0.5–6.5 mm) and the mean diameter of ACoA was 2.07 ± 0.83 mm (0.8–4.3 mm). The RAHs were found as a single vessel in 41 (56.9%), two vessels in 24 (33.3%), three in 4 (5.6%), and absent in 3 (4.2%) of the 72 hemispheres dissected. The 96 (95.0%) of the RAHs could be identified within 4 mm proximal or distal from ACoA in all 101 RAHs. After elevating the ACoA, the lamina terminalis exposure area achieved the 59.87 ± 12.88 mm², and promoted 80.1% comparing before elevating the ACoA (33.11 ± 17.75 mm², *p* < 0.001).

Conclusion: A higher incidence of variations in the anterior communicating artery complex can be encountered in the endoscopic transplanum–transtuberular approach. The relationship between the ACoA complex and the optic chiasm has different meaning for reaching ACoA complex and exposure lamina terminalis through suprachiasmatic corridor in endoscopic transplanum–transtuberular approach.



A256. Comparative Analysis of Microsurgical Techniques for the Exposure of Internal Maxillary Artery: A Cadaver Study of a Major Donor for Cerebral Revascularization
 Xiong Li^{1,2}, Atakan Orscelik², Ivan H. El-Sayed^{2,3}, Adib A. Abl^{2,4}, Roberto Rodriguez R. Rubio^{2,3,4}

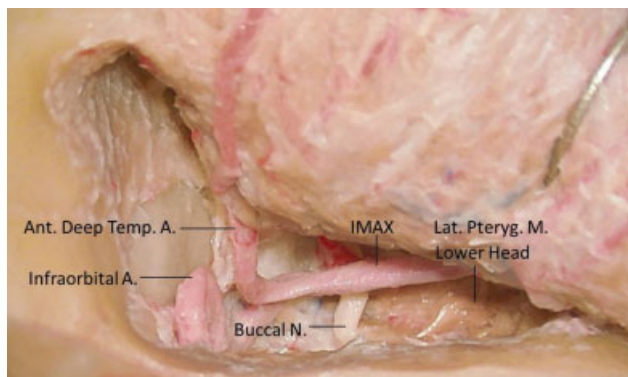
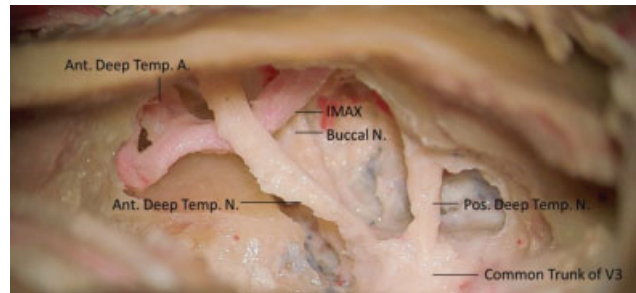
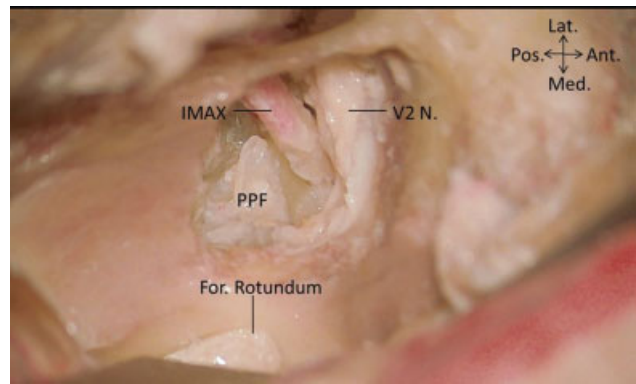
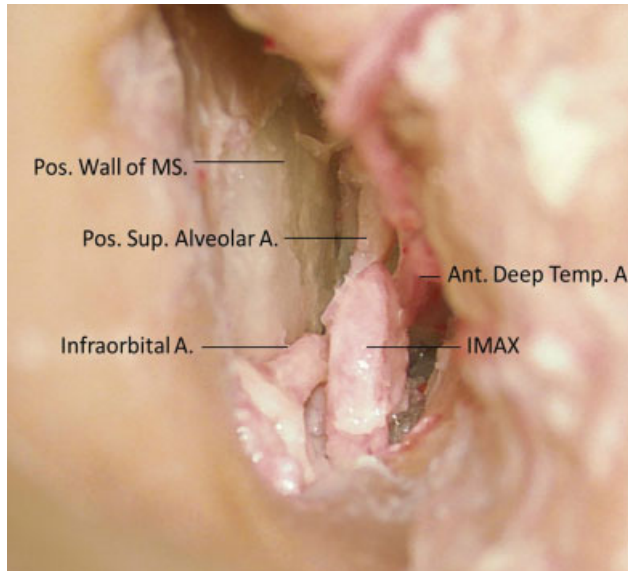
¹Department of Neurosurgery, Beijing Chao-Yang Hospital, Capital Medical School, Beijing, China
²Skull Base and Cerebrovascular Laboratory, University of California, San Francisco, California, United States
³Department of Otolaryngology – Head and Neck Surgery, University of California, San Francisco, California, United States
⁴Department of Neurological Surgery, University of California, San Francisco, California, United States

Background: Internal maxillary artery (IMAX) has been used as a donor vessel in extracranial-to-intracranial bypass surgery. In literature, four different approach methods have been described as techniques of exposing different segments of IMAX: anterior medial infratemporal fossa (AMITF), middle infratemporal fossa (MITF), anterior lateral middle fossa (ALMF), and lateral middle fossa (LMF) approaches. However, the advantages and limitations between these techniques were not compared. We aimed to compare the anatomical measurements of these four effective techniques for exposing IMAX as a bypass donor vessel and also measurements of AMITF and MITF methods without zygomatic bone.

Methods: Each approach technique was performed on 10 cadaveric specimens. The length, branches, caliber of targeted segments of IMAX, and depth from operating plane to IMAX were recorded. The surgical area of each technique was measured by assessing surrounding landmark with a navigation system. The time of surgical dissection of each technique has been calculated in five specimens. The downward reflected length of temporal muscle after zygomatic bone dissection was also recorded in 10 specimens. All data were analyzed by SPSS statistic software.

Results: The method of MITF provided the greatest operating area of exposure (3.88 ± 0.97 cm²), while the ALMF method provided the smallest one (1.08 ± 0.34 cm²). The method of LMF and MITF provided the largest caliber of IMAX (3.1 ± 0.4 mm, 3.0 ± 0.3 mm). The method of ALMF provided the shortest road from the operating plane to the exposed segment and the least time for exposure (21.8 minutes). The method of MITF exposed the longest segment of IMAX (18.8 ± 3.5 mm). The MITF method without zygomatic bone provided significantly longer segment than MITF method (19.5 ± 3.8 mm).

Conclusion: The AMITF and MITF methods can make the whole anastomosis procedure easier than ALMF and LMF methods with advantages such as less complex structure, less skull base drilling, and less muscle dissection. Identification of the pattern of IMAX is important before decision of the approach method in bypass operation. Our research can provide evidence for neurosurgeon to decide which one method would be better for their surgeries, plan their procedures preoperatively, and also to understand better the advantages and limitations of these methods.



A257. Crista Galli Pneumatization: Anatomical Variations and Clinical Consideration in Neurosurgery

Osamu Akiyama¹, Akihiko Kondo¹, Hajime Arai¹

¹Department of Neurosurgery, Juntendo University, Tokyo, Japan

Objective: To investigate the variations of crista galli pneumatization and to describe the classification, anatomical measurement, and surgical attention of crista galli pneumatization.

Background: Cerebrospinal fluid leakage caused by frontal sinus exposure is a serious complication of bifrontal craniotomy using the anterior interhemispheric approach for the treatment of skull base tumors. Especially with the basal interhemispheric approach, the crista galli is a structure that must be encountered. Crista galli pneumatization is often observed, and exposure of the crista galli pneumatization can cause cerebrospinal fluid leakage when the basal interhemispheric approach is used.

Methods: We examined the computed tomography (CT) images of 300 consecutive patients with brain tumors treated with surgery between January 2016 and January 2019. We performed a morphological analysis of the crista galli and the incidence of crista galli pneumatization. Crista galli was classified according to its location in relation to the cribriform plate and presence of pneumatization. Cells adjacent to the paranasal sinus were investigated as the origin of the crista galli pneumatization[A1]. Thirty consecutive patients who underwent bifrontal craniotomy using the basal interhemispheric approach for tuberculum sellae and planum sphenoidale meningiomas were included in the study as

clinical cases. In these clinical cases, we demonstrated the basal interhemispheric approach and assessed the range of skeletonization of the crista galli and considered the route of cerebrospinal fluid leakage through the crista galli.

Results: Crista galli pneumatization was found in 28 (9.3%) of the 300 CT scans as follows: 4 (14.3%), upper type; 10 (35.7%), middle type; and 14 (50%), lower type. The origin of the pneumatizing air cell was the frontal sinuses in 17 patients (right: 8, middle: 3, and left: 6) and the ethmoid sinuses in 11 (right: 4, left: 7). The primary origins of the crista galli pneumatization were the frontal sinus. In all the cases, pneumatization was of the anterior type, which means that the pneumatization was located in the anterior half of the crista galli. Of the 30 consecutive clinical cases, 23 had tuberculum sellae meningiomas, 4 had craniopharyngiomas, and the remaining 3 had other pathologies. The preoperative height of the crista galli was 12.3 mm (range, 7.9–15.3 mm). On the postoperative CT scan, the distance from the top of the skeletonization of the crista galli to the cribriform plate was 5.2 mm (range: 0–11.6 mm).

Conclusion: Crista galli pneumatization from paranasal sinuses can be a route of cerebrospinal fluid leakage. In this study, the pneumatization was located in the anterior half of the crista galli. In case of pneumatization of the crista galli from the ethmoid sinus, we should take care of the sealing of the exposed crista galli intradurally.

A258. The Role of Endoscopic Condylectomy in Endonasal Inferior Clivectomy and Extended Far Medial Approaches: Demonstration of Stereotactic CT Landmarks in Cadaveric Dissection with Clinical Correlation

Giuliano S. Bertazzo-Silveira¹, Sunil V. Manjila², Rafael Martinez-Perez¹, Thiago F. Albonette¹, Luciano M. Prevedello¹, Ricardo L. Carrau³, Daniel M. Prevedello⁴

¹Department of Neurological Surgery, The Ohio State University Wexner Medical Center, Columbus, Ohio, United States

²Department of Neurosurgery, McLaren Hospital, Bay Region, Bay City Michigan, United States

³Department of Otolaryngology and Head and Neck, The Ohio State University Wexner Medical Center, Columbus, Ohio, United States

⁴Departments of Neurosurgery and Head and Neck Surgery, Wexner Medical Center, The Ohio State University, Columbus, Ohio, United States

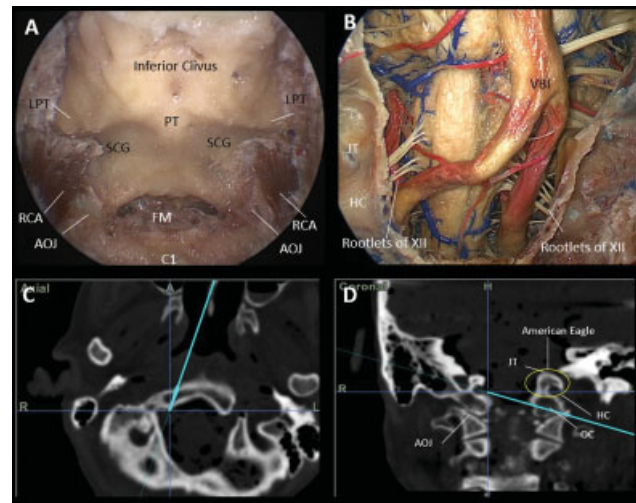
Background: Exposing the inferior clivus, the tubercular and the condylar compartments through a narrow sinonasal corridor is a challenging task reserved for specifically trained endoscopic skull base surgeons and requires an excelsior knowledge of anatomy. We offer a comprehensive update on the role of endoscopic condylectomy in expanded endoscopic transclival approach, with special references to stereotactic intraoperative landmarks, that can help in the avoidance and mitigation of surgical complications.

Methods: In the current study, stepwise image-guided dissections were performed in 11 colored latex-injected human heads and morphometric measurements on the inferior clival region were performed verified by two independent observers. The greatest area of neurosurgical exposure was defined as the quadrangular area bounded by the most lateral accessible point at the lacerum level and at the level of the anterior arch of C1, bilaterally. The angle of attack was calculated at the level of the hypoglossal nerve and glossopharyngeal nerve. All these data points were verified by stereotactic scan thin-slice CT images.

Results: The expanded endoscopic techniques involve a deep endonasal corridor (100.1 mm ± 8.1 mm) and provide a valuable area of surgical exposure of the lower clivus (677 ± 158 mm²). The narrowest transverse length of the

ventral foramen magnum (anterior intercondylar distance) was 19.1 mm ± 1.51 mm, with an average gain of 6 mm, making it ~25.5 mm ± 1.64 mm after bilateral transcondylar approach. The transverse length measured from either medial side of the ICA at the lacerum level representing the superolateral limit of the exposure was 22.8 mm ± 2.53 mm, and the mean lower clivus exposure from the floor of the sphenoid sinus to the anterior arch of C1 was 31.1 mm ± 2.04 mm. The stereotactic intraoperative landmarks were also studied by two independent observers and we have elucidated some cardinal signs for ensuring surgical safety: for example, the correlation between the radiological landmark such as the “American eagle” beak and the endoscopic landmark offered by the supracondylar groove.

Conclusion: We have demonstrated stepwise and meticulous utilization of intraoperative stereotactic CT landmarks in endonasal inferior clival surgery such as the eustachian tube, lateral pharyngeal tubercle, supracondylar groove, hypoglossal canal, and the occipital condyle. The additional area of surgical exposure obtained by bilateral endoscopic condylectomy has been demonstrated with the help of CT-guided stereotaxis in silicon injected cadavers. Customization of each anteromedial skull base lesion is hence mandated for EEA, especially in the hypoglossal canal and jugular foramen regions.



A259. Volumetric Assessment of Endoscopic Endonasal Anterior Clinoidectomy

Pierre-Olivier Champagne¹, Georgios Zenonos¹, Eric E. Wang¹, Carl H. Snyderman¹, Paul A. Gardner¹

¹University of Pittsburgh Medical Center, Pittsburgh, Pennsylvania, United States

Background: Transcranial removal of the anterior clinoid (AC) allows access to the clinoidal segment of the internal carotid artery (ICA) as well as laterosuperior decompression of the optic nerve in the optic canal. Endoscopic endonasal approaches (EEAs) can access the entire medial and inferior portions of the optic canal, but no data exists to support what proportion of the anterior clinoid could be safely resected via an EEA.

Methods: A prospective cadaveric anatomical study was performed. Removal of the AC followed three major steps in order of difficulty and risk. Following medial canal decompression, the first step consisted of drilling the optic canal

roof maximally into the medial anterior clinoid; the second step consisted of drilling the optic strut (via the lateral opticocarotid recess) and sphenoid wing attachment; the third step consisted of opening of the proximal dural ring and medial transposition of the ICA. At each step, the removal was stopped when no more bone of the AC could be seen without traction on neural structures. After each step, a CT scan was performed to allow volumetric measurement of the remaining AC.

Results: Twenty ACs in 10 cadaveric heads were removed to various degree using the described stepwise technique. The mean percentage of resection of the AC provided by each step was 21, 46, and 29%, respectively ($p < 0.001$). The mean percentage of removal at the end of the three steps was 96%, with complete removal achieved in 40% of the specimens only at the end of the third step. The most common locations for bony remnant were the lateral optic canal and the tip of the AC.

Conclusion: Using the safe route above the optic canal, removal of only 21% the AC can be achieved via an endoscopic endonasal approach, allowing medial and superior decompression of the optic nerve. Although substantially more of the AC can be drilled by accessing the optic strut, the benefits of pursuing additional removal must be weighed against the significant risks of drilling in this narrow corridor bordered by the ICA, third cranial nerve, and optic nerve.

A261. Morphometric Analysis of the Petroclival Region and the Effects of Clival Dimensions on Surgical Approach Selection

Zaid Aljuboori¹, Ahmad Alhourani¹, Candice Nguyen¹, Heegok Yeo¹, Brian Williams¹, Norberto Andaluz¹

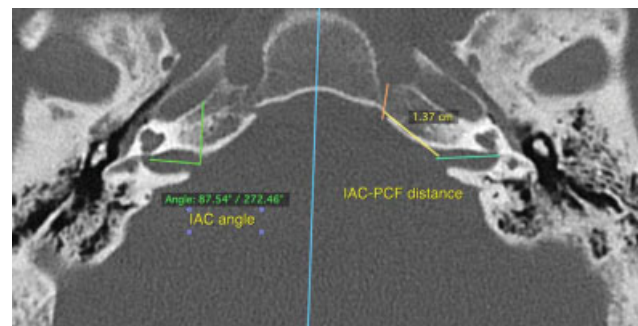
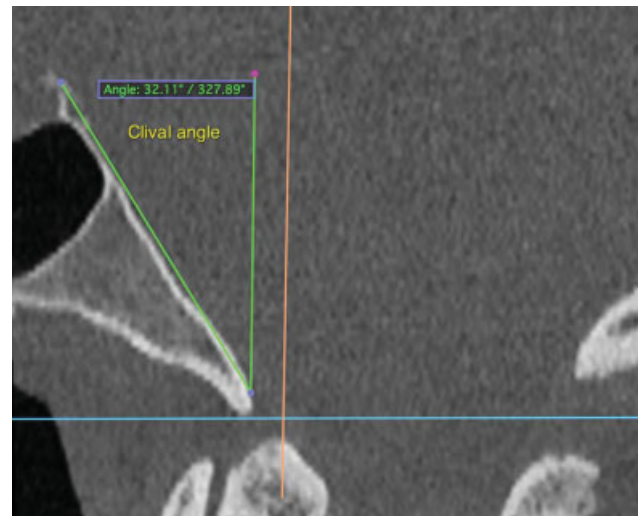
¹University of Louisville, Louisville, Kentucky, United States

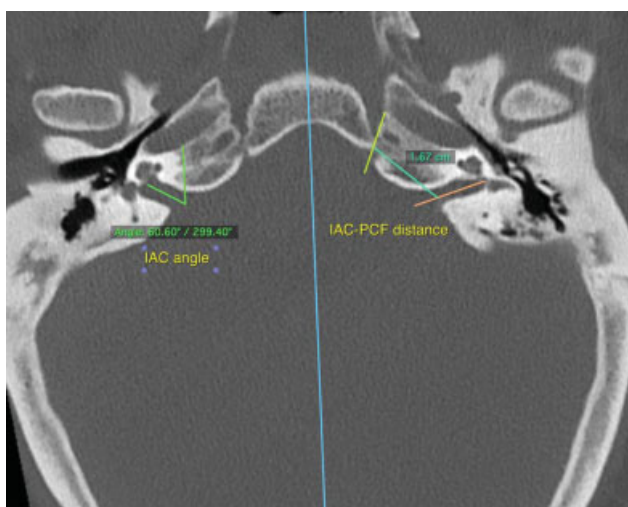
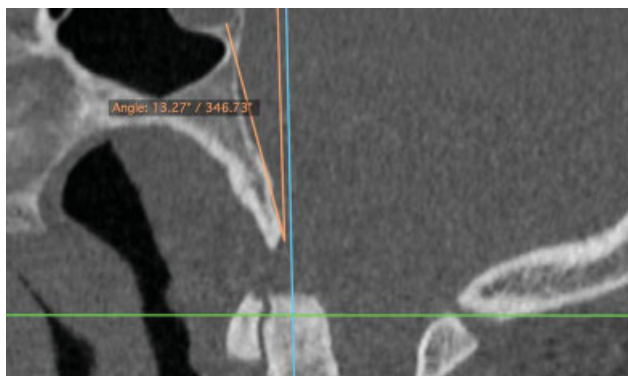
Introduction: Cranial base pathologies are challenging group of neurosurgical diseases. Since the adoption of the surgical microscope and later the endoscope, the field of cranial base surgery has become an integral part of neurosurgery. The central dogma of this field is the use of cranial base osseous structures for surgical advantage. This means, by removing parts of the osseous cranial base, the surgeon can create surgical corridors to minimize or avoid brain retraction. The petroclival region is a special area of the cranial base as it can harbor different pathologies, and it is considered a gateway to the clivus, petroclival junction, and cerebellopontine angle. Multiple surgical approaches have been described to address pathologies in this region. The choice between these approaches is based on surgeon's experience and preference, lesion size and location, the neurovascular anatomy, and patient's symptomatology. In this study, we present the results of the morphometric analysis of the clivus, petrous apex, and the internal acoustic canal in adults and its relevance to cranial base surgical approach selection.

Patients and Methods: One hundred adult patients were selected. All patients had 1-mm slice thickness computed tomography scan of the temporal bone. Exclusion criteria included patients younger than 18 years, radiographic evidence of trauma, neoplastic, inflammatory disease, infection, or previous surgery at the region of interest. The images were analyzed using OsiriX MD (Bernex, Switzerland). We recorded clival length, clival vertical angle, clival central depression angle, internal acoustic canal (IAC) angle, IAC to petroclival fissure distance (IAC-PCF), and IAC to jugular foramen distance (IAC-JF).

Results: The average age was 49.8 with 57% males and 85% whites. The median clival length, clival vertical angle, and central clival depression angle were 44.3 mm (IQR: 39.2–

49.4), 28 mm (IQR: 14.4–41.6), and 142.6 (IQR: 128.6–156.6) degrees, respectively. Females had shorter clivus (42 vs. 46 mm, $p < 0.05$), shorter IAC-IAC distance (48 vs. 50.4 mm, $p < 0.05$), and shorter IAC-PCF distance (15 vs. 15.8, $p < 0.05$) in comparison to males. The correlation analyses showed that clival length correlated negatively with the clival vertical angle ($\rho = -0.2$, $p < 0.05$). Also, it correlated positively with the IAC-PCF distance ($\rho = 0.24$, $p < 0.05$) and the IAC-JF distance ($\rho = 0.41$, $p < 0.05$). The clival vertical angle correlated positively with the IAC angle ($\rho = 0.26$, $p < 0.05$), and negatively with the IAC-PCF distance ($\rho = -0.2$, $p < 0.05$). We conclude that a longer clivus with a narrow vertical angle is associated with longer petrous apex and a larger distance between the IAC and the jugular foramen. IAC angle is variable. Clival length, vertical angle, and thickness are interconnected (Figs. 1–4); these indices should be considered especially for transclival approaches. Finally, the surgical treatment of cranial base pathologies is associated with certain morbidity because of proximity to critical structures. Besides other factors, the utilization of anatomical variability of clival dimensions and IAC angle can be used to choose an optimal surgical approach.





A262. Bony Dehiscence in the Lateral Wall of the Sphenoid Sinus: Prevalence and Its Implication

Sung-Woo Cho¹, Kihwan- KihwanHwang¹, Tae-Bin Won¹

¹Seoul National University Bundang Hospital, Seongnam, South Korea

Objective: According to the literature, bony dehiscence at the lateral wall of the sphenoid sinus is reported to be rare. However, authors have experienced frequent bony dehiscence of sphenoid sinus in patients with sphenoid fungus ball. Therefore, this study evaluated the prevalence of bony dehiscence of sphenoid sinus according to pathology.

Methods: This is a single-center study with retrospective analysis during January 2017 to January 2019. First, patients who had been treated with sphenoid fungus ball (SFB) were recruited. This was followed by recruitment of age- and sex-matched patients with bilateral chronic rhinosinusitis (CRS) or with pituitary adenoma (PA). Presence and width of the bony defect were measured in the coronal section of paranasal sinus CT scan with 2 mm thickness in the bone setting. For sphenoid fungus ball, the ipsilateral side was selected for analysis, and for others, side of analysis was selected randomly.

Results: In total, 65 patients were analyzed (27 SFB, 15 PA, 23 CRS). All bony defects were located medial to foramen rotundum and superior orbital fissure, just anterior to opti-

cocarotid recess. In SFB, bony defects were present in 74.1% (20/27) and were significantly more frequent compared with PA (20%) and CRS (26.1%; $p < 0.001$). The width was highest in SFB (1.24 ± 6.96 mm) followed by CRS (0.79 ± 0.18 mm) and PA (0.72 ± 0.32 mm). However, the difference was not significant ($p = 0.304$). Bony otitis was most frequently observed in SFB (88.8%) followed by CRS (56.5%) and PA (0%). Logistic regression revealed that the presence of bony defect was more dependent on the presence of otitis rather than on sinus pathology. During the study period, three patients with SFB presented with invasive fungal sinusitis. In two patients, lateral wall defect was the route on invasion to the skull base.

Conclusion: Sphenoid sinus lateral wall defect is more frequently observed when the bony otitis is present. In SFB in which bony otitis is common, this bony defect could be a route of skull base invasion.

A264. Pediatric Endonasal Endoscopic Skull Base Surgery: An Institutional Experience of 54 Patients

Cem Meco¹, Gokmen Kahilogullari¹, Suha Beton¹, Murat Zaimoglu¹, Onur Ozgural¹, Hazan Basak¹, Melih Bozkurt¹, Agahan Unlu¹

¹Ankara University, Ankara, Turkey

Objective: Endonasal endoscopic approach to the skull base in pediatric age group could be challenging. Our aim is to discuss its advantages and disadvantages.

Methods: Retrospective analysis of 54 pediatric patients who are operated purely via endonasal endoscopic approach in Ankara University between 2012 and 2018 were done.

Results: Thirty-three patients (61.1%) were male and 21 were female (38.8%). The main age was 10.4 (1–17). Sixteen cases had craniopharyngioma (29.6%), 12 had pituitary adenoma (22.2%), 5 had meningocele (9.3%), 4 had traumatic CSF rhinorrhea (8%), 2 had germinoma (4%), 2 had malign tumors (4%), 2 had hypophysitis (4%), 2 had pilocytic astrocytoma (4%), 1 had basilar invagination (2%), 1 had fibrous dysplasia (2%), 1 had hemangiopericytoma (2%), 1 had neurocytoma (2%), 1 had dermoid cyst (2%), 1 had chordoma (2%), 1 had hamartoma (2%), 1 had abscess (2%), and 1 had capillary hemangioma (2%). Gross total resection was achieved in 33 (76.7%) of patients who underwent surgery because of the presence of tumors. All visual deficits improved, although one patient sustained olfactory deterioration. Sixteen (29.6%) patients presented with complications such as transient diabetes insipidus and temporary visual loss.

Conclusion: Endonasal endoscopic approach is an effective method for surgery in managing various pathologies of the pediatric age group. Due to its less invasive nature, it protects the developing bony structures of the face and the skull, while achieving satisfactory outcomes. Nevertheless, narrow transnasal corridor as well as inadequate sphenoid sinus pneumatization could be the main handicaps of this approach in pediatric patients.

A265. Sinonasal Symptom Outcomes following Endoscopic Anterior Cranial Base Surgery in the Pediatric Population

Taylor R. Carle¹, Anthony P. Heaney¹, Harvey K. Chiu¹, Jeffrey D. Suh¹, Marilene B. Wang¹

¹University of California, Los Angeles, Los Angeles, California, United States

Objectives: Endoscopic anterior cranial base surgery in the pediatric population has been shown to be safe and

feasible without significant morbidity. Most studies to date have focused on outcomes related to complications such as CSF leak, endocrinopathy, epistaxis, and hyposmia, as well as impact on craniofacial development. The objective of this study was to evaluate the impact of endoscopic anterior cranial base surgery on sinonasal symptoms in the pediatric population utilizing the Sino-Nasal Outcome Test (SNOT)-22 questionnaire.

Design: Retrospective review.

Setting: Tertiary academic medical center.

Participants: Thirty-four consecutive patients, age <18 years, underwent endoscopic anterior cranial base surgery from July 2008 to August 2019. The age range was 6 to 17 years, 13 males and 21 females. The most common surgical pathologies included are pituitary adenoma (12), craniopharyngioma (7), and Rathke's cleft cyst (6). Ten patients had baseline and a minimum of two subsequent postoperative (SNOT)-22 questionnaires available for analysis. Historical data previously published by our institution regarding adult (SNOT)-20 and (SNOT)-22 scores, in the setting of endoscopic anterior cranial base surgery, was used for comparison.

Main Outcome Measures: Baseline and postoperative (SNOT)-22 scores were compared. The mean change between baseline and postoperative sinonasal symptom scores in the pediatric and adult cohorts were compared.

Results: The mean baseline (SNOT)-22 score for our 10-patient pediatric cohort was 0.46 for each of the first 10 sinonasal symptom-specific (rhinologic, extranasal rhinologic, and ear/facial) questions, and 1.08 for the 12 quality of life (psychological and sleep dysfunction) questions. The mean sinonasal symptom score worsened slightly to 1.69 and the mean quality-of-life score improved slightly to 0.91, at an average of 37 days postoperative. At an average of 82 days postoperative, the mean sinonasal symptom score improved to near baseline, at 0.7, and the mean quality-of-life score improved to better than baseline, at 0.6. The mean changes from baseline for the following specific items at an average of 87 days postoperatively in our pediatric cohort were as follows: (1) need to blow nose, 0.5; (2) runny nose, 1; (3) postnasal discharge, 0.2; (4) thick nasal discharge, 0.1; (5) wake up at night, -0.5; (6) reduced concentration, -0.6; and (7) frustrated/restless/irritable, -0.5, respectively. These mean changes were similar to those found in our historical adult cohort scores at 3 months postoperatively. All but two patients were able to undergo postoperative sinonasal debridement in clinic. The following complications occurred in our 34-patient pediatric cohort: postoperative CSF leak, 2 (5.8%); new postoperative diabetes insipidus, 7 (20.6%); new postoperative pituitary dysfunction, 6 (17.6%); DVT/PE, 1 (3%); fat graft site hematoma, 1 (3%).

Conclusion: Endoscopic anterior cranial base surgery in the pediatric population results in increased sinonasal symptom morbidity in the early postoperative period; however, symptoms return to near baseline by ~3 months. Most pediatric patients tolerate postoperative sinus care well, including debridements in clinic.

A266. Juvenile Nasopharyngeal Angiofibroma: A Retrospective Institutional Surgical Case Series

Salomon Cohen-Cohen¹, Michael J. Link¹, Jeffrey R. Janus², Garret W. Choby², Eric J. Moore², Jan Kasperbauer², Jamie J. Van Gompel¹

¹Department of Neurologic Surgery, Mayo Clinic, Rochester, Minnesota, United States

²Department of Otorhinolaryngology Mayo Clinic, Rochester, Minnesota, United States

Background: Juvenile nasopharyngeal angiofibromas (JNA) are highly vascular benign tumors that originate in the pterygoid space and often involve multiple compartments. It is the most common tumor presenting in the nose and nasopharynx and is seen exclusively in young men, typically between the ages of 9 and 19 years. Surgery remains the main treatment modality, particularly when coupled with preoperative embolization. We report our experience with a series of 20 patients with JNA treated between 2005 and 2019.

Methods: After Institutional Review Board approval, a retrospective review was preformed to identify all patients with JNA with surgery at our institution during the study period 2005–2019. Only those patients who underwent either primary or secondary surgical treatment at our institution and had a confirmed pathologic diagnosis of angiofibroma were included in the study. Data abstraction included demographics, clinical presentation, operative technique, and postoperative outcomes.

IRB 19-008145.

Results: Twenty patients, all males, were included, with an overall median age at diagnosis of 18 years (range, 9–26). Sixteen (80%) patients received primary diagnosis and treatment at Mayo Clinic, and four (20%) were treated after previous unsuccessful treatment at another institution. The most common presenting symptoms were nasal obstruction in 15 (75%) epistaxis in 14 (70%), and headache/facial pain in 5 (20%). In 65% of the cases, the tumor was right sided. All patients underwent preoperative embolization before surgical resection. The internal maxillary artery was predominant in all 20 patients. All patients were operated within 24 to 48 hours following embolization. Tumor size (maximum dimension) ranged from 1.6 to 10.7 cm with a median size of 4.4 cm. Based on the Radkowski classification, there was two (10%) stage IA, three (15%) stage IB, two (10%) stage IIA, five (25%) stage IIIB, seven (35%), and one (5%) stage IIIB. All tumors were confirmed as JNA on pathological analysis. In 16 patients (80%), an endoscopic approach was used and 4 patients (20%) had open approaches. Gross total resection was achieved in all patients. One patient (5%) presented with recurrence. This patient had an atypical angiofibroma and required multiple interventions. There were no mortalities associated with the procedures. One patient (5%) had a postoperative CSF leak that was managed with reconstruction of the middle fossa and a lumbar drain. The average estimated blood loss was 736 mL (range: 50–6750 mL). Two patients required blood transfusions (10%). No patient underwent radiotherapy or radiosurgery.

Conclusion: The EEA is a safe and effective technique even for large JNAs. A multidisciplinary team consisting of a skull base neurosurgeon and an otorhinolaryngologist with extensive expertise in endoscopic surgery is required for optimal results.

A267. Anterior Skull Base Sarcomas: Report on Characteristics and Outcomes

Sallie Long¹, Panagiotis Asimakopoulos², Marlina McGill², Marc A. Cohen², Snehal G. Patel², Jatin P. Shah², Ian Ganly²

¹Department of Otolaryngology Head and Neck Surgery, NewYork-Presbyterian Hospital Columbia and Cornell, New York, New York, United States

²Department of Surgery, Head and Neck Service, Memorial Sloan Kettering Cancer Center, New York, United States

Introduction: Sarcomas of the head and neck region are uncommon malignancies, accounting for ~1% of all head and neck cancers. The aim of this study is to describe our experience on characteristics and treatment outcomes of skull base sarcomas.

Methods: Thirty-one patients with sarcomas of the anterior skull base treated with primary surgery presenting from 1979 to 2015 at a single institution were retrospectively reviewed. Patient, tumor, and treatment characteristics were recorded. Survival and recurrence outcomes were determined using the Kaplan–Meier method.

Results: The median age was 44 years (13–69). Eleven patients were female (35%). The majority of patients presented with clinical T4 tumors (28, 91%). Seven patients had a previous history of retinoblastoma, one patient had neurofibromatosis type 1, and one patient had a history of fibrous dysplasia. All patients underwent open anterior craniofacial resection apart from two who had endoscopic resection. The most frequent pathologies were leiomyosarcoma (19%), osteosarcoma (16%), chondrosarcoma (10%), and myxofibrosarcoma (10%).

Positive or close margins were present in 14 patients (45%), and 18 (58%) had high-grade tumors. Twenty-three patients (74%) received adjuvant radiation and four patients (13%) received adjuvant chemotherapy. There were nine postoperative complications (29%) including one mortality and three cerebrospinal fluid leaks. With a median follow-up of 74 months (range: 1–310), the 5-year overall survival (OS) and disease-specific survival (DSS) were 72 and 70%, respectively. There were 10 local, two regional, and five distant recurrences. The 5-year local (LRFS), regional (RRFS), and distant (DRFS) recurrence free survivals were 70, 91, and 72%, respectively. Patients with positive and negative margins had a 5-year DSS of 60 and 64%, respectively. Patients with high- and low-grade tumors had a 5-year DSS of 74 and 86%, respectively.

Discussion: Skull base sarcomas are rare. Disease-specific survival is ~70% at 5 years. Due to the rarity of these tumors, management should be determined by a multidisciplinary team (Fig. 1).

Conclusion: This study contributes to an updated analysis of sarcomas of the head and neck. The accumulation of only 31 cases in such a large time period highlights the rarity of these tumors.

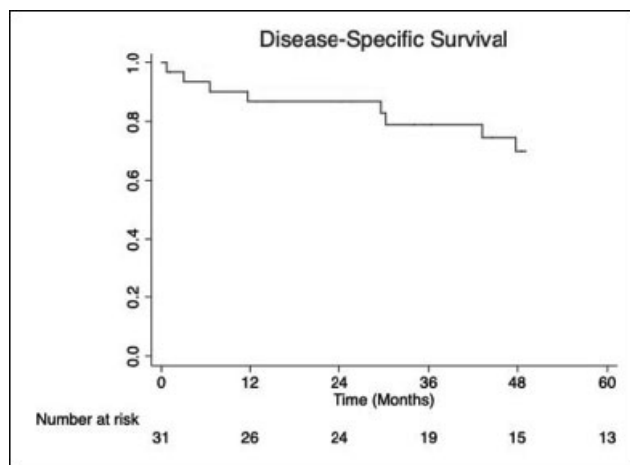


Fig. 1 Disease-specific survival rates, all cases.

A268. Surgical Management of Class C and D Glomus Jugulare Tumors: Fisch Infratemporal Fossa Type A Approach

Yin Xia¹, Yubin Xue¹, Ting Ye¹, Xiaopeng Qu¹, Xukun Yan¹, Wenyang Zhang¹

¹Department of Otorhinolaryngology, Beijing Tiantan Hospital, Capital Medical University, Beijing, China

Objective: To analyze retrospectively the indications and the results obtained with the Fisch infratemporal fossa Type A approach in a series of patients with Class C and D glomus jugulare tumors.

Methods: The study included 39 patients admitted to our hospital from July 2007 to July 2019 with Class C and D glomus jugulare tumors that were removed with the Fisch infratemporal fossa Type A approach. All patients underwent preoperative pure-tone audiometry, evaluation of facial function, CT and MR imaging, and digital subtraction angiography (DSA). Fourteen males (35.8%) and 25 females (64.2%), with an average age of 42.7 years, were analyzed.

Results: Thirty-six cases (92.3%) presented pulsatile tinnitus and hearing loss as the main symptoms. According to the Fisch classification 1981, the tumors in 31 ears were class C, and Class D in 8 ears. The tumor was totally removed in 37 (94.9%) and near-totally removed in 2 (5.1%) of the patients. The facial nerve was permanently anteriorly transposed in 36 (92.3%) of the patients. The postoperative facial function after 6 weeks was House-Brackmann grade ? in 8 (20.5%), grade ? in 16 (41.0%), grade ? in 9 (23.1%), grade ? in 4 (10.3%), grade ? in 2 (5.1%) patients. There were two patients who required revision surgery, one with a CSF leak and another with a postoperative tumor recurrence. Dysphagia and hoarseness were seen in three cases, respectively. There were no deaths and no severe complications such as hemiplegia or intracranial infections. Of the 39 patients followed up with a mean time of 5.9 years (range: 0.2–12.1 years).

Conclusion: Fisch infratemporal fossa Type A approach allows complete resection of the tumor. Surgical approach can supply a wide exposure of surgical field and make the surgeon to protect the large blood vessels and nerve, which leads to low rates of complications.

A269. Craniopharyngiomas: The Advantage of an Infratemporal Approach with Posterior Clinoidectomy

Ariel Kaen¹, Eugenio Cardenas¹, Edinson Najera¹, Pablo Remon², Ignacio Martin Schrader¹, Alfonso Soto²

¹Department of Neurological Surgery, Hospital Universitario Virgen del Rocío, Sevilla, Spain

²Department of Endocrinology and Nutrition, Hospital Universitario Virgen del Rocío, Sevilla, Spain

Background: Location classifications of craniopharyngiomas for the infundibulum have been used to guide various approach strategies. However, approaching Type III tumors (retroinfundibular) with a narrow chiasm-pituitary corridor (CPC) has been considered a contraindication to an endonasal endoscopic approach (EEA) due to the high risk of visual deterioration and consequent subtotal resection (STR). Posterior clinoidectomy may allow direct retrosellar and retroinfundibular access without the manipulation of the neurovascular structures that lie around the perimeter of this region. In this study, we describe the advantage of using an infratemporal approach with posterior clinoidectomy in retroinfundibular craniopharyngiomas.

Methods: A retrospective review was conducted to determine the outcome of 15 consecutive patients with retroinfundibular craniopharyngiomas who underwent endonasal endoscopic resections between February 2018 and February 2019. The topographical relationship of the tumor to the third ventricle, stalk, and optic chiasm was investigated, with special attention paid to clinic outcomes and how the posterior clinoidectomy improved the resections.

Results: Gross and near-total resections were achieved in 11 patients (73.3%) and 4 patients (26.6%), respectively. No postoperative complications were found related to the posterior clinoidectomy. Narrow CPCs and large CPCs were found

in 5 patients (33%) and 10 patients (66%), respectively. Posterior clinoidectomy allowed not only for an increased surgical area in the sagittal plane, but also in the coronal plane. This advantage was observed especially in patients with narrow CPCs ($p < 0.05$).

Conclusion: An EEA is an effective surgical approach for retroinfundibular craniopharyngiomas. Posterior clinoidectomy is safe and useful, especially in patients with narrow CPCs.

A270. Endoscopic Endonasal Surgery for “Inoperable” Craniopharyngiomas: Intraoperative Challenges and Management of Complications

Juan C. Fernandez-Miranda¹, Ahmed Moyheldin¹, Zara Patel¹, Jayakar Nayak¹, Peter Hwang¹

¹Stanford University, Stanford, California, United States

Introduction: Craniopharyngiomas are among the most challenging intracranial tumors. Compared with well-established transcranial approaches, endoscopic endonasal surgery combines the virtues of the caudocranial and midline approaches, allowing for appropriate infrachiasmatic exposure without the need for manipulation of surrounding neurovascular structures to access the tumor.

Methods: Here we present several highly complex craniopharyngioma cases operated by the author at Stanford University Medical Center and Lucile-Packard Children’s Hospital, which had been previously labeled as “inoperable” or “unresectable” based on imaging characteristics (size, calcification), behavior (multiple recurrence), or patient’s age.

Results: Five patients were included in the study, three adults and two children. Two of the adults had undergone a total of 12 previous operations and 4 radiation treatments, while the remaining adult patient was left untouched based on the presence of a large calcification in spite of progressive growth. The two pediatric patients had giant tumors and had undergone transfrontal cyst drainage without attempted resection secondary to huge size and/or very young age (2 years old).

In four out of five patients, gross-total resection was achieved, with near-total resection (+95%) in the remaining case. There were two intraoperative vascular injuries involving the posterior circulation that were successfully managed with bipolar coagulation or aneurysm clip placement, with vessel preservation in both cases. One patient had evidence of a small stroke on postoperative MRI (anterior thalamus) with no obvious neurological deficits. One patient had postoperative CSF leakage secondary to necrotic nasoseptal flap that required a temporoparietal fascia flap reconstruction.

Conclusion: Here we emphasize the importance of new surgical planning platforms, “live-cadaver” vascular injury exercises, virtual reality simulation, and 3D-printed models, as adjuncts to training in the surgical neuroanatomy laboratory in preparation for these challenging cases. There is an absolute need for advanced expertise and dedication for safe, effective, and live-changing treatment of complex adult and pediatric craniopharyngiomas.

A271. Surgical Management of Petroclival Meningiomas Based on a Radiographic Classification with Updated Follow-up

Zhen Wu¹, Da Li¹, Jun-Ting Zhang¹

¹Beijing Tiantan Hospital, Capital Medical University, Beijing, China

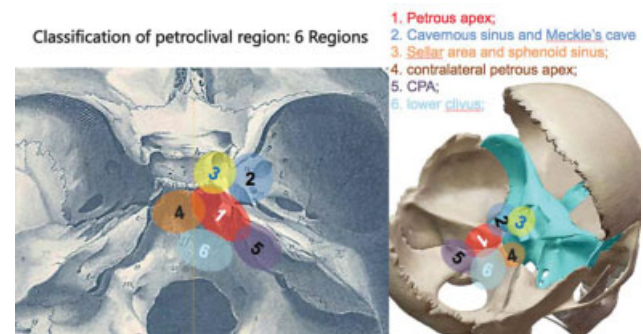
Background: Surgical management of petroclival meningiomas (PCMs) was challenging accompanied with relatively high morbidity. Treatment selection was quite surgeon dependent, and no consensus-based strategy was proposed.

Objective: The study aimed to propose a radiographic classification of PCMs to facilitate treatment selection and predict neurological outcomes.

Methods: Clinical and radiographic data of 513 cases of surgically treated PCMs between May 2011 and August 2018 were retrospectively reviewed, and follow-up was accomplished in 483 (94.2%) cases. Skull base compartments surrounding petrous apex included (1) petrous apex itself; (2) Meckel cave, cavernous sinus, and/or middle cranial fossa; (3) sellar area and/or sphenoidal sinus; (4) contralateral clivus and/or petrous apex; (5) invasion to CPA region and lateral to internal auditory meatus; and (6) lower third clivus. All PCMs were classified into seven subtypes based on the regions potentially involved by PCMs: type I (region 1); type II (region 1 plus 2); type III (region 1 plus 3); type IV (region 1 plus 4); type V (region 1 plus 5); type VI (region 1 plus 6); and type VII (region 1 plus 2 regions or more). Surgical approach was selected based on the classification, and the association with outcome was evaluated.

Results: This consecutive cohort included 372 females (72.5%) with a mean age of 49.7 years. Mean preoperative and postoperative KPS at discharge was 78.5 and 66.2, respectively, and recent KPS was 77.8. Retrosigmoid approach ($n = 47$), anterior transpetrosal ($n = 289$), presigmoid retrolabyrinthine approach ($n = 81$), far lateral approach ($n = 23$), frontal-temporal approach ($n = 42$), and others ($n = 31$). Gross total resection was achieved in 293 cases (57.1%) which was a bit greater than that of our early series. Surgical mortality and morbidity rates were 1.4% ($n = 7$) and 48.0% ($n = 246$), respectively. Mean follow-up duration was 46.5 months, and the recurrent rate was 2.7% (13/483). Surgical morbidity was different between various subtypes but that was significantly higher in type VII group ($p < 0.001$) as well as the lesion size that was largest in type VII group ($p = 0.003$). Other adverse factors for neurological outcome included brainstem edema, subarachnoid space, extent of surgical resection, preoperative KPS score, and intraoperative findings (adhesion to neurovascular structure and/or vessel encasement). The association between subtypes and neurological outcome was significant ($p = 0.013$) but compromised after adjustment for surgical approach ($p = 0.116$).

Conclusion: The radiological classification facilitated surgical approach decision, and total resection could be improved via suitable approach. Follow-up duration should be prolonged to validate the reasonability of the classification.



Poster Presentations

P001. Early Investigation Assessing the Feasibility of Electrospinning of Cyanoacrylate Glue for Endonasal Skull Base Repair

Ivanna Nebor¹, Daewoo Han¹, Kora Montemagno¹, Rebecca Fumagalli¹, Ikrame Labiad¹, Alice Xu¹, Andrew J. Steckl¹, Ahmad Sedaghat¹, Mario Zuccarello¹, Jonathan Forbes¹

¹University of Cincinnati Medical Center, Cincinnati, Ohio, United States

Background: The expanded endonasal approach (EEA) helps to minimize neurologic morbidity by eliminating brain retraction and the need to work through corridors bordered by cranial nerves. However, despite numerous technologic and surgical innovations, post-operative CSF fistula following EEA continues to be associated with considerable morbidity. Cyanoacrylate glues offer enhanced strength and durability for skull base repair compared with fibrin and polyethylene glycol alternatives. However, problems with unwieldy deposition and inhomogeneity have limited options for clinical application. Electrospinning is a novel method that uses electric force to draw together charged threads of polymer solutions. Such a method facilitates precise deposition of ultrathin continuous nanofibers, which may make skull base repair with cyanoacrylate glue a promising alternative. In this study, we investigate the application of electrospinning cyanoacrylate glue as a promising future method for endonasal skull base repair.

Methods: A piece of calvarial bone measuring approximately 5 cm² in size was removed from a fresh frozen cadaver. A central defect, measuring approximately 1 cm, was created in the calvarial bone to simulate a skull base defect. Temporalis fascia obtained from a fresh frozen cadaver was placed as an inlay graft. An endoscope-like extended electrospinning device was then utilized to apply a thin film of ethyl cyanoacrylate (ECA) glue fibers on bone and fascia surfaces. A rhodamine red dye was added to glue solution for better visualization. High voltage of 7 to 10kV was applied to the needle and the distance between the needle and the target was adjusted between 10 and 15 cm to control the glue deposition area. Cyanoacrylate glue was fed at the constant rate of 1 mL/h using the syringe pump. Scanning electronic microscopy (SEM), EVEX miniSEM SX-30, was used to evaluate the ECA fibers. Samples were coated with gold using Denton Desk II bench-top sputter coater for SEM observation.

Results: ECA fibers were deposited successfully on the fresh cadaver bone and fascia model. Deposition areas of 250 and 78 cm² were conveniently controlled by adjusting the electrospinning distance from 15 to 10 cm, respectively. Deposition on 78 cm² area only required 50 uL of glue for approximately 3 minutes of electrospinning. Based on SEM observation, electrospun glue fiber forms a film structure embedding ECA nanofibers which congealed satisfactory with the temporalis fascia over the bone defect.

Conclusion: The method of electrospinning investigated facilitated precise and meticulous deposition of ECA glue on fresh cadaveric tissue. Developed endoscope-like electrospinning device have demonstrated the potential for the surgical use in EEA. Excellent film homogeneity and adhesive characteristics have obtained for dural repair purpose. Data from this investigation will pave the way for additional research into endonasal application of glue and skull base repair using the electrospinning glue nanofibers.

P002. Managing CSF Leak with Temporalis Muscle Flap for Challenging Skull Base Defect after Radiation Therapy

Wei-Hsin Wang¹, Ming-Ying Lan²

¹Department of Neurosurgery, Taipei Veterans General Hospital, National Yang-Ming University, Taiwan

²Department of Otolaryngology, Taipei Veterans General Hospital, National Yang-Ming University, Taiwan

Introduction: The presence of CSF leak after radiation therapy is very challenging for repair. We reported a case of 56-year-old male with right temporal base osteoradionecrosis and dura radionecrosis presented with CSF leak, 10 months after Boron Neutron Capture Therapy for the treatment of recurrent buccal squamous cell carcinoma, following wide excision and CCRT.

Methods: The CSF leak through the foramen ovale was localized by images. The temporalis muscle flap was harvested according the size of defect measured on the 3D printing skull. A pterional craniotomy was performed to resect necrotic right temporal tip tissues to subside uncal herniation. A free pericranial flap was used to cover the foramen ovale intracranially. The temporalis muscle flap was rotated into infratemporal fossa to cover the foramen ovale extracranially.

Results: After wide debridement of the necrotic skull bone and the dura, the temporalis muscle flap was covered on the right temporal base. Though the embolization of right internal maxillary artery had been performed in prior surgery, this temporalis muscle flap still survived on the recipient site and CSF leak was improved.

Conclusion: The temporalis muscle flap is a useful and reliable flap to repair challenging defects of the lateral skull base. Having satisfactory size of the flap relative to the defect, the temporalis muscle flap still can survive and provide strong support even in the condition of prior embolization and radiotherapy had been performed on the recipient site.

P003. Microsurgical Anatomy of the Labyrinthine and Subarcuate Arteries and Clinical Implications

Laura Salgado-Lopez¹, Maria Peris-Celda¹

¹Department of Neurosurgery, Albany Medical Center, Albany, New York, United States

Objective: The labyrinthine and subarcuate arteries are two small arteries that are usually exposed during the approaches to cerebellopontine angle. Both arteries arise most frequently from the anteroinferior cerebellar artery (AICA), but they may have different origins, as well as trajectories, and relationships with the surrounding neurovascular structures. Being able to identify and differentiate them is crucial due to the different clinical implication of their surgical compromise as sacrifice of the labyrinthine artery (LA) can result in hearing loss, whereas no clear clinical implications have been related to the subarcuate artery (SA) injury. The objective of the present work is to study the surgical anatomy and anatomical variations of the LA and the extrapetrous portion of the SA and their anatomical relationships.

Methods: 10 formalin-fixed latex-injected specimens were dissected (20 sides). After a retrosigmoid craniotomy was performed, the dura mater was opened and dissection of the neurovascular structures was achieved under microscopic magnification. A 4 mm, 0- and 30-degree endoscopic lenses (Storz) were then used to improve the exposure, visualization, and assessment of the vascular anatomy. The results were statistically analyzed.

Results: The LA was identified as the artery following the vestibulocochlear nerve into the internal auditory canal;

its distal portion was posteroinferior to the vestibulocochlear nerve in 85.7% of the cases and in 14.3% was anterosuperior. The SA ended blindly in the dura mater around the subarcuate fossa and its distal portion was anterosuperior to the vestibulocochlear nerve in all cases. The origin of the LA was also posteroinferior to the vestibulocochlear nerve in the majority of the cases (57.1%), inferior in 28.6% and anterosuperior in the remaining 14.3%. The origin of the SA was posterosuperior to the vestibulocochlear nerve in 50% of the specimens, and posterior and between the facial and vestibulocochlear nerves in the remaining 50%. The main distance between the origin of the LA and SA was 7 mm. The LA branched off from the AICA in all cases but one, in where it arose from the basilar artery. The LA arose from the AICA loop in 85.7% of the cases and from the pre-loop AICA in the remaining 14.3% whereas the SA branched off from the preloop AICA in all cases. The average length of the LA was 13.6 mm (7–24 mm). It was found to be a single artery in 83% and two arteries in 17%. The SA was present in 33.3% of the specimens; its average length was 8.5 mm (5–12 mm) and it was a single artery in all cases.

Conclusion: The LA is a constant artery that follows the vestibulocochlear nerve into the internal auditory canal whereas the SA ends in the dura mater of the subarcuate fossa and is only present in 33% of the cases. Both arteries arise mainly from the AICA. The LA is usually posteroinferior to the vestibulocochlear nerve at its distal aspect, whereas the SA is anterosuperior to the vestibulocochlear nerve. Understanding the surgical anatomy of the labyrinthine and subarcuate arteries and their anatomical relationships is important in approaches to the cerebellopontine angle.

P004. Classification of the Suprameatal Tubercle and Morphometric Analysis with Surgical Approach to the Temporal Bone

Humberto Reyna¹, Sergio Reyna¹, Jose Espinoza¹, Enrique Lopez¹, Diego Mendez¹

¹CMN 20 Noviembre ISSSTE

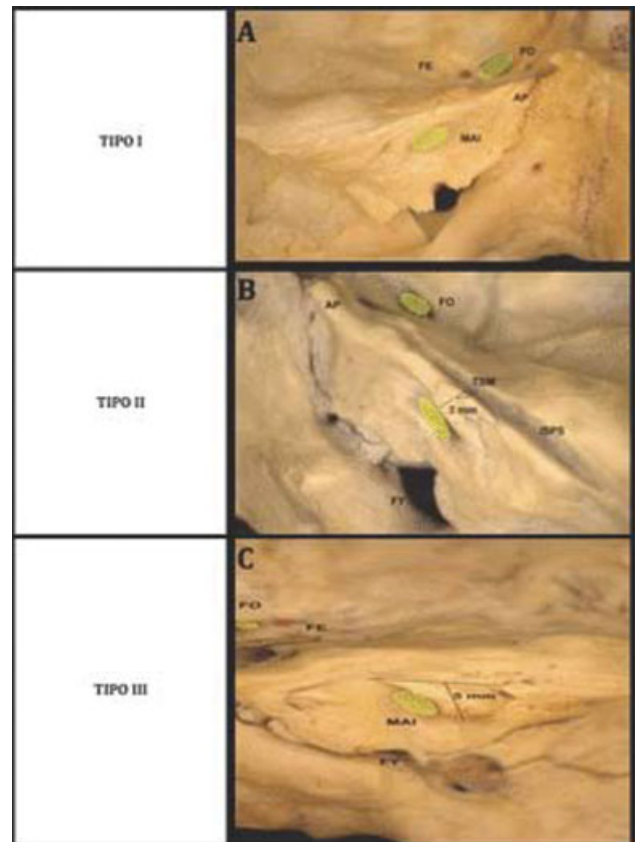
Abstract: The temporal bone is a valuable structure in the approach of intracranial pathologies to the middle and posterior fossa, sometimes requiring the performance of anterior, posterior, or combined approaches for resection of tumors in these regions. The purpose of this study is to perform morphometric analysis with a surgical approach to the temporal bone, in adult skulls, with emphasis on the suprameatal tubercle (SST) taking into account their anatomical relationships.

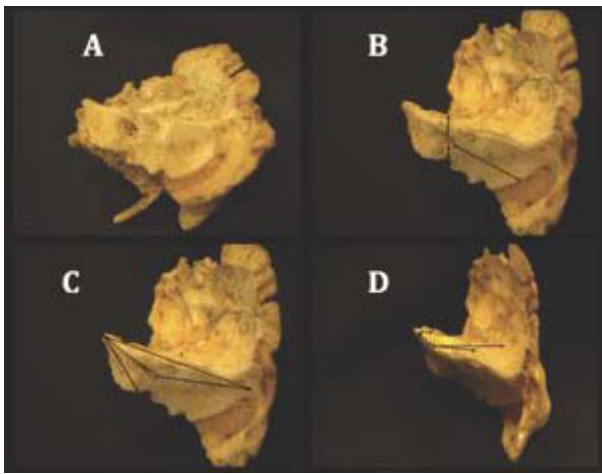
Material and Methods: The present study was developed in the facilities of the Faculty of Medicine of the National Autonomous University of Mexico (UNAM). A total of 200 temporal bones from 100 adult human skulls were analyzed. The TSM was emphasized according to its location and size, classifying it as: middle or posterior anterior and type I (0–1 mm), type II (2–3 mm), and type III (>3mm). In addition, measurements were made with a surgical approach of the petrosal portion of the temporal bone and the supramastoid crest.

Results: The SST was observed in 171 specimens studied (85.5%). Among them, the posterior position was the most frequent 85 of 171 (49.70%), followed by the average position 43 (25.14%), and finally the previous position 43 (25.14%). In terms of size, type II was more frequently found in 99 of the specimens (49.5%), type I in 82 specimens (41%), and type III were found in 19 (9.5%). The asterion was reflected within the impression of the breasts in the majority 48.5%; the union of the supramastoid crest with squamous suture was reflected in 98.5% of the cases to the middle fossa.

Discussion: In our search for information there is no data to make a comparison with that obtained in this study of the suprameatal tubercle, the findings found seems to indicate that there is a direct relationship with the presence of the impression of the groove of the upper petrosal sinus. The distribution according to its position is important when it is in grade III, since it poses a technical difficulty in approaches such as petrosectomies or Meckel's cavum from a retrosigmoid approach.

Conclusion: The anatomical observation and classification that we perform of the suprameatal tubercle, a very poorly evaluated structure, gives us preoperative and transoperative considerations when we perform an approach that involves the posterior aspect of the petrosal portion of the temporal bone.





avoid bleeding complications. There have been few studies reporting the presence and dimensions of the anterior (AIS), posterior (PIS), and inferior (IIS) intercavernous sinuses. We therefore performed a cadaveric study to better understand these structures.

Methods: Colored latex was injected into the arterial and venous trees of fifteen cadaveric heads. Dissections were then performed to assess the presence and dimensions of the anterior, posterior, and inferior intercavernous sinuses.

Results: In nine specimens (60%), all three sinuses were identified. In five specimens (33%), only the anterior and posterior intercavernous sinuses could be identified, and in one specimen, only anterior and inferior sinuses were identified. An anterior intercavernous sinus was identified in 100% of specimens, posterior intercavernous sinus in 93%, and an inferior intercavernous sinus in 66%. In two specimens (13%), the anterior intercavernous sinus covered the entire face of the sella. The average dimensions for the sinuses were as follows: AIS, 1.7 ± 0.8 mm anterior-posterior, 11.7 ± 2.2 mm medial-lateral, 2.8 ± 1.2 mm dorsal-ventral; PIS, 1.5 ± 0.5 mm anterior-posterior, 10.8 ± 2.3 mm medial-lateral, 1.7 ± 0.6 mm dorsal-ventral; IIS, 8.7 ± 3.4 mm anterior-posterior, 11.8 ± 4 mm medial-lateral, 1.0 ± 0.8 mm dorsal-ventral.

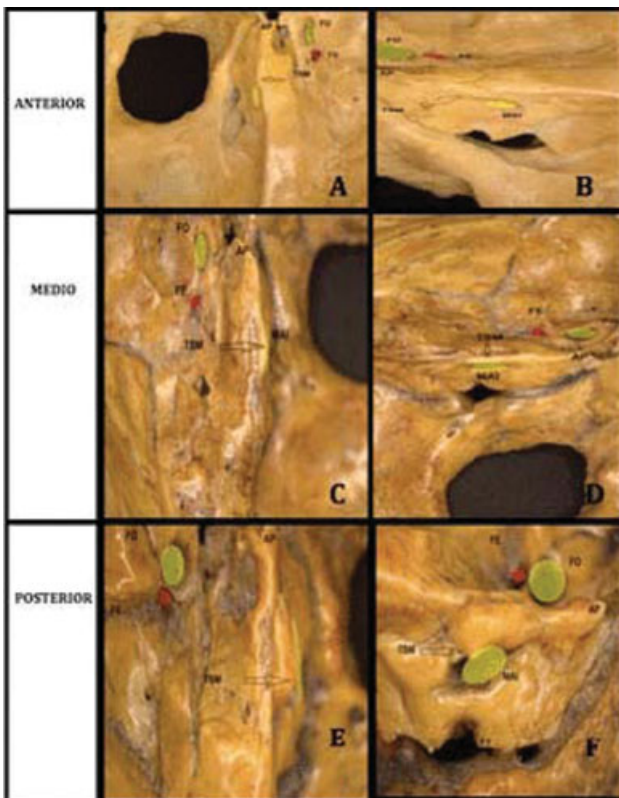


Table 1 Intercavernous sinus frequencies in the literature

Citation	Number of Samples	Method of Assessment	Anterior Intercavernous Sinus	Inferior Intercavernous Sinus	Posterior Intercavernous Sinus
Knott JF, 1881	44	Macroscopic evaluation	97%	41%	41%
Green HT, 1957	18	Serial microscopic sections	100%	94%	89%
Berglund et al., 1968	225	Macroscopic evaluation	85%		
Renn and Khotan, 1975	50	Macroscopic evaluation	76%		32%
Aquini et al., 1994	32	Serial microscopic sections	100%	97%	100%
Tubbs et al., 2014	35	Macroscopic evaluation	97%	17%	83%
Deng et al., 2015	18	Macroscopic evaluation	78%	61%	28%
Deng et al., 2015	24	Contrast enhanced MRV	29%	29%	8%
Mizutani, et al., 2016	97	CTV	53%	29%	78%

Conclusion: All examined specimens in our study demonstrated the presence of an anterior intercavernous sinus, and most also had a posterior intercavernous sinus. The presence of an inferior intercavernous sinus was more variable.

P006. Anatomical Step-by-Step Dissection of Complex Skull Base Approaches for Trainees: Surgical Anatomy of the Retrosigmoid Approach

Christopher S. Graffeo¹, Maria Peris Celda², Avital Perry¹, Lucas P. Carlstrom¹, Colin L. Driscoll¹, Michael J. Link¹
¹Mayo Clinic, Rochester, Minnesota, United States
²Albany Med, Albany, New York, United States

Introduction: Neurosurgical anatomy is traditionally taught via anatomic and operative atlases; however, these resources present the skull base using views that emphasize 3D relationships rather than operative perspectives, and are frequently written above a typical resident's understanding. The goal of current study was to outline, step-by-step, a retrosigmoid dissection, presented from an operative perspective and described in accessible language, to aid junior

P005. An Anatomic Study of the Intercavernous Sinuses
 Timothy Banks¹, Jennifer Kosty¹, Racheal Wolfson¹, Rimmal Dossani², Bharat Guthikonda¹
¹Louisiana State University HSC Shreveport, Shreveport, Louisiana, United States
²University at Buffalo, Buffalo, New York, United States

Background: As expanded endoscopic endonasal approaches are gaining popularity, a thorough understanding of the anatomy of the intercavernous sinuses is pertinent to

level trainees with a valuable resource for laboratory and preoperative study alike.

Methods: Six sides of three formalin-fixed latex-injected specimens were dissected under microscopic magnification. A retrosigmoid craniotomy was performed by each of three neurosurgery residents, under supervision by the senior authors (C.L.D. and M.J.L.) and a graduated skull base fellow, neurosurgeon, and neuroanatomist (MPC). Dissections were supplemented with representative case applications (**Fig. 1**).

Results: The retrosigmoid craniotomy (aka, lateral suboccipital approach) affords excellent access to CN IV–XII, with corresponding applicability to numerous posterior fossa operations. Key steps include: positioning and skin incision, scalp and muscle flaps, burr hole and parasigmoid trough, craniotomy flap elevation, initial durotomy and deep cystern access, completion durotomy, and final exposure (**Fig. 2**).

Conclusion: The retrosigmoid craniotomy is a work-horse skull base exposure, particularly for lesions located predominantly in the cerebellopontine angle. Operatively oriented neuroanatomy dissections provide trainees with a critical foundation for learning this fundamental skull base technique. We outline a comprehensive approach for neurosurgery residents to develop their familiarity with the retrosigmoid craniotomy in the cadaver laboratory in a way that simultaneously informs rapid learning in the operating room, and an understanding of its potential for wide clinical application to skull base diseases (**Figs. 3 and 4**).

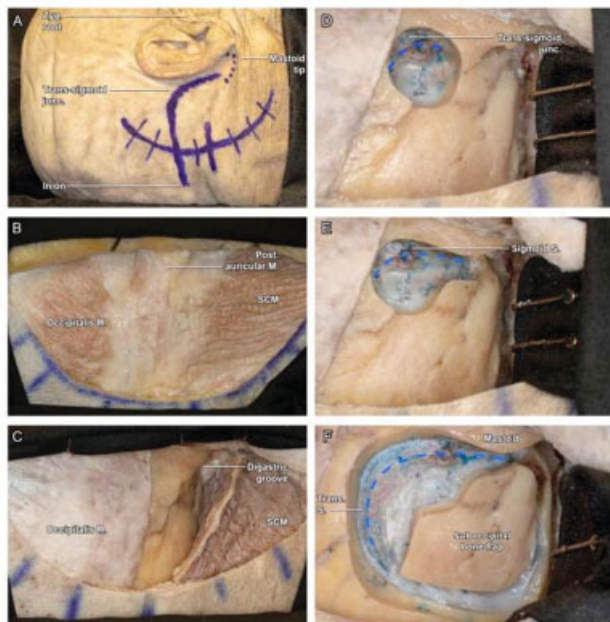


Fig. 1



Fig. 2

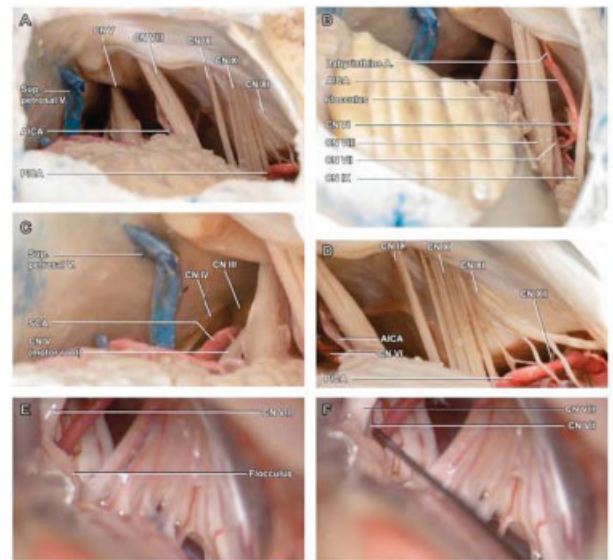


Fig. 3

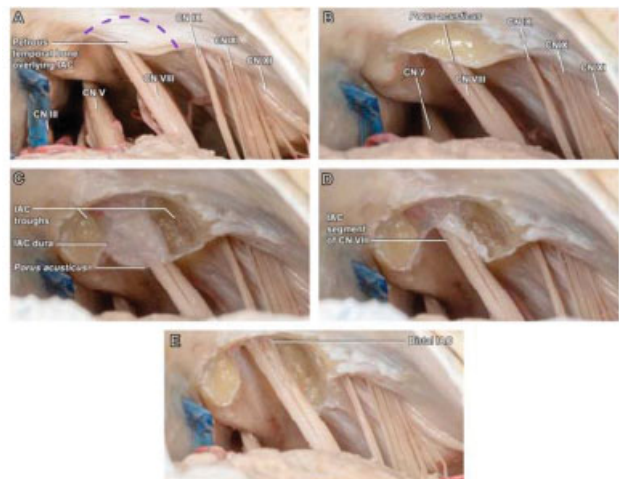


Fig. 4

This document was downloaded for personal use only. Unauthorized distribution is strictly prohibited.

P007. Skull Base Anatomy in Charge Patients with Bilateral Choanal Atresia

Christopher Pool¹, Roshan Nayak², Meghan Wilson¹

¹Penn State Hershey Medical Center, Hershey, Pennsylvania, United States

²Icahn School of Medicine at Mount Sinai, New York, New York, United States

Background: Bilateral choanal atresia (BCA) repair is necessary in neonates as they are obligate nasal breathers. The risk of skull base injury during choanal atresia repair can be mitigated via thorough understanding of skull base anatomy. There is a paucity of data describing differences in skull base anatomy between patients with CHARGE syndrome and those without.

Objectives: To measure nasal and skull base anatomy in patients with isolated bilateral choanal atresia, CHARGE syndrome, and other severe congenital abnormalities to provide low-risk surgical repair.

Methods: A retrospective chart review was conducted of all patients with bilateral choanal atresia with computed tomography images of the maxillofacial region between 2001 and 2019. Choanal width, height, midnasal height, and skull base slope were measured radiographically. Differences in anatomy between healthy patients, those with CHARGE syndrome, and those with other congenital anomalies were compared.

Results: A total of 21 patients with BCA and relevant imaging were identified: 7 with isolated BCA, 6 with CHARGE syndrome, and 8 with other congenital abnormalities of varying severity. The small sample size of this study did not demonstrate significant differences between the groups with respect to choanal height or skull base slope ($p > 0.05$). With equal variance between CHARGE and normal groups, a *t*-test indicated insignificant difference between CHARGE skull base slope and normal patient skull base slope. A similar result of insignificant difference in skull base slope was found between CHARGE and the congenital abnormality group. When comparing CHARGE group to congenital abnormality group and normal patient group (separately), with equal variance, a *t*-test indicated insignificant difference in midnasal skull base height. Patients with concurrent significant congenital abnormalities, not including CHARGE, were found to have a higher incidence of bony atresia versus membranous. Two patients in the congenital anomaly group were found to have skull base defects preoperatively.

Conclusion: Currently, this study represents the largest description of skull base and nasal anatomy in patients with CHARGE syndrome and BCA. While no statistical significant difference was identified due to the small sample size of this study, these measurements may approach significance with larger sample size and aid in the avoidance of skull base injury during BCA repair.

P008. Microsurgical Anatomy of the Inferior Petroclival Vein: An Anatomic and Radiologic Study

Satoshi Matsuo¹, Noritaka Komune², Sojiro Yamashita¹, Yuichiro Miyamatsu¹, Toshiyuki Amano¹, Akira Nakamizo¹

¹Department of Neurosurgery, Clinical Research Institute, National Hospital Organization Kyushu Medical Center, Fukuoka, Japan

²Department of Otorhinolaryngology, Graduate School of Medical Sciences, Kyushu University, Fukuoka, Japan

Objective: The inferior petroclival vein courses along the extracranial surface of the petroclival fissure. It is occasionally involved in vascular diseases and has recently been used for vascular access to the cavernous sinus. However, detailed descriptions of its anatomy are currently lacking.

This study aimed to define the anatomic relationship between the inferior petroclival vein and its surrounding structures based on cadaveric dissection and radiologic analysis.

Methods: A cadaver was dissected step-by-step to reveal the relationships between the inferior petroclival vein and the surrounding structures. The existence of the inferior petroclival vein and its relationships with other venous structures were also examined retrospectively by contrast-enhanced, fat-suppressed T1-weighted magnetic resonance imaging (MRI) in 26 adult Japanese patients (51 sides).

Results: Stepwise cadaveric dissection defined the three-dimensional network of venous structures around the craniocervical junction comprising the jugular bulb, sigmoid sinus, inferior petrosal sinus, suboccipital cavernous sinus, petrosal confluence (also known as the anterior condylar confluence), and inferior petroclival vein, and the posterior, lateral, and anterior condylar veins. The inferior petroclival vein was identified on all sides and was shown to originate from the venous plexus around the carotid artery in all cases. The vein coursed along the petroclival fissure and drained into the petrosal confluence in most cases (39/51, 76.5%), or into the end of the inferior petrosal sinus (10/51, 19.6%), or anterior condylar vein (2/51, 3.9%).

Conclusion: Contrast-enhanced, fat-suppressed T1-weighted MRI allows profound visualization of the venous network at the craniocervical junction, including the inferior petroclival vein. This examination, combined with stepwise cadaver dissection, will aid our understanding of the three-dimensional anatomy in terms of both the venous relationships and the relationships between the vein and surrounding structures. A precise understanding of this anatomy will enable endovascular and skull base surgeons to gain safe access to lesions involving the inferior petroclival vein.

P009. Histology of the Vertebral Artery–Dural Junction: Relevance to Posterolateral Approaches to the Skull Base

Robert Rennert¹, Martin Powers¹, Jeffrey Steinberg¹, Takanori Fukushima², John Day³, Alexander Khelessi¹, Michael Levy¹

¹UCSD

²Carolina Neuroscience Institute, Raleigh, North Carolina, United States

³University of Arkansas, Fayetteville, Arkansas, United States

Objective: The far lateral, extreme lateral infrajugular transcondylar–transtuberular exposure (ELITE), and extreme lateral transcondylar transodontoid (ELTO) approaches provide access to lesions of the foramen magnum, inferolateral-to-mid clivus, and ventral pons and medulla. A subset of pathologies in this region requires manipulation of the vertebral artery (VA)–dural interface. Although a cuff of dura is commonly left on the artery to avoid vessel injury during these approaches, there are varying descriptions on the degree of VA–dural separation that is safely achievable. We herein provide a detailed histologic analysis of the VA–dural junction to guide microsurgical technique for posterolateral skull base approaches.

Methods: An ELITE approach was performed on six preserved adult cadaveric specimens. The VA–dural entry site was resected, processed for histologic analysis, and qualitatively assessed by a neuropathologist.

Results: Histologic analysis demonstrated a clear delineation between the intima and media of the VA in all specimens. No clear plane was identified between the connective tissue of the dura and the connective tissue of the VA adventitia.

Conclusion: The VA forms a contiguous plane with the connective tissue of the dura at its dural entry site. When

performing posterolateral skull base approaches requiring manipulation of the VA-dural interface, maintenance of a dural cuff on the VA is critical to minimize the risk of vascular injury.

P010. Ear through Nose: An Endoscopic Endonasal Approach to IAC and Cochlea—Anatomic Study

Yury Anania¹, Ricardo Gomez Arroyo¹, Eric W. Wang², Georgios Zenonos³, Carl H. Snyderman², Gardner A. Paul³

¹Center for Cranial Base Surgery, University of Pittsburgh, Pittsburgh, Pennsylvania, United States

²Department of Otolaryngology, University of Pittsburgh Medical Center, Pittsburgh, Pennsylvania, United States

³Department of Neurosurgery, University of Pittsburgh Medical Center, Pittsburgh, Pennsylvania, United States

Background: Endoscopic endonasal surgery has become a widely accepted and increasingly adopted approach for skull base surgery in the last decades. It has become relatively widely applied for midline to skull base regions, decreasing morbidity and providing direct access for deep tumors which displace neurovascular structures laterally. While surgical limitations along the sagittal plane have been well-described, coronal/lateral limitations are not as well defined, other than avoiding crossing cranial nerves. The aim of this study was to understand the lateral-most petrous structures accessible endonasally, namely the IAC and cochlea, which might become relevant in level IV–V surgeries for tumors expanding into the petrous bone.

Methods: The IAC and cochlear anatomy were evaluated relative to neighboring structures through an endoscopic endonasal transnasal, infrapetrous, and contralateral transmaxillary (CTM) approach in 10 colored silicon-injected human head specimens (20 sides). Semicircular canals and otic capsule were excluded from this anatomical description, since their location lateral to the IAC obviates their access from an endonasal perspective. The relationship between the IAC/cochlea and trigeminal nerve, Gasserian ganglion, foramen lacerum, posterior genu and petrous portion of ICA and GSPN were evaluated with the aid of image guidance (**Fig. 1**).

Results: The trigeminal nerve at the porus trigeminus remained one of the most important landmarks: it was identifiable (i.e., visible or barely visible) through its dural covering in 19/20 sides (**Fig. 2**). The IAC was always located above (left, 8.63 ± 0.97 mm; right, 8.36 ± 0.93 mm), a plane passing through the foramen lacerum, near or at the level of the lateral margin of the porus segment of the trigeminal nerve (left, 2.55 ± 0.384 mm; right, 2.11 ± 0.335 mm). However, in their anterior course, the trigeminal and facial-cochlear complex separate, creating an angle (left trigeminofacial angle, 56.9 ± 6.0 degrees; right trigeminofacial angle, 57.8 ± 12.5 degrees) where, anteriorly, lies the basal turns of the cochlea. The mean distance from the lateral porus segment of the trigeminal nerve and the cochlea was 10.45 ± 1.651 mm and 10.5 ± 1.547 mm on the left and right side respectively. In all of our specimens the basal turn of the cochlea was always located posterior or posterolateral to the posterior genu of the petrous ICA: in all of our dissections, the cochlea was not reachable through a CTM alone without unsafe manipulation of the paraclival ICA (**Fig. 3**).

Conclusion: The cochlea and IAC remain the most lateral structures which can be visualized from an endoscopic endonasal perspective, and as a result of our dissection, they are unlikely to be damaged. These are not surgical targets, but rather anatomical structures at the lateral limit of access for endoscopic endonasal and CTM approaches to the petrous bone.

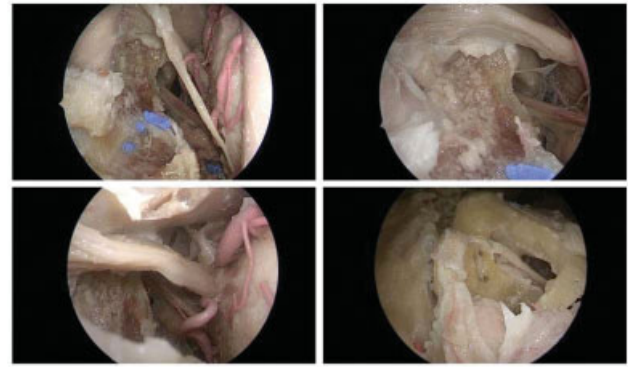


Fig. 1

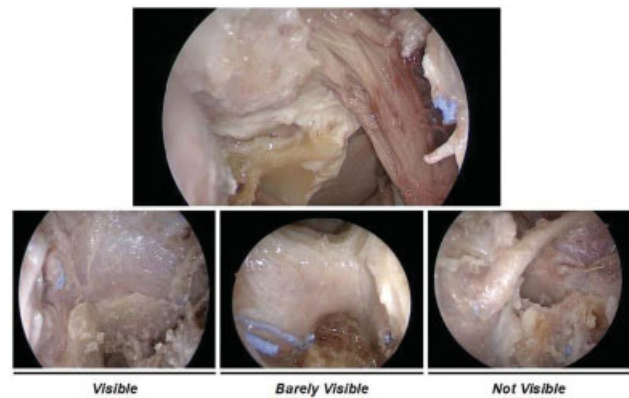


Fig. 2

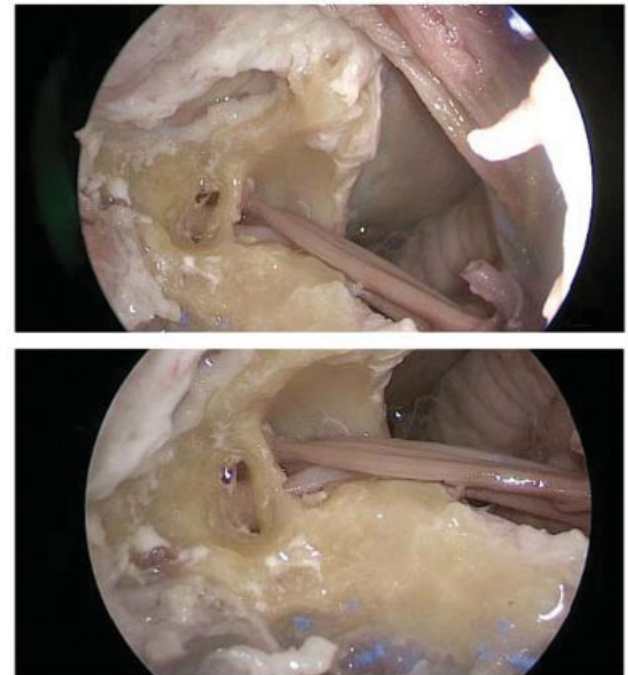


Fig. 3

P011. Morphometric Analysis of the Petroclival Angle in Adults Using High Resolution CT Scans

Ahmad Alhourani¹, Zaid Aljuboori¹, Candice Nguyen¹, Heegok Yeo¹, Brian Williams¹, Norberto Andaluz¹

¹University of Louisville, Louisville, Kentucky, United States

The Petroclival region is an integral part of skull base surgery. It can harbor different pathologies and can be used to access important areas such as the petroclival angle, cerebellopontine angle, and other areas. Lesions of this area pose a challenge to surgeons due to proximity to critical structures. Different surgical approaches are available to treat lesions in this region. The choice between different approaches is based on surgeon's experience and preference, the neurovascular anatomy, and lesions' characteristics. Here, we present the results of the morphometric analysis of the petroclival angle using high resolution computed tomography images in adults.

One hundred adult patients who underwent a computed tomography scan of the temporal bone at our institution were selected. Exclusion criteria included patients <18 years of age, radiographic evidence of trauma, neoplastic, infection, or previous surgery at the region of interest, and congenital deformities of the skull base. Images were acquired with a resolution of 512×512 , and 1 mm slice thickness. The images then were analyzed using OsiriX MD (Bernex, Switzerland). We measured clival central depression angle, petroclival angle at the level of the carotid foramen, the internal auditory meatus (IAC), and the carotid canal. We also measure the inter IAC distance, and inter jugular foramen distance.

The average age was 49.8 with 57% males. The median central clival depression angle was 142.6 (IQR: 128.6–156.6) degrees. The median petroclival angle at the level of carotid canal (CC), IAC, and carotid foramen (CF) were 142.7 (IQR: 130.7–154.7), 154.31 (IQR: 142–166.5), and 167.5 (IQR: 155.8–179.1) degrees, respectively. The comparison analysis between males and females showed that females have a shorter inter IAC distance (48 vs. 50.4 mm, $p < 0.05$), and narrower petroclival angle at the carotid canal level (141 vs. 144.5 degrees, $p < 0.05$). The correlation analyses of different parameters showed that the central clival depression angle correlated negatively with the petroclival angle at every level (CF: $\rho = -0.39$, IAC $\rho = -0.55$ and CC $\rho = -0.23$, $p < 0.05$; **Fig. 1**). The petroclival angle at the level of the IAC and the carotid canal correlated positively with the inter IAC distance (IAC $\rho = 0.3$, CC $\rho = 0.32$, $p < 0.05$; **Figs. 2 and 3**). The inter IAC distance correlated positively with the interjugular foramen distance ($\rho = 0.39$, $p < 0.05$; **Fig. 4**).

The anatomical variability of the petroclival angle among patients can be used to guide surgical approach selection. For clival and petroclival angle lesions a narrow petroclival angle can limit the working corridor for retrosigmoid approaches, which can be circumvented by opting for anterior petrosal or transclival approaches.

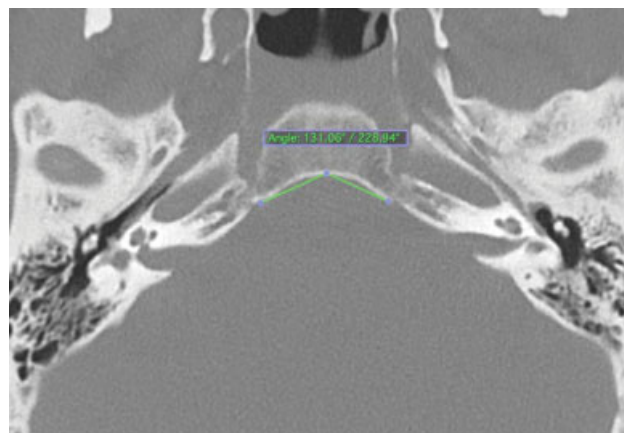


Fig. 1

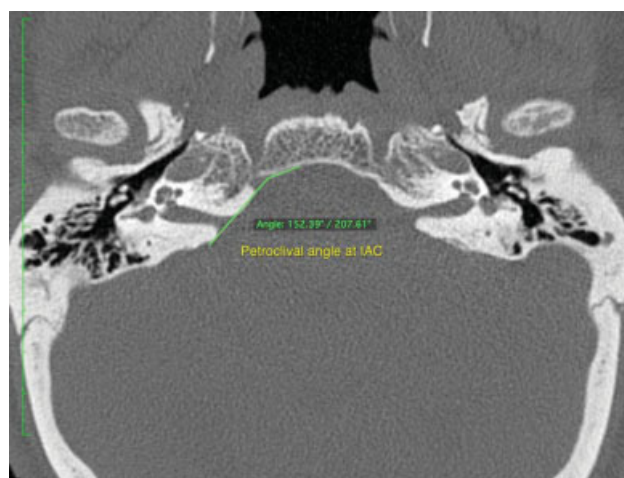


Fig. 2

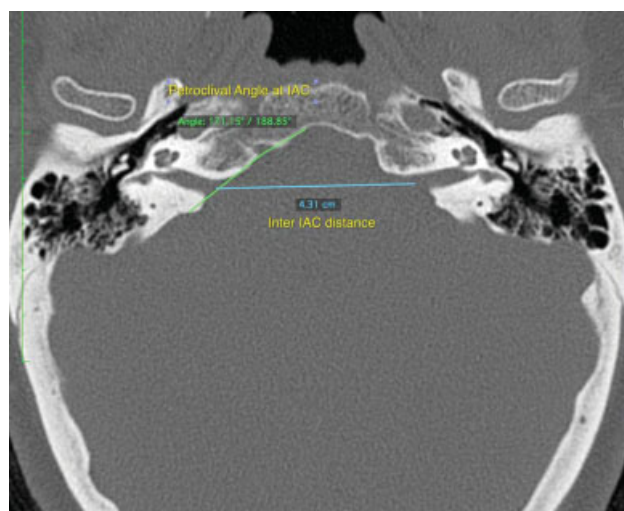


Fig. 3

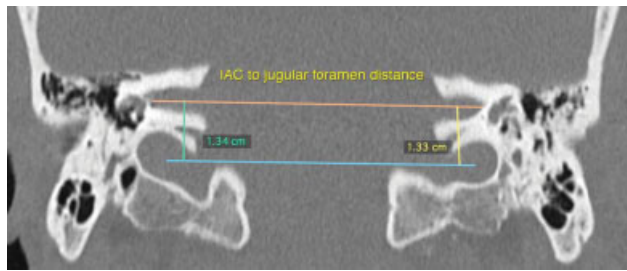


Fig. 4

P012. Anatomical Study of the Jugular Foramen in Cadaverous Specimens in the Mexican Population, Varieties and Constants

Alfredo Espinosa Mora¹, Humberto Reyna Mendez¹, Enrique Lopez Berumen¹, Carlos Erosa Velázquez¹, Diego Méndez Rosito¹

¹CMN 20 DE Noviembre

Background: The jugular foramen (FY) described since 1934 by Hovelacque, in two compartments: one anteromedial called the nerve part (pars nervosa) and another posterolateral, called the venous part (pars vascularis), terms that are still valid to date.

Recently Katsuta has made a division into three compartments: posterolateral, anteromedial and an intermediate or neural, a method that has been well received by current anatomists.

The jugular foramen (FY) has been described as the most complex of all the forages of the skull base, and the one with the greatest challenge for surgical approaches, located in the posterior fossa formed by the union of the temporal and occipital bones, in the back of the petroccipital fissure.

It represents a communication between the posterior fossa of the base of the skull and the superolateral region of the neck, connecting between these a third of the cranial nerves and the greater cerebral venous drainage system.

Its complexity lies in the deep location, variability in shape and size in each skull, and even from side to side within the same skull, in addition to its irregular shape, the neurovascular structures that pass through it and the structures through which it is surrounded.

The purpose of this work was to carry out a laboratory study of anatomical specimens, identifying the various neural structures of the jugular foramen.

The main neural structures that cross it and the main differences in the Mexican population with respect to their comparison in world literature were to properly understand the predominant anatomy to help plan the ideal approach route.

Material and Methods: Measurements were taken with digital caliper of a total of 120 adult skulls, with a total of 240 jugular forages, measurements of the anteroposterior, and laterolateral diameter and measurements of the intrajugular process were made, the distance from the upper edge of the foramen to the lower edge of the duct was measured Internal auditory, from the lower edge of the FY to the foramen magno, from the most anterior edge of the FY to the trigeminal impression, the largest size between each foramen was taken into account.

Digital photographs were subsequently taken with a high-definition camera, exemplifying the measurements made; shots were taken from superior, posterior oblique, lateral views, and from the exocranial face.

The measurements found were analyzed using the SPSS software and plotted to obtain the results of the investigation. Surgical approaches to the jugular foramen were performed in cadaveric specimens.

Discussion and Conclusion: It will be important variations which are commented more specifically in the complete work, the data obtained serve as the basis for further studies, as well as support for decision making, regarding surgical approach.

P013. Microsurgical Anatomy of the Triangles of the Posterior Fossa: Neurosurgical Relevance

Alejandro Monroy-Sosa¹, Srikant Chakravarthi¹, Jonathan Ortiz Rafael¹, Austin Epping¹, Richard Rovin¹, Melanie Fukui¹, Amin Kassam¹

¹Aurora Neuroscience Innovation Institute, Milwaukee, Wisconsin, United States

Introduction: Tumors of the posterior fossa, which often distort regional anatomy, can be located either dorsal/lateral or ventral/medial to the cranial nerves. Further identification of anatomical landmarks and assigning a relative relationship to neurovascular elements be an important adjunct during surgical decision-making.

Objectives:

1. To describe a system of three anatomically-based triangles of the posterior fossa according to the relative position of neurovascular complexes.
2. To describe these triangles with clinical cases.

Method: Ten fully embalmed cadaveric specimens injected with colored silicon were studied bilaterally (20 sides). Retrosigmoid, extended retrosigmoid and far lateral approaches were studied and triangles were projected from key osseous landmarks (asterion, superior nuchal line (SNL), mastoid emissary vein foramen (MEVF) and condylar emissary vein foramen (CEVF). Neurovascular complexes, as previously described by Rhoton, forming these triangles consisted of the following components: cranial nerves, superior petrosal vein, tentorium, petrous bone, and brainstem. Clinical cases were described (Fig. 1).

Result: Topographic anatomy was divided in superior, middle, and inferior regions.

Superior: Formed by the asterion and SNL and corresponds with the upper neurovascular complex. The asterion was found superior to the SNL in seven sides, and at the same level to the SNL in three sides. In addition, it was found in the same position of the transversal sinus in 8 sides and above to the transversal sinus in two sides. The distance between the asterion and the (MEVF) was on average 19.75 mm. The petrous-tentorial triangle, formed by the superior petrosal venous complex, tentorium, petrosal and tentorial surfaces of the cerebellum. The petrous-acousticofacial triangle (PAFT), formed by the superior petrosal venous complex, acousticofacial complex, petrous bone, and pons.

Middle: formed by the MEVF and corresponds with the middle neurovascular complex. The MEVF was present in eight sides and absent in two sides; distance to the SNL was on average 13.25 mm. The MEVF was found laterally to the sigmoid sinus in all sides (average 10 mm). Acousticofacial-trigeminal triangle (AFTT), formed by the acousticofacial complex trigeminal nerve-cerebellar petrosal surface. The Acousticofacial-Glossopharyngeal triangle (AFGT), formed by the acousticofacial complex, CN IX, petrous bone, and brainstem (Figs. 2-4).

Inferior: formed by the CEVF and the occipital condyle and corresponds with the lower neurovascular complex. It was present in all sides and the distance between the MEVF and CEVF tracing a perpendicular line was on average 32.25 mm. The distance between SNL and CEVF was on average 47.10 mm and the distance between the SNL and occipital condyle was on average 50.70 mm. The vagoaccessory triangle formed by the cisternal segment of the vagus-spinal root of the accessory nerve and the medulla. The

suprahypoglossal triangle (SHT) formed by the vagus, spinal, and the hypoglossal cranial nerves. The infrahypoglossal triangle (IHT) formed by the spinal, hypoglossal, and the medulla.

Conclusion: The development of anatomically based triangles in navigation in the posterior fossa may facilitate in organization and categorization of regional anatomy. Explicitly, these triangles may serve as a reliable in deciding the appropriate surgical route in addressing pathologies of the cerebellopontine angle.

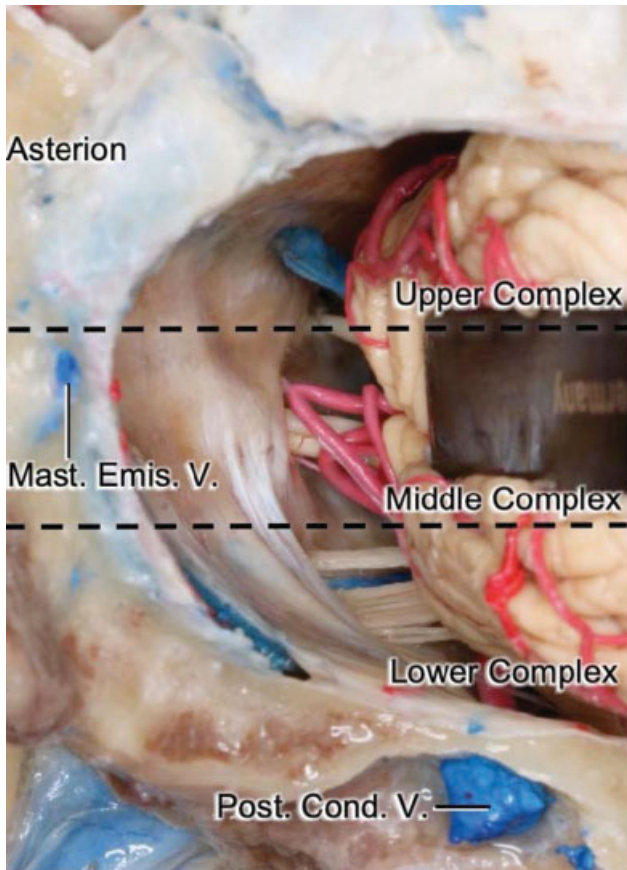


Fig. 1

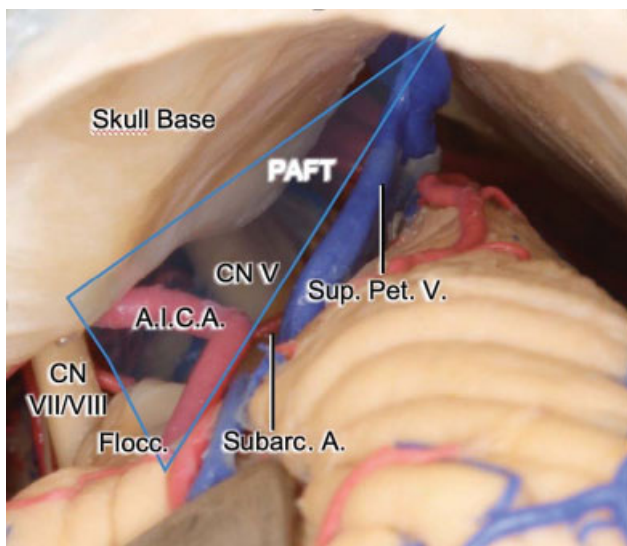


Fig. 2

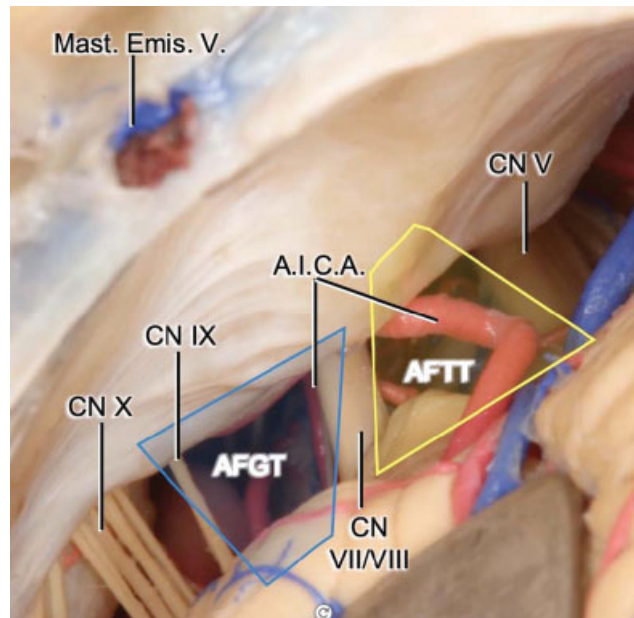


Fig. 3

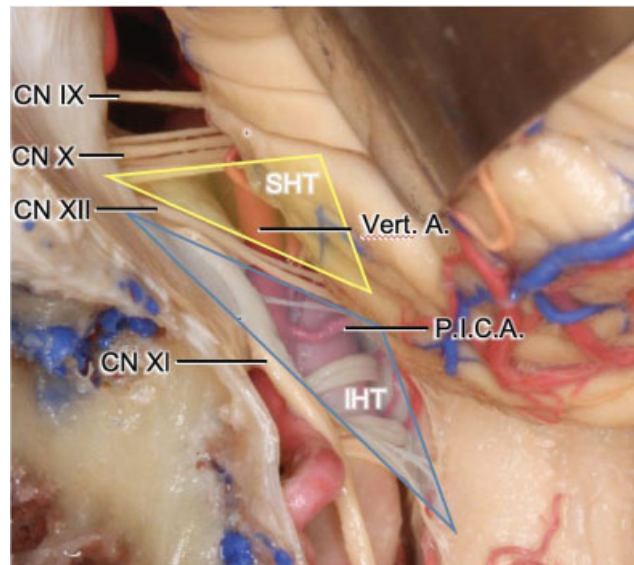


Fig. 4

P014. Surgical-Anatomical Pillars of Posterior Petrosectomy: A Tridimensional View

Alejandro Monroy-Sosa¹, Srikant Chakravarthi¹, Austin Epping¹, Richard Rovin¹, Melanie Fukui¹, Amin Kassam¹

¹Aurora Neuroscience Innovation Institute, Milwaukee, Wisconsin, United States

Introduction: Tumors, localized in the petroclival region and jugular foramen, are commonly accessed via a posterior petrosectomy. Due to complex nature of posterior fossa anatomy, surgery can be difficult, requiring enhanced technical ability. Tumors in the posterior fossa often distort the normal anatomy; this is of critical importance, especially when locating the vessels and cranial nerves. As such, enhanced and organized anatomical knowledge of the

petrosectomy, which is often required for access, may be helpful in surgery.

Objectives:

1. To describe relevant anatomical landmarks for performing the posterior petrosectomy.
2. To create a coordinate-projection system in localizing the structures deep to the mastoid.
3. To represent these landmarks in clinical cases.

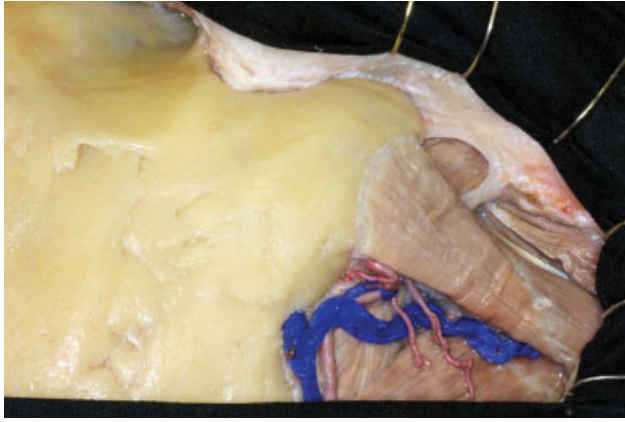


Fig. 1

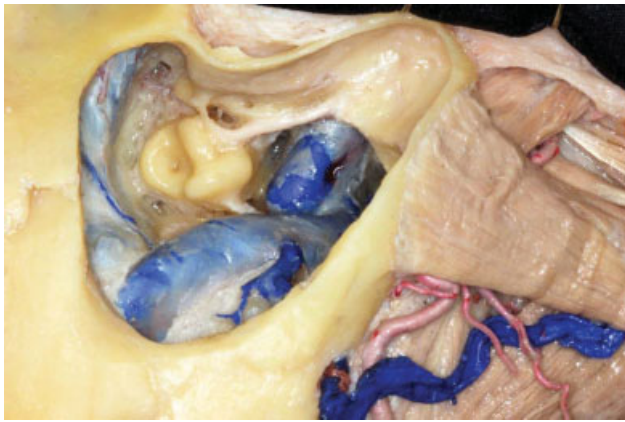


Fig. 2

Method: 10 formalin-fixed cadaver heads, injected with blue and red silicon, were used. Cadavers were also CT-scanned and images were co-registered to allow for real-time navigation of the osseous structures. We projected the superficial soft tissues (muscle) and relevant bony landmarks to important deep structures in the mastoid. Three clinical cases were described to apply this projection system to surgical practice.

Result: We described three anatomical lines as follows: (1) superior: the insertion of the nuchal muscles in the superior occipital line projects with the asterion and supramastoid crest. These landmarks are important in delineating the mastoidectomy. These landmarks project to the temporal dura, the superior part of the mastoid antrum and the sinodural angle; (2) middle: the insertion of the preauricular muscle, the spine of Henle and the suprameatal triangle projects to the horizontal semicircular canal, and tympanic segment of the facial; and (3) inferior: the mastoid tip and insertion of the posterior belly of the digastric muscle projects to the jugular bulb. The main anatomical landmarks of

the superior line allow us to understand the superior limit of the mastoidectomy; the middle line is a safe zone for drilling and to localize relevant anatomical structures (i.e., facial nerve canal), and the inferior line corresponds to the mastoid tip that corresponds to contents of the jugular foramen.



Fig. 3

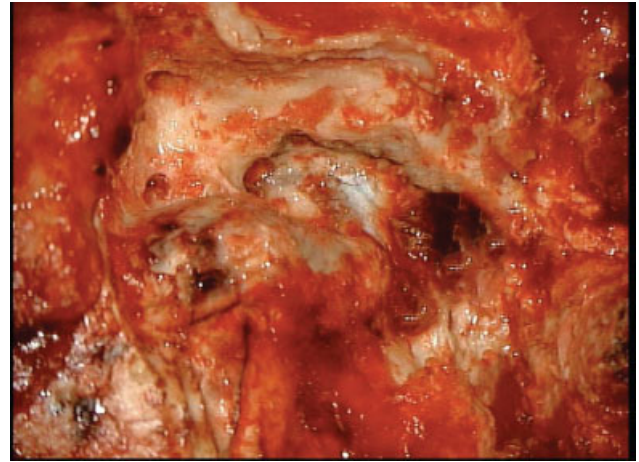


Fig. 4

Conclusion: The proposed posterior petrosectomy projection system using three anatomic lines, from superficial to deep, permitted reliable and reproducible localization of the inner anatomical structures, especially with a more confident ability to locate the facial canal intraoperatively.

P015. Nuances of the Surgical Management of the Paranasal and Ventral Cranial Base Malignancies: The Endonasal Endoscopic Approach

Alejandro Monroy-Sosa¹, Srikant Chakravarthi¹, Austin Epping¹, Juanita M. Celix¹, Richard A. Rovin¹, Melanie B. Fukui¹, Amin B. Kassam¹

¹Aurora Neuroscience Innovation Institute, Milwaukee, Wisconsin, United States

Introduction: Malignancies of the ventral cranial base can often extend into the sinuses, paranasal sinuses, orbit and extracranial fossa. As such, surgical management can be more difficult and often requires enhanced technical ability.

Traditionally, two routes are employed to reach these tumors: (1) transfacial, cranial and craniofacial (combined) approaches, and (2) endonasal endoscopic approaches. Malignancies in the ventral cranial base often distort the nasal cavity making it difficult to locate the internal carotid artery (ICA), and an inadvertent damage could lead to serious complications.

Objectives: The objectives of this study are: (1) to describe relevant anatomical landmarks for localizing the ICA, (2) to create a projection system in localizing the ICA, and (3) to validate these landmarks in clinical cases.

Method: Ten formalin-fixed cadaver heads, injected with blue and red silicon, were used. The cadavers were CT-scanned and images were coregistered to allow for real-time navigation of the osseous structures. The anatomical dissections were performed by endoscopic vision (0o lens). Relevant anatomical landmarks are the vertical lamella of the superior turbinate, palatine bone, vidian canal, and Eustachian tube were analyzed for localizing the segments of the ICA.

Result: We described three anatomical landmarks: (1) superior: projects to the paraclinoid internal carotid artery (ICA), (2) middle: projects to the genu of the ICA, and (3) inferior: projects to the parapharyngeal ICA. The superior landmark is the basal lamella of the middle turbinate and the lacrimal crest, which projects laterally to the lamina papyracea. The lamina papyracea allows for an understanding of the orbit anatomy and reaches to the paraclinoid ICA, through the orbitosellar line which connects the orbit to the sellar region. The middle landmarks: the posterior adhesion of the middle turbinate to the ethmoidal crest; this bony structure allows for identification of the sphenopalatine foramen and the vidian canal is above and medial to the pterygopalatine foramen, and provides a guide to the genu of the ICA. In addition, we created a vertical line from the vidian canal to the lateral opticocarotid recess for localizing the paraclinoid carotid. The main anatomical landmarks of the inferior pillar, is the posterior adhesion of the inferior turbinate with the conchal crest and the Eustachian tube. The distance from the Eustachian tube to the carotid was on average 22 mm. Three clinical cases were shown to exemplify each anatomical landmark.

Conclusion: The correlation of the three anatomical landmarks allowed for reliable localization of the ICA, with a more confident ability to control the ICA intraoperatively, especially in the event that anatomy is distorted by surrounding tumor.

P016. The Role of the Petroclival Fissure as a Surgical Landmark for the Hypoglossal Canal

Roberto M. Soriano¹, Gustavo Pradilla¹, C. Arturo Solares¹
¹Emory University (SSO), Atlanta, Georgia, United States

Background: With advances in anatomical knowledge, surgeon expertise and the use of extended or transoral approaches, endoscopic surgery may be indicated for varied pathologies and can be used for more extensive resections. When extracranial dissection in the petroclival region extends posteriorly, it is important to have a good understanding of its relation to surrounding structures. Among these structures, the location of the hypoglossal canal (HC) is particularly important to avoid injury to the hypoglossal nerve (XII). In this study, we investigate the anatomical relations of the petroclival fissure (PCF) and its use as a landmark for locating the HC.

Study Design: Cadaveric study.

Methods: Endoscopically assisted transoral dissection was performed bilaterally on three latex-injected cadaveric

specimens. Following parapharyngeal space dissection and Eustachian tube removal, remaining musculature and fibrous tissue were removed from the skull base, exposing the foramen lacerum (FL), clivus, petrous bone (Pe), and PCF. Measurements, using a surgical ruler, were made as part of the evaluation of the spatial relation between the PCF and HC. High definition endoscopic images were also obtained demonstrating this relation.

Results: The PCF runs between the clivus and petrous bone and extends from the FL to the jugular foramen (JF). The PCF can be divided, by creating a vertical line from the FL to the PCF, into a descending and lateral segment. The descending segment takes an anterior to posterior and cephalic to caudal direction, and extends from the FL to the intersection of the line and PCF. The lateral segment courses in a medial to lateral and anterior to posterior direction, and extends from the line to the termination of the PCF at the jugular foramen. The HC was identified bilaterally in all specimens by creating a straight line from the FL along the petrous border of the descending PCF. The HC lies directly along the trajectory of this line. The distance from the FL to the HC (FL-HC), along this line, was measured bilaterally on all specimens (six sides), with a mean of 20 mm (SD = 1 mm; **Figs. 1-3**).

Summary: The PCF serves as a reliable landmark in the location of the HC. It can be divided into two segments and can be used to locate the HC by using a line created from the FL to the HC along its descending portion at a distance of 20 ± 1 mm. Detailed knowledge of this anatomical relationship is necessary for safe dissection of the petroclival region, especially when in proximity to the HC.



Fig. 1



Fig. 2

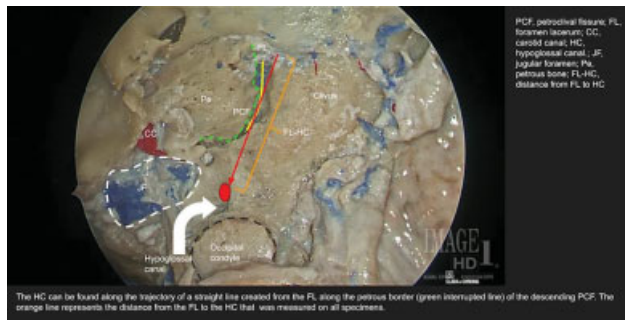


Fig. 3

P017. Periclinoid and Pericavernous Surgical Corridors to the Cavernous Sinus: An Extensive Anatomical Analysis

Alexander I. Evins¹, Giovanni Barbagli¹, Lukasz Przepiórka¹, Michael G. Kim¹, Jimmy J. Xia¹, Gabriel M. Longo¹, Paolo Di Russo¹, Philip E. Stieg¹, Antonio Bernardo¹

¹Department of Neurological Surgery, Weill Cornell Medicine, New York, New York, United States

Background: Lesions involving the cavernous sinus (CS) represent some of the most challenging pathologies of the skull base due to the dense surrounding neurovasculature. Extradural exposure and preparation of this region, whether as initial preparation for a combined intra-extradural approach or as the main avenue of surgical exposure, can enlarge surgical corridors and minimize retraction. We describe the surgical approaches to this region, the entry corridors to the CS that are available within each approach, and the surgical exposure provided by each of these corridors. Additionally, we describe and demonstrate how extradural and intradural preparation of these surgical corridors can be used to widen the available working space and facilitate surgery of the CS.

Methods: Pterional, frontotemporal-orbital, fronto-orbitozygomatic, frontozygomatic, conservative perilabyrinthine transtentorial, and endoscopic transnasal transsphenoidal approaches were performed on cadaveric heads to access the periclinoid and pericavernous regions. Periclinoid techniques (cutting of the meningo-orbital band, anterior clinoidectomy, unroofing of the superior orbital fissure, unroofing of the optic canal, displacement of the extra-annular structures, opening of the annulus of Zinn, and extradural dissection of the CS), pericavernous techniques (cutting of the distal dural ring, falciform ligament, and optic sheath; mobilization of the supraclinoid ICA, opening of the porus oculomotorius, and mobilization of CN III), and peritrigeminal techniques (mobilization of CN's V2 and V3), along with other maneuvers were performed. The CS was divided into eight anatomical compartments and nine entry corridors were described, and exposure was assessed accordingly.



Fig. 1

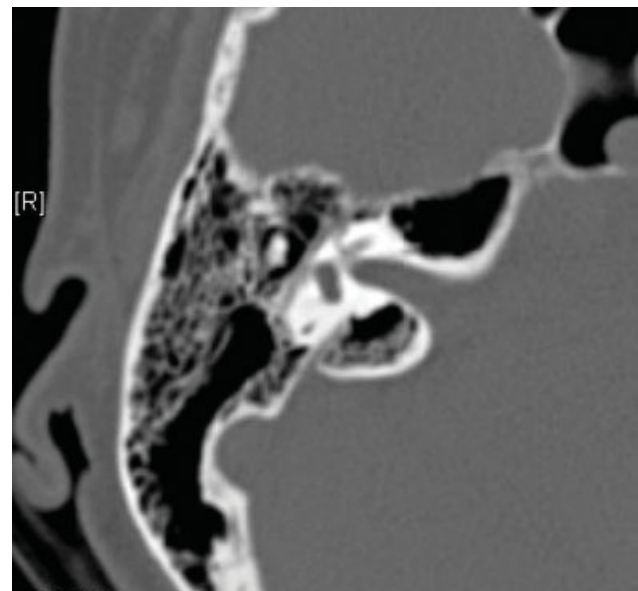
Results: The standard pterional transsylvian approach provided access solely to the intradural parasellar entry corridor into the superior wall of the CS. Extending this approach with an extradural anterior clinoidectomy and unroofing of the optic canal allowed for application of the pericavernous maneuvers and enlargement of the entire parasellar corridor and exposure of the carotid cave. The extradural pterional approach, with or without removal of the anterior clinoid, was allowed for limited access, only one of the six corridors, into the lateral wall of the CS. The frontotemporal-orbital approach also provided access extradurally to one entry corridor and intradurally to the posterior portion of the parasellar corridor. Extending this approach with the periclinoid and pericavernous maneuvers allowed for full exposure of three of the lateral wall corridors and an enlarged parasellar corridor. The fronto-orbitozygomatic approach provided access extradurally to four of the corridors into the wall, as well as the posterior portion of the intradural parasellar corridor. Application of periclinoid, pericavernous, and peritrigeminal maneuvers, allowed for exposure of all six lateral wall entry corridors, as well as an enlarged parasellar corridor. The frontozygomatic approach provided access to three lateral wall corridors extradurally, and the posterior parasellar window intradurally, all of which were expanded following pericavernous and peritrigeminal maneuvers. The conservative perilabyrinthine transpetrosal transtentorial approach to the posterior wall was enlarged with opening of Dorello's canal and the endoscopic transnasal transphenoidal approach was enlarged with opening of the optic canal.

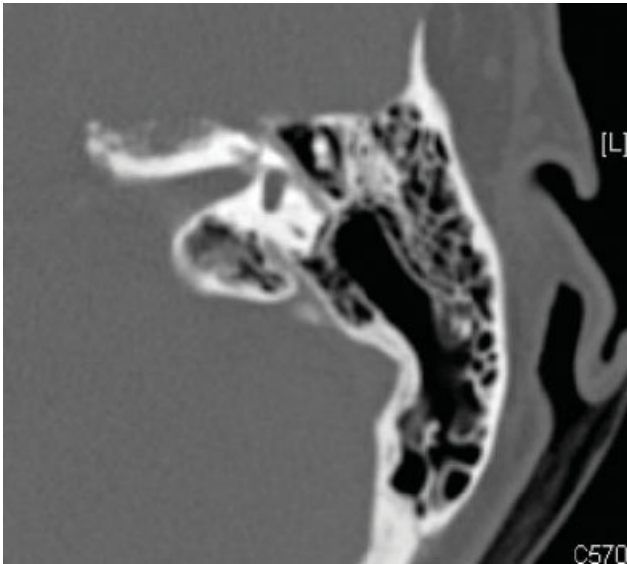
Conclusion: Extradural exposure is essential whether as initial preparation for a combined intra-extradural approach or as the main avenue of CS surgical exposure.

P018. Near Dehiscence of the Endolymphatic Duct and SAC

Neal M. Jackson¹

¹Tulane University, New Orleans, Louisiana, United States





This radiographic case report showcases bilateral near-dehiscence of the endolymphatic duct and sac on imaging of the temporal bone. The endolymphatic duct and sac are structures of the temporal bone and posterior cranial fossa that are normally well protected in bone. They are critical to inner ear function and can be at risk if exposed during skull lateral base surgery. In this case, the structures are near-zero-dehiscent and at greater risk during temporal bone drilling. Axial, sagittal, and coronal views on high definition computed tomography scans are available for display. The endolymphatic duct can clearly be seen in the hyperpneumatized temporal bone as a soft-tissue density linear structure communicating from the otic capsule to the posterior fossa. Bilateral images are included and show the entire course of the duct in single image. This patient underwent infralabyrinthine approach to a jugular foramen chondrosarcoma, and hearing preservation was achieved. Lateral skull base surgeons should be aware of the possibility of dehiscence or near-dehiscence of the endolymphatic sac and duct as injury with high speed drill could lead to complete hearing and vestibular loss.

P019. Anatomical Step-by-Step Dissection of Complex Skull Base Approaches for Trainees: Surgical Anatomy of the Translabyrinthine Approach

Avital Perry¹, Christopher S. Graffeo¹, Lucas Carlstrom¹, Colin L. Driscoll¹, Michael J. Link¹, Maria Peris-Celda²

¹Mayo Clinic, Rochester, Minnesota, United States

²Albany Med, Albany, New York, United States

Introduction: Surgical neuroanatomy is the cornerstone of skull base education. However, although a large number of anatomic and operative atlases have been published both in print and online, most utilize illustrations rather than cadaveric dissections, focus on nonoperative views, or are written for a higher level target audience, rather than junior-level residents. Our objective is to describe, step-by-step, a translabyrinthine approach dissection, in a way that is educationally valuable for trainees at numerous levels.

Methods: Six sides of three formalin-fixed latex-injected specimens were dissected under microscopic magnification. A translabyrinthine approach was performed by

each of three neurosurgery residents, under supervision by a senior skull base team (C.L.D. and M.J.L.) and the primary investigator, a graduated skull base fellow, neurosurgeon, and neuroanatomist (MPC). Dissections were supplemented with representative case applications.

Results: The translabyrinthine approach provides excellent access to the entire ipsilateral posterior fossa, via a more lateral and less acute trajectory than the standard retrosigmoid. This correspondingly shortens the working distance to areas of the ventrolateral brainstem, and affords wide applicability to a large number of posterior fossa operations. Key steps include: Positioning and skin incision, myocutaneous flap elevation, superficial mastoidectomy, sigmoid sinus skeletonization, mastoid antrostomy, dural elevation and retractor placement, semicircular canal resection, facial nerve skeletonization, opening of the vestibule, exposure of the jugular bulb and transection of the endolymphatic duct, circumferential skeletonization and un-roofing of the IAC, dural opening, and final intradural exposure.

Conclusion: The translabyrinthine craniotomy is one of the most versatile and widely used lateral skull approaches, with particular utility in the cerebellopontine angle. Neuroanatomic education is a critical aspect of skull base training, which promotes safe, accurate, and gentle surgery, to paraphrase Professor Rhoton. In the current study, we have described and demonstrated with 3D image capture techniques a step-by-step approach to completing a translabyrinthine approach, which will helpfully inform resident and fellow education in the laboratory and in the operating room alike.

P020. Extreme Hyperpneumatization of the Skull Base and C-Spine Associated with Meningitis: Mechanisms and Management

Keonho A. Kong¹, Emily Pascal², Kevin McLaughlin¹, Dwayne Anderson³, Daniel W. Nuss¹

¹Louisiana State University Health Sciences Center - New Orleans, Louisiana, United States

²Tufts University, Medford, Massachusetts, United States

³Department of Radiology, Our Lady of the Lake Regional Medical Center, Baton Rouge, Louisiana, United States

Introduction: Skull base pneumatization varies widely across populations, and patterns of air cell development are unique to each individual, originating from both sinonasal and temporal bone sources. “Hyperpneumatization” of the skull base is seen with some frequency in clinical practice, yet its precise incidence is not well known, perhaps due to lack of uniformity of definition. Specific causes of hyperpneumatization are also not known, but in published case reports and series, it has been theorized that hyperpneumatization of the temporal bone may occur as a result of increased pressures from the middle ear; it seems also likely that certain sinonasal conditions may similarly predispose to hyperpneumatization of the sinuses and anterior skull base. We present a rare case of a patient with “extreme hyperpneumatization” of the skull base, including the temporal bone, sphenoid bone, occipital bone and condyle, the majority of foramen magnum, and the C1 cervical vertebrae, who presented with clinical signs of meningitis. Mechanisms of hyperpneumatization and associated risk of meningitis will be discussed, along with literature review and recommendations for diagnosis and treatment. Implications for avoidance of long-term complications including future meningitis, CSF leakage, and fracture or instability of the craniocervical junction will also be presented.

Case: A 54-year-old female with a history of asthma, aspirin sensitivity, and chronic rhinosinusitis/nasal polyposis

presented with nausea, diplopia, imbalance, and progressive somnolence over 7 to 10 days. She was confused, having difficulty finding her words, and slurring her speech. She had a history of two prior endoscopic sinus surgeries for extensive polyposis. She also reported a habit of frequent, vigorous, high-pressure nose blowing. Physical exam did not reveal photophobia or specific cranial neuropathy, but her cognition, memory and balance were severely disturbed. The clinical impression was that this patient likely had early meningitis. Imaging showed chronic inflammatory-polypoid changes throughout the paranasal sinuses, with absence of bone of the posterior sphenoid sinus and clivus. There was "extreme" hyperpneumatization of the clivus, temporal bone, occipital bone (including the condyle and much of the circumference of foramen magnum), and the right lateral C1 vertebra, notably with both intra- and extradural air at the craniocervical junction (See images). Initial management focused on medical therapy for the meningitis, and the patient responded to intravenous antibiotics, fully returning to her baseline mental, neurological, and functional status within a few days. She was discharged on day 6, and IV antibiotics were continued for 6 weeks. Surgical management 8 weeks later included revision bilateral maxillary, ethmoid, frontal and sphenoid sinusotomies, and placement of right tympanostomy tube. The patient has been clinically well since completing treatment, but we believe that there is clearly significant risk for future complications of this extreme hyperpneumatization. These risks include future meningitis and CSF leakage from dural exposure, and fracture or instability at the craniocervical junction due to fragile osseous structures. Strategies designed to limit these risks, and multidisciplinary evaluation and treatment options, will be discussed.

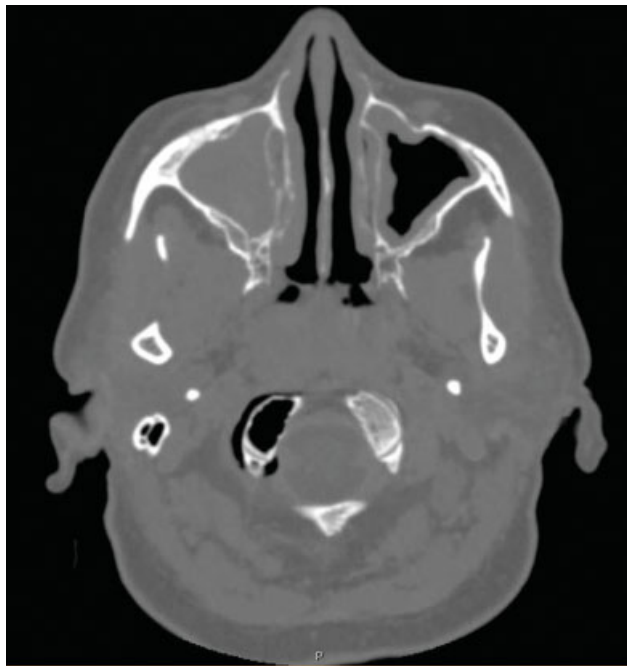


Fig. 1

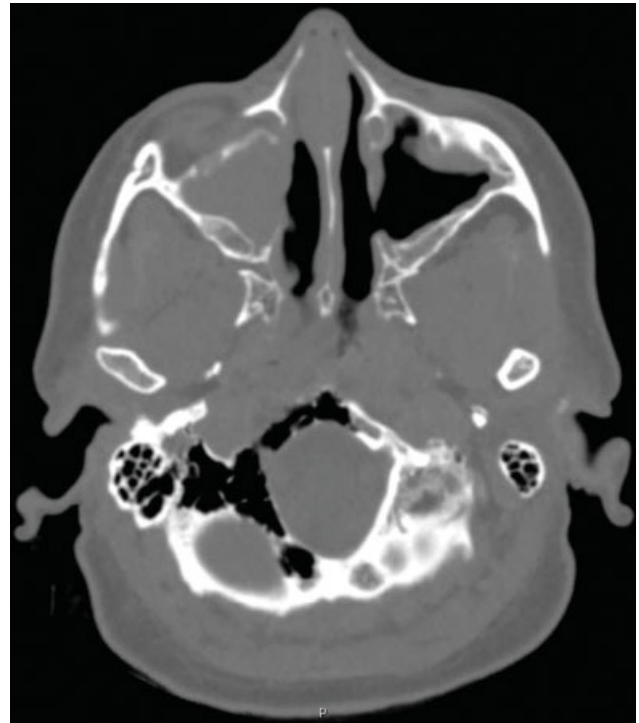


Fig. 2

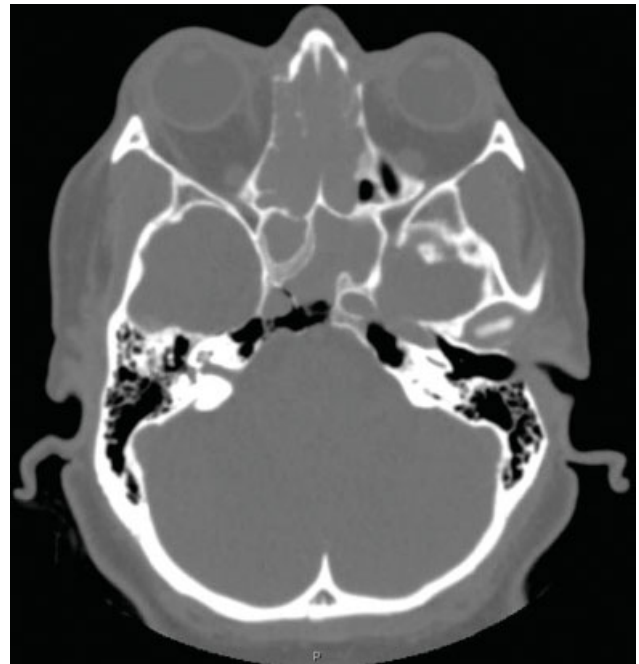


Fig. 3

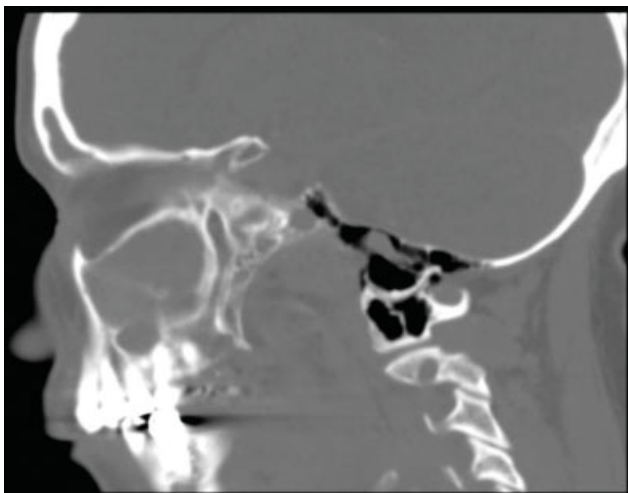


Fig. 4

P021. The Anterior Tentorial Folds: Surgical Significance and Management

Michael G. Kim¹, Alexander I. Evins², Philip E. Stieg², Antonio Bernardo²

¹Department of Neurosurgery, Westchester Medical Center, Valhalla, New York, United States

²Department of Neurological Surgery, Weill Cornell Medicine, New York, New York, United States

Background: As the tentorium curves anteromedially, it gives rise to several ligaments or folds of dura that collectively form a complex architecture around critical neurovascular structures in the sellar region. We describe the surgical significance of this dural architecture and strategies for managing these folds in several different surgical windows.

Methods: Anterior and anterolateral approaches were performed on cadaveric heads to explore the anterior, posterior, and interclinoid folds and their correlating anatomy; proximal and distal dural rings; carotid collar; and the falciform, petrosphenoidal, and petrolingual ligaments. The management of each of these structures when performing periclinoid and pericavernous maneuvers is evaluated in each approach and described accordingly.

Results: The anterior, posterior, and interpetroclinoid folds span between the anterior and posterior clinoid processes and the petrous apex. The anterior petroclinoid fold is encountered when approaching the perisellar area from anterior or anterolateral, whereas the posterior petroclinoid fold is seen when approaching from laterally through a subtemporal approach or posterior through a combined transtentorial approach. The surgical management of these folds depends entirely on the direction from which they are approached.

Conclusion: Understanding the tentorial folds is essential for safely navigating the complex and tightly packed neurovasculature of the anterior and middle skull base and maximizing surgical exposure. Surgical manipulation of these structures can allow for mobilization of the internal carotid artery, exposure of the carotid cave, opening the carotid-oculomotor or opticocarotid window, and exposure of the perisellar area from multiple surgical perspectives.

P022. A Skull Base Surgeon's GPS: 27 Anatomical Triangles of the Anterior, Posterior and Middle Fossae

Dimitri Benner¹, Benjamin K. Hendricks², Mark C. Preul², Michael T. Lawton²

¹Medical University of Vienna, Vienna, Austria

²Barrow Neurological Institute, Phoenix, Arizona, United States

Procedures at the skull base are technically challenging and demand a thorough knowledge of anatomy. Anatomical triangles created by the natural intersection of nerves and vessels have been described to guide the surgeon during delicate dissections along the skull base. These geometrical corridors improve the safety of approach by orientating the surgeon in the operative field, helping to locate the lesion, and protecting critical structures, such as cranial nerves and vasculature. Review of the literature identified 27 anatomical triangles of the skull base. The eight anterior fossa triangles include: interoptic triangle, carotid-oculomotor triangle, optic-carotid triangle, supracarotid-infracarotid triangle, oculomotor-tentorial triangle, precommunicating triangle, junctional triangle, and falcofrontal triangle. The 14 middle fossa/cavernous sinus triangles include: clinoidal/anteromedial triangle (Dolenc), oculomotor/medial triangle (Hakuba), supratrochlear/paramedian triangle, infratrochlear triangle (Parkinson), Anteromedial Triangle (Mullan), Anterolateral Triangle, Posterolateral Triangle (Glasscock), Posteromedial Triangle (Kawase), inferolateral triangle, inferomedial triangle, superior petrosal triangle, parapetrosal triangle, parasellar triangle, and internal carotid artery triangle. The five posterior fossa triangles include: vagoaccessory triangle, suprahypoglossal triangle, infrahypoglossal triangle, Trautmann's triangle/retromental trigone, and Guillain-Mollaret Triangle. Our goal was to create a comprehensive review of skull base triangles, with borders, contents and surgical applications, to increase anatomical knowledge and inform microsurgical dissection.

P023. The Clinoid Space: Surgical Anatomy and Relevance for Endoscopic Approaches

Pedro Augusto Sousa Rodrigues¹, Ayoze Doniz-Gonzalez¹, Ahmed Mohyeldin¹, Guillermo Blasco Garcia de Andoain¹, Lingzhao Meng¹, Qingguo Meng¹, Kumar Abhinav¹, Juan C. Fernandez-Miranda¹

¹Stanford University, Stanford, California, United States

Objective: A carotid injury is a major complication in endoscopic endonasal surgery and the clinoid segment is the most susceptible area. This segment is delimited by the distal and proximal dural rings and is well described from traditional open approaches but is less understood from an endoscopic endonasal perspective. The objective of this study was to provide a detailed investigation of the surgical anatomy and anatomical relationships of this segment from an endonasal and open perspective.

Methods: 6 fresh human silicon-injected heads underwent an endonasal transsellar approach. 12 clinoid segments were dissected to expose the dural rings and their relationship with the pituitary gland, surrounding bone structure and associated ligaments. The clinoid segments were measured and the anatomical variation was recorded (**Figs. 1 and 2**).

Results: we show that the clinoid segment is delimited superiorly by the distal dural ring and inferiorly by proximal dural ring. From a transcranial perspective, the proximal ring is formed by carotidoculomotor membrane, lateral to the carotid artery, and carotidoclinoidal ligament (CCL) medially. Endoscopically, CCL attaches the medial wall of the cavernous sinus (CS) to the anterior clinoid process (**Fig. 3**). We identified several anatomical variations of the clinoid space: (1)

Continuous and thick CCL; (2) fenestrated CCL with direct communication between the clinoid space and the CS; (3) CCL continuous with the inferior parasellar ligament in the CS; and (4) multiple bands of CCL extending and attaching in a vertical orientation to the medial wall of the CS. The morphology of the CCL and dimension of the clinoid space were correlated with the presence and size of the middle clinoid. The caroticoclinoid ligament is the boundary between the clinoid space and the roof of the cavernous sinus, endoscopically. From a transcranial perspective this limit correspond a caroticoculomotor membrane (Fig. 4).

Conclusion: This study provides an important anatomic comprehension of the clinoid space in the endonasal perspective that may facilitate its safe exposure for removal of lesions, minimizing the risk of injury to the internal carotid artery.

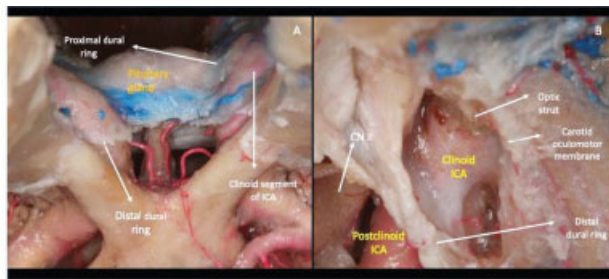


Fig. 1

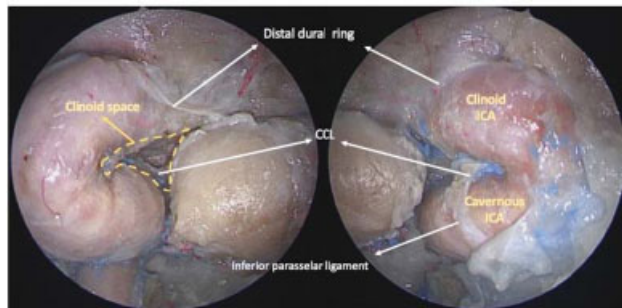


Fig. 2

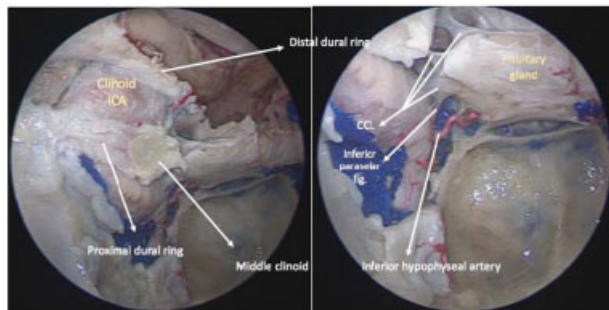


Fig. 3

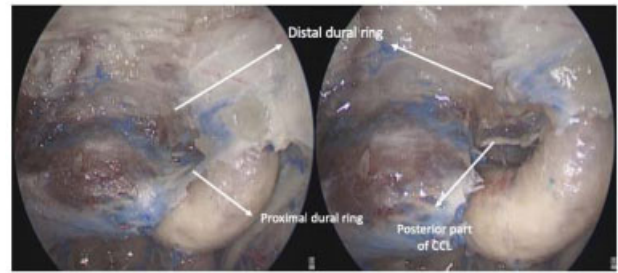


Fig. 4

P024. The Petrous Process of Sphenoid Bone: A Surgical Landmark for the Identification of Abducens Nerve in Endoscopic Endonasal Surgery

Ayoze Doniz-Gonzalez¹, Pedro Augusto Sousa Rodrigues¹, Guillermo Blasco Garcia de Andoain¹, Ahmed Mohyeldin¹, Qingguo Meng¹, Lingzhao Meng¹, Juan C. Fernandez-Miranda¹
¹Stanford University Medical Center, Stanford, California, United States

Objective: The abducens nerve is the most medial of the midline cranial nerves and has several segments; from its origin in the pontomedullary fissure to the lateral rectus muscle. Its identification during expanded endonasal approaches in the coronal plane can be challenging, with the interdural segment being at most risk. The objective of this study was to provide a detailed investigation of the surgical anatomy and anatomical relationships of the interdural segment of the abducens nerve, based on anatomical dissections, anatomical models and imaging studies. In addition, we describe and study the petrous process of sphenoid bone (PPsb), as we believe it could be a key and reproducible landmark to safely identify the abducens nerve during endoscopic endonasal surgery.

Method: Eight fresh human silicon-injected heads underwent an endonasal transclival approach. 16 cranial nerves were dissected to expose the interdural segment of the 6th nerve and its relationship with the petrous process of the sphenoid bone. The distance between the sphenoid sinus floor and petrous process and from petrous process to sellar floor was measured, and anatomical relationships and variations were recorded. The length of the interdural segment was registered. Additionally, we compared the findings with an open transcranial approach (Fig. 1).

Results: The petrous process of the sphenoid bone (PPsb) is a bony prominence in the lateral aspect of the sphenoid body on either side of the dorsum sellae that could be identified in all 8 specimens. It articulates with the apex of the petrous portion of the temporal bone laterally. The sixth nerve was located above the PPsb in all the specimens, just above the petroclival dural fold. Its identification proved to be reliable, as none of the nerves were damaged during the procedure or PPsb drilling. The average height from the sphenoid sinus floor to the PPsb apex was 7 mm and the average distance to the sellar floor was 6 mm. The interdural segment had an oblique trajectory and the average length from its dural entry point to PPsb apex was 8 mm. PPsb was located posteromedial to the paraclival ICA and medial to the foramen lacerum. Gruber's ligament was located posterior to the abducens nerve in all 16 sides, running from the petrous apex to posterior clinoid process (Figs. 2 and 3).

Conclusion: This study identifies the PPsb as an important and reproducible landmark in the early identification of the abducens nerve in endoscopic endonasal

procedures, which should potentially minimize the risk of injury.

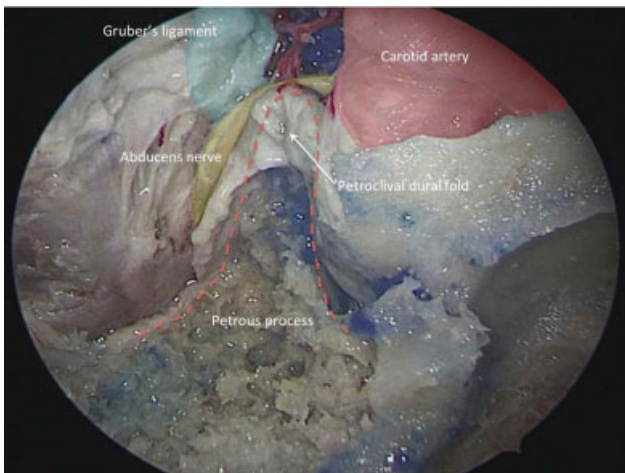


Fig. 1

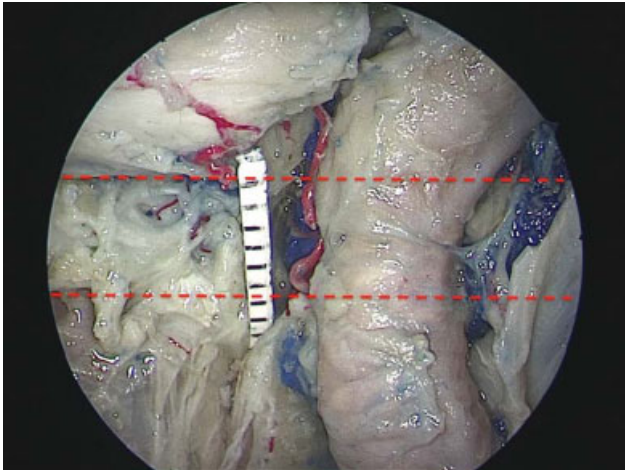


Fig. 2



Fig. 3

P025. The Extended Retrosigmoid Approach for High-Riding Posterior Inferior Cerebellar Artery Aneurysms—Part I: A Quantitative Anatomical Analysis of the Glossopharyngo-Cochlear Triangle

Xiaochun Xiaochun Zhao¹, Ali Meybodi¹, Komal Naeem¹, Engenii Belyk¹, Mohamed Labib¹, Mark Preul¹, Michael Lawton¹
¹Barrow Neurological Institute, Phoenix, Arizona, United States

Object: An extended retrosigmoid approach can offer sufficient space for clip reconstruction of high-riding posterior inferior cerebellar artery aneurysms. We conducted a quantitative anatomical analysis on the glossopharyngo-cochlear triangle (GCT) and structures within it.

Methods: Extended retrosigmoid craniotomies were performed on ten sides of cadaveric heads, and the GCT was identified in each specimen. The length of the base and the area of the GCT were measured. The depth of the vertebro-basilar system and the abducens nerve to the GCT were measured. The proximal and distal exposable and controllable points on the vertebrasilar system were identified. The length from those points to the dural entry point of the vertebral artery were measured, and the superoinferior distance from those points to the inferior edge of the foramen magnum were recorded to establish approach algorithms based on the preoperative imaging. Other factors related to accessibility via the GCT were investigated.

Results: The mean (\pm SD) area of the GCT was 45.7 ± 12.55 mm². Through the GCT, the mean depths of the proximal exposable point, proximal controllable point, distal controllable point, and distal exposable point of the vertebrasilar system were 12.2 ± 4.79 , 14.7 ± 5.22 , 18.9 ± 3.68 , and 22.3 ± 4.01 mm, respectively; the mean depth of the abducens nerve was 14.3 ± 1.42 mm. The mean lengths between the dural entry point of the vertebral artery to the proximal exposable point, proximal controllable point, distal controllable point, and distal exposable point of the vertebrasilar system were 30.5 ± 8.09 , 33.8 ± 9.00 , 43.1 ± 8.74 , and 48.0 ± 7.86 , respectively; the mean superoinferior distances from the foramen magnum to those points were 23.1 ± 7.39 , 24.7 ± 8.25 , 30.0 ± 9.56 , and 32.6 ± 7.79 mm, respectively. The lower segment of the vertebrasilar system was more superficial in the setting of a high-lying vertebrasilar junction (VBJ) than a low-lying VBJ.

Conclusion: We describe the parameters of the GCT in an extended retrosigmoid approach for high-riding posterior inferior cerebellar artery aneurysms and evaluate the spatial relationship of the neurovascular structures within it, its relationship to the position of the vertebrasilar junction, and the effect of a protruding jugular tubercle on this approach. Finally, two potential algorithms are offered for preoperative patient selection.

P026. The Anterior Incisural Width as a Preoperative Indicator for Intradural Space Evaluation: An Anatomical Investigation

Xiaochun Zhao¹, Mohamed Labib¹, Komal Naeem¹, Preul Mark¹, Michael Lawton¹, Lopez Gonzalez Miguel¹
¹Barrow Neurological Institute, Phoenix, Arizona, United States

Objective: The opticocarotid triangle (OCT) and the caroticooculomotor triangle (COT) are two anatomical triangles used in accessing the basilar region. We conducted a morphometric study to evaluate the anterior incisural width (AIW) as an indicator to predict the intraoperative exposure via both triangles.

Methods: Twenty sides of ten cadaveric heads were dissected and analyzed. The heads were divided into groups: group A, narrow anterior incisura and group B, wide anterior incisura, using 26.6 mm as a cut-off distance of the AIW. The area of the COT and the OCT in the transylvian approach was measured. The maximum widths via the two trajectories in a modified superior transcavernous approach were measured. The areas and the widths of the triangles were compared between the narrow and wide groups.

Results: The COT in the wide group was shown to have a significantly larger area compared with the COT in the narrow group (38.4 ± 12.64 vs. 58.3 ± 15.72 mm, $p < 0.01$). No difference between the two groups was reported in terms of the area of the OCT (50.9 ± 19.22 mm vs. 63.5 ± 15.53 mm, $p = 0.20$), the maximum width of the OCT (6.6 ± 1.89 vs. 6.5 ± 1.38 mm, $p = 1.00$), or the maximum width of the COT (11.7 ± 2.06 vs. 12.2 ± 2.32 mm, $p = 0.50$).

Conclusion: An AIW less than 26.6 mm is an unfavorable factor related with a limited COT area in a transylvian approach for pathologies at the interpeduncular fossa such as basilar apex aneurysms at the level of the posterior clinoid process. Preoperative identification and measurement of a narrow AIW can suggest the need to add a transcavernous approach. The approach selection should be individualized based on multiple related factors comprehensively.

P027. Dolenc Approach for the Craniotomy Clipping of a Carotid-Ophthalmic Giant Aneurysm: A Case Report

Gaoyang Fan¹, Lei Zhao², Yanchun Sun¹, Hao Han¹, Chunhai Su¹, Lijian Zheng¹, Lei Feng¹

¹Jining No.1 People's Hospital, Shandong, China

²Air Force Medical University, Xincheng, China



Fig. 1

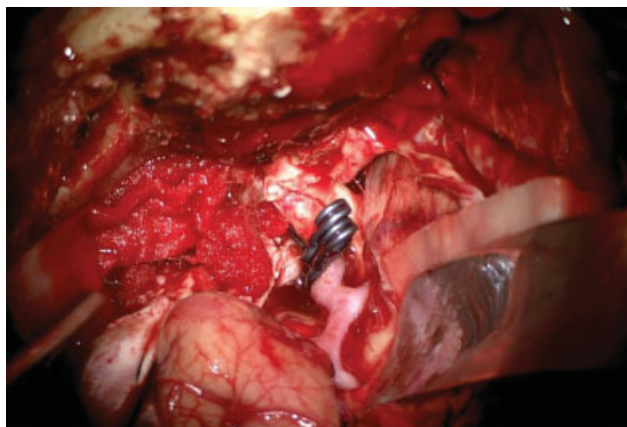


Fig. 2



Fig. 3

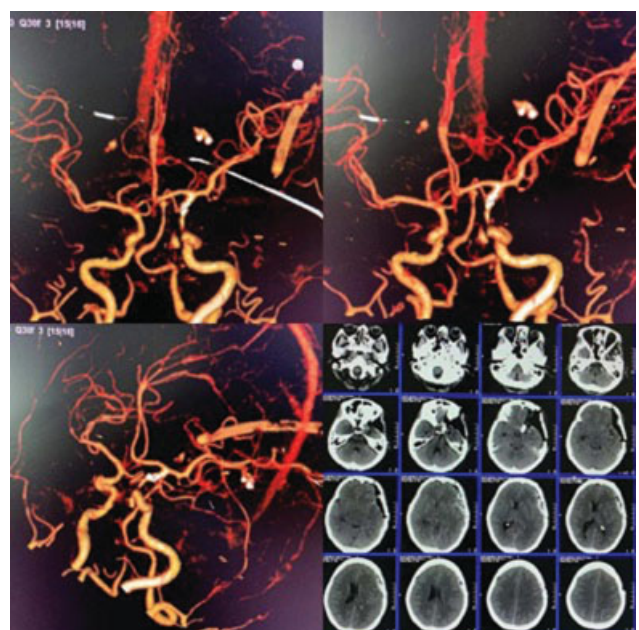


Fig. 4

A 66-year-old woman presented with severe headache. The angiography suggested a carotid-ophthalmic giant aneurysm. The size is 10.4 mm × 9.4 mm × 8.6 mm, and the neck width is 5.7 mm.

Dolenc's approach was performed to clip the aneurysm.

One day postoperatively, the patient was awake, and coordinated with the physical examination. The ocular movement is normal. And the patient also presented with middle tongue extension, and symmetrical nasolabial sulcus. Two days postoperatively, CT scan showed that there was no bleeding in the operation area and local bone defect was observed in the lateral skull base. CTA suggested that the aneurysm disappeared, and the internal carotid artery was unobstructed.

The transcavernous approach, as initially described by Dolenc, is a useful technique for microsurgical clipping of carotid–ophthalmic aneurysms.

P028. Comparative Anatomical Analysis between Minipterional and Supraorbital Approaches in the Treatment of Anterior Circulation Aneurysms

Rafael Martinez-Perez¹, Thiago Albonette-Felicio¹, Giuliano Silveira-Bertazzo¹, Luis Requena¹, Ruichun Li¹, Douglas Hardesty¹, Ricardo Carrau¹, Daniel Prevedello¹

¹Wexner Medical Center, The Ohio State University, Columbus, Ohio, United States

Introduction: In vascular neurosurgery, most of recent discussions regarding the applicability of MIA included the comparative analysis between minipterional (MPT) and supraorbital (SO) approaches for the treatment of anterior circulation aneurysms. There exists a trend toward the treatment of middle cerebral artery (MCA) aneurysm through a MPT approach, while the SO technique is usually preferred to treat anterior communicating artery (ACoM) aneurysms. The aim of this work is to establish indications and limits of both techniques in the treatment of anterior circulation aneurysms, through a pertinent comparative anatomical analysis.

Methods: Area of exposure and surgical maneuverability provided by the SO and MPT were compared in five cadaveric heads. The area of exposure was selected based in the most relevant points in the anterior circulations that can be reached throughout the pterional approach. Surgical maneuverability was calculated by means of the Ammirati and Bernardo score that assess from how many directions the target can be approach, as such as the permissibility to perform microvascular dissection maneuvers. The surgical maneuverability was assessed for three selected target points, namely, (1) ipsilateral bifurcation of the middle cerebral artery (MCA); (2) ipsilateral bifurcation of the internal carotid artery (ICA); and (3) the anterior communicating artery (ACoM). The points were selected to characterize the most representative surgical targets in the anterior circulation so that the exposure of these structures in both approaches could be evaluated.

Results: The MPT provided an increase of 21% in the area of exposure, in comparison to the SO ($p < 0.05$). Additionally, the MPT provided a better surgical maneuverability along the MCA (4 vs. 2.7, $p = 0.005$) and ICA bifurcation (4 vs. 2.1, $p < 0.005$). The SO affords a slightly better maneuverability around the ACoM, although the statistical analysis did not reach significant differences (4 vs. 3.8, $p > 0.05$).

Conclusion: Our results demonstrate that the MPT is a versatile and minimally invasive approach that affords a larger area of exposure and better surgical maneuverability than the MSO to approach most of the anterior circulation aneurysms, including MCA, and ICA bifurcation aneurysms. ACoM can be approach through both approaches, although limitations in the maneuverability and exposing parasellar and parasellar structures should be considered when choosing a SO. While SO provides a straight forward approach to ACoM, the MPT offers the possibility to proximally dissect

the Sylvian fissure, reducing the brain retraction and improving the surgical maneuverability.

P029. Reimplantation Bypass Using One Limb of a Double-Origin Posterior–Inferior Cerebellar Artery for Treatment of a Ruptured, Fusiform PICA Aneurysm

Fabio Frisoli¹, Joshua S. Catapano¹, Stefan Koester¹, Gabriella Paisan¹, Michael Lang¹, Michael T. Lawton¹

¹Barrow Neurological Institute, Phoenix, Arizona, United States

Background and Importance: PICA aneurysms are uncommon, and aneurysms associated with anatomical PICA variants are even more rare. Although often treated endovascularly, aneurysms associated with anatomical PICA variants may not be suitable for endovascular intervention given the risk of compromise of brainstem perforators and may be more amenable to open techniques. In this case report, we describe the successful treatment of an aneurysm associated with a double origin PICA (DOPICA) by distally reimplanting one of its limbs.

Clinical Presentation: We report the case of a 78-year-old male with a Hunt and Hess grade 3 and Fisher's grade 4 subarachnoid hemorrhage secondary to a ruptured distal right PICA aneurysm associated with a DOPICA. This was treated with PICA-PICA bypass and trapping of the aneurysm. This is the first reported case in the literature of successful bypass of a DOPICA-associated aneurysm. Radiographically, the bypass remained patent with successful obliteration of the aneurysm, and on discharge, the patient was noted to have a GCS 15 and mRS 3.

Conclusion: This case demonstrates a novel reimplantation bypass for a ruptured aneurysm that exploits this rare variant anatomy of a DOPICA.

P031. Flow Diversion of a Traumatic Middle Cerebral Artery Pseudoaneurysm with the Pipeline Flex Embolization Device

Zaid Aljuboori¹, Nicolas Khattar¹, Dale Ding¹, Robert James¹

¹University of Louisville, Louisville, Kentucky, United States

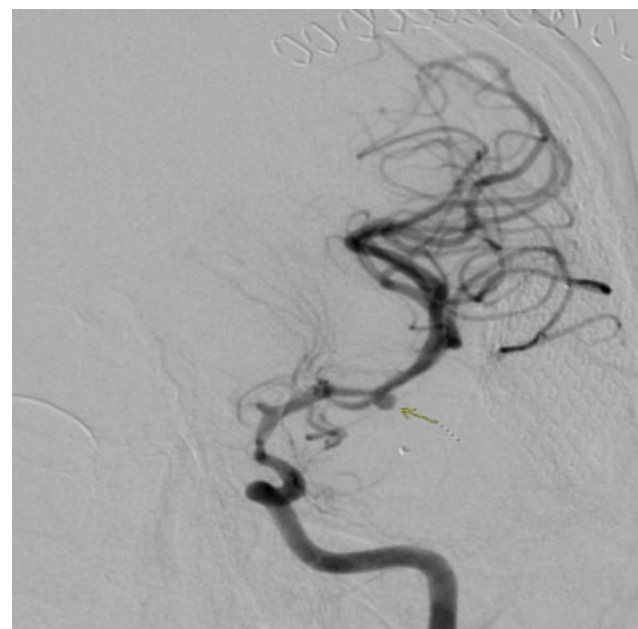


Fig. 1

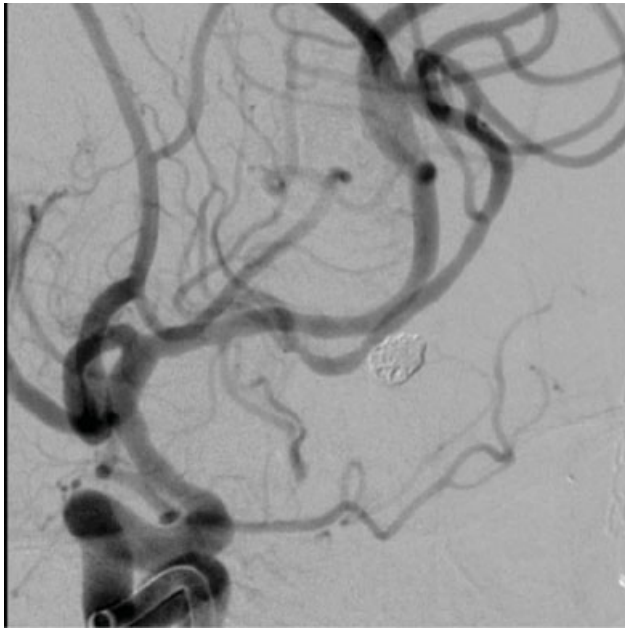


Fig. 2

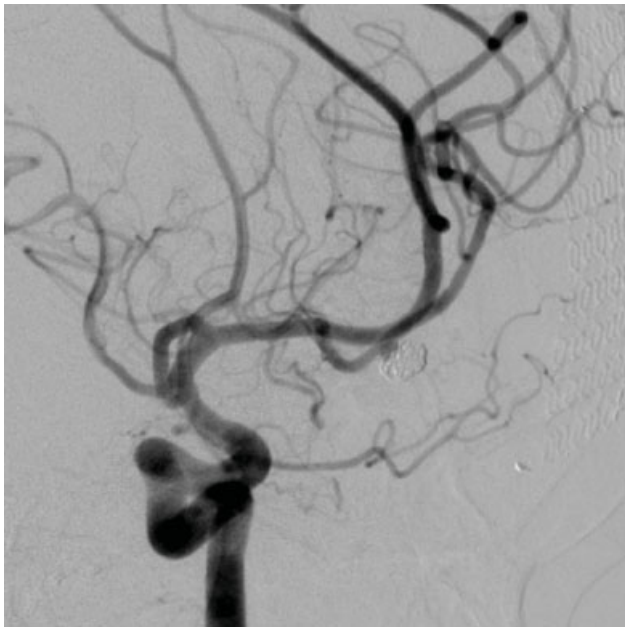


Fig. 3



Fig. 4

Introduction: Traumatic middle cerebral artery (MCA) pseudoaneurysms are rare cerebrovascular lesions which can be challenging to safely treat when they are localized to proximal segments of the vessel which cannot be sacrificed. Multiple endovascular and surgical treatment options have been described with varying degrees of efficacy.

Methods: We Describe The endovascular management of traumatic internal carotid artery (ICA) and MCA M1 superior division pseudoaneurysms with flow diversion.

Results: A 19-year-old male sustained a gunshot wound to the head. initial computed tomography angiogram showed only mild vasospasm of the left ICA and MCA. Catheter digital subtraction angiography (DSA) on post-injury day (PID) 7 showed a 1.4 mm × 2.0 mm pseudoaneurysm arising from the ophthalmic segment of the left ICA and a second 3.6 mm × 3.2 mm arising from the left MCA superior division. on PID 9, we performed coil embolization of the left MCA pseudoaneurysm. follow-up DSA 2-weeks after the coiling procedure showed recurrence of the left MCA pseudoaneurysm, with unchanged appearance of the left ICA pseudoaneurysm. At this time, we performed flow diversion of both the left ICA and recurrent MCA pseudoaneurysms using two pipeline flex embolization devices (Medtronic Neurovascular, Irvine, CA, United States). The patient was maintained on a dual antiplatelet regimen of (aspirin, 325 mg daily and Brilinta, 90 mg twice a day). Postembolization DSA 6 months after the flow diversion procedure showed complete obliteration of both pseudoaneurysms with preserved patency of left the ICA and MCA. The patient was neurologically intact at follow-up, without evidence of ischemic symptoms.

Conclusion: Flow diversion is an efficacious treatment for traumatic MCA pseudoaneurysms, with a favorable risk to benefit profile in appropriately selected cases. the use of dual antiplatelet therapy necessary to minimize the risk of thromboembolic complications after flow diversion must be balanced against the risk of hemorrhagic complications in the setting of recent trauma.

P033. Effects of Preoperative Embolization on Petroclival Meningiomas: Operative Impact, Outcomes, and Complications

Sam Emerson¹, Jake Ruzevick¹, Rajeev Sen¹, Kate Carroll¹, Manuel Ferreira Jr¹

¹University of Washington, Forks, Washington, United States

Clival and petroclival meningiomas are among the most formidable of all meningiomas owing to their rarity, crucial location and insidious progression. As benign entities, the goal of surgery is total resection, as this can be curative for some tumors. Even for atypical and malignant meningiomas, gross total resection is a significant predictor of improved survival. Pursuit of gross total resection can result in significant blood loss and other morbidity. One contributing factor is deep and poorly accessible vascular supply to petroclival meningiomas. This can preclude devascularization until late in the operation. Preoperative embolization can contribute to the feasibility of complete resection by targeting vascular pedicles, thus reducing operative time and intraoperative blood loss. However, this procedure is not without its own attendant risks, which must be weighed against any potential benefits intraoperatively for the neurosurgeon. Complete embolization is often difficult to achieve as these tumors often receive dual blood supply from the ICA and ECA, sometimes with anastomoses between the two that are difficult to visualize and increase the risk of complication.

Due to the relative rarity and complex vascular supply of petroclival meningiomas, the true risk-benefit profile of preoperative embolization remains nebulous, as there is a paucity of high-level evidence. A deeper understanding of outcomes and complications will help guide skull base neurosurgeons in the treatment algorithm for these tumors. In this series we retrospectively review our institution's experience with preoperative embolization of petroclival meningiomas. In particular, we analyze effects on estimated blood loss, need for transfusion, and operative time and recurrence. Procedure-related complications, including cranial nerve deficits and other neurologic deficits, are also presented. Based on these data, neurosurgeons will be better equipped to tailor their approach in terms of aggressiveness of devascularization versus complication avoidance.

P034. Ectopic Rathke's Cleft Cysts: Review of an Unusual Entity

S. Newman¹, R. Rindler², A. Boucher², S. Neill¹, G. Pradilla²

¹Emory University School of Medicine, Atlanta, Georgia, United States

²Department of Neurosurgery, Emory University, Atlanta, Georgia, United States

Introduction: Rathke's cleft cysts (RCCs) are benign intracranial cysts typically found in the sella turcica or in the suprasellar space. Ectopic RCCs are rare but have been found in a variety of locations with varying presentations, interventions, and outcomes. As of yet, an RCC has not been identified in the anterior cranial fossa, specifically along the olfactory groove. We report the first case of histologically confirmed RCC in the anterior skull base and present a review of all reported ectopic RCCs identified in the literature.

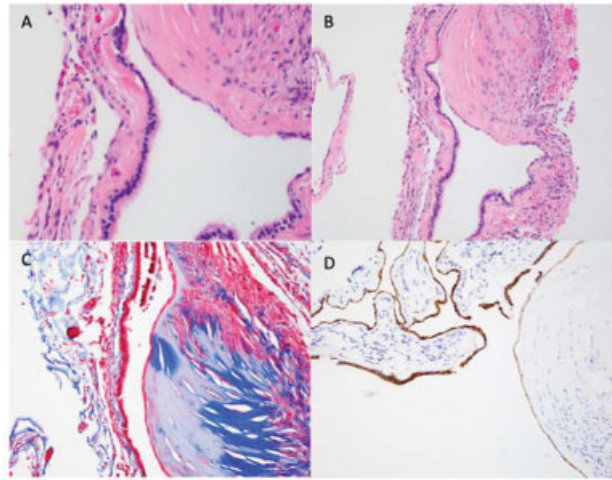


Fig. 1

Methods: A complete review of the available literature was performed along with evaluation of reference lists of included articles to identify all case reports of ectopic Rathke's cleft cysts. The current case report of olfactory groove RCC was included for a total of eight cases. Data points including demographics, characteristics of the lesion, radiographic evaluation, intervention, and outcomes were collected and analyzed.

Results: There were three pediatric cases (37.5%) and five adult cases reported with a median age of 41 years. Two of the eight case reports were male patients (25%). The locations identified were left olfactory groove (one), upper half of the prepontine cistern (two), cerebellopontine angle (two), sphenoid sinus (two), and temporo-frontal-parietal region (one). Seven of the eight patients presented with headache (87.5%) with headache being the only presenting symptom in 25%. The second most common presenting symptoms were vertigo, nausea, and vomiting all present in two patients. The MRI features of the lesions were widely variable with relation to intensity on T1 and T2 series. In all cases, gross total resection was achieved of the primary lesions. In all cases where clinical outcomes were reported (87.5%), there was complete resolution of presenting symptoms. Histopathological evaluation was universally consistent with RCCs.

Table 1 Demographics of the studies

Author, Year	Age (yr), Sex	Presentation	Location	Size (mm)	MRI Features	Outcome	Histology
Hemonds, 2005	41, M	HA, ptosis, diplopia	Sphenoid sinus*	Not reported	T1, isointense T2, hypointense No CE	Transsphenoidal resection, preservation of neurohypophyseal cyst IIS	Columnar ciliated epithelium
Zhou, 2000	32, F	HA, vertigo, nausea, vomiting	Cerebellopontine angle	Not reported	T1, hyperintense T2, hypointense No CE	L-ethmoidal suboptimal resection**	Columnar ciliated epithelium
Kim, 2012	41, F	HA	Upper half of prepontine cistern	25	T1, hyperintense T2, hypointense No CE	Planned craniotomy for resection IIS	Columnar ciliated epithelium
Fan, 2004	25, M	HA, R hearing loss, tinnitus, vertigo, facial numbness	Cerebellopontine angle	30 x 30 x 25	T1, hypointense T2, hyperintense No CE	R suboptimal retrograde resection IIS	Columnar ciliated epithelium with areas of squamous epithelium
Agarwal, 2017	8, F	HA, W vision loss, nausea, vomiting	R temporo-frontal-parietal region	30 x 30 x 45	T1, hypointense T2, hyperintense Peripher of CE	R craniotemporo-parietal craniotomy for resection IIS	Plasmociliated squamous epithelium with chronic inflammation
Kames, 2017	34, F	HA, dizziness	Upper half of prepontine cistern	34 x 10 x 9 → 38 x 13 x 10†	T1, hypointense T2, isointense No CE	Subtransphenoidal approach for resection IIS	Columnar ciliated epithelium
Papkov, 2013†	65, F	HA	Sphenoid sinus	25 x 18 x 24	T1, isointense T2, not reported No CE	Transnasal total resection IIS	Columnar ciliated epithelium
Present Study	54, F	Incidentally discovered epidermoid	Left olfactory groove	25 x 18 x 24	T1, hypointense T2, hyperintense Heterogeneous CE	Minifrontal craniotomy for resection IIS Resolution of papilloedema	Columnar ciliated epithelium

CE = Contrast enhancement; IIS = Total resolution of symptoms.
*With accompanying smaller contiguous cyst on posterior wall of neurohypophysis.
**No clinical outcomes reported.
†Initial growth at 10-month follow-up.
‡Report of ectopic RCC adjacent to compression with ectopic pituitary adenoma

This document was downloaded for personal use only. Unauthorized distribution is strictly prohibited.

Conclusion: Rathke's cleft cysts are rare, benign lesions that should be considered in the differential diagnosis of cystic lesions identified on imaging especially considering the radiographic presentation which, according to the results of this study, are variable on T1- and T2-weighted MRI. These ectopic RCCs can mimic other aggressive lesions in one of the several ectopic locations in which they have been identified.

LOs: By the conclusion of this session, participants should be able to (1) understand the embryological origins of Rathke's cleft cysts, (2) discuss in small groups the possible origins of ectopic RCCs, and (3) incorporate ectopic RCCs into differential diagnoses of cystic, extra-axial lesions without a clear radiographic diagnosis.

P035. Volumetric Growth Rates of Untreated Cavernous Sinus Meningiomas

Carolina Benjamin¹, Donato Pacione², Reed Mullen², Eman Kazi², Kimberly Ashayeri², Donato Pacione², Chandra Sen², John G. Golfinos², Dimitris Placantonakis², Douglas Kondziolka², Jafar Jafar²

¹University of Miami, Miami, Florida, United States

²NYU Langone Medical Center, New York, New York, United States

Cavernous Sinus Meningiomas are indolent tumors that initiate within the cavernous sinus and can expand along the skull base as well as intracranially. Given the involvement of vital neurovascular structures within the cavernous sinus including the internal carotid artery as well as cranial nerves II–VI, cavernous sinus meningiomas can have significant neurologic deficits. Management includes observation with serial imaging, stereotactic radiosurgery, or microsurgical debulking of the extracavernous components and decompression of neural elements. Prior studies suggest that such tumors are indolent, and favor observation with symptomatic medical management.¹

Between January 2013 and July 31, 2017, 38 patients with cavernous sinus meningiomas were retrospectively evaluated. The average age of patients was 60 years. There was a female preponderance in this cohort, with 82% of patients being females. Most patients (79%) were asymptomatic. All MR images preceded any intervention. Of the 38 patients analyzed, 66% never underwent treatment, 21% underwent stereotactic radiosurgery (SRS), 8% underwent microsurgical resection, and 5% underwent a combined approach with SRS, and craniotomy. To precisely calculate tumor volumes, the tumor area was outlined on every slice, and the products of the area and slice thickness were summed (55% of scans were done). The mean cavernous sinus volumetric growth rate was 35% per year. An assessment of the frequencies of individual tumor annual growth rates revealed that 21% demonstrated growth (5% fast growing), 79% were stable on an average interval of 51 months. There was no relationship between patient age and tumor growth rate.

This study is a comprehensive measure of cavernous sinus meningioma volumetric growth rates using high-resolution imaging. The majority of the tumors remained stable over time, as predicted in previous studies. These findings provide volumetric data regarding the tumor behavior which can assist in the clinical decision making for the management of cavernous sinus meningiomas.

P036. Treatment Strategy and Clinical Outcome for Cavernous Sinus Lesion

Takashi Sugawara¹, Yoji Tanaka¹, Taketoshi Maehara¹

¹Department of Neurosurgery, Tokyo Medical and Dental University, Tokyo, Japan

Objective: The surgery for the lesions around the cavernous sinus is still challenging, especially for the lesion

invading cavernous sinus, optic sheath, and oculomotor cave. The exposure of these region is sometimes necessary but have a risk of cranial nerve injury. In this presentation, we show the surgical strategies and techniques with video and also clinical outcome for these lesions.

Materials and Methods: Surgical resection is indicated for benign cases with neurological symptoms or tumor growth. For malignant cases, considering resection according to individual circumstances. Surgical strategy: the benign tumors invading cavernous sinus are removed as much as possible while preserving cranial nerves. For malignant tumors, preoperative symptoms and prognosis assessment are taken into account, and when necessary, the tumor is removed with sacrifice of cranial nerves followed by adjuvant therapy. Preoperative symptom and their postoperative course, adjuvant therapy, postoperative complication, degree of removal, recurrence were investigated in 22 surgical cases with cavernous sinus invasion (16 meningiomas [13 grade I and 3 grade II], 3 schwannomas, 1 squamous cell carcinoma, 1 chondrosarcoma, and 1 angiofibroma) between January 2013 and August 2019.

Results: Major preoperative symptoms were external ophthalmoplegia, visual disturbance, facial dysesthesia, brain swelling in 10, 8, 5, and 4 cases, respectively. And these symptoms recovered in 7 (70%), 7 (88%), 2 (40%), and 4 (100%) cases, respectively. Facial dysesthesia deteriorated in two schwannoma cases. Postoperative complications were temporary oculomotor paresis in three cases, facial dysesthesia in three cases, contralateral visual deterioration in one case, and brief transient hemiparesis by IC dissection or vasospasm in one case. Gross total removal was achieved in 12 lesions but 10 meningioma cases were partially removed (mainly remnant in cavernous sinus). One squamous cell carcinoma underwent chemoradiotherapy after total resection of tumor and cranial nerves in cavernous sinus. Two residual atypical meningioma in cavernous sinus underwent IMRT. One atypical meningioma recurred and underwent γ -knife radiosurgery.

Conclusion: In surgical resection of cavernous sinus lesion, sacrifice of cranial nerves is acceptable for malignant tumor, but that is not acceptable for benign tumor. Except for intentional sacrifice of V2 in trigeminal schwannoma and angiofibroma cases, almost all of the tumors can be well controlled with only acceptable transient insult by careful and delicate procedure, and accurate judgment of possibility of resection.

P037. Another Cavernous Sinus Syndrome

Steven A. Newman¹

¹University of Virginia, Charlottesville, Virginia, United States

Introduction: The cavernous is the prototypical skull base location besides containing the carotid artery, it also contains the lateral wall of the third, fourth, and fifth cranial nerves responsible for facial sensation and largely responsible for ocular motility and deep within its substance the sixth nerve and the sympathetic, responsible for lid position and abduction.

Materials and Methods This is a 67-year-old gentleman seen in July of 2019 who presented to the Emergency Room complaining of diplopia. He was also found to have a vestibular rash involving the v1 distribution bilaterally. Neurophthalmic evaluation revealed limitation in abduction on the right side compatible with a right sixth nerve palsy. On evaluation 2 days later had an abduction deficit but also now had ptosis on the right side and marked limitation in vertical gaze on the right, as well as a slightly enlarged pupil. He was diagnosed as having a partial sixth and third nerve palsy.

Imaging studies done at that time revealed changes of abnormalities in both cavernous sinuses.

Results: Review of the MRI scan did show bilaterally cavernous sinus abnormalities. The most important piece of information here was the previous history. The patient had been diagnosed as having ulcerative colitis in 2000, treated with Imuran and Mesalamine. In April of 2009, he developed cirrhosis and hypertension, and was diagnosed as having primary sclerosing cholangitis. In May of 2012, he underwent a liver transplant complicated by incarcerated hernia repair. Postoperative he developed anemia and polio and in March of 2016 underwent bile stone duct removal and percutaneous drainage. He had additional imaging studies done when he presented with diplopia, including an MRI scan of the liver which revealed hypodensity of the medial aspect of the transplanted liver. Fine needle aspiration biopsy showed lymphocytes that were characterized as being B cell.

Discussion: This patient was diagnosed as having posttransplant lymphoproliferative disorder, this time with B-cell lymphoma involving the liver and the cavernous sinus, as well as the clivus presenting with diplopia involving the right cavernous sinus. His immune modulation was reduced and he was treated with rituximab which did not have a particularly beneficial effect. He was then started on chemotherapy for lymphoma with improvement in function. Post-transplant proliferative disorders have been recognized for several years, often associated with Epstein-Barr virus abnormalities common with hepatitis C. Interestingly it seems to occur less frequently with transplant of the liver than with other solid organs. It is clearly demonstrated that immune suppression used to treat these patients have a causative effect and one of the first treatments is to reduce the immune suppression as much as possible. As in this case, various modalities of treating the lymphoproliferative disease may be necessary.

P038. Bilateral Sequential Spontaneous Otogenic Pneumocephalus: Lessons in Pathophysiology and Management

Scott B. Shapiro¹, Noga Lipschitz¹, Parker Tumlin¹, Bryan Krueger¹, Jonathan A. Forbes¹, Ravi N. Samy¹

¹University of Cincinnati College of Medicine, Cincinnati, Ohio, United States

Background: Spontaneous intradural pneumocephalus is an extremely rare but serious condition related to defects in the temporal bone and dura. The precise mechanism by which this otogenic complication occurs is poorly understood.

Objective: Report the details of an unusual case of initially unilateral spontaneous otogenic pneumocephalus followed by contralateral pneumocephalus which presented after surgical repair of temporal bone and dural defects on the initial side.

Case: A 73-year-old obese male presented with bilateral retroorbital pain and headache; he was found to have unilateral intradural pneumocephalus in the temporal lobe with an adjacent defect in the temporal bone. He underwent surgical repair of the initial defect in the temporal bone and dura via a middle cranial fossa approach with obliteration of the mastoid cavity. His symptoms and degree pneumocephalus on this side decreased initially after surgery. Two weeks after surgery, he developed worsening pneumocephalus on the contralateral side in the left temporal and frontal lobes with weakness and somnolence. This side was repaired via a similar technique without mastoid obliteration. Two weeks after surgery the patient recovered to a normal level of consciousness.

Conclusion: Spontaneous otogenic intradural pneumocephalus is an extremely rare but serious condition; unfortunately, the pathophysiology is incompletely understood. This unusual case, in which repair of the initial defect may have predisposed to development of pneumocephalus via a defect in the skull base on the contralateral side, offers insight to the complex underlying pathophysiology.

P039. Polymicrobial Intracerebral Abscess Growing *Achromobacter xylosoxidans* and *Mycobacterium Avium* Complex

Juliana Rotter¹, Christopher S. Graffeo¹, Hannah E. Gilder¹, Lucas P. Carlstrom¹, Avital Perry¹, Michael J. Link¹

¹Mayo Clinic, Rochester, Minnesota, United States

Introduction: *Achromobacter xylosoxidans* (AX) is an uncommon cause of intracerebral infection with only thirteen reported cases of meningitis or vasculitis and, to our knowledge, no published reports of intracerebral abscess. *Mycobacterium avium* complex (MAC) is also a rare source of intracerebral infection, with only four cases of intracranial MAC abscess reported in previously healthy patients. We report the index case of intracranial AX abscess, and the first instance of polymicrobial AX-MAC abscess, which arose 10 years after a preceding skull base surgery.

Case Report: Ten years before presentation, the patient underwent endoscopic resection of a left frontal sinus and zygomaticomaxillary mucocele via Caldwell-Luc approach, complicated by CSF leak and subsequent frontal lobe *Streptococcus pneumoniae* abscess, which were managed via temporalis fascia graft, surgical abscess drainage, and IV antibiotics. His history was notable for grade-3 colorectal adenocarcinoma, in remission after resection and chemotherapy. He presented with 2 weeks of sinus congestion and headache, which progressed rapidly in spite of cefdinir to fever, diaphoresis, worsening congestion, and severe headache, as well as a mild right lower facial droop, and subtle word-finding difficulties with paraphasic errors. Noncontrast CT head demonstrated a ring-enhancing, centrally necrotic, proteinaceous, bilobed, frontal lesion, associated with marked edema and mass effect causing 12 mm of midline shift (**Fig. 1**). Dexamethasone was initiated, along with broad spectrum antibiotics including vancomycin, cefepime, and metronidazole. Magnetic resonance imaging (MRI) confirmed that the bilobed left frontal lesion was most consistent with a large, intraparenchymal abscess, with extra-axial extension to the left cribriform plate, ethmoids, and posterior table of the frontal sinus (**Fig. 2**). The patient was initially treated via stereotactic needle decompression of both cystic spaces from a lateral inferior trajectory (**Fig. 3**). Fifty-five mL viscous, yellow-green, purulent fluid was aspirated, postoperative CT demonstrated excellent decompression, and the patient rapidly recovered to his preinfection neurologic baseline. Intraoperative cultures predominantly grew AX, as well as *Staphylococcus epidermidis*, *Streptococcus mitis*, and *Streptococcus salivarius*, and the antibiotic regimen was narrowed to IV ertapenem for 6 weeks. Twelve days later, cultures grew *M. Avium* complex and the treatment plan was modified again, to ceftriaxone and sulfamethoxazole/trimethoprim. Follow-up MRI was scheduled, with a surgical plan to include bifrontal craniotomy, left frontal intracranial abscess resection, and anterior skull base repair with fascia lata and vascularized pericranium.

Conclusion: Intracranial infections caused by AX or MAC are exceedingly rare, with no documented instances of cerebral abscess attributable to AX, and very few cases associated with MAC. Additionally, while intracranial infections are a relatively well-described complication of skull

base surgery, particularly in the setting of CSF leak, they generally occur in close proximity to the index operation. Correspondingly, the present case highlights the potential for insidious infections to arise in a dramatically delayed fashion, via the transnasal route.

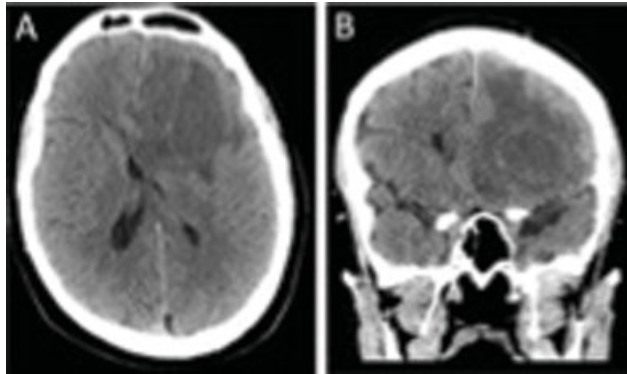


Fig. 1 (A) Axial, (B) coronal CT demonstrating left frontal lobulated lesions.

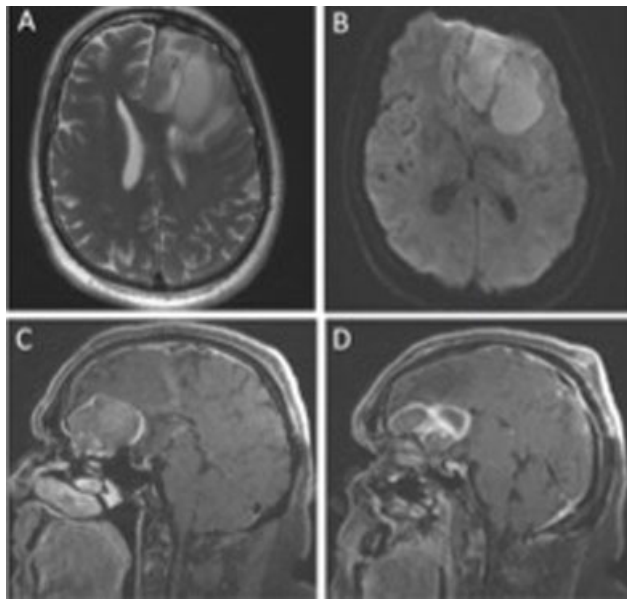


Fig. 2 (A) Axial T2 with contrast and (B) DWI MRI revealing a complex bilobed left frontal abscess with 5.6 cm × 3.1 cm × 4.4 cm medial lobe and 5.7 cm × 3.3 cm × 3.5 cm lateral lobe. (C), (D) Sagittal T1 MRI demonstrating mostly intra-axial lateral lobe and medial lobe extending anteriorly in cranial fossa.

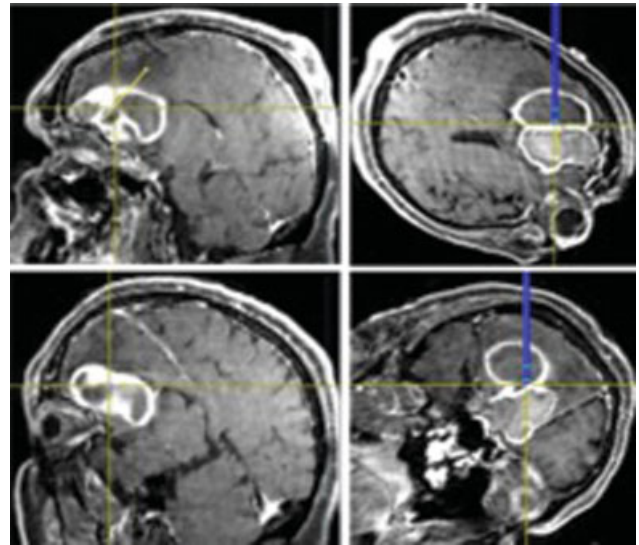


Fig. 3 T1 MRI with intraoperative neuronavigation tracks.

P040. Fetal Bovine Collagen Grafts for Repair of Tegmen Defects and Encephaloceles via Middle Cranial Fossa Approach

Anand Patel¹, Matthew R. Bartindale², Jehad A. Zakaria², Anand V. Germanwala², Douglas E. Anderson², Sam J. Marzo², Matthew L. Kircher², John P. Leonetti², Vikram C. Prabhu²
¹Stitch School of Medicine, Maywood, Illinois, United States
²Loyola University Medical Center, Hines, Illinois, United States

Objectives: To determine whether allogenic materials using fetal bovine collagen that are commercially available (Durepair, DuraMatrix, and DuraGen) provide outcomes and infection rates comparable to autologous grafts.

Design: Retrospective, single-center case series.

Participants: Patients who underwent surgical repair of a tegmen defect associated with ipsilateral cerebrospinal fluid (CSF) otorrhea using a middle cranial fossa approach between 2004 and 2018 at Loyola University Medical Center.

Main Outcome Measures: Resolution of CSF otorrhea, audiologic outcomes, facial nerve outcomes, and complications.

Results: Thirty-seven patients were included in the study, with an average age of 55 years and average body mass index of 35 kg/m². All patients had some degree of hearing loss preoperatively. Repairs were made with combinations of allograft and autograft in 17 patients, allograft only in 15 patients, and autograft only in 5 patients. The CSF otorrhea resolved in all 36/37 patients, and the other patient's otorrhea resolved with a revision surgery. Three patients had significant complications requiring readmission. There was no statistically significant association between repair graft and surgical outcome.

Conclusion: The use of the middle cranial fossa approach coupled with the use of fetal bovine collagen grafts is an effective and viable method to repair lateral skull base defects. This is a treatment modality that affords a cost-effective solution with salutary outcomes and low morbidity.

P041. Presentation and Management of Wound Closure Failure after Sphenoclival Expanded Endonasal Surgery: Single Institution Experience

Abel David¹, Nicole Jiam¹, Jose Gurrola II¹, Manish Agh¹, Philip Theodosopoulos¹, Michael W. McDermott¹, Ivan H. El-Sayed¹
¹University California San Francisco, San Francisco, California, United States

While surgical approaches and techniques of expanded endonasal approach (EEA; surgery have been well described over the past 16 years, data regarding the sequelae of EEA is evolving. Defects of the skull base after EEA are different in size and nature than those that arise from spontaneous CSF leaks. We reviewed the experience at a minimally invasive skull base center with a single OHNS surgeon from 2006 to 2018 and analyzed the closure to help provide clinical insight into diagnosis and management.

Objective: describe the presentation and management of CSF leak after EEA of the sphenoclival axis. **Methods:** retrospective chart review of single surgeon (OHNS) experience from 2006 to 2018.

Results: Eleven patients were identified in the patient series requiring return to the operating room. Indications for primary surgery included chordoma (three), pituitary adenoma (two), tuberculoma meningioma (one), radionecrosis (one), supracellar cyst (one), craniopharyngioma (one), basilar aneurysm (one), epidermoid (one). Nine of eleven surgeries were performed prior to 2012. Malignant etiologies were present in 4/10 cases. The original defect size was a median of 3.75 cm²; (range, 0.05–6.5 cm²) and defects were located in the sella (four), sella clivus (one), clivus (four), clivus planum (one), and planum (one). Nine of 11 defects were categorized as high-flow leaks intraoperatively. Median time to presentation of CSF leak was 20 days (range, 1–542 days). Only three (27%) patients presented within 7 days of surgery and seven (63%) patients presented between 15 to 40 days after surgery.

Presentation: rhinorrhea (eight), meningitis (six), pneumocephalus (one). Overall 10/11 required endoscopic repair and 2/12 required two surgeries. Endoscopic inspection revealed evidence of infection (three), flap necrosis (five), and reversed nasal septal flap (one). CSF leak undetected in operative inspection (one), or repaired with fat graft alone (three), fat graft + inferior turbinate flap (two), inferior turbinate flap alone (one), nasal septal flap + fat graft (three), nasopharyngeal roof mucosa flap + fat graft (one). All CSF leaks were closed without taking down the entire initial repair. Nine of 11 were live at last follow-up. One of 11 Died during admission due to progressive basilar artery aneurysm and 1 of 11 died due to recurrence of malignant disease at 6 months.

Conclusion: The majority of post EEA wound failures present between 15 to 40 days in our experience with either rhinorrhea of clear fluid or signs of meningitis. The majority of cases occurred prior to 2012 after which the authors changed their closure techniques. The majority of closure failures (63%) occur outside the sella reflecting the direct relation to intracranial cisterns. Operative repair is the treatment of choice and involved sealing the defect and using a vascularized flap in the majority of cases (63%), although fat graft alone sufficed in two-thirds of cases. Correct placement of vascularized flap is essential and we now mark the non-epithelialized surface upon flap elevation. Knowledge of alternate flaps is important when the NSF is no longer available.

P042. Iatrogenic Cerebrospinal Leak Arising from a Persistent Foniculus Frontalis

William C. Harris¹, Edward D. McCoull²

¹Department of Otorhinolaryngology, Tulane University, New Orleans, Louisiana, United States

²Department of Otorhinolaryngology, Ochsner Clinic Foundation, Tulane University, New Orleans, Louisiana, United States

Congenital midline nasal anomalies are rare; however, when present the typical result is a glabellar mass that presents in childhood. The persistence of an asymptomatic foniculus frontalis in an adult is thought to be a rare event. We report a case of a 71-year-old man with chronic rhinosinusitis who underwent image-guided endoscopic sinus surgery including Draf 2A frontal sinusotomy. During frontal sinus dissection, a suspected cerebrospinal fluid leak was encountered anteromedial to the right frontal ostium. Image-guided navigation demonstrated the defect was not adjacent to the cribriform plate. The defect was repaired intraoperatively using a free mucosal graft from the septum. Upon review of the sagittal and axial CT imaging, the patient was noted to have a persistent foniculus frontalis that was encountered while enlarging the medial aspect of the frontal ostium. This case calls attention to the potential relevance of a persistent foniculus frontalis as a risk factor for cerebrospinal fluid leak in adults undergoing endoscopic sinus surgery. Identification of this anatomic variant should be considered during the preoperative assessment.

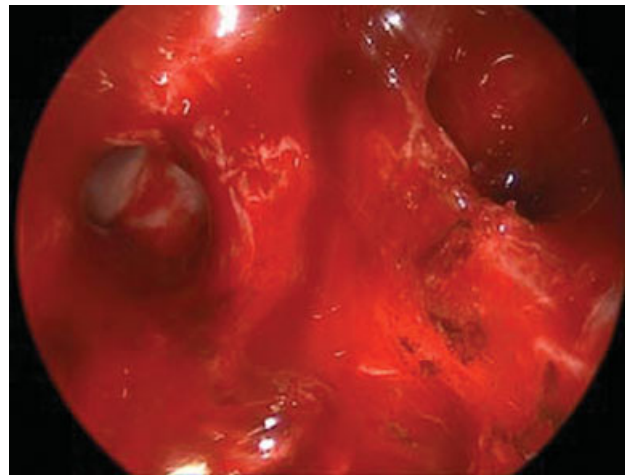


Fig. 1

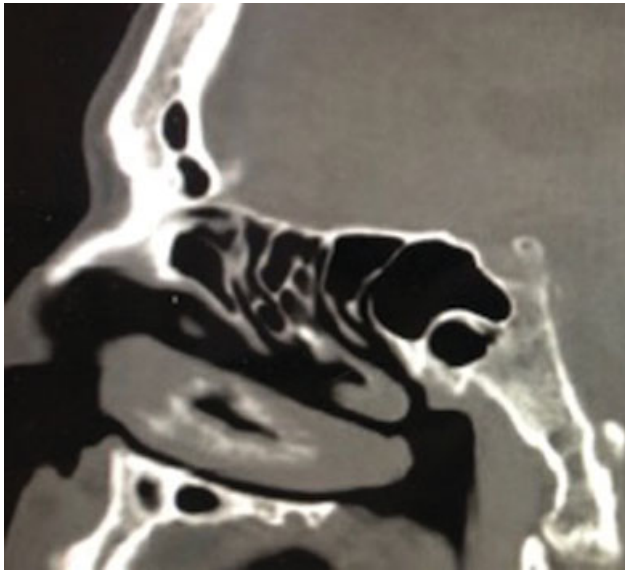


Fig. 2

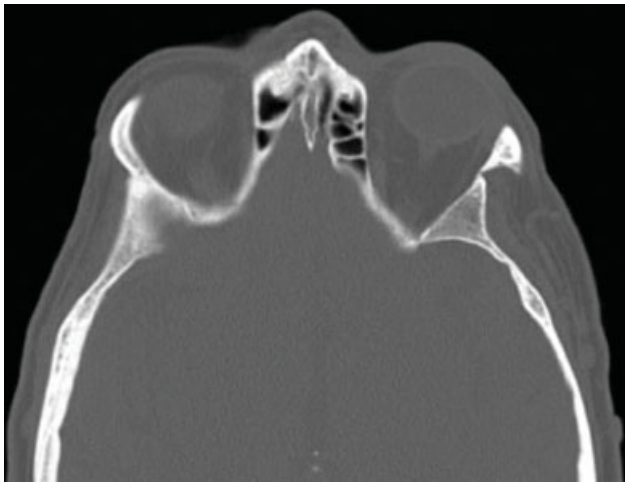


Fig. 3

P043. Liquorhoea—Conservative or Surgery, or Both of Them Is True?

Jan Hemza¹

¹Department of Neurosurgery Faculty Hospital at Saint Ann, New Jersey, United States

Our group has more than 493 patients: the anterior skull base, middle, posterior open trauma. During anterior skull base reconstruction we protected the olfactory structures in 91%. Mortality v our series is 1.7%, morbidity post-traumatic 17%, postoperative 0,6%.

Follow-up in this series is 27 years.

In our series, we preferred acute operations and reconstructions of open skull base fracture with very effective goal. In reconstruction method, we preferred vascularized flaps for reconstruction of dura. Author discussed problems of acute and delay reconstruction, discussed mortality and morbidity. Authors have experiences 27 years with acute operations and reconstructions, diagnostic technics, treatment, and follow-up of patients.

Concurrently with timing surgery study of open skull base fracture, we have constituted group nonsurgery treatment open skull base fracture. Our study group have together 116 cases, which come into being first 5 years. We have follow-up of the group 20 years. We were all eyes on complications, which developing during 15 to 20 years under different diagnosis: meningitis, meningoencephalitis, abscessus cerebri, liquorrhea, pneumocephalus, Pott's tumor, mucocele, meningoencephalocele, "polyps of paranasal sinuses," "polyps of middle ear," and "cholesteatoma of middle ear."

The criteria— our characteristics of choices to the nonsurgery group: only intradural pneumocephalus intradural pneumocephalus and liquorrhea, which stop during 24 to 48 hours only liquorrhea, which stop during 24 to 48 hours.

The first group have maximum between half and 1 year after trauma after diagnosis (15.5%), the second group between 5 and 6 years (12.1%), the third group between 11 and 13 years, (13.9%) and fourth group between 16 and 18 years. (9.4%).

We need to do exchanges conservative treatment to surgery treatment in 58.6% during 20 years. under different diagnosis. If became the diagnosis after trauma late, the diagnosis have not immediate relation to traumatic diagnosis.

We study different pathological problems posttraumatic on olfactory structures - destruction or contusion or hematoma into olfactory bulb, destruction of olfactory tract and destruction or contusions in olfactory trigonum.

In lecture author will be discussed about new anatomical aspect of skull base, the biomechanical aspect of dura mater, the technical notes of different approaches of reconstruction, problems of timing of reconstruction or the controversies between conservative and surgery treatment.

In our series, we preferred acute operations and reconstructions of open skull base fracture with very effective goal. In reconstruction method, we preferred vascularized flaps for reconstruction of dura. Author discussed problems of acute and delay reconstruction, discussed mortality and morbidity. Authors have 27 years of experiences with acute operations and reconstructions, diagnostic technics, treatment, and follow-up of patients.

P044. Idiopathic Intracranial Hypertension Presenting as Spontaneous CSF Leak

Christopher S. Hong¹, Eugenia M. Vining¹, R. P. Manes¹, Sacit B. Omay¹

¹Yale University School of Medicine, New Haven, Connecticut, United States

Introduction: Spontaneous cerebrospinal fluid (CSF) leaks may represent a unique clinical presentation of idiopathic intracranial hypertension (IIH), secondary to skull base erosion from chronically elevated CSF pressures. However, patients with spontaneous CSF leaks may not present with the classical symptoms of IIH, including severe headaches, papilledema, elevated opening pressures, and slit ventricles on imaging. As such, we retrospectively reviewed our own recent institutional experience and performed a literature review to further characterize patients presenting with spontaneous CSF leak and previously undiagnosed IIH.

Methods: Following a single-institution retrospective review of the last five patients treated for spontaneous CSF leak with delayed measurement of opening pressures after leak repair, we performed a systematic literature review of spontaneous CSF leak in patients previously undiagnosed with IIH, utilizing a PubMed query of "CSF leak," and "hypertension."

Results: Including our last five patients, the literature review yielded 21 total studies, comprised of 476 total patients meeting criteria for presentation with spontaneous CSF leak without prior history of IIH. Patient demographics included an average age of 52.1 years, 84.8% female predominance, and an average body mass index of 27.8. Out of 322 patients with available data, presenting symptoms in addition to CSF leak included significant headaches (38.5%), visual disturbances (6.5%), and signs of meningitis (6.5%). Out of 101 patients undergoing formal ophthalmologic examination, papilledema was reported in 18.8% of patients. Radiographic findings revealed empty sella in 58.9% of 331 patients and normal ventricular configuration (i.e., absence of slit ventricles) in 96.5% of 57 patients with available imaging for review. Opening pressures measured either at time of CSF leak repair or in the immediate postoperative period demonstrated an average of 21.7 cm H₂O among 427 patients with available data. While the majority of patients underwent medical treatment postoperatively with acetazolamide, 14.3% of patients were ultimately treated with a ventriculoperitoneal shunt, due to recurrent CSF leak, significantly elevated opening pressures post-CSF leak repair, and/or intolerance of acetazolamide therapy.

Conclusion: An underlying diagnosis of IIH must be strongly suspected in patients presenting with spontaneous CSF leaks. Our experience and review of the literature suggests that these patients may present differently from typical IIH patients, including absence of a significant headache history and lack of subjective or objective evidence of visual deficits. Opening pressures may range from normal to mildly elevated ranges, reflective of attenuation of intracranial hypertension via the CSF leak. In addition, in contrast to slit ventricle morphology characteristic of typical IIH, imaging in these patients may reveal a normal ventricular configuration, as well as an empty sella, the latter reflective of long-standing undiagnosed intracranial hypertension. At our institution, we routinely perform a delayed measurement of opening pressure within 1 to 3 months after spontaneous CSF leak repair to evaluate for IIH. Additionally, all patients should undergo neurovascular imaging to rule out cerebral venous thrombosis. While medical therapy with acetazolamide for IIH is commonplace, definitive treatment via permanent CSF diversion or venous stenting may be indicated in patients exhibiting significantly elevated opening pressures postoperatively, or experiencing recurrent CSF leaks.

P045. A Simplified Transpterygoid Technique to Lateral Sphenoid Encephaloceles: A Shorter Run for a Longer Slide
Dennis M. Tang¹, Jonathan Y. Ting², Troy D. Woodard¹, Pablo F. Recinos¹, Varun R. Kshetry¹, Elisa Illing², Kolin Rubel², Aaron Cohen-Gadol², Raj Sindwani¹

¹Cleveland Clinic Foundation, Cleveland, Ohio, United States

²Indiana University Health, Indiana, United States

Introduction: Encephaloceles and cerebrospinal fluids (CSF) leaks in the lateral sphenoid sinus have traditionally been difficult to repair. The originally described endoscopic transpterygoid approach affords a direct trajectory, but is burdened with an involved and time-consuming dissection of the pterygopalatine fossa (PTF) and related risks. We have developed a modified transpterygoid approach which involves a subperiosteal dissection maintain the integrity of the PTF contents retracting them inferiorly and laterally allowing access to the lateral sphenoid recess.

Methods: Patients who underwent the endoscopic modified transpterygoid-contents intact technique (EMTCIT) for lateral sphenoid recess encephaloceles at two academic centers between 2014 and 2019 were identified. Patients

with any other pathologies (iatrogenic CSF leaks, skull base tumors) were not included. Patient demographics, repair techniques, and outcomes were recorded. The primary endpoint was successful repair of the CSF leak, with secondary outcomes including dry eye, bleeding, or trigeminal nerve related symptoms. The technique begins with removal of the posteromedial wall of maxillary sinus. The palatine bone is drilled and the anterior aspect of the bony sphenopalatine foramen is removed to permit mobilization of the medial aspect of the PTF contents. The sphenoid face is opened maximally in the lateral dimension. Dissection in a subperiosteal plane is performed for mobilization of the PPF contents inferiorly and laterally. This permits further bone removal of the lateral sphenoid face and pterygoid wedge, permitting access to the lateral recess. If necessary, the Vidian nerve and/or the distal aspect of the sphenopalatine artery may be sacrificed to provide further exposure. Using a 30degree endoscope with a malleable bipolar or angled coblator, the encephalocele is resected. The skull base defect is then prepared and reconstructed with free or pedicled nasal mucosal grafts.

Results: Twenty-one patients underwent the EMTCIT. The average BMI was 46.4. Skull base defects were reconstructed using free mucosal grafts in the large majority of cases (15/21). A nasoseptal flap was used in four patients and fat in two patients. There were no persistent or recurrent CSF leaks occurred for a 100% success rate. Complications included three patients with temporary V2 anesthesia that recovered (14.3%), and 1 patient with subjective eye dryness which improved over several months (4.8%). There were no cases of epistaxis or hemorrhage requiring intervention. Average follow-up was 1.1 years.

Discussion: The modified transpterygoid technique described allows for access to the lateral sphenoid sinus without exposure of the PPF contents, greatly simplifying the approach and minimizing damage to neurovascular structures. Although the exposure afforded is not a straight-line trajectory to the defect site, our results suggest that with the aid of angled endoscopes and instruments, successful management of encephaloceles in this area can be reliably performed. For more aggressive pathologies, a traditional transpterygoid approach with PTF dissection may be preferred.

Conclusion: The EMTCIT greatly simplifies exposure of the lateral sphenoid sinus for management of encephaloceles, without compromising access. This technique obviates the need for PTF dissection and should be considered for the management of benign lesions involving the lateral sphenoid sinus.

P046. Management of Cerebellar Dysplasia, Chiari I Malformation, Syringomyelia, and Hydrocephalus in a Patient with Bannayan–Riley–Ruvalcaba Syndrome
Ali O. Jamshidi¹

¹Kaiser Permanente, Portland, Oregon, United States

Background: Bannayan–Riley–Ruvalcaba syndrome thought to be caused by PTEN tumor suppressor gene mutations. Similar to Cowden's syndrome, these patients can develop hamartomas and other benign lesions, as well as malignancy. In addition these patients are known to have macrocephaly and macrosomia at birth and genital freckling in males. The author presents a case of a patient with this syndrome and the triad of a posterior fossa tumor, Chiari I malformation and hydrocephalus.

Case Report: A 27-year-old male presented to our facility after suffering a first-time generalized tonic-clonic seizure. The patient had initial head CT that showed florid

obstructive hydrocephalus associated with a right cerebellar hemisphere mass and tonsillar herniation. After recovering from his seizure, the patient admitted to a history of worsening headaches and intermittent hiccups over approximately two to three months but no focal neurologic complaints. An MRI of the brain recapitulated the findings of the CT scan and also suggested that the mass was most consistent with Lhermitte Duclos; a cervical spine MRI revealed a syrinx. The patient proceeded with a right frontal external ventricular drain, posterior fossa craniectomy, C1 laminectomy, expansile duraplasty, and debulking of his dysplastic tumor; he was advised that he may need a staged procedure for CSF diversion. The tumor was infiltrative and had no discrete borders, consistent with the diagnostic impression from the MRI. Postoperatively, the patient had no new deficits and his drain was kept clamped. He could not tolerate his clamp trial. A postoperative MRI evaluating for CSF flow showed a persistent blockage roughly at the level of the rostral fourth ventricle and craniovertebral junction. As such, the patient was counseled to proceed with another procedure for definitive CSF diversion. After a ventriculoperitoneal shunt was placed, the patient's condition improved and he was discharged home.

Discussion: The cause of the patient's hydrocephalus was assumed to be multifactorial. The preoperative MRI did not show significant mass effect on the fourth ventricle from the cerebellar mass. It was thought that the Chiari decompression would help resolve the hydrocephalus because the tonsillar crowding was the presumed culprit. On pathology, the patient was found to have cerebellar dysplasia; more specifically, he had slightly enlarged granule cells that were largely restricted to the ribbons of the cerebellar cortex internal granule cell layer. These neurons were smaller and blander compared with the bizarre ganglion cells associated with Lhermitte Duclos. As such, this type of dysplasia may be unique to the patient's syndrome or specific PTEN deletion that is associated with it.

Conclusion: The patient presents with a complex history that is typically not associated with hydrocephalus

or hamartomas of the cerebellum. This case underlies the importance of imaging in patients with PTEN hamartoma tumor syndromes, as well as the optimal strategy, in managing Chiari-I malformation in this population. Because the patient did not improve with the craniectomy and duraplasty, it is possible that exploring the obex could have revealed another source of the obstruction.

P047. Endoscopic Surgery for Chondrosarcoma of the Nasal Cavity and Sinus

Jianbao Ju¹

¹Affiliated Hospital of Qingdao University, Qingdao, China

Objective: To investigate the surgical treatment of chondrosarcoma of the nasal cavity and sinus under nasal endoscope, and to summarize the clinical manifestations, diagnosis, treatment, and prognosis of this disease.

Methods: the clinical data of seven patients with chondrosarcoma of the nasal cavity and sinus treated with nasal endoscopic surgery were retrospectively analyzed, and the surgical techniques and clinical characteristics of chondrosarcoma of the nasal cavity and sinus were summarized.

Results: Seven patients underwent nasal endoscopic resection, and the follow-up effect was good. The clinical features of chondrosarcoma of the nasal cavity and sinus are complex and varied, and it is difficult to make a definite diagnosis. Early chondrosarcoma of the nasal cavity and sinus is limited to the nasal sinus, the operation is easier, the treatment effect is better. The advanced lesions are extensive and even easy to involve the orbital and skull base. The operation is difficult and risky, and the prognosis is poor. Irregular plaque calcification is a typical imaging feature of this disease.

Conclusion: Endoscopic radical resection is the first choice for the treatment of chondrosarcoma of the nasal cavity and sinus. Early diagnosis of chondrosarcoma of the nasal cavity and sinus is difficult, which should be combined with CT, MR imaging, and histopathology.

Table 1 Clinical data of seven patients

	Sex	Age (y)	Primary site of tumor	Main symptoms	Pathology and S-100	Follow-up
1	F	28	Posterior septum involving sphenoid sinus	bilateral nasal obstruction for 3 months	Chondrosarcoma, ? level, (+)	4 years without recurrence
2	F	56	The posterior septum involves the base of the skull	Blurred vision in the right eye with diplopia for 20 days	Chondrosarcoma, ? level, (+)	No recurrence in 2 years
3	F	77	The maxillary sinus involves the base of the skull	Left nasal congestion for 5.5 years left eye vision loss for 20 days	Chondroma with a tendency to malignancy	4 years of progression
4	F	81	The posterior septum involves the base of the skull	Left nasal obstruction for 1 year left nasal bleeding for 4 days	Chondrosarcoma, ? level, (+)	No recurrence in 1 year
5	M	34	Maxillary sinus	Left nasal congestion for 5 months	Chondrosarcoma, ? level, (+)	No recurrence in 1 year
6	M	56	The maxillary sinus involves the base of the skull	Repeated right nasal bleeding for 2 months	Chondrosarcoma, ? level, (+)	No recurrence in 2 years
7	F	40	The maxillary sinus involves the base of the skull	Repeated right nasal bleeding for 2 months	Chondrosarcoma, ? level, (+)	No recurrence in 3 years

P049. Combined Transoral, Transnasal Endoscopic Surgery with Immediate Craniocervical Fusion for Giant Chordomas of the Clivus and Craniocervical Junction—State of the Art Team Work

Alessandra Cataldo Russomando¹, Ron Eliashar¹

¹Hadassah Medical Center, Jerusalem, Israel

Introduction: Chordoma is a rare aggressive, locally invasive tumor, arising from remnants of notochord. Complete surgical resection followed by radiation offers the best chance of long-term local control and survival. Treatment of clival chordomas is exceptional with emphasis on vascular protection and preservation of neurological function, typified by a concept of maximally aggressive safe surgery and advanced radiation techniques, such as proton beam. The craniocervical stability should be addressed during surgery of giant tumors.

Methods: Review of the operative technique and surgical results of giant clival chordomas requiring combined trans-oral, trans-nasal endoscopic surgery with immediate craniocervical fusion in the past 2 years.

Results: Three giant clival/craniocervical junction chordoma cases underwent a combined trans-oral, trans-nasal endoscopic surgery with immediate posterior craniocervical fusion. There were one male and two females in the ages of 30, 16, and 17 years. Surgery was staged as required and lasted up to a total of 30 hours in 3 days. Complete surgical excision was achieved in all with no vascular sequela. A hypoglossal nerve, involved by the tumor in two cases, was damaged. There were no other neurological deficits. The 6 to 8 cm skull base defect was reconstructed using multilayer closure with one post-operative CSF leak managed conservatively. Craniocervical fusion was uneventful in all cases, demanding 3 months of fixation in a rigid collar. The third, most complicated and demanding case, will be presented.

Conclusion: Endoscopic surgery of giant clival/craniocervical junction chordomas is very challenging but feasible. It should be performed by an experienced endoscopic skull base team.

P050. Endoscopic Endonasal Approach to Large Anterior Skull Base Chondrosarcoma: Case Report

Tural Hidayetov¹, Tural Rahimli¹

¹Baku Medical Plaza, Baku, Azerbaijan

Background: Chondrosarcomas are rare, infiltrative, progressive lesions that occur at the cranial base. Their intimate association with cranial nerves and major vessels of the head and neck often make it very hard to complete surgical resection.

Methods: We present a 59-year-old female patient with headache and 5-year deterioration of visual acuity. The radiologic investigation with a head magnetic resonance image had shown massive anterior skull base neoplasm filled sphenoid and maxillary sinuses and extended to right orbital fossa.

Results: Surgery was done by endoscopic endonasal approach, tumor was removed totally. Anterior skull base was kept intact, so there were no need skull base reconstruction. Patient's postoperative period followed without any complication. Visual acuity improved slightly. Pathology confirmed a chondrosarcoma grade I.

Conclusion: EEA may be considered a good option for managing anterior skull base chondroid tumors without significant damage to skull base. However one route approach is highly selective according to the skull base occupation by tumor



Fig. 1

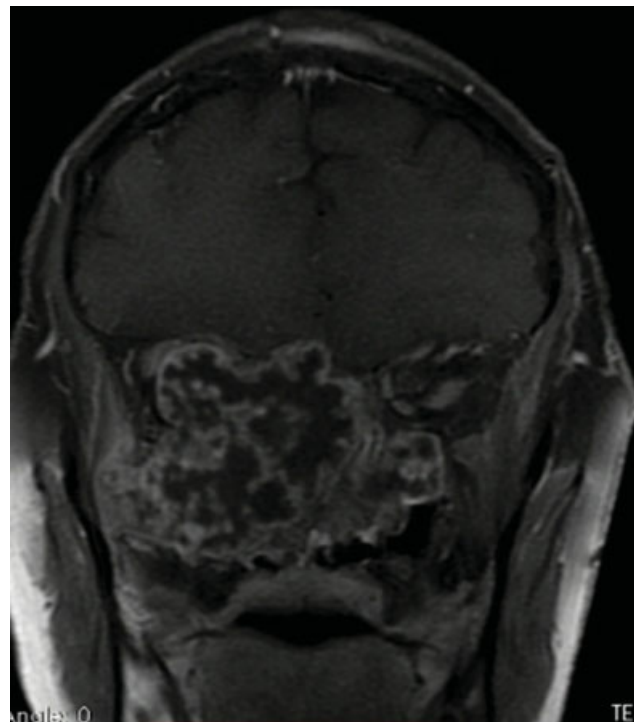


Fig. 2

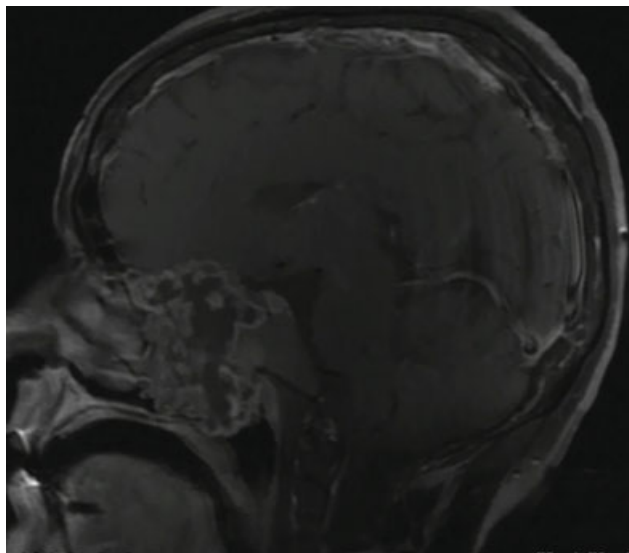


Fig. 3

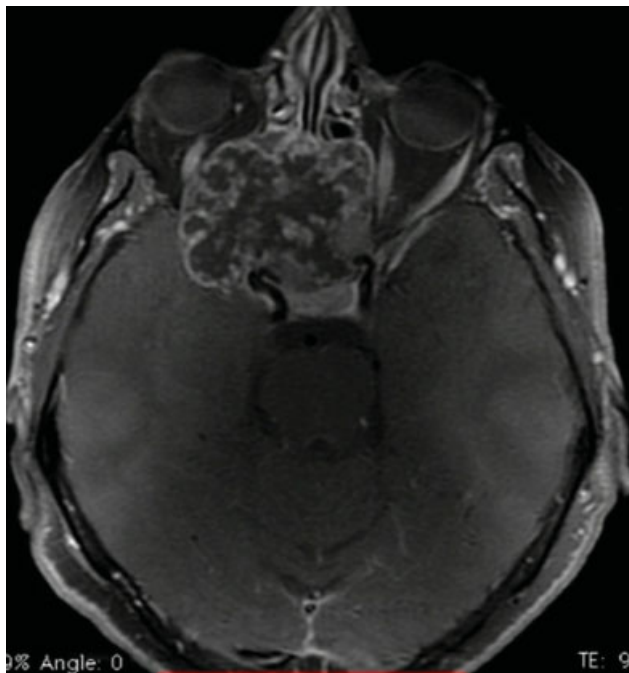


Fig. 4

P051. Cranial Nerve VI Palsy as a Presenting Sign of Previously Undiagnosed Metastatic Prostate Adenocarcinoma to the Clivus

Jennifer E. Douglas¹, John Y. K. Lee², Karthik Rajasekaran¹

¹Department of Otorhinolaryngology - Head and Neck Surgery, University of Pennsylvania Health System, Philadelphia, Pennsylvania, United States

²Department of Neurosurgery, University of Pennsylvania Health System, Philadelphia, Pennsylvania, United States

Introduction: Prostate adenocarcinoma is the most common cancer in males in the United States with an annual incidence of 110 per 100,000 males annually. Typically, highly curable prostate adenocarcinoma is the second leading cause

of cancer-related death due to metastatic disease to the bone in 86% of cases. There has, however, been only three reported cases of metastatic prostate adenocarcinoma to the clivus. Here we present the case of a male who presented with a cranial nerve VI palsy with imaging showing an infiltrative skull mass, who was ultimately diagnosed with prostate adenocarcinoma metastatic to the clivus.

Case Report: An 81-year-old male with history of prostate adenocarcinoma status-post radiation three years prior presented to the emergency department for evaluation of diplopia. Of note, the patient was on enzalutamide for rising prostate-specific antigen in the absence of known active disease. His examination showed partial right abducens palsy on extreme lateral gaze, and he had no other focal neurological deficits. A noncontrast computed tomography scan of the sinuses was performed which showed a 2.5 × 3.5 × 3.9 cm midline skull base mass involving the sella and suprasella (image 1) and he was subsequently admitted to the hospital for further work-up. He was unable to undergo a magnetic resonance imaging at that time as it was thought his stainless prostate seeds were a contraindication. Therefore, based on CT scan, differential included pituitary adenoma, meningioma, hematologic malignancy, chondrosarcoma, chondroma, and metastatic disease. Endocrinology was consulted given concern for secreting pituitary adenoma, with no evidence of endocrine dysfunction. Due to inability to perform further imaging, decision was made to take the patient to the operating room and obtain a biopsy for definitive diagnosis. An anterior skull base approach was performed, the sella was entered, and biopsies were taken. Intraoperative frozen section showed atypical epithelioid neoplasm, with final pathology confirming a diagnosis of metastatic prostatic adenocarcinoma. He was subsequently cleared to undergo MRI, which demonstrated an infiltrative mass of the clivus extending to the petrous apices, cavernous sinus, petrous and cavernous internal carotid arteries, prepontine cisterns, and abutting the pituitary gland (image 2). The patient was thus referred to radiation oncology for palliative radiation.

Conclusion: Prostate adenocarcinoma is the leading cause of cancer in males and metastatic disease can involve the skull base in unique circumstances. Few case reports exist of prostate adenocarcinoma metastatic to the clivus. Here we add to this literature by presenting a case of a patient with isolated cranial nerve VI palsy as the presenting sign of previously undiagnosed metastatic prostate adenocarcinoma involving the clivus. The skull base surgeon should maintain a high clinical suspicion for metastatic disease as a cause of atypical sellar and suprasellar lesions.

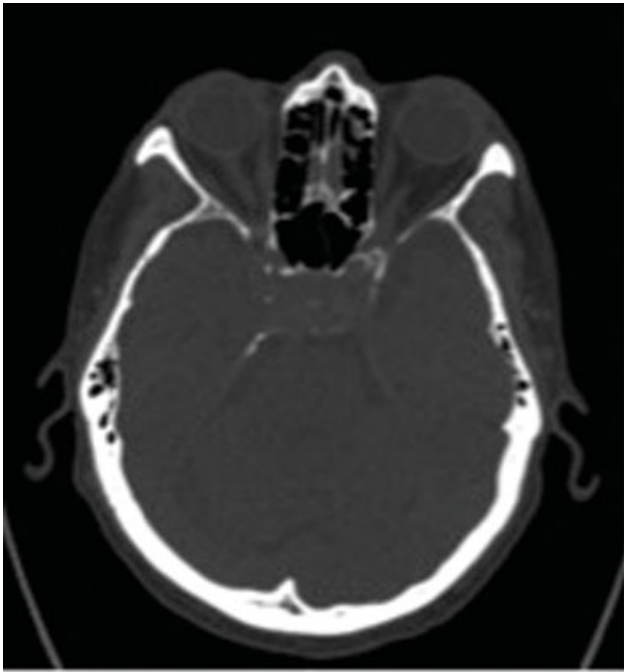


Fig. 1 Noncontrast enhanced CT at the level of the pituitary gland shows a $2.5 \times 3.5 \times 3.9$ cm midline skull base mass involving the sella and suprasella.

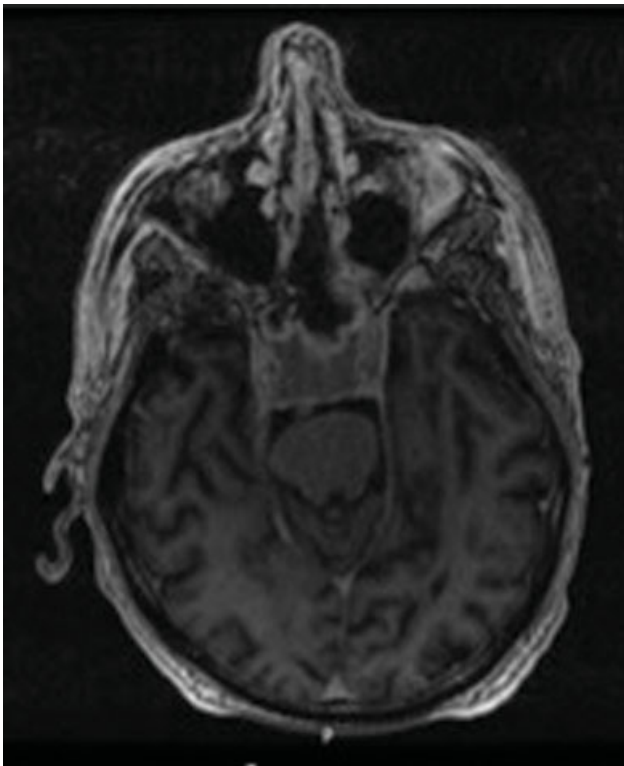


Fig. 2 MRI of the head with and without IV contrast demonstrating diffuse metastatic infiltration and destruction of the clivus.

P052. Intraoperative Evaluation of Sigmoid Sinus Velocity in Translabyrinthine Craniotomies for Vestibular Schwannomas using Doppler Ultrasound

Zachary R. Barnard¹, Anne K. Maxwell¹, Tommy J. Muelleman¹, William H. Slattery¹, Guatam U. Mehta¹, Gregory P. Lekovic¹
¹House Institute, New Delhi, India

Introduction: Sigmoid sinus (SS) occlusion or compression is a known complication of the translabyrinthine approach. Velocity changes in the SS measured by intraoperative Doppler ultrasound, may help in identifying patients at risk for sinus occlusion.

Methods: SS velocity was measured using Doppler ultrasound prior to opening dura and again prior to placement of the abdominal fat graft. Data collected included patient age, side of surgery, sigmoid sinus dominance, tumor volume, intra-operative Doppler ultrasound measurements, postoperative venous sinus imaging, use of anticoagulation, morbidities and mortalities. Statistical analysis was performed using Wilcoxon signed rank test (IBM SPSS Statistics 24).

Results: A total of eight patients were included for analysis. Age ranged from 22 to 69 years old. Four had left-sided and four had right-sided craniotomies. Sigmoid sinuses were either right-side dominant or co-dominant. The mean velocity + SD prior to dura opening and abdominal fat packing was $23.2 + 11.3$ and $25.5 + 13.9$ cm/s, respectively, $p = 0.575$. Postoperative MRV imaging showed four sigmoid sinus occlusions; seven patients showed sigmoid sinus compression, and one internal jugular vein occlusion. One patient only had postoperative CTV. On the four patients with MRV occlusions, CTVs were performed with three showing occlusion and all four showing compression. There were no occluded internal jugular veins on CTV. The one patient with internal jugular vein occlusion on MRV received warfarin anticoagulation. There was one CSF leak requiring ear closure and one small cerebellar infarct.

Conclusions: SS velocity changes before and after tumor resection were not predictive of sinus occlusion. We hypothesize that sinus occlusion may be caused by related factors other than thrombosis, such as external compression of the sinus secondary to abdominal fat grafting.



P053. Skull Base Meningioma Surgeries: How Aggressive Is Aggressive Enough?

Sebastian Liao¹, Shao-Ching Chen², Sanford Hsu²

¹Taichung Veterans General Hospital, Taichung, Taiwan

²Taipei Veterans General Hospital, Taipei, Taiwan

Introduction: Skull base surgeons frequently sink into a dilemma while dealing with skull base meningiomas because of the involvements of crucial neurovascular structures: “Shall we be aggressive to reduce tumor recurrence rate or shall we be conservative to diminish the postoperative neurological deficits?” The present study aims to clarify the correlation between the resection rate, neurological outcomes, and clinical results in patients with skull base meningiomas.

Material and Methods: Patients who underwent surgeries for skull base meningiomas by our senior author during 2010–2018 were included. The first postoperative image would be obtained within 3 days postoperatively for evaluation of resection rates, and then followed by every 3 or 6 months, depending on the pathological grading of the tumor. Medical records and clinic data were retrospectively reviewed for statistical analyses.

Results: A total of 143 patients with a median follow-up time of 27.3 months were included. The mean resection rate is 93.4% (33.3–100%). Postoperatively, 23 patients (16%) presented with new-onset or worsen cranial nerve deficits (CNDs), of which were smelling disturbance (4%), eye symptoms (43%), facial numbness (17%), facial palsy (22%), and swallowing difficulties (13%). Fifty-seven patients (39.8%), including postoperative cranial nerve deficits, experienced postoperative complications. Main symptoms were hydrocephalus (23%), infarctions (21%), eye symptoms (18%), and infections (9%). In our series, a resection rate over 93% for Grade I meningiomas was associated with prolonged progression-free survival ($p = 0.018$). For Grade II or Grade III meningiomas, a resection rate over 97% was associated with prolonged progression-free survival ($p = 0.031$). The correlation between resection rates and postoperative CNDs or complications were not statistically significant. ($p = 0.47$ and 0.35)

Conclusion: Extensive resection for skull base meningioma may be encouraged under the premise that the surgeon is confident of avoiding postoperative deficits, especially while operating high-grade tumors.

P054. Management of Frontal Mucocele after Pericranial Flap Reconstruction of Anterior Skull Base Resection Defect

Matthew Kim¹, Carl Snyderman², Andrew Tassler¹

¹Weill Cornell Medical College, New York, New York, United States

²University of Pittsburgh School of Medicine, Pittsburgh, Pennsylvania, United States

Introduction: Over the past two decades, techniques for endoscopic resection of ventral skull base lesions and reconstruction of resulting skull base defects has progressed significantly. The benefits of the endoscopic endonasal approach (EEA) include decreased postoperative morbidity with hastened recovery, the absence of an external incision, and improved intraoperative visualization—all without compromising oncologic resection in appropriately selected patients. While literature supports this approach as safe and effective, recognized complications include cerebrospinal fluid leak, meningoencephalocele, delayed healing and skull base crusting, donor site morbidity, and mucocele formation. Mucocele, in particular, is a rare complication, with published rates well below 5%. We describe a case of frontal mucocele formation after skull base resection and vascularized reconstruction, and a novel approach to its management.

Case Presentation: A 31-year-old male presented with a 1-month history of progressive left forehead swelling and pain, with related complaints of numbness radiating to the occiput. His past surgical history was notable for Hyams grade 3 right olfactory neuroblastoma, treated 3 years previously with endoscopic resection followed by pericranial flap reconstruction and adjuvant radiation. Interval imaging following treatment had revealed bilateral opacification of the frontal sinuses without associated findings, and no evidence of recurrence. Magnetic resonance imaging revealed bilateral frontal opacification, with expansion of the left frontal sinus associated with disruption of the anterior table, consistent with mucocele. Computed tomography revealed a heterogeneous collection spanning both frontal sinuses with a bony defect of the left anterior table. The patient underwent endoscopic drainage and marsupialization of the frontal mucocele under general anesthesia. Nasal endoscopy revealed extensive postoperative changes and scarring with an intact vascularized skull base reconstruction. Stereotactic image guidance was utilized to identify the left bony frontal outflow tract, and a blunt-tipped angled suction was gently advanced into the mucocele cavity. Moderate mucopurulent drainage was suctioned and irrigated. The neofrontal drainage pathway was widened anteriorly with through-cutting hand instruments and a curved microdebrider, taking care not to violate the posterior table or skull base reconstruction. The left frontal sinus was then brought into continuity with an intersinus septal cell, likely communicating with the right frontal sinus. A steroid-eluting bio-absorbable stent was then placed into the neo-frontal ostium to prevent scarring and maintain patency. The stent was removed at the first nasal debridement, and the frontal sinus drainage pathway remained patent at follow-up 4 weeks after surgery.

Discussion: Mucoceles are rare complications following vascularized reconstruction of skull base defects. We present a case of frontal mucocele following endoscopic resection of esthesioneuroblastoma and pericranial flap reconstruction, managed by endoscopic drainage and marsupialization with placement of a steroid-eluting bioabsorbable stent.



Fig. 1 Sagittal image from noncontrast CT revealing left anterior table erosion by mucocele.



Fig. 2 Coronal image from noncontrast CT revealing erosion of left orbital roof.

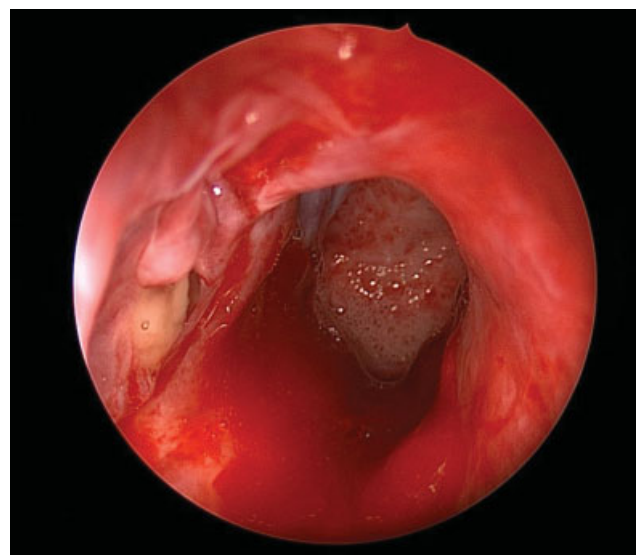


Fig. 3 Endoscopic view into left frontal mucocele cavity with mucopurulent secretions in a communicating intersinus septal cell.

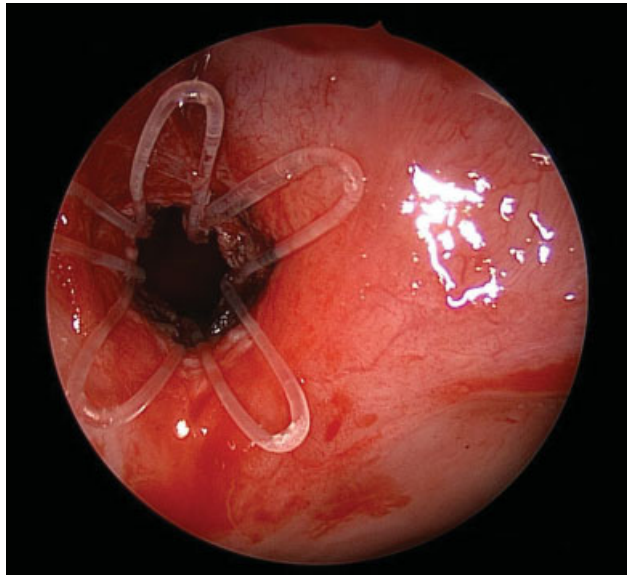


Fig. 4 Endoscopic view of steroid-eluting bioabsorbable stent in neofrontal ostium.

P055. Hemifacial Spasm: Surgical Strategies and Complications

Sam Emerson¹, Jake Ruzevick¹, Rajeev Sen¹, Kate Carroll¹, Manuel Ferreira Jr¹

¹University of Washington, Forks, Washington, United States

Hemifacial spasm is a unilateral movement disorder of the facial nerve characterized by intermittent twitching of the muscles of the face. This progressive disorder can cause significant embarrassment and social withdrawal, and in severe cases lead to functional blindness. The most common cause is direct compression of the root entry zone by an ectatic blood vessel leading to local demyelination. How this demyelination leads to hyperactivity of the nerve is not precisely known, though multiple putative mechanisms exist. Here we review our institutional series of microvascular decompression of the facial nerve for the treatment of hemifacial spasm. We discuss the surgical setup, neurophysiological monitoring (including lateral spread for the purposes of predication of resolution) and postoperative complications. Potential complications include: facial palsy, gustatory or vestibular dysfunction, hearing loss, hoarseness, dysphagia, or recurrence of spasm.

P056. Defining the Complication Landscape of Internal Neurolysis for the Treatment of Trigeminal Neuralgia via a Systematic Review of the Literature

Jacob Mazza¹, Victor Sabourin¹, Jeffery Head¹, Pascal Lavergne¹, Tomas Garzon¹, Anthony Stefanelli¹, Fadi Al-Saiegh¹, James J. Evans¹

¹Thomas Jefferson University, Philadelphia, Pennsylvania, United States

Introduction: Trigeminal neuralgia (TN) is considered one of the most debilitating facial neuropathic pain syndromes that can affect an individual. Medical treatment remains first line therapy, with microvascular decompression (MVD) being the primary surgical intervention for patients with underlying neurovascular compression (NVC) of the trigeminal nerve. Internal neurolysis (IN) has recently shown promising results for trigeminal neuralgia pain-relief in

patients with absent or low-grade NVC. However, the complications profile of IN has not been well defined.

Methods: A literature search of PubMed was performed using the search terms “Trigeminal Neuralgia,” “Internal Neurolysis,” and “Microvascular Decompression,” as well as common permutations of free text terms along with appropriate indexation terms. This search resulted in 57 articles, which were then reviewed for duplicates, non-English articles, and articles with alternative treatment methods. Articles without results differentiating treatment with IN versus other modalities were also excluded. A total of nine articles were considered for analysis, and PRIMSA guidelines were followed throughout the systematic review.

Results: The systematic review resulted in nine studies including a total of 459 people, 323 (70.4%) of which underwent IN. The mean/median range of follow-up was 12–90 months. Primary complications relating to trigeminal nerve manipulation included facial hypoesthesia, corneal numbness, corneal ulcer and anesthesia dolorosa. Immediate postoperative rates of facial numbness in all patients receiving IN was 46%, with individual studies showing rates of immediate postoperative facial numbness between 20 and 96%. This decreased at last follow-up to anywhere from 3.75 to 67.6%. The overall rate of corneal numbness/ulcer or loss of corneal reflex was 1.2%, although one study specifically did not report corneal symptoms postoperatively. One instance of anesthesia dolorosa was reported (0.3%).

Conclusion: Compared with standard MVD, the rate of facial hypoesthesia is higher with internal neurolysis. However, the rate of severe complications remain low and is comparable to other interventions for trigeminal neuralgia. More studies are warranted to compare the efficacy of IN and analyze the cost-benefit of long-term facial numbness and robust pain outcomes.

P057. Combined Pipeline Embolization Device with Endoscopic Endonasal Fascia Lata/Muscle Graft Repair as a Salvage Technique for Treatment of Iatrogenic Carotid Artery Injury and Pseudoaneurysm

Jordina Rincon-Torroella¹, Ann Liu¹, Matthew T. Bender¹, Cameron G. McDougall¹, Anthony P. Tufaro¹, Alexander L. Coon¹, Douglas D. Reh¹, Gary L. Gallia¹

¹Johns Hopkins Hospital, Baltimore, Maryland, United States

Introduction: The incidence of internal carotid artery (ICA) injury associated with endoscopic endonasal approaches to the pituitary is 0.2–2%. While parent vessel sacrifice has historically been the choice of treatment, vessel-preserving endovascular techniques have been reported. We describe the use of a combined pipeline embolization device (PED) with endoscopic endonasal repair using a fascia lata/muscle graft to treat an iatrogenic ICA pseudoaneurysm.

Case Presentation: A 77-year-old woman with a non-secreting pituitary macroadenoma treated at another institution was transferred to our hospital due to intraoperative ICA injury during ultrasonic bone removal. She was emergently packed with pledgets and three Foley catheters. Once resuscitated and hemodynamically stabilized, she was transferred from the OR to our institution. Upon arrival, she underwent an angiogram showing a 1.4 × 2 mm right medial cavernous segment pseudoaneurysm. She subsequently underwent a balloon test occlusion (BTO) with left arm weakness after 9 minutes of occlusion. Due to the failed BTO, she was started on aspirin 325 mg and prasugrel 5 mg daily in anticipation for flow diversion. She underwent endovascular flow diversion on day of admission (DOA) 5. Three telescoping PED were deployed using a standard triaxial catheter. Repeat angiography on DOA12 showed good

stent-vessel wall apposition but continued residual filling of the pseudoaneurysm (2.9 mm). The patient developed fevers and increased white counts despite broad spectrum antibiotics and packing/Foley removal was planned given concern this was the source of her fevers. Due to residual filling, repair of her ICA was necessary. A fascia lata/muscle graft was harvested at the beginning of the case. Superficial packing was removed and the sphenoidotomy was expanded for increased access. Brisk arterial bleeding was noted from the region of the anterior genu of the carotid while attempting to dissect the final pledgets. Hemostasis was obtained by gentle pressure on a pledget over the rupture site. This was removed and the graft was placed over the pseudoaneurysm/wall of the ICA with excellent hemostasis. The site was packed with Gelfoam wrapped in Surgicel. Two nasopores were positioned into the sphenoid sinus and a gloved merocel was placed in each nostril. Angiography on DOA19 showed complete obliteration. Aspirin dose was decreased to 81 mg. She was weaned off the ventilator and transferred to the floor being discharged to rehab soon after. Follow-up angiography at 6 months and 2.5 years confirmed complete obliteration of the pseudoaneurysm with no in-stent stenosis or thrombosis.

Discussion: Pseudoaneurysms lack true walls and have increased risk of rupture during manipulation. Flow diversion offers endoluminal treatment without accessing the aneurysm. The major limitation is the delay in obtaining complete occlusion. Close follow-up for continued filling of the pseudoaneurysm is necessary and additional treatment may be needed. As the false wall of the pseudoaneurysm remodels, fascia lata/muscle grafting can help reinforce the false wall, rather than opting for vessel sacrifice. Further investigation into the utility of directed endoscopic endonasal repair of traumatic pseudoaneurysms after PED is necessary, especially given the need of post-PED anticoagulation and the rate of permanent neurological deficit after ICA sacrifice.

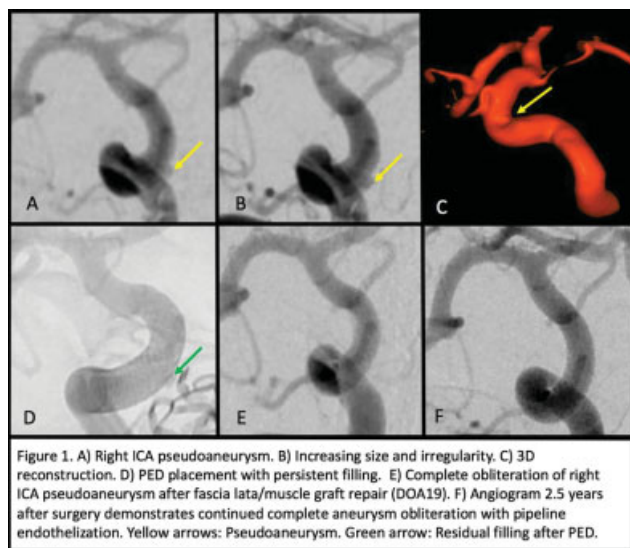


Figure 1. A) Right ICA pseudoaneurysm. B) Increasing size and irregularity. C) 3D reconstruction. D) PED placement with persistent filling. E) Complete obliteration of right ICA pseudoaneurysm after fascia lata/muscle graft repair (DOA19). F) Angiogram 2.5 years after surgery demonstrates continued complete aneurysm obliteration with pipeline endothelialization. Yellow arrows: Pseudoaneurysm. Green arrow: Residual filling after PED.

P058. Complications of Endoscopic Endonasal Skull Base Surgery for Sellar Pathology—An Institutional Experience

Amey Savardekar¹, Tim Banks¹, Jennifer Kosty¹, Bharat Guthikonda¹

¹Department of Neurosurgery, LSUHSC, Shreveport, Louisiana, United States

Background: Endoscopic endonasal surgery is the preferred approach for most sellar pathologies and with the advent of nasoseptal flap reconstruction, major complications have been effectively countered. We present our institutional experience in the management of sellar pathologies with the endoscopic endonasal approach.

Methods: Patients who underwent endoscopic endonasal skull base surgery for sellar pathology between 2012 and 2018 were retrospectively evaluated. Complications reviewed were divided into major and minor. Major complications included new-onset and continuing CSF leak and meningitis. Minor complications included long-standing crust formation, synechia, epistaxis, septal perforation, sinusitis, and anosmia.

Results: Fifty-nine patients with managed with EES for their sellar pathologies. The mean age was 56.4 years (\pm 8.9) and M:F = 26:33. The most common pathology was pituitary macroadenoma, seen in 42 (71%) patients. Intraoperative CSF leak was observed in 19 patients; however, postop leak was noted only in four patients. Preop and postop lumbar drainage placement was required in seven patients. DI was noted in 14 patients and managed effectively. Minor complications were noted in eight (12%) patients requiring local treatment and observation.

Conclusions: EES is an extremely effective approach for sellar tumors. While it is associated with a low rate of major complications, minor complications are frequent, but require only local (nasal) treatment and conservative management. CSF leaks can be effectively managed with temporary lumbar drain placement

P059. Economics of the Treatment of Craniospinal Chordoma and Chondrosarcoma and the Feasibility of using the Bundled Payment Model

Zaid Aljuboori¹, Beatrice Ugiliweneza¹, Norberto Andaluz¹, Maxwell Boakye¹, Brian Williams¹

¹University of Louisville, Louisville, Kentucky, United States

Healthcare expenditures are continuously rising in the United States. The current fee-for-service (FFS) system reimburses health care providers based on the volume of services performed. Due to the risk of performing unnecessary tests, the Centers for Medicare and Medicaid Services (CMS) created a new reimbursement model called the “Bundled Payment for Care Improvement (BPCI).” This model reimburses providers a prespecified bundled payment in advance to cover all possible services rendered to patients within a specified time window around the treatment, including eventual complications. Chordoma/chondrosarcoma are slow-growing and locally aggressive malignant primary bony tumors. Treatment includes maximum safe surgical resection and radiotherapy with substantial risk for recurrence which necessitates observation and further treatment. These factors make these conditions valuable to explore the feasibility of the BPCI model. Data were obtained from the United States MarketScan database, patients were identified using the International Classification of Diseases 10 codes. A total of 1,755 patients were included, 1,412 had cranial (group 1) and 343 had a mobile spine (group 2) chordoma/chondrosarcoma. For Index hospitalization, the median length of stay (days) was 4 and 6, median total payments were 35401\$ and 42303\$, complication rates were 30% and 33.5%, for group 1 and 2. Three months postdischarge period, hospital readmission rates were 21% and 39%, and payments were 29824\$ and 28969 \$, for group 1 and 2. Combined median payments for the index hospitalization and 90 days postdischarge were 79752\$ and 102366\$ for group 1 and 2. For the second 3 months payments were 87% and 93% of the

first 3 months for groups 1 and 2. For the first 6 months after discharge, readmission rates were 30% and 45% for group 1 and 2. For the second 6 months after discharge, readmission rates dropped to 14% and 7% for groups 1 and 2. This was associated with a decline in payments. Payments during the second 6 months after discharge were 52% and 62% of payments during the 1st 6 months for group 1 and 2. These findings indicate that the excessive cost needed to manage craniospinal chordoma and chondrosarcoma extend over an extended period. The BPCI may not be feasible for conditions with a high rate of complications and readmission, and an increased need for outpatient services. It poses a risk of monetary loss to the hospital. The success of BPCI requires a joint effort between insurers and hospitals. It should consider patients' comorbidities, the complexity of the disease, inherent risk for complications. Also, it is well-documented centers with high case volume is associated with lower complications, better outcomes, and lower cost. Therefore, it may be of importance for certain complex neurosurgical conditions to be managed at centers of excellence. From the hospital side, the adoption of programs like Enhanced Recovery After Surgery or Enhanced Perioperative Care which aimed at decreasing length of stay, complications, and readmissions may be valuable to improve outcomes and decrease cost.

P060. An Orbital Floor Implant Angulation Guide with 3D-Printed Customization

Henry Bair¹, Giancarlo A. Garcia², Emily Charlson², Andrea Kossler², Benjamin P. Erickson²

¹Stanford University School of Medicine, Stanford, California, United States

²Byers Eye Institute, Stanford University School of Medicine, Stanford, California, United States

Introduction: Achieving optimal implant angulation can be challenging in orbital fracture repair, and the posterior edge may wind up low without support from a well-defined bony ledge, resulting in under-correction of enophthalmos. There may be intrinsic difficulties in judging angulation, particularly as perception is influenced by operative head tilt, as well as technical challenges in further elevating the posterior aspect of a cantilevered implant once the anterior aspect has been anchored to the rim. We present a simple patient-customizable intraoperative guide that addresses both potential concerns.

Method: One arm of a Castroviejo caliper was machined to produce a contoured implant elevator, while the other was replaced with a stabilizing orbital rim footplate, custom 3D printed with P430XL ABSplus material (Stratasys, Eden Prairie, MN) via a uPrint SE 3D printer (Stratasys) to match the external rim contour in a parasagittal section (Fig. 1A). Once screwed to the anterior rim, the anterior-posterior contour of the implant can then be adjusted to the optimal angle determined by preoperative scan analysis by placing the elevator under the implant (Fig. 1B), the footplate on the exposed anterior rim, and turning the thumbscrew until the desired position is achieved.

Results: In a cadaveric model, an orbital fracture without a stable posterior bony ledge was created via a swinging eyelid approach. Periosteum overlying the anterior rim was then raised with a Freer elevator, exposing the desired resting position for the custom footplate. A contoured titanium floor implant (3D Titan, Stryker, Kalamazoo, MI) was then secured to the rim using 4-mm self-drilling titanium screws, with the posterior aspect depressed within the maxillary sinus. The implant angulation guide was then positioned as described (Fig. 2) and the thumbscrew manip-

ulated to elevate the posterior implant, which remained appropriately positioned after the guide was removed.

Conclusion: While intraoperative navigation can assist with implant placement for complex fractures, such setups entail obtaining specially formatted CT scans and may be inconvenient for routine use. Likewise 3D-printed custom implants are produced from expensive materials with demonstrated long term biocompatibility and, when not well positioned, lose their volumetric advantage over conventional implants. We foresee that this simple intraoperative guide with inexpensive customization based on routine scans (Fig. 3) can help ensure appropriate implant position, thereby improving volumetric correction without the use of navigation or custom implants.

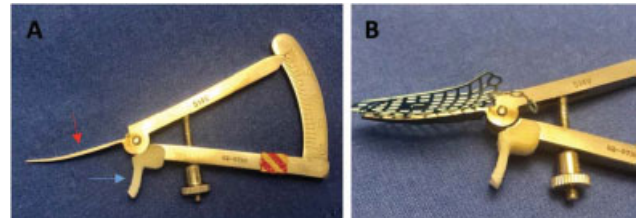


Fig. 1 Orbital implant angulation guide (A), showing the contoured implant elevator (red arrow) and 3D printed footplate (blue arrow). Elevator with implant (B).



Fig. 2 Implant angulation guide in situ with printed footplate resting on external bony rim.

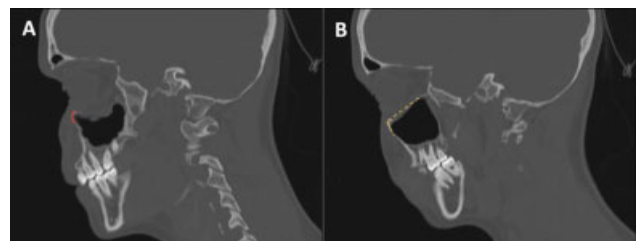


Fig. 3 CT scan demonstrating fractured (A) and unaffected contralateral orbit (B). 3D printed footplate is customized to the contour of the patient's anterior orbital rim (red). The angle formed by the intact orbital floor and anterior rim (dashed yellow) determines optimal retractor angle setting.

P061. Surgical Strategy Using Extended Endoscopic Transsphenoidal Approach for Craniopharyngioma: Single-Center Experience

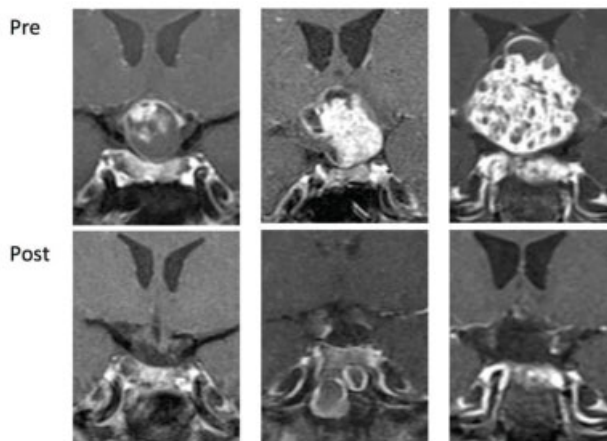
Masahiko Tosaka¹, Rei Yamaguchi¹, Masanori Aihara¹, Takaaki Miyagishima¹, Yuhei Yoshimoto¹

¹Gunma University Graduate School of Medicine

Craniopharyngioma is a benign brain tumor, however it is difficult to treat because of its proximity to critical structures at the base of the skull. Craniopharyngioma originates mainly in the pituitary stalk. It shows different size, shape, mode of progression. It may be associated with cyst formation, and calcification. Extended endoscopic transsphenoidal surgery (EETSS) is useful because it has wider angle of view. Our institution started EETSS for craniopharyngioma since 2012. EETSS was the first choice for suprasellar craniopharyngioma. We present our cases of suprasellar craniopharyngioma resected by purely endoscopic extended transsphenoidal approach.

Twenty-one patients (19 cases: 9–68 years old, average 48 years old, male: female = 9:10) of suprasellar craniopharyngioma (preoperative diagnosis) who underwent EETSS from April 2012 to February 2018 were included. One of them was pathologically diagnosed as xanthogranulomatosis. Six cases were recurrent cases after removal with open craniotomy. Four patients were irradiated with gamma knife. During this period, there were no cases of craniopharyngioma removed by craniotomy, and all cases were treated by endoscopic nasal surgery in our institution. Average tumor size was 28.5 mm (11–45 mm). Gross total removal (GTR) or near total removal (NTR) was achieved in 17 patients (81%). In three cases, 90% removal was achieved. Pre- and postoperative gadolinium enhanced MRI in 3 representative cases are shown in Figures (left, and center: GTR, right: 90% removal). One case had partial removal. Of the 90% of the resected cases, one pathologically had xanthogranuloma. The patient with partial removal, received a gamma knife after two times of craniotomy. There was one postoperative cerebrospinal fluid leak, but it was successfully repaired. Complications such as postoperative pneumonia occurred in one patient and subdural hematoma in one patient. Both showed complete recovery. Two patients underwent reoperation by the same route for recurrence, and four patients had small recurrence after surgery, and were treated with stereotactic radiotherapy. As regard visual function, 11 patients improved, 6 patients remained unchanged, and 3 patients deteriorated. Two of the worsening cases were cases that had not undergone intraoperative visual evoked monitoring (VEP), and the remaining one was xanthogranuloma. All but one patient returned to their normal life. In one case of xanthogranuloma, short-term memory impairment worsened. In this series, all patients needed some endocrinological compensation.

The prevention of cognitive and visual dysfunction is the major challenge during operation of craniopharyngioma. For this reason, it is necessary to observe midsagittal MRI before surgery to carefully identify the position of the optic chiasm, and mammillary bodies. The dissection between optic nerve and tumor should be performed carefully. We believe that avoiding any neurological deficit and safe gross total removal has a higher priority than preserving endocrinological function in many cases as this may be compensated medically.



P062. Endoscopic Endonasal Transsphenoidal Surgery for Craniopharyngiomas: Pearls and Pitfalls from a Large Case Series

Andrew B. Boucher¹, Sarah Newman¹, Bray P. David¹, Nelson M. Oyesiku¹

¹Emory University, Atlanta, Georgia, United States

Introduction: Craniopharyngiomas are rare, sellar/suprasellar tumors of embryologic origin that are histologically benign but clinically aggressive presenting with neuroendocrine abnormalities, hydrocephalus, or visual disturbance with high rates of recurrence. The preferred management of craniopharyngiomas is complete surgical resection, though the surgical challenge of proximity to neurovascular structures and extension into deep-seated spaces limits this goal. Classically, open, transcranial approaches have been utilized; in recent decades, there has been increased utilization of endoscopic endonasal transsphenoidal surgery (EETS) which provides a more direct route and less brain manipulation. Characteristics of patients and tumors that might be best treated by the EETS approach have not been clearly delineated. In this project, we analyze our experience with EETS approaches to craniopharyngiomas at a high volume center to determine surgical and treatment strategies.

Methods: A complete review of a single-surgeon, single-institution case series for EETS for craniopharyngiomas from 1994 to 2019 was completed using the clinical, operative, and radiographic records within the electronic medical record. Data collected included patient demographics, radiographic findings, patient presentation, surgical intervention, adjuvant therapy, and outcomes.

Results: There were 21 patients who underwent an endoscopic endonasal transsphenoidal surgery for craniopharyngioma. Most of these patients (13/21) had gross total resection. Only 19% (4/21) had recurrence or progression of residual tumor. All patients treated with radiation therapy for residual or recurrence (6/21) had either stable or regression of their disease. Rates of intraoperative CSF leaks were expectedly high (20/21) but postoperative meningitis rates were low at 14%, and there were no incidents of new cranial nerve injury. 52% of these tumors were large (>5 cm³) and 48% extended into the third ventricle.

Conclusions: Craniopharyngiomas remain a formidable disease entity given their intricate location, proximity to critical neurovascular structures and size at presentation. Our series adds to the growing evidence that the endoscopic

endonasal corridor is a safe and effective means to resect these tumors. The use of radiation therapy for residual or recurrence provides excellent disease control and should be used in combination with surgical resection when appropriate.

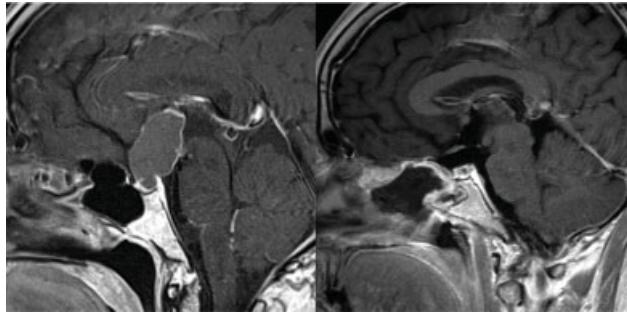


Fig. 1 Preop and postop sagittal MRI imaging of a craniopharyngioma resected using the endoscopic endonasal trans-sphenoidal approach.

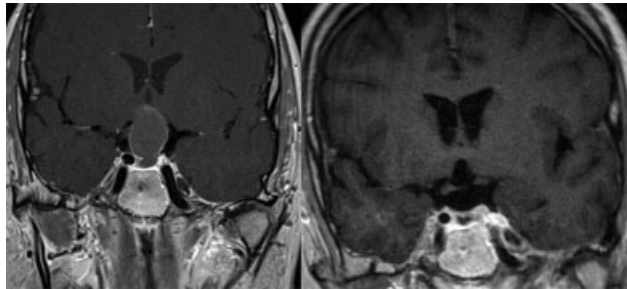


Fig. 2 Preop and postop coronal MRI imaging of a craniopharyngioma resected using the endoscopic endonasal trans-sphenoidal approach.

P064. Endonasal Endoscopic Surgery of Craniopharyngiomas: A Case Series

Bakhtiyar Pashaev¹, Dmitriy Bochkarev¹, Valeriy Danilov², Andrey Alekseev¹, Gulnar Vagapova³

¹Interregional Clinical Diagnostic Center, New Delhi, India

²Kazan Medical State University, Kazan, Russia

³Kazan Medical State Academy, Kazan, Russia

Objects: To present the results of endoscopic endonasal surgery of craniopharyngiomas.

Methods: A retrospective review including surgical technique, extent of resection, complications and outcomes was performed. All patients were operated between 2011 and 2019 in department of neurosurgery of Kazan Interregional Clinical Diagnostic Center.

Results: Twenty-two patients with craniopharyngiomas were operated. All procedures were performed under frameless image-guidance control, purely endoscopic. There were 9 (31%) males and 13 (59%) females. Patient's age was between 20 and 76 years, with mean age of 40.5 years. In four patients (18.2%) it was a repeat surgery due to residual tumor progression in the period of 5 to 56 months postoperatively. One of them underwent initial transcranial surgery in another medical center. Gross-total resection was achieved in 12 patients (54.5%), near total in 4 (18.2%), subtotal in 5 (22.7%). In three patients after a repeat surgery a gross-total resection was achieved in one case and subtotal in three rest cases. All patients with gross-total resection have no signs of tumor

recurrence at follow-up. The mean period of follow-up is 63 months. Prior to surgery 18 patients had a visual disturbance, 13 (59%) of them improved and 4 (18.2%) remained unchanged postoperatively. In one patient (4.5%) the worsening of visual function was marked. A postoperative cerebrospinal fluid (CSF) leak occurred in seven (31%) patients and was a reason of meningitis in 4 (18.2%) of them (two aseptic and two bacterial), all were cured. Six patients with cerebrospinal fluid leak underwent a surgical reconstruction of CSF-fistula (one patient twice, and one for three times), in this particular case a usage of free pericranial flap allowed get a final water-tide reconstruction. In one patient a CSF leak resolved on lumbar drain. Four (18.2%) patients developed a diabetes insipidus in one it was transient, 1 (4.5%) patient showed a panhypopituitarism, and 1 (4.5%) patient had a cerebral salt-wasting syndrome postoperatively. One patient had an acromegaly and after subtotal tumor removal receiving octreotide for growth hormone relief without residual tumor progression. In one patient a short memory loss was determined postoperatively which completely resolved 6 month later. In one patient a cognitive impairment remained at the same level postoperatively with minor improvement 1 year later. Mortality rate in series was zero.

Conclusions: Expanded endoscopic endonasal approaches allowed make a microsurgical resection of craniopharyngiomas in safe mode and with good visual control. Postoperative CSF leak remains a significant complication. Learning curve impacts on extent of tumor resection and postoperative CSF-leak frequency.

P066. Minimally Invasive Tubular Approach for Occipital Condylar Biopsy and Resection

Andrew Platt¹, Melissa Stamates², Ricky Wong²

¹University of Chicago, Chicago, Illinois, United States

²Evanston Hospital, Evanston, Illinois, United States

Occipital condyle syndrome describes the presentation of a patient with unilateral occipital headache and ipsilateral hypoglossal nerve palsy. The clinical significance of occipital condyle syndrome is that it is frequently the first sign of bony metastasis to the occipital condyle and can many times be discovered prior to the primary malignancy. Surgical approaches to the craniovertebral junction are inherently challenging and have traditionally involved far-lateral craniotomies, open posterior approaches, and transoral approaches. Few cases of minimally invasive surgical approaches specifically to the occipital condyle have been described.

We present the case of a 38-year-old African-American female with past medical history of breast cancer (DCIS, ER+, PR+, HER2-) status post right breast simple mastectomy and left breast modified radical mastectomy and treatment with letrozole and leuprolide 3 years prior to admission, who presented to an outside hospital with a two month history of headache localizing to the right occipital area, and right tongue deviation. Neurologic exam was notable for a right hypoglossal nerve palsy. MRI revealed a 1.3 cm × 1.1 cm heterogeneously enhancing mass within the right occipital condyle which was noted to be lytic on CT (image 1). After multidisciplinary discussion between the patient's oncologist and neurooncologist it was decided to pursue tissue diagnosis via an excisional biopsy. The patient was brought to the OR and placed in three-point cranial fixation in the prone position. A 3-cm paramedian incision was made on the right ~2.5 cm off midline at the level of C1. Sequential dilation using a tubular retractor system was performed under fluoroscopic guidance (image 2). Using a penfield #4 dissector, a subperiosteal plane was identified and carefully followed

laterally and anteriorly until the condylar fossa was visualized (image 3). Once the posterior surface of the occipital condyle was seen, the cortex was entered (image 4) at which point tumor was immediately visualized and resected. Specimen was sent for pathology. A combination of pituitary rongeurs, curettes, and suction dissection was used to debulk the condylar mass while minimizing bony destruction. Operative time was 65 minutes and estimated blood loss was 5 cc. The patient was able to be discharged less than 24 hours after surgery.

We present the first case of a minimally invasive tubular retractor system-based approach for biopsy and resection of a breast metastasis causing occipital condyle syndrome. The majority of patients in the literature found to have isolated occipital condyle metastases have been treated with radiotherapy without surgical biopsy or intervention. Biopsy and resection with a plan to adjust chemotherapy limits the risks of radiation including development of radiation induced tumors which is small however not negligible. The biopsy results in this case were also significant as the final pathology was different from the outside hospital pathology report from the patient's original surgeries. The benefits of a minimally invasive approach to the craniocervical junction include decreased operative time, decreased blood loss, decreased postoperative pain, and decreased hospital length of stay.

P067. Retro-odontoid Intradural Synovial Cyst Decompressed via an Endoscope-Assisted Far Lateral Approach C1-C2 Hemilaminectomy without Fusion: Use of Denticulate Ligament as Intraoperative Landmark

Christos F. Deamont¹, Michael Fana², Donald Labarge², Sunil Manjila²

¹Norton Community Hospital, Norton, Virginia, United States

²McLaren Bay City Hospital, Bay City, Michigan, United States

Background: Purely intradural (retro-odontoid) synovial cysts are rarely reported in neurosurgical literature, especially with no bony erosions. We present the case of a middle aged male with a retro-odontoid cyst associated with a history of chronic refractory neck pain, decompressed via an endoscope-assisted far lateral approach C1-C2 hemilaminectomy without fusion.

Case Summary: A 57-year-old male presented to our clinic with a several month history of neck, shoulder, and hand pain. Magnetic resonance imaging (MRI) findings revealed an intradural cyst at the level of C2 behind the odontoid process, which impinged on the medulla and caused vertebral artery displacement. The differential diagnosis of a cystic meningioma, chordoma and echordosis physaliphora was entertained. Considering the patient's progressively worsening symptoms and interval growth in size of the cyst and increasing mass effect, it was decided to decompress the cyst surgically and obtain histological diagnosis. A far lateral approach with endoscopic assistance was employed, without transposition of vertebral artery segment over C1. C1-C2 hemilaminectomy without fusion was employed for access and denticulate ligament served as an intraoperative surgical landmark. There was a thick walled intradural cyst containing greenish yellow fluid with waxy cyst contents,, encountered after cutting the first denticulate ligament. The final pathology was reported as a synovial cyst. The patient remained neurologically intact, same as preoperative status. This article highlights the surgical trajectory obtained by a left hemilaminectomy and endoscopic guidance.

Conclusion: This case represents a rare case of retro-odontoid synovial cyst with review of literature on surgical approaches with and without fusion. The utility of planning

surgical trajectory using Stealth neuronavigation and endoscopic assisted "fish eye" view visualizing contralateral aspect of the lesion are well-illustrated. An endoscope-assisted far lateral approach using C1-C2 hemilaminectomy without fusion is demonstrated using first denticulate ligament as the landmark.

P068. Inferolateral Transorbital Approach to the Petrous Apex. An Adjunctive Approach to the EEA

Moustafa Ali^{1,2}, Janmaris Marin¹, Daniel Prevedello¹, Bradley Otto¹, Ray Cho¹, Ricardo Carrau¹

¹Ohio State University, Columbus, Ohio, United States

²Assiut University, Egypt

Introduction: Many approaches to reach the petrous apex have been used open as well as endoscopic and more recently, endoscopic ear surgery approaches. However, there is a lot of morbidity and access limitation with anterior endoscopic endonasal approaches regarding lateral access with probable need to excise the eustachian tube, jeopardizing the middle ear aeration and probable delayed complications.

Aim of Work: Providing a safe corridor to completely eradicate tumors that arise and/ or extend into the petrous apex laterally trying to spare the eustachian tube and avoiding unnecessary complications to the middle ear.

Materials and Methods: Five cadaveric latex injected heads were used in the study Nora define landmarks and properly describe the Corredor as required. The trigeminal ganglion lies anatomically on top of the petrous apex on the anterior and middle portions of it, two branches (V2 and V3) pierce the pterygoid process to reach the pterygopalatine, and infratemporal fossae. An inferolateral transorbital approach was used to gain access to the maxillary sinus, ION was traced posteriorly to reach foramen rotundum, posterior maxillary wall is dissected, periosteal covering of the pterygoid base at the lateral side of foramen rotundum is identified, and the lateral pterygoid plate is dissected inferiorly subperiosteally, going superiorly to reach foramen ovale and V3. Posterior dissection is continued and performed till the eustachian tube is identified. Bleeding from the pterygoid plexus can be controlled by Surgiflo, if encountered.

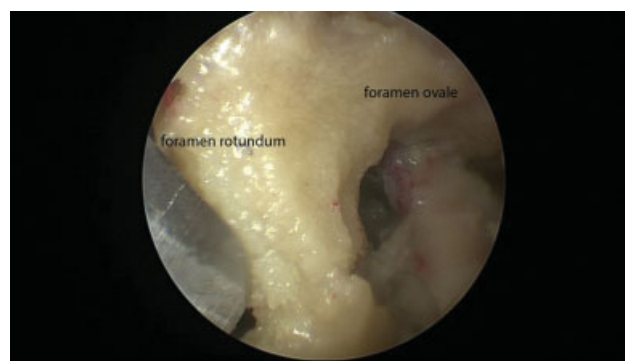


Fig. 1 Showing the space between v2 and v3.

By tracking v2 to its origin in the trigeminal ganglion, a point between v2 and v3 is reached using an anterolateral trajectory.

Drilling the lateral pterygoid plate is done in an inferolateral fashion superior to the eustachian tube, which can provide a safe corridor to remove the lesions extending all the way into the posterior part of the petrous apex till the carotid genu if needed.

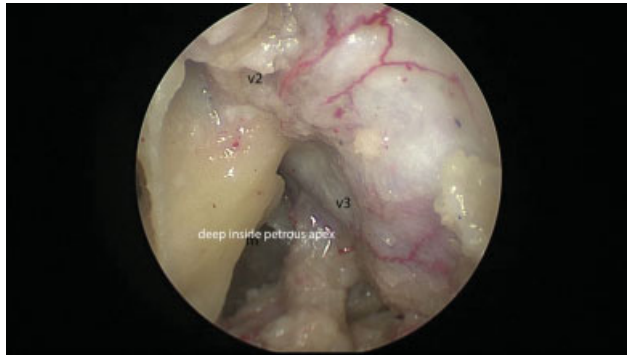


Fig. 2 Transorbital view of the space between v2 and v3 and drilling of the petrous apex following drilling.

Careful drilling of the lateral pterygoid plate inferior to foramen ovale in a posteromedial trajectory (identifying and preserving the anterolateral and inferior surfaces of Meckel's cave) toward the eustachian tube is done. In this fashion any lesion lateral to Meckel's cave posterior or superior to the cartilaginous part of eustachian tube is detected, eradicated and cleared.

The distances between foramen ovale, foramen rotundum, posterior genu of ICA, eustachian tube are measured and used as landmarks if needed.

Results: The inferolateral transorbital corridor to petrous apex can be a safe, efficient addition as an adjunctive technique to eradicate laterally located lesions of the petrous apex or extending into it from the petroclival fissure sparing the eustachian tube, maximizing surgical dominance and tumor control.

P069. Transorbital Approach to the Internal Carotid Artery—A Novel Adjunctive Approach to the EEA

Moustafa Ali^{1,2}, Ricardo L. Carrau¹, Daniel Prevedello¹, Bradley Otto¹, Tekin Baglam², Janmaris Marin¹, Thiago Albonette¹, Ray Cho¹

¹Ohio State University, Columbus, Ohio, United States

²Assiut University, Egypt

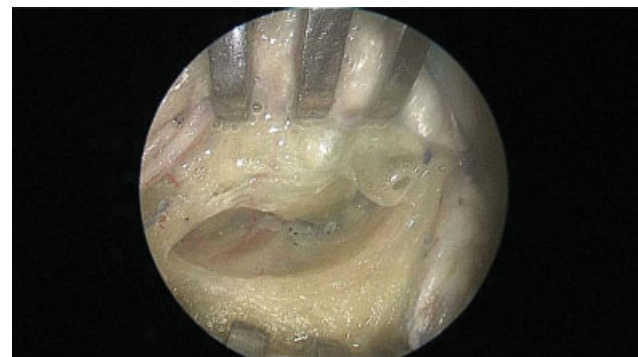
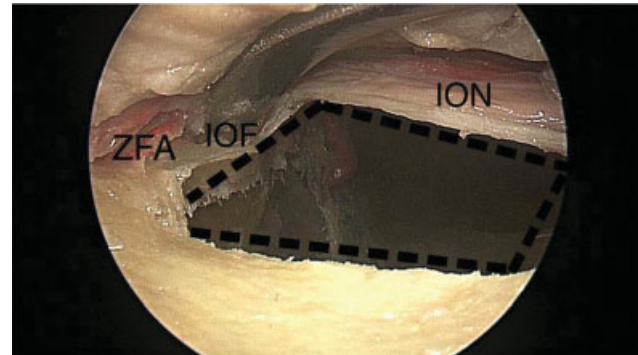
Introduction: The EEA in the recent years has largely replaced many of the more morbid techniques to remove lesions in the midline of skull base. The extended EEA approaches to the coronal plane has helped a lot to gain access to lesions in that are around the anterior genu of the internal carotid artery. However, lesions extending lateral and posterior in the petrous bone toward the posterior genu, are a lot more challenging and almost non accessible by EEA.

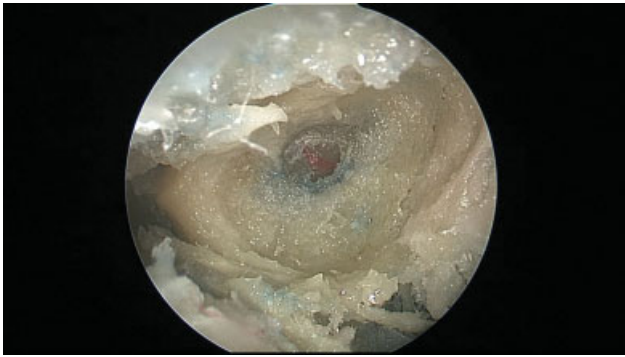
Aim of Work: To have a new technique adjunct to the EEA to help eradicate lesions with extension toward the posterior genu with minimal morbidity.

Materials and Methods: Four cadaveric latex injected heads were used in this study where landmarks and measurements were taken to gain a safe access to the posterior genu of the internal carotid artery. An inferolateral transorbital approach was performed, the posterior wall of the maxillary sinus was dissected, identification the lateral pterygoid plate was done, subperiosteal dissection of the infratemporal fossa muscles was done starting at the inferior part of the lateral pterygoid plate going superior and lateral till the TMJ muscle attachment is reached. Identifying the foramen ovale and foramen spinosum is done, the middle meningeal artery is identified, dissected, and coagulated, and the mandibular nerve is identified, dissected, and secured. Sacrificing the nerve was done to take the measurements, but it is not

required for the approach. Further dissection is done posteriorly until the lateral pterygoid plate posterior rim is reached and the sphenoid wing is identified superiorly. And the eustachian is identified inferomedially. Drilling of the petrous bone posteromedial to the foramen spinosum in making the (Ali triangle) the apex is the foramen spinosum the anterior border is the line joining the foramen spinosum and the eustachian tube inferiorly, the posteromedial border is the line from foramen spinosum to the posteromedial junction of the pterygoid plate and the greater wing of sphenoid. Drilling is started using a 3-mm diamond burr in a fashion directed inferomedially, taking in consideration that laterally and superiorly to the described triangle the middle ear and lateral surface of the posterior genu of the ICA is located. The distances between the different available landmarks (foramen ovale to spinosum, foramen spinosum to the posterior genu, and TMJ to the posterior genu) were measured in the four heads used in the study.

Results: The transorbital corridor to the posterior genu of the ICA can be a valuable addition for safe and proper access of the lesions extending posterolateral surrounding the petrous ICA. It can serve as an adjunctive port to allow tumor eradication in petroclival tumors as chondrosarcomas.





P070. Quantification Analysis of Minimally Invasive Techniques to the Infratemporal Fossa

Moustafa Ali¹, Nyall London², Daniel Prevedello³, Tekin Baglam³, Ray Cho³, Bradley A. Otto³, Ricardo L. Carrau³

¹Ohio State University/Assiut University, Egypt
²Johns Hopkins Hospital, Baltimore, Maryland, United States
³Ohio State University, Columbus, Ohio, United States

Introduction: The infratemporal fossa has always been an anatomically challenging location with several neurovascular elements, The maxillary artery and its branches as well as its close proximity to trigeminal ganglion and its branches and connections to the orbit via the inferior orbital fissure, pterygopalatine fossa, and the nose. Lesions and tumors of the infratemporal fossa have been either arising from these structures or extending into it through fissures from the nose or the orbit.

Aim of Work: In this study, comparison of transnasal transmaxillary, as well as the endoscopic transorbital approach, will be conducted to find out the best suitable approach for lesions in each quadrant of the four quadrants of the infratemporal fossa. Four cadaveric heads were used, both sides right and left. Endoscopic endonasal approach with maximal exposure possible was performed associated with medial maxillectomy to be able to reach as lateral as possible. A transmaxillary approach was done, an endoscopic transorbital approach was performed to dissect the infratemporal fossa and expose the parapharyngeal fascia. Using the navigation system, Cartesian coordinates were collected via Stryker navigation system in Altvision laboratory, and the surgical freedom area of exposure and angle of attack were calculated.



Fig. 1 A panoramic view of the infratemporal fossa through a transorbital approach. Five anatomical points were chosen to compare between the three approaches regarding surgical freedom and area of exposure and angle of attack. Each point would represent a quadrant of the infratemporal fossa and the fifth point is to represent depth while operating. These

points are foramen ovale, the TMJ, inferior alveolar foramen, the inferior most portion of the pterygoid process. The fifth point is the point of intersection of the diagonals of the rectangle created by these points.

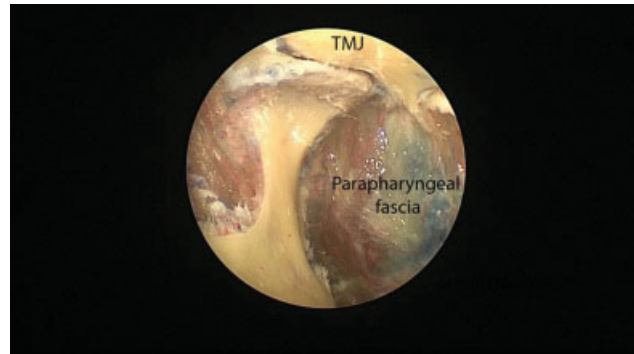


Fig. 2 Showing the TMJ through—a transorbital view.

Results: Statistical data analysis was performed using a statistical software program (SPSS for Windows, version 21, United States), data were presented as mean with standard deviation. To compare the used approaches (transorbital transmaxillary and transnasal) One-Way ANOVA test was conducted. If there is a statistically significant difference between the used methods, Tukey's multiple comparison posthoc test was done to know which of the specific groups differed. Inf alveolar foramen was not reachable through transnasal method, so in such case, paired t-test was conducted to compare between the two used methods; transorbital and transnasal. For all statistical analysis, results were considered significant at $p < 0.05$.

Table 1. Freedom

	Trans-orbital (n =)	Trans-maxillary (n =)	Trans-nasal (n =)	P - value
Ovale	46.49 ± 10.76 *	101.82 ± 28.12 ^b	100.06 ± 32.02 ^b	0.021
TMJ	88.55 ± 76.16	94.40 ± 33.13	99.65 ± 50.31	0.962
Inf alv	131.29 ± 68.10	92.67 ± 41.44	-	0.340
Inf pterygoid	94.43 ± 70.78	74.36 ± 27.90	120.25 ± 91.50	0.652
Intersection point	103.61 ± 50.71	103.29 ± 53.86	108.39 ± 47.89	0.987

Table 1 summarizes the freedom. For ovale, there was a statistically significant difference between trans-orbital, trans-maxillary, and trans-nasal as determined by one-way ANOVA ($F(2,9) = 6.143, p = 0.021$). A Tukey post hoc test revealed that both trans-maxillary ($101.82 \pm 28.12, p = 0.032$) and trans-nasal ($100.06 \pm 32.02, p = 0.037$) was significantly higher compared with trans-orbital (46.49 ± 10.76). However, there was no statistically significant difference between the three used methods for TMJ ($p = 0.962$), inf alv ($p = 0.340$), inf pterygoid ($p = 0.652$), and intersection point ($p = 0.987$).

	Trans-orbital (n =)	Trans-maxillary (n =)	Trans-nasal (n =)	P - value
Ovale	52.82 ± 23.69 *	124.73 ± 35.08 ^b	81.27 ± 36.36 ^{ab}	0.034
TMJ	72.12 ± 41.15	98.31 ± 50.93	132.01 ± 67.49	0.339
Inf alv	118.63 ± 57.79	94.11 ± 38.91	-	0.520
Inf pterygoid	102.35 ± 101.30	74.26 ± 26.11	108.88 ± 74.41	0.787
Intersection point	105.47 ± 55.97	118.12 ± 68.72	101.90 ± 42.10	0.918

Table 2 summarizes the exposure. For ovale, there was a statistically significant difference between trans-orbital, trans-maxillary, and trans-nasal as determined by one-way ANOVA ($F(2,9) = 5.054, p = 0.034$). A Tukey post hoc test revealed that trans-maxillary ($124.73 \pm 35.08, p = 0.028$) was significantly higher compared with trans-orbital (52.82 ± 23.69) and there is no statistically significant difference between trans-nasal and trans-orbital ($p = 0.456$) and trans-maxillary and trans-nasal ($p = 0.192$). However, there was no statistically significant difference between the three used methods for TMJ ($p = 0.339$), inf alv ($p = 0.520$), inf pterygoid ($p = 0.787$), and intersection point ($p = 0.918$).

P072. Extended Endoscopic Transnasal Transsphenoidal Removal of Tuberculum Sellae Meningiomas: Illustrative Reports on the Importance of Preoperative Case Selection and Planning in Extent of Resection and Outcomes

Ness Jerold A. Justo¹, Michael N. Sabalza¹, Peter Jarin¹

¹The Medical City Philippines, Quezon City, Philippines

Introduction: Tuberculum sellae meningiomas frequently arise from the tuberculum sellae, chiasmatic sulcus, planum sphenoidale, and diaphragma sellae and comprise 4–10% of all intracranial meningiomas. These tumors are managed traditionally using open cranial approaches. The present developments in different approaches however make it possible to resect these tumors thru the endoscopic transnasal transsphenoidal route. Endoscopic management of these tumors allow for minimal brain retraction and minimal manipulation of neurovascular structures. In this present study, we reviewed our management of five patients by an extended endoscopic endonasal transsphenoidal approach to resect tuberculum sellae meningiomas.

Methods: All patients were selected on the basis of a histopathologically diagnosed tuberculum sellae meningiomas. Approach to resection are all endoscopic and spanning three institutions with the team being comprised of one neurosurgeon and one ENT. Initial MRI and CT scan were done for all patients as part of their preoperative planning. Intraoperative neuronavigation (Brainlab) was utilized to guide the team during the resection. Skull base defect reconstruction consistently involved the use of the Hadad-Bassagasteguy flap, tensor fascia lata, and fat. Patients were followed up immediately postoperatively and continuously for developments of new outcomes.

Results: All five patients were females with a mean age of 44 years old. Initial presentation involved visual disturbances and headache. Visual disturbance involved an initial bitemporal hemianopia in four patients, and symptoms of headache for all five patients. No postoperative CSF leak, no ICU admissions, and one transient bitemporal hemianopia postop were noted. In the five patients, gross total tumor resection was accomplished.

Conclusion: The different cases elucidate that extended endoscopic transnasal transsphenoidal approach is an effective minimally invasive approach for the resection of tuberculum sellae meningiomas. This approach is best executed with a proper and well-coordinated neurosurgical team. Intraoperative imaging as well as proper endoscopic equipment such as angled scopes and suction tips are crucial in achieving gross total tumor resection. The rates of CSF leaks have been greatly augmented by the use of the Hadad-Bassagasteguy flap in combination with other means of cranial flap reconstruction. The cases provide us with lessons on patient selection as well as the importance of other technical nuances involving optic canal invasion and presence of a cortical cuff. Familiarity and expertise is greatly emphasized as this contributes greatly to the extent of resection and complications. The approach provides a dynamic and panoramic view of the operative field which makes identification of relevant anatomy and pathology easier leading to successful and complication-free outcomes that should eventually be passed on to the next generation as part of the standard of care for these patients.

P073. Do We Need Prophylactic Antibiotic Use in Endoscopic Transsphenoidal Pituitary Surgery?

Ioana D. Moldovan¹, Charles Agbi², Shaun Kilty², Fahad Alkherayf²

¹Ottawa Hospital Research Institute, Ottawa, Ontario, Canada

²University of Ottawa, Ottawa, Ontario, Canada

Background: The benefit of prophylactic antibiotic use in endoscopic endonasal transsphenoidal surgery (EETS) for pituitary lesions is controversial. Many surgeons administer antibiotics perioperatively not based on clear guidelines but “to be safe.”

Objectives: Determine if antibiotic prophylaxis use reduces the risk of infection (e.g., meningitis, sinusitis) within 30 days after the surgery, in adult patients with pituitary lesions undergoing EETS.

Methods: A systematic review was performed to assess the effectiveness of perioperative antibiotic use in preventing infectious complications in patients undergoing EETS. Data sources: Ovid Databases, Scopus, PubMed, Cochrane Library, Gray Literature. The inclusion criteria were: randomized controlled trials, systematic reviews, observational studies, and case series of prophylactic antibiotic perioperative use for EETS. The study end points were the rates of meningitis and sinusitis as infectious complications after EETS.

Results: A total of 282 articles were identified by the initial literature search. Four studies met the inclusion criteria: three retrospective cohort and one prospective case series studies. All patients included in each study received different antibiotic regimens perioperatively. The quality of studies did not permit performance of a meta-analysis.

Conclusion: Even though there are no clear practice guidelines regarding the antibiotic prophylaxis need in EETS, various antibiotic regimens have been used by surgeons. Our systematic review identified a limited number of published studies assessing this question, all observational. Randomized control trials are needed to evaluate the effectiveness of prophylactic antibiotic use in patients with pituitary lesions undergoing EETS.

P074. Endoscopic Endonasal Approach to the Orbit: An Anatomical and Clinical Study

Matteo Zoli¹, Thiago Albonette Felicio², Giuliano Schmidt Bertazzo Silveira², Rafael Martinez-Perez², Gustavo Guimarães Rangel³, Mostafa Shahein^{2,4}, Marcus Zachariah², Douglas Hardesty², Bradley A. Otto³, Ricardo L. Carrau³, Daniel M. Prevedello²

¹Department of Neurosurgery, Center of Surgery for Pituitary Tumors, IRCCS Istituto delle Scienze Neurologiche of Bologna, Bologna, Italy

²Department of Neurological Surgery, The Ohio State University Wexner Medical Center, Columbus, Ohio, United States

³Department of Otolaryngology and Head and Neck, The Ohio State Wexner Medical Center, Columbus, Ohio, United States

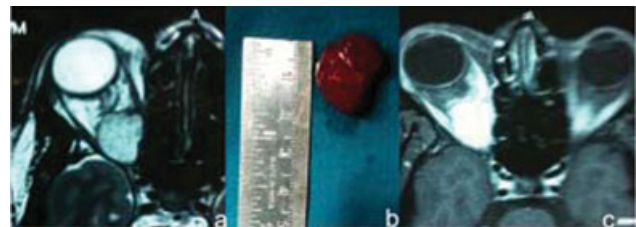
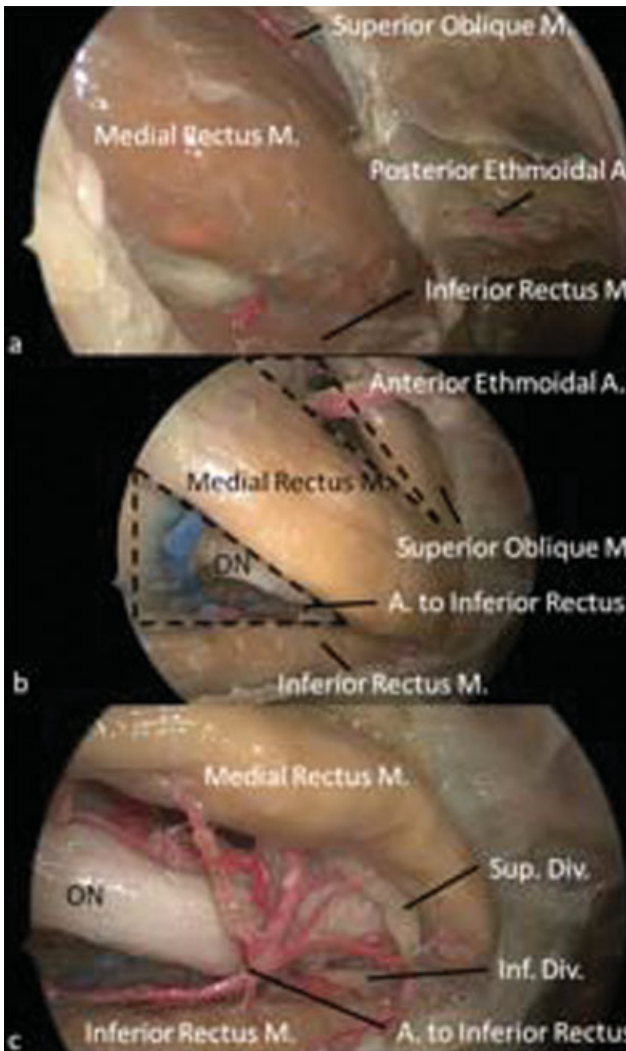
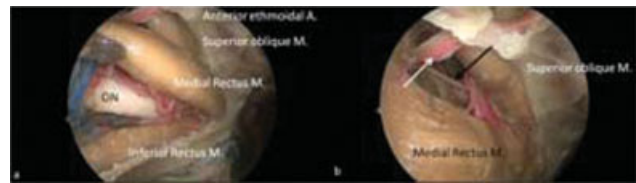
⁴Department of Neurological Surgery, Aswan University, Aswan, Egypt

Background: Recently, some cases have been reported of endoscopic endonasal resection of intraorbital intraconal retrobulbar lesions. In a few anatomical regions, the knowledge of anatomy is so relevant to orient and guide the surgeon. The aim of this study is to describe the anatomy of the orbit from the endoscopic endonasal perspective, comparing this route to the transcranial one for lesions located in the medial compartment. Two surgical cases are reported to enlighten the advantages and limits of this approach.

Materials and Methods: Anatomical dissection of 12 orbits was performed in 6 fixed and injected cadaveric specimens with both endoscopic endonasal and transcranial approaches.

Results: In all specimens the endoscopic endonasal approach allows us to expose the medial compartment of the orbit and the apex region. Differently from the transcranial approach, which offered also the view of the lateral and superior compartments of the orbit, the endoscopic endonasal avoids any brain retraction, and gives a more direct and straightforward vision of the medial compartment of the orbit, allowing to reduce the manipulation of optic and oculomotion nerves for lesions located in the medial compartment.

Conclusion: The endoscopic endonasal approach resulted in safe and effective for selected orbit lesions located medially to the optic nerve. It provided excellent access to the medial orbit compartment, which exposure trough the transcranial approach requires brain retraction and an angled view. Finally, we believe that every approach could present advantages and limits and that the surgical route should be chosen considering the location and extension for the tumor, to maximize its efficacy and reduce the morbidity rate.



P075. Endonasal Endoscopic Management of a Craniopharyngeal Canal Meningoencephalocele in a 6-Month-Old Patient

Hazan Basak¹, Suha Beton¹, Gokmen Kahilogullari¹, Cem Mecoc¹
¹Ankara University, Ankara, Turkey

Background: Endonasal endoscopic approach (EEA) for managing even large skull base defects have become a routine and effective method in adults and increasingly in older pediatric populations despite their challenging narrow transnasal corridors. For the first time in a six-month-old boy, we report management of a huge craniopharyngeal canal (CC) meningoencephalocele using this minimal invasive approach.

Case: A 6-month-old baby with known intrauterine large arachnoid cyst had nasal breathing difficulties since birth. Neurologic examination was normal. Flexible endoscopic examination revealed a pulsatile mass obliterating the nasopharynx. Various imaging methods showed a bony CC defect at central sphenoid region and a protruded meningoencephalocele through this defect. Using an EEA we first prepared a pedicled nasoseptal mucoperiosteal flap and parked in maxillary sinus at the beginning of the surgery. Since the transnasal working corridor was too narrow, posterior septectomy was performed to enable binostril dissection and visualization of the origin of meningoencephalocele and bony defect at skull base. After careful cauterization and resection of the meningoencephalocele sac, metal clips were used to additionally seal the dura of CC. Then additionally bony defect was closed in a multilayer fashion using cartilage, allograft dura and nasoseptal flap as the last layer. Nasal breathing became normal right after surgery and no

recurrence of meningocele or CSF leak was seen during the follow-up period of 10 months.

Conclusion: For the huge CC meningoencephalocele of the 6-month-old baby, EEA achieved a perfect visualization of skull base defect and enabled a watertight closure after resection of the pathology.

P076. Endoscopic Approach of Metastatic Renal Clear Cell Carcinoma in Infratemporal Fossa

Hana Caroline Morais Higa¹, Miguel Soares Tepedino¹, Daniel Herchenhorn², Ricardo José Lopes da Cruz³

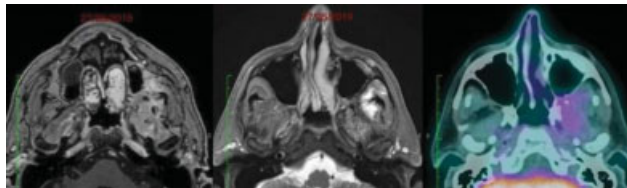
¹Policlínica de Botafogo, Rio de Janeiro, Rio de Janeiro, Brazil

²Centro de Oncologia de D'Or, Rio de Janeiro, Rio de Janeiro, Brazil

³Hospital Samaritano—UHG, Rio de Janeiro, Rio de Janeiro, Brazil

Representing 2 to 3% of adult cancers, renal cell carcinoma (RCC) accounts for 90% of renal malignancies and affects one and a half times more men than women. Clear cell RCC is the most common type. It is the third most common cancer of the genitourinary tract, following prostate and bladder tumors. At diagnosis, one-third of the patients usually have distant metastases. The most common sites are lungs (50%), bones (33%), skin (11%), liver (8%), and brain (3%). In this article, we report a case of metastatic RCC in infratemporal fossa (ITF), an unusual site of dissemination which was treated with endoscopic endonasal approach (EEA).

A nonsmoker 69-year-old male was presented with a history of left nephrectomy for RCC in 2001. He was subsequently diagnosed with multiple metastases. The patient underwent right lung metastases resection, right adrenal gland metastases resection, right cuboid bone metastases radiosurgery, and left maxillary sinus partial resection in 2018. Magnetic resonance imaging (MRI) performed for clinical follow-up detected suspicious left ITF lesion after 18 years of primary tumor treatment. Positron emission tomography with 18F-fluorodeoxyglucose (PET 18F-FDG) images corroborated the hypothesis of tumor metastases, showing radiotracer uptake in the left ITF region. The patient underwent multiple lines of systemic therapy (e.g., sunitinib, immunotherapy, and axitinib). We chose to perform EEA of the left ITF lesion for tumor resection. Histopathological study and immunohistochemistry confirmed the diagnosis of metastatic clear cell RCC.



Late recurrence of RCC several years after initial treatment may occur. But metastatic spread of RCC to the head and neck region is rarely seen. Such metastases can be observed in approximately 15% of cases, almost always associated with other lesions in other common sites. The main goal of the ITF surgery was the resection of the metastatic lesion for subsequent treatment plan with radiotherapy to the resected cavity. The close proximity of the ITF to the intracranial structures, orbit, paranasal sinuses, nasopharynx, and the facial area demands careful planning of surgical excision. Several ways of approaching the ITF have been described, such as the orbitozygomatic approach, mid-

facial degloving, and the maxillary swing. However, in selected cases, EEA may provide lower morbidity, shorter recovery time and induce less physiological impact compared with the techniques described above.

Patients previously diagnosed with RCC and who subsequently underwent surgical resection, the possibility of metastatic tumor should always be considered as a differential diagnosis when a solitary lesion develops on the head and neck region, even long time after primary surgery. Endoscopic endonasal approaches to the skull base allow excellent visualization, eliminate or significantly reduce the need for craniofacial soft tissue dissection, skeletal alteration and brain retraction for tumor access. For well-selected cases and appropriate adjuvant therapy, endoscopic resection results in acceptable oncological outcomes.

P077. Expanded Exposure and Detailed Anatomic Analysis of the Superior Orbital Fissure and the Associated Neurovascular Structures

Lifeng Li¹, Jr. Nyall R. London², Daniel M. Prevedello³, Ricardo L. Carrau⁴

¹Department of Otolaryngology-Head and Neck Surgery, Beijing Tongren Hospital, Capital Medical University, Beijing, China

²Department of Otolaryngology-Head and Neck Surgery, Johns Hopkins School of Medicine, Baltimore, Maryland, United States

³Department of Neurological Surgery, the James Cancer Hospital at the Wexner Medical Center of The Ohio State University, Columbus, Ohio, United States

⁴Department of Otolaryngology-Head and Neck Surgery, the James Cancer Hospital at the Wexner Medical Center of The Ohio State University, Columbus, Ohio, United States

Introduction: The superior orbital fissure (SOF) lies between the greater and lesser wings of the sphenoid bone and can be accessed through either an endonasal or trans-orbital approach. The purposes of this study were to maximize the exposure of SOF and its transmitting neurovascular tract using an endonasal combining a trans-orbital approach.

Methods: Six cadaveric specimens (12 sides) were dissected using an endonasal and trans-orbital approaches. Via an endonasal approach, cranial nerves III through VI were visualized in the lateral wall of the cavernous sinus and traced forward to the inferomedial SOF. Through the trans-orbital approach, the superolateral SOF and the transmitting structures were explored.

Results: Through an endonasal approach, the inferomedial one-third of the SOF including the proximal segment of the oculomotor, ophthalmic and abducens nerves could be accessed; the terminal branches of the oculomotor nerve and nasociliary nerve within intraconal space could also be accessed. Through a transorbital approach, the superolateral two-thirds of the SOF could be explored, including the superior ophthalmic vein, lacrimal nerve and abducens nerve located at the lateral aspect; the nasociliary nerve and divisions of oculomotor nerve centrally; and the frontal and trochlear nerves located at the dorsal aspect of levator palpebrae superioris.

Conclusion: A combined endonasal and trans-orbital approaches provide expanded exposure of the SOF and its transmitting neurovascular structures. The endonasal approach was better for exposure of the inferomedial one-third of the SOF. The trans-orbital approach provided good exposure of the superolateral two-thirds of the SOF. The detailed anatomical knowledge presented here will be helpful for managing lesions in this challenging region.

P078. Comparison of Endoscopic Transthyroid and Prelacrimal Approaches for Exposure of the Medial Intraconal Space: A Cadaveric Study

Lifeng Li¹, Jr. Nyall R. London², Daniel M. Prevedello³, Ricardo L. Carrara⁴

¹Department of Otolaryngology-Head and Neck Surgery, Beijing Tongren Hospital, Capital Medical University, Beijing, China

²Department of Otolaryngology-Head and Neck Surgery, Johns Hopkins School of Medicine, Baltimore, Maryland, United States

³Department of Neurological Surgery, The James Cancer Hospital at the Wexner Medical Center of The Ohio State University, Columbus, Ohio, United States

⁴Department of Otolaryngology-Head and Neck Surgery, The James Cancer Hospital at the Wexner Medical Center of The Ohio State University, Columbus, Ohio, United States

Introduction: Both the transthyroid and prelacrimal approaches can be utilized to access the medial intraconal space (MIS). The purposes of this study were to compare the advantages and drawbacks of each approach for exposure, and to explore the appropriate indications for management of lesions at varying locations within the MIS.

Methods: Six injected cadaveric specimens were dissected using an endonasal approach. For each specimen, a transthyroid approach was performed on one side, while a prelacrimal approach on the contralateral side. The exposure provided by these two approaches to various zones within the MIS as well as structures included was assessed.

Results: The MIS was divided into three zones based on horizontal lines crossing the superior and inferior borders of medial rectus muscle (MRM). Zone 1 was defined as the area above the superior border of MRM, zone 2 defined as the area between the MRM and optic nerve, and zone 3 as the area below the inferior border of MRM. Both approaches provided adequate exposure of zones 2 and 3; however, the prelacrimal approach provided direct exposure of the posterosuperior aspect of zone 2 without retraction of MRM, while retraction of MRM was unavoidable using a transthyroid approach. Access to zone 1 was best achieved through the corridor between superior oblique and medial rectus muscles.

Conclusion: Subdivision of the MIS into three zones will be beneficial in selecting the optimal approach for lesions restricted to each specific zone. Both a transthyroid or prelacrimal approach could access zones 2 and 3; however, the prelacrimal approach is more suitable for direct exposure of the posterosuperior aspect of zone 2 given the reduced need for retraction of the MRM. For lesions restricted to zone 1, the transthyroid approach is best indicated.

P079. Oropharyngeal Reconstruction after Transoral Robotic Radical Tonsillectomy: When Reconstruction is Indicated?

Katherine P. Lipinski¹, Randall S. Ruffner², Karthik S. Shastri², Lisa Galati², Carlos D. Pinheiro-Neto³

¹Albany Medical College, Albany, New York, United States

²Division of Otolaryngology/Head and Neck Surgery, Department of Surgery, Albany Medical Center, Albany, New York, United States

³Division of Otolaryngology/Head and Neck Surgery, Department of Surgery, Department of Neurosurgery, Albany Medical Center, Albany, New York, United States

Background: Transoral robotic surgery (TORS) has become an important treatment modality for oncologic resection of oropharyngeal cancers. While reconstruction of post-resection defects is not traditionally performed, scarring and contracture may lead to stenosis and velopharyngeal insufficiency (VPI). The nasoseptal flap (NSF) has been

shown as a viable option for reconstruction of oropharyngeal defects after TORS. Additionally, the NSF may also expand the indication of TORS for patients with soft palate involvement. Here we review a series of patients who underwent TORS for oropharyngeal cancer and compare indications and outcomes between patients who received no reconstruction and those who underwent oropharyngeal reconstruction with NSF.

Methods: A retrospective chart review was performed for patients at our institution who underwent TORS for oropharyngeal cancer between 2015 and 2019.

Results: A total of $n = 23$ patients received TORS for radical tonsillectomy. Ten patients had no reconstruction (five males and five females), mean age: 63 years (range: 28–88 years); four patients had buccal fat flap (BFF) reconstruction of the tonsillar defect (three males and one female), mean age: 62 years (range: 47–74 years); and nine patients had reconstruction of the oropharyngeal defect with NSF (eight males and one female), mean: 65 years (range: 53–78 years). Patients who had NSF had larger oropharyngeal defects, partial soft palate resection, or exposure of the internal carotid artery (ICA). Patients who had no reconstruction or had BFF presented with smaller tumors limited to the tonsillar fossa and did not require major soft palate resection. All 14 patients with no reconstruction or BFF had some degree of palatal retraction, but none had stenosis or VPI postoperatively (**Fig. 1**). In the NSF group, the four last patients had extended dissection of the flap pedicle to PPF and internal maxillary artery (IMAX) to improve the flap reach. Only one patient out of nine developed mild VPI despite much larger defects resulting from the palatal resection (**Fig. 2**). None of the patients in the NSF group had palatal retraction or stenosis. The most common complication of the nasoseptal flap was nasal crusting. In addition to nasal crusting, one patient had partial necrosis of the NSF. There was no postoperative Eustachian tube dysfunction or serous otitis media in patients reconstructed with an NSF. The presence of the pedicle in the nasopharynx may function as a pharyngeal flap, occupying space in the area and preventing VPI in this patient population.

Conclusion: Soft palate involvement should not limit the resection achieved with TORS. Reconstruction with NSF has shown to prevent major complications associated with soft palate resection, such as severe VPI, palate retraction, or stenosis. It also offers excellent coverage when the parapharyngeal ICA is exposed. Pedicle dissection toward the PPF and IMAX offers a great improvement of the flap reach. Although all patients who had no reconstruction after TORS for tumors limited to the tonsillar fossa had some degree of palatal retraction, no clinical VPI was noticed in this group.

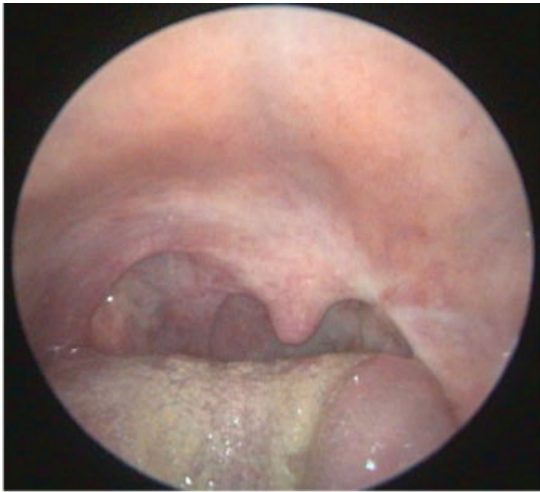


Figure 1. Postoperative image 5 years post-TORS left radical tonsillectomy, no reconstruction. The tumor was limited to the tonsillar fossa. Observe the resultant soft palate retraction with deviation of the uvula. This patient has no VPI or dysphagia, but complains of trismus.



Figure 2. Postoperative image 1 year post-TORS right radical tonsillectomy with partial resection of the soft palate. Observe the well-healed nasoseptal flap covering right tonsil and soft palate defect (arrow).

P080. Transseptal Transsphenoidal Approach to Hypophysectomy: Comparisons of Sinonasal Quality of Life and Complications

Alexander Zhu¹, Jonathan Simmonds², Brian Duff¹

¹Brown University, Providence, Rhode Island, United States

²Tufts University, Massachusetts, United States

Background: The transsphenoidal approach to pituitary and sellar lesions has evolved drastically with the use of endoscopy. The most common approaches today, incorporating posterior septectomy, as well as a great deal, of mucosal

manipulation that have been associated in the literature with high rates of sinonasal complaints such as crusting. Though the transseptal approach had been described more than a century ago, the adaptation of the technique using endoscopy as well as the resulting outcomes and complications have not been well-described.

Methods: A retrospective chart review was performed of patients who underwent primary endoscopic, transseptal, transphenoidal hypophysectomy at Rhode Island Hospital between April 2015 and December 2018. Rates of sinonasal complaints and complications, including nasal crusting, congestion, epistaxis, septal perforations, septal hematomas, synechiae, impaired olfaction, dysesthesia, and postoperative sinusitis were collected and compared with those found in the literature.

Results: Forty-five patients underwent transsphenoidal hypophysectomy for a primary pituitary lesion over the 3.5 year study period. In our cohort, a single patient had nasal crusting and no patients were found to have hematoma, septal perforation, synechiae, or require debridement. Epistaxis occurred at a rate of 10.5% postoperatively, but always resolved without surgical management.

Conclusions: The transseptal transsphenoidal approach to pituitary lesions provides a safe option to surgeons and patients who prioritize the minimization of postoperative complaints and complications.

P081. Discordant Radiographic and Endoscopic Findings Regarding Orbital Invasion in Esthesioneuroblastoma: Case Report and Review of the Literature

Prashanth J. Prabakaran¹, Tyler J. Willman¹, Timothy M. McCulloch¹, Azam S. Ahmed¹, Ian J. Koszewski¹

¹University of Wisconsin School of Medicine and Public Health, Madison, Wisconsin, United States

Endoscopic resection plays an important and expanding role in the surgical management of esthesioneuroblastomas (ENB). Preoperative planning, including high-resolution CT and MRI, is crucial for accurate patient selection and to inform optimal surgical modality. Orbital invasion is generally considered to be a relative contraindication to endoscopic-only resection, particularly if orbital exenteration may be required for oncologic margins. Preoperative imaging is considered the sole opportunity for informing decisions regarding orbital preservation, but may not always delineate the presence or degree of orbital invasion. Here we present a case of discordant radiographic and intraoperative, endoscopic findings during endoscopic ENB resection that allowed for avoidance of orbital exenteration.

A 42-year-old male presented with initial left-sided followed by bilateral nasal obstruction progressing over one year, copious left-sided nasal drainage, and most recently left-sided tearing with proptosis. Anterior rhinoscopy showed a soft, fleshy mass in the left nasal passage which on biopsy was confirmed to be ENB. Initial MRI showed a $7.2 \times 7.2 \times 3.2$ cm mass in the left nasal cavity with intracranial extension and invasion through the left medial orbit with involvement of the left medial rectus and superior oblique making this a modified-Kadish C esthesioneuroblastoma. Repeat imaging after neoadjuvant chemotherapy yielded equivocal findings regarding orbital involvement, though proptosis was still present. After tumor board discussion, surgical intervention was favored with a combined endoscopic and open approach including orbital exenteration. Intraoperatively, however, we did not detect any obvious left orbital involvement and disease was readily freed off of the lamina papyracea and periorbita with no obvious defects noted. The left medial orbit was negative for malignancy on intraoperative biopsy after

gross total tumor resection. With these findings, we were able to avoid orbital exenteration and preserve meaningful visual function without compromising on an oncologically sound resection.

There is a paucity of literature comparing radiologic and intraoperative, endoscopic visualization for invasive sinonasal malignancies, including ENB. While increasing consideration in the literature is being given to orbital preservation even in the setting of modest orbital invasion, preoperative imaging is often considered the sole opportunity for such crucial decision making. Endoscopic endonasal approaches allow for superior visualization, including the utilization of intraoperative image guidance and, as such, may provide an additional opportunity for operative decision making, surgical optimization, and avoidance of unnecessary procedures. Here we provide an example of careful intraoperative visualization allowing for reduction in patient morbidity.

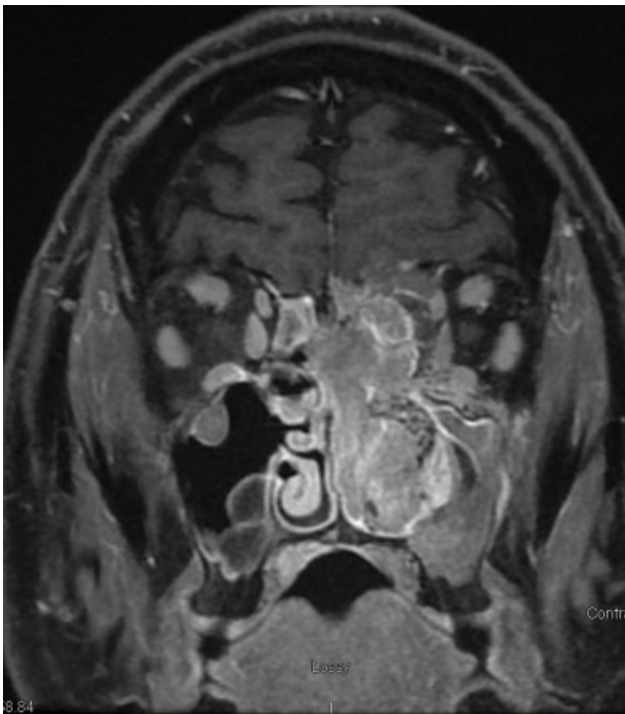


Fig. 1 Preoperative MRI, coronal view.

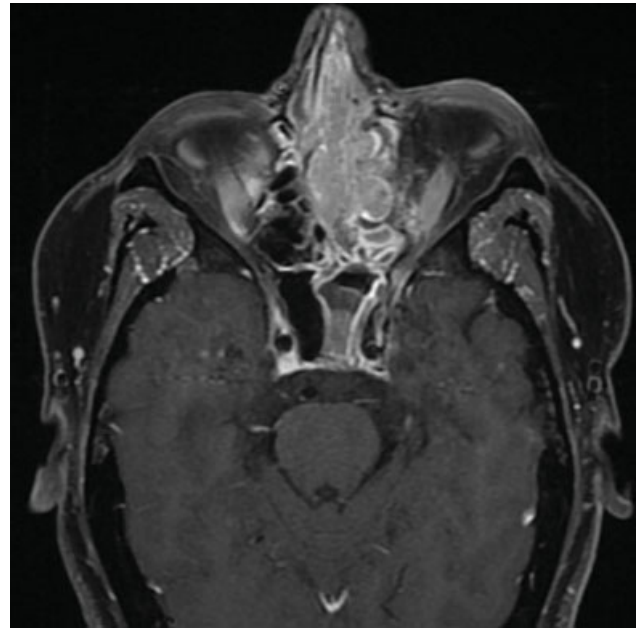


Fig. 2 Preoperative MRI, axial view.

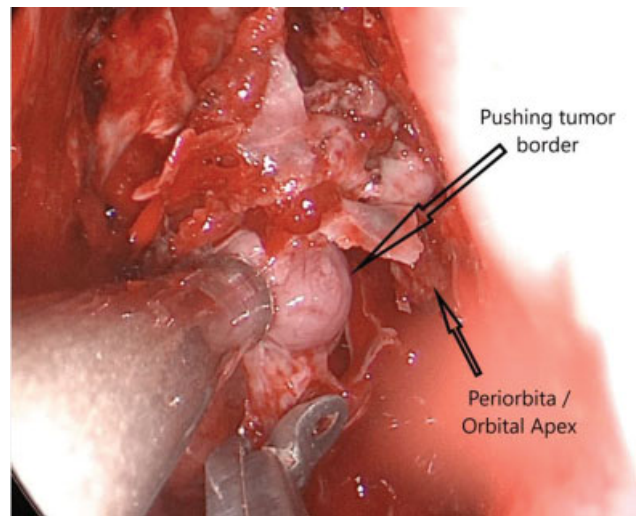


Fig. 3 Endoscopic view of pushing tumor border.

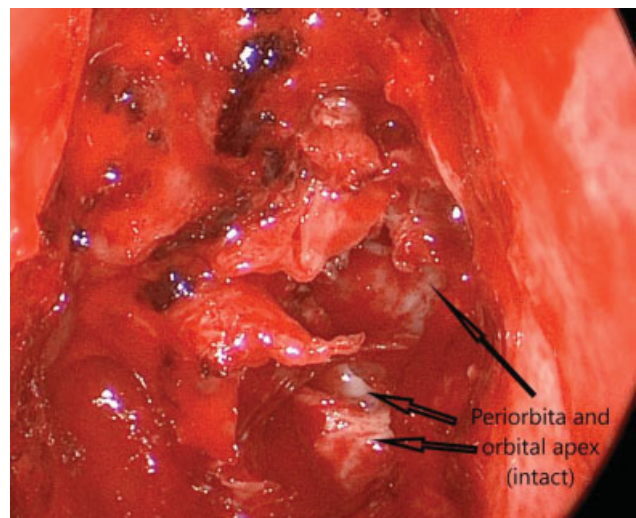


Fig. 4 Endoscopic view of intact periorbita.

P082. Endoscopic Endonasal Transtuberulum Transplanum Approach for Resection of Giant Pituitary Adenoma: The Second Floor Strategy to Avoid Postoperative Pituitary Apoplexy

Dante L. Pezzutti¹, Daniel M. Prevedello¹

¹The Ohio State University College of Medicine, Columbus, Ohio, United States

Giant pituitary adenomas (GPAs) have widely been defined as those tumors with a maximum diameter of >4 cm and represent 5 to 20% of pituitary tumors. These lesions are typically removed surgically unless identified as a prolactinoma, however, pituitary apoplexy is a rare and fatal complication that can sometimes ensue during the perioperative or postoperative period. Over the years, authors have noticed that during endoscopic endonasal approach (EEA) for resection of a GPA, using the traditional approach of starting the removal of tumor from the floor of the sella and then going progressing superiorly causes the tumor to suffer intraoperative apoplexy. We suspect that the partial resection of giant pituitary adenomas causes venous stasis in the residual tumor leading to tumor venous infarct and hemorrhagic transformation. This is likely because the traditional strategy of removing the lower part of the tumor initially when coming from a transsphenoidal approach leads to early disconnection of the suprasellar component in relation to the venous drainage that was established to the cavernous sinus. Consequently, the suprasellar tumor becomes quickly and progressively firmer making a complete resection less favorable and more likely to be associated with residual tumor postoperative apoplexy, deficits and possibly death.

We hypothesize that by accessing the tumor from the suprasellar portion first via a transplanum transtuberulum approach, and then resecting the inferior sellar portion via a transsellar approach secondarily allows the surgeon to completely remove the lesion without subsequent pituitary apoplexy.

We re-examined three cases at our home institution of The Ohio State University Wexner Medical Center to illustrate the problems with the traditional endoscopic endonasal transsellar approach in contrast to our newly proposed surgical method.

Case 1: A 62-year-old male experienced partial GPA resection using an endoscopic endonasal transsellar approach. A component of the tumor lateral to the right optic nerve was left for posterior treatment, which led to apoplexy of the residual tumor and vision deterioration. The patient was taken back and a craniotomy was performed to remove the enlarged residual. The patient ultimately recovered but lost vision in his right eye due to the apoplexy.

Case 2: A 46-year-old male underwent partial resection of a GPA via endoscopic endonasal transsellar approach at an outside institution first, which led to a long and complicated hospital course accompanied by postoperative suprasellar tumor apoplexy, meningitis, and frontal lobe brain infarction. After being referred to our home institution, a year later, we recommended surgery. We were able to successfully resect the remaining residual tumor via endoscopic endonasal transtuberulum approach without complication.

Case 3: A 21-year-old male underwent complete resection of the GPA using our proposed surgical technique of a primary transtuberulum transplanum approach, followed by a secondary transsellar approach. The patient experienced no postoperative complications.

The proposed study introduces a new surgical approach for GPAs that led to the complete resection of a GPA without complication. We recommend that surgeons utilize this "Second Floor" technique when managing giant pituitary adenomas.

P083. Endoscopic Endonasal Fenestration and Marsupialization of Petrous Apex Cholesterol Granulomas Using Silastic "Cigarette" Stent-Assisted Nasoseptal Flap

Kevin Zhao¹, Grant Arzumanov¹, Christopher Markosian¹, Pankaj Agarwalla¹, Giant Lin¹, Wayne D. Hsueh¹, Jean A. Eloy¹, James K. Liu¹

¹Rutgers New Jersey Medical School, Newark, New Jersey, United States

Background: The endoscopic endonasal approach (EEA) has become a popular approach for the treatment of petrous apex cholesterol granulomas (PACGs). Compared with open skull base approaches, such as the middle fossa approach or the infracochlear approach, the EEA offers the advantage of direct exposure of the cyst, shorter operative times, minimal bone drilling, and marsupialization into the nasal cavity. Surgical management of PACGs typically involves drainage, aeration and occasional cyst wall resection. Successful prevention of recurrence of PACGs relies on maintaining patency of the cyst fenestration.

Objective: We describe the use of an endoscopic endonasal expandable silastic "cigarette" stent-assisted nasoseptal flap technique to help maintain patency and prevent recurrence after endoscopic fenestration and drainage of PACGs. The technique and surgical outcomes are described.

Methods: A retrospective study was conducted for the treatment of PACG using the described technique. After an EEA exposure, the anterior cyst wall is opened and excised to maximize the width of the fenestration. A small nasoseptal flap is rotated into the PACG defect, lining the cyst wall. A silastic sheet is then rolled up like a cigarette and placed into the long axis of the PACG. After the stent is released, the silastic sheet uncoils and radially expands to keep the nasoseptal flap opposed to the cyst wall lining. The stent is removed 2 weeks after surgery. Serial nasal endoscopy and magnetic resonance imaging is performed to assess the patency of the PACG marsupialization.

Results: Five patients (two females, three males; mean age = 45 years) with PACG underwent the described technique. Three patients were primary cases, and two patients presented as recurrences after prior procedures (one middle fossa, one infracochlear approach). All patients experienced improvement of preoperative symptoms. There were no recurrences of PACG after a mean follow-up of 13.2 months (range: 2–48 months). There were no complications of CSF leakage, carotid injury, or infection.

Conclusions: Endoscopic endonasal fenestration and marsupialization of PACG using the silastic "cigarette" stent-assisted nasoseptal flap is a safe and effective technique for maintaining patency and preventing recurrences of cholesterol granulomas. The nasoseptal flap promotes mucosalization and marsupialization of the cyst while the silastic stent prevents migration of the nasoseptal flap. This technique helps ensure continuous drainage and aeration of the PACG.

P084. Use of Endoscopic Technique in Resection of Trigeminal Schwannoma

Alice E. Huang¹, Garret W. Choby², Jacob Dey², Matthew L. Carlson², Jamie J. Van Gompel³, Janalee K. Stokken²

¹Mayo Clinic School of Medicine, Rochester, Minnesota, United States

²Department of Otolaryngology, Mayo Clinic, Rochester, Minnesota, United States

³Department of Neurosurgery, Mayo Clinic, Rochester, Minnesota, United States

Objectives: To investigate the outcomes of endoscopic endonasal surgery for trigeminal schwannomas and the anatomical determinants of a combined surgical approach.

Methods: Seven patients who underwent resection of trigeminal schwannoma involving an endoscopic endonasal approach at the authors' institution between January 2006 and May 2019 were reviewed.

Results: Four lesions (57%) involved V2, 1 (14%) lesion involved V3, and 2 lesions extended into the sphenoid sinus (29%). Three tumors (43%) extended intracranially (**Table 1**). Two patients underwent combined intracranial approaches with frontotemporal ($n = 1$) and subtemporal craniotomy ($n = 1$). Both of these tumors had considerable intracranial extension into Meckel's cave (**Fig. 1**). Three patients underwent a combined endoscopic and Caldwell–Luc approach. Two of the three tumors extended into the infratemporal fossa (**Fig. 2**), while one demonstrated extensive involvement of the orbital floor (**Fig. 3**). Two cases (29%) required endoscopic endonasal medial maxillectomy alone. The two purely endoscopic resections occurred in patients who were completely asymptomatic and without physical exam deficits, while the remainder of the patients reported preoperative facial numbness, pain, or both. Moreover, these two lesions were the smallest tumors of the cohort as measured by greatest overall image-based dimension (mean = 2.7 vs. 5.1 cm for the other five lesions). Gross total resection was felt to be achieved in six of seven cases, with no postoperative cerebrospinal fluid leaks. At initial postoperative follow-up (mean = 1.1 months following surgery), all patients with preoperative facial numbness had persistent numbness. Of the three patients without preoperative numbness, two demonstrated new sensory deficits. The mean total duration of follow-up was 14.1 months. By most recent follow-up, resolution of facial numbness was reported in one patient who had exhibited new early postoperative numbness.

Conclusions: An endoscopic approach is safe for resection of smaller V2/V3 lesions with minimal to no intracranial extension. The addition of a Caldwell–Luc approach can assist in dissection, particularly with tumor extension into the infratemporal fossa or orbital floor.

Table 1 Tumor characteristics and surgical approach

Case	Location	Maximum length (cm)				Surgical approach
		AP	SI	ML	Overall	
A	MF, PF	4.9	3.5	3.03	4.9	EEA, frontotemporal craniotomy
B	MF, V2	6.54	6.13	6.01	6.54	EEA, Caldwell Luc
C	MF, PF	4	3.7	3.8	4	EEA, subtemporal craniotomy
D	V3	2.48	2.8	2.1	2.8	EEA
E	V2	2.59	2.02	2.12	2.59	EEA
F	V2	5.5	4.3	3.8	5.5	EEA, Caldwell Luc
G	V2	3.43	4.67	3.48	4.67	EEA, Caldwell Luc

Abbreviations: middle fossa (MF), posterior fossa (PF), anterior-posterior (AP), superior-inferior (SI), medial-lateral (ML), endoscopic endonasal approach (EEA)

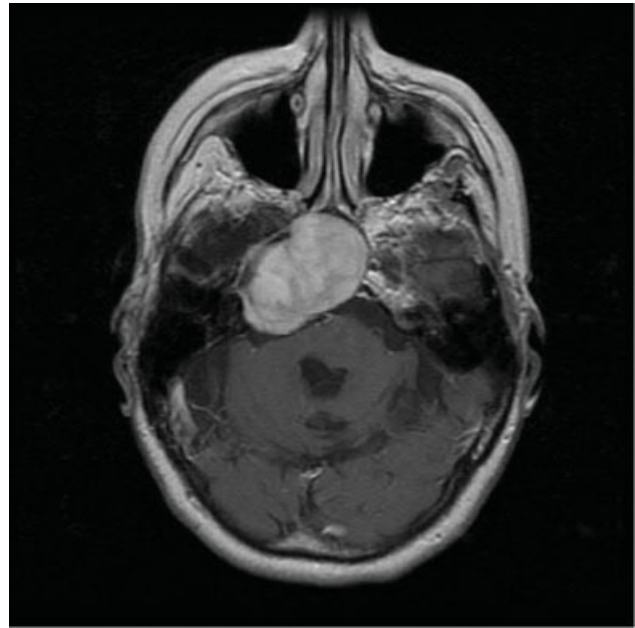


Fig. 1 Trigeminal schwannoma with intra- and extracranial components.

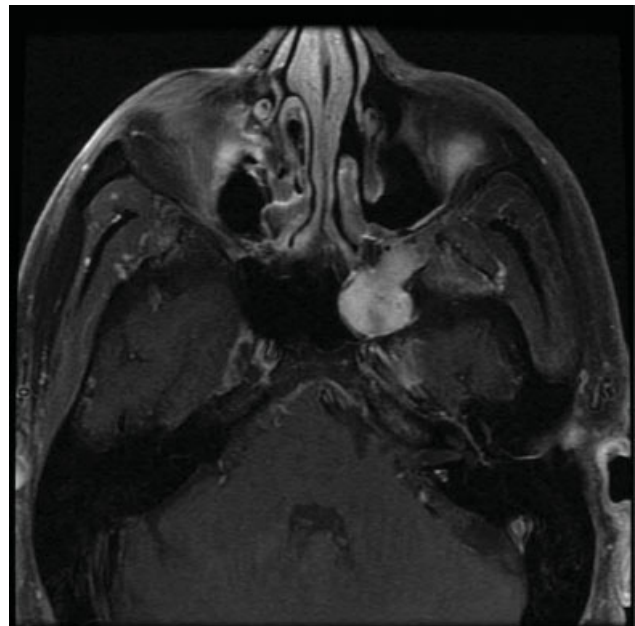


Fig. 2 V2 schwannoma extending into the infratemporal fossa.

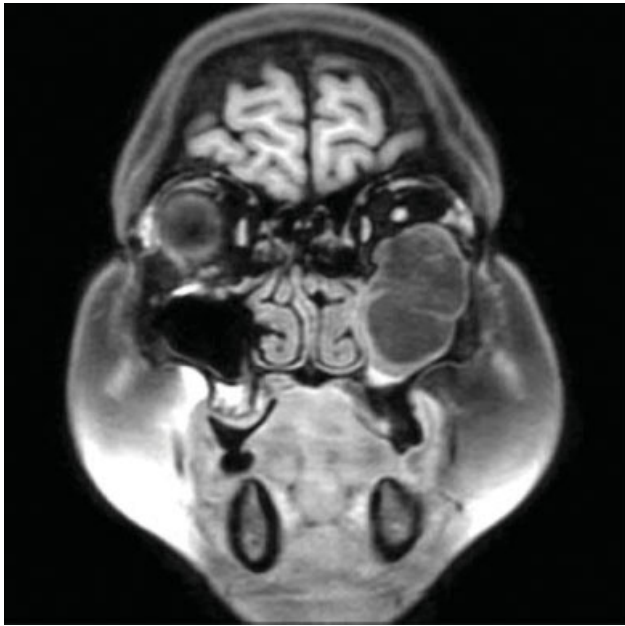


Fig. 3 V2 schwannoma with intraorbital extension.

P085. The Role of Endoscopic Endonasal Approach to the Axis Combined with Inferior Clivectomy and Extended Far Medial Approaches: Correlation of Morphometric Data with Stereotactic CT Landmarks in Cadaveric Dissection

Giuliano S. Bertazzo-Silveira¹, Sunil V. Manjila², Rafael Martinez-Perez¹, Thiago F. Albonette¹, Ricardo L. Carrau³, Daniel M. Prevedello¹

¹Department of Neurological Surgery, The Ohio State University Wexner Medical Center, Columbus, Ohio, United States

²Department of Neurosurgery, McLaren Hospital, Bay Region, Bay City, Michigan, United States

³Department of Otolaryngology and Head and Neck, The Ohio State University Wexner Medical Center, Columbus, Ohio, United States

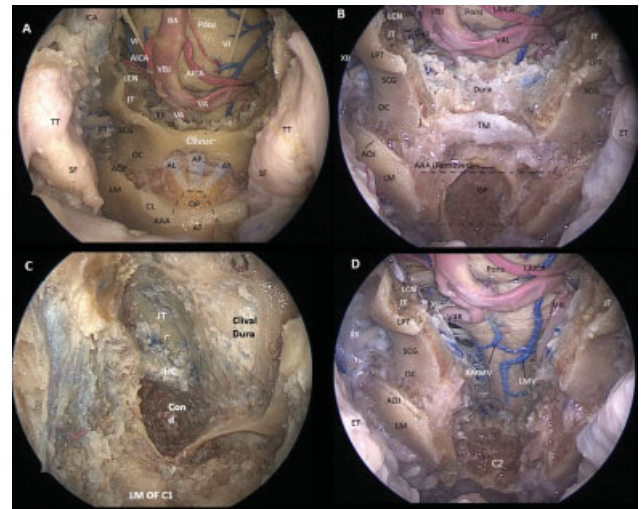
Background: The inferior clival and CCJ region is an anatomically complex and difficult-to-access area and endoscopic skull base surgeons would require detailed knowledge of the surgical anatomy and nuances while performing lower clivectomy with further caudal extension to involve C2 body/dens.

Methods: In the current study, stepwise image-guided dissections were performed in eleven colored latex-injected human heads. Morphometric measurements on the ventral foramen magnum, depth of the corridor, surgical exposure and the surgical freedom were verified by stereotactic CT scan thin-slice images. We describe an expanded endonasal transclival transodontoid approach to the C2 vertebra, highlighting the surgical key points with a stepwise image-guided cadaveric dissection to enhance surgical safety. The authors have performed a comprehensive literature review pertinent to the indications, limitations, outcomes along with technical pearls and pitfalls to avoid complications. Special attention is given to the endoscopic visualization of the landmarks on the posterior nasopharyngeal region.

Results: The bony depression of the occipital condyle labeled as the supracondylar groove was a reliable external reference to locate the hypoglossal canal and bilateral condyles which articulates with the lateral masses of the atlas. To approach the axis, drilling the anterior arch of C1 in between the medial borders of the lateral masses, to avoid injury to the vertebral artery situated lateral to the lateral masses at the

C1–C2 level. We observed that dissecting in between the Eustachian tubes using the midpoint of the posterior pharyngeal wall as the guiding landmark will reduce the risk of carotid injury as the parapharyngeal ICA often runs posterolaterally. The maximum diameter corresponding to the safe bony drilling area on the anterior arch of C1 presented an average of 17.5 ± 1.6 mm. The widest odontoid diameter, the thickness, and the height (measured from the body of C2 up to the tip of the odontoid process) was an average of 10.1 ± 1.05 mm, 10.04 ± 1.05 mm and 14.3 ± 2.4 mm, respectively. The depth of the nasal corridor measured from the anterior nasal spine to the posterior aspect of C2 along the plane of the hard palate was 96.7 ± 7.6 mm.

Conclusion: The endoscopic endonasal approach to the craniocervical junction uses a minimally invasive endonasal route instead of the traditional transoral approach, reducing morbidity and complications such as dysphagia, phonation dysfunction, and pharyngeal dehiscence. A stepwise procedure and deep knowledge of the anatomical landmarks are essential for complication avoidance.



P086. Morphometric Data on the Working Angle and Area of Neurosurgical Exposure for Anteromedial Skull Base Lesions Using Extended Endoscopic Transclival Approaches: Validation Using Ammirati's Maneuverability Grading System and Neuronavigation

Giuliano S. Bertazzo-Silveira¹, Sunil V. Manjila², Rafael Martinez-Perez¹, Thiago F. Albonette¹, Ricardo L. Carrau³, Daniel M. Prevedello¹

¹Department of Neurological Surgery, The Ohio State University Wexner Medical Center, Columbus, Ohio, United States

²Department of Neurosurgery, McLaren Hospital, Bay Region, Bay City, Michigan, United States

³Department of Otolaryngology and Head and Neck, The Ohio State University Wexner Medical Center, Columbus, Ohio, United States

Background: The “Far medial” and “Extreme Medial” are challenging approaches reserved for specifically trained endoscopic skull base surgeons and no published literature is available on the intraoperative maneuverability grading combined with stereotaxic navigation. We offer a comprehensive update on the morphometric data of the working angle and area of neurosurgical exposure for anteromedial skull base lesions using expanded endoscopic endonasal far medial and extreme medial approaches.

Methods: In the current study, stepwise image-guided dissections were performed in eleven colored latex-injected human heads and morphometric measurements on the inferior lateral clivus region (Fig. 1). The stereotactic angle of attack and the maneuverability of all relevant neurovascular structures exposed were scored using a modified Ammirati numerical grading system for further comparison and statistical analyses. The authors have performed a comprehensive literature review pertinent to the indications, limitations as well as outcomes along with technical pearls and pitfalls to avoid complications. The working angle is calculated by the degree of exposure, level of manipulability and surgical freedom, while the area of exposure is calculated by quadrangle bounded by the most lateral accessible point at the lacerum level and the most lateral accessible point at the level of the anterior arch of C1, bilaterally.

Results: The comparative results of Ammirati maneuverability score and exposure of most relevant anatomical structures from each compartment were 432 (Mean \pm SD 3.92 ± 0.26) for the ventromedial compartment and 285 (Mean \pm SD 2.59 ± 0.82) for the dorsolateral compartment ($p < 0.05$). The surgical freedom of $15.0^\circ \pm 1.9^\circ$ was noted at the level of the hypoglossal nerve and $9.0^\circ \pm 1.87^\circ$ at the level of the glossopharyngeal nerve, respectively ($p < 0.05$).

Conclusion: The extended endoscopic approaches to the ventral foramen magnum and jugular foramen using endonasal route have distinct advantages obviating brain retraction and the need for crossing major neurovascular structures in the posterior fossa. We have demonstrated cadaveric morphometric data on the working angle and area of neurosurgical exposure for anteromedial skull base lesions using endoscopic endonasal far medial approaches, with validation combining the use of Ammirati maneuverability grading system and neuronavigation.

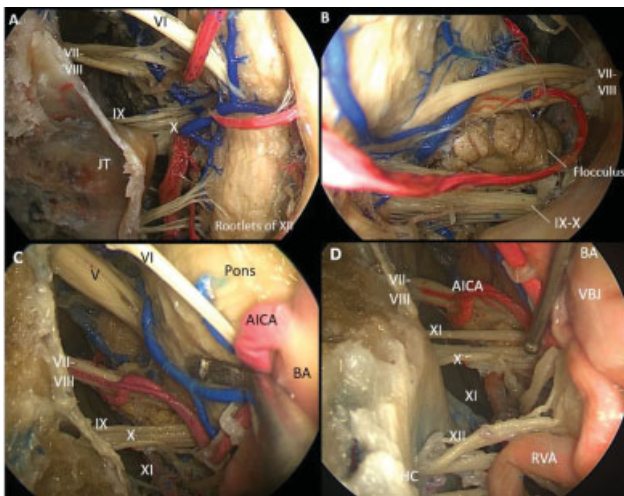


Fig. 1

P087. Endoscopic Endonasal Surgery (EES) for Craniopharyngiomas: Experience of the Neurosurgery Institute Dr. Alfonso Asenjo, Chile

Patricio Sepúlveda¹, Matías Gomez¹, Homero Sario¹, Patricia Walker¹, Cristian Naudy¹

¹Neurosurgery Institute Dr. Alfonso Asenjo, Chile

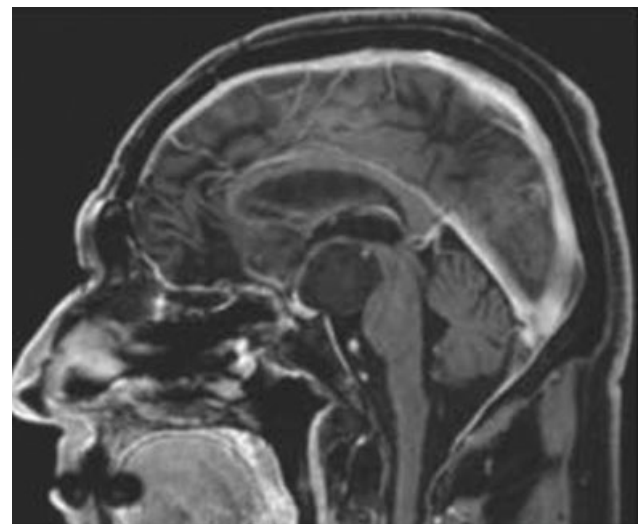
Introduction: Conventionally, the transsphenoidal approach (TE) has been considered as an effective surgical method for craniopharyngiomas that originated and developed in the sella turcica. However, recently, extended TE

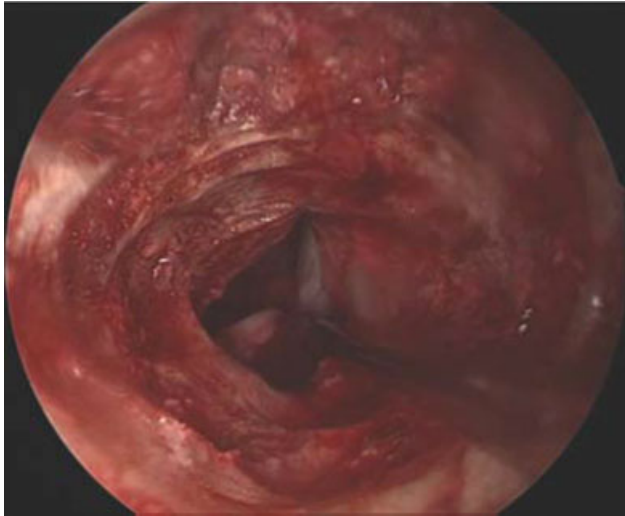
surgery with endoscopy has subsequently expanded its range of indication, which allows its use in suprasellar craniopharyngiomas. The purpose of this paper is to show our experience in endonasal endoscopic surgery for craniopharyngiomas.

Methods: Data were obtained from patients diagnosed with craniopharyngioma and who underwent endoscopic endonasal surgery (EES) at the Dr. Alfonso Asenjo Institute of Neurosurgery, Santiago-Chile, between November 2011 and May 2019, to analyze them retrospectively. The diagnosis of craniopharyngioma was histologically confirmed. We consider pre and postoperative evaluations for neurophthalmology, endocrinology, and skull base repair in operative protocol.

Results: We included 16 patients, average age 32.2 (6–69) years, 50% male and 50% female. They were classified into two groups; Primary surgery and reintervention (transcranial or transsphenoidal). The 47.3% (9/16) received primary surgery; 11.1% presented panhypopituitarism prior to surgery and 33.3% presented it in the postoperative period. 66.6% had visual field disturbance prior to surgery, of which four improved after surgery and two remained with the same postoperative deficit. Of the eight patients in the reintervention group, there were two with more than one EES, and the rest previously underwent transcranial surgery. Of these, 62.5% had panhypopituitarism, and after surgery 75%. Also, 87.5% had altered visual field, two with postoperative deterioration. Of the 20 surgeries, 17 used nasoseptal flap with vascular pedicle and bone in situ to repair the skull base defect, the rest; one was repaired with a titanium plate-abdominal subcutaneous fat-Duraseal; one with Surgicel-abdominal subcutaneous fat; one with abdominal subcutaneous fat-Bone-Beriplast. Three of the patients presented CSF leak after surgery. All of them were repaired with the nasoseptal flap, previously in de EES. As for other complications, six had diabetes insipidus, three transiently. One of our patients evolved with CNS infection associated with acute hydrocephalus that required external ventricular drainage. Another of our patients presented CSF fistula, which required reoperation, then evolved with meningitis, multisystem failure, and died.

Conclusion: The surgical approach is challenging in craniopharyngioma. The use of the endoscopic endonasal technique provides great exposure for the neurosurgeon. The injury of the endocrine and visual function should be considered. The septal flap with vascular pedicle and bone in situ, for the reconstruction of the skull base defect, was used in the majority of our surgeries with an acceptable number of CSF leakage.



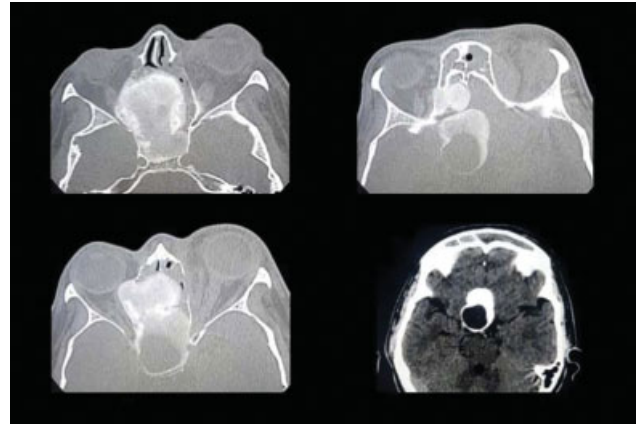


P088. Giant Ossifying Fibroma of the Ethmoid Sinus, Orbit, and Anterior Skull Base: Endoscopic Endonasal Approach
Danielle de Lara¹, Thiago B. Sonogo², Beatriz Sartori², Alaina E. Sordi¹, João G. Valim¹

¹Universidade Regional de Blumenau, Santa Catarina, Brazil

²Hospital Santa Isabel, São Paulo, Brazil

Introduction: Ossifying fibroma (OF) is a benign fibro-bone tumor that affects the bones of the face, but rarely involves the ethmoid sinus and orbit. The lesion is asymptomatic in most cases until growth produces facial deformity.



Case Report: A 45-year-old previously healthy woman presented to the emergency department complaining of headache and nasal discharge, evolving with ocular proptosis, pain and right periorbital edema. CT scans demonstrated a lesion centered on the skull base and ethmoid sinus, with involvement of drainage pathways and right orbit. The patient underwent endoscopic endonasal skull base surgery for tumor removal. Surgery was uneventful and patient was dismissed from hospital on the fifth postoperative day. Pathology confirmed a cementoossifying fibroma.

Discussion: OF are fibroosseous lesions that mainly involve facial bones and usually present with a slightly exuberant clinical picture. However, as tumor growth advances, facial asymmetry and neurological symptoms may occur due to compression of vital structures. In the reported case, there was visual field impairment and oculomotor nerve palsy due to extrinsic cranial nerve compression. Endoscopic endonasal surgery was effective to remove the tumor offering a straightforward approach.

Conclusion: Although a benign tumor, in this case the OF presented as an aggressive lesion due to the extension of the mass and compression of adjacent structures. Endoscopic endonasal approach for ossifying fibromas has proved to be an excellent therapeutic option, providing direct visualization and the absence of facial scars.

P092. Skull Base Tumors Treated via Endonasal Endoscopic Approaches. Case Series

Bakhtiyar Pashaev¹, Dmitriy Bochkarev¹, Valeriy Danilov², Andrey Alekseev¹, Gulnar Vagapova³, Vladimir Krasnozhon³

¹Interregional Clinical Diagnostic Center, Kazan, Russia

²Kazan Medical State University, Kazan, Russia

³Kazan Medical State Academy, Kazan, Russia

Objective: A different tumors of the skull base could be treated via endoscopic endonasal routes. Due to the small number of each neoplasm we consolidate those heterogenic pathologies according to the type of surgical approach. The aim of this paper is to emphasize the effectiveness of endoscopic endonasal approach (EEA) in different skull base tumors treatment.

Methods: A retrospective review of patient's data with non-pituitary skull base tumors treated via EEA in the department of neurosurgery at Interregional Clinical Diagnostic Center in the period of 2010 to 2019 was made. Type of

pathology, extent of resection, reconstruction technique, complications and outcomes were collected.

Results: A total of 54 patients with 19 different pathologies were operated. Among them were 17 meningiomas, 8 chordomas, 3 neuroendocrin carcinoma, 3 chondromyxoma, 3 metastasis, 3 SNAC, 2 SNUC, 2 ENB, 2 chondrosarcoma, 2 plasmocytoma, aggressive fibromatosis, angiofibroma, cylindroma, hemangiopericytoma, lymphoma, neurinoma, neuroenteric cyst, RCC, and vidian nerve neurooma by 1 case per pathology. There were 21 males and 33 females. Patient's age was between 19 and 76 years, with median of 51.8 years. With regard to the pathology's location different types of endonasal approaches to the anterior, central and posterior skull base were used. Most of them were extended and required a multilayer reconstruction as a final step of surgery. With regard to extent of resection there were 7 biopsies, 12 partial removals, 14 STRs, 6 NTRs, and 17 GTRs. In a vast majority of cases, a skull base reconstruction with pedicle vascularized nasoseptal flap was made. Reconstruction with pedicle vascularized pericranial flap was made in four cases and in one case with free pericranial flap. A postoperative CSF diversion with external drainage was applied in 20 (37.03%) patients and one of them required a subsequent shunting. Five patients (9.25%) developed a postoperative CSF leak and in two (3.7%) of them a meningitis was marked. Both were cured with delay extracranial complication in one case. Among other complications two (3.7%) patients had visual deteriorations, two (3.7%) cases of vascular injury including one basilar artery injury with brain stem stroke, two (3.7%) cases of CN VI palsy, two (3.7%) cases of brain tissue injury, five (9.25%) cases of excessive blood loss, two (3.7%) cases of DVT, and three (5.5%) patients developed a DI. Perioperative mortality rate was a 1.8% in this series.

Conclusions: Different skull base pathologies could be treated via EEA. Depends on their biology surgical treatment could be as a treatment of chose or provide the disease diagnosis and be a part of combined treatment. A learning curve is a critical point impacting on effectiveness of surgery and its outcomes.

P093. Integration of an Enhanced Recovery after Anesthesia Program for Patients Undergoing Skull Base Tumor Surgery
Stephanie Flukes¹, Ilya Laufer¹, Martin Hanson¹, Jennifer Cracchiolo¹, Eliza Geer¹, Vivian Tabar¹, Marc A. Cohen¹

¹Multidisciplinary Pituitary and Skull Base Tumor Program, Memorial Sloan Kettering Cancer Center, New York, New York, United States

Background: Utilization of evidence-based perioperative management paradigms has been demonstrated to improve outcomes and shorten length of stay. The benefits of early recovery after surgery (ERAS) programs have been established in several surgical specialties, including orthopedics, colorectal surgery, and head and neck surgery. There is sparse literature on the adoption of an ERAS program for patients with pituitary and other skull base tumors.

Objective: To assess the ability to implement an ERAS program for skull base surgery

Methods: An evidence-based, systematic review of the literature was performed with the manuscript accepted for publication. The best practices as outlined in the systematic review, which involved several elements of perioperative care, were discussed with all stakeholders, including surgeons, physicians involved in perioperative management (anesthesia, endocrine), nurse practitioners, inpatient and outpatient nursing, social work, physical therapy, nutrition, and administrative project managers. Utilizing these data, preoperative and postoperative order sets were developed and established as the standard of care in our institution.

Intraoperative guidelines were adopted by the anesthesiology department. Milestones by hospital day were identified. Patient reported outcome surveys were initiated via an online portal. Educational materials were created by nursing and physician staff and were edited by the patient education group at our institution for the average reader to comprehend preoperatively.

Results: The standardized order sets are utilized in presurgical testing and postoperatively by the house staff. The care items include: preoperative consultation with endocrinology for assistance with hormonal and diabetes management, notice for patients with acromegaly and Cushing's disease to be aware of anesthesia challenges with intubation and postoperative obstructive sleep apnea, early cessation of antibiotics, avoidance of systemic steroids in the presence of an intact hypothalamic-pituitary-adrenal axis and in the setting of Cushing's, early Foley's catheter removal, and early ambulation. Other best practice milestones were identified for retrospective review and to track prospectively to measure success of our endeavors. Information technology infrastructure to track clinical milestones, patient reported outcome data, perioperative complication rates, and length of stay are underway.

Conclusion: The integration of ERAS protocols for pituitary and other skull base tumors has been demonstrated to be feasible with multidisciplinary engagement. This enables best evidence-based perioperative management, with prospective data collection that provides ample opportunity for assessment of quality of care and quality improvement initiatives.

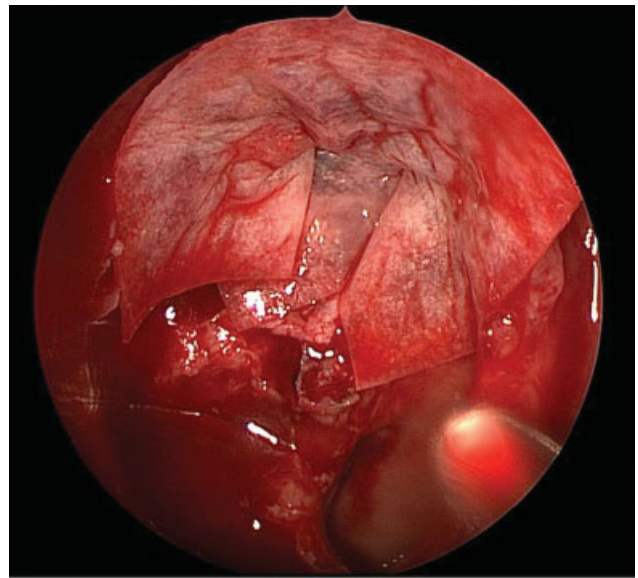
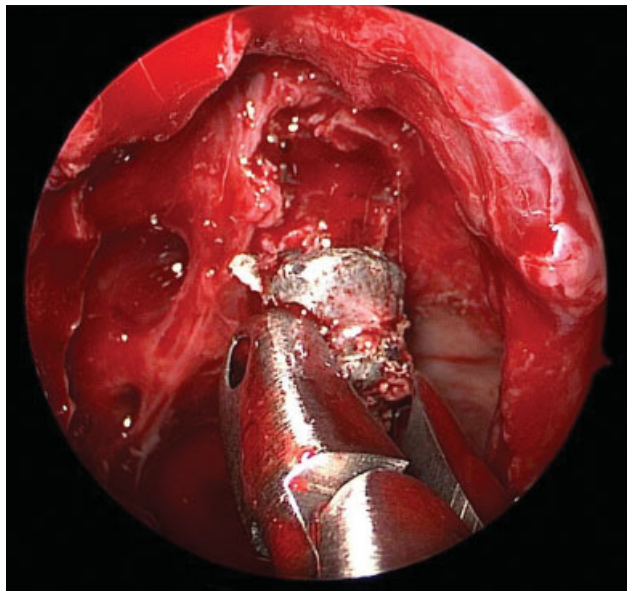
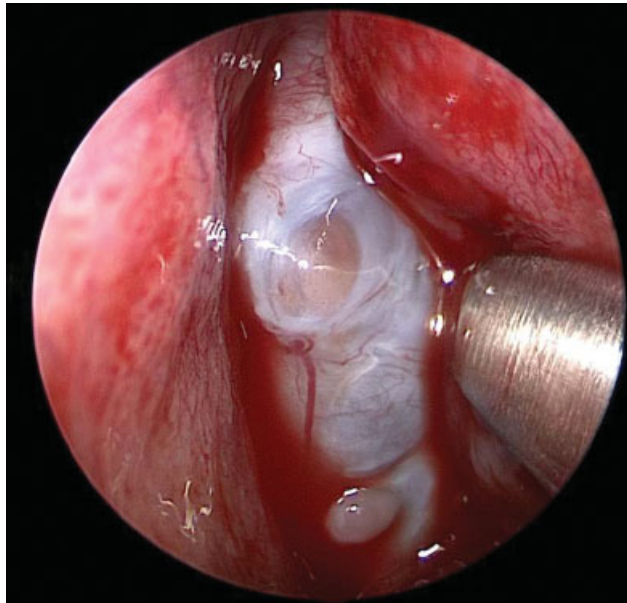
P094. Endoscopic Removal of a Retained Bullet from the Planum Sphenoidale

William C. Harris¹, Edward D. McCoul²

¹Department of Otorhinolaryngology, Tulane University, New Orleans, Louisiana, United States

²Department of Otorhinolaryngology and Ochsner Clinic Foundation, Tulane University, New Orleans, Louisiana, United States

A retained bullet within the sphenoid sinus is an unusual entity as it is unlikely for an individual to survive the initial traumatic event. To this point, there are several critical structures that a bullet must pass through or narrowly avoid to reach this location. Furthermore, attempted removal of a foreign body from this site requires meticulous avoidance of several vital structures. We present the case of a 40-year-old male with a remote (25 years prior) history of a gunshot wound to the head and subsequent repair of cerebrospinal fluid leak who presented with persistent headaches, clear rhinorrhea, as well as several emergency room visits for suspected meningitis during the past year. CT imaging demonstrated an apparent retained metallic fragment within the roof of the left sphenoid sinus. MRI revealed a complex fluid collection within the sphenoid sinus, a portion of which was isointense to cerebrospinal fluid. A navigation-guided endoscopic approach was used to remove a bullet from the planum sphenoidale, evacuate a mucopyocele of the sphenoid sinus, and reduce a meningocele adjacent to the orbital apex. Subsequently, a multilayered closure consisting of a collagen matrix graft, calcium phosphate cement, fibrin sealant, and nasoseptal flap was used to repair the dural defect. This case calls attention to this rare finding as well as the important considerations related to operative intervention.



P095. Endoscopic Surgery for Tumors in and around the Third Ventricle

Kenichi Oyama¹, Toshio Hirohata¹, Keisuke Onoda¹, Shigeyuki Tahara², Akira Teramoto³, Akio Morita², Akira Matsuno¹

¹Department of Neurosurgery, Teikyo University School of Medicine, Tokyo, Japan

²Department of Neurological Surgery, Nippon Medical School, Tokyo, Japan

³Shonan University of Medical Science, Kanagawa, Japan

Objectives: To show the current activities and future perspectives of the endoscopic surgery for tumors in and around the third ventricle.

Method: During five years, 23 consecutive patients with tumor in and around the third ventricle underwent endoscopic tumor resection. We used both a flexible-

(VISERA video scope, Olympus Co. Ltd., Japan) and a rigid endoscope (Endoarm, Olympus Co. Ltd., Japan) depending on the lesion.

Results: Seven patients were operated on via the single burr-hole approach using a flexible endoscope to perform a biopsy of the tumor, as well as the third ventriculostomy. In all seven patients, a sampling of tumor tissue was successfully performed. Sixteen patients underwent endoscopic surgery using a rigid scope via various entry routes (endonasal: 6, transventricular: 4, combined endonasal and transventricular: 1, infratentorial supracerebellar: 1, occipital transtentorial: 3, and interhemispheric: 1 toward the third ventricle. Using a rigid endoscope, we could achieve extensive removal of the tumor with a clear vision, and 81.3% underwent gross total (10/16) and subtotal (3/16) resection.

Conclusions: The endoscopic surgery is safe and feasible for the third ventricle tumors. Using endoscope, we can choose 360-degree surgical corridor to the third ventricle depending on the tumor characteristics.

P097. Endoscopic Endonasal Free Flap Reconstruction after Failed Cranialization: A Case Report

Patrik Pipkorn¹, Adam P. Liebendorfer¹, Jake Lee¹

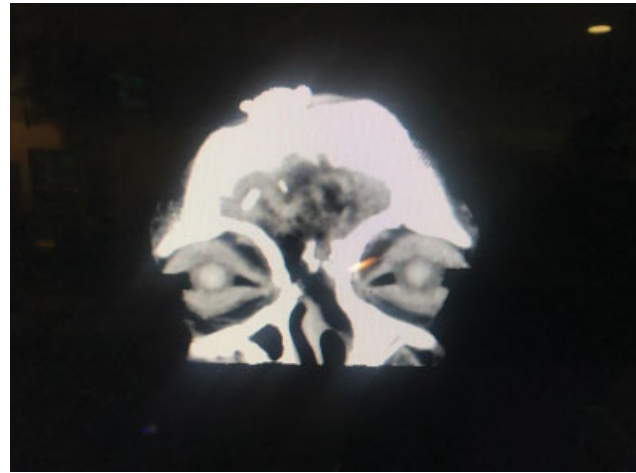
¹Washington University in St. Louis School of Medicine, St. Louis, Missouri, United States

Objective: Cerebrospinal fluid leak after craniofacial resection can be a difficult problem to manage. Standard reconstructive efforts include local and locoregional flaps, as well as various allopathic materials. Although endoscopic surgery for skull base procedures has gained recognition in recent years, few approaches exist for delivering such flaps endoscopically. In this study, we present one case demonstrating a novel and unusual method of for reconstructive of a difficult CSF leak after skull base surgery.

Methods: A 67-year-old male with persistent cerebrospinal fluid leaks following a craniotomy and gamma knife procedure for aggressive meningioma. He and the neurosurgeon were reluctant doing a revision craniotomy and cranialization due to unsuccessful previous attempt for providing separation between the cranium and sinonasal cavity. Thus, he underwent a reconstruction of the anterior skull base with a left forearm free flap used to cover the defect. To create space for the fibrofatty flap, we conducted a Draf's III bilateral frontal sinusotomy and medial maxillectomy. A Caldwell-Luc procedure was performed to provide a corridor through which the flap was inserted. We then removed the flap from the left distal forearm, passed it through the Caldwell-Luc and placed it on the anterior skull base. The flap vessels were the tunneled through down to the left neck. We approximated the facial artery and the radial artery and coupled the facial vein and vena comitantes from the radial artery.

Results: During the procedure, the flap appeared well-seated and provided a watertight seal. The patient's remaining hospital courses were unremarkable for further CSF leaks. The patient reports no new CSF leaks during 6 months of follow-ups, and no evidence for flap failure or necrosis on follow-up examinations.

Conclusions: We present a promising novel endoscopic free flap solution for complex skull base defects with a demonstrated efficacy for treating postcraniotomy CSF leaks. Further work can elucidate other potential uses for such an approach.



P098. Endoscopic Transnasal Combined Transoral Approach for Giant Parapharyngeal Space Tumors

Xicai Sun¹, Huan Wang¹, Quan Liu¹, Weidong Zhao¹, Yurong Gu¹, Houyong Li¹, Chunquan Zheng¹, Hongmeng Yu¹, Dehui Wang¹

¹Department of Otolaryngology, Eye, Ear, Nose and Throat Hospital, Shanghai Medical College of Fudan University, Shanghai, China

Background: Surgical treatment of parapharyngeal space tumors is challenging. With the development of endoscopic skull base surgery, various endoscopic-assisted surgical approaches have become one of the options for parapharyngeal space surgery. The purpose of this study was to compare the anatomical characteristics of parapharyngeal space between endoscopic transnasal and transoral approaches, and to explore the application of endoscopic-assisted transnasal combined with transoral approach in giant parapharyngeal space occupying surgery.

Materials and Methods: Six fresh cadaveric heads (12 sides) perfused with silicon gel were dissected under endoscopy, and possible surgical anatomical markers were found. Three cases of giant parapharyngeal space lesions treated by endoscopic transnasal and transmaxillary sinus combined with transoral approach were reported.

Results: The anatomical details of parapharyngeal space could be displayed through both transnasal and transoral approaches. Transnasal and transmaxillary sinus approaches are more direct in exposing the parapharyngeal space, and have advantages in resecting tumors invading the skull base. But its exposure range is limited, the lower boundary is hard palate, the lateral boundary is medial pterygoid muscle and temporal muscle. The structure of the parapharyngeal space exposed directly through the transoral approach, but the exposure to the anatomical structure around the Eustachian tube was limited. The stylopharyngeal muscle and stylohyoid muscle can be used as the anatomical markers for locating the parapharyngeal internal carotid artery through the transoral approach. Endoscopic-assisted transnasal transmaxillary sinus and combined with transoral approach were used to complete the resection of three patients with giant parapharyngeal space tumors. No obvious complications occurred.

Conclusion: Endoscopic-assisted transnasal maxillary sinus and combined with transoral approach can be used for giant parapharyngeal space tumor surgery. This approach can clearly show the important neurovascular structures in the

parapharyngeal space. Endoscopic-assisted transoral approach is more direct in exposing the parapharyngeal internal carotid artery.

P099. Endoscopic Endonasal Transsphenoidal Resection of Pituitary Apoplexy: Assessment of Visual and Endocrine Outcomes

Rosemary T. Behmer Hansen¹, Kevin Zhao¹, Christine Yen¹, Grant Arzumanov¹, Wayne D. Hsueh², Jean Anderson Eloy², James K. Liu³

¹Rutgers New Jersey Medical School, Newark, New Jersey, United States

²Department of Otolaryngology Head and Neck Surgery, Rutgers New Jersey Medical School, Newark, New Jersey, United States

³Department of Neurological Surgery and Otolaryngology, Center for Skull Base and Pituitary Surgery, Neurologic Institute of New Jersey, New Jersey, United States

Background: Pituitary apoplexy (PA) is a rare clinical syndrome typically caused by acute hemorrhage or infarction of a pituitary adenoma. We analyzed a series of patients with PA who underwent endoscopic endonasal transsphenoidal surgery (EETS) and assessed clinical outcomes.

Methods: A retrospective chart review was performed on 28 patients diagnosed with PA between August 2009 and June 2019. Data was collected regarding patient demographics, presenting symptoms, postoperative complications, pathology, and clinical outcomes.

Results: Twenty-eight patients (12 females, 16 males; mean age, 50.19 ± 14.40 years; mean follow-up, 5.67 ± 6.33 months) underwent EETS. Common presenting symptoms included headache (89.3%), visual acuity deficit (60.7%), nausea/vomiting (50.0%), ocular paresis (46.2%), and visual field deficit (35.7%). Most common presenting endocrine abnormalities included hypothyroidism (60.7%), and hypoprolactinemia (28.6%). All adenomas were macroadenomas, either hemorrhagic (25.0%) or necrotic (28.6%), or both. Sphenoid sinus mucosal thickening was present in 53.6% of cases. After EETS, improvement or normalization in visual function was noted in at least 80% and improvement in ocular paresis in 100%. Endocrine outcomes varied. Hormone replacement therapy was administered to 61.5% of patients postoperatively. Five patients had temporary diabetes insipidus (DI), and two had long-term DI. There were no postoperative CSF leaks and no deaths.

Conclusion: EETS is a safe and effective approach for the surgical treatment of PA, where visual and ocular paresis symptoms were more likely to improve or normalize than endocrine. Timely recognition of PA may further improve patient visual outcomes after EETS.

P100. Establishment and Characterization of Two Novel Olfactory Neuroblastoma Cell Lines

Tianna Zhao¹, Lisa M. Rooper², Debraj Mukherjee¹, Nicholas R. Rowan³, Masaru Ishii³, Christine L. Hann⁴, Gary L. Gallia¹

¹Department of Neurosurgery, Johns Hopkins University School of Medicine, Baltimore, Maryland, United States

²Department of Pathology, Johns Hopkins University School of Medicine, Baltimore, Maryland, United States

³Department of Otolaryngology, Johns Hopkins University School of Medicine, Baltimore, Maryland, United States

⁴Department of Oncology, Johns Hopkins University School of Medicine, Baltimore, Maryland, United States

Background: Olfactory neuroblastoma (ONB), also known as esthesioneuroblastoma, is a malignant neoplasm of the sinonasal cavity accounting for approximately 6% of all

sinonasal malignancies. ONBs are locally aggressive neoplasms and can metastasize to the neck, central nervous system, and bone. Currently, there are no effective systemic therapies available for ONB patients and there is little progress in understanding the pathogenesis of ONB, largely due to the lack of model systems which accurately maintain the genetic and pathophysiologic characteristics of ONB. In this study, we aim to establish and characterize two ONB cell lines, to develop novel therapies with translational potential.

Methods: Specimens were obtained from patients with ONB including both intranasal and/or intracranial components of tumors. Specimens were transported directly from the operating room to the laboratory and were minced and digested with collagenase IV. After passing through a 70-µm nylon mesh, the cells were maintained in growth medium at 37°C, 5% CO₂ in a humidified incubator. Short tandem repeat (STR) analysis was used to characterize established ONB cell lines and their parental ONB tumors, while immunofluorescence staining in ONB cell lines and immunohistochemical staining in their parental tumors were used to compare the expression of ONB molecular markers.

Results: Cell lines were established from two patients, with one line derived from an intranasal specimen (JHH_ONB_1903) and the other from an intracranial specimen (JHH_ONB_1904). Genomic analysis using STR profiling revealed that the intranasal ONB cell line showed 100% identity and the intracranial ONB cell line showed 98.4% identity to their parental ONB samples, respectively. In addition, the expression of ONB molecular markers, including synaptophysin, INSM1 and neuron-specific enolase, were detected in both ONB cell lines and their parental ONB samples in similar patterns: the expression of synaptophysin was detected in a punctate pattern; the expression of INSM1 was detected in nucleus; and the expression of neuron-specific enolase was detected diffusely throughout the cytoplasm.

Conclusion: Two novel ONB cell lines were established. These lines accurately maintain the genetic and immunohistochemical characteristics of their parental ONB samples. These lines provide reliable models to further study the pathophysiology underlying ONB and to evaluate therapeutic strategies.

P101. Malignant Peripheral Nerve Sheath Tumor of the Intratemporal Facial Nerve: A First Case Report and Review of the Literature

Eric N. Appelbaum¹, Nathan R. Lindquist¹, Alex D. Sweeney¹

¹Baylor College of Medicine, Houston, Texas, United States

Objective: To report a novel case of an intratemporal malignant peripheral nerve sheath tumor (MPNST) arising from the mastoid segment of the facial nerve and a review of the relative literature.

Design: Case report and review of the relevant literature.

Setting: A large public county hospital and level-1 trauma center.

Participants: A 54-year-old female with a history of stage-III cervical carcinoma presenting with otorrhea, facial palsy, and an external auditory canal mass.

Main Outcome Measures: Description of clinical case presentation, diagnosis, and treatment of MPNST of the intratemporal facial nerve. Review of the existing peer-reviewed literature for prior similar cases and treatment strategies.

Results: Biopsy of the mass showed MPNST. The patient underwent lateral temporal bone resection, facial nerve decompression and sacrifice, dissection of the jugular foramen, total auriculectomy, total parotidectomy, selective

neck dissection and microvascular free flap reconstruction. Tumor was noted to be filling the mastoid cavity confluent with the mastoid segment of the facial nerve with extension to the jugular bulb and jugular foramen. Pathology results confirmed MPNST. Ipsilateral neck dissection revealed no existing cervical metastases. After a short inpatient stay, the patient recovered well and underwent adjuvant chemoradiation. At most recent follow up, there appears to be no evidence of malignancy. Review of the literature was performed using Medline and Google Scholar. There are few previous reports of MPNST involving the lateral skull base and none reporting primary MPNST of the intratemporal facial nerve.

Conclusions: MPNST is a rare entity within the head and neck with limited reports in the literature of involvement of the lateral skull base. This is the first reported case of a primary MPNST arising from the intratemporal facial nerve.

P103. Parotid Mass and Orofacial Granulomatosis—A Diagnostic Dilemma with Review of Literature Shaswati Sengupta Datta¹

¹Jagannath Gupta Institute of Medical Sciences, Budge Budge, Kolkata, West Bengal, India

Introduction: Parotid mass and facial nerve palsy are common clinical presentations in hospital and clinic-based practice. But when presented together they usually point to the possibility of malignancy or inflammatory pathogenesis. Melkersson–Rosenthal Syndrome is one of the diseases in the spectrum of orofacial granulomatosis characterized by bilateral alternate facial nerve palsy, swelling of lips and fissured tongue. We present a study of two cases where the spectrum of disease consisted of parotid mass, alternating facial nerve palsy, characteristic features of Melkersson–Rosenthal syndrome, ultimately leading to the diagnosis of Wegener's granulomatosis.

Study Design: Retrospective case study of two subjects, in the span of 9 years, presenting with unilateral parotid mass, lower motor neuron-type facial palsy, characteristic facial changes and clinicopathological features of Wegener's granulomatosis.

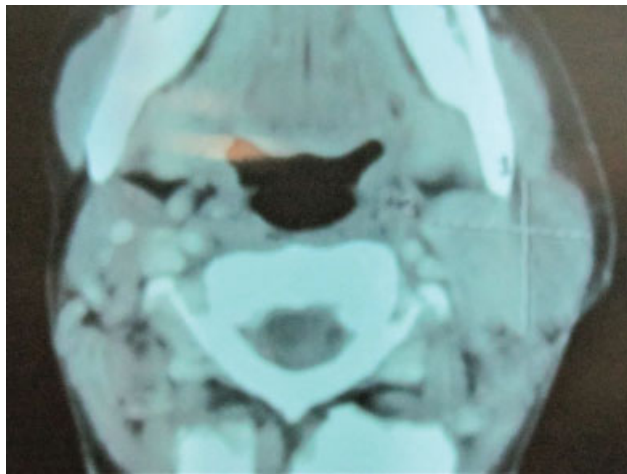
Materials and Methods: Data related to clinical features, pathological and radiological parameters were evaluated in each patient for 15.5 months (range, 7–24 months). Experience from the first case helped us to initiate necessary management plan tailored to second patient. Modified American College of Rheumatology criteria for the classification of Wegener's granulomatosis was followed for assessment.

Results: The primary complaint of both patients was recently developed facial palsy and mild facial puffiness with preexisting parotid mass and otitis media with effusion (OME). Facial palsy improved with parotidectomy and steroid therapy, though OME persisted. Histopathology showed non-caseating granulomatous disease of parotid. Blood levels of c-ANCA and p-ANCA were negative initially, though in the first case there was rising titer of c-ANCA in later stage of disease. After an apparently smooth postoperative recovery there was relapse of facial palsy on opposite side with swollen lips, face and constitutional symptoms. This time lip biopsy showed chronic inflammatory cell predominance with granuloma formation (case 2). The first patient had weight loss, arthralgia, hemoptysis with multiple lung nodules on radiography and was treated with anti-tubercular drugs. She had little improvement and underwent CT guided FNAC from mediastinal mass and pleural biopsy that again showed noncaseating granulomatous lesion, along with high normal level of c-ANCA. Unfortunately, she succumbed to massive hemoptysis within 3 days of starting cytotoxic therapy. In the second case,

patient improved dramatically with steroid and methotrexate therapy with only two relapses of facial palsy with lip swelling and epistaxis in last seven years. Renal function and urinalysis were absolutely normal in both cases.

Conclusion: Wegener's granulomatosis can present in generalized or limited form with or without systemic involvement in later period of disease spectrum. Parotid mass is its rare presentation and association with facial palsy and features of orofacial granulomatosis (Melkersson–Rosenthal syndrome) is even rarer. High degree of clinical suspicion and meticulous follow up is needed to establish the diagnosis. Tuberculosis is a common compounding factor in countries like India and must be ruled out to prevent delay in treatment and mortality. Dependence upon antineutrophilic cytoplasmic antibody should be weighed judiciously against clinical symptoms and biopsy reports.





P104. Locoregional Skull Base Recurrence Masked by Chronic Otomastoiditis in a Patient with HPV-Related Oropharyngeal Squamous Cell Carcinoma Treated with Primary Chemoradiation

Christie McGee¹, Giovana Thomas¹

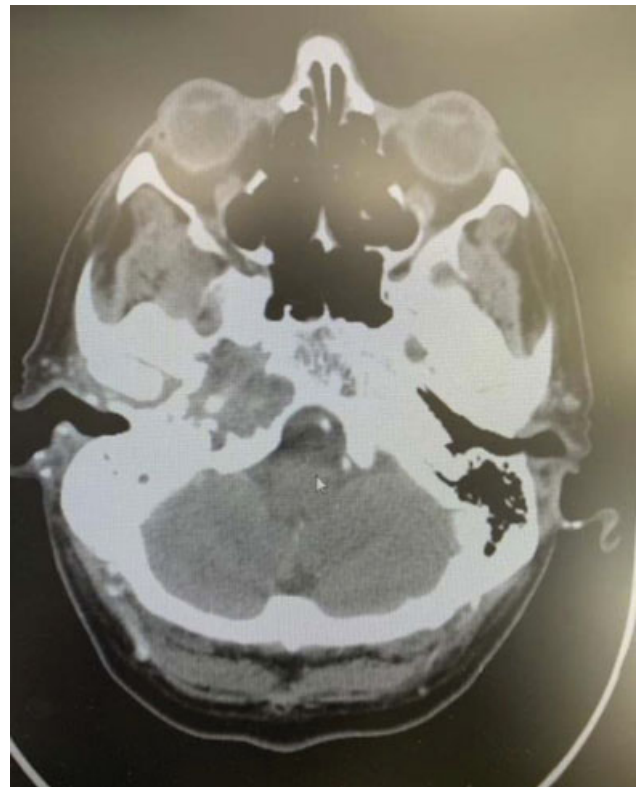
¹Department of Otolaryngology, University of Miami Miller School of Medicine, Miami, Florida, United States

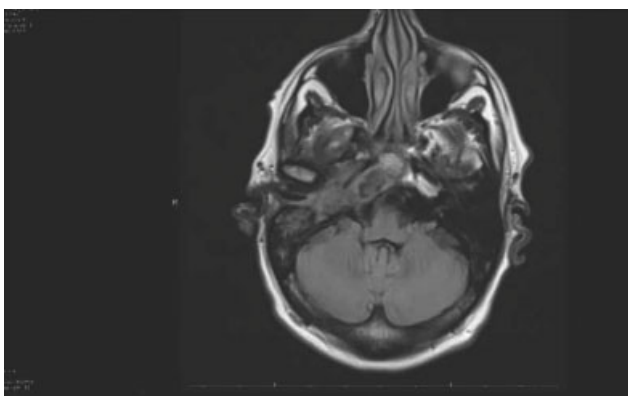
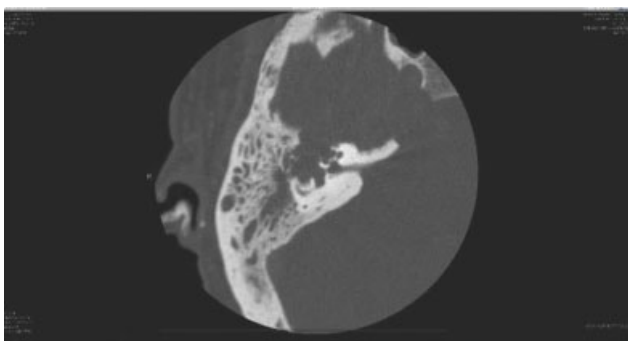
Background: HPV-related oropharyngeal squamous cell carcinoma (OPSCC) presents at more advanced stages than HPV-negative OPSCC, but since it is more responsive to chemotherapy and radiation has better overall survival. Interestingly, outcomes differ between HPV-related OPSCC smokers as compared with non-smokers, with studies indicating locoregional and distant recurrence rates of 37 versus 21% at 24 months respectively. Additionally, the recurrence patterns of smokers with HPV-positive disease mirror those of HPV-negative patterns with primarily (70–79%) locoregional disease recurrence.¹

Case: A 61-year-old male with 20 pack-year smoking and drinking history, and 20-year history of chronic right otomastoiditis, presented to a community otolaryngologist in 2017 with odynophagia. An indurated soft palate lesion was

identified and biopsy revealed p16+ invasive moderately differentiated OPSCC. Initial staging PET-CT showed FDG-avid mass of SUV 8.6 involving right soft palate with extension beyond the nasopharynx, into the petrous apex, floor of middle cranial fossa, lateral margin of the sphenoid and anterolateral basiocciput, with high probability for perineural involvement at the level of the vidian canal and foramen rotundum. Staged as T3N1M0 after imaging, he was definitively treated with concurrent weekly Cisplatin and intensity-modulated radiation therapy. The oncologic physician at the time of diagnosis recommended further Otolaryngology evaluation to address the mastoiditis; however, no surgery or biopsy was done. Six-month surveillance imaging showed ongoing skull base lesion involving the petrous bone (**Fig. 1**), although notes mention this could be secondary to chronic otomastoiditis. In January, 2019 the patient developed diplopia with lateral gaze palsy and subsequent right facial nerve paralysis prompting repeat imaging. CT and MRI showed an expansile invasive mass at right petrous apex extending to midclivus and right mastoid bone (**Figs. 2 and 3**), with critical finding of encasement of the mastoid portion of the right ICA. The patient underwent BTO with right carotid embolization by interventional neurosurgery, followed by right transcranial biopsy with mastoidectomy and petrous apicectomy. Intraoperative biopsies showed p16+ OPSCC disease of the EAC, as well as in the deep mastoid segment. He was treated with 2 weeks of IV antibiotics with improved House-Brackmann score at follow-up, and returned to home oncologists for chemoradiation treatment.

Discussion: It is possible that in this case the patient had locoregional extent to the skull base initially, and with history of otomastoiditis potentially masking malignancy, no tissue diagnosis of skull base was completed at the time. It is important to be vigilant about diagnosis and disease extent, especially in smokers with HPV+ disease, as this may have warranted more expanded radiation or chemotherapy regimen.





the clivus posteriorly. The jugular fossa, the carotid canal and the petrous sinus delimitate the inferior border. The superior petrous sinus marks the limit between the middle cranial fossa and the posterior cranial fossa. The internal auditory canal bisects the petrous apex, this is important to consider surgical techniques.

These lesions can present with several symptoms, the most common that have been reported are hearing loss followed by vestibular dysfunction, headache, tinnitus, facial spasm, diplopia, facial paralysis and otorrhea; this presented months or years before diagnosis. Incidental discovery is not unusual.

The patient is then referred for a guided imaging study, which allows characterizing the lesions detected incidentally or by their symptoms in previous studies. The first line of study is the MR because it allows delineating the extension, demonstrating if there is a compromise of the cavernous sinus, and the relationship of the lesion with the cranial nerves and vessels. It also allows a definitive diagnosis of certain apex lesions that have characteristic signal intensities, such as cholesterol granuloma. On the other hand, CT is useful in characterizing bone involvement better than MR, determining if the lesion is osteolytic or if it results in bone remodeling, which helps intuit the degree of aggressiveness.

To make a pictorial description of the different pathologies that may occur in this region, we performed a retrospective and anonymous review of the images by MR and/or CT of sixteen patients in whom pathologies of the petrous apex have been identified at the Chilean Institute of Neurosurgery Dr. Asenjo.

Reference

1. Liu C, Talmor G, Low GM, et al. How does smoking change the clinicopathological characteristics of human papillomavirus-positive oropharyngeal squamous cell carcinoma?? One medical center experience. Clin Med Insights Ear Nose Throat 2018;11:1179550618792248

P105. Lesions of the Petrous Apex: Pictographic Distinction at CT and MR Imaging

Andres Rojas¹, Matias Gomez¹, Katherine Walker¹, Homero Sario¹, Aaron Vidal², Roberto Marileo², Francisca Montoya²

¹Department of Otolaryngology, Chilean Neurosurgical Institute Asenjo

²Department of Neuroradiology, Chilean Neurosurgical Institute Asenjo

The petrous apex is the medial region of the temporal bone, it is divided by the internal auditory canal (IAC), and is surrounded by neurovascular structures, from which, various pathological lesions originate. They can cause severe symptoms by invasion or compression of the cranial nerves, brain stem or internal carotid artery.

This structure is defined laterally by the otic capsule and the petrous carotid artery, it is the floor of the middle cranial fossa and extend from the eminentia arcuata to Meckel's cave anteriorly and from the semicircular canal to

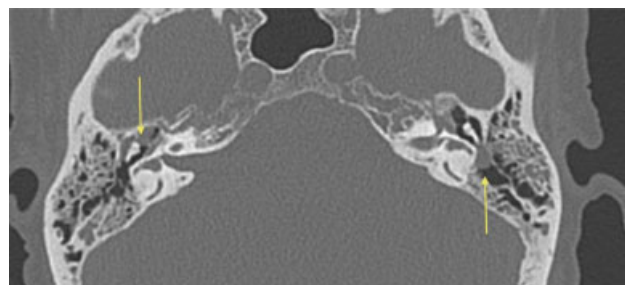
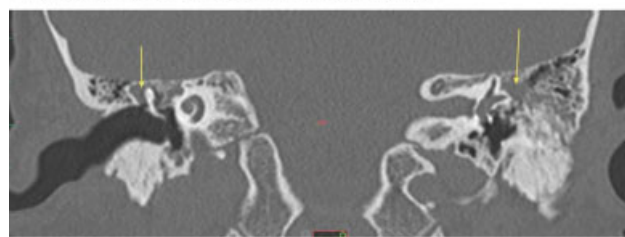
P106. Bilateral Middle Cranial Fossa Encephaloceles Showcasing Tegmen Tympani and Tegmen Mastoideum Defects

Neal M. Jackson¹

¹Tulane University School of Medicine, New Orleans, Louisiana, United States

Neal M. Jackson¹

¹Tulane University School of Medicine, New Orleans, Louisiana, United States



This radiographic case report showcases one patient with

This document was downloaded for personal use only. Unauthorized distribution is strictly prohibited.

bilateral middle cranial encephaloceles: one of the tegmen mastoideum defects on right and another of the tegmen tympani defect on the left. The patient underwent transmastoid repair of both encephaloceles. On the left, the meningoencephalic herniation was adjacent to the body of the incus, and this was easily reduced with bipolar cautery. On the right, the meningoencephalic herniation filled the epitympanum and reached the middle ear space; encephalocele repair required removal of the incus and the head of the malleus, with later ossicular chain reconstruction. Bilateral CT and MR images are available on axial, coronal, and sagittal views. This case highlights the radiographic differences between tegmen tympani and tegmen mastoideum defects and herniation of intracranial contents.

P107. Interrater Reliability and Accuracy of CISS versus Contrasted T1 Vibe for the Presence of Optic Canal Invasion in Tuberculum Sella Meningiomas

Hamid Borghei-Razavi¹, Baha`eddin A. Muhsen¹, Ingrid Wu², Alankrita Raghavan³, Jeniffer Bullen², Christopher Karakasis², Sarah Stock², Matthew Poturalski², Jonathan Lee², Varun Kshetry³, Pablo Recinos³

¹Department of Neurosurgery, Cleveland Clinic Florida, Weston, Florida, United States

²Imaging Institute, Cleveland Clinic, Cleveland, Ohio, United States

³Department of Neurosurgery, Cleveland Clinic, Cleveland, Ohio, United States

Background: A recent study has shown that constructive interference steady state (CISS) is better correlated with intraoperative cavernous sinus invasion than post contrast T1 volume-interpolated breath-hold examination (VIBE). However, we are unsure if that result can be extrapolated to other important anatomic locations, such as the optic canal. Our current study was to determine if CISS has better interrater agreement and is more accurate at predicting optic canal invasion than post contrast T1 VIBE.

Materials and Methods: Presurgical diagnostic MRI studies containing both CISS and post-contrast T1 sequences from 27 patients (54 optic canals) were analyzed retrospectively. Five neuroradiologists blinded to the radiology reports and surgical results were recruited. Each optic canal was divided into four visual quadrants and was evaluated at two anatomic locations, the tip of the anterior clinoid and the optic strut. Each quadrant was considered positive for tumor invasion if there is tumor invasion at either of the two anatomic locations. The reference standard at quadrant level was each patient's presurgical Humphrey visual test result. Each optic canal was considered positive for tumor invasion if any of the four quadrants at either of the two anatomic locations was positive. The reference standard at canal level was both presurgical Humphrey visual test result and intraoperative observation of gross optic canal invasion by tumor.

Results: There was good inter-rater agreement on the presence/absence of tumor involvement at a particular quadrant, 0.635 for CISS and 0.643 for post-contrast T1 (95% CI for difference: -0.086, 0.010). At the quadrant level with the Humphrey visual test as the standard reference, the readers' mean sensitivity and specificity of predicting tumor invasion were 0.724 and 0.742 with CISS and 0.768 and 0.692 with postcontrast T1, respectively. At the canal level with the Humphrey visual test result as the standard reference, the readers' mean sensitivity and specificity were 0.775 and 0.632 with CISS and 0.758 and 0.640 with postcontrast T1, respectively. At canal level with the intraoperative findings as the standard reference, the readers' mean sensitivity and specificity were 0.643 and 0.438 with CISS and 0.643 and 0.454 with postcontrast T1, respectively. There is no statisti-

cal difference between the two MRI sequences at either level in terms of reader accuracy with either Humphrey visual test or intraoperative findings as the standard reference.

Conclusions: There was good interreader agreement on optic nerve tumor involvement for both CISS and post-contrast T1. Both CISS and postcontrast T1 sequences have good accuracy at predicting optic canal tumor invasion at both visual quadrants and optic canal levels without statistical difference in accuracy between the two MRI sequences.

P108. Tolosa–Hunt Syndrome: Case Report

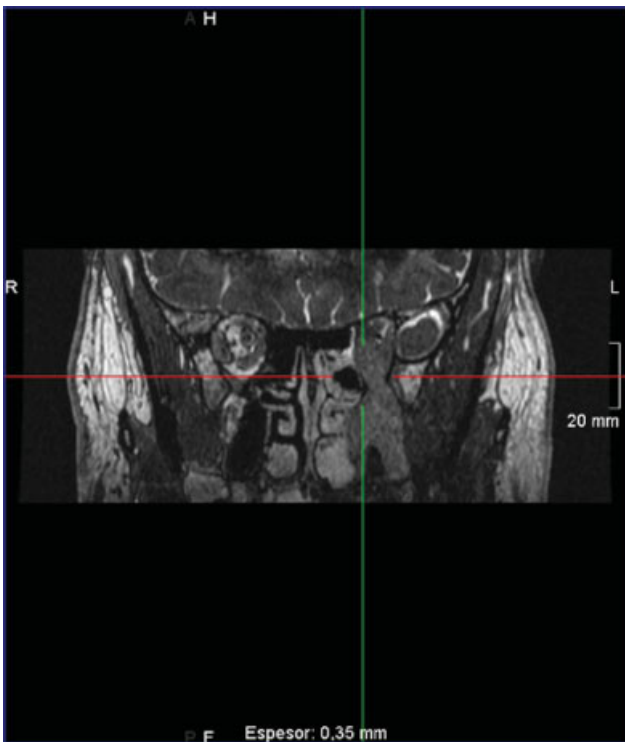
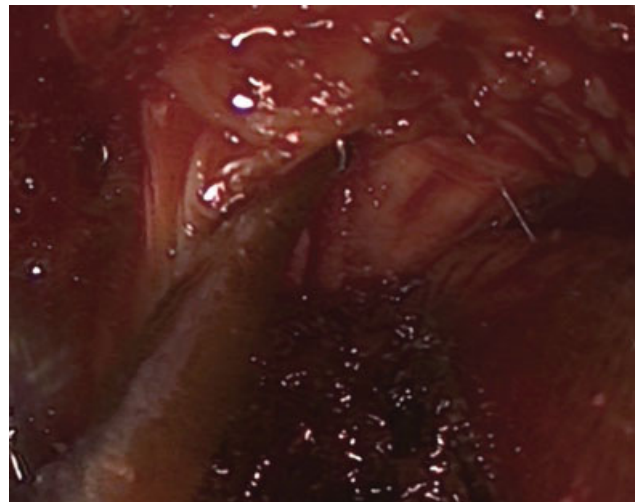
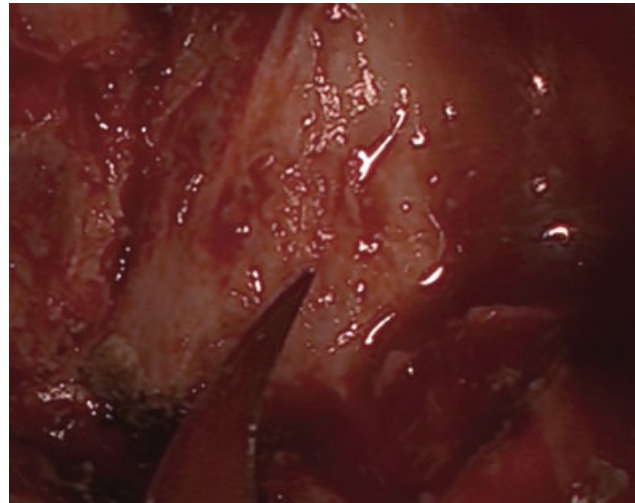
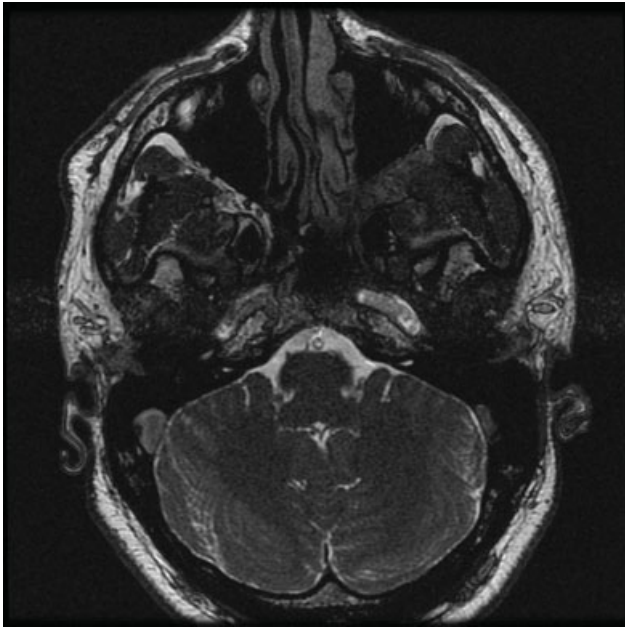
Jesus Gimeno Hernandez¹, Ricardo Ginestal Lopez¹, Marta Vanesa Garcia Yepes¹, Alberto Francisco Gomez Esteban¹, Pablo Perez Alonso¹, Ana Sanchez Prieto¹, Rosario Garcia Monescillo¹, Maria Cruz Iglesias Moreno¹

¹Hospital Clinico San Carlos, Madrid, Spain

Introduction: Tolosa–Hunt syndrome is an idiopathic granulomatous inflammation of the cavernous sinus, superior orbital fissure, or orbit, and is primarily a diagnosis of exclusion. The majority of patients present with unilateral orbital or periorbital pain associated with paresis of one or more of the III, IV, and/or VI cranial nerves. Tolosa–Hunt syndrome is a very rare diagnosis. Was first classified by the International Headache Society in 2004 and now is a part of Classification ICHD-3. Physicians should rule out the more common causes of cavernous sinus syndrome, including cavernous sinus thrombosis, intraorbital or intraparenchymal tumors, vasculitis, basal meningitis, systemic granulomatous diseases such as sarcoidosis and tuberculosis, diabetes mellitus or more recent diagnosis like IgG4-related disease. MRI of the head may show unilateral enhancement of the cavernous sinus and orbital apex. For accuracy diagnosis, endoscopic transnasal image-guided approach biopsy to orbital apex, optic canal or pterygopalatine fossa lesions can be realized by an ENT surgeon. High-dose glucocorticoids are the first line treatment considering its inflammatory pathology, initially with high-dose intravenous steroids followed by tapering oral steroids. There is not sufficient evidence for the appropriate dose, route of administration and duration of therapy. For steroid-resistant patients, antimetabolic agents such as methotrexate, infliximab, and mycophenolate mofetil have also been shown to cause dramatic improvement.

Materials and Methods: A 30-year-old previously healthy man presented with a 2-month history of moderate to severe pain in cheek and retroocular left side, sharp and continuous. This was associated with subsequent development of left horizontal diplopia, without vomiting, dizziness, loss of consciousness or limb weakness 24-hour previously. He was afebrile, alert, conscious, and oriented to time, place and person. Examination of the left eye revealed partial ptosis, left horizontal diplopia, normal visual acuity and visual field. The rest of the neurological and systemic examination was unremarkable. CT was normal and MRI showed enhancement of the left cavernous sinus, orbital apex, inferior part of Meckel's cave, V2 and left pterygopalatine fossa. Transnasal endoscopic biopsy was performed to rule out malignancy from pterygopalatine fossa. Absence of adipose tissue with intense fibrosis was observed. Pathological reports show inflammatory and sclerosing lesions, with fusiform cells without atypia and granulomatous tissue without signs of malignancy that did not fulfill the criteria of IgG4-related disease. Hematological malignancy was excluded. Postoperative day 9, severe epistaxis was observed and angiography embolization on left maxillary artery with coils was performed. High-dose intravenous steroids followed by tapering oral steroids were performed with resolution of facial pain and diplopia. One year after diagnostic, the patient still continues asymptomatic.

Discussion/Conclusions: Tolosa–Hunt syndrome is a diagnosis of exclusion. Neurologists should rule out the more common causes of cavernous sinus syndrome. ENT surgeon can play a role making differential diagnosis using endoscopic transnasal image-guided approach biopsy from affected tissues. Steroids have both diagnostic as well as therapeutic significance in Tolosa–Hunt syndrome. Patients should be followed-up regularly to ensure resolution of symptoms and signs, and also for early detection of relapse, which happens in nearly 50% of the patients.



P109. Pseudomonas Osteomyelitis of the Anterior Skull Base: Case Report and Review of the Literature
 Daniel Zhu¹, Amanda Wong¹, Daniel Russo¹, Tristan Tham², Aron Pollack²
¹Donald and Barbara Zucker School of Medicine at Hofstra/Northwell, East Garden City, New York, United States
²New York Head and Neck Institute, New York, New York, United States

Background: Skull base osteomyelitis (SBO) is a rare, life-threatening infection of the bone caused by either bacterial or fungal pathogens and most commonly associated with patients in immunocompromized states. Some reports have highlighted only 8.4 cases per year. SBO has a mortality rate of around 10% and a recurrence rate of 10 to 15%. Studies have reported similar incidence rates of fungal (52%) and bacterial (48%) etiologies for all types of SBO. However, the profile of causative organism changes drastically by anatomical site. For example, temporal SBO is commonly caused by *Pseudomonas aeruginosa* (90–98% incidence), often as a complication of otitis externa in diabetes mellitus patients.

Meanwhile, central skull base osteomyelitis has a more diverse distribution, with *Staphylococcus aureus* (21%), *Pseudomonas aeruginosa* (19%), and all fungal sources (17%) as the most common pathogens. Here, we present a case of a patient with *Pseudomonal* SBO and review the literature to raise awareness of this uncommon clinical entity.

Case: In this report, we describe the case of a 51-year-old patient with a history of chronic lymphocytic leukemia complicated by chemotherapy-induced neutropenia, treated for *Pseudomonal* SBO. He presented with persistent nasal drainage and right sided facial and eye pain. Treatment included bone marrow stimulants for his neutropenia, multiple rounds of surgical debridement and removal of necrotic bone, and intravenous antibiotic and antifungal therapy. Cultures were conducted following surgical intervention to obtain identification of the causative organism and obtain antimicrobial sensitivities. After identifying that the source was *Pseudomonas aeruginosa*, culture-directed antibiotics were modified accordingly, with persistent prophylactic antimicrobial therapy due to the patient's immunocompromized state.

Discussion and Conclusion: *Pseudomonal* SBO is a rare and potentially life-threatening condition that is clinically indistinguishable from fungal etiologies. Compared with other bacterial etiologies of SBO, *Pseudomonal* SBO is associated with higher recurrence rates, increased likelihood of treatment failure, and decreased overall prognosis. Due to the aggressive nature of the disease, rapid empiric therapy and subsequent tissue biopsy with culture and sensitivities is recommended. After initial empiric treatment, rapid identification of the causative microorganism is suggested, as the evidence surrounding surgical resection is equivocal in cases of bacterial SBO, but is widely recommended in fungal etiologies. Following biopsy and surgical resection (if indicated), long-term intravenous antibiotics for 6 months duration tailored to microorganism's sensitivities is recommended in both bacterial and fungal etiologies to reduce the risk of infection recurrence. In immunocompromized patients with neutropenia, especially those post-chemotherapy, therapies that increase absolute neutrophil counts are also advised to improve chances for complete resolution of SBO. Through this case and literature review, we conclude that early diagnosis and subsequent aggressive treatment, both surgical and medical, are necessary for patients with suspected SBO to reduce the potentially life-threatening complications associated with the condition.

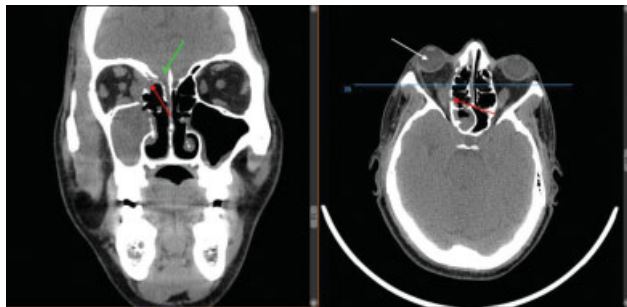


Fig. 1 Computed tomography showing right lamina papyracea multifocal dehiscence (red arrow) with intraorbital extension of disease, resulting in proptosis (white arrow). There is right anterior skull base dehiscence (green arrow), which raises suspicion for intracranial extension of disease.

Parameter	Day 1	Day 2	Day 3	Day 4	Day 5	Day 6	Day 7	Day 8	Day 9	Day 10	Day 11	Day 12	Day 13	Day 14	Day 15
WBC Count (WBC)	2.87	2.5	2.9	2.8	2.5	2.4	1.8	1.8	4.1	5.7	1.8	2.2	2.1	3.5	2.9
% Neutrophils	81.0	86.0	85.0	46.1	50.0	27.7	-	9.8	45.8	48.8	26.0	29.8	28.0	36.0	47.2
Antibiotic	Vancomycin (100mg q12h)		Tobramycin (200mg q8h)		Tobramycin (200mg q8h)		Colistin/Imipenem (1.5mg q8h)						Colistin/Imipenem (1.5mg q8h)		
Antifungal	Mergafon (100mg q8h)		Pip-Tazo (2.5g q8h)												
Antifungal	Amphotericin B (200mg q8h)		Voriconazole (200mg q12h)		Isavuconazole (300mg q12h)										
Other Drugs							Ergosterol		G-CSF (200mcg over 6 weeks)		Ergosterol (200mcg over 6 weeks)		Pip/Tazo		
Culture Results			2 strains of <i>P. aeruginosa</i>						2 strains of <i>P. aeruginosa</i>						<i>P. aeruginosa</i>
Surgical Interventions	Debridement #1						Debridement #2								Debridement #3

Fig. 2 Timeline of events.

P110. Outcomes of Early Functional Endoscopic Sinus Surgery for Orbital Complications of Acute Rhinosinusitis
 Saangyoung E. Lee¹, Mark W. Gelpi¹, William C. Brown¹, Adam M. Zanation¹, Brent A. Senior¹, Jr. Charles S. Ebert¹, Adam J. Kimple¹, Brian D. Thorp¹

¹Department of Otolaryngology/Head and Neck Surgery, University of North Carolina at Chapel Hill, Chapel Hill, North Carolina, United States

Background: Acute sinusitis affects millions of patients each year and is most often self-resolving or managed with antibiotics and/or steroid treatments with good resolution of symptoms. Though rare, complications of acute sinusitis can have serious consequences due to the proximity of numerous important anatomic structures. Extension of disease into the orbit is one such serious complication and can occur through direct extension or via shared venous connections. This can manifest as cranial nerve palsies, optic nerve involvement, and/or periorbital soft tissue inflammation, all of which can contribute to visual changes in the patient. If untreated, these sequelae can lead to significant morbidity including permanent visual impairment or loss. Because of this risk, rapid initiation of treatment is paramount for these patients. Currently, the mainstay of initial management is intravenous antibiotics; however, the utility of early surgical intervention has been poorly studied. This study aims to assess the orbital outcomes of functional endoscopic sinus surgery (FESS) and orbital decompression for patients with orbital complications of acute sinusitis and to evaluate the effect of prompt surgical intervention on visual outcomes.

Methods: An 8-year retrospective chart review was performed of patients who presented with subjective visual complaints in the setting of acute sinusitis and subsequently underwent FESS with orbital decompression and serial comprehensive ophthalmologic exams. Seven patient charts were identified and reviewed. Data from physical exam and ocular tests conducted by ophthalmology were collected from initial presentation and followed to symptom resolution or to the present.

Results: Seven patient charts met inclusion criteria. Average time from symptom onset to FESS was 7.6 days. Average time from tertiary hospital admission to FESS was 0.6 days. All seven patients had complete resolution of subjective visual complaints. Objective ocular exam findings including light reflex, visual acuity, intraocular pressures, and extraocular movements returned to baseline.

Conclusion: Prompt surgical intervention for orbital extension of rhinosinusitis is associated with positive outcomes and return to baseline orbital function. With orbital extension of rhinosinusitis, early surgical intervention should be considered in lieu of a watchful waiting approach with IV antibiotics.

P111. Pain is Temporary, EBV is Forever: Epstein-Barr Virus-Associated Lymphoproliferative Disorder Causing Trigeminal Neuropathy

Cheyenne Silver¹, Lucas P. Carlstrom², Christopher S. Graffeo², Avital Perry², Michael J. Link²

¹Department of Otorhinolaryngology, Mayo Clinic, Rochester, Minnesota, United States

²Department of Neurologic Surgery, Mayo Clinic, Rochester, Minnesota, United States

Background: Compressive lesions of the trigeminal nerve may cause debilitating trigeminal neuropathy. In addition to classic vascular compression, common compressive lesions are schwannomas or meningiomas, although lymphoma and lymphoproliferative disorders (LPD) have been reported. Epstein-Barr virus (EBV) infects over 90% of the world population and is associated with the development of various lymphoproliferative disorders (LPDs). EBV-LPDs can occur from either a B cell or T cell line, typically presenting as a lymphoma with systemic symptoms, with B cell predominant disease being far more common and extra-nodal occurrence noted chiefly in immunosuppressed patients. We present a case of an immunocompetent woman who was found to have an extra-nodal EBV-associated T-cell LPD of Meckel's cave causing trigeminal neuropathy

Methods: Case Report.

Results: A 62-year-old immunocompetent woman initially presented with progressive left V2-3 numbness and burning face pain over 4 weeks. MRI showed enhancement within left Meckel's cave, with direct involvement of the trigeminal nerve root to the brainstem. Blood tests and CSF examination was unremarkable for an infectious or inflammatory process. A PET scan showed avid FDG in the Meckel's cave lesion, along with sub centimeter enhancement of the right lower lobe of the lung, and in the T12 vertebral body. The patient underwent a biopsy of the thoracic spine which was inconclusive. As a result, the patient was taken to the operating room for a left sided middle fossa craniotomy and exploration of the Meckel's cave lesion. The lesion appeared to directly involve the trigeminal ganglion and V2-3 fascicles; an aggressive subtotal resection was completed. In the post-operative period, the patient's pain improved, and she noted increased numbness along V2 and V3 distributions. Pathology confirmed Epstein-Barr virus-associated lymphoproliferative disorder with CD2+, CD3+, CD8+, and TCR β 1+, but CD5- and CD7-, T-cell infiltrate.

Conclusion: Trigeminal neuropathy can be caused by solid lesion, such as schwannomas or meningiomas, with LPDs remaining a rare cause. Currently, primary EBV+ LPDs of the cavernous sinus are reported in patients with autoimmune disorders, or immunosuppression, and almost always of a B-cell origin. Lymphomatous involvement of the trigeminal nerve has also been documented as a metastatic complication of lymphoma, but remains rare in immunocompetent patients. We present the first reported case of T-cell EBV-LPD causing focal left trigeminal neuropathy in a healthy immunocompetent patient, which improved with surgical debulking, highlighting the role of operative intervention to not only obtain diagnostic tissue but also treat the neuropathy.

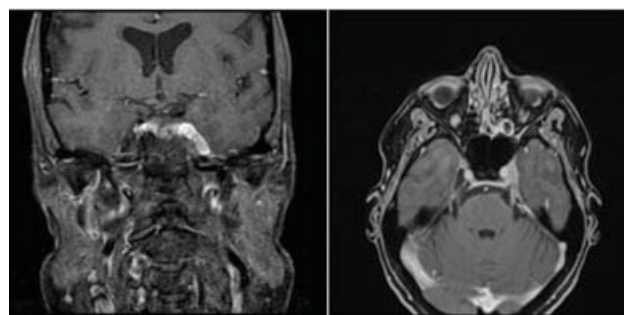


Fig. 1 Left: preoperative coronal MR with Gadolinium. **Right:** preoperative axial MR with gadolinium.

P114. Evaluating the Clinical, Medicolegal, and Economic Impact of Continuous Tracking of Multidisciplinary Skull Base Conference Disease and Patient Metrics

Perry T. Mansfield¹, Hannah G. Goldman¹, Kathryn M. Liang¹, Allison A. Nguyen¹, Riley C. Henderson¹

¹Senta Clinic, San Diego, California, United States

Objective: To evaluate the utility of tracking various disease, patient metrics and treatment paradigms at regular multidisciplinary skull base tumor conferences through prospective documentation, retrospective database analysis, and literature review. Data discussion with an emphasis on medicolegal risk and economic impact to both patient and health care provider was done.

Methods: Patients were presented at regional biweekly CME accredited multidisciplinary skull base conferences. Disease-specific data were recorded and organized by factors including physician presenter, radiographic/pathologic interpretation, tumor staging, p16 testing, photo documentation, and recommended treatment paradigm. These metrics were recorded and analyzed. In addition, the legal and financial implications of these multidisciplinary meetings were examined within the context of our experience and a literature review analyzing the benefits and drawbacks of multidisciplinary tumor board conferences.

Results: Over the course of 300 conferences in a 15-year period, a total of 3,754 cases were presented by physicians at biweekly tumor conference meetings, 1,889 of which were new patients. This patient population, comprised of 51.78% women and 48.22% men, had a mean age of 55.23 years and a median age of 59.00 years ranging from ages 14 to 100. A total of 11 disciplines were represented at the meetings with the majority of cases presented by surgeons (67.44%). This study consisted of a wide range of 260 distinct diagnoses. While squamous cell carcinomas were the most prevalent multisite pathology, constituting 25.99% of cases, the most prevalent single-site pathology was vestibular schwannoma of the CPA, with 11.33% of the total prospective case volume. Furthermore, the brain was the most common tumor location, accounting for 424 cases. Our analysis suggests that tracking of multidisciplinary skull base tumor conferences provides a platform and assurance that nationally standardized best practices are followed based on accurate diagnosis, tumor staging, and treatment paradigms.

Discussion: The tracking of disease metrics creates a database that provides insight on successful treatment recommendations through the organization of quantitative diagnostic and therapeutic information, particularly given the broad diagnostic base and frequency of subtleties associated with anatomic location. It is difficult to establish correlation between successful multidisciplinary meetings and overall quality of patient care. The demand on physician time is ever-increasing and hindrances in implementing the multidisciplinary conferences are evident, although CME accreditation may work to improve physician attendance. Medicolegal concern derives from provider documented presence supporting a treatment path in which the outcome may not be optimal or may be deleterious. While the overall financial impact remains unclear, it can be reasonably concluded that reduction in patient medical expense due to more accurate diagnostic and treatment path makes multidisciplinary tumor board meetings and database tracking economically advantageous for both patients and physicians.

Conclusion: Multidisciplinary tumor board meetings and disease metric tracking foster beneficial cross-specialty interaction, clarify diagnostic, and treatment paradigms, and promote conversation about patient-specific considerations. The authors intend to discuss medicolegal and economic implications as analyzed through both literature review and long-term conference presentation experience.

P115. Qualitative Assessment of Intranasal Pressures during Incentive Spirometry

Swar Vimawala¹, Erin Reilly², Colin Huntley², Maurits Boon², Gurston Nyquist², Marc R. Rosen², James Evans³, Mindy R. Rabinowitz²

¹Cooper Medical School of Rowan University, Camden, New Jersey, United States

²Department of Otolaryngology Head and Neck Surgery, Thomas Jefferson University Hospital, Philadelphia, Pennsylvania, United States

³Department of Neurological Surgery, Thomas Jefferson University Hospital, Philadelphia, Pennsylvania, United States

Introduction: Incentive spirometry is routinely prescribed after surgery as a component of pulmonary rehabilitation, aimed to decrease the rate of lung atelectasis postoperatively. It has been suggested that incentive spirometry may negatively affect the pressure within the nasal cavity, and for this reason, it is discouraged in patients who have undergone reconstruction of the skull base. In this study, we seek to measure the intranasal pressures of healthy subjects when using incentive spirometry.

Methods: A previously validated cadaveric model using intracranial sensor catheters has proved to be a reliable technique for measuring sinonasal pressures. These sensors were placed halfway down the nasal cavity floor of 20 healthy individuals without a history of sleep apnea or nasal surgery. Subjects were asked to forcibly inhale, forcibly exhale, and perform 10 consecutive breaths with an incentive spirometer. The subjects were then asked to repeat these tasks while pinching their noses to simulate nasal obstruction. Additionally, each subject was asked to blow their nose. Each set of measurements were performed in triplicate. The average, maximum, and minimum pressures were recorded in mm Hg. The values recorded were corrected for the zero value, and then a Student's *t*-test was used to compare nopinching (NP) versus pinching (P).

Results: The mean pressure in NP for inhalation was -0.5 ± 1.0 compared with -0.8 ± 1.1 for exhalation and -0.5 ± 1.2 for breathing. The mean pressure in P for inhalation was -1.3 ± 1.3 compared with 1.1 ± 1.4 for exhalation

and 1.1 ± 2.6 for breathing. Within (VSN11) NP, mean (-0.5 ± 1.0 vs. -0.8 ± 1.1 , $p = 0.407$), maximum (0.1 ± 1.1 vs. -0.1 ± 1.1 , $p = 0.638$), and minimum (-1.6 ± 1.3 vs. -2.2 ± 2.4 , $p = 0.345$) pressures for inhalation and exhalation were not significantly different. The minimum pressure on forceful inhalation was significantly lower in P (-1.6 ± 1.3 vs. -6.1 ± 2.6 , $p < 0.001$). The maximum pressure on forceful exhalation was significantly greater in P (-0.1 ± 1.1 vs. 6.6 ± 3.5 , $p < 0.001$). The mean (-0.5 ± 1.2 vs. 1.1 ± 2.6 , $p = 0.017$), maximum (-0.1 ± 1.6 vs. 5.1 ± 5.3 , $p < 0.001$), and minimum (-1.1 ± 1.2 vs. -4.1 ± 3.5 , $p < 0.001$) pressures were all significantly different when subjects performed 10 consecutive breaths between NP and P. Analysis of intranasal pressures with nose-blowing revealed maximum pressures of 24.6, significantly greater than those experienced with maximal exhalation in the NP ($p < 0.001$) or P ($p < .001$) groups.

Conclusions: Compared with no obstruction (NP), simulation of nasal obstruction (P) significantly increases the absolute pressure experienced in the nasal cavity with maximal inhalation and exhalation during incentive spirometry. As maximum intranasal pressures are much lower than those found with nose-blowing in both NP and P groups, it may be safe to restart patients on incentive spirometry postoperatively, but further investigation is warranted.

P116. Anatomic Considerations of Microvascular Free Tissue Reconstruction of Clival Defects: Expanding the Algorithm for Skull Base Reconstruction in Endoscopic Endonasal Surgery

Leila J. Mady¹, Thomas M. Kaffenberger¹, Katie L. Melder¹, Paul A. Gardner¹, Carl H. Snyderman¹, Shaum Sridharan¹, Eric W. Wang¹

¹University of Pittsburgh Medical Center, Pittsburgh, Pennsylvania, United States

Objective: To describe anatomical considerations of endoscopic endonasal inset of radial forearm free tissue transfer (RFFTT) of clival defects and its clinical relevance in reconstruction of ESBS defects.

Materials and Methods: Full transclival defects averaging 17.2 cm^2 were dissected in four cadaveric specimens. A RFFTT model was used to characterize reconstruction technique and flap inset. Bilateral neck explorations were performed for identification of recipient vessels. Descriptive measures for pedicle orientation, pedicle length, and recipient vessel intraluminal diameter were obtained.

Results: Mean facial artery intraluminal diameter was significantly smaller on the right ($2.1 \pm 0.3 \text{ mm}$) compared with the left ($2.5 \pm 0.0 \text{ mm}$) ($p = 0.02$). There was no difference between mean facial vein intraluminal diameter on the right ($2.8 \pm 0.6 \text{ mm}$) compared with the left ($2.5 \pm 0.4 \text{ mm}$). Bilateral anterior and lateral maxillotomies preserving the zygomaticomaxillary buttresses and endoscopic medial maxillectomies were prepared as corridors for flap passage. For tunneling of the pedicle to the facial vessels, premaseteric space tunnels were created. In all specimens, the RFFTT was folded lengthwise and introduced via the anterior maxillotomy and passed through the medial maxillectomy. Through an endoscopic endonasal approach, the RFFTT pedicle was oriented cranially with the remainder of the flap placed against clival defect. The mean pedicle length required for anastomosis from the skull base to the neck was $13.2 \pm 0.5 \text{ cm}$ on the right and $13.1 \pm 0.4 \text{ cm}$ on the left.

Conclusion: Anatomical characterization of RFFTT repair of clival defects is critical in developing a roadmap for the reconstructive surgeon as part of team-based approach to endoscopic endonasal surgery. The primary options for

reconstruction of ESBS defects include multilayer fascial grafts, vascularized pedicled flaps, and locoregional flaps, notably the temporoparietal fascial and extracranial pericranial flap. With a greater understanding of the anatomical factors related to successful preoperative planning of free flap design and inset, microvascular free tissue transfer may be added to the reconstruction ladder for ESBS defects.

P117. Primary Dural Repair Using Titanium Microclips following Lateral Skull Base Surgery

Camille K. Milton¹, Panayiotis Pelargos¹, Ali Palejwala¹, Griffin Ernst¹, Rachad Mhaweji¹, Greg A. Krempf¹, Alexander G. Bien¹, Chad A. Glenn¹

¹University of Oklahoma Health Sciences Center, Oklahoma City, Oklahoma, United States

Objective: Standard techniques for primary dural repair following lateral skull base surgery are both technically challenging and time consuming. However, inadequate closure may result in postoperative CSF leak and local infection. Numerous methods and techniques have been described to address this issue. Here we report a novel technique for primary dural closure following lateral skull base surgery using nonpenetrating titanium microclips. A case example is provided.

Technique: Following completion of surgical tumor resection, the margins of the dural opening were identified. A free tissue synthetic dural graft was tailored to the dural defect. Using nonpenetrating titanium microclips, a primary dural repair was performed. As the clips do not penetrate the dura or the synthetic dural graft, clips are applied along all margins of the defect without concerns for damaging adjacent neurovascular structures.

Case Report: A 17-year-old male presented to our institution with a large vagal schwannoma extending into the carotid sheath. He presented acutely with diplopia, nystagmus, papilledema, and obstructive hydrocephalus. Gross total resection was achieved using a trans-temporal trans-jugular approach, and surgical pathology confirmed the diagnosis of schwannoma. As an adjunct to standard surgical repair techniques, primary dural closure was performed using nonpenetrating titanium microclips and a free tissue synthetic dural graft. Postoperative MRI demonstrated minimal clip artifact. No postoperative complications were observed.

Conclusion: To our knowledge, this is the first report on the use of microclips in repairing dural defects following lateral skull base surgery. Surgical outcomes for this small case series suggest that dural repair of the lateral skull base with nonpenetrating, titanium microclips is a feasible alternative to suturing dura in confined spaces with limited maneuverability.

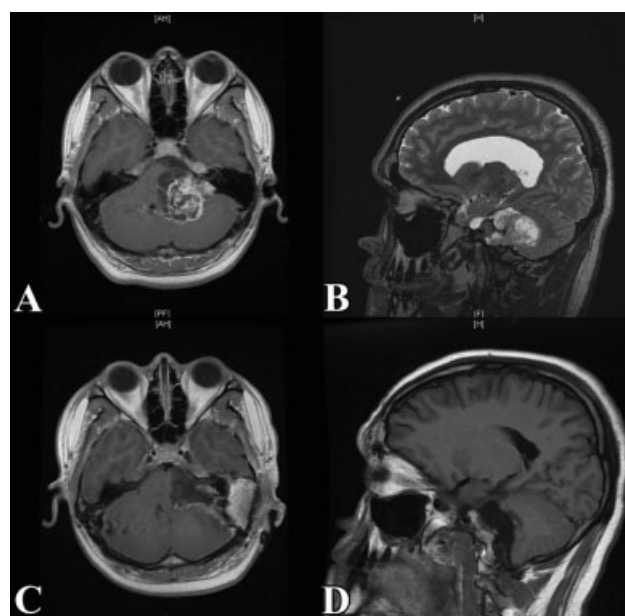


Fig. 1 Case Report MRI. Preoperative axial T1 MRI (A) and sagittal T2 MRI (B). Postoperative axial T1 MRI (C) and sagittal T1 FLAIR MRI (D) for resection of large vagal schwannoma. Minimal postoperative clip artifact is demonstrated.

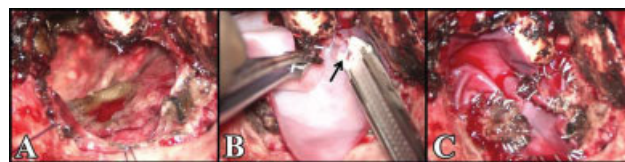


Fig. 2 Primary dural repair with nonpenetrating titanium microclips. Sequential intraoperative photographs (A-C) demonstrate the use of our novel dural closure technique following lateral skull base surgery. Black arrow indicates clip applicator.

P118. Vertical Vector Surgical Knot in Endoscopic Endonasal Surgery and Repair: An Exonasal Knot for Endonasal Application

Karam Asmaro¹, Jack Rock¹, John Craig¹

¹Henry Ford Health System, Detroit, Michigan, United States

Developing innovative surgical approaches through narrow anatomic corridors requires continual adaptation surgical techniques and maneuvers. Regarding skull base surgery, endoscopic endonasal approaches have become extremely popular, resulting in lower patient morbidity, without sacrificing clinical outcomes. Although surgical approaches have changed dramatically over the last few decades, suturing and knot tying in these narrow corridors have not been developed at the same pace. Endoscopic repair of skull base defects after endoscopic endonasal surgery is often achieved with 90–95% success through multilayered reconstruction with a variety of grafts or flaps, sealants, and possibly sinonasal packing to avoid postoperative cerebrospinal fluid leaks. These high success rates are achieved without any direct suturing of the grafts/flaps to adjacent tissues. In some situations, perhaps suturing could limit the risk of graft/flap migration, and increase the chance of graft/flap water-tight closure and integration. The utility of

endonasal suturing of grafts/flaps is largely unknown because intranasal geometry restricts the hand and instrument movements needed to achieve traditional surgeons' or square knots. The current study demonstrates a suturing technique resulting in a facile surgical knot through vertical vector motions, making it an ideal candidate when operating through narrow corridors. The advantages of this technique are its cost-effectiveness, the ability to use any type of needle or suture for tissue approximation, and the elimination of horizontal vectors and maneuvers which are limited in endonasal. This facile knot can be employed during endoscopic endonasal surgery potentially to facilitate watertight closure in scenarios where it is felt necessary or when repairing vascular structures.

P119. Fenestration of a Symptomatic Intrasellar Arachnoid Cyst through an Eyelid Incision

Zaid Aljuboori¹, Jeremy Clark Brian Williams¹

¹University of Louisville, Louisville, Kentucky, United States

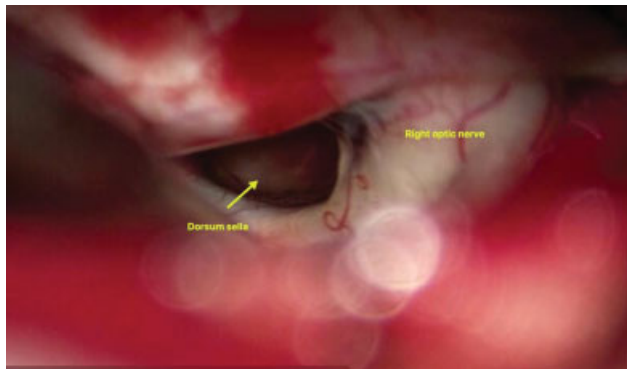


Fig. 1

Intracranial arachnoid cysts (AC) are benign lesions, forming ~1% of all intracranial space-occupying lesions. Intrasellar arachnoid cysts (IAC) constitute ~3% of all intracranial arachnoid cysts. Two pathophysiologic mechanisms have been proposed for the development of IAC. Both hypotheses rely on the presence of anatomic variation of the diaphragma sellae that permits herniation of the basal arachnoid layers into the sellar compartment. The first hypothesis proposes that closure of the arachnoid diverticulum due to either meningitis, hemorrhage, or inflammation result in a non-communicating intrasellar cyst. The second hypothesis suggests that cyst enlargement occur through a ball-valve mechanism. Generally, IACs are asymptomatic and requires no intervention. Surgical treatment indicated for cysts that cause chiasmatic compression, pituitary dysfunction, and/or severe headaches. We present a 63-year-old female with history of hypercalcemia and diabetes insipidus (DI) for 7 years. She presented with headache and blurriness of vision for ~2 years. Her headaches are severe, persistent, aching in nature, and deep bifrontal in location. Neurological exam was normal except for left sided temporal hemianopsia. MRI brain showed intrasellar non enhancing cystic lesion consistent with arachnoid cyst. She underwent a fronto-orbital craniotomy with fenestration of the cyst through an eyelid crease incision. On 6 months follow up her headaches had significantly improved from daily to 2–3 times a month, left visual field deficit improved, and her DI had resolved. Intrasellar arachnoid cysts usually found incidentally. Symptomatic ones require surgical fenestration either through transcranial or

transsphenoidal route. Establishing a communication between the cyst and the normal cerebrospinal fluid circulation is the single most important determinant of success.

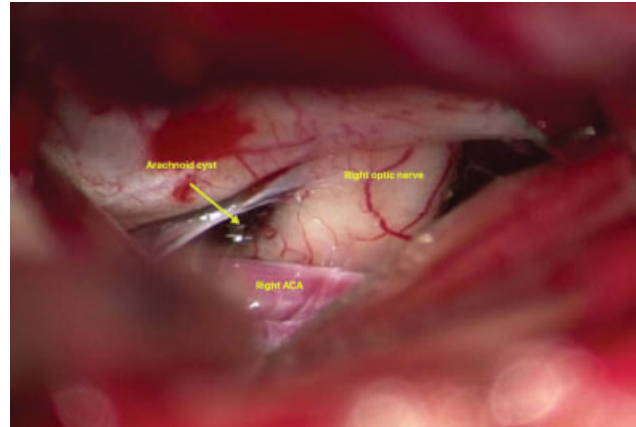


Fig. 2

P120. Prevalence of Pediatric Orbital Roof Fractures as a Function of Orbital Dimensions

Stephen C. Dryden¹, Adrianna Eder¹, Andrew G. Meador¹, Mason Schofield¹, James C. Fleming¹, Brian T. Fowler¹

¹University of Tennessee Health Science Center, Hamilton Eye Institute, Memphis, Tennessee, United States

Purpose: Orbital roof fractures are more likely to occur in younger children, specifically less than 7 years of age.^{1,2} It has been well stated that cranium-to-face ratio decreases with age.² In addition, development and pneumatization of sinuses relates to the increased incidence of orbital roof fractures in children less than 7 years of age.^{3,4} We propose a novel idea that length of the orbital roof is a representative of the neuro cranium and length of the orbital floor is a representative of midface. The purpose of this study is to examine if simple measurements of orbital dimensions as defined above are correlated with rates of orbital roof fractures within the pediatric population.

Methods: A retrospective review of maxillofacial and orbital imaging was performed from October 1, 2011 to October 31, 2014 at a major pediatric trauma center. Patients with orbital roof fractures were identified. Patients were stratified into two groups by age <7 and ≥7. Images were reviewed, and the lengths of the orbital roof (superior orbital rim to anterior clinoid process) and orbital floor (inferior orbital rim to anterior clinoid process) were measured for each patient using McKesson imaging software by the primary author (SCD) (Fig. 1). Statistical analysis was performed using a student *t*-test with significance determined by $p < 0.05$. The main outcome measures were the ratio of orbital roof length to floor length compared with age.

Results: Sixty-six patients with orbital roof fractures were identified. There were 40 males and 26 females. Patient ages ranged from 2 months to 17 years. 31 patients were younger than 7 years and 35 patients were 7 years or older. Mean orbital roof length was 43.4mm, standard deviation 3.06 mm and 45.1 mm, standard deviation 3.94 mm for patients <7 and ≥7, respectively ($p = 0.023$). Mean orbital floor length was 41.3 mm, standard deviation 2.99 mm and 47.7 mm, standard deviation 4.19 mm for patients <7 and ≥7 respectively ($p < 0.00001$; Fig. 2). The mean roof to floor ratio (RTFR) for patients <7 was 1.051, standard deviation 0.039 and for patients ≥7 was 0.947, standard deviation 0.031 ($p < 0.00001$).

Conclusion: As children age, the relative length of the orbital roof decreases when compared with the length of the orbital floor. The RTFR was greater than 1.0 in children younger than seven. These differences were statistically significant when compared with children 7 and older. This may help explain the differences noted in orbital fracture patterns between early and late childhood described in previous studies.¹⁻⁴

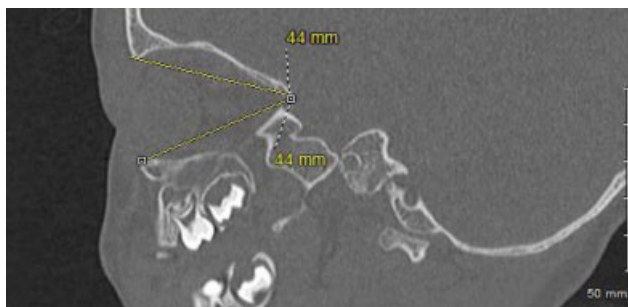


Fig. 1

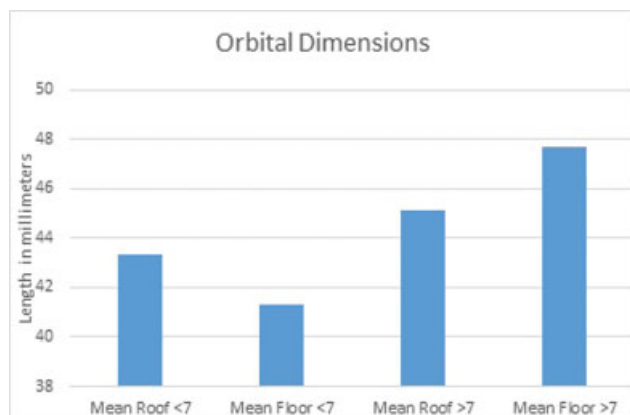


Fig. 2

References

- Hink EM, Wei LA, Durairaj VD. Clinical features and treatment of pediatric orbit fractures. *Ophthal Plast Reconstr Surg* 2014;30(2):124-131
- Koltai PJ, Amjad I, Meyer D, Feustel PJ. Orbital fractures in children. *Arch Otolaryngol Head Neck Surg* 1995;121(12):1375-1379
- Kozak FK, Ospina JC, Cardenas MF. Characteristics of Normal and Abnormal Postnatal Craniofacial Growth and Development. In: Flint PW, ed. *Cummings Otolaryngology*. 6th ed. Philadelphia: Saunders, 2015: 2865-2890.
- Messinger A, Radkowski MA, Greenwald MJ, Pensler JM. Orbital roof fractures in the pediatric population. *Plast Reconstr Surg* 1989;84(2):213-216, discussion 217-218

P121. Skull Base Approaches to Cerebrovascular Pathologies: Surgical Strategies and Outcome Analysis

Mohsen Nouri¹, Julia R. Schneider¹, Amrit K. Chiluwal¹, Timothy G. White¹, Amir R. Dehdashti¹

¹Department of Neurosurgery, North Shore University Hospital, Northwell Health, Manhasset, New York, United States

Background: Recent advances in endovascular techniques have diminished neurosurgeons' exposure to common vascular pathologies and cerebrovascular surgeons have been treating more challenging cases in recent years. Therefore, expertise in skull base approaches seems inevitable for those treating such complex pathologies. In this study, we reviewed all vascular lesions treated with skull base approaches in our hospital and analyzed their outcome considering our strategies in selecting surgical approaches.

Methods: Operative notes, pre- and postoperative images, and follow up notes of all the patients with vascular pathologies operated in the last five years were reviewed and those patients operated with skull base approaches were enrolled. Clinical and radiological outcomes were collected.

Results: Among the patients treated for vascular pathologies, 29 patients underwent skull base approaches (7 males, mean age: 53.7 ± 13.0). Patients were approached for aneurysm clipping (10 cases), cerebral revascularization (2 for vertebrobasilar insufficiency, 1 for moyamoya, 6 for giant or dissecting aneurysms), arteriovenous fistulae (4 cases), or brain stem cavernomas (6 cases). These approaches included far lateral, orbitozygomatic, retrolabyrinthine, and fronto-basal in descending order of frequency. No major approach related complication was observed.

Conclusion: Our results showed that excellent outcome can be achieved for treating aneurysms, cavernoma, arteriovenous fistulae, or performing intra-cranial extra-cranial arterial revascularization with using skull base approaches. Less brain retraction and wider surgical exposure are the advantages that cannot be achieved with conventional approaches.

P122. The Role of Intraoperative MRI in Excision of Clival Chordoma

Salman Al Qazlan¹, Muath Alfalaj², Mody Almarshad², Abdullah Alobaid²

¹King Saud University, Riyadh, Saudi Arabia

²King Fahad Medical City, Riyadh, Saudi Arabia

Introduction: Chordoma is a rare aggressive bone cancer that originates from the remnants of notochord and accounts for 1-4% of all bone malignancies. The basisphenoidal region constitutes 35-40% of all chordoma sites mainly the clival region.¹ Clival chordomas are slowly growing tumors, but due to their location adjacent to important skull base structures, invasive nature and recurrence rate, they are considered to be malignant. The use of Intraoperative MRI (iMRI) provides high accuracy and precision specially when dealing with skull base tumors. The impact of iMRI in clival chordoma surgeries are not well studied as in pituitary surgeries.

The main objective is to evaluate the effect of iMRI in chordoma surgeries.

Method: A retrospective cohort study conducted at King Fahad Medical City (KFMC), Riyadh, Saudi Arabia which compares two groups of clival chordoma patients:

- **Group A:** Surgical resection with the use of iMRI.
- **Group B:** Surgical resection without the use of iMRI.

In terms of the Degree of surgical resection; using preoperative and postoperative volume assessment; hospital stay and functional status; using modified Ranking Scale

(mRS)² at last follow-up. All operated clival chordoma cases from January 2008 to July 2018 were included, chordomas not involving skull base & redo surgeries were excluded.

Results: A total of 24 patients were included. Group A were 9 patients (37.5%) and Group B were 15 (62.5%). 58% of the sample were males. Headache and visual disturbance were the most presenting symptoms.

Mean preoperative tumor volume in both groups was 49.1mm³, in group A the mean preoperative tumor volume was 41mm³ whereas in group B it was 53.9mm³.

The mean degree of resection in group A was 64.58% while in group B it was 58.63% with a p-value of 0.65. Hospital stay mean was 53 days in group A, in group B it was 97 days with a p-value of 0.12.

Most of the patients (88.8%) in group A were scaled 0 in mRS at their last follow-up while only (46.7%) of group B were scaled 0.

Discussion: Group A had a better degree of surgical resection (Fig. 1) and far shorter hospital stay compared with group B (Fig. 2). Although it was not statistically significant, it can be attributed to the small sample size. Patients' long-term functional status was much better in group A as most of the patients were scaled 0 which supports the safety of the resection aided by iMRI guidance.

Conclusion: iMRI has a great potential in clival chordoma. However, further studies and more data are needed to confirm its utility.

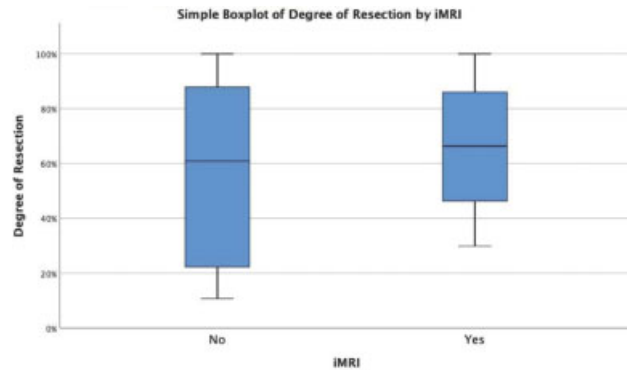


Fig. 1 Mean degree of resection.

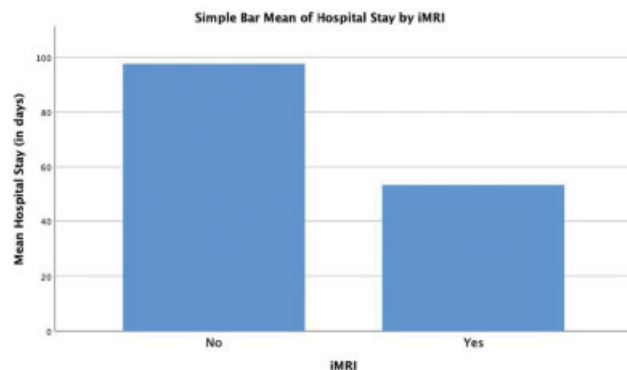


Fig. 2 Mean hospital stay.

References

1. Gay E, Sekhar LN, Rubinstein E, et al. Chordomas and chondrosarcomas of the cranial base: results and follow-up of 60 patients. *Neurosurgery* 1995;36(5):887–896,

discussion 896–897

2. Banks JL, Marotta CA. Outcomes validity and reliability of the modified Rankin scale: implications for stroke clinical trials: a literature review and synthesis. *Stroke* 2007;38(3):1091–1096

P123. Role of Intraoperative MRI in Endoscopic Endonasal Transsphenoidal Pituitary Surgery

Yosef Dastagirzada¹, Carolina G. Benjamin², Julia Bevilacqua¹, Jason Gurewitz¹, John G. Golfinos¹, Dimitris Placantonakis¹, Chandra Sen¹, Jafar Jafar¹, Girish Fatterpekar¹, Seth Lieberman¹, Rich Lebowitz¹, Donato Pacione¹

¹NYU Langone Medical Center, New York City, New York, United States

²University of Miami, Coral Gables, Florida, United States

The transsphenoidal corridor for pituitary adenoma surgery was established as early as 1906 by Schloffer and was subsequently refined by Cushing throughout the early 20th century [1]. The use of intraoperative magnetic resonance imaging (iMRI) in endoscopic endonasal transsphenoidal resections, however, is a relatively contemporary addition to the surgical treatment of pituitary tumors. The morbidity of these cases has decreased over the years in light of advances in intraoperative navigation as well as improvements in endoscope dynamics and surgical instruments. Despite such improvements, a substantial number of patients require repeat surgeries or subsequent radiotherapy for residual and/or recurrent disease. This can be largely attributed to cavernous sinus invasion or suprasellar extension, which pose technical challenges to achieving gross total resections (GTRs). The rate of GTR for pituitary tumors cited in the literature varies from 59–88%.[2–3] The advantage of iMRI is that it provides the surgeon with immediate feedback regarding their progress and ability to safely achieve GTR which, in pituitary surgery, is critical for long term cure. Additionally, although there is concern for increased risk of postoperative endocrine dysfunction, Zhibin et al prove that this is not necessarily the case. In their series, 133 patients who underwent iMRI had higher rates of GTR and did not have a significant difference in postoperative hypopituitarism. [4]

This study includes a combined retrospective and prospective comparative analysis of 238 patients who underwent transsphenoidal resection of a pituitary tumor from January 2013 until May 2019. All patients were operated on by one of four experienced neurosurgeons and one of three experienced otolaryngologists. There were 203 patients who did not undergo iMRI and 25 patients who did. A 3 tesla MRI magnet was used in all cases. All intraoperative images were read and interpreted by a senior neuroradiologist at our institution. Amongst the two groups, there was no statistically significant difference in patient age ($p = 0.488$), tumor size (microadenoma versus macroadenoma, $p = 0.878$), and primary versus recurrent tumor ($p = 0.837$). The use of iMRI did not yield a decrease in the length of stay (4.84 days in the no iMRI group and 5 in the iMRI group, $p = 0.777$). There were zero cases of a return to the OR for residual tumor in the intraoperative MRI group versus the non-MRI group. However, this did not reach statistical significance. This study did not yield a statistically significant difference in GTR ($p = 0.75$), near total resection (NTR, $p = 0.167$), or subtotal resection ($p = 0.083$). This is likely secondary to a low sample size and therefore power in the iMRI group. Finally, there was no significant difference in the number of patients requiring postoperative DDAVP ($p = 0.099$) or hydrocortisone ($p = 0.873$) after discharge.

Preliminary results reveal a potential benefit of iMRI use to assess for residual disease which can be addressed

immediately during the initial operation, thus decreasing the need for re-operations. Furthermore, the ability to correlate intraoperative findings with an intraoperative structure may lead to more precise identification and preservation of normal gland, which can possibly decrease the incidence of postoperative endocrine dysfunction.

P124. Frameless Stereotactic Placement of Brachytherapy Seeds within a Pituitary Adenoma via Endoscopic, Endonasal Approach: A Technical Note

Aaron R. Plitt¹, Ashleigh Halderman¹, Robert Timmerman¹, Samuel L. Barnett¹

¹UT Southwestern, Dallas, Texas, United States

Introduction: Recurrent pituitary adenomas are challenging lesions. The standard second-line treatment after surgery is radiotherapy. After radiotherapy, there is no standard third-line treatment. At our institution, we have utilized I-125 seeds as brachytherapy for treatment-refractory pituitary adenomas. The placement of the seeds requires precision to maximize target tissue exposure and minimize radiation dose to surrounding structures; therefore, the seeds must be placed under stereotactic navigation. For pituitary adenomas, stereotactic placement of seeds presents a unique challenge given the safest, and easiest exposure is in a narrow corridor via an endonasal approach. Here we present a technical note on the use of frameless stereotactic guidance for placement of brachytherapy seeds within a pituitary adenoma.

Case Description: A 67-year-old male with a non-secreting pituitary adenoma presented with imaging progression. He had undergone three prior surgeries, two prior treatments with photon radiotherapy, and three cycles of temozolomide. The decision was made to pursue brachytherapy with I-125 seeds. A preoperative MRI with thin slices through the sella was utilized to create the target for each of the two planned seeds. The targets were chosen by the radiation oncology team. A thin slice CT head was performed on the day of surgery and merged with the planning MRI in the Brainlab (Brainlab, Munich, Germany) interface. The patient was taken to the operating room and placed under general anesthesia. He was positioned in a standard fashion for an endoscopic, endonasal approach to the sella in cranial pin fixation in the head holder. Facial registration was performed with the Brainlab soft-touch. The typical endoscopic, endonasal approach was then performed. The Variguide Brainlab frameless stereotactic navigation device was then brought into the field. A safe trajectory was chosen to the preplanned targets. The first I-125 seed was then placed under stereotactic guidance at the first target. The second seed was then placed in similar fashion. The small defects in the dura were covered with fibrin glue. The patient was then extubated and admitted to the floor overnight. Postoperative CT confirmed appropriate placement of the seeds. The patient tolerated the procedure well and was discharged the following day.

Conclusion: Brachytherapy is a viable treatment option for treatment-refractory pituitary adenomas. Frameless stereotactic navigation provides excellent accuracy for placement of the radioactive seeds through a small aperture such as the nasal passage while obviating the technical challenges of a stereotactic frame.

P125. The Extended Minipterional Approach: A Modification to Approach the Insular Region

Rafael Martinez-Perez¹, Giuliano Silveira-Bertazzo¹, Thiago Albonette-Felicio¹, Marcus Zachariah¹, Gustavo G. Rangel¹, Douglas Hardesty¹, Ricardo L. Carrau¹, Daniel Prevedello¹
¹Wexner Medical Center, The Ohio State University, Columbus, Ohio, United States

Background: For its versatility and wide acceptance, the pterional craniotomy has become the mainstay of treatment for most of the anterior circulation aneurysms, parasellar lesions and tumors located in the anterior cranial fossa. Minipterional approach (MPTa) was introduced as a less invasive alternative to treat anterior and middle fossa lesions and anterior circulation aneurysms. As in other minimally invasive approaches, the MPT offers better cosmetic results, protection of the underlying brain parenchyma, shorter operative times, and less soft tissues injury. Nonetheless, soon after its first description, several authors raised their concerns regarding the reduced surgical freedom of movement and the limited operative view using the MPTa. In fact, one limitation of the MPTa is the reduced exposure of the distal Sylvian fissure, which preclude a wide dissection, limiting the access to lesions located deep at the Sylvian cistern.

We describe a modification of the MPTa, the extended minipterional approach (eMPTa), that improves access to the distal Sylvian fissure with minimal additional bony removal. We define the ideal posterior landmark for this craniotomy based on an anatomic cadaveric study.

Methods: Insular and sylvian linear exposure offered by the MPTa and eMPTa were compared among 6 heads of cadaveric specimens. Surgical anatomy of the eMPTa and its relationship with representative neurovascular landmarks were also evaluated.

Results: By minimally expanding the bone removal up the preauricular line, the eMPTa affords a threefold increase in the linear exposure of the insular and linear exposure ($p = 0.001$ and $p < 0.001$, respectively). The frontal precentral artery, an important landmark for performing a distal-to-proximal Sylvian dissection, is 17 ± 5.2 mm anterior to the preauricular line, the posterior limit of the eMPTa, whereas it is 6.5 ± 3.6 mm posterior to pterion, the posterior limit of the MPTa.

Conclusion: The eMPTa provides an increased sylvian and insular exposure while maintaining a minimally invasive approach. Importantly, this bony expansion achieved an expanded insular view that offers potential increasing applications to vascular (i.e., giant MCA aneurysms, thalamic cavernous malformation) and neoplastic (i.e., insular gliomas) pathologies that are classically treated via a pterional approach. Potential disadvantages of this technique, in comparison to the classic MPTa, are the use of a larger skin incision and the risk of damaging certain eloquent areas given the increase in the brain exposure (i.e., Broca's area in the left side).

P126. Role of the Extradural Anterior Clinoidectomy to Approach the Paraclinoid Region Using Minimally Invasive Approaches: An Anatomic Study

Rafael Martinez-Perez¹, Thiago Albonette-Felicio¹, Giuliano Silveira-Bertazzo¹, Marcus Zachariah¹, Douglas Hardesty¹, Ricardo Carrau¹, Daniel Prevedello¹

¹Wexner Medical Center, The Ohio State University, Columbus, Ohio, United States

Background: The eAC is a standard technique that enhances the extradural corridor and provides a broad access

to the entire parasellar region, while reducing brain retraction. However, its role in expanding the surgical corridor in minipterional approach has not been addressed yet.

We sought to illustrate the microsurgical anatomy of the MPT + eAC and to evaluate the effect of eAC on surgical exposure and maneuverability along the paraclinoid region.

Methods: Area of exposure, surgical freedom, and surgical maneuverability provided by the MPT and MPT + eAC along the paraclinoid region were compared in six cadaveric heads. The area of exposure was determined by the length and width of a pentagonal-shaped region defining the area of interest within the paraclinoid region. Area of surgical freedom and maneuverability were calculated at 4 points considered to be representative of the paraclinoid region (Optic chiasm, origin of the posterior communicating artery, origin of the ophthalmic artery, and internal carotid bifurcation).

Results: In comparison to the MPT, the MPT + eAC enlarges the area of exposure in the paraclinoid region up to twofold (90 vs. 192 cm², $p < 0.001$). Likewise, the MPT + eAC afforded a larger area of surgical freedom and better maneuverability at all selected targets in the paraclinoid area ($p < 0.05$).

Conclusions: The evidence provided in this study establishes that the ACP affords improved surgical exposure and maneuverability when added to the MPT. The MPT offers a less invasive alternative to the traditional pterional or orbitozygomatic approach, while the eAC is a well established technique that overcomes some of the previous limitations of the standard MPT, improving surgical exposure and maneuverability within such narrow corridor.

P127. Anatomic Assessment of the Limits of an Endoscopically Assisted Retrolabyrinthine Approach to the Internal Auditory Canal

Thomas J. Muelleman¹, Anne K. Maxwell¹, Kevin A. Peng¹, Derald E. Brackmann¹, Gregory P. Lekovic¹, Gautam U. Mehta¹
¹House Ear Institute, Los Angeles, California, United States

Objective: The retrolabyrinthine approach is a hearing preservation approach that can be applied to internal auditory canal (IAC) pathology with endoscopic assistance. Information regarding the surgical advantages and anatomic constraints of this approach is lacking. This study aims to define the minimum amount of retrosigmoid dural decompression necessary for exposure of the entire IAC and the degree of surgical freedom afforded by this approach.

Methods: Presigmoid retrolabyrinthine approaches were performed on fresh cadaveric heads. The IAC was exposed under endoscopic guidance. The retrosigmoid posterior fossa dura was decompressed in a step-wise fashion until the fundus of the IAC was exposed and successive measurements were made. Degree of surgical freedom at the fundus of the IAC was calculated for each specimen after both the retrolabyrinthine approach and translabyrinthine approach.

Results: The IAC was entirely exposed in 9 specimens with a median length of 12 mm (range: 10–13 mm). Complete IAC exposure could be achieved with 1 cm of retrosigmoid dural decompression in eight of nine mastoids. One mastoid required 2 cm of dural decompression to expose the entire IAC. For the retrolabyrinthine approach, the median anterior-posterior surgical freedom was 13° (range: 6–23°) compared with 46° (range: 36–53°) for the translabyrinthine approach ($p = 0.014$). For the retrolabyrinthine approach, the median superior-inferior surgical freedom was 40° (range: 33–46°) compared 47° (range: 42–51°) for the translabyrinthine approach ($p = 0.022$).

Conclusions: Using endoscopic assistance, the retrolabyrinthine approach can expose the entire length of the IAC. We recommend that at least 1.5 cm of posterior fossa dura is exposed for this approach. Compared with the translabyrinthine approach, this strategy provides significantly less instrument freedom in both the horizontal and vertical axes. This approach may be appropriate for carefully-selected patients with intact hearing and small- to medium-sized tumors involving the IAC.

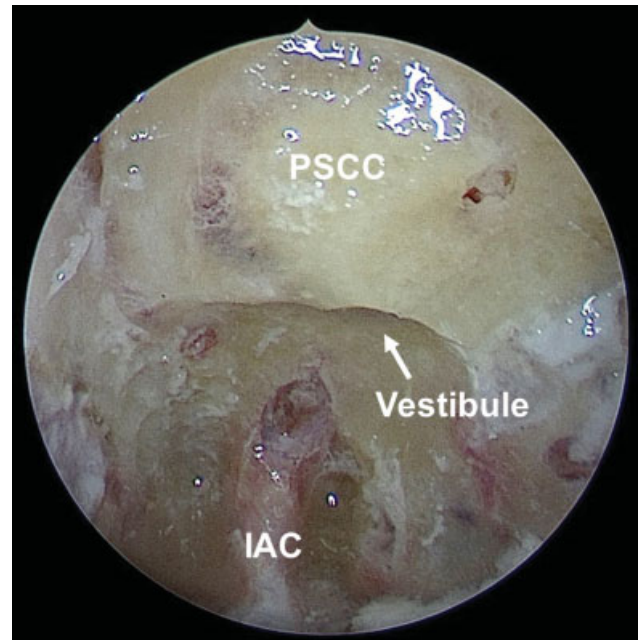


Fig. 1

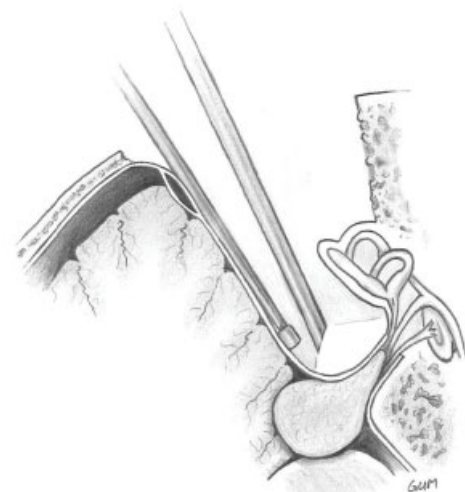


Fig. 2

P128. From Cholesteatoma to Squamous Cell Carcinoma: A Case Report

Juan Carlos Yanez-Siller¹, Carissa Wentland¹, Norman S. Litofsky¹, Arnaldo L. Rivera¹

¹University of Missouri-Columbia, Columbia, Missouri, United States

Squamous cell carcinoma of the temporal bone (SCCTB) is a rare malignancy with relatively poor prognosis. Affected patients typically present with locally advanced disease. Although a few reports have implicated cholesteatoma as an etiologic factor for SCCTB, a formal association between both entities remains unproven.

We present a case of SCCTB in a 62-year-old female, who underwent surgery for cholesteatoma of the left ear, 54 years prior. The patient presented at our institution with a long history of left-sided hearing loss as well as persistent ipsilateral otorrhea and vertigo. All symptoms had reportedly been present since her ear surgery but had intensified significantly over several months prior to her first visit. Imaging revealed a large left temporal bone mass with dural involvement and tegmen erosion. The decision was made to take the patient to the operating theater to approach the lesion via a left middle cranial fossa approach and left mastoidectomy.

Intraoperative frozen sections came back positive for squamous cell carcinoma. The tumor was continuous with the skin of the external acoustic canal and also extended into the left jugular bulb and sigmoid sinus. The vestibule and facial nerve remained uninvolved. Given the confirmed dural invasion, complete excision of the lesion was not pursued. The patient was started on radiation therapy, but due to intolerance of side effects, the patient chose to undergo comfort measures.

This case demonstrates that long-standing cholesteatoma may degenerate to SCCTB. Early detection may increase the likelihood of successful surgical and adjuvant management. A high index of suspicion should be kept in patients with prior history of cholesteatoma and evidence of temporal bone mass with persistent symptoms.

P129. The Retrolabyrinthine Presigmoid Approach: An Underutilized Approach for Safe Resection of Expansive CP Angle Tumors

Jacob Ruzevick¹, Sam Emerson¹, Kate Carroll¹, Manuel Ferreira¹

¹University of Washington, Seattle, Washington, United States

Purpose: We present our outcomes for patients undergoing a retrolabyrinthine presigmoid approach for tumor resection, and its benefit over retrosigmoid versus more lateral approaches.

Background: Pathologies of the CP angle amenable to the retrolabyrinthine presigmoid approach include vestibular schwannomas and meningiomas, amongst others. MRI remains the gold standard for assessing mass effect on adjacent brainstem and cranial nerves, invasion of bony foramina, as well as location of vascular structures. CT is helpful for understanding petrous bone anatomy. Intra-operative navigation and neuromonitoring is helpful for identifying cranial nerves which may be encased or displaced within a tumor mass.

Methods: A retrospective review of illustrative patients presenting between July 2015 and January 2019 was performed. Clinical data and radiographic parameters were reviewed using electronic medical records.

Results: A total of 20 illustrative patients were reviewed. Fifteen (75%) patients were women and the average age was 46 years (16–74). Pathologies included vestibular schwannoma ($n = 8$), meningioma ($n = 6$), epidermoid

($n = 3$), chordoma ($n = 1$), cranial nerve 4 schwannoma ($n = 1$), and cranial nerve 5 schwannoma ($n = 1$). The average tumor size was $18.9 \pm 14.1 \text{ cm}^3$. Gross total resection was accomplished in 14 (70%) of cases with an average estimated blood loss of $264 \pm 161 \text{ cc}$. Average surgical time was 13:47. Complications associated with the approach included cranial neuropathies that were temporary in 4 patients (20%) and permanent in 4 patients (20%), CSF leak ($n = 2$, 10%), pseudomeningocele ($n = 2$, 10%), and wound dehiscence ($n = 1$, 5%). Need for permanent CSF diversion was required in two patients (10%).

Conclusion: As compared with the retrosigmoid and more lateral approaches, the retrolabyrinthine presigmoid approach allows for ample exposure and freedom of surgical manipulation of the sigmoid sinus, tentorium, and tumor mass without the morbidity associated with significant retraction or violating middle ear structures.

P130. Anatomical Step-by-step Dissection of Complex Skull Base Approaches For Trainees: Surgical Anatomy of the Anterior Petrosal Approach

Laura Salgado-Lopez¹, Christopher S. Graffeo², Lucas P. Carlstrom², Avital Perry², Carlos D. Pinheiro-Neto³, Collin L. W. Driscoll⁴, Michael J. Link², Maria Peris-Celda¹

¹Department of Neurosurgery, Albany Medical Center, Albany, New York, United States

²Department of Neurologic Surgery, Mayo Clinic, Rochester, Minnesota, United States

³Division of Otolaryngology and Head and Neck Surgery, Department of Surgery, Albany Medical Center, Albany, New York, United States

⁴Department of Otolaryngology, Mayo Clinic, Rochester, Minnesota, United States

Background: The anterior petrosal approach is a challenging approach that provides access to the posterior fossa through the middle fossa floor and petrous apex between the petrous portion of the internal carotid artery, the internal acoustic meatus and the lateral aspect of Meckel's cave. Although many descriptions of the anterior petrosal approach have been published, a practical step-by-step surgical guide that allows an easy understanding for skull base and neurosurgical trainees at different levels in their training is needed.

Methods: Three formalin-fixed, colored-injected specimens were utilized (six sides). The specimens were dissected under microscopic magnification. A middle fossa craniotomy and drilling of the petrous apex was performed and the anatomical dissection was documented in stepwise 3D photographic images. Following dissection, representative case applications were reviewed.

Results: The middle fossa exposure with anterior petrosotomy provides excellent access to lesions located in the trigeminal porus, Meckel's cave, superior petroclival area, superior cerebellopontine angle and ventrolateral midbrain and upper pons. The area to drill in the anterior petrosotomy approach forms a pentagon limited by the petrous internal carotid artery, cochlea, internal auditory canal, petrous ridge, and lateral border of V3. Key steps include: positioning and skin incision, scalp and muscle flap dissection, burr holes, craniotomy flap elevation, dura dissection along the petrous ridge, division of the meningeal artery, exposure of the greater superficial petrosal nerve, tegmen tympani, arcuate eminence and mandibular division of the trigeminal nerve. The anteromedial petrosotomy is performed, posterior fossa dura exposure and durotomy (in a T fashion: parallel to the superior petrosal sinus followed by dural division perpendicular and through the superior petrosal sinus) and final exposure.

Conclusions: The anterior petrosectomy is a complex approach that allows access to the posterior fossa through the middle fossa. Operatively oriented neuroanatomy dissections provide trainees with a critical foundation for learning this fundamental skull base technique. We describe a comprehensive step-by-step approach to learning this technique, intended to be easy to understand by an audience of all levels of knowledge and experience in a way that simultaneously assists with rapid learning in the operating room, and an understanding of its potential for wide clinical application to skull base diseases.

P132. The Asterion to Transverse Process of the Atlas Line as a Surgical Landmark: Anatomical and Radiological Study

Jaafar Basma¹, Dom E Mahoney², Christos Anagnostopoulos³, L. Madison Michael¹, Jeffrey M Sorenson¹, Nickalus R Khan¹, Sanjeet Rangarajan⁴, Angelo Pichierri³

¹Department of Neurosurgery, University of Tennessee Health Science Center, Memphis, Tennessee, United States

²Faculty of Health Sciences, University of Bristol, Bristol, United Kingdom

³Department of Neurosurgery, North Bristol Trust, Bristol, United Kingdom

⁴Department of Otolaryngology, University of Tennessee Health Science Center, Memphis, Tennessee, United States

Introduction: Several landmarks have been proposed to predict the anatomical location and trajectory of the sigmoid sinus, with variable degrees of reliability. Even with the advent of neuro-navigation technology, such landmarks continue to be crucial in planning and performing complex approaches to the posterolateral skull base. By combining two major dependable structures, asterion (A) and transverse process of the atlas (TPC1), we studied the utility of the A-TPC1 line in relation to the sigmoid sinus and in partitioning surgical approaches to the region.

Methods: Six cadaveric heads (12 sides) were dissected to expose the posterolateral skull base, including the mastoid and suboccipital bone, TPC1 and suboccipital triangle, distal jugular vein and internal carotid artery and lower cranial nerves in the distal cervical region. We inspected the line between the asterion and TPC1, before and after drilling the mastoid and occipital bones exposing the sigmoid sinus. We studied the relationship of the sigmoid sinus trajectory and major muscular elements related to the line. We also retrospectively reviewed 31 CT angiograms of the head and neck (total 61 sides) from our PACS system, excluding posterior fossa or cervical pathologies. Using the Fujitsu Synapse 3D segmentation software, bone and vessels were reconstructed in three-dimensions. We measured the distance between the A-TPC1 line and sigmoid sinus at different levels: digastric point (DP), and maximal and minimal distances above and below the digastric notch. The Rhoton collection and clinical cases were reviewed to further illustrate the utility of the A-TPC1 line.

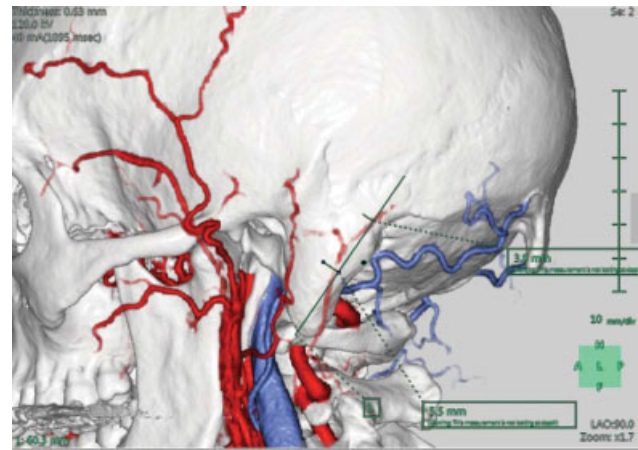


Fig. 1

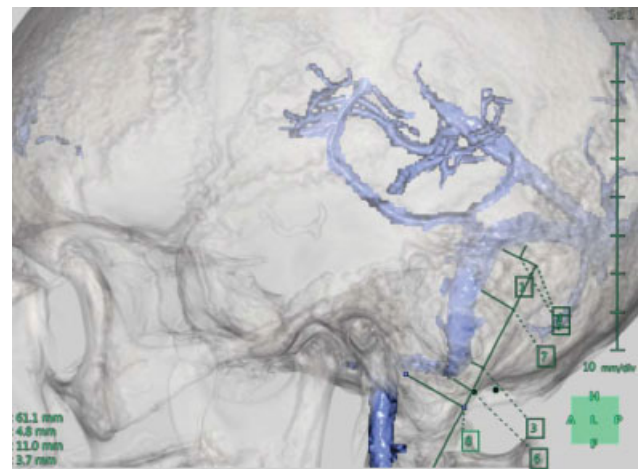


Fig. 2

Results: The A-TPC1 line averaged 65 mm in length, and was found to be consistently posterior to the sigmoid sinus in all cadaver specimens, coming closest to it at the level of the digastric notch. Using the transverse-asterion line and the skull base as a horizontal plane, we divided the major surgical approaches to the posterolateral skull base into four quadrants: distal cervical/extreme lateral and jugular foramen (anteroinferior), presigmoid/petrosal (anterosuperior), retrosigmoid/suboccipital (posterosuperior) and far lateral/foramen magnum regions (posteroinferior). Case illustrations were found to illustrate its utility in planning the surgical approach. From a radiographic perspective, the A-TPC1 line was also posterior to the sigmoid sinus in all sides. It came closest to the sinus at the level of digastric point (DP) (average 7 mm posterior, range 0–18.7 mm). The maximal distance above the DP averaged 10.1 mm (3.6–19.5 mm), and that below the DP 8.8 mm (–2 to 20 mm).

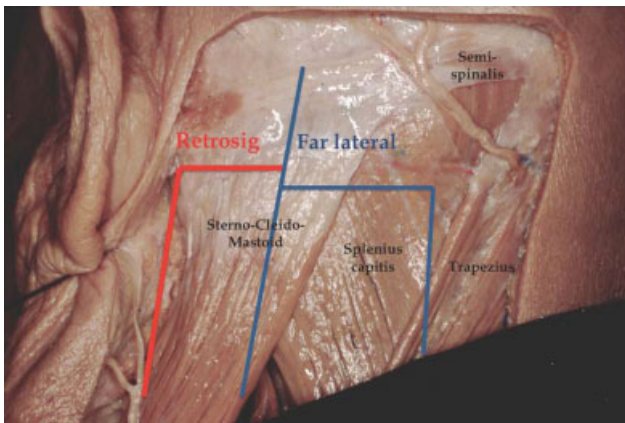


Fig. 3

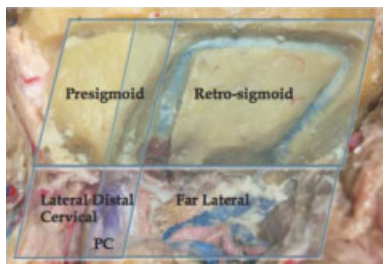


Fig. 4

Conclusion: The A-TPC1 line is a helpful landmark that is reliably found posterior to the sigmoid sinus in cadaveric specimens and radiographic CT scans. It can corroborate the accuracy of neuronavigation, assist in minimizing the risk of sigmoid sinus injury, and is a useful tool in planning surgical approaches to the posterolateral skull base, both preoperatively and intraoperatively.

P133. Glioblastoma in the Cerebellopontine Angle in a Patient with Neurofibromatosis Type I: A Case Report and Review of the Literature

Mohammad K. Shukairy¹, Andrea Ziegler², Douglas Anderson², John Leonetti²

¹Wayne State University School of Medicine, Detroit, Michigan, United States

²Loyola University Medical Center, Maywood, Illinois, United States

Glioblastoma Multiforme (GBM) is the most common primary brain malignancy in adults and is typically in the supratentorial cerebral hemispheres. It has been reported to occur in the posterior fossa at the cerebellopontine angle (CPA), but the incidence is extremely rare. We report a case of a patient with a history of neurofibromatosis type I (NFI) diagnosed with a GBM arising in the CPA after presenting with facial numbness and pain. Patients with NFI are known to have an increased risk of developing both benign and malignant tumors, including a propensity for brainstem gliomas. However, there is no known association between NFI and tumors of the CPA. We believe this is the first reported case of a GBM of the CPA in a patient with NFI. Although rare, GBM should be included in the differential diagnosis of a patient with a CPA tumor especially in patients with increased risk of malignant pathology.

P134. Antibiotic Use in Lateral Skull Base Surgery: A Survey of the North American Skull Base Society

K. L. Li¹, C. H. Fang¹, V. S. Hawn¹, V. Agarwal², V. R. Kshetry³, E. Bellile⁴, N. A. Akbar¹, E. L. McKean⁵, W. M. Abuzeid¹, H. S. Moskowitz¹

¹Department of Otorhinolaryngology-Head and Neck Surgery, Albert Einstein College of Medicine, Bronx, New York, United States

²Department of Neurosurgery, Albert Einstein College of Medicine, Bronx, New York, United States

³Department of Neurosurgery, Cleveland Clinic, Cleveland, Ohio, United States

⁴Department of Biostatistics, University of Michigan, Ann Arbor, Michigan, United States

⁵Department of Otolaryngology-Head and Neck Surgery, University of Michigan, Ann Arbor, Michigan, United States

Introduction: Antibiotic use in lateral skull base surgery (LSBS) has not been thoroughly investigated in the literature. As such, there is wide variability in antibiotic use and insufficient data to guide management. This study aims to describe the factors and patterns influencing antibiotic use in LSBS.

Methods: An online-based survey was designed and distributed to the membership of the North American Skull Base Society. Data were analyzed using multivariate analysis.

Results: The survey response rate was 25.6%, with a total of 208 respondents. 143 (68.8%) respondents performed LSBS, and 58.0% practice full-time in an academic institution. The majority of respondents (79.0%) are fellowship trained in skull base surgery. Most are neurosurgeons (68.5%) with the remaining being otolaryngologists (31.5%). 92.3% of respondents prescribe intraoperative antibiotics, and 89.4% cite reduction in the risk of postoperative infection risk as the motivating factor. Bivariate analysis showed that compared with academic surgeons, private practice surgeons are 13.3 times less likely to prescribe intraoperative antibiotics (OR 0.075 [95% CI: 0.012–0.455]; $p = 0.011$). Postoperative antibiotics were prescribed at a lower rate (61.5%) and were most commonly used to prevent postoperative infection (51.7%) or for the presence of purulence (14.0%). European surgeons were 4.7 and 1.5 times less likely to prescribe postoperative antibiotics than the Midwest United States and Central American surgeons, respectively (OR 0.214 [95% CI: 0.062–0.746]; $p = 0.013$; OR 1.5 [95% CI: 0.945–2.381]; $p = 0.047$). Asian surgeons are 4.3 times more likely to prescribe postoperative antibiotics than surgeons in the Western United States (OR 4.308 [95% CI: 0.987–18.796]; $p = 0.044$), and 10.9 times more likely than surgeons in Europe (OR 10.889 [95% CI: 2.262 – 52.416]; $p = 0.001$). The presence of active cerebral spinal fluid leak was associated with a 24.4 times increase in postoperative antibiotic use (OR 0.041 [95% CI: 0.008–0.207]; $p < 0.0001$).

Conclusion: This study demonstrates significant variations in intraoperative and postoperative antibiotic use in LSBS. Future prospective randomized studies are needed to evaluate effective perioperative antibiotic use.

P135. Advanced Cutaneous Squamous Cell Carcinoma Extending to the Temporal Bone

Michael Schachtel¹, Ben Panizza¹, Arturo Solares², Mitesh Gandhi¹, Mark Midwinter³, James Bowman¹

¹Princess Alexandra Hospital, Brisbane, Australia

²Emory University Hospital, Atlanta, Georgia, United States

³University of Queensland, Brisbane, Australia

Introduction: Primary temporal bone tumors are rare and aggressive, with an estimated incidence of 1–6 cases per 1 million population. However, cutaneous malignancies

extending to the temporal bone, particularly squamous cell carcinomas (SCC), are a problem that deserves more attention. These tumors can be as difficult to manage and are often quoted to be more common than the primary subtype around the world. This certainly holds true in regions such as Queensland (Australia) and southern United States, where nonmelanoma skin cancer (NMSC) rates are extraordinarily high. Yet, a greater paucity of evidence exists on cutaneous malignancy involving the temporal bone, with very few series exclusively examining this specific disease entity. Thus, staging systems, treatment protocols, survival data, and prognostic factors, which are often applied interchangeably for all temporal bone tumors regardless of origin, may be unreliable and not entirely applicable for cutaneous malignancy extending to the temporal bone.

Objective: To evaluate the epidemiology, patterns of spread, survival outcomes, and prognostic factors of patients with advanced periauricular cutaneous SCC extending to the temporal bone managed with temporal bone resection.

To develop a unique staging system for preauricular cutaneous SCC extending to the temporal bone, leading to more accurate prognostication and standardized operative recommendations.

Methods: This is a multi-institutional retrospective study of 150 patients* who underwent temporal bone resection for advanced periauricular cutaneous SCC at 2 tertiary care centers between 2000 and 2019. Data were collected on demographics, disease extent, treatment, histopathology, and survival outcome. All patients were staged according to the modified Pittsburgh Staging System (mPSS) and AJCC 8th edition TNM Staging System. Kaplan–Meier survival analysis was performed, and prognostic factors were identified through uni- and multivariate analysis.

A human cadaveric dissection series was conducted to identify potential fascial planes of dissection and barriers of spread in relation to advanced preauricular cutaneous malignancies. Relevant planes were mapped on cross-sectional imaging and correlated with survival outcomes. These findings, together with other prognostic factors identified, were used to formulate a novel staging system. The predictive accuracy of this staging system was compared with the mPSS and AJCC systems.

Results: This is the largest ever case series of cutaneous SCC extending to the temporal bone. Data collection is being finalized and analysis will be completed before the end of 2019.

The most cranial part of the carotid sheath, specifically the tensor-vascular styloid fascia, is an important barrier to medial spread of disease, and could be a useful plane of dissection in extirpative surgery (see picture as example of dissection).

Conclusion: Conclusions will be drawn once data analysis is complete.

*Final patient numbers TBD but will be at least 150.



Fig. 1

P136. Perineural Spread of the Facial Nerve from Cutaneous Squamous Cell Carcinoma of the Head and Neck: Epidemiology and Survival Outcomes

Michael Schachtel¹, Ben Panizza¹, James Bowman¹, Mitesh Gandhi¹

¹Princess Alexandra Hospital, Brisbane, Australia

Introduction: Perineural spread (PNS) from cutaneous head and neck malignancies has traditionally been a rare disease that is poorly understood. This has led to diagnostic delays, resulting in poorer outcomes and more debilitating treatments. In areas such as Queensland (Australia), where nonmelanoma skin cancer (NMSC) rates are extraordinarily high, PNS is becoming more prevalent, likely in part due to an increased awareness of the disease. While understanding of the disease process is becoming clearer, PNS still poses unique therapeutic challenges and can be associated with poor outcomes. Multiple previous studies have investigated outcomes of patients with PNS from cutaneous squamous cell carcinoma (SCC) of the head and neck, however few have exclusively studied PNS of the facial (VII) nerve.

Objective: To evaluate the epidemiology, patterns of spread, survival outcomes, and prognostic factors of patients with PNS of the VII nerve from cutaneous squamous cell carcinoma of the head and neck.

Methods: This is a retrospective cohort study of 60 consecutive patients* with PNS of the VII nerve from cutaneous squamous cell carcinoma of the head and neck managed at a tertiary care center between 2000 and 2019. Data were collected on demographics, primary tumor, disease extent, treatment, histopathology, and survival outcome. All patients were staged according to the Williams Zonal Classification for PNS and the AJCC 8th edition TNM Staging System. Kaplan–Meier survival analysis was performed, and prognostic factors were identified through uni- and multivariate analysis.

Results: This is the largest ever case series on PNS of the VII nerve from cutaneous squamous cell carcinoma of the head and neck. Data collection is being finalized and analysis will be completed before the end of 2019.

Conclusion: Conclusions will be drawn once data analysis is complete.

*Final patient numbers TBD but will be at least 60.

P137. Hematologic Malignancies Affecting the Skull Base: Two Unique Cases and a Literature Review

Eric Barbarite¹, Shekhar K. Gadkaree¹, Anuraag S. Parikh¹, Kevin S. Emerick¹, Derrick T. Lin¹, Stacey T. Gray¹
¹Massachusetts Eye and Ear Infirmary, Boston, Massachusetts, United States

Objective: Hematologic malignancies affecting the skull base are rare and may present with nonspecific symptomatology. The objectives of this study were to characterize the manifestations and clinical outcomes of two cases of lymphoma at the cranial base where initial diagnoses were missed, and to review the pertinent literature.

Methods: Case reports and review of the literature.

Case 1: A 47 year-old female with an incoming diagnosis of granulomatosis with polyangiitis presented with worsening facial edema despite high dose steroids. Exam was notable for severe left-sided proptosis with restricted extraocular movements. Imaging demonstrated severe pansinusitis, left subperiosteal abscess, diffuse pachymeningeal enhancement and focal leptomeningeal enhancement in the frontal lobe with a subdural empyema. She underwent endoscopic biopsy and drainage of the subperiosteal and subdural collections. Pathology demonstrated extranodal NK/T cell lymphoma, nasal type. She was started on systemic chemotherapy with good clinical and radiographic response. She is currently undergoing radiation therapy with plans for future autologous stem cell transplant.

Case 2: A 50 year-old male who experienced an episode of aphasia and confusion while overseas and initially diagnosed with a cerebrovascular occlusion. On presentation to our institution, he was neurologically intact with left-sided hearing loss, however subsequently developed left facial palsy. CT demonstrated opacification of the left mastoid air cells and middle ear, hyperdensity in the left posterior and middle cranial fossae and a mass-like density along the left temporal lobe. MRI showed dural thickening and enhancement overlying left posterior fossa and bilateral middle cranial fossae. After reteropitoneal node biopsy, he was diagnosed with stage IV Burkitt lymphoma with CNS involvement. Systemic chemotherapy was initiated with complete facial nerve recovery and oncologic remission.

Conclusions: Hematologic malignancies may mimic a variety of more common skull base pathologies, thus posing a diagnostic challenge. Presentation may be nonspecific, including diplopia, nasal obstruction or facial nerve weakness. The literature shows that the anterolateral skull base is most commonly involved, and poor survival is associated with central nervous system involvement. Prompt identification of these cases is dependent upon appropriate clinical suspicion, which is necessary to ensure proper treatment with the assistance of a multidisciplinary oncologic team.

P139. Population-Based Database Survival Analyses of Intracranial Meningiomas

Zaid Aljuboori¹, Ahmad Alhourani¹, Alexandra Schaber¹, Shiao Woo¹, Eyas Hattab¹, Mehran Yusuf¹, Megan Nelson¹, Norberto Andaluz¹, Dale Ding¹, Brian Williams¹
¹University of Louisville, Louisville, Kentucky, United States

Study Design: National database analysis.

Introduction: Intracranial Meningiomas are the most common primary intracranial tumors. There are several treatment options available (observation, radiotherapy, surgery, and combination of surgery and radiotherapy) with different outcomes. Patient and tumor related factors affect the choice of treatment method as well as patient's survival.

Here we present a population-based database survival analysis of patients with intracranial meningioma.

Methods: We surveyed the National Cancer Database (NCDB) for the years 2004–2015 to identify patients with a diagnosis of intracranial meningioma using the International Classification of Disease 9 code. We then performed survival analyses of the retrieved data.

Results: A total of 199,096 patients with a diagnosis of intracranial meningioma met the inclusion criteria, 73.3% were females, and 76.4% were white. Mean age was 61 years, and mean Karnofsky score was 74.5. 73.4% of patients had no comorbidities. Patients treated at community hospitals had increased mortality in comparison to academic institutions for all treatment modalities. Increasing age and the presence of comorbidities were associated with increased mortality. Female gender was associated with increased survival. Tumors size >3 cm, and high tumor WHO grade was associated with increased mortality.

Conclusion: There is a multitude of factors that affect survival of patients with intracranial meningioma. Nonacademic institutions, comorbidities, advanced age, larger tumor size, and higher WHO grade are associated with increased mortality.

P141. Chromosome Instability and Transcriptomic Subpopulations Underlie Intratumor Heterogeneity in Meningioma

Stephen T. Magill¹, Harish N. Vasudevan¹, Kyounghee Seo¹, S. John Liu¹, Stephanie Hilz¹, Javier E. Villanueva-Meyer¹, Abrar Choudhury¹, Benjamin Demare¹, Steve E. Braunstein¹, Nancy Ann Oberheim Bush¹, Manish K. Aghi¹, Philip V. Theodosopoulos¹, Penny K. Sneed¹, Adam R. Abate¹, Mitchel S. Berger¹, Michael W. McDermott¹, Daniel A. Lim¹, Erik M. Ullian¹, Joseph F. Costello¹, David R. Raleigh¹
¹University of California, San Francisco, California, United States

Meningiomas are the most common primary intracranial tumor, and high grade meningiomas are resistant to most cancer therapies. As intratumor heterogeneity is a driver of cancer resistance, we hypothesized that investigating intratumor heterogeneity in meningiomas would elucidate biologic drivers and shed light on tumor evolution. Thus, we performed multiplatform molecular profiling of 86 spatially distinct samples from 13 meningiomas to discover that alterations in chromosome structure underlie evolution of synchronous tumor subpopulations in high grade meningiomas. To understand the impact of genomic instability on gene expression in meningioma, we used single nucleus RNA sequencing, single cell RNA sequencing of meningioma cells in co-culture with human cerebral organoids, and RNA sequencing of paired primary and recurrent tumors to develop a single cell transcriptomic atlas of meningioma. These data reveal that clonal genomic instability and subpopulations of cells delineated by misactivation of mesenchymal and immediate early genes define intratumor heterogeneity in meningioma.

P142. Middle Fossa Meningioma Presenting with External Auditory Canal Mass, Conductive Hearing Loss, and Facial Weakness

Joseph Lockwood¹, Kendra Harris¹, Rizwan Aslam¹, Peter Amenta¹, Neal Jackson¹
¹Tulane Medical Center, New Orleans, Louisiana, United States

Introduction: Meningiomas account for 13–18% of primary brain tumors, with, temporobasal lesions accounting for 4% of all such tumors. Extracranial extension occurs in 20%

of meningiomas, but increases to 43% with temporal bone involvement. We describe a rare presentation of meningioma with an external auditory canal (EAC) mass, conductive hearing loss, and facial nerve weakness. Only 8 additional cases of meningioma extension into the EAC are found in the literature. We highlight meningiomas as part of the differential diagnosis in EAC lesions and conductive hearing loss. Our case also underscores the importance of multidisciplinary teams in the management of complex skull base lesions.

Case: A 38-year-old female presented to neurotology clinic with 1 year of progressive right-sided hearing loss and facial weakness. She complained of a dry right eye secondary to her inability to fully close the eye. On examination, she had right-sided House-Brackmann grade IV facial nerve weakness. Otolaryngologic examination demonstrated a soft, compressible mass occupying the right ear canal and obscuring visualization of the tympanic membrane. An audiogram confirmed a significant right-sided conductive hearing loss with 45 dB air-bone gap and normal left-sided auditory function.

CT of the head revealed diffuse hyperostosis of the petrous temporal bone and bone of the floor of the middle cranial fossa. The middle ear, mastoid, and medial ear canal were filled with contiguous soft tissue density material. MRI demonstrated an extensive intraosseous meningioma of the right petrous temporal bone with a large middle fossa soft tissue component displacing the inferior right temporal lobe. The tumor extended inferiorly through the floor of the middle cranial fossa to fill the middle ear, extend into the medial ear canal, and encase the distal internal carotid artery.

The patient underwent a combined middle fossa craniotomy, radical mastoidectomy, and decompression of the facial nerve within the fallopian canal. A lumbar drain was placed to facilitate brain relaxation and temporal lobe retraction. Tumor was found to fill the tympanic cavity, obliterate the tympanic membrane, dislodge the incus, and extend into the ear canal. The tumor was resected, and the ear canal was oversewn. A radical mastoidectomy was performed, and the facial nerve was identified and decompressed. Extensive bony resection of the middle fossa floor was performed with a diamond burr. The intracranial tumor was resected, with a small residual left encasing the distal carotid artery. Pathology was consistent with a WHO grade I meningioma. The patient was discharged with stable right-sided facial paralysis and complete hearing loss.

Three-month MRI demonstrated minimal residual meningioma encasing the distal extracranial carotid artery. Facial nerve function did not significantly improve, and the patient underwent gold weight placement in the right eyelid for lagophthalmos. She has received external whole beam radiation to the floor of the middle fossa and small residual extracranial tumor.

Conclusion: Middle fossa meningiomas should be included in the differential of EAC lesions and in those patients presenting with facial nerve weakness and conductive hearing loss. Multidisciplinary teams consisting of otology/otolaryngology, neurosurgery, and radiation oncology maximize patient care.

P144. Endoscopic Endonasal Treatment of Frontal Sinus Meningoencephalocele

Jesus Gimeno Hernandez¹, Carla Fernandez Garcia¹, Melchor Saiz Pardo-sanz¹, Manuel Gomez Serrano¹, Ivan Muerte Moreno¹, Jose Roan Roan¹, Eduardo Castillo Serrano¹, Andrea Lopez Salcedo¹

¹Hospital Clinico San Carlos, Madrid, Spain

Introduction: Meningoceles, encephaloceles, and meningoencephaloceles may develop through defects associated with congenital anomalies or through defects produced

by tumors, trauma, or surgery. Their initial management, surgical indications, and repair techniques are not globally standardized.

The incidence of specific types of encephalocele varies by geographic location and race. Anterior encephaloceles are the most common type and occur most frequently in Southeast Asia, parts of Russia, and central Africa, where they are seen in up to 1 in 3,500 live births. In contrast, in North America 85% of all encephaloceles are occipital, while anterior encephalocele is seen in only 1 in 35,000 live births.

Materials and Methods: We present the case of a 65-year-old male patient with a meningoencephalocele diagnosed and treated at our academic hospital. He complained of daily right frontal headache and spontaneous ipsilateral rhinorrhea several months previous to diagnosis. No previous history of trauma or surgery was reported. CT scan and MRI were performed prior to surgery, revealing a 9 mm bone defect of the posterior table of the frontal sinus and a 46 mm encephalocele.

Transnasal endoscopic repair (Draf 3 procedure) with free grafts was performed. Nasal packing was removed 2 days after surgery. Intravenous perfusion of a third-generation cephalosporin was continued for 3 days. No lumbar drainage was applied and no CSF leakage postoperatively occurred. The patient was discharged 5 days after surgery and instructed to avoid any activity that could raise intracranial pressure such as Valsalva maneuvers or nose blowing. The patient remains asymptomatic 2 years following surgery.

Discussion / Conclusions: EES is a well-established treatment modality for a variety of anterior skull base pathologies including congenital or acquired meningoencephaloceles. It is a minimally invasive single stage surgery, with advantages in terms of hospital stay, cost of treatment, and cosmesis. The reported complication rate is low. The repair technique should be tailored to the size and site of the defect to provide a water-tight seal for better outcome. The presence of hydrocephalus was significantly related to poor surgical outcomes.¹⁻⁵

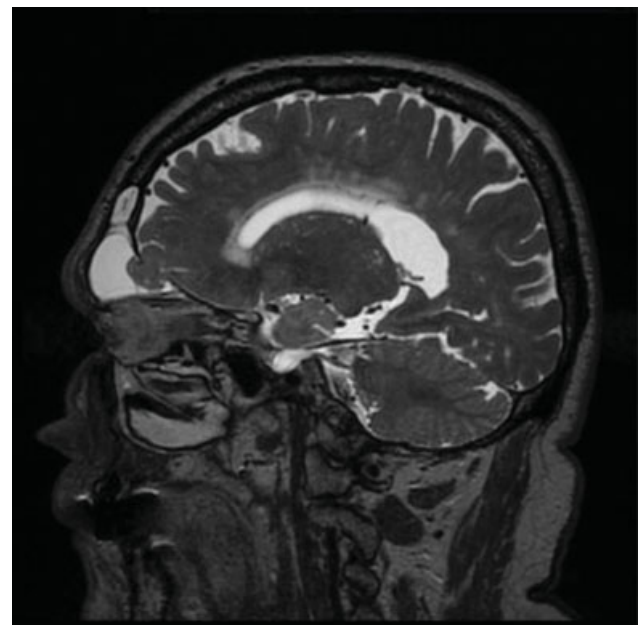


Fig. 1 MRI preop.

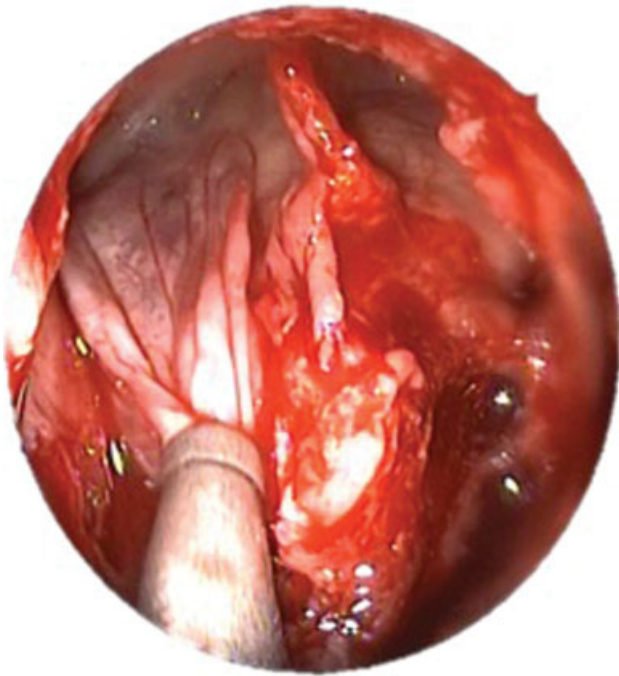


Fig. 2 Intraoperative view of right frontal sinus meningocele.

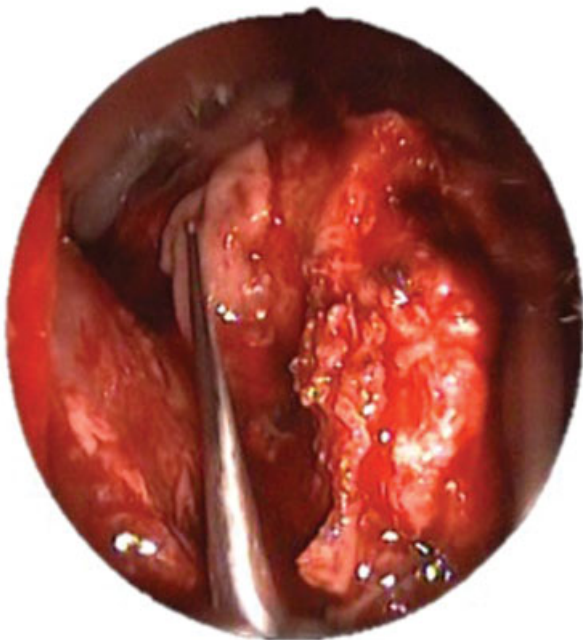


Fig. 3 Intraoperative view. Free graft over posterior table defect.

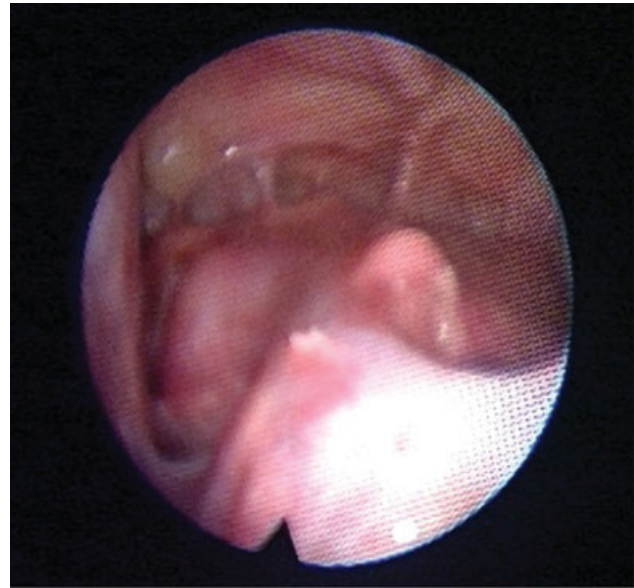


Fig. 4 Endonasal view of Draf 3 procedure 1 year postop.

References

1. Zweig JL, Carrau RL, Celin SE, Snyderman CH, Kassam A, Hegazy H. Endoscopic repair of acquired encephaloceles, meningoceles, and meningo-encephaloceles: predictors of success. *Skull Base* 2002;12(3):133-139
2. Keshri AK, Shah SR, Patadia SD, Sahu RN, Behari S. Transnasal endoscopic repair of pediatric meningoencephalocele. *J Pediatr Neurosci* 2016;11(1):42-45
3. Kapitanov D, Shelesko E, Potapov A, et al. Endoscopic endonasal diagnosis and treatment of skull base meningoencephalocele. *Vopr Neirohir.* 2017
4. Snyderman CH, Kassam A, Hegazy H. Endoscopic Repair of Acquired and Meningo-Encephaloceles? Predictors of Success. *Laryngoscope.* 2002;12(3):133-140
5. Rawal RB, Sreenath SB, Ebert CS Jr, et al. Endoscopic sinonasal meningoencephalocele repair: a 13-year experience with stratification by defect and reconstruction type. *Otolaryngol Head Neck Surg* 2015;152(2):361-368

P145. Management of Cholesteatoma and Tegmen Dehiscence: Complexities and Nuance

Isaac D. Erbele¹, Gauri Mankekar², Moises A. Arriaga¹

¹Louisiana State University Health Sciences Center, New Orleans, Louisiana, United States

²Louisiana State University Health Sciences Center Shreveport, Shreveport, Louisiana, United States

Objectives: Cholesteatoma and bony tegmen dehiscence may coexist in the same patient, occasionally with cholesteatoma causing the dehiscence. Surgical management of coexistent disease is poorly explored in the literature. The purpose of this study is to identify characteristics of safe surgical intervention.

Study Design: Case series.

Setting: Tertiary care centers.

Materials and Methods: Patients were identified in chart review at two tertiary care centers between 2011 and 2019 as having coexistent cholesteatoma and tegmen dehiscence. Patient were included if surgery had been performed to address both pathologies.

Results: Thirty cases were identified in 28 patients. Average patient age was 49 years (range 10–81 year), and average follow up was 29 months (range: 2.5 to 84 months). Tegmen dehiscence repair was performed via transmastoid approach in 21 cases and via middle cranial fossa approach in nine patients. Decision making for the approach was based on the apparent size and location of the tegmen dehiscence, as well as the presence of encephalic herniation through the dehiscence. Postoperative skull base complications were identified two patients.

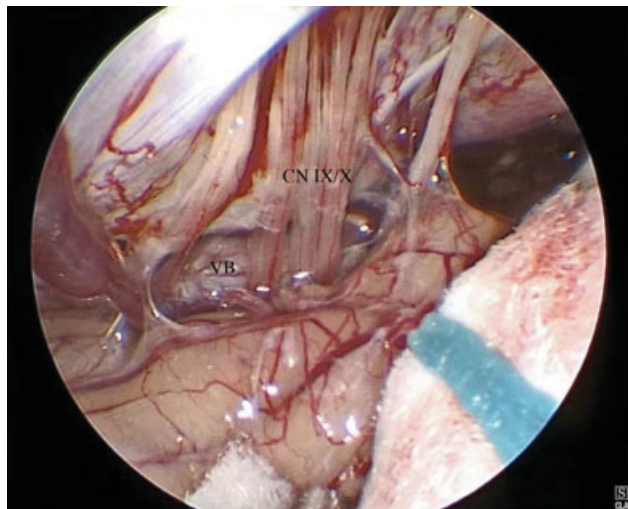
Conclusions: Management of tegmen dehiscence in the setting of cholesteatoma is a challenging problem. Careful preoperative planning may help prevent complications.

P146. Endoscopic Microvascular Decompression for Cardiac Syncope/Arrhythmia: Vasoglossopharyngeal Neuralgia

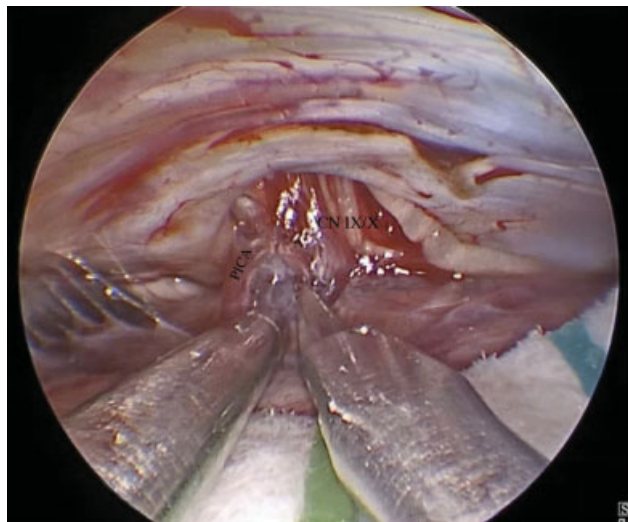
Rachel Blue¹, Michael F. Spadola¹, Michael McAree², John Y.K. Lee¹

¹University of Pennsylvania, Philadelphia, Pennsylvania, United States

²Rowan School of Medicine, Stratford, New Jersey, United States



Patient 2: Compression of the glossopharyngeal nerve by a dolichoectatic vertebrabasilary artery (VB)



Patient 1: Compression of the glossopharyngeal nerve by posterior inferior cerebellar artery

Introduction: Glossopharyngeal neuralgia (GN) is a rare cra-

nial nerve compression, with an annual incidence of 0.8/100,000 and classically characterized by paroxysms of unilateral lancinating pain involving the throat, tongue, soft palate, posterior and lateral pharynx, and ear. Rarely, this syndrome is associated with arrhythmias, cardiac syncope, and cardiac arrest leading to significant disability. This condition, termed vasoglossopharyngeal neuralgia (VGPN), occurs in ~4/217 patients with GN and is often misdiagnosed as cardiac or cerebral episodes. We review our experience of MVD surgery in patients with symptomatic, medication-refractory cardiac syncope secondary to VGPN successfully treated with endoscopic-microvascular decompression (E-MVD).

Methods: Chart abstraction was performed and cases were identified from a prospective database collected by senior surgeon. From 2006 to 2019, 17 patients have undergone E-MVD for ninth/tenth nerve symptoms. Of these, two were identified with cardiac episodes.

Results: The first patient was a 53-year old male with right-sided glossopharyngeal neuralgia symptoms that became associated with syncopal episodes 10-years after the onset of symptoms. The second patient was a 61-year old female with a history of Ehlers–Danlos syndrome and malignant vasovagal syndrome that became associated with painful, shooting left anterior neck spasms consistent with glossopharyngeal neuralgia. Both patients underwent extensive medical and cardiac work-up prior to surgical consideration. Patient 1 was diagnosed with supraventricular tachycardia, underwent cardiac ablation, but continued to have symptoms. Patient 2 underwent bilateral styloidectomy for concern for eagle syndrome, but continued to have both neuralgia and syncopal symptoms. Ultimately, both underwent craniotomy for E-MVD. Patient 1 underwent a right retrosigmoid craniotomy. The glossopharyngeal nerve was noted to be compressed by the posterior inferior cerebellar artery, which was decompressed using Teflon. Patient 2 underwent a left retrosigmoid craniotomy, which showed compression secondary to the dolichoectatic vertebrabasilary artery, which was also decompressed using Teflon. Both had uncomplicated postoperative courses and were seen at follow-up without return of neuralgia or syncopal episodes. At 1.5 years and 0.75 years of follow-up, both patients have not had recurrence of cardiac syncope.

Discussion: The pathogenesis of vasoglossopharyngeal neuralgia is largely unknown and a variety of mechanisms have been proposed. One theory suggests irritation of glossopharyngeal nerve causes reflex bradycardia or asystole via the tractus solitarius to the dorsal motor nucleus of the vagal nerve. Another proposes artificial synapses between the Hering nerve (carotid sinus nerve) and the Jacobson nerve (tympanic branch of glossopharyngeal nerve). Direct neurovascular compression of the root entry zone of both the glossopharyngeal and vagal nerves has also been observed, which was noted in both of these patients. For some, this rare condition can be managed with medical therapy alone. But here, we present two cases demonstrating safe and successful management of VGPN with E-MVD after failure of therapy. These outcomes support previously published case reports of successful treatment of VGPN using microvascular decompression of the glossopharyngeal nerve, and is the first report in the literature using an endoscopic technique.

P147. Teflon or Ivalon®: A Scoping Review of Implants Used in Microvascular Decompression for Trigeminal Neuralgia
 Elliot Pressman¹, R. Tushar Jha¹, Gleb Zavadskiy², Jay I. Kumar¹, Ivo Peto¹, Harry van Loveren¹, Jamie J. van Gompel³, Síviero Agazzi¹

¹Department of Neurosurgery and Brain Repair, University of South Florida, Tampa, Florida, United States

²Muma College of Business, University of South Florida, Tampa, Florida, United States

³Department of Neurosurgery, Mayo Clinic, Rochester, Minnesota, United States

Background: Trigeminal Neuralgia (TN) is characterized by jolts of pain along the distribution of the trigeminal nerve. If patients fail conservative management, microvascular decompression (MVD) is the next step in treatment. MVD is largely done by placing implant pads between the nerve and compressing vessels. We conducted a literature review to assess effectiveness and safety of Teflon and Ivalon sponges for treatment of TN with MVD.

Methods: In January 2019, PubMed was searched for manuscripts published in English using permutations of, "Microvascular decompression," "Teflon," "Ivalon," "Granuloma," "Polytetrafluoroethylene," "Polyvinyl acetal," "Trigeminal Neuralgia," and "Exploration." Success and relapse rates, causes of relapse, and complication rates were analyzed. We analyzed for relationships with ANCOVA at an α threshold of 0.05.

Results: 36 studies representing 4273 patients fit inclusion criteria. 25 dealt with initial MVD, 12 with re-do MVD. Initial MVD initial success rates were 85% in patients receiving Teflon (57–100%), and 91% in patients receiving Ivalon (79–100%). Recurrence rates were 12% in Teflon patients (0*–30%) and 9.1% in Ivalon patients (0*–19%). In patients with relapses, implants were the cause in 49% of Teflon patients (0*–100%) and 50% of Ivalon patients (0*–100%). Complication rates for patients receiving Teflon was 12% (0*–34%) and 19% for patients receiving Ivalon (0*–40%).

Conclusion: Teflon and Ivalon are two materials used in MVD for TN. It is an effective treatment with long-term symptom relief and recurrence rates of 1–5% each year. Ivalon has been used less than Teflon though is associated with similar success rates and similar complication rates.

P148. Micro-RNA Mutations Across Multiple Resections of a Giant Nonfunctional Pituitary Adenoma

Abhijeet Gummadavelli¹, Lily McCarthy¹, Zeynep Erson¹, Eugenia Vining¹, Murat Gunel¹, S. Bulent Omay¹

¹Yale University SOM, New Haven, Connecticut, United States

Introduction: Nonfunctional pituitary adenomas are one of the most common types of brain tumors, but the landscape of genomic alterations is not well understood. Despite widespread genetic disruptions in pituitary adenomas, they are known to harbor few focal events. Increasingly, epigenetic factors are thought to play a role in pituitary adenoma tumorigenesis. MicroRNAs are noncoding RNAs that modulate posttranscriptional gene expression by affecting stability and translation of messenger RNAs, thought to control 30–50% of protein-coding genes. A variety of miRNAs have been previously implicated in functional and nonfunctional microRNAs but has never been shown to be preserved during tumor development.

Methods: High throughput sequencing was performed to analyze a giant pituitary adenoma specimen for somatic mutations in three different time points.

Results: We present a 41-year-old patient who presented with headache and 2 months of visual changes and

galactorrhea, found to have 3.7 cm × 5.2 cm pituitary giant adenoma. Patient underwent three staged operations using different approaches and whole-exome sequenced at a different site with each resection, over a 13-month period. She initially had a right supraorbital craniotomy, followed by endoscopic endonasal transsphenoidal approach, and lastly an endoscopic endonasal trans-planum approach. Her headaches and visual impairment improved after treatment.

The first sample had a growth hormone secretagogue receptor mutation, and all three samples of tissue had a conserved mutation in microRNA MIR1268A. Prior studies have not identified this microRNA involved in pituitary adenomas.

Conclusions: This case serves as a novel example of a pituitary adenoma biopsied at several time points at different locations. All samples show a similar somatic mutation burden with only a single conserved miRNA mutation and similar somatic copy number profiles pointing to intratumoral genetic homogeneity.

P149. A Case of the Use of Genomic Signatures in the Diagnosis of Cushing Disease

Keerti Murari¹, Mona Gossman¹, Amit Mahajan¹, Zeynep Erson¹, Silvio Inzucchi¹, S. Bulent Omay¹

¹Yale University SOM, New Haven, Connecticut, United States

Case Presentation: A 31 year-old female presented with headaches and left sided facial pain. On exam she was found to have a cranial nerve (CN) VI palsy and some Cushingoid features. MRI revealed a 2.5 cm sellar/suprasellar mass with left cavernous sinus invasion and extension into the superior orbital fissure and optic foramen. Her presentation was concerning for pituitary apoplexy. Due to the need for urgent intervention, her preoperative evaluation was limited but demonstrated elevated random cortisol levels and failure to adequately suppress cortisol with 4 mg dexamethasone (8 am cortisol 2.3 mcg/dL). She subsequently underwent endoscopic endonasal resection which revealed a large sellar, suprasellar tumor with visible normal pituitary pushed to the right side of the cavity. Intraoperative pathology revealed a pituitary adenoma with infarction. The majority of the specimen was necrotic tissue with viable cells staining positive for synaptophysin and negative for all pituitary hormones including ACTH. Whole exome sequencing (WES) of the patient's tumor and blood control showed a USP8 missense mutation. Postoperative MRI at 3 months showed no residual tumor. Patient had resolution of her CN VI palsy and noted a decrease in weight and improvement in acne, AM cortisol normalized, and the remainder of her pituitary hormones were normal.

One year following her surgery, she developed recurrent headaches and left sided facial pain during the first trimester of pregnancy. Soon after delivery, she developed double vision and a third nerve palsy. MRI then revealed a partially hemorrhagic enlarging mass in the left cavernous sinus. Given the rapid tumor expansion, she began radiation therapy and received a total of 52 GY. Her double vision resolved and imaging showed decrease in tumor size. Hormonal evaluation now revealed elevated Urine Free Cortisol, salivary cortisol, ACTH, and failure to suppress with dexamethasone. She was diagnosed with CD and was started on cabergoline but this was discontinued due to persistent hypercortisolism and replaced by pasireotide.

Discussion: Our case highlights the challenge in making an accurate diagnosis of CD. Clinically our patient's history was suspicious, but, since her tumor did not stain for ACTH and since her initial cortisol levels were obtained while on oral contraceptives, a diagnosis of CD was not

initially confirmed. On subsequent testing, however, after tumor regrowth, evidence of hypercortisolism was unequivocal.

Mutations in USP8, a deubiquitinating enzyme, have been described in cases of CD. The mechanism for stimulating ACTH production is thought to be due to impaired EGF signaling and increased transcription of the POMC gene that encodes the precursor peptide of ACTH. The presence of USP8 mutation is thought to suggest a more aggressive adenoma with an increased probability of recurrence. In our patient, it appeared to correlate with the patient's course. Our patient's WES result revealing the USP8 mutation, which is only seen in CD, helped confirm the diagnosis of CD where biochemical and pathological methods had initially failed. Molecular diagnosis may become an important adjunct in the diagnosis and management of pituitary tumors as it has become in the field of neuro-oncology.

P150. Retrieval of an Intracranially Migrated Dental Injection Needle through the Foramen Ovale Using an Extradural Approach

Salah Aoun¹, Tarek El Ahmadieh¹, Vin Shen Ban¹, Hunt Batjer¹, Sam Barnett¹

¹The University of Texas Southwestern, Dallas, Texas, United States

Dental injection needle migration is a rare complication of orthodontal procedures. When these needles fracture, they typically dislodge into the cervical space or the facial musculature. We report a rare case of intracranial migration of an anesthetic injection needle through the foramen ovale. A 59-year-old man underwent the extraction of a right maxillary molar. The distal end of a 25 gauge injection needle broke into his pterygoid musculature causing him pain while chewing. Repeat cranial imaging showed that the needle had migrated, potentially because of his efforts of mastication, and had traversed the foramen ovale into the middle cranial fossa.

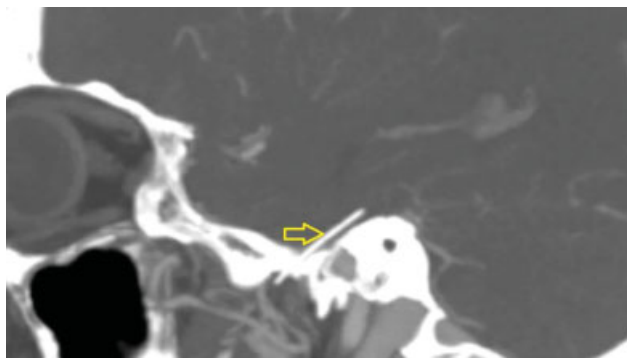


Fig. 1

The patient started experiencing intermittent right facial numbness, likely due to compression or injury to the right trigeminal nerve. Our oral and maxillofacial colleagues did not believe that the needle could be retrieved from its facial end. The patient elected to undergo recovery of the needle through a craniotomy, given the fact that the object was contaminated, and because he was becoming increasingly symptomatic. A right pterional craniotomy was planned.

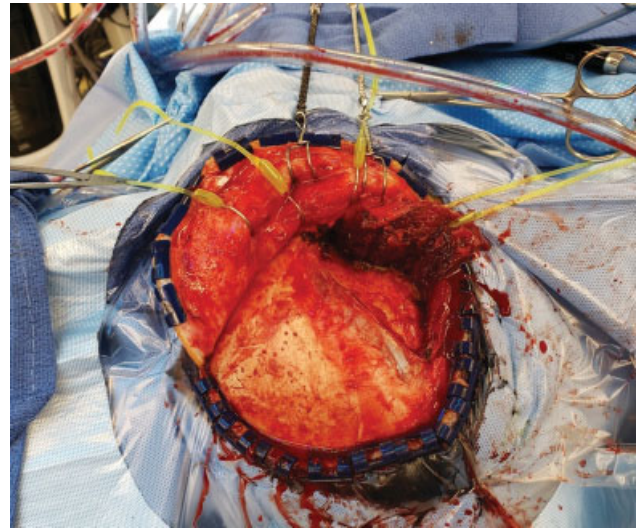


Fig. 2

Extradural dissection was performed until the dura going into the foramen ovale was revealed. We could feel the metallic needle under the dural sheath of the trigeminal nerve.

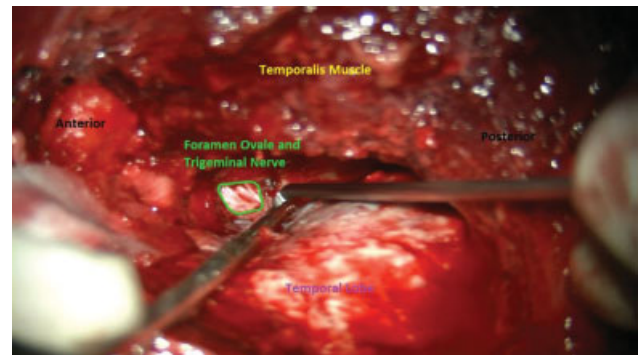


Fig. 3

The dura was opened sharply directly over the needle. We then proceeded to mobilize the needle into the face, and then pulled it out completely through the craniotomy, to avoid injury to the temporal lobe.

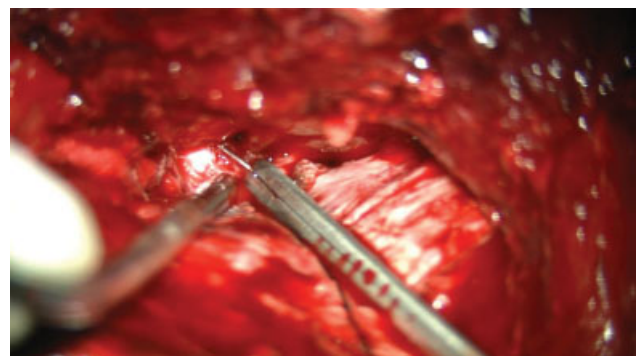


Fig. 4

The patient recovered well and was asymptomatic at the time of discharge.

P151. The Perforator Bone Chip as a Convenient and Effective Autologous Bone Graft for Middle Fossa Encephalocele Repair: A Technical Report

Timothy A Webb¹, Weston Northam², Matthew Dedmon², Nofrat Schwartz², Deanna Sasaki-Adams²

¹Virginia Commonwealth University, Richmond, Virginia, United States

²University of North Carolina, Chapel Hill, North Carolina, United States

Spontaneous middle fossa encephaloceles can precipitate classic symptoms of spontaneous cerebrospinal fluid rhinorrhea or otorrhea, as well as recurrent bouts of meningitis. Additionally, patients may experience years of frustratingly persistent middle ear effusions and infections, conductive hearing loss, and drug-resistant epilepsy prior to recognition of the underlying cause. We describe one such patient who underwent surgical repair, which can be performed using a variety of techniques and materials, some costly and/or time-consuming. During the procedure we utilized an as-yet undescribed technique of bony repair utilizing the bone chip created from the perforator drill as an autologous graft. The perforator drill bit is widely utilized and creates up to a 14-mm bone chip which we felt would be convenient, effective, and economical for use as a bone graft, rather than allograft, split thickness calvarial graft, or other synthetic and biological adjuncts.

The patient discussed is a 55-year-old female with a right sided middle fossa defect discovered in the setting of chronic Beta-2 transferrin positive otorrhea and tegmen erosion demonstrated on computed tomography with an accompanying encephalocele on magnetic resonance imaging. Neurosurgery and Otolaryngology performed a transmastoid/right middle fossa craniotomy for resection of the encephalocele and repair of the skull base defects. A perforator drill was utilized to create burr holes around the circumference of the middle fossa craniotomy in standard fashion. The nature of the automatic clutch mechanism of this widely available drill bit results in an eggshell wafer of bone, the "bone chip," to remain once the drill disengages. Intraoperatively, the decision was made to save the bone chips created by the drill, and use them as autologous bone grafts to repair the skull base defects. At the time of skull base repair, the bone chips were harvested and placed intracranially such that they fully covered the bony defects. These were then reinforced with fascia harvested from the temporalis muscle. The opposing sides of the defects were reinforced from the transmastoid aspect using bone pate and additional temporalis fascia.

The patient had an uncomplicated postoperative course and has since enjoyed sustained resolution of symptoms, further demonstrating the efficacy of perforator bone chip grafting. We posit that the use of perforator bone chips as autologous graft is reasonable as a practical, expedient, far less expensive alternative to commercial products for bony defect repair in encephalocele where the defect is of smaller diameter than the perforator graft.

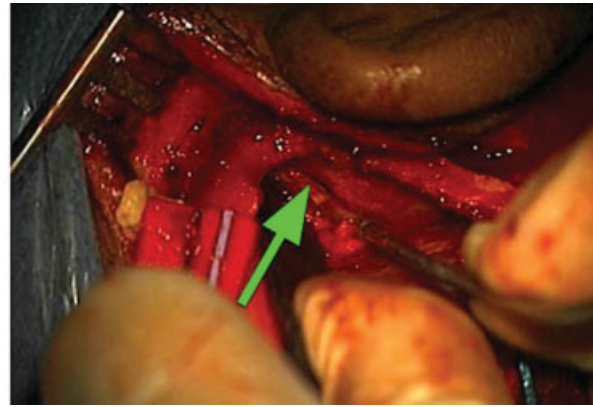


Fig. 1 Middle fossa craniotomy revealing defect (arrow) in the skull base after encephalocele is resected.

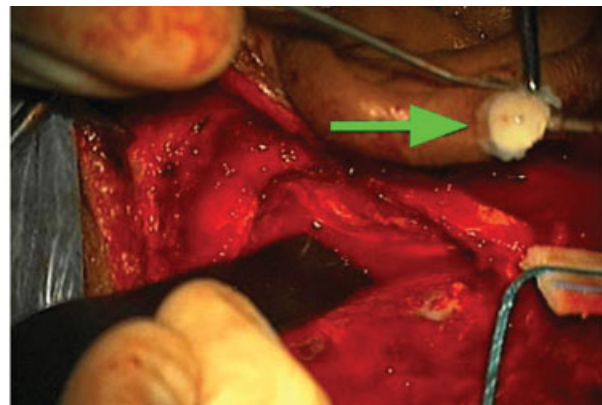


Fig. 2 The perforator bone chip (arrow) is brought into the field in preparation for placement across the skull base defect.

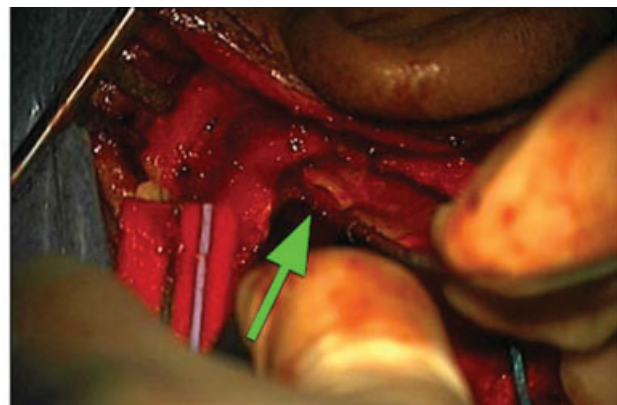


Fig. 3 The perforator bone chip (arrow) provides convenient, adequate bony coverage over the skull base defect.

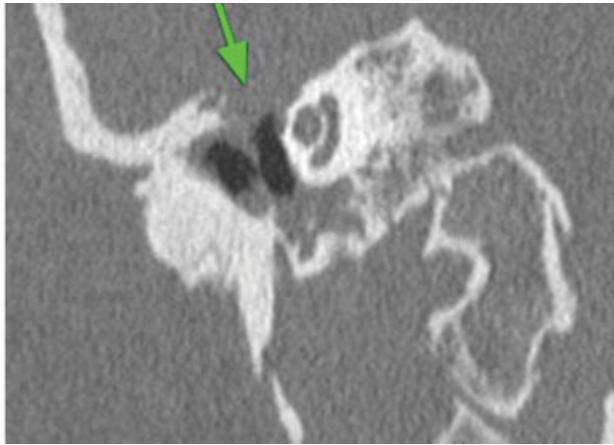


Fig. 4 Right-sided middle fossa skull base dehiscence (arrow) visualized on coronal CT of the right temporal bone.

P152. The Value of 68GA-DOTATATE PET/CT in Sinonasal Neuroendocrine Carcinoma Management and Detection of Local and Distant Metastases: Case Study and Review of Literature

Katherine Liu¹, Sen Ninan¹, David Goldrich¹, Andrey Filimonov¹, Joshua Zeiger¹, Satish Govindaraj¹, Alfred Marc Illoreta¹
¹Mount Sinai, New York City, New York, United States

Background: 68Gallium-dotatate (Netspot) is a newer somatostatin analogue that can be used as a PET tracer to successfully identify neuroendocrine tumors (NETs). It has been shown to detect neuroendocrine tumors that traditional imaging failed to identify and offers superior image quality, spatial resolution of small lesions, and diagnostic utility. Due to the rarity of sinonasal NETs there are few recommendations for 68Ga-dotatate imaging and management options in these patients.

Case Presentation: We report the cases of four patients diagnosed with sinonasal NETs and discuss their management utilizing 68Ga-dotatate imaging. The first patient had a left sinonasal mass identified on CT. 68Ga-dotatate PET/CT identified a NET and revealed a pancreatic primary. Biopsy and immunostaining confirmed sinonasal small cell neuroendocrine carcinoma (SNEC). The second patient had a right sinonasal mass identified on MRI. 68Ga-dotatate PET/CT staging demonstrated NET primary malignancy, as well as T3 vertebral metastatic disease. Biopsy and immunostaining confirmed sinonasal SNEC. The third and fourth patients both had right-sided sinonasal NETs, confirmed by biopsy to be esthesioneuroblastomas (ENBs). 68Ga-dotatate PET/CT was used after surgical resection in these patients to scan for residual tumor and metastases, and the third patient was found to have potential residual tumor. Neither had evidence of local nor distant metastases. **CONCLUSIONS:** 68Ga-dotatate is a superior imaging modality for extrapulmonary sinonasal NETs, with potential to improve diagnostic accuracy and clinical decision making. This report demonstrated the utility of 68Ga-dotatate in sinonasal NET detection. Future studies are required to determine the role 68Ga-dotatate in sinonasal NET management.

P153. Use of Advanced Digital Technology to Enhance Subtotal Schwannoma Resection

Holly E. Oemke¹, Leslie Schlachter¹, Joshua Bederson¹
¹Mount Sinai Hospital, New York City, New York, United States

The use of advanced digital tools in the operating room has increased immensely over the last few years to target tumor resection with a specific aim to help the surgeon to identify preoperatively planned areas where the tumor can be left behind. As more data about the advantages and benefits of a subtotal resection IE: preserving function, these tools can be leveraged in very specific ways. (1–3) Preoperatively a patient-specific simulation is created by fusing volumetric MRI, CTA and Fiesta sequences to create a Heads Up Display (HUD), model. This model can be manipulated intraoperatively throughout the resection process with the use of software tool Intraoperative Structure update, with the aim of calculating the amount of tumor resected and updating the intraoperative model.

A 62-year-old female presented with right-sided facial paralysis and intermittent hearing. The MRI demonstrated a 6-cm facial schwannoma pressing gains her brainstem and cerebellum. Using Brainlab Smartbrush the sinus, tumor, facial nerve V (orange), and Basilar artery were outlined. In conjunction with ENT a trans condylar approach was taken. The painted critical structures were utilized with HUD, an Augmented reality overlay that allows the surgeon to “look ahead.” Both Navigation Update and Intraoperative update software were utilized to maintain the accuracy of navigation as well as update tumor resection.

Navigation Update was performed after dural opening when an error in the accuracy of registration was determined. The tool allowed for an adjustment of approximately 0.5 cm anterior and lateral superiorly the tumor displaced and compressed the Vth nerve near its origin, the tumor was carefully dissected free from the nerve and transected at the superior margin of the internal auditory meatus. After the initial phase of the resection 22% tumors were calculated to be resected with ISU. A second update was done to get the deep portions of the tumor showing 52% tumor remaining. The final calculation of tumor volume was compared with postoperative imaging. The MRI demonstrated a small amount of tumor that was left to preserve nerve function. Initial tumor volume from preoperatively painted objects was calculated to be (24.6 cm³) while Remaining tumor volume on postoperative MRI was calculated (1.38 cm³) and compared with intraoperative findings (12.8 cm³).

Initial experience with the Intraoperative Structure Update tool has shown that there are still improvements that need to be made to accommodate for brain shift. The ability to create a new registration with Navigation update cannot solve for this alone. The ability to use this tool postoperatively to plan for radiosurgery seems promising with future improvements in translating from the OR to the clinic. There are limitations in this experience due to the comparison of a 3 month postoperative MRI as well as challenges collecting proper data points in the surgical cavity. This was due to brain shift and limitations with angulation of pointer in the tumor cavity.

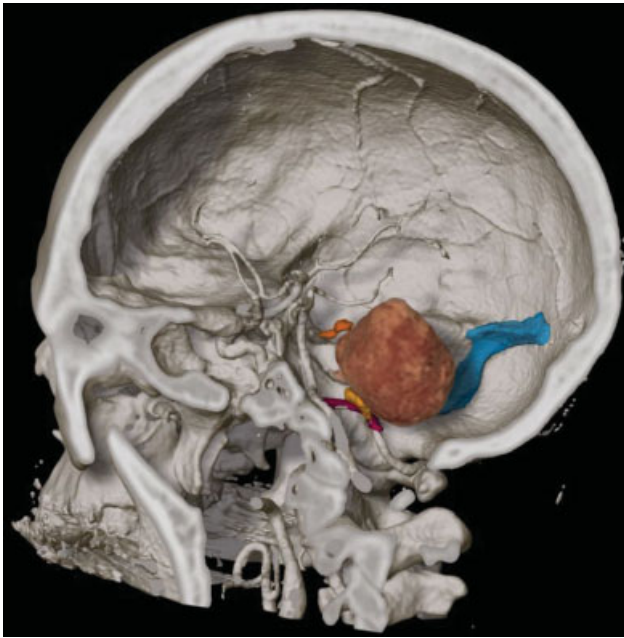


Fig. 1

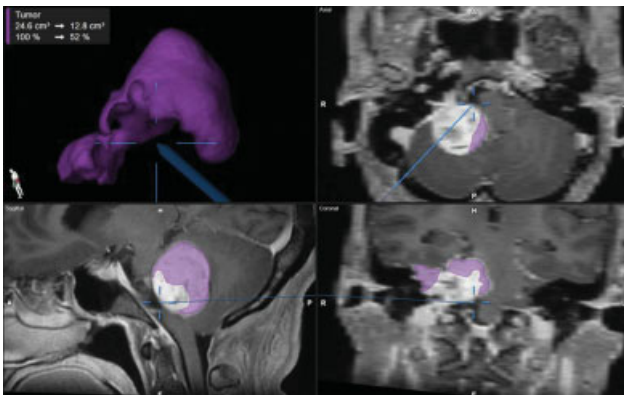


Fig. 2

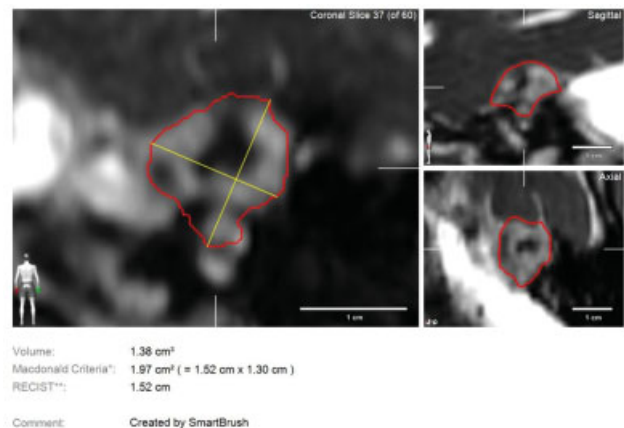


Fig. 3

P156. Endonasal Resection of the Cartilaginous Eustachian Tube with Nasoseptal Flap Closure for Refractory CSF Fistula Following Previous Mastoid and Middle Ear Obliteration
 Stephen Hernandez¹, Vilija Vaitaitis¹, Kevin McLaughlin¹, Daniel Nuss¹

¹Louisiana State University Health Sciences Center, New Orleans, Louisiana, United States

Background: Lateral skull base approaches or previous temporal bone trauma can lead to persistent encephaloceles or CSF fistula despite appropriate management with mastoid obliteration and attempted occlusion of the bony eustachian tube through the middle ear space. These patient scenarios may present a reconstructive dilemma.

Objective/Case Presentation: We present a challenging case of a young male with a remote history of penetrating injury to the lateral skull base. He had resultant cholesteatoma and encephalocele requiring transmastoid repair and obliteration with closure of the external auditory canal. He had persistent infectious complications and subcutaneous emphysema over the temporal scalp when blowing his nose, indicating a persistently patent eustachian tube. There was also some concern for intermittent CSF rhinorrhea on history and examination.

Technique: A submucous resection and partial turbidectomy was first performed to facilitate appropriate exposure and uniaxial two-handed technique. Cuts were designed around the torus, extending into the fossa of Rosenmuller posteriorly. The cartilaginous eustachian tube was then resected and surrounding mucosa meticulously removed. The remaining visible lumen was packed with Surgicel. An ipsilateral nasoseptal flap was then harvested and rotated for inset with excellent coverage. Care was taken to avoid covering any native mucosa as to avoid mucocele formation.

Results: The cavity was carefully packed and the patient observed overnight. He has done well in the immediate postoperative setting with no recurrent subcutaneous emphysema and no evidence to suggest CSF rhinorrhea.

Conclusions: Endonasal closure of the eustachian tube may be an option in cases of recalcitrant CSF fistula and infectious complications. Employing a vascularized septal flap ensures optimal wound healing and ample closure.

P157. Composite Reverse Septal Flap Following Subtotal Septectomy: A Novel Technique for Re-establishing Tip Support Following Oncologic Resection
 Stephen Hernandez¹, Griffin Santarelli², Adam Kimple², Charles Ebert², Brian Thorp², Adam Zanation²

¹LSU Health Sciences Center, New Orleans, Louisiana, United States

²University of North Carolina, Chapel Hill, North Carolina, United States

Background: Resection of neoplasms involving the septal mucosa often includes removal of the involved mucosa and underlying septal cartilage and/or bone. When located anteriorly in the nasal cavity, this can lead to total loss of tip support with collapse of the lower third of the nose.

Objective: We present a case illustrating subtotal septal resection with preservation of the contralateral septal mucoperiosteum and remaining vomer, which can be utilized for reconstruction.

Technique: A 59-year-old male underwent resection of a nasal cavity squamous cell carcinoma in situ, resulting in total cartilaginous septal resection and partial bony resection with complete loss of structural nasal tip support. The contralateral septal mucoperiosteum remained intact and attached to the residual vomer posteriorly. An osteotomy was

designed at the rostrum freeing the remaining vomer from the sphenoid bone, and posterior septal cuts were made to mobilize the composite as an anteriorly based flap. The vomer was then secured in between the medial crural footplates in a tongue-in-groove fashion.

Results: Intraoperatively and in the immediate post-operative setting, he had excellent maintenance of tip support. His final margin status revealed no evidence of tumor or compromise of oncologic resection. He has followed up at the 3-month interval with preserved structural support and no evidence of recurrent disease.

Conclusion: In the appropriately selected patient, the reverse septal composite flap can be considered as an option for reconstruction of the nasal tip support mechanisms following oncologic resection.

P158. Triplicity—Threefold of Skull Base Tumor—Atypical Meningioma Sphenoidal Wing Left, Low-Grade Olfactory Neuroblastoma of Sphenoidal Sinuses, Neurinoma N VIII. SIN. Very Rare Case Report

Jan Hemza¹

¹Department of Neurosurgery Faculty Hospital at Saint Ann, England, United Kingdom

Author described one case of threefold skull base tumor on one lady. This patient had 3 skull base tumors— atypical meningioma sphenoidal wing meningioma left, low-grade olfactory neuroblastoma, and intrameatal neurinoma N VIII. left. The patient have surgery procedure in one step of atypical meningioma sphenoidal wing left side and trans-basal lateral approaches to sphenoidal sinuses, because we mean that is growing meningioma to sphenoidal sinuses, but is not true. The small intrameatal neurinoma now we are following on MRI and waiting with surgery.

P159. Risk Factors Impacting Operative Mortality and Overall Survival in Adults Treated for Skull Base Chordoma and Chondrosarcoma

Adam L. Holtzman¹, James E. Bates¹, Christopher G. Morris¹, Michael S. Rutenberg¹, Ronny L. Rotondo¹, Daniel J. Indelicato¹, Daryoush Tavaniaepour², William M. Mendenhall¹

¹Department of Radiation Oncology, University of Florida College of Medicine, Jacksonville, Florida, United States

²Department of Neurosurgery, University of Florida College of Medicine, Jacksonville, Florida, United States

Purpose/Objective(s): To evaluate the impact of type of treatment center and access to care on mortality and survival in patients treated for skull base chordoma and chondrosarcoma.

Materials/Methods: We queried the National Cancer Database (NCDB) for patients over the age of 18 years with chondrosarcoma or chordoma of the skull base as defined by ICD-O-3 codes for histology and primary disease site. Of 1,241 skull base chordoma and chondrosarcoma patients, 1102 had available follow-up data (chordoma, 488; chondrosarcoma, 614 patients). Facilities were also stratified by volume into low-, medium-, and high-volume centers based on <10 cases, 10–20, and >20 cases, over the period of 2004 to 2014.

Results: Overall 30-day and 90-day mortality rates for the 925 patients who had surgery and available mortality data were 0.9 and 1.5%, respectively. On univariate analysis, only lower levels of education were associated with an increased risk of operative mortality. With a median follow-up 52 months (0.03–152 months), log-rank analysis demonstrated the following factors were associated with higher survival: metro size ($p = 0.0294$), academic center

($p < 0.0001$), age < median ($p < 0.001$), and having private insurance ($p < 0.0001$). Comparing across high-, medium-, and low-volume centers respectively: High-volume centers were most likely to be academic (63% vs. 57% and 41%), deliver radiotherapy (54% vs. 45% and 43%), escalate dose over 70Gy (37% vs. 10% and 7%), and utilize proton radiotherapy (29% vs. 8% and 4%).

Conclusion: While level of education was the only socioeconomic factor significant in univariate analysis of 30- or 90-day operative mortality for skull-base chordoma and chondrosarcoma, treatment and access to an academic facility, high-volume center including being from a metro area, younger age, and private insurance were associated with a statistically significant increase in overall survival.

P160. Osteoplastic Flap without Obliteration for Massive Fronto-orbital Fibrous Dysplasia: A Novel Surgical Approach, Case Report, and Literature Review

Zachary D. Urdang¹, Sallie Long², Marc Otten³, David Gudis³

¹OHSU, Portland, Oregon, United States

²Cornell/Columbia, United States

³Columbia, United States

Fronto-orbital fibrous dysplasia is a rare condition with complex management. We report a case of massive frontal sinus fibrous dysplasia with extensive orbital involvement treated with osteoplastic flap without frontal sinus obliteration. We also review and discuss the literature regarding the management of these lesions with attention to malignant conversion.

A 20-year-old male initially presented with acute right orbital ptosis, diplopia, swelling, edema, and erythema. Emergent imaging demonstrated a right superior orbital mucopyocele in the setting of a massive fibro-osseous lesion involving the entire frontal bone and both orbits, concerning for fibrous dysplasia. He underwent a right anterior orbitotomy with removal of the mucocele to decompress the orbit. The patient elected conservative observation and serial evaluation of the primary fibro-osseous lesion.

Over the subsequent two years, his right ptosis progressed and frontal bossing developed. At age 22 he reported progressive worsening of symptoms including orbital asymmetry and periorbital swelling. He remained neurologically intact with no visual deficits. Surveillance CT imaging demonstrated interval growth of the fibro-osseous lesion. He elected surgical management.

The patient underwent a bicoronal osteoplastic flap without frontal sinus obliteration, including resection of the frontal lesion, bilateral orbital roof decompression, and a concurrent endoscopic Draf 3 frontal sinusotomy with mucosal grafting of the frontal sinus posterior table. He tolerated the procedure well and was discharged home on the first postoperative day. Pathology revealed benign fibrous dysplasia. Postoperative imaging revealed bilateral orbital decompression and wide lesion resection with residual disease in the most lateral portions of the frontal sinuses.

This lesion the final pathology did not indicate malignant conversion. Malignant change in fibrous dysplasia is very rare, and its frequency was estimated to be just 0.5% for monostotic fibrous dysplasia and 4% for McCune–Albright syndrome (Hoshi 2006). This case highlights the importance of close follow-up and surveillance imaging in FD malignant.

P161. Benign Granular Cell Tumor Masquerading as Thyroid Eye Disease

Ryan Larochelle¹, Tadhg Schempf², Peter Hwang³, Benjamin Erickson³

¹University of Colorado, Colorado, United States

²University of Pittsburgh, Pittsburgh, Pennsylvania, United States

³Stanford University, Stanford, California, United States

Introduction: Granular cell tumor (GCT) is a benign neoplasm of Schwann cell origin that occasionally arises within the periocular tissues. Tumors have been reported in the lacrimal sac, eyelid, caruncle, orbicularis muscle, orbit, extraocular muscles, conjunctiva, anterior uvea, and ciliary body. While rectus muscle involvement with associated diplopia has been reported in several cases, imaging typically reveals a discrete mass emanating from the muscle of origin. We present an unusual case of GCT with fusiform inferior rectus muscle enlargement masquerading as thyroid eye disease (TED), managed using a multidisciplinary surgical approach.

Methods: Case report.

Results: A 48-year-old female with a history of hyperthyroidism presented with two years of vertical diplopia. Exam revealed hyperglobus, proptosis, and lid retraction of the left eye (OS), with diminished supraduction ($-3.5/4$) and infraduction ($-2/4$). Orbital MRI demonstrated fusiform enlargement of the inferior rectus with tendinous sparing, and signal isointense to normal muscle on T1 and heterogeneously hyperintense on T2 (Fig. 1). Also noted by the interpreting radiologist were mild medial rectus enlargement and proliferation of postseptal fat. The patient was diagnosed with TED. During attempted strabismus surgery, a firm, homogenous, yellow-white mass was discovered diffusely infiltrating the inferior rectus, including its anterior insertion. The planned muscle recession was therefore aborted and a muscle biopsy performed. Pathologic analysis revealed abnormal connective tissue composed of large polygonal cells with disorganized, granular, eosinophilic cytoplasm. The nuclei appeared dark, mildly pleomorphic, and distorted. No high-grade cytologic features or necrosis were evident to suggest malignancy. Cells were positive for S-100 and CD-68 and negative for AE1/AE3, CD45, melan-A, desmin, and caldesmon. Given these features, a diagnosis of benign granular cell tumor was made. The patient subsequently underwent combined tumor resection with the oculoplastics and otolaryngology services. Trans-conjunctival orbitotomy with orbital floor decompression was performed and the tumor was transected at the anterior insertion. It was subsequently depressed into the maxillary sinus, sectioned at the orbital apex, and delivered via a Caldwell-Luc antrostomy. The orbital floor was reconstructed with a porous polyethylene/titanium implant, which was later removed due to episodic inflammation. Biopsy at this time demonstrated no evidence of tumor recurrence/progression. Despite the absence of an inferior rectus muscle, the patient is close to orthophoric in primary gaze awaiting consideration of strabismus surgery.

Conclusion: In this case, history and imaging initially suggested a diagnosis of TED, which draws attention to the previously unrecognized possibility of GCT masquerading as an orbital inflammatory disorder. It also highlights a novel interdisciplinary strategy for surgical management of large orbital GCTs, with only one prior report of trans-sinus resection.

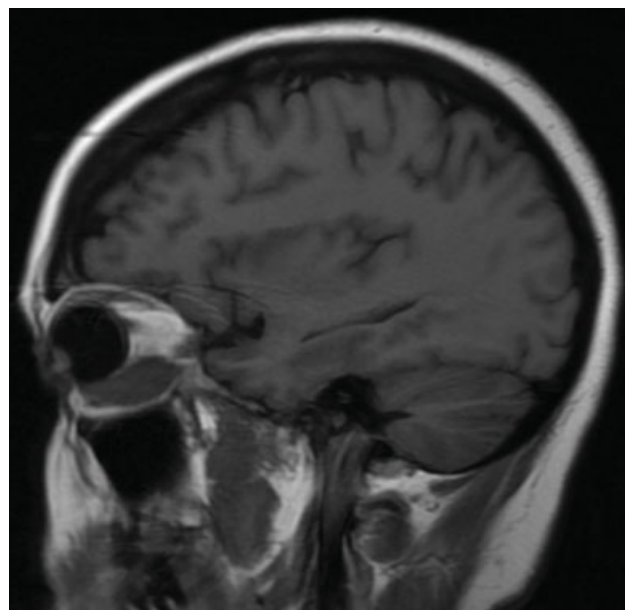


Fig. 1 Orbital MRI demonstrated fusiform enlargement of the inferior rectus with tendinous sparing, and signal isointense to normal muscle on T1 and heterogeneously hyperintense on T2.

P162. Unusual Postoperative Outcomes of Vagal Nerve Lesions: A Case Series

Mackenzie O'Connor¹, Kira Murphy¹, Chandala Chitguppi¹, Joseph Curry¹, Adam Luginbuhl¹

¹Thomas Jefferson University, Philadelphia, Pennsylvania, United States

Introduction: Vagus nerve tumors are rare entities that typically present as slowly developing lateral neck masses that are often clinically silent but may present with symptomatology. Here we discuss vagal nerve pathology with intriguing clinical presentations and postsurgical sequelae.

Methods: Retrospective case series and presentation of initial and postoperative symptoms of surgical management of vagal nerve pathology.

Results: We present a case series involving patients with vagal tumors. In particular, a 44-year-old woman presented with a lower vagal schwannoma with associated syncope and other reported various vague symptoms, such as intermittent heart racing. Enucleation of schwannoma, with preservation of the nerve, resulted in complete resolution of her symptomatology and conservation of vagal nerve function. Additionally, a 47-year-old female with chronic neurogenic cough, failing medical management with nortriptyline and Lyrica, presented for evaluation. A paraganglioma emanating off the lower vagus nerve was identified. There was no vocal cord weakness or elevated metanephrines. Intraoperative decision was made not to resect the tumor due to good vocal fold function, but rather ligation of arterial vessels to the lesion was undertaken. Postoperatively, her cough resolved and vocal fold function remained intact.

These cases are in contrast to a 74-year-old female with a large, high vagal schwannoma with significant growth. She underwent enucleation with preservation of vagal nerve and confirmed function with neuromonitoring at the completion of the resection. Surgery resulted in new onset neurogenic cough that remains recalcitrant to treatment. Use of multiple neuroleptic medication (nortriptyline and

gabapentin) have not resolved her symptoms. Cough only started postoperatively.

Conclusion: These cases offer distinctive presentations of presenting and postoperative course due to vagal tumors, providing interesting insight into these rare tumors and the preoperative and postoperative considerations.

P163. Facial Nerve Schwannoma Complicated by Acute Hemorrhage Posttreatment with Stereotactic Radiosurgery

Mohammad Hassan A. Noureldine¹, R. Tushar Jha², Ivo Peto³, Patrick Malafronte⁴, Kyle Allen³, Siviero Agazzi³

¹Johns Hopkins University School of Medicine, Baltimore, Maryland, United States

²Boston University School of Medicine and Boston Medical Center, Boston, Massachusetts, United States

³University of South Florida Morsani College of Medicine, Tampa, Florida, United States

⁴Ruffolo, Hooper & Associates, MD, PA, Tampa, Florida, United States

Background: Facial nerve schwannomas (FNSs) are rare benign tumors arising from Schwann cells of the facial nerve. In the last decade, stereotactic radiosurgery (SRS) has shown promise in stabilizing or shrinking FNSs.

Case Description: A 71-year-old female patient presented with left facial palsy [House-Brackmann (H-B) 3/6]. MRI showed a 1.85 cm left cerebellopontine angle (CPA) mass that follows the facial nerve trajectory to the geniculate ganglion, most consistent with FNS (Fig. 1A). After 5 months of watchful waiting, a serial MRI demonstrated interval increase in tumor size to 2.15 cm (Fig. 1B).

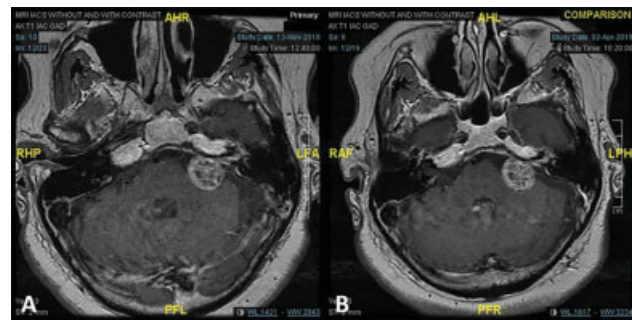


Fig. 1

Treatment with CyberKnife® was recommended (21 Gy/3 fractions) (Fig. 2A). Three days after receiving the first fraction, the patient presented to the emergency department with sudden onset of severe headache, dizziness, imbalance, and worsening of facial palsy (H-B 6/6). She was somnolent; an urgent CT showed a hemorrhagic left CPA mass measuring 3.5 cm, with displacement and compression of the brainstem and fourth ventricle (Fig. 2B).

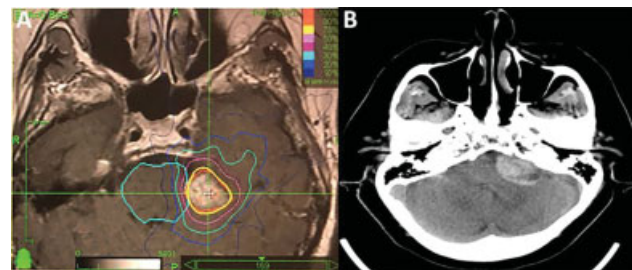


Fig. 2

Surgical intervention was recommended. A transotic approach achieved a successful near-total resection of the FNS (Fig. 3A), where a small remnant was left over a loop of the AICA. The involved facial nerve segment was resected, and a cadaveric donor was used to connect the midportion of the tympanic segment and the stump originating from the brainstem (Fig. 3B).

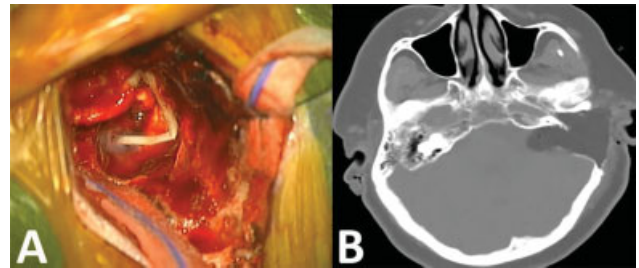


Fig. 3

Histological examination demonstrated schwannoma with infiltration of tumor cells into the facial nerve fascicles (Fig. 4).

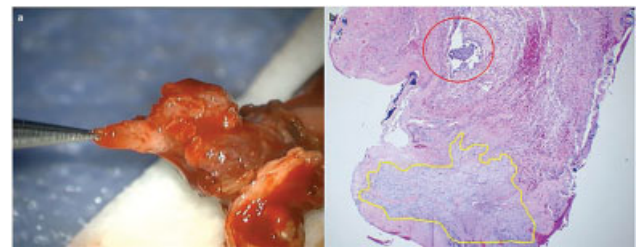


Fig. 4

As expected, the patient progressed to a complete H-B 6/6 facial palsy; Platinum-Gold eye weight insertion was performed to protect the left eye from dryness and injury. The patient was sent to rehab and stayed for 10 days until she regained her baseline functional independence, except for facial palsy, after which she was discharged home.

Discussion: To our knowledge, this report documents the first case of intratumoral hemorrhage in a patient with FNS, which occurred acutely (within 3 days) after receiving SRS with CyberKnife.

Intratumoral hemorrhage in vestibular schwannomas (VSs) is estimated at around 0.4%.¹ However, a rate as high as 18% has been reported following SRS.² By extrapolating hemorrhage rates from VSs, we wonder whether the hemorrhagic occurrence in our patient was due to the pathophysiologic effects of SRS on the tumor or it was a simple coincidence.

In hemorrhagic VSs, facial nerve dysfunction is much more common (33%) upon presentation compared with non-hemorrhagic VSs (6%), and mortality is significantly increased as well (10% vs 0.2%).² Our patient's clinical deterioration due to the acute posterior fossa hemorrhage necessitated surgical intervention, the promptness of which, we believe, was the main factor for the patient's quick return to baseline status.

Conclusion: While SRS remains the treatment of choice for FNSs, symptomatic hemorrhagic transformation may be life-threatening, yet can be successfully managed with

prompt surgical resection and cable nerve anastomosis with good functional outcome, except for the expected facial palsy.

References

1. Carlson ML, Tombers NM, Driscoll CLW, et al. Clinically significant intratumoral hemorrhage in patients with vestibular schwannoma. *Laryngoscope* 2017;127(6):1420–1426
2. Niknafs YS, Wang AC, Than KD, Etame AB, Thompson BG, Sullivan SE. Hemorrhagic vestibular schwannoma: review of the literature. *World Neurosurg* 2014;82(5):751–756

P164. Skull Base Nodular Fasciitis in and Adolescent Male

Conor M. Devine¹, Mark D. Rizzi¹, Tricia Bhatti¹

¹Children's Hospital of Philadelphia, Philadelphia, Pennsylvania, United States

Objectives: To report a case of nodular fasciitis (NF) arising from the skull base of an 11-year-old male.

Study Design: This was a case report and review of the literature.

Case: An 11-year-old male with a history of cranio-spinal radiation for medulloblastoma presented with severe epistaxis and a rapidly growing right nasal mass. Since presentation was consistent with possible secondary malignancy or vascular tumor, preoperative angiography was performed for consideration of embolization. The mass was removed through a transnasal endoscopic approach and found to arise from the right cribriform plate. Frozen section assessment favored a benign process, so a small fragment was left along the skull base to minimize the risk of CSF leak. Final pathologic diagnosis was consistent with NF.

Discussion: NF is a benign myofibroblastic lesion known to mimic sarcoma—the lesions are often rapidly progressive soft tissue masses that demonstrate increased cellularity and mitotic activity on histology. NF has long been suspected to be a reactive process resulting from local tissue injury; however, recent associations with MYH9-USP6 gene fusion have led to the idea that NF may instead be a neoplastic process. In the present case, the first reported originating from the skull base, several aspects of the patient's history suggested a more aggressive diagnosis. Fortunately, NF responds to surgical resection alone and recurrence is rare.

Conclusion: This is the first documented case of NF arising from the cribriform plate. The unusual location in addition to the concerning clinical characteristics made this a challenging diagnostic dilemma. Fortunately, with frozen pathology, and the use of highly specific molecular testing, the correct diagnosis was made and the patient was spared potentially significant morbidity.

P165. Removal of Intracranial K-Wire through Combined Endoscopic and Pterional Approach

Reginald Fong¹, Christoph Griessenauer¹, Andrew Conger¹

¹Geisinger, Germany

Introduction: Cleft palate is a congenital abnormality that has been treated by numerous strategies. One such method involves a Kirschner wire, also referred to as K-wire, placed through the maxilla and vomer to fixate the cleft palate. The K-wire is typically removed after several months because they can migrate. Here we describe the removal of an intracranially migrated K-wire from the anterior skull base through a combined approach.

Methods: A 17-year-old female with history of a cleft palate and maxillary fixation with a K-wire sometime before turning 1-year-old presented to our clinic. She was being evaluated by oral maxillofacial surgery for further cleft palate repair and computed tomography of the head demonstrated that the K-wire migrated intracranially. She had no neurological findings, but requested that the K-wire be removed. Computed tomography angiography was obtained that suggested the K-wire may be adherent or eroding through the left internal carotid artery. Further migration could prove deleterious and the patient was counseled on the risks and benefits and wished to proceed with surgery. The patient was planned for a simultaneous pterional craniotomy and transnasal endoscopic approach in our hybrid operating room equipped with endovascular capabilities.

Results: Intraoperative findings revealed that the K-wire had migrated through the patient's optic nerve. It pierced the optic nerve without any large vessel involvement. The K-wire was removed transnasally without any significant disruption of surrounding structures. The patient tolerated the procedure well and was discharged home after being monitored for any possible CSF leak. No leak was observed. Patient returned for a follow up visit after 2 weeks and 3 months without any complications.

Conclusion: Removal of foreign objects in the skull base can prove to be challenging and sometimes require a combined approach. This case of a migrating K-wire that was found to pierce the optic nerve demonstrates how a combined approach can provide an optimal and safe outcome. In hindsight, a preoperative Goldmann perimetry or other formal visual field test would have allowed an objective measure of visual field deficits. Fortunately for the patient, she remained at her neurological baseline postoperatively without any reported deficits.

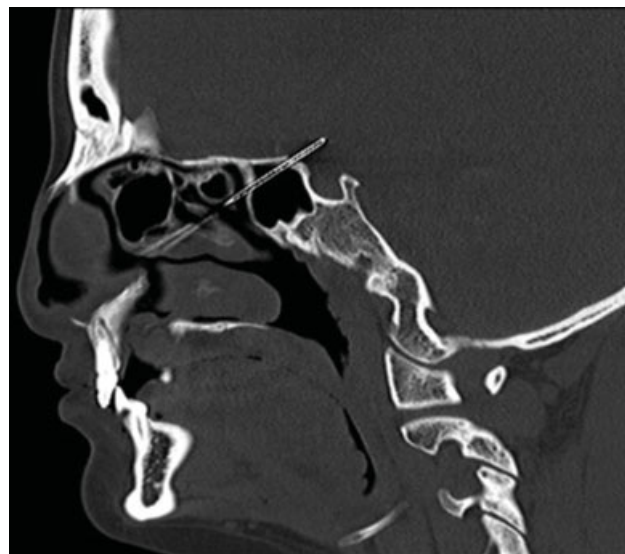


Fig. 1



Fig. 2



Fig. 3

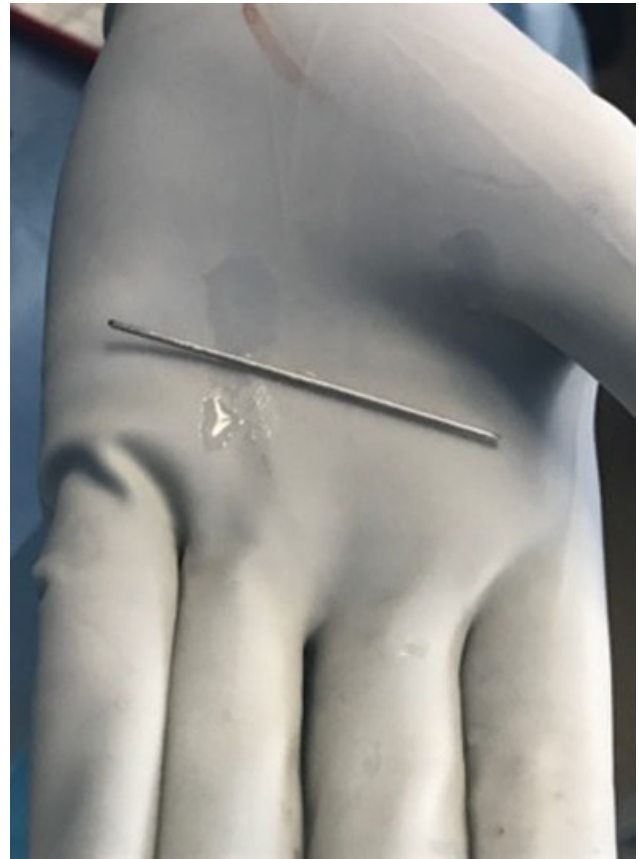


Fig. 4

P167. Novel Pineal Germinoma Model Demonstrates Sensitivity to mTOR Inhibition

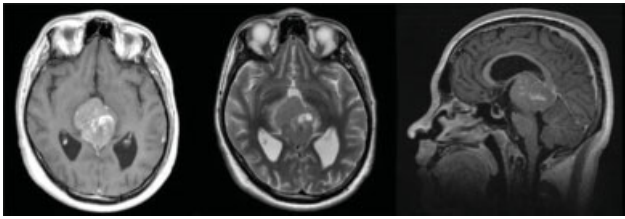
Dominique Higgins¹, Pavan S. Upadhyayula¹, Alexander A. Sosunov¹, George J. Zanazzi², Aayushi Mahajan¹, Nelson Humala¹, Stergios Zacharoulis¹, Peter Canoll¹, Guy M. McKhann II¹, Neil A. Feldstein¹, Jeffrey N. Bruce¹

¹Columbia University Medical Center, New York City, New York, United States

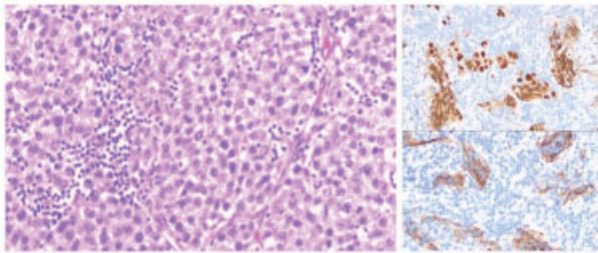
²Dartmouth-Hitchcock Medical Center, Lebanon, New Hampshire, United States

Germinomas are the most common pineal region tumor. Epidemiologically most patients with pineal germinomas are below the age of 20 and males. Patients generally present with symptoms of headache, nausea, and visual disturbances. Although radiation is a mainstay of treatment, long-term impacts on the central nervous system can be profound. These include both behavioral and cognitive deficits. Previous work has linked somatic mutations in the AKT/mTOR pathway to a subset of intracranial germ cell tumors. Our goal here was to determine whether targeted inhibition of the mTOR pathway was effective in pineal germinomas. Ultimately, we aim to determine whether mTOR inhibition is a feasible treatment method for decreasing the radiation doses needed without decreasing treatment efficacy.

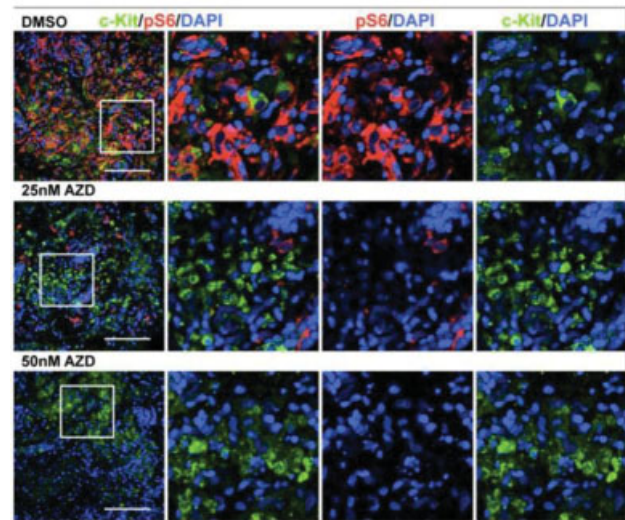
We describe the case of a 19-year-old male with two months of impaired balance and back pain. He began to have visual disturbances along with altered mentation and was thus taken for an MRI. A heterogeneously enhancing 4.4 cm pineal region mass was discovered.



Pathologic examination showed large epithelioid cells with strongly positive Oct-4 and c-Kit staining.



The patient underwent biopsy with subtotal resection through a supracerebellar infratentorial approach. We generated ex-vivo organotypic slice cultures from the surgically resected specimen. Briefly, the surgical specimen was kept in ice-cold artificial CSF solution and then cut to a thickness of 300–500 μ m. These sections were then cultured over a semipermeable membrane insert in a serum free media (DMEM/F12 + N2 supplement). This ex-vivo method allows for study of the intact tumor microenvironment. Furthermore, drug perturbations of tumor tissue can be directly studied. At baseline, the ex-vivo sections demonstrated strong Oct-4 and c-Kit staining; this recapitulated the molecular phenotype observed in-vivo. Moreover, these sections were strongly phospho-S6 positive. Treatment with AZD8055 led to an inhibition of the phospho-S6 staining. Furthermore, this inhibition occurred in a dose-dependent manner and was pronounced at low doses of AZD8055 treatment, with complete inhibition occurring at a dose of 50nM.



From the primary sample, we also dissociated the tumor cells to form a primary cell line. This primary cell line was used for in-vitro assays to determine the efficacy of AZD8055 treatment on cell viability. To determine cell viability an ATP-luminescence assay was used. This cell line showed a clear dose dependent effect of AZD8055 treatment. Importantly, the cells had a robust response to even low doses of AZD8055 highlighting the potential therapeutic benefit that may be achieved in combination of AZD8055 and radiation

Pineal Germinoma Dose Response to AZD

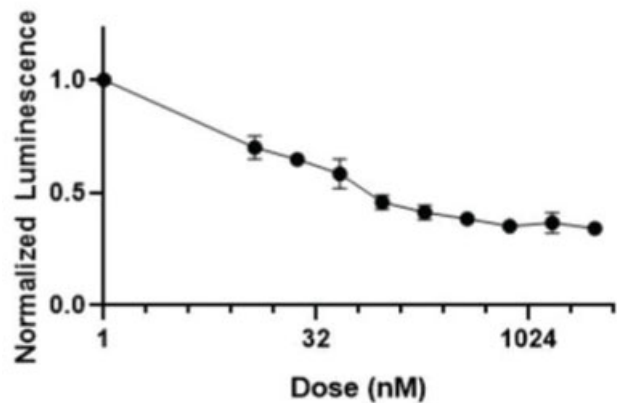


Fig. 4

Given the strong clinical relevance of mTOR inhibitory chemotherapeutics, this is an area that warrants further research. Taken together, we show that AZD8055 treatment has a profound molecular effect and can even impact cell survival and proliferation. Future studies examining the interaction between mTOR inhibition and standard of care radiation are warranted.

P168. Pituitary Macroadenoma Presenting with Complete Nasal Obstruction: A Case Report and Literature Review

Mitchell McDonough¹, Andre A. Le Roux², Christopher J. Chin²

¹Dalhousie Medicine New Brunswick, Saint John, New Brunswick, Canada

²Dalhousie University, Halifax, New Brunswick, Canada

Case: A 58-year-old lady presented with worsening congestion, nasal obstruction, and hyposmia. After failing medical therapy, imaging demonstrated a massive tumor (6.1 cm × 3.9 cm × 5.2 cm) in the nasal cavity with erosion through the skull base superiorly and the clivus inferiorly (Fig. 1). At this point she was referred to our center where she underwent urgent biopsies that demonstrated a pituitary adenoma. Formal visual testing showed decreased visual acuity in the right eye. She then underwent successful endoscopic resection of the tumor with significant improvement clinically.



Fig. 1 A large mass obliterates the sphenoid and posterior ethmoidal air cells.

Review of the Literature: The literature on pituitary adenomas was reviewed. Pituitary adenomas are relatively common lesions and represent ~15% of all intracranial neoplasms. The presentation can be varied, but often patients present with headache, endocrinological disturbances, or visual changes. Nasal obstruction is a very rare presentation of a pituitary adenoma, but has been described in the literature, first being described in 1910.

In the workup of a large nasal mass, imaging and histological exam is essential. The differential for nasal obstruction is rare, but pituitary tumors (including adenoma) should be on the differential and kept in the back of the mind whenever a patient presents with a large posteriorly-based sinonasal mass.

P169. Expanded Endoscopic Endonasal Transtuberulum Transplanum Resection of a Giant Thyroid-Stimulating Hormone Producing Macroadenoma: A Case Report

Dante L. Pezzutti¹, Daniel M. Prevedello¹

¹The Ohio State University College of Medicine, Columbus, Ohio, United States

Thyroid-stimulating hormone (TSH) secreting tumors of the pituitary gland (TSHomas) are a rare tumor that represent up to only 1–2% of all pituitary lesions. TSHomas are often misdiagnosed by clinicians for disorders such as Grave's disease and it is not until patients complain of vision changes/loss that they present to a neurosurgeon. By this time, the tumor can be progressed to a giant macroadenoma (>4 cm) and is complicated by suprasellar extension and invasion. The first line treatment for TSHomas remains surgical resection of the tumor via the endoscopic endonasal approach (EEA), with the goal of removing the neoplastic tissue and returning normal pituitary function and subsequent thyroid hormone levels. We present the following case in support of endoscopic endonasal surgical resection as the first line treatment for TSHomas.

A 21-year-old male presented with a chief complaint of left vision loss and increased blurriness over the course of two months. MRI of the brain and orbits revealed a giant pituitary macroadenoma with suprasellar subarachnoid extension that mainly compressed the left optic nerve. Although no abnormal endocrinopathies were noted in the history and physical examination, laboratory values displayed an elevated TSH (7.936 uIU/mL) and free T4 (1.78ng/dL), thus the diagnosis of a TSHoma was made. Because of rapidly declining vision, we elected to pursue surgical resection of the tumor via endoscopic endonasal transtuberulum transplanum and transellar approaches. Intraoperative MRI demonstrated complete resection of the tumor with no signs of residual tumor. Immediately postoperatively, the patient's TSH levels began to normalize and vision improvement was noted. At 6 weeks follow-up, vision was completely restored and TSH and T4 levels were normalized (2.063 uIU/mL and 0.88 ng/dL, respectively). The patient experienced mild weight gain likely due to a decrease in TSH and subsequent T4 decrease. The patient is confirmed to be in remission with 6 months follow up.

The present case demonstrates an expanded endoscopic endonasal surgical success in achieving complete tumor removal, vision restoration, and re-normalization of TSH/T4 levels in a patient with a TSH-secreting macroadenoma. We recommend surgery as the first line management for TSHomas. Longer period of follow up is necessary to evaluate possible recurrence.

P170. Case Report of Internal Carotid Artery Aneurysm and Pituitary Adenoma: Causal or by Chance Relationship?

Mostafa Shahein^{1,2}, Douglas A. Hardesty¹, Ricardo L. Carrau³, Bradley A. Otto³, Daniel M. Prevedello¹

¹Department of Neurological Surgery, The Ohio State University, Wexner Medical Center, Columbus, Ohio, United States

²Department of Neurosurgery, Aswan University, Qism Aswan, Egypt

³Department of Otolaryngology–Head and Neck Surgery, The Ohio State University, Wexner Medical Center Columbus, Ohio, United States

Background: Unruptured Intracranial aneurysms have the prevalence of 3% in the general population. Pituitary adenomas, meningioma and gliomas have been associated with higher prevalence of aneurysm formation. they hypothesized a causal relationship either resulting from the changes related to the hormone production, or by mechanical compression. In this case the ICA aneurysm has occurred twelve years before a pituitary adenoma has been diagnosed. This question the casual relationship between the ICA aneurysm and the pituitary adenoma.

Case Presentation: A 64-year-old women presented to the clinic with a headache and blurred vision. She has a family history of aneurysm formation in her brother. She underwent

a left frontotemporal craniotomy for ICA aneurysm clipping 12 years earlier. During the follow up period, the patient complained of blurry vision and headache that drew attention to undergo further investigations. Ophthalmologic evaluation revealed a bitemporal superior quadrant hemianopsia. The fact that the patient had two Sugita aneurysm clips no.37 and no.33, MRI brain could not be obtained. Initial CT non contrast images (Fig. 1 A, B) showed a slightly enhancing lesion in the sellar and suprasellar region. Conventional angiography (Fig. 1 C, D) that showed a normal flow in the left ICA with evidence of two aneurysm clips in the left supra-clinoid region in close proximity to the posterior communicating artery. No residual or recurrent aneurysm was detected elsewhere. The patient was planned to undergo an endoscopic endonasal surgery with the use of intraoperative image guidance. The tip of the aneurysm clip (Fig. 2) was noted close to this area and the tumor was dissected from around the clip. Last portion of the tumor extending posteriorly on the top of the dorsum sellae was removed. The patient tolerated surgery well with no postoperative complications. Follow up CT scan (Fig. 1 E, F) after surgery showed no residual tumors. No recurrence was encountered in 8 year follow up period. She is neurologically intact with no need for hormonal replacement.

Conclusion: The association between the ICA aneurysm and pituitary adenoma has been discussed in the literature. Though previous theories explained this as a hormonal or mechanical effect on surrounding vasculature that cause the aneurysm. This case showed the reverse. This question the causal relationship of such association. Surgeons should be aware of this possible association to avoid complications.

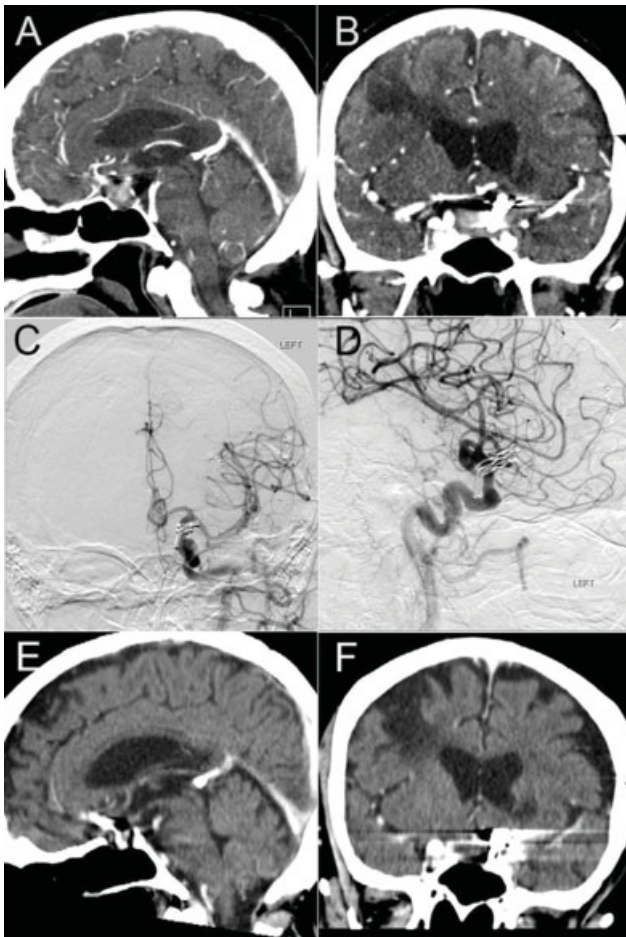


Fig. 1 CT scans sagittal (A) and coronal (B) sections showing hyperdense sellar lesions in close proximity to an aneurysm

clip. DSA coronal (C) and sagittal (D) showing no residual or recurrence of previously clipped aneurysm. Postoperative CT scans sagittal (E) and coronal (F) sections showing gross total resection of the tumor with no residuals.

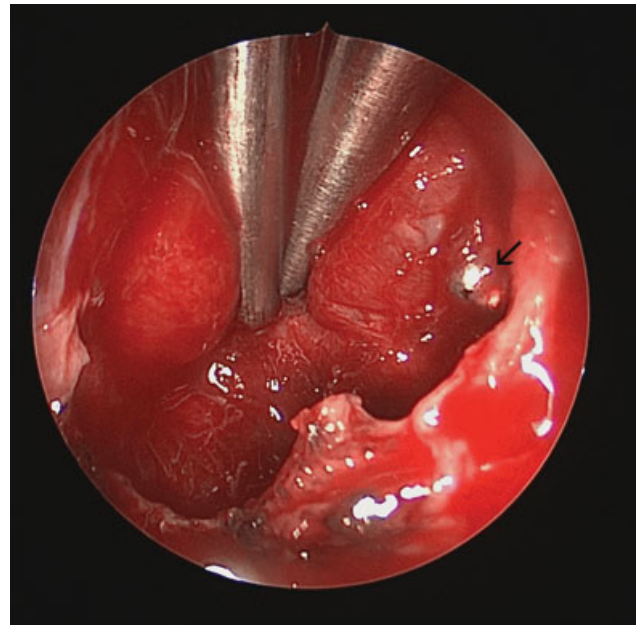


Fig. 2 Intraoperative endoscopic view of the tip of the aneurysm (arrow) clip encroaching on the sellar space.

P171. Cyclic Cushing's Disease in Mixed Gangliocytoma-Pituitary Adenoma Tumor: Case Report

Yury Anania¹, Venteicher S. Andrew², Pearce M. Thomas³, Gardner A. Paul⁴

¹Center for Cranial Base Surgery, University of Pittsburgh, Pittsburgh, Pennsylvania, United States

²Department of Neurosurgery, University of Minnesota, Minneapolis, Minnesota, United States

³Department of Pathology, University of Pittsburgh, Pittsburgh, Pennsylvania, United States

⁴Department of Neurosurgery, University of Pittsburgh Medical Center, Pittsburgh, Pennsylvania, United States

Background: Cushing's disease can be a challenging diagnosis and is independent of radiographic findings. A 70 year-old woman was referred for surgical consultation after an incidental finding of a sellar lesion. Despite an absence of symptoms, on physical examination she appeared Cushingoid. Following extensive laboratory evaluation and inferior petrosal sinus sampling, a diagnosis of cyclic Cushing's disease was finally made. She then underwent endoscopic endonasal resection of the lesion.

The specimen was evaluated intra-operatively by touch preparation, revealing large ganglion cells with abundant cytoplasm and large nucleoli as well as dyscohesive adenomatous anterior pituitary cells. The impression of a bimorphic cell population was confirmed on frozen and permanent sections, with ganglion cells intimately admixed with adenomatous cells. The majority of adenomatous cells were positive for ACTH. The ganglion cells, in contrast, showed cytoplasmic and weak nuclear immunoreactivity for NeuN.

Mixed gangliocytoma-pituitary adenoma is a rare lesion, mostly described in literature through case reports

and small case series. It has been recently classified as a distinct entity in the 4th edition (2017) of the WHO Classification of Pituitary Tumors, and most reported cases are somatotrophs. The histogenesis of these biphasic gangliocytoma-pituitary adenoma tumors is still a matter of debate, and many theories have been proposed: 1) transdifferentiation of adenomatous cells into neuronal/gangliocytic cells; 2) a common progenitor/stem cell capable of transformation of the two cellular components; 3) abnormal migration of ganglion cells from the hypothalamus within the adenohypophyseal parenchyma during the early phase of embryogenesis.

Twelve cases of mixed gangliocytoma-pituitary corticotroph adenoma were reported in a recent review of the literature, but none of them showed clinical features of cyclic Cushing's disease. To our knowledge, this is the first described case of coexistence of these two rare entities.

It is possible that the presence of a gangliocytic population in the context of the adenomatous parenchyma might influence secretion of ACTH.

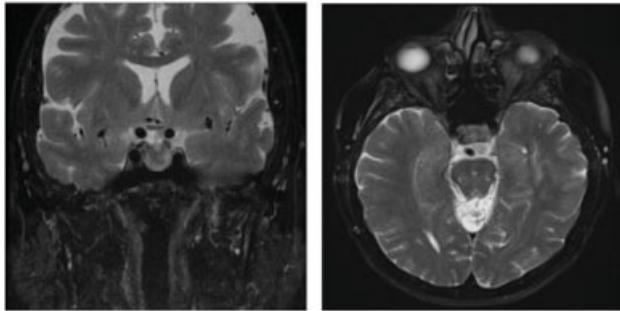


Fig. 1

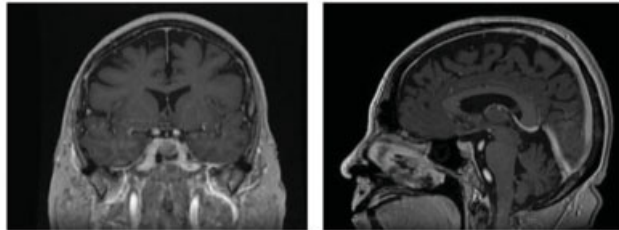


Fig. 2

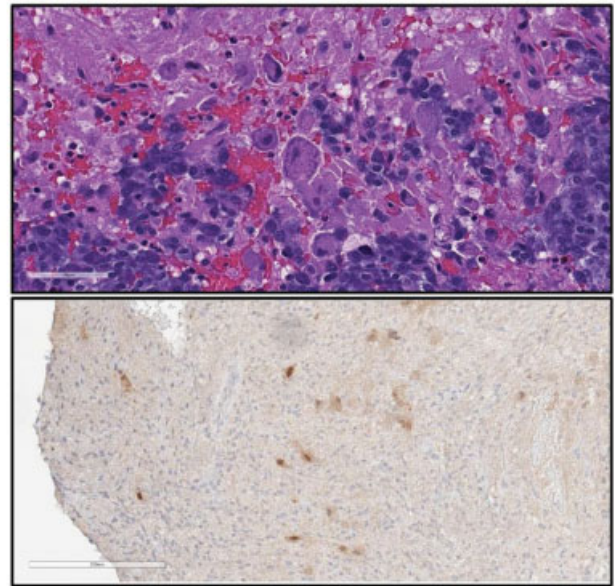


Fig. 3

P172. Pituitary Stalk Gangliogliomas

Oluwaseun Omofoye¹, Griffith Harsh¹

¹ University of California Davis, Davis, California, United States

Background and Importance: Gangliogliomas rarely occur in the sella or parasellar region and are almost never seen in the pituitary stalk. Seven cases of gangliogliomas occurring in this region have been reported, and only one case involved a tumor within the pituitary stalk. Of the other six tumors, two occurred in the neurohypophysis, one was in the adenohypophysis, the location of one was unspecified, and two extensively invaded the optic chiasm, hypothalamus and brainstem. To our knowledge, this is only the second reported case of a pituitary stalk ganglioglioma.

Clinical Presentation: A 51-year old woman with an eleven-month history of polydipsia, polyuria and diagnosis of diabetes insipidus presented for evaluation. Magnetic Resonance Imaging of the brain revealed contrast-enhanced thickening and anterior bowing of the hypophyseal stalk. Transsphenoidal exploration found a firm, white mass, integral to the right side of the enlarged pituitary stalk. Pathologic analysis of the biopsy showed WHO grade I ganglioglioma. The patient tolerated the procedure well and required no endocrinologic treatment other than desmopressin.

Results: Including the 6 other reports of gangliogliomas presenting in the pituitary sella, the patient's ages ranged from 7 to 89 with a mean of 45.7 years. The most common presenting symptoms were headaches and vision changes. Three cases reported pathology grades, which was WHO grade 1 for all those cases. The most common endocrine abnormality was hyperprolactinemia, and there was only one other report of decreased vasopressin, though this occurred in a ganglioglioma of the neurohypophysis. The surgical approaches were evenly divided between endoscopic endonasal approach and craniotomy; with three cases each, while one patient was diagnosed on autopsy. Five cases reported the extent of resection; three had a gross total resection, and there were two cases of subtotal resection.

Discussion: Multiple theories have been postulated regarding the pathogenesis of gangliogliomas and ganglion cell tumors. Neuronal differentiation, pluripotent cells, or malformative neuronal lesions with glial components representing hamartomatous elements have all been suggested as

origin pathways. Ongoing research studies into the molecular basis of gangliogliomas are shedding light on possible prognostic factors and therapeutic options. However, the predominant treatment modality for pituitary stalk gangliogliomas is surgical resection when possible. Two cases of pituitary stalk gangliogliomas with tumor extension to the optic-chiasm and hypothalamic pathway have utilized adjuvant radiotherapy. There have been reports of high-precision stereotactic conformal radiation therapy to a dose of 54 Gy in 30 fractions. Despite a reported 15-year overall survival rate of 94 percent, the rate of malignant degeneration of gangliogliomas have been noted to vary between 4 and 32 percent. Though adjuvant radiotherapy has been shown to prolong recurrence time without improving overall survival, a controversy with its use is the risk of accelerating malignant transformation of a previously benign ganglioglioma, several cases of which has been reported.

Conclusion: Pituitary stalk gangliogliomas are extremely rare entities. The diagnosis should be considered in patients who present with enlargement of the pituitary stalk. Since management differs for possible alternative diagnoses, biopsy should be performed for pathologic certainty.

P174. The Effectiveness of Endoscopic Endonasal Surgery for Pituitary Adenomas: Clinical Outcomes and Postoperative Complications at a Single Institution

Edinson Najera¹, Eugenio Cardenas¹, Ariel Kaen¹, Pablo Remon², Ignacio Martin Schrader¹, Alfonso Soto²

¹Department of Neurological Surgery, Hospital Universitario Virgen del Rocío, Sevilla, Spain

²Department of Endocrinology and Nutrition, Hospital Universitario Virgen del Rocío, Sevilla, Spain

Background: The endoscopic endonasal approach (EEA) has become the gold standard for the surgical treatment of pituitary adenomas due to the wide-angle view and exposure it provides. In this study, the authors seek to evaluate the EEA's real contributions to the prognosis and survival of pituitary adenoma patients.

Methods: A retrospective analysis was conducted of all endoscopic pituitary surgeries for adenomas completed between 2015 and 2018 at a single tertiary referral institution. 129 patients met the inclusion criteria. Patient complications, resection, and remission rates were assessed.

Results: Out of 129 patients, 63 (49%) had nonfunctional adenomas and 73 (51%) had functional adenomas, including 39 with growth hormone-secreting tumors and 27 with adrenocorticotropic hormone-secreting tumors. Amongst the 39 patients with growth hormone-secreting adenomas, 5 had microadenomas and 34 had macroadenomas. Radiographically, 46% of the cases were Knosp Grades 3 and 4. A cure (IGF-1 <100) was obtained in 100% of the microadenomas and 67.6% of the macroadenomas, with a global cure rate of 72%. Amongst the 27 patients with adrenocorticotropic hormone-producing adenomas, 21 had microadenomas and 6 had macroadenomas. Radiographically, 14% of the cases were Knosp Grades 3 and 4. A cure (salivary and free urine cortisol) was obtained in 81.8% of the microadenomas and 80% of the macroadenomas, with a global cure rate of 81.4%. Out of the 63 cases with nonfunctional macroadenomas, 45 were under 25 mm and 9 were over 40 mm. Radiographically, 63.4% of the cases were Knosp Grades 3 and 4. Gross total resection was achieved in 64.5% of the cases. 40 (63.5%) of the patients presented prior campimetric deficit. Total improvement was obtained in 26, partial improvement in 12, and stability in 2. The mean follow-up was 20 months for patients with functional adenomas and 15 months for those with nonfunctional adenomas. One patient

developed a postoperative CSF leak, 2 patients presented epistaxis, and no postsurgical visual disorder or cranial nerve palsies were detected.

Conclusions: Endoscopic endonasal surgery in experienced hands can provide a better prognosis for patients diagnosed with pituitary adenomas. Aggressive cavernous sinus surgery can provide a cure rate even higher than those published to date.

P175. Pituitary Hyperplasia Causing Complete Bitemporal Hemianopsia with Resolution Following Surgical Decompression: Case Report

Nataly Raviv¹, Tyler J. Kenning¹, Carlos D. Pinheiro-Neto¹, Maria Peris-Celda¹

¹Albany Medical Center, Albany, New York, United States

Introduction: Pituitary hyperplasia (PH) may occur in the setting of pregnancy or end-organ insufficiency, as well as with medications such as oral contraceptives and antipsychotics, or may be idiopathic.¹ Pituitary size may vary according to gender and age, and gland enlargement in a young and healthy woman may be defined with a height of >9 mm.² PH is often found incidentally and surgical intervention is usually unnecessary, as it rarely progresses and may be managed by treating the underlying etiology.¹ The objective of this clinical case report is to demonstrate a case of a patient with idiopathic PH who developed complete bitemporal hemianopsia and amenorrhea despite benign imaging and laboratory findings.

Case Description: We present the case of a twenty-four year old woman with no significant past medical history, who presented with a 3-week history of visual disturbances. The patient was evaluated by a neuroophthalmologist who identified a left temporal visual field defect on visual field testing. Brain MRI revealed a 4–5 mm hypoenhancing focus within the inferior pituitary gland that was concerning for a pituitary microadenoma. The gland appeared to be enlarged, touching and abutting the chiasm, but no significant anatomical compression was noted. The patient also reported amenorrhea over the previous seven months with a negative pregnancy test. Pituitary function tests were within normal limits. Follow-up visual field testing 2 weeks after the initial evaluation showed progression of the visual field defect to complete bitemporal hemianopsia. Repeat MRI imaging did not show significant changes, with exception of the complete disappearance of the 4–5 mm hypoenhancing lesion. The patient was offered sellar decompression, biopsy and gland exploration, and elected to proceed with surgery. She underwent surgical decompression of the anterior and inferior walls of the sella turcica, dural opening, biopsy, and exploration of the gland through an endoscopic endonasal transsphenoidal approach. No tumor was identified. The patient's vision immediately improved after surgery and a follow-up visual field exam revealed complete resolution of the bitemporal hemianopsia. Menstruation resumed three days later, and postoperative cortisol levels were within normal limits. The patient remains asymptomatic. Pathology results demonstrated pituitary hyperplasia.

Conclusion: In this report, we illustrate how PH can cause complete bitemporal hemianopsia, even in the setting of mild anatomical compression of the optic chiasm. In these cases, complete resolution of the symptoms can be achieved with surgical decompression.

References

1. De Sousa SM, Earls P, McCormack AI. Pituitary hyperplasia: case series and literature review of an under-recognized and heterogeneous condition. *Endocrinol Diabetes Metab Case Rep* 2015;2015:150017

2. Chanson P, Daujat F, Young J, et al. Normal pituitary hypertrophy as a frequent cause of pituitary incidentaloma: a follow-up study. *J Clin Endocrinol Metab* 2001;86(7):3009–3015

P176. Tumor Consistency as a Predictor of Successful Pseudocapsular Dissection of Pituitary Adenomas

Giyarpuram N. Prashant¹, Won Kim¹, Marilene Wang¹, Marvin Bergsneider¹

¹ University of California, Los Angeles, California, United States

Pseudocapsular dissection is a well described technique for the separation of pituitary tumors from the normal pituitary gland. It has been suggested that this surgical technique may allow for improved tumor identification and gross-total resection of these lesions. It is well known that smaller pituitary adenomas tend to have a higher proportion of intact pseudocapsules and therefore tend to have more successful extracapsular dissections. However, tumor consistency and firmness has not been evaluated as a predictor of successful pseudocapsular dissection. Therefore, we evaluated whether the intra-operative consistency of the tumor predicted the rate of successful pseudocapsular dissection. Exclusionary criteria included final pathology that was not consistent with pituitary adenoma, imaging or clinical evidence of apoplexy, prior endoscopic endonasal surgery, and cases in which pseudocapsular dissection was not planned or attempted. This resulted in a series of 475 consecutive pituitary adenomas. Tumors were classified as a “complete” pseudocapsular dissection if the tumor was removed en bloc with the capsule, or in the case of larger tumors if the tumor was initially centrally debulked then a complete pseudocapsular dissection was performed. All tumors in which this was attempted but could not be performed were classified as a failed pseudocapsular dissection attempts. At the same time, tumors were classified as “soft” if they could be removed with suction, “semi-firm” if they could be removed with curettes, and “firm” if sharp dissection was required. There was no significant difference in gender or age of either group. Both groups consisted of 57% nonfunctional adenomas and 43% functional (secreting) adenomas. Rate of intra-operative CSF leak was 31% in the failed pseudocapsular dissection group and 20% in the successful pseudocapsular dissection group. In the group with failed pseudocapsular dissections, 76% of tumors were soft, 17% were semi-firm, and 7% were firm. In the group with successful pseudocapsular dissections, 72% of tumors were soft, 22% were semi-firm, and 6% were firm. There was no statistical difference with respect to success of pseudocapsular dissection and tumor consistency. In this study, pituitary tumor consistency was not a statistically significant predictor of the success of pseudocapsular removal of tumor. Further studies are needed to determine what factors may play a role in the success of an extracapsular dissection of pituitary adenomas.

P177. Completely Resected Pituitary Macroadenomas Have a Low Risk of Long-Term Radiographic Progression

Jennifer A. Kosty¹, Yair M. Gozal², Mario Zuccarello³, Norberto O. Andaluz⁴, Lee A. Zimmer⁵, Bharat Guthikonda¹

¹Louisiana State University HSC Shreveport, Shreveport, Louisiana, United States

²Mayfield Clinic, Cincinnati, Ohio, United States

³University of Cincinnati, Cincinnati, Ohio, United States

⁴University of Louisville, Louisville, Kentucky, United States

⁵Mercy Health, Cincinnati, Ohio, United States

Background: In 2017, the FDA issued a warning regarding the risk of chronic retention of gadolinium in several

body tissues, including brain, following the administration of gadolinium-based contrast agents. This risk is heightened in patients requiring multiple lifetime doses, such as those who have undergone pituitary adenoma surgery. In this study, we assessed the long-term risk of radiographic recurrence of pituitary macroadenomas in an attempt to define patients at low risk for progression, in whom fewer surveillance scans may be warranted.

Methods: The records of all patients undergoing endoscopic endonasal transsphenoidal resection of pituitary macroadenomas between 2007 and 2011 at our institution were reviewed. Only patients with more than 3 years of clinical and radiographic follow-up were included.

Results: 45 patients with at least 3 years of follow-up were identified, 33 of whom had at least 5 years of follow-up. The average age was 53 ± 18 years. Twenty patients were male, 26 were female. Thirty-two had non-functioning adenomas (average diameter 2.5 ± 1.3 cm), and 14 had hormone-secreting tumors (average diameter 2.4 ± 0.7 cm). The most common presenting symptoms were visual loss (42%), endocrinopathy (29%), and headache (16%).

Among patients with non-functioning tumors, tumor resection was complete in 18. One-hundred percent of these patients had no evidence of tumor recurrence 3 years after surgery. More than 5 years of follow-up was available for 10 of these patients (average 8 ± 1.6 years). No tumor recurred over this time period. In contrast, only 8/12 (66%) patients with subtotal resections and no additional treatment remained progression-free at 3 years. This was significantly less than patients with complete resections ($X^2 = 4.28$, $p = 0.04$). Four patients with subtotal resection and stable imaging at 3 years were followed more than five years (average ± 2 years). Two of these demonstrated progression, and two did not.

Among the 13 patients with functioning tumors, only 4 (26%) had complete resections. All 4 had greater than 5 years of follow-up demonstrating no radiographic recurrence. In contrast, of 7 patients with subtotal resections and no additional treatment, 5 (66%) demonstrated stable tumor size at 3 years after surgery. Four of these patients had greater than 5 years of imaging follow-up (average 8.5 ± 2 years), and all demonstrated stability of their lesions.

Conclusions: These preliminary results suggest that patients with completely resected pituitary lesions are at a low risk of progression and surveillance imaging may safely be widely spaced. In contrast, those with subtotal resections require more frequent surveillance imaging.

P178. Endoscopic Ethmoido-Pterygoido-Sphenoidal Approach to the Cavernous Sinus in Recurrent Invasive Pituitary Adenoma

Rafael Martinez-Perez¹, Giuliano Silveira-Bertazzo¹, Bradley A. Otto¹, Ricardo L. Carrau¹, Daniel Prevedello¹

¹Wexner Medical Center, The Ohio State University, Columbus, Ohio, United States

Background: Sellar region is an anatomically complex region in close relationship with important neurovascular structures. As such the surgical treatment of recurrent aggressive pituitary adenomas invading the cavernous sinus represents an operative challenge, especially when a re-intervention is warranted. Scar tissue and previous interventions materials hinders a clear visualization and understanding of the surgical anatomy through the endoscopic endonasal corridor.

Methods: Throughout a 2D surgical video, we describe in detail the surgical technique of the ethmoido-ptyerygoido-sphenoidal approach (EPSa) for the surgical re-operation of a

recurrent pituitary adenoma in the context of a Nelson’s syndrome after bilateral adrenalectomy.

Results: This video details the surgical anatomy of the sellar region to facilitate the identification of surgical landmarks and anatomic boundaries with the goal of avoiding injury to the neurovascular structures involved in this approach. Anatomically, the authors would like to highlight the importance of few surgical anatomical landmark for getting access to the cavernous sinus: (1) the lateral orbital optic carotid recess (LOCR) is a bony depression that corresponds intracranially to the optic strut, a bony extension inferior to the anterior clinoid process, that separates the carotid artery from the optic nerve (2) the medial optic canal recess located at the inferomedial margin of the paraclinoid ICA; (3) the carotid protuberance; and (4) the vidian canal, which is considered to be the most critical landmark to accessing the anterior genu of the petrous horizontal segment of ICA. It is localized in the pterygoid wedge at the intersection between the sphenoid sinus floor and the medial pterygoid plate

Conclusion: The EPSa is a versatile approach that uses the endoscopic transsphenoidal route and thereby, reduces brain retraction. Anatomic landmarks offer a good sense of the area that is exposed in reoperations and reduce the risk of injury of important neurovascular structures located within the cavernous sinus and the parasellar region.

P179. Postoperative Care Coordination for Acoustic Neuroma Patients: Improving Patient Satisfaction

Allie Mains¹, Mario Zuccarello¹, Ravi Samy¹, Scott Shapiro¹
¹University of Cincinnati, Cincinnati, Ohio, United States

Background: Treating patients with acoustic neuroma (AN) requires a multidisciplinary approach that includes many subspecialties including neurosurgery, otolaryngology, physical therapy and rehab, facial rehabilitation and vestibular therapy. This care is unique to this patient population and is different than other types of brain tumors. Patients often feel misunderstood and lost in navigating their postoperative care and expectations. We work closely with the Acoustic Neuroma Association to assess patient needs and work with our patients to improve their care and outcomes. Our goal is to provide care coordination specific to acoustic neuroma patients to improve outcomes and patient satisfaction.

Objective: At the University of Cincinnati we performed over 60 acoustic neuroma resections a last fiscal year. Our aim is to have a Nurse Navigator dedicated specifically to these patients to assist them in navigation of their unique preoperative and postoperative care. Along with providing written recommendations and guidance in the form of a booklet for preoperative and postoperative care.

Method: This presentation will explore the multidisciplinary approach to the management of AN patients. The unique pre and postoperative needs of patients with acoustic neuroma. We will propose a description of a specialized Nurse Navigator along with the role of the Nurse Navigator in the care of these patients. We will also outline the development and use of a booklet to assist with patient and caregiver education and support.

Results: We will discuss the impact this specialized care will have on the post op outcomes of these patients along with the improved patient satisfaction.

Conclusion: Specialized nurse navigation for patients with skull base tumors, specifically acoustic neuroma’s, is an essential part of improving patient satisfaction and outcomes.

P180. Utility of Postoperative Nasal Steroid Irrigations in Sinonasal Tumor Patients

Theodore C. Lin¹, Cameron P. Heyd², Sylvia Horne³, Auddie M. Sweis¹, Tran B. Locke¹, Heather Ungerer¹, George Gardner¹, James N. Palmer¹, Nithin D. Adappa¹
¹Department of Otorhinolaryngology - Head and Neck Surgery, University of Pennsylvania, Philadelphia, Pennsylvania, United States
²Lake Erie College of Osteopathic Medicine, Bradenton, Florida, United States
³State University of New York Downstate Medical Center, Brooklyn, New York, United States

Introduction: Postoperative care for endoscopic sinus surgery (ESS) often includes nasal saline and/or steroid irrigations to effectively control symptoms. Though topical corticosteroid use has been well characterized for managing inflammatory sinus diseases, their role in managing symptoms after ESS for sinonasal tumors is unclear. We seek to quantify the impact of postoperative steroid irrigations on the quality of life in patients with sinonasal tumors who have undergone ESS.

Methods: All patients who underwent surgical resection of a sinonasal tumor at this institution from 2000 to 2019 were included in the study. The electronic medical record was reviewed for patient factors, postoperative steroid irrigation use, and 22-item Sino-nasal Outcome Test (SNOT 22) scores and unpaired *t*-tests were performed.

Results: 101 patients were assessed (64% males) and divided into (1) no steroid irrigation (NSI) and (2) steroid irrigation (SI) cohorts. The groups were similar in number (NSI *n* = 44, SI *n* = 57) and baseline preop SNOT 22 scores did not differ significantly (NSI: 28.8 ± 23.7, SI: 23.5 ± 20.2; *p* = 0.2784). 3-, 6-, 12-, 18-, and 24-month post-op SNOT 22 scores did not significantly differ between groups (Table 1), though the steroid group showed a greater improvement in SNOT 22 scores compared with the NSI cohort.

Conclusions: Though corticosteroid irrigations are a routine part for managing inflammatory sinus disease, their role in postoperative management after ESS for sinonasal tumors is unclear. Further studies should be performed to investigate the costs and benefits of steroid irrigations in this patient population.

Table 1 Postoperative SNOT 22 scores (mean ± SD) in patients with or without steroid irrigations

Snot 22 scores	No steroid irrigation	Steroid irrigation	<i>p</i>
Pre-op	28.8 ± 23.7	23.5 ± 20.2	0.2784
3 months post-op	16.7 ± 16.6	12.1 ± 12.1	0.2403
6 months post-op	18.7 ± 18.4	12.6 ± 13.3	0.1511
12 months post-op	16.9 ± 20.8	11.3 ± 13.8	0.2809
18 months post-op	18.4 ± 18.3	14.2 ± 16.0	0.4505
24 months post-op	16.7 ± 18.0	10.2 ± 11.0	0.1421

This document was downloaded for personal use only. Unauthorized distribution is strictly prohibited.

P181. Improved Sinonasal Quality of Life Outcomes Following Endoscopic Endonasal Repair of Spontaneous Cerebrospinal Fluid Leaks

Feras Y. Ackall¹, Lyndon Chan¹, Kevin Choi¹, Jordan Teitelbaum¹, Patrick Codd¹, Ali Zomorodi¹, Ralph Abi Hachem¹, David W. Jang¹

¹Duke University Medical Center, Durham, North Carolina, United States

Introduction: Spontaneous cerebrospinal fluid (CSF) rhinorrhea is a rare condition associated with idiopathic intracranial hypertension (IIH). The endoscopic endonasal approach is often utilized for repair of skull base defects in CSF rhinorrhea. However, endoscopic repair can often lead to significant disruption in sinonasal anatomy and physiology. Our objective is to evaluate sinonasal quality of life (QOL) following endoscopic endonasal repair of spontaneous CSF leaks.

Methods: This is a retrospective study of patients with spontaneous CSF leaks who underwent endoscopic endonasal repair from January 2014 to May 2019 at our institution. Patients with complete SNOT-22 data were included. Electronic medical records were reviewed for demographic and operative data. Total and individual item pre- and post-operative (3 and 6 months) SNOT-22 scores were compared using a two-tailed, paired *t*-test.

Results: Twenty patients with spontaneous CSF leaks were identified as having undergone endoscopic endonasal repair with complete pre- and postoperative SNOT-22 data. Nineteen of the twenty patients were female with a median age of 54 years. Four patients had defects in the cribriform, 5 had defects in the ethmoid roof, 1 had a defect in the frontal, and 10 had defects in the sphenoid [DJM1]. Repair was performed with a free mucosal graft in 14 cases, middle turbinate flap in 2 cases, and a nasoseptal flap in 3 cases. Two patients required revision repair.

The mean preoperative total SNOT-22 score was 33.0 ± 19.8 . At 3 and 6 months postoperatively, patients had significant improvement with a mean total score of 15.1 ± 15.1 ($p < 0.0002$) and 14.2 ± 16.0 ($p < 0.006$), respectively. Assessment of individual items preoperatively revealed that “runny nose” (mean 3.6 ± 1.6) was the worst symptom, but improved significantly at 3 (0.8 ± 1.0) and 6 months (0.4 ± 0.7). “Wake up at night” (mean 2.6 ± 1.6) was the second worst symptom, but also improved significantly at 3 (0.8 ± 1.1) and 6 months (0.7 ± 1.3). No single item had significantly worse scores postoperatively.

Conclusion: Spontaneous CSF rhinorrhea has a significant impact on QOL, especially as it relates to sinonasal and sleep-related symptoms. Patients undergoing endoscopic endonasal repair of spontaneous CSF leaks exhibited significant improvement in sinonasal QOL at 3 and 6 months postoperatively. SNOT-22 scores reached “normal” levels for these patients.

P182. Have Influence of Postsurgery Quality of Life Choice of Surgery Approach?

Jan Hemza¹

¹Department of Neurosurgery Faculty Hospital at Saint Ann, England, United Kingdom

The surgery approach and philosophy of them choice can be influence to postoperative quality of life and postoperative complications after surgery procedure too.

The postoperative bleeding is important complication, with temporary artificial pulmonary ventilation, subsequently problem with TBI and postoperative massive pulmonary embolization with next therapy on ECMO and Trendelenburg pulmonary embolectomy. The postoperative

bleeding can be after surgery procedure with delay, postponed provided that surgery approach permit for tumor resection in maximal safety degree or radically and bleeding will be started into tumor residuum with mortality resultant. The problems of complications are leucorrhoea too after different surgery approaches and understanding principles of healing and mending dura nad skull base.

Author supplement philosophical problem of choice different approaches patient case history illustration.

P183. Sinonasal Morbidity Following Chemoradiation in Nasopharyngeal Carcinoma Patients

Matthew Stewart¹, Chandala Chitguppi¹, Kira Murphy¹, Tawfiq Koury¹, Mackenzie O'Connor¹, James J. Evans², Mindy Rabinowitz¹, Marc Rosen¹, Gurston G. Nyquist¹

¹Department of Otolaryngology – Head and Neck Surgery, Thomas Jefferson University Hospital, Philadelphia, Pennsylvania, United States

²Department of Neurological Surgery – Thomas Jefferson University Hospital, Philadelphia, Pennsylvania, United States

Background and Purpose: The majority of nasopharyngeal carcinomas are treated by radiation therapy. Some of the common sinonasal complications in these patients are sinusitis, crusting, and adhesions. The objective of the study was to determine the risk factors for sinonasal morbidity patients of NPC post chemoradiotherapy.

Methods: A single center, retrospective chart review of patients who underwent radiation therapy treatment for nasopharyngeal carcinoma between 2015–2019 was performed. Patients were evaluated for complications of sinusitis, adhesions, and crusting.

Results: 43 patients were included in the study. Mean age at presentation was 56 ± 14.6 years and majority were males (83.3%). The mean total dose of radiation was 68.5 ± 6.4 Gy, and mean fraction of radiation treatment was 35 ± 6.1 . Average duration of follow up was 20.1 ± 14.5 months.

20 patients (46.5%) had at least 1 of the sinonasal complications analyzed – either crusting, sinusitis or adhesions – following radiation treatment. Six patients (14.0%) required treatment for sinusitis at 5.4 ± 5.3 months after completion of radiation treatment. Of those treated, 3 were treated with antibiotics and 3 received FESS.

Three patients (7.0%) experienced adhesions requiring treatment at 5.3 ± 5.8 months after completion of radiation treatment. Sinusitis was found to be 75 times more likely in patients who developed adhesions ($p = 0.002$, OR = 75.00, 95% CI: 3.18–1766.46).

Eight patients (18.6%) experienced extensive nasal crusting that required debridement and crusting was noted to present at average 7.1 ± 4.0 months after completion of radiation treatment. All patients with crusting were able to be debrided in-office.

We did not observe any significant correlation between sinusitis, adhesions, or crusting and groups stratified by: gender, race, age, smoking history, primary vs recurrent tumor, tumor skull base involvement, pterygopalatine invasion, infratemporal fossa invasion, xerostomia, chemotherapy treatment, radiotherapy treatment, fractions of radiation, radiation dosage, immunotherapy treatment, EBV status, p16 status, TNM stage, or 30 day readmission. Crusting did not correlate with either adhesions or sinusitis.

Conclusions: Sinonasal morbidity—either crusting, adhesions, or sinusitis—are seen in one in 5 patients of NPC following chemoradiotherapy. The majority of these complications are seen at 6.1 ± 4.5 months following treatment completion. Although none of the patient or tumor related factors are a reliable predictor of sinonasal morbidity,

development of adhesions increased the risk of development of sinusitis 75-fold.

P184. Repeat Gamma-Knife Radiosurgery for Recurrent Glossopharyngeal Neuralgia: Case Report and Literature Review

Joel Kaye¹, Lekhaj C. Daggubati², James McInerney²
¹Robert Wood Johnson Medical School, New Brunswick, New Jersey, United States
²Penn State Hershey Medical Center, Hershey, Pennsylvania, United States

Glossopharyngeal neuralgia (GPN) is a rare facial pain syndrome, but its symptoms are debilitating. For medication-resistant idiopathic GPN, stereotactic radiosurgery (SRS) is an emerging treatment option with a promising role; however, recurrence after SRS is not uncommon. SRS for recurrent GPN is rarely reported. We present a patient who underwent repeat SRS for recurrent GPN and subsequently maintained over 3 years of complete pain relief. A review of literature of recurrent GPN treated with repeat SRS revealed only 9 previous cases. Six patients (66.7%) had adequate pain relief at 12 months. Four patient (44%) had adequate pain relief at their last follow-up at a median of 24.5 months. Four patients (44%) had recurrence at a median of 25 months. Only two patients (22%) experienced mild adverse radiation effects. Repeat SRS is a viable and minimally invasive alternative to open surgery for the treatment of recurrent GPN; however, it may be associated with a low risk of adverse radiation effects. Limited by the small cohort of patients, response to initial SRS of >5 months, maximum doses greater than 75 Gy, and a target at the glossopharyngeal meatus provide the best predictors for an effective second treatment.

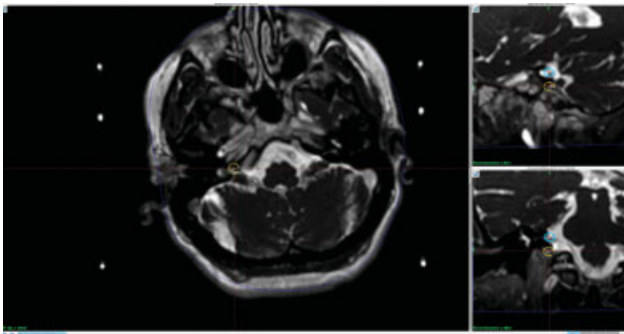


Fig. 1

Study Author Year	Patients	Age (yr)	Site	ICP (mmHg)	Target	Dose (Gy)	Time to pain relief after 1 st SRS	Time to pain relief after 2 nd SRS	Relief onset after 2 nd SRS	Duration of pain relief after 2 nd SRS	Additional surgery	Comments
Kaye, 2018	1-4	N/A	N/A	N/A	Meatus	75-85Gy	N/A	Median 22 months (21-36)	N/A	12 months* 18 months* 30 months* one patient had no follow-up	No	Limited info on individual cases one patient developed hyperphagia of postoperative week 8 months after repeat SRS
	5	N/A	N/A	N/A	Meatus	80 Gy	No relief after initial SRS	7 months	No initial relief	No relief	No	developed hyperphagia of the postoperative week 8 months after repeat SRS
Berens, 2018	6	63F	L	N/A	CS	80Gy	5 months	19 months	N/A	38 months (38-38)	No	Recurred after 1 st SRS was 38. Significant improvement w/ reduction in attack frequency* underwent 2 nd SRS 38 months after 1 st and remained SRS free until 74. 38 months later
	7	75M	L	N/A	CS	80Gy	12 months	17 months	N/A	12 months*	Yes	same target used both times 80-100Gy, 80-70Gy had TC 23 months and 22 months after 2 nd SRS, remained SRS free an additional 20 years
Wang, 2018	8	63F	L	Yes	Meatus	70Gy	2 months	7 months	"Dry"	4 months*	Yes	same target used both times 80-100Gy, 80-70Gy had TC 23 months and 22 months after 2 nd SRS, remained SRS free an additional 20 years
Parvathani, 2018	9	52F	L	Yes	Meatus	80Gy	36 Months	36 months	3 weeks	32 months (32-32)	No	
Kaye, 2018	10	63F	R	Yes	Meatus	80Gy	9 Months	18 months	3 weeks	30 Months (30-30)	No	
Total	17	61.2	L	80%	Meatus	80Gy	10	19	3	24.5	0	

Fig. 2

P185. A Cure for Pains? A Novel Approach to Management of Proton-Associated Internal Nasal Stenosis (Pains)

Stephanie Flukes¹, Matthew Bott¹, Martin Hanson¹, Marc A. Cohen¹
¹Department of Surgery, Memorial Sloan Kettering Cancer Center, New York City, United States

Background: Acquired anterior nasal stenosis is a challenging problem. Stenosis as a result of direct trauma to the nasal valve region during nasal packing and instrumentation is well described in the literature. Indirect trauma, such as that occurring during thermal burns and radiotherapy treatment, is less well recognized but similarly difficult to correct.

Regardless of the etiology, surgical management is the mainstay of treatment. Repair can be difficult due to the tendency of the area to cicatrize and re-stenose. Several techniques have been proposed including excision and split skin grafting, CO2 laser resection with stenting, local flap rotation, Z-plasty techniques, and composite graft reconstruction. Balloon dilatation of congenital pyriform aperture stenosis has been described in the neonatal population but its utility in the setting of acquired anterior stenosis has never been reported.

Case Report: We describe the case of a 65-year-old female patient who developed complete anterior nasal stenosis following proton radiotherapy for treatment of a sino-nasal undifferentiated carcinoma. She was treated with induction chemotherapy with cisplatin and etoposide and then following partial response was treated with concurrent cisplatin and proton radiation. She has been without evidence of disease for approximately two years but with anterior nasal stenosis related to treatment. She was interested in minimally invasive intervention to improve her nasal breathing. The patient underwent an endoscopic-assisted trans-nasal balloon dilatation using the Boston Scientific TM CRE endoscopic balloon dilation catheter, followed by silicone stenting of the region. The stenting was maintained for two weeks. The patient had complete resolution of obstructive symptoms without evidence of restenosis at last follow-up.

Conclusion: The balloon dilatation procedure offers a low-morbidity alternative to the management of acquired anterior nasal stenosis. It is of particular value in the irradiated patient, where poor tissue healing may be considered a relative contraindication to more involved reconstructive techniques.

This document was downloaded for personal use only. Unauthorized distribution is strictly prohibited.

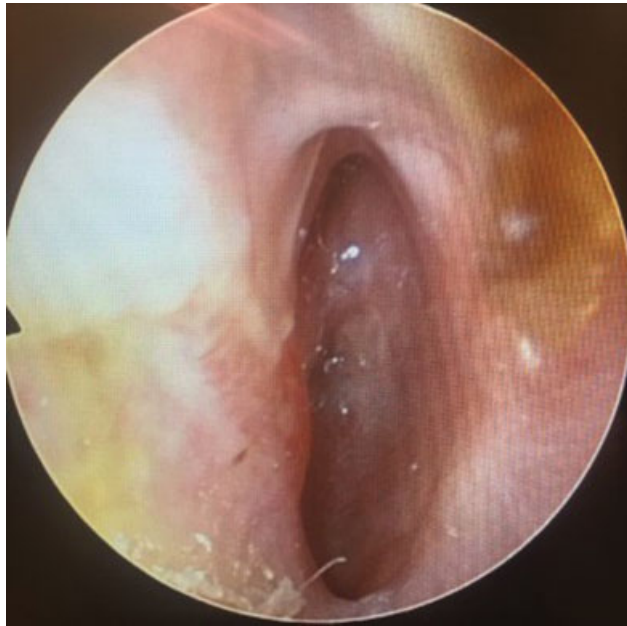


Fig. 1 Preoperative photograph showing complete left-sided nasal stenosis.

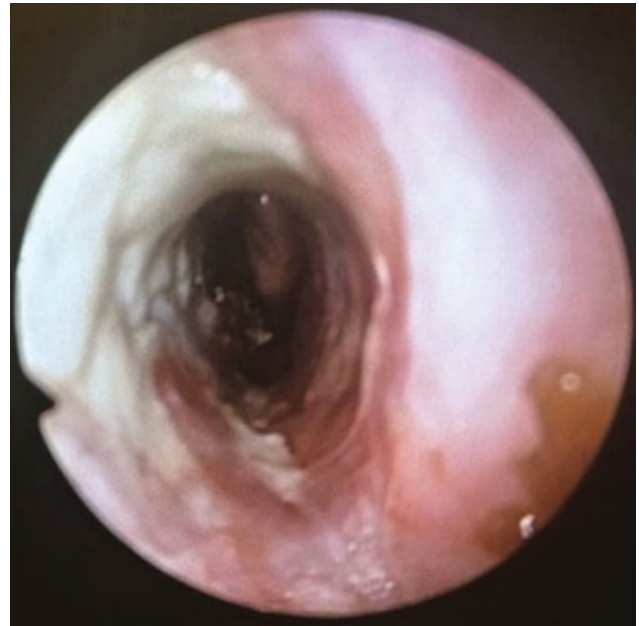


Fig. 3 Postoperative photograph showing a widely patent nasal passage.



Fig. 2 Intraoperative photograph showing the Boston Scientific CRE endoscopic balloon dilating the area of stenosis.

P186. Sinonasal Adenocarcinoma with Neuroendocrine Differentiation: Case Report and Review of Literature
 Khalil Issa¹, John Madden², David Jang¹, A.R. Zomorodi³,
 Ralph Abi Hachem¹

¹Department of Head and Neck Surgery & Communication Sciences, Duke University Medical Center, Durham, North Carolina, United States

²Department of Pathology, Duke University Medical Center, Durham, North Carolina, United States

³Division of Neurosurgery, Duke University Medical Center, Durham, North Carolina, United States

Background: Sinonasal mixed adenocarcinoma with neuroendocrine features is a rare tumor with no treatment guidelines. These tumors can be very aggressive, with locoregional and distant spread. Adenocarcinomas are generally non-responsive to chemotherapy unless an intestinal-type with a retained functional p53 protein. Neuroendocrine differentiation might be another indication to include chemotherapy in the management of these tumors.

Case Presentation: 64-year-old Jehovah's witness wood-worker presented with right sided epistaxis and right facial swelling. Imaging showed a sinonasal mass with an epicenter in the right olfactory cleft and the biopsy was consistent with high grade sinonasal adenocarcinoma with neuroendocrine differentiation. A PET/CT scan did not show any loco-regional or distant metastasis and he was staged as cT4aN0M0. Immunohistochemical studies were positive for CK7, chromogranin, synaptophysin and CDX-2. EGFR, TP53 and CK20 were all negative. He underwent endoscopic endonasal anterior skull base resection with negative margins and completed adjuvant intensity modulated radiation therapy. One year later, he presented with a right cervical mass and the fine needle aspiration confirmed the presence of neuroendocrine cells consistent with metastasis. He underwent definitive chemotherapy. One year later the patient presented with hilar metastasis.

Discussion: Mixed adenoneuroendocrine carcinoma (MANEC) have been poorly described, with only 5 cases published in the English literature. MANECs are mostly found

in males with a mean age of 60.6 years and these tumors are considered aggressive neoplasms associated with poor prognosis. An important prognostic factor remains the differentiation grade. Management and sequence of therapy is not well described but some reports suggest induction chemotherapy followed by either surgery with chemoradiation or definitive chemoradiation. Other reports show that chemotherapy does not improve overall survival in neuroendocrine carcinomas and the main treatment consists of surgery followed by radiation therapy.

Conclusion: Neuroendocrine differentiation in sinonasal adenocarcinomas should be properly detected by experienced pathologists and quantified as the percentage of the tumor. No optimal treatment strategy has been described. Despite not improving overall survival, chemotherapy could be considered to aid in prevention of locoregional and distant spread and as a biomarker to determine the sequence of therapy when a neoadjuvant treatment strategy.

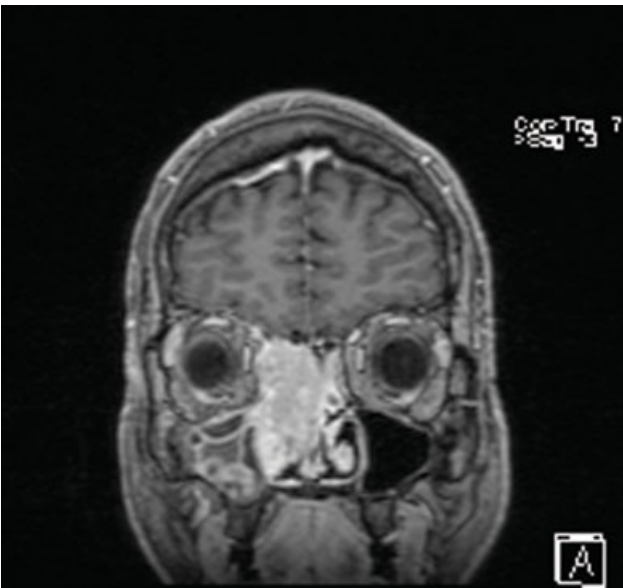


Fig. 1 MRI T1 with contrast showing a large enhancing mass centered within the right nasal cavity abutting the orbit and the anterior base of skull.

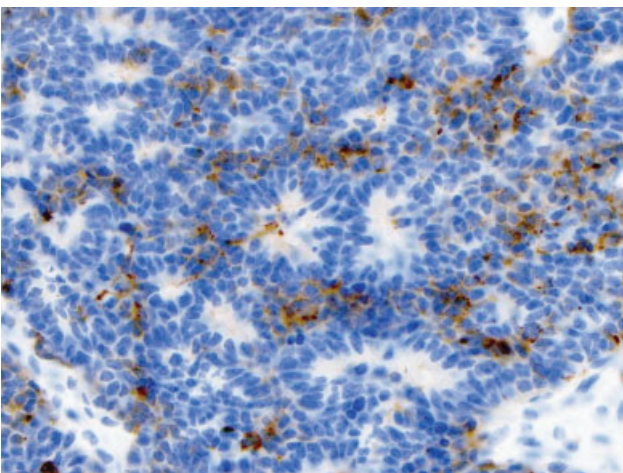


Fig. 2 40× close-up synaptophysin immunoperoxidase stain population of synaptophysin (+) cells (brown).

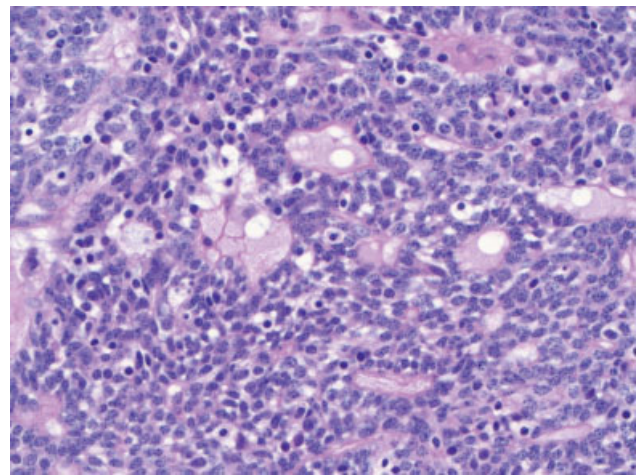


Fig. 3 40× close-up H&E, area with glandular lumina.

P187. Medically Refractory Cushing's Syndrome as a Paraneoplastic Manifestation of Esthesioneuroblastoma
 Jordan A. Malenke¹, Justin Morse, Lola Chambless¹, Justin Turner¹

¹Vanderbilt University Medical Center, Nashville, Tennessee, United States

Background: Esthesioneuroblastoma or olfactory neuroblastoma (ONB) is a rare malignancy of the sinonasal cavity derived from the olfactory epithelium. There are scattered reports of ectopic or paraneoplastic hormone secretion from these tumors.

Objectives: To report a case of medically uncontrollable ectopic Cushing's Syndrome necessitating prompt surgical management and a review of the literature surrounding this unique diagnosis and management.

Methods: This report describes a case of esthesioneuroblastoma presenting with acute hyperglycemia and electrolyte abnormalities. A review of the literature (PubMed and Medline) was performed with an emphasis on tumors with ectopic adrenocorticotropic hormone (ACTH) and management.

Results: A 52-year-old male presented with acute altered vision and new onset hyperglycemia. A head CT discovered an erosive skull base mass. Endoscopic biopsy revealed esthesioneuroblastoma and the patient was discharged pending further workup. Prior to tumor board evaluation and other consultations, the patient returned to the hospital with profound weakness, edema, and severe electrolyte abnormalities. Further workup revealed blood glucose of 342 mg/dL and ACTH of 344 pg/mL. The patient was aggressively medically managed for presumed paraneoplastic Cushing's syndrome. He ultimately failed medical management, necessitating surgical resection. Following surgery, the patient progressed well and was able to achieve resolution and medical control of his Cushing syndrome, with undetectable postoperative ACTH levels. The patient underwent adjuvant treatment with combined radiation and chemotherapy and recovered endocrine function. 5 year follow up demonstrated no evidence of disease.

A review of the current literature demonstrates fewer than 20 cases describing esthesioneuroblastoma with ectopic ACTH production. We present a unique case of acute onset Cushing's syndrome in a patient without typical Cushingoid features refractory to medical management. Ultimately surgical resection lead to resolution of endocrine symptoms related to excess ACTH.

Conclusion: Esthesioneuroblastomas are rare skull base tumor that can present with acute paraneoplastic secretion of ACTH. Treatment consists of medical management and surgical resection if indicated.

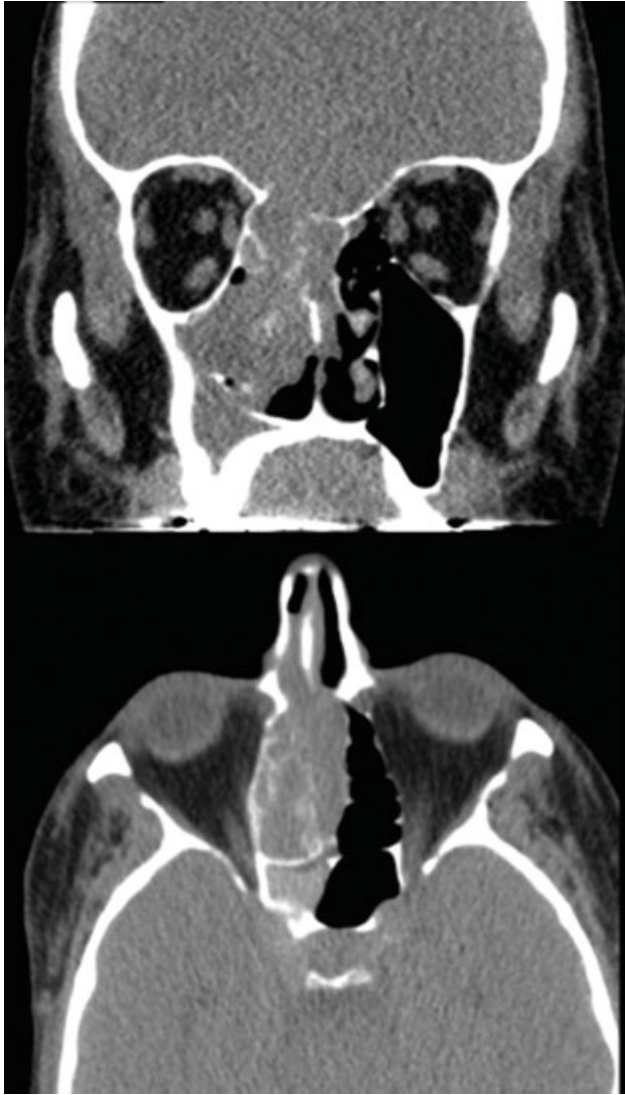


Fig. 1 Computerized tomography demonstrating cribriform erosion and skull base extension.

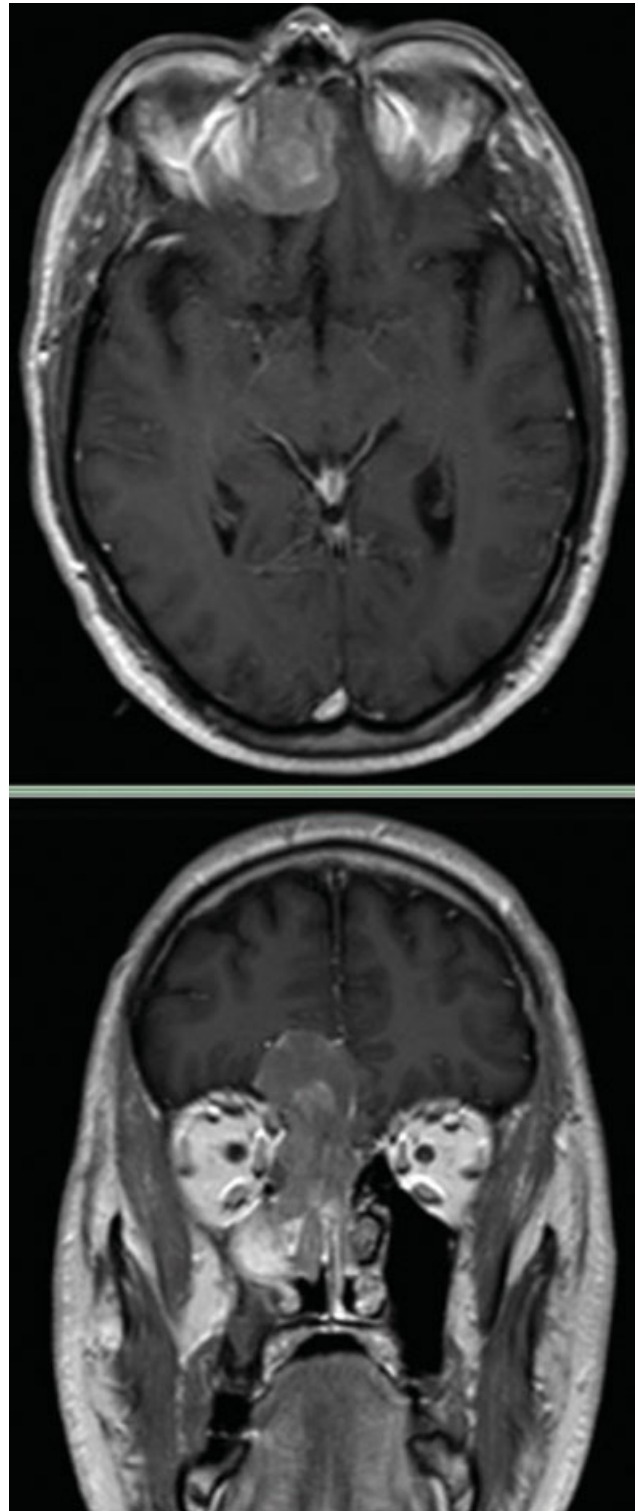


Fig. 2 Magnetic resonance imaging showing skull base erosion and intracranial extension.

P188. Aggressive Neurocranial Juvenile Psammomatoid Ossifying Fibroma

Cheyenne M. Silver¹, Lucas P. Carlstrom², Christopher S. Graffeo², Avital Perry², Garret W. Choby¹, Michael J. Link²

¹Department of Otorhinolaryngology, Mayo Clinic, Rochester, Minnesota, United States

²Department of Neurologic Surgery, Mayo Clinic, Rochester, Minnesota, United States

Background: Juvenile ossifying fibromas are a group of benign craniofacial neoplasms, divided into histologically juvenile psammomatoid ossifying fibromas (JPOF) or juvenile trabecular ossifying fibroma (JTOF). JPOF is predominantly sinonasal, with rare intracranial extension; aggressive subtypes are associated with aneurysmal bone cyst (ABC) formation. Recurrence is high in JPOF, occurring in 30–65% of patients — particularly following subtotal resection. We report a novel case of extensive, hyper-acute JPOF progressing over 3 months, in association with new meningoencephalocele development.

Methods: Case Report

Results: A 26-year-old woman initially presented elsewhere with headache, fever, and jaw pain radiating to the ear. MRI demonstrated a large, destructive, heterogeneous mass involving the anterior fossa, with erosion through the cribriform plate and extension into the ethmoid sinus, tuberculum sellae and bilateral orbits. The patient underwent endonasal biopsy which diagnosed JPOF with ABC changes. Correspondingly, the patient underwent a right pterional craniotomy and subtotal resection, elsewhere. Residual tumor was left on the tuberculum sellae and left skull base.

The patient presented to our institution for second opinion regarding ongoing management. Repeat imaging, 3 months after the initial operation elsewhere, demonstrated remarkable interval tumor growth, as well as the development of a large meningoencephalocele extending from the left skull base into the resection cavity. We performed a combined bifrontal craniotomy with endonasal sphenoidotomy and aggressive JPOF and ABC resection to the tuberculum sellae, with decompression of the left optic nerve, amputation of the meningoencephalocele, and skull base reconstruction with autologous fascia lata and vascularized pericranium. The operation proceeded without complication, and as of the patient's last follow-up at four month post-repeat resection, the patient's neurologic deficits had resolved, and MRI demonstrated no evidence of tumor or meningoencephalocele recurrence.

Conclusion: JPOF are rare neoplasms with marked risk of recurrence—particularly following subtotal resection, with prior reports documenting recurrence as early as 6 months. The current report demonstrates the potential for dramatic regrowth in these lesions, suggesting that a more aggressive approach may be indicated at primary resection. If clinical circumstances or patient-specific considerations mandate a staged approach, we recommend updating intracranial imaging at a shorter postresection interval, ideally 4–6 weeks following the initial operation.

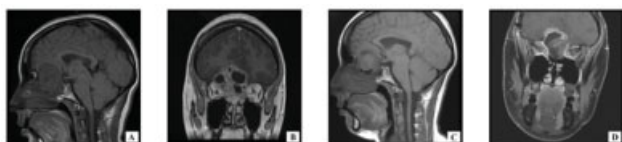


Fig. 1 (A) Preoperative sagittal T1 MRI. (B) Preoperative coronal MRI. (C) Postoperative showing recurrent tumor and meningoencephalocele on sagittal T1 MRI. (D) Postoperative showing recurrent tumor and meningoencephalocele on coronal T1 MRI with gadolinium

P189. Aggressive Juvenile Angiofibromas

Steven A. Newman¹, Spencer Payne¹, Jose Mattos¹

¹University of Virginia, Charlottesville, Virginia, United States

Materials and Methods: Two case reports of patients presenting with nasal obstruction epistaxis found to have masses of the skull base with unusual amount of bone erosion found to represent juvenile angiofibromas.

Discussion: Angiofibromas may originate in the nasopharynx or the pterygomaxillary area. They often cause local bone destruction but with extension into the sinuses. Extensive bone involvement suggests more rapidly expanding aggressive tumors.

Conclusions: In young males, the presence of mass lesions involving either primarily or secondary the paranasal sinuses may represent juvenile angiofibroma. Because of dual supply, it is essential that original surgery be performed to remove the major supply of the pterygomaxillary artery, but also to make sure that no additional supply off the internal carotid artery, particularly to the cavernous sinus branches is taken care of.

P190. Nonneoplastic Etiologies of Erosive Disease of the Frontal and Ethmoid Sinuses

Jose L. Mattos¹, Steven A. Newman¹, Mark J. Jameson¹

¹University of Virginia, Charlottesville, Virginia, United States

Introduction: Most cases of erosive disease of the frontal or ethmoid sinuses are related to carcinoma. This may be diagnosed with open or fine needle aspiration biopsy.

Materials and Methods: This is a single case report of a 66 year old patient who presented to the otolaryngology service with a bump on her forehead. Her visual afferent system seemed to be normal with 20/40 and 20/30 vision, no afferent pupillary defect, trace nuclear sclerosis, and applanation tensions of 12 and 16. Her funduscopic evaluation was unremarkable. Her motility did demonstrate some subtle abnormalities in elevation on the right side, better seen on the Hess screen with binocular single vision fields revealing diplopia ~45 degrees up. Her previous ophthalmic history included glaucoma for 2 years and early nuclear sclerosis and posterior vitreous detachment.

Results: Because of the bump on her forehead, a CT scan was obtained which showed a “heterogeneous soft tissue mass which appeared to arise in the right anterior ethmoid air cell of frontal sinuses causing osseous destruction extending into the orbit and anterior cranial fossa. The impression radiographically was this was a malignancy. Patient underwent a fine needle aspiration biopsy. Two passes were made which showed evidence of histiocytes and inflammatory cells, but no evidence of malignancy. Because of the “abundance of histiocytes” a differential diagnosis included infectious process, Langerhans, histiocytosis, Rosai-Dorfman disease, rhinoscleroma, and Erdheim-Chester disease. There was no evidence of organisms and had negative Steiner stain, which failed to support a diagnosis of rhinoscleroma. S 100 was also negative for Rosai-Dorfman, and Braf was also negative. Because of the question about the etiology of this inflammatory lesion, an open biopsy was obtained on July 26, 2019 which showed “dense fibrous tissue diffusely infiltration with a mixture of lymphocytes, abundant plasma cells, and forming macrophages. Infiltrate was negative for CD1A and Langerhan’s.

Discussion: Although most bone destructive processes involving the sinuses are a result of rapidly expanding lesions, most commonly neoplastic, in this particular case, the short history masked the presence of an inflammatory non-neoplastic

P191. Nasal Obstruction in a Patient with SchwannomatosisThomas Yusin¹, Cinthia Orlov², Debraj Mukherjee²,
Nicholas R. Rowan²¹Tulane University School of Medicine, New Orleans, Louisiana,
United States²Johns Hopkins Medical Institute, Baltimore, Maryland, United States

Purpose: Describe a rare presentation of a patient with schwannomatosis, highlighting the involvement of the central skull base.

Introduction: Schwannomatosis is the newest recognized form of neurofibromatosis, an extremely rare disease with an estimated prevalence of 1 in 40,000 and an incidence of 0.58 per 1,000,000 people. This disease characteristically presents in the 3rd-6th decade of life with multiple peripheral schwannomas, benign Schwann cell tumors of the peripheral nervous system. Patients with schwannomatosis, typically present with subcutaneous, cranial, and spinal nerve root schwannomas with associated symptoms of muscular atrophy and chronic pain. Schwannomatosis is an increasingly recognized entity, but the least well characterized form of neurofibromatosis.

This case report describes a unique presentation of a patient with schwannomatosis who presented with progressive, benign sinonasal symptomatology, and was found to have a large schwannoma with destruction of the central skull base.

Case: A 77 year old woman with a personal and family history of schwannomatosis who had previously undergone resection of schwannomas of the brachial plexus, spine, and pleura, as well as a papillary thyroid carcinoma, presented with a 2–3 month history of progressive unilateral nasal airway obstruction and intermittent blood-tinged nasal drainage that failed to improve to medical therapy for rhinosinusitis. Nasal endoscopy revealed a large, pulsatile, left sinonasal tumor emanating from the sphenothmoidal recess. Magnetic resonance imaging (MRI) revealed a destructive, 5.4 cm × 3.6 cm × 2.5 cm, T2-hyperintense sinonasal mass centered in the left posterior nasal cavity with transcavernous involvement, partial carotid encasement, perineural invasion along foramen ovale and extension through the pterygopalatine fossa to the pterygoid musculature (Fig. 1). Biopsy confirmed diagnosis of schwannoma.

Discussion: This case highlights an uncommon presentation of schwannomatosis, the least well characterized form of neurofibromatosis. Though schwannomas of the sinonasal tract and central skull base are rare, the combination a sinonasal schwannoma in the setting of schwannomatosis is an even less common finding. In addition to review of our patient, we herein review the published literature of this unique, but increasingly recognized entity. In this report, we detail the most common clinical presentation and treatment strategies of sinonasal and anterior skull base schwannomatosis. Multidisciplinary management of patients with schwannomatosis is essential, and gross total resection of skull base schwannomas is achievable and effective.

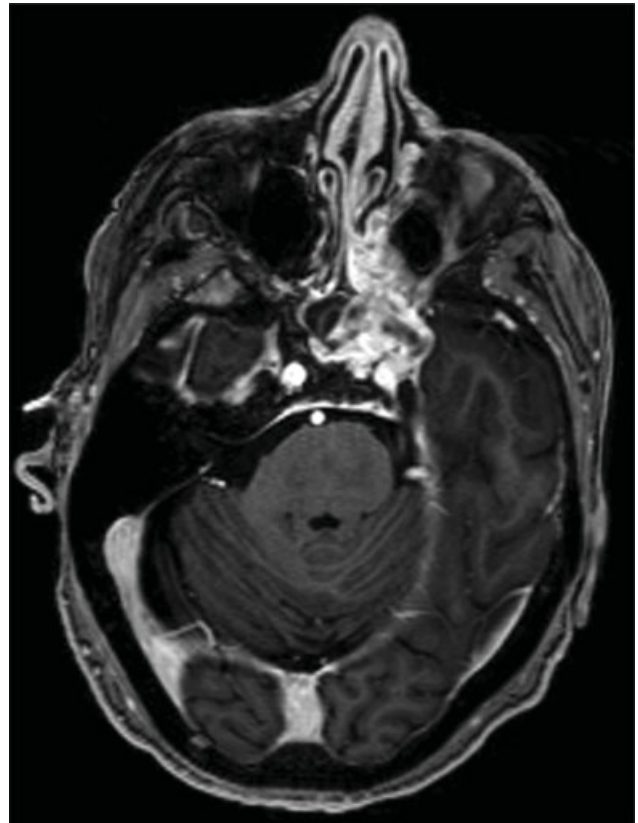
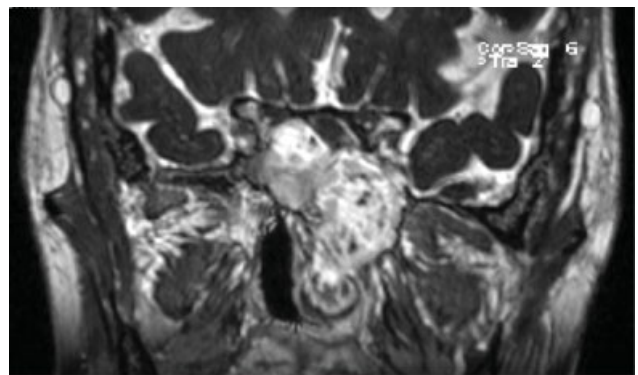


Fig. 1 T1-weighted (a) axial and (b) coronal postcontrast MRI demonstrating destructive, hyperintense sinonasal lesion with left cavernous involvement and partial encasement of left internal carotid artery.

(A)



(B)

P193. Primary Neuroendocrine Tumor of the Sphenoid Sinus: Three Case ReportsIdoya Zazpe¹, Daniel De Frutos¹, Carlos Beaumont¹, Coro
Zubimendi¹, Juan Carlos Garcia¹, Onditz Arechaga¹¹Hospital of Navarre, Navarre, Florida, United States

Objective: Presentation of three cases of primary intracranial neuroendocrine tumor of the sphenoid sinus, with a review of the most recent literature published.

Method: We report three cases that occurred in our center, with a bibliographic search performed in PubMed

using the keywords “neuroendocrine tumor,” “intracranial” and “primary.”

Results: *Case 1:* A 44-year-old patient presented with headaches over the last 3 months. A MRI of the skull base demonstrated a mass lesion in the sphenoid sinus. An extension study was performed, which was negative. Acromegaly and Cushing’s syndrome were also discarded. Biopsy of the lesion was performed, resulting in neuroendocrine tumor with hormonal expression for GH, LH, and HCG.

Case 2: 63-year-old patient presented with pathological visual field. A cranial MRI is performed where a neoplastic mass is seen in the sphenoid sinus suggestive of tumor lesion with aggressive local behavior (Fig. 1). The presence of macroprolactinemia and central hypothyroidism stands out in blood samples. Subtotal resection of the lesion is performed, resulting in low histological grade neuroendocrine tumor.



Case 3: A 60-year-old patient with a history of melanoma and prostate cancer, consulted because of a long-standing headache. A sphenoid sinus mass is seen in cranial MRI. A biopsy is performed with the result of neuroendocrine carcinoma of intermediate degree of malignancy. Given these findings,

surgical intervention is performed with macroscopically complete resection.

Conclusions: Intracranial neuroendocrine tumors without evidence of a primary tumor are extremely rare, mostly metastatic from the gastrointestinal tract or respiratory tract. During the past 40 years, 75 cases of small cell neuroendocrine carcinoma of the nasal and paranasal cavities have been reported in the literature.

Therefore, a full body imaging that discards an origin away from the CNS is essential. The radiological findings are not specific, obtaining similar images as in meningiomas, schwannomas, glomus tumor or metastasis. That is why the combination of anatomical and functional techniques is recommended. In this sense, scintigraphy has demonstrated its usefulness for the location of radiologically occult tumors.

Pathological diagnosis is the gold standard. The neuroendocrine tumor must be distinguished from squamous cell carcinoma, melanoma, esthesioneuroblastoma or pituitary adenoma, among others. Synaptophysin and chromogranin A are sensitive but not specific markers, and several immunohistochemical markers must be combined to arrive at the diagnosis.

The malignancy of these tumors is divided into 3 parts, according to the Ki-67 index: under 1–3%; 3–20% medium, >20% high.

The treatment must be multidisciplinary. At present there is no systematic treatment due to its low incidence and the little literature published in this regard, but it seems that surgical resection followed by radiotherapy and chemotherapy treatment is the one with better disease control and overall survival.

P194. Outcomes of Aggressive Surgical Resection of Sinonasal Inverted Papilloma with Removal of Bone at the Attachment Site

Yufan Lin¹, Carlos D. Pinheiro-Neto¹

¹Albany Medical Center, Albany, New York, United States

Objectives: In current literature, sinonasal inverted papillomas (IP) have a high risk of recurrence (14–21%) and are associated with malignant transformation (9–13%). The mainstay management of IP is complete local resection. Despite this, most recurrences are attributable to inadequate resection at the attachment site. The aim of this study is to present our experiences with aggressive surgical management of IP with wide bone drilling and removal at the tumor attachment site.

Table 1 Tumor characteristics

Tumor extension	Krouse staging:(cases)	Cannady staging:(cases)	Attachment site	Recurrences
N	T1:(4)	A:(4)	NS-post; SR,NS-post; SR; SR	0
M	T3:(2)	B:(2)	M-ant; M-lat	0
F	T3:(1)	B:(1)	F	0
N+M	T2:(1)T3:(5)	A:(1)B:(5)	M-med; M-ant; M-ant; M-post; M-post; M-lat	0
N+E+M	T3:(2)	B:(2)	M-post; M-lat,ant	0
N+E+S	T3:(2)	B:(2)	S; T-sup, S, NS-post	0
N+E+F	T3:(2)	B:(2)	F; F	0
N+F+EN/ES	T4:(1)	C:(1)	F	0
N+E+M+F+EN/ES	T4:(1)	C:(1)	F	0

Abbreviations: ant, anterior; E, ethmoid sinus; EN/ES, extra-nasal/extra-sinus; F, frontal sinus; inf, inferior; lat, lateral; M, maxillary sinus; med, medial; N, nasal cavity; NS, nasal septum; post, posterior; S, sphenoid sinus; SR, sphenoid rostrum; sup, superior; T, turbinate.

Methods: We present 21 consecutive patients with histopathological diagnosis of IP who received surgical management with bone resection from March 5, 2013 to June 24, 2019. Results are based on the experiences of one surgeon at one clinical center. Data collected include staging, extension of tumor, tumor attachment site, surgical approach, complications, and recurrences.

Results: All patients underwent endoscopic sinus surgery with wide resection of bone underlying the tumor attachment site. Twelve patients (57%) were referred to our institution due to recurrence or incomplete resection. Eight patients (38%) required a combined external approach (5 Caldwell-Luc, 2 external brow, 1 bicoronal). Tumor involved the anterior skull base in 6 cases (29%) and orbit in 1 case. Three tumors had multiple attachments. Median follow-up time was 6.5 months (range: 1–36.3). Intraoperative cerebrospinal fluid leak was observed in two cases; one required repeat surgery for repair. Seven patients required medial maxillectomy. One patient had transient epiphora postoperatively. No recurrences were observed in this case series.

Conclusion: Resection of bone at the tumor attachment site seems to contribute toward minimizing the risk of recurrence. Combined endoscopic and external approaches may be required for tumors with attachment sites in the anterior or lateral walls of the maxillary sinus and frontal sinus.

P195. Ectopic Olfactory Neuroblastoma: A Case Report

Gregory D. Disse¹, Matthew Bobinski², Mirna Lechpammer³, Toby O. Steele⁴, Kiarash Shahlaie¹

¹Department of Neurological Surgery, University of California, Davis, California, United States

²Department of Radiology, University of California, Davis, California, United States

³Department of Pathology, University of California, Davis, California, United States

⁴Department of Otolaryngology, University of California, Davis, California, United States

Introduction: Olfactory neuroblastoma (ONB) is a rare intranasal tumor arising from olfactory epithelium. The mass classically originates in the olfactory recess, between the nasal septum and the insertion of the vertical portion of the middle turbinate on the anterior skull base. History, physical exam, and imaging are largely nonspecific and often confused with benign and more frequent processes including inflammatory polyps. Ectopic cases have even been reported, further complicating not only the understanding of the tumor, but its diagnosis and management. While rare, this malignancy's penchant for aggressive local invasion and even metastasis make its early identification crucial for optimal patient outcomes. We present a case of ONB of middle turbinate origin *without* olfactory recess involvement and summarize the literature regarding non-classical ONB origin.

Methods: Case Report

Results: A 50-year-old man presented with an eight month history of progressive left-sided nasal obstruction and intermittent severe epistaxis. Nasal endoscopy revealed a hypervascular mass filling the left nasal cavity, with origin at the middle turbinate and vascular supply near the posterior ethmoid artery. A thin cut sinus computed tomography scan (Fig. 1) demonstrated a mass centered within the middle turbinate, encroaching on the ethmoid labyrinth, and a clear olfactory recess with no intracranial or orbital extension. Pathological analysis of biopsy specimens (Fig. 2) was immunopositive for S100 and synaptophysin and negative for cytokeratin AE1, AE3, and CD45, resulting in a diagnosis of olfactory neuroblastoma (grade 1, Kadish stage A). The pa-

tient underwent endoscopic endonasal left anterior cranial base resection for tumor resection with circumferential negative margins.

Discussion: The cellular origin of ONB remains controversial, yet current research identifies the basal cells of the sensory neuroepithelium as the likely site of origin. These stem cells continuously replace neurosensory cells in the olfactory epithelium throughout life and thus are reasonable sites for malignant transformation. To date, there are 18 published cases of "ectopic ONB" involving various anatomic regions, including the sphenoid bone, sella, pituitary, maxillary sinus, nasopharynx, nasal floor, anterior ethmoid, and inferior meatus. ONB originating from the middle turbinate has not been previously described. Ectopic ONB exclusively originating from an area that lacks olfactory epithelium is a paradox that may be explained by three hypotheses. First, impaired migration of olfactory placode neuronal cells during embryologic development may establish ectopic olfactory neuroepithelial cell rests. Second, fetal accessory olfactory systems, such as those containing the vomeronasal nerve and terminal nerve, may fail to degenerate during development. Lastly, tumor cells may spread submucosally to their final destination.

Conclusion: While olfactory neuroblastoma is uncommon, clinicians should consider ONB in cases of nasal obstruction or epistaxis with masses even outside the olfactory recess to hasten diagnosis and prevention of possible tumor invasion into the orbit or cranial vault.



Figure 1. (A) Coronal and (B) Axial Head computed tomography scan showing left nasal mass (4.5 x 2.1 x 3.9 cm) without osseous destruction abutting and slightly extending into the left maxillary antrum ostium.

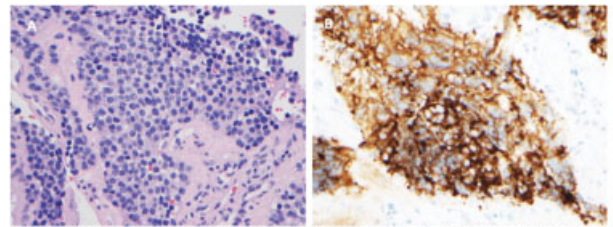


Figure 2. Pathology results from biopsy, both at 400x magnification. (A) Hematoxylin and eosin staining demonstrating nests and sheets of neoplastic cells separated by vascular and hyalinized stroma. (B) Immunohistochemistry result showing synaptophysin expression of neoplastic cells.

P196. Biphenotypic Sinonasal Sarcoma a Newly Recognized Sinonasal Neoplasm: Case Report and Review of the Literature

Somtochi Okafor¹, Ashleigh Halderman¹, Justin Bishop¹, Matthew Ryan¹, Bradley Marple¹

¹University of Texas Southwestern Medical Center, Dallas, Texas, United States

First described in the literature in 2012, biphenotypic sinonasal sarcoma represents a newly recognized neoplastic entity of the sinonasal cavities. As such, differential diagnosis of sinonasal masses may overlook this rare neoplasm. We present a case report of biphenotypic sinonasal sarcoma of the left ethmoid skull base and review the literature to better define the typical presentation, histologic appearance, and treatment outcomes of this rare tumor.

A 54 year old man presented with a 4–5 month history of left sided nasal airway obstruction. Nasal endoscopy showed a large mass occupying the left nasal cavity and displacing the septum to the right. The surface had both a smooth mucosal surface as well as a stippled appearance more suggestive of an inverted papilloma. Computed tomography (CT) sinus demonstrated an expansile mass occupying the majority of the left nasal fossa and extending laterally into the maxillary antrum and superiorly to occupy the ethmoid sinuses and the region of the frontal recess. In addition, imaging showed extreme thinning versus loss of cortical continuity related to the left vertical cribriform plate and left anterior aspect of the lamina papyracea. The patient underwent endoscopic excision. Intraoperative frozen section was read as consistent with sinonasal papilloma, however, this was changed on final pathology to low-grade biphenotypic sinonasal sarcoma. The tumor was focally positive for S100 and smooth muscle actin (SMA) staining. Subsequently, the patient underwent a second surgery to fully clear margins including resection of the ethmoid skull base and repair of the skull base defect. All margins were negative upon final pathology.

Biphenotypic sinonasal sarcoma (BSS) is a rare, slow-growing sarcoma of the sinonasal cavities. The mean age at diagnosis is 50 years old and shows a predilection for women with a female to male ratio of 2:1. BSS most commonly involves the ethmoid cavity and typically involves multiple sinonasal subsites. Intracranial extension can occur in up to 10% of cases and intraorbital involvement is seen in 25%. Histologically, the tumor consists of a highly cellular proliferation of purely spindled cells arranged as fascicles and in a herringbone pattern. The tumor nuclei are uniform, hypochromatic, wavy, and bland. Necrosis is absent and the mitotic rate is low. The tumor is further characterized by co-expression of both S100 and SMA (hence, “biphenotypic”) and PAX3 gene rearrangements. Clinically, BSS is regarded as a low-grade sarcoma. Treatment consists of surgical resection with or without adjuvant radiation. Despite treatment, the recurrence rate is relatively high at 40–50%. Nonetheless, prognosis remains good with no reported cases of metastasis and only one reported death due to intracranial involvement.

P197. Anterior Cranial Base Meningeal Hemangiopericytoma

Jesus Gimeno Hernandez¹, Juan Manuel Revuelta Barbero¹, Carla Fernandez Garcia¹, Andres Camilo Vargas Jimenez¹, Manuel Gomez Serrano¹, Pablo Sarrio Solera¹, Diana Hernanperez Hidalgo¹, Melchor Saiz Pardo-sanz¹, Maria Cruz Iglesias Moreno¹

¹Hospital Clinico San Carlos, Madrid, Spain

Introduction: Central nervous system (CNS) meningeal hemangiopericytoma (MHPC) is a rare entity accounting

less than 0,5–1% of all CNS tumors. MHPC present a mesenchymal origin, arising from pericytes of the meningeal capillaries. There are classified as solitary fibrous tumors grade II-III (WHO CNS tumors classification 2016).

Although MHPC can arise along the entire CNS the supra tentorial location is more common in close relation with the meninges. MHPC are more often observed in young population, with an average age presentation around 30–50 years-o and with a slight male predisposition.

Material and Methods: A 61y-o male was admitted in our department with a personal history of anosmia and an anatomopathological report of hemangiopericytoma based in a endoscopic endonasal biopsy performed in a different institution.

A CT and MRI showed an intense contrast enhancement lesion (4 × 5 × 4.5 cm) center at the frontal sinus eroding its posterior table and with a bilateral expansion into both frontoethmoidal recesses. Besides, a multilobulated posterior extension toward both frontal lobes was observed.

24 hours before surgery endovascular procedure was performed aiming to reduce the tumoral vascular supply. A single-stage combined bicoronal-bifrontal assisted by endoscopic endonasal approach was performed. A gross-total resection was achieved. There were no intra- or postoperative complications and the patient was discharged in the 7 day post op. Histopathological examination confirmed a MHPC WHO grade II.

Following the recommendations of the Radiation Oncology department, hypofractionated adjuvant radiotherapy was provided to the patient (total dose: 54 Gy). The patient remains asymptomatic and no recurrence on 12 months follow-up.

Discussion: MHPCs are very unusual CNS tumors.

MHPC and angioblastic/anaplastic meningioma present clinical, pathological and imaging similarities. Because they receive different treatment and have different prognosis, it is essential to make a precise differential diagnosis. Immunohistochemical studies are crucial in that aim.

MHPC are distinguished due to their hypercellularity, higher mitotic index, and microscopic tendency to bulge into vascular lumens; additionally, they have a strong tendency to local recurrence and until 20% can metastasize, typically to liver, lung and bone.

Patients with a gross-total total resection and post-operative radiation have demonstrated the best prognosis.

Conclusions: A single-stage combined bicoronal-bifrontal assisted by endoscopic endonasal approach followed by hypofractionated adjuvant radiotherapy it is safe and effective strategy in the MHPC treatment. Further studies are necessary to confirm this observation.

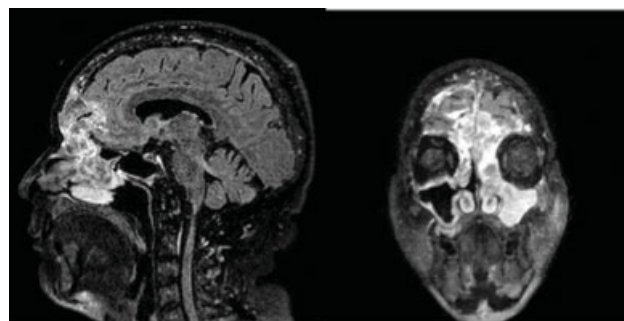


Fig. 1 MRI preop.

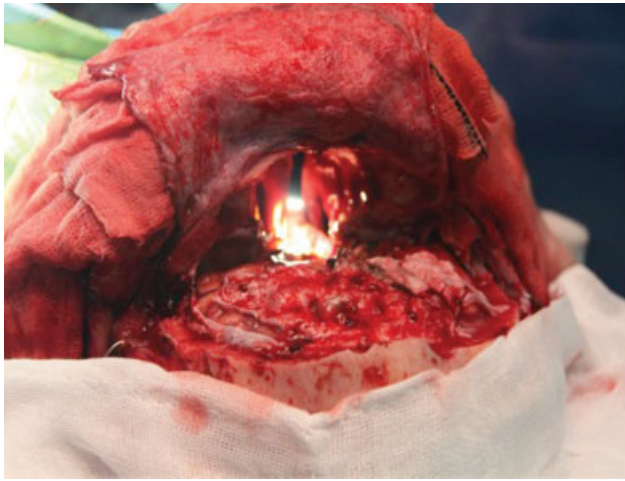


Fig. 2 Combined approach.

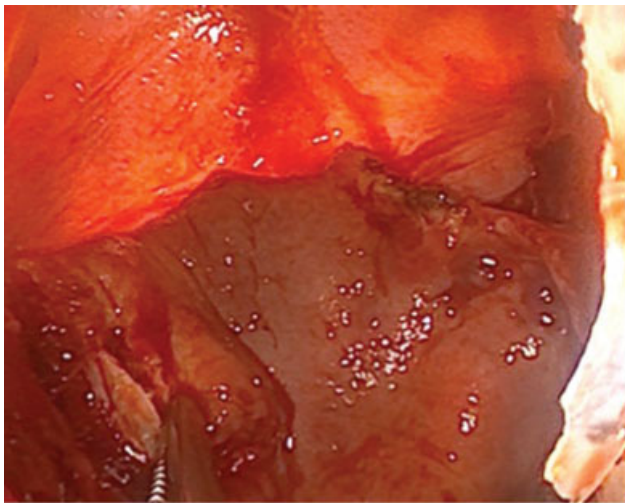


Fig. 3 Nasoseptal flap over pericranial flap.

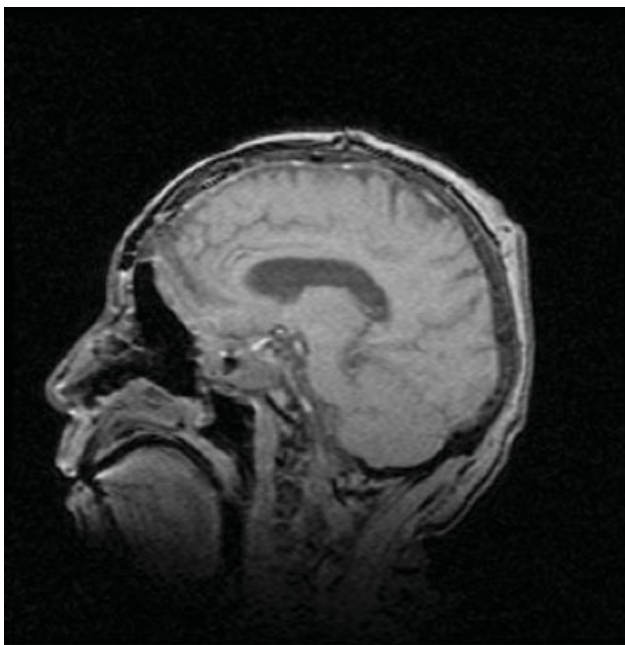


Fig. 4 MRI postop.

P198. SMARCB1-Deficient Sinonasal Carcinoma: A Case Report and Systematic Review

Sean M. Parsek¹, Basit A. Jawad¹, Edward D. McCoull²

¹Tulane University, New Orleans, Louisiana, United States

²Ochsner Clinic Foundation, Jefferson, Louisiana, United States

Introduction: Carcinoma arising from the paranasal sinuses is uncommon, accounting for only 3% of all head and neck malignancies. Prognosis is generally dependent on tumor histology, with poorly differentiated carcinomas being particularly aggressive. These tumors typically present at advanced stages due to nonspecific symptoms and prognosis is poor. Recently basaloid squamous cell carcinoma displaying complete loss of nuclear SMARCB1/INI-1 has been described. This subtype accounts for ~6% of sinonasal carcinomas. In this report, we present a case of SMARCB1-deficient sinonasal carcinoma (SDSC) and systematically review the literature.

Case Presentation: A 21-year-old male presented to the emergency department for severe progressive headache and diplopia of three months duration. Computed tomography revealed a large skull base neoplasm arising from the cribriform plate and extending into the sphenoid sinus, obliterating the bony architecture. His examination was notably only for left medial rectus palsy. The process was initially presumed to be an esthesioneuroblastoma with no evidence of metastatic disease on imaging and was he was taken for endoscopic resection and skull base reconstruction with a combined neurological surgery and otolaryngology approach. The tumor was noted to extend over the cribriform plate with near total erosion of the bilateral ethmoid sinus roof with extension into the planum sphenoidale and left orbital apex with a small dural defect. Histologic examination of the tumor revealed epithelioid cells with loss of INI1 on immunohistochemistry. The final diagnosis was SDSC. The patient subsequently underwent stereotactic radiation therapy for residual disease.

Systematic Review: Systematic search was performed on July 26, 2019 and yielded 13 studies for final review. All studies were either case series or case reports with 82 cases of SDSC published since 2014. Age on presentation ranged from 19 to 75 years with the majority of patients being male. Surgical resection was the primary modality of treatment with adjuvant radiation or chemoradiation therapy. Overall, the prognosis was poor with most tumors presenting at advanced stages with median survival of 24 (15–26) months with 50% of patients dying of the disease and high rates of distant metastases (43.3% [27.1–66.7%]). Only 33.3% (20.8–43.3%) of patients had no evidence of disease at follow up with a median survival of 10.5 (8.8–40.5) months. Studies comparing SNUC to SDSC reported worse prognosis for SDSC and increased risk for locoregional recurrence in the latter cohort.

Discussion: SDSC represents a rare subtype of undifferentiated sinonasal carcinoma with only 82 reports of cases described in the literature. In general, this is a highly aggressive tumor presenting at advanced stage with propensity of metastasis. The majority of patients are treated with primary surgical resection and adjuvant radiation therapy or chemoradiotherapy though have poor prognosis with average survival at ~2 years from diagnosis. Given the nascent description of this entity in the literature and the unfavorable outcomes, it is important to recognize its presence and differentiate it from other undifferentiated carcinomas arising in the paranasal sinuses. More research is necessary to determine the optimal treatment modality and management

P199. Management of Ethmoid Biphenotypic Sarcoma—A Rare Skull Base Malignancy

Justin C. Morse¹, Jordan Malenke¹, Jacob Snyder¹, Eric Succar¹, Mitra Mehad¹, Rakesh Chandra¹

¹Vanderbilt University Medical Center, Nashville, Tennessee, United States

Background: Biphenotypic sinonasal sarcomas (BSNS) are a recently described entity within the latest WHO edition on Head and Neck tumors. Diagnosis is challenging due to similar histologic features of other sinonasal malignancies. Recent work describes improved diagnostic utility utilizing several biomarkers for improved immunoprofiling. Given the scarcity of this pathology, management remains variable and to our knowledge no studies have reviewed treatment techniques in the current literature.

Objectives: To report a case of ethmoid biphenotypic sarcoma and a review of the literature on diagnosis and management of these rare tumors.

Methods: This retrospective case report describes a case of ethmoid biphenotypic sarcoma and treatment. A systematic review of the literature (PubMed and Medline) was performed with an emphasis on management and treatment of these rare malignancies. Data collected included tumor location, treatment techniques, including need for adjuvant therapy, duration of follow up, and reported recurrence.

Results: A 52-year-old female presented with gradual onset double vision and headache with MRI revealing a left ethmoid skull base mass. Endoscopic biopsy revealed BSNS. The patient underwent complete endoscopic resection of the BSNS with skull base repair utilizing a gasket flap composed of Cook Medical BioDesign Duraplasty graft and KLS-Martin Resorb X plating system, followed by nasoseptal flap overlay. Lumbar drain was placed for postoperative CSF diversion for 5 days. Patient was referred to both medical oncology and radiation oncology and recommended for adjuvant radiation but ultimately declined electing for endoscopic and imaging surveillance.

A review of the current literature demonstrates just over 100 reported cases of BSNS, yet treatment is infrequently described. Treatment modality is reported in less than 40 patients. Surgical therapy remains mainstay of treatment. 33% of reported patients received adjuvant therapy including combined chemotherapy and radiation therapy. Local recurrence is high and metastatic disease is rare. There are no clear differentiating factors on which patients should receive adjuvant therapy in the current literature.

Conclusion: BSNS are a rare skull base tumor with a unique diagnostic immunoprofile. Treatment consists of surgical excision. There is no clear consensus in the current literature on selection of patients requiring adjuvant therapy after excision, however, given high reported local recurrence, adjuvant radiation therapy should be highly considered in most cases. The value of combination adjuvant therapy remains uncertain.

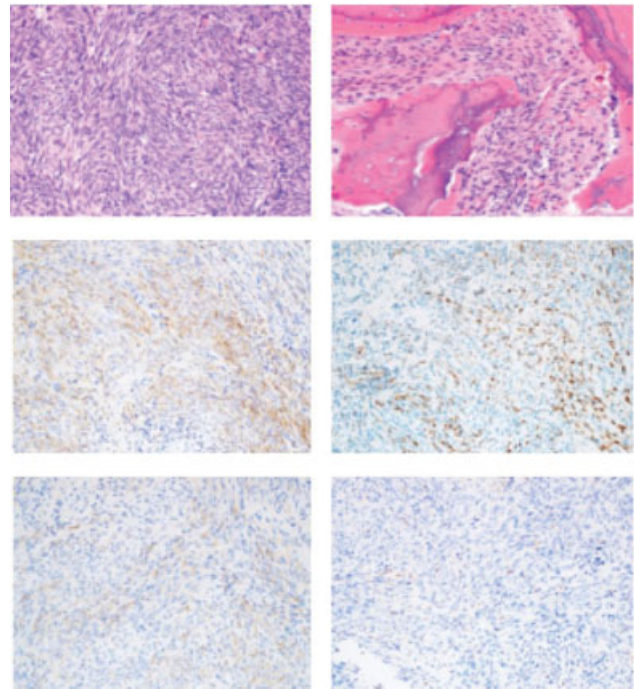


Fig. 1 Biphenotypic sinonasal sarcoma has a fascicular and herringbone growth pattern (A), a subset of cases show bone invasion (B). By immunohistochemistry, they are positive for smooth muscle actin (C), calponin (D), muscle specific actin (E) and focally for S100 (F).

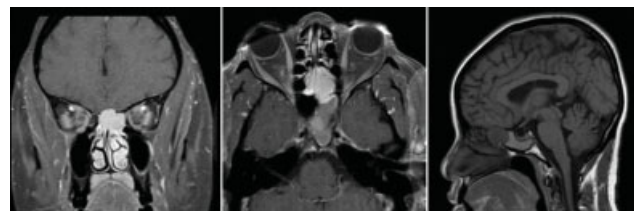


Fig. 2 Magnetic resonance imaging demonstrating contrast enhancement (part A & B) and ethmoid involvement.

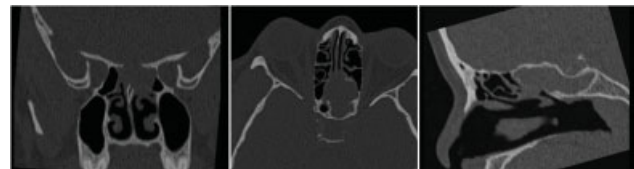


Fig. 3 Computerized tomography imaging showing mass invasion of the ethmoid cavity and vomer.

P200. Combined Synthetic and Nonautologous Gasket Seal for Skull Base Repair after Endoscopic Transsphenoidal Surgeries

Justin C. Morse¹, Jordan Malenke¹, Shanik Fernando¹, Chris Puchi¹, Rakesh Chandra¹, Naweed Chowdhury¹, Lola Chambless¹, Justin Turner¹

¹Vanderbilt University Medical Center, Nashville, Tennessee, United States

Background: Transsphenoidal surgery (TSS) is a highly prevalent surgery that in many cases requires skull base repair. This is particularly important in the setting of

intraoperative cerebrospinal fluid (CSF) leak. Multiple repair techniques exist for repair of CSF leaks after TSS. The gasket seal is often employed for CSF leak repair and commonly utilizes autologous tissue for reconstruction that may lead to donor site morbidity. We present a single intuition's experience utilizing a combined synthetic and non-autologous gasket seal for repair of CSF leaks following TSS.

Objectives: To report the use of combined synthetic and non-autologous gasket seal for skull base repair after TSS.

Methods: This retrospective case series reviewed TSS surgeries at a single institution. Demographics of the patient population, readmission rate, perioperative complications, postoperative leak rates, skull base repair technique, and pathology were all recorded for patients repaired with a combined synthetic/non-autologous gasket seal (decellularized porcine small intestinal submucosa combined with Poly-D, L-lactic acid (PDLLA) resorbable plate) during TSS.

Results: A total of 13 patients (31% female) with an average age of 45 and BMI of 30.6 kg/m² underwent TSS with combined synthetic/non-autologous gasket seal repair over the past 12 months. Pathology was consistent with 11 pituitary adenomas (84.8%), 1 Rathke cleft cyst (7.6%), and 1 craniopharyngioma (7.6%). 6 of 11 (55%) pituitary adenomas resected were secreting tumors. All patients demonstrated intraoperative CSF leak after tumor resection. Average tumor size was 2.29 cm. Combined synthetic/non-autologous gasket seal showed no evidence of postoperative leak in any patient post operatively at most recent follow up.

Conclusion: A combined synthetic/non-autologous gasket seal is a unique and efficient skull base repair using readily available products that has potential to limit donor site morbidity from autologous graft harvest. No patients demonstrated postoperative leak. This study serves as a pilot on the efficacy of this technique while longer term follow up and cost efficacy will be necessary to fully determine its utility.

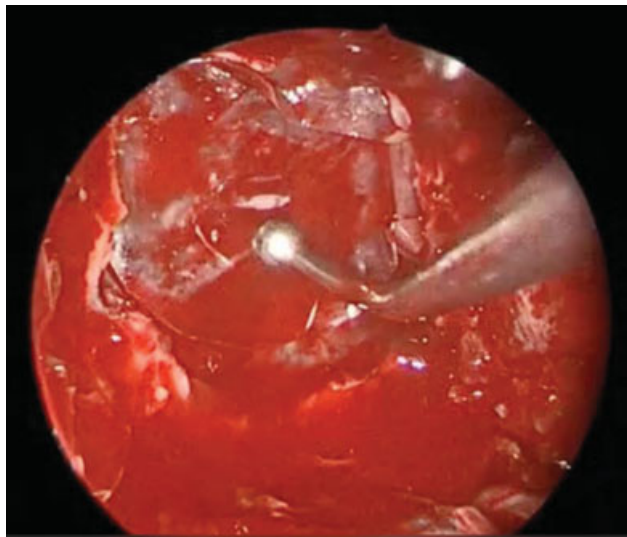


Fig. 1 Gasket seal repair of CSF leak utilizing decellularized porcine small intestinal submucosa combined with PDLLA resorbable plate.

P201. The Application of “in Situ Bone Flap” Combined with Free Middle Turbinate Mucosa in Skull Base Reconstruction after Extended Endoscopic Endonasal Approaches for Craniopharyngioma

Gang Yang¹

¹Department of Neurosurgery, The First Affiliated Hospital of Chongqing Medical University, P.R.China

Objective: To introduce the experience of application of “In Situ Bone Flap” (ISBF) combined with free middle turbinate mucosa to reconstruct skull base after extended endoscopic endonasal approaches (EEAs) for craniopharyngioma.

Background: EEAs for craniopharyngioma cause large skull base bone defects, resulting in high-flow cerebrospinal fluid (CSF) leaks intraoperatively. The vascularized pedicled nasoseptal flap (PNSF) is the classic skull base soft reconstruction method. Our group has confirmed the role of ISBF combined with PNSF in reconstruction of skull base for EEA for craniopharyngioma. With the application of ISBF, is PNSF really indispensable to the reconstruction of EEA?

Methods: ISBF combined with free middle turbinate mucosa was used to reconstruct the Skull base for 3 craniopharyngioma patients who underwent EEA at the First Affiliated Hospital of Chongqing Medical University of P. R. China.

Results: 3 cases of craniopharyngioma recovered evenly. No CSF leaking occurred of these 3 cases. The follow-up MRI and CT images revealed good healing in the surgical region and no neurovascular complications were observed.

Conclusions: ISBF combined with free middle turbinate mucosa is feasible and safe in the reconstruction of EEA for craniopharyngioma. PNSF and fascia lata are not indispensable for the reconstruction of EEA for craniopharyngioma.

P202. Comparative Analysis of Autograft and Xenograft Based Multilayer Lateral Skull Base Reconstruction for Encephalocele And CSF Leaks

Nauman F. Manzoor¹, Douglas J. Totten², Kristen Yancey¹, Alexander D. Sherry², Marc L. Bennett¹, David S. Haynes¹, Alejandro Rivas¹

¹Department of Otolaryngology, Vanderbilt University Medical Center, Nashville, Tennessee, United States

²Vanderbilt University School of Medicine, Nashville, Tennessee, United States

Objective: To compare the use of porcine small intestine submucosal grafts (PSISG, Biodesign) and standard autologous material (fascia) as a reconstructive material in multilayer repair of lateral skull base (LSB) defects.

Setting: Tertiary skull base center

Methods: Retrospective chart review. After IRB approval, a retrospective cohort study was performed including patients who underwent LSB defect repair in a multilayer fashion using either fascia autograft or porcine small intestinal submucosal grafts (PSISG, Biodesign). Demographics were summarized with descriptive statistics. The Kruskal-Wallis and Fisher's exact tests compared the cohorts. Single-predictor binary logistic regression evaluated the association of covariates with outcomes.

Results: 45 patients (mean age = 56 years (range 26–73) and female= 30 (67%) underwent LSB defect repair in a multilayer fashion using either fascia autograft (26 patients; 58%) or porcine small intestine submucosal grafts (Biodesign) (19 patients; 42%) from 2016–2019. Patients were followed for a minimum of six months after surgery. The mean BMI

across all cohorts was 36 kg/m² (range 22–57). BMI did not differ significantly between the Biodesign and fascia autograft cohort ($p = 0.2232$). The most common location of defect was the tegmen mastoideum (39, 87%) followed by the tegmen tympani (19, 42%) and posterior fossa plate (2, 4%). Intraoperatively, 21 patients (47%) were noted to have dural defects, 41 patients (91%) were noted to have encephalocele present and 34 (76%) were noted to have an active CSF leak. Intra-operative lumbar drains were used in 5 (26%) Biodesign cases and 13 (50%) fascia autograft cases (Biodesign vs. autograft: OR 0.357, 95% CI 0.099–1.282, $p = 0.114$).

There was no significant difference in defect location or intraoperative findings between the fascia autograft and Biodesign groups. There were no primary operative failures and recurrent CSF leaks in either cohort (0.0%).

Conclusion: Porcine small intestinal submucosal grafts (Biodesign) appear to provide an effective barrier as a component of multilayer reconstruction after surgical repair of LSB defects. Biodesign performs well in preventing recurrent CSF leaks and appears non-inferior to fascial autografts in LSB reconstruction.

P203. Middle Fossa Encephaloceles Treated via the Transmastoid Approach

Tyler Scullen¹, Peter S. Amenta¹, Zane Freeman², Mansour Mathkour¹, Joseph Lockwood¹, Neal Jackson²

¹Department of Neurosurgery, Tulane University, New Orleans, Louisiana, United States

²Department of Otolaryngology, Tulane University, New Orleans, Louisiana, United States

Table 1.

N	Age	Sex	Etiology	Presentation	Defect	Side	Follow-up(mo)	LOS(d)
1	34	F	Spontaneous	cHL_otoerha	T	L	3	3
2			Spontaneous	cHL_otoerha	M	R	1	4
3	58	F	Spontaneous	cHL_otoerha	M	R	3	5
4			Spontaneous	cHL_otoerha	T	L	1	5
5	77	F	Mastoiditis	Bacterial meningitis,cHL_otoerha	M	L	1	5
6	42	M	Iatrogenic	cHL_chronic mastoiditis	M	R	3	3
7	65	M	Osteoradionecrosis	cHL_otoerha	PF	L	2	6
8	72	M	Chronic otitis media	cHL_otitis	M	R	1	5

cHL denotes conductive hearing loss, M tegmen mastoideum, T tegmen tympani, PF posterior fossa, and LOS length of stay.

Introduction: Middle fossa, or less commonly, posterior fossa, encephaloceles are rare lesions resulting from herniation of the inferior temporal lobe through bony defects in the tegmen tympani or mastoideum. Clinical manifestations include meningitis, epilepsy, cerebrospinal fluid(CSF) leak, and conductive hearing loss. Etiology is variable, with known causes including trauma, iatrogenic injury, long-standing infection, and idiopathic intracranial hypertension(IIH). A significant number of cases are idiopathic. Surgical goals include obliteration of the intracranial-extracranial communication, resection of non-functioning parenchyma, and dural and bony dehiscence repair. The middle fossa craniotomy (MCF), transmastoid (TM), and combined approaches have been described. The minimally invasive TM route provides excellent exposure of the pathology and allows for ample working room to repair the defect. The approach avoids the morbidity of craniotomy and temporal lobe retraction, and allows direct evaluation of middle ear structures. Skull base reconstruction can be facilitated by TM placement of an autologous mastoid cortical bone graft. We describe short-term follow-up in patients treated via TM repair at our facility.

Methods: We retrospectively reviewed patients with symptomatic encephaloceles treated via the TM approach. All procedures were performed by our multidisciplinary neurosurgery and neurotology team. In all cases, a lumbar drain was placed for temporary CSF diversion. Otology harvested graft materials and performed the TM exposure. The neurosurgeon then performed the resection of the encephalocele

and dural defect and bony dehiscence repair. Reconstruction was accomplished with dural substitute and fascia, hydroxyapatite cement, and either a mastoid cortical bone plate or a porous polyethylene implant.

Results: A total of eight encephaloceles in six patients were treated (Table 1). Defect etiologies included spontaneous (50%), iatrogenic(12.5%), and secondary to chronic infection (25%) or osteoradionecrosis(12.5%). One case was iatrogenic following prior tympanomastoidectomy at an outside facility. One patient presented with bacterial meningitis and all with conductive hearing loss. Defects were most often within the tegmen mastoideum (62.5%). On short-term follow up (average 2.25 months) no patients experienced postoperative CSF leak and all experienced preservation of hearing and facial nerve function as well as significant symptom improvement.

Conclusions: Middle fossa encephaloceles have multiple etiologies and can present with a wide range of clinical manifestations. Surgical repair is required to eliminate the communication between the intracranial and extracranial compartments. The TM approach effectively exposes the pathology and allows for a durable repair while avoiding the morbidity of a MCF craniotomy. Our short-term results support the more widespread use of this approach for the treatment of these lesions.

P204. Sellar Trough Trap Door Transclival Reconstruction

Andrew K. Wong¹, Joseph Raviv², Ricky H. Wong²

¹Rush University, Chicago, Illinois, United States

²Northshore University HealthSystem, Evanston, Illinois, United States

Object: The clival and paraclival region are surgically challenging areas to access. Traditional open approaches are limited by the need for brain retraction and traversing neurovascular structures.¹ The endoscopic endonasal trans-clival approach allows for the use of a natural orifice to access what would otherwise be a deep-seated lesion. Cerebrospinal fluid (CSF) leak is a common and serious complication after endonasal approaches and of particular concern with trans-clival approaches. Here we report our modification of a previously described “gasket closure” technique adapting it to the unique anatomy of the clivus by utilizing a sellar trough and porous polyethylene (PP) implant

Methods: The charts of two patients who underwent endoscopic endonasal trans-clival approaches for tumor resection were reviewed. One patient was treated for a clival chordoma while the other for a petroclival meningioma. A nasal-septal flap was raised in the right nare and a transseptal approach was utilized on the left. After clival drilling and tumor resection was complete, the anterior aspect of the sellar floor was resected – creating a trough to allow the sliding of the PP implant into the sellar extradural space. An abdominal fat graft was sized and placed into the prepontine space extending through the clival defect with some mild extrusion into the sphenoid sinus. The PP implant (Medpor; Stryker; Kalamazoo, MI) is tailored and advanced into the region of the defect. The inferior edge of the implant is seated into the caudal clival defect that then acts as a fulcrum as the superior edge of the implant is advanced until it snaps into the trough. The abdominal fat graft extrudes from the circumferential recess of our buttress (PP implant) such that the graft’s sealing function also acts as its anchoring point. The nasal septal flap is then placed over the implant (Fig. 1A–H).

Results: A 21-year-old male with an incidentally found growing chordoma and a 71 year-old female with an abducens nerve palsy found to have a petroclival meningioma were taken for an endoscopic endonasal transclival resection of their tumors with a sellar trough trap door clival closure

and reconstruction. Operative duration was 171 and 178 minutes, hospital length of stay was 4 and 7 days, and follow up was 23 and 17 months, respectively. No postoperative CSF leak was noted. Pre and post op MRI demonstrated complete resection of the tumors (Figs. 2–3)

Conclusions: Postoperative CSF leak is a known complication of endonasal approaches with reported rates as high as 21%. Various methods including a nasoseptal flap and a “gasket-seal” closure have been used to mitigate this risk.² We modified and adapted these methods for a transclival approach with good results.

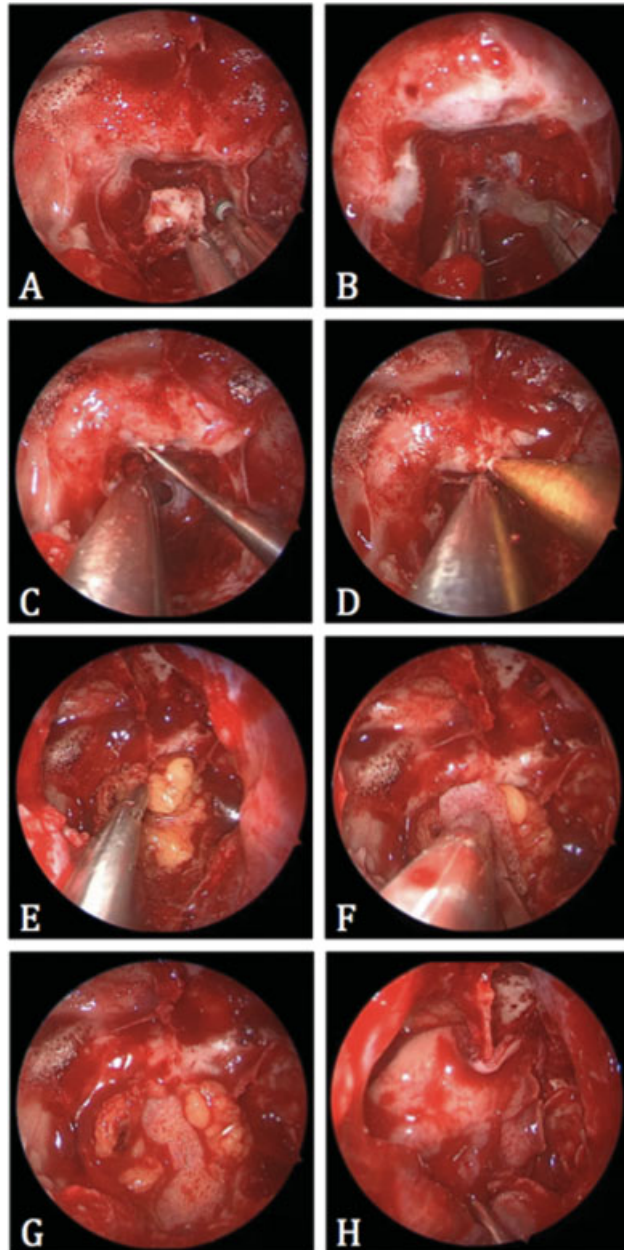


Figure 1 (A) clival skeletonization; (B) tumor resection; (C,D) creation of sellar trough; (E) fat graft placement; (F-G) porous polyethylene implant placement; (H) nasoseptal flap placement

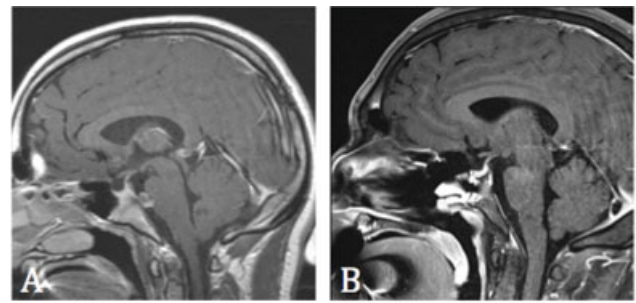


Figure 2 (A) MRI of preoperative chordoma; (B) Postoperative MRI with gross total resection

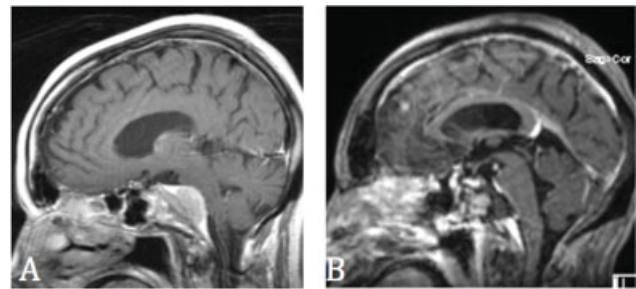


Figure 3 (A) MRI of preoperative meningioma; (B) Postoperative MRI with near total resection

References

1. Carrabba G, Dehdashti AR, Gentili F. Surgery for clival lesions: open resection versus the expanded endoscopic endonasal approach. *Neurosurg Focus* 2008;25(6):E7
2. Leng LZ, Brown S, Anand VK, Schwartz TH. “Gasket-seal” watertight closure in minimal-access endoscopic cranial base surgery. *Neurosurgery*. 2008;62(5 Suppl 2): ONSE342–3

P205. Utilizing the Transpterygoid/Parapharyngeal Corridor for Free Flap Reconstruction of Cranio-orbital Defects: A Case Series

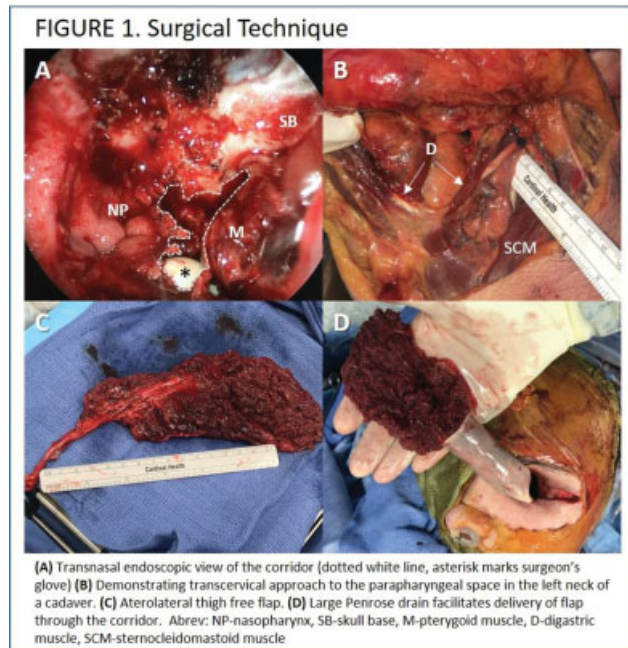
Ricardo J. Ramirez¹, Jake J. Lee¹, Patrik Pipkorn¹

¹Washington University in St. Louis, St. Louis, Missouri, United States

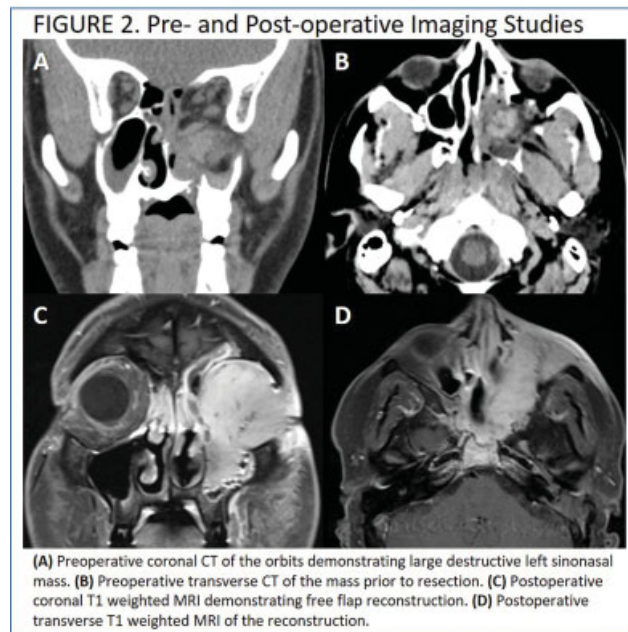
In cases that require large reconstruction of the skull base, a free flap may be considered. During planning, surgeons should be aware of available pedicle corridors. In this report, we describe our experience with the transpterygoid/parapharyngeal corridor for reconstruction of cranio-orbital defects in two patients.

This corridor was first described in a cadaver study by Rivera-Serrano and colleagues. Similar to their description, we create the corridor endoscopically through a transpterygoid approach. Removal of the posterior maxillary wall and pterygoid plate enables access to the pterygopalatine fissure and infratemporal fossa. Neck exploration is performed for vessel exposure and the dissection is carried medially to the pterygomasseteric sling at the mandibular angle to identify the medial pterygoid muscle. With blunt dissection through

the parapharyngeal space, the corridor is completed. A large Penrose drain facilitates tunneling of the flap through the corridor for microvascular anastomosis. Herein, we describe two cases in which we utilized this corridor for cranio-orbital reconstruction.



The first patient is a 32-year-old male who presented with sudden onset epistaxis, blurred vision, and left retro-orbital pain. His imaging revealed a large destructive sinonasal mass with skull base erosion. Biopsy was consistent with a malignant peripheral nerve sheath tumor. He received neoadjuvant chemotherapy and subsequently underwent left orbital exenteration, transorbital extradural resection of the anterior and middle fossa skull base tumor, and resection of infratemporal fossa contents. Due to the large cranio-orbital defect with dural and carotid exposure, a transpterygoid/parapharyngeal tunnel was created for anterolateral thigh free flap reconstruction with facial artery anastomosis. The patient's postoperative course was uncomplicated, and he was discharged on postoperative day 6. He has since undergone adjuvant chemoradiation and at 6-month follow-up was noted to have a completely mucosalized flap with no evidence of CSF leak.



The second patient is a 52-year-old male with history of adenoid cystic carcinoma of the right posterior ethmoid and sphenoid sinuses. He previously underwent anterior cranio-facial resection with orbital reconstruction followed by radiation. He experienced local recurrence treated with gamma knife radiosurgery and additional radiation. He subsequently developed a frontal brain abscess which was aspirated and treated with chronic antibiotic suppression. He experienced recurrent infectious bouts despite chronic antimicrobial therapy and ultimately experienced total loss of vision. Due to these complications, the decision was made to proceed with right orbital exenteration and resection of necrotic neoplastic tissue. Because of the defect size, and due to a significant prior radiation history; recruitment of non-radiated tissue was performed for safe reconstruction. A corridor was created, and a right anterolateral thigh free flap was tunneled through the orbital defect. The facial artery was

used for anastomosis. The postoperative course was uncomplicated, and he was discharged on postoperative day 7. Four-month follow-up revealed an intact flap covering the skull base with no evidence of CSF leak.

To our knowledge, this is the first in-vivo case series reporting successful skull base reconstruction utilizing the transpterygoid/parapharyngeal corridor. This technique is feasible and allows for safe skull base reconstruction with tunneling of the pedicle for microvascular anastomosis.

P206. The Use of Composite Cartilagomucosal Nasoseptal Flap for Skull Base Reconstruction after Resection of a Suprasellar Mass

Kent V. Curran¹, Tyler J. Kenning², Maria Peris-Celda², Carlos Pinheiro-Neto³

¹Albany Medical College, Albany, New York, United States

²Department of Neurosurgery, Albany Medical Center, Albany, New York, United States

³Division of Otolaryngology/Head and Neck Surgery, Department of Surgery, Albany Medical Center, Albany, New York, United States

Introduction: The nasoseptal flap (NSF) is the main reconstructive option in endonasal skull base surgery. This reliable reconstruction is effective to seal cranial base defects and avoid CSF leak. However, the bone removal resultant from the approach is not replaced with this technique. Here we present a novel technique based on semi-rigid reconstruction that can be used not only to prevent CSF leak but also to reinforce and protect the intracranial structures. The composite cartilagomucosal NSF is designed leaving part of the quadrangular cartilage of the septum attached to the mucosal flap. This extra strength obtained with the cartilage may be interesting to protect important neurovascular structures, particularly in young patients where medical nasal intrusion may be necessary.

Case Report: The patient is a 17-year-old female who presented with primary amenorrhea. Images showed a suprasellar mass. It showed a lobulated mass within the suprasellar cistern with extension into the floor of the third ventricle that measured 16 × 8 × 12 mm. No other acute intracranial findings were noted. Preoperative laboratories showed hyponatremia and decreased pituitary hormones consistent with hypopituitarism. The patient's suprasellar mass showed reactive lymphoid hyperplasia; the pituitary gland was infiltrated by lymphocytes, resulting in impaired hormone release.

Surgical Technique: After the regular incisions for the NSF are performed, the anterior edge of the flap, next to the caudal border of the septum is carefully elevated. This elevation is carried posteriorly up to ~5 mm of the incision. Superiorly, next to the nasal dorsum incision, the mucosa is elevated from the cartilage only ~5 mm from the nasal dorsum. The goal is to expose an "L" strut to support the septum and leave the mucosa of the center of the quadrangular cartilage still attached. At that point, the septal cartilage is transected parallel to the caudal border of the septum and parallel to the nasal dorsum. Then the cartilage is elevated from the contralateral mucosa in a subperichondrial plane until identification of the perpendicular plate of the ethmoid posteriorly and the maxillary crest inferiorly. At that point, the cartilage is detached from those two structures and the harvest continues on the initial side as usual for the NSF with the elevation of the mucosa from the vomer. At the end, the NSF will have a piece of septal cartilage attached to it. After the tumor was resected with a transplanum/transuberulum approach, the high flow intraoperative CSF leak was reconstructed with inlay/onlay fascia lata button graft and onlay composite cartilagomucosal NSF.

Results: Patient is 4-months out from surgery. No postoperative CSF leak. No complications related to the composite flap. Nasal endoscopy in clinic shows the flap well healed to the cranial base but no pulsation due to transmission of brain pulsation as usually seen with the regular NSF.

Conclusions: The reconstruction of a suprasellar defect with a composite cartilagomucosal NSF was feasible. No complications related to the flap were noticed. Further surgical cases and longer follow-up are needed for a better assessment of the benefits of this technique.

P208. Anterior Skull Base Reconstruction Using Nasoseptal Flap: Cadaveric Feasibility Study

Ju Hyung Moon¹, Kyoung Su Sung², Jaejoon Lim³, Chang Ki Hong⁴

¹Severance Hospital, Yonsei University, Seoul, South Korea

²Dong-A University Hospital, Busan, South Korea

³Bundang CHA Medical Center, Seongnam, South Korea

⁴Gangnam Severance Hospital, Yonsei University, Seoul, South Korea

Objectives: There is limited cadaveric data regarding the feasibility of pedicled nasoseptal flap (PNSF) for anterior skull base (ASB) reconstruction. The purpose of this study is to assess the feasibility of PNSF for ASB reconstruction and to describe a method to compensate the shortage of flap length using a cadaveric model.

Methods: Using 10 formalin-fixed and 5 fresh adult cadaver specimens, ASB dissection without sphenoidotomy was performed, and sufficiency of the PNSF to cover the ASB was assessed. After sphenoidotomy, the insufficient length to the posterior wall of the frontal sinus, extent of anterior coverage from the limbus of the sphenoid bone (CL) using PNSF was measured.

Results: Without sphenoidotomy, mean length of the remaining PNSF after coverage of the posterior wall of the frontal sinus (CPFS) was 0.67 cm (standard deviation [SD] = 0.38 cm); all dissections showed sufficient coverage of ASB using PNSF without sphenoidotomy. After sphenoidotomy, mean insufficiency in the length of PNSF to the posterior wall of the frontal sinus was 2.10 cm (SD = 0.41 cm), CL: 1.86 cm (SD = 0.51 cm). Correlations between CPFS without sphenoidotomy and CL were not positive ($r = 0.165$, $p = 0.557$).

Conclusion: The use of PNSF for ASB reconstruction can be associated with cerebrospinal fluid leakage. The length of ASB coverage using PNSF can be increased by remaining the anterior wall of sphenoid sinus as it can support the pedicle of PNSF, so it can raise success rate of ASB reconstruction using PNSF. For large tumors which need a wide sphenoidotomy for tumor resection, additional methods could be needed for ASB reconstruction.

P209. Sinonasal Morbidity Following A Regenerated Oxidized Cellulose Onlay for Sellar Reconstruction

Mark B. Chaskes¹, Tawfiq Khoury¹, Pascal Lavergne¹, Gurston C. Nyquist¹, Mindy R. Rabinowitz¹, Christopher Farrell¹, Marc R. Rosen¹, James J. Evans¹

¹Thomas Jefferson University Hospital, Philadelphia, Pennsylvania, United States

Background: A variety of endonasal sellar repair techniques have been described, many of which are complex, expensive, and carry potential morbidity. We have previously shown that an onlay of layered sheets of regenerated oxidized cellulose is an inexpensive, simple, and adequate reconstruction for repair of the sella in appropriately selected pituitary adenoma patients. The objective of this study is to review

overall sinonasal morbidity associated with this simple and effective reconstruction technique.

Methods: Retrospective review of patients who underwent endoscopic transsphenoidal surgery for pituitary adenoma between 2005–2018 at a tertiary center. Postoperative sinonasal morbidity and SNOT-22 scores in patients who underwent sellar reconstruction with an onlay of regenerated oxidized cellulose were compared with those who were reconstructed via any other technique and to the literature. Criteria used to assess postoperative morbidity included crusting, synechia formation, septal perforation, sinusitis, epistaxis, sellar hemorrhage, cerebrospinal fluid (CSF) leak, meningitis, and unplanned 30-day readmission.

Results: A total of 686 patients were reviewed, 186 were reconstructed with a regenerated oxidized cellulose onlay. Eleven of these patients (5.9%) had significant crusting, 21 (11.3%) had synechia formation, and there were no instances of septal perforation noted on postoperative nasal endoscopy. Twenty-five patients (13.4%) had postoperative sinusitis treated with antibiotics; no patients required further endoscopic sinus surgery. Two patients (1.1%) experienced new onset postoperative epistaxis requiring packing or operative cauterization. There was one case of sellar hemorrhage. There were two postoperative CSF leaks (1.1%). There were no cases of meningitis. Pre- and postoperative SNOT-22 scores were 12.9 ± 11.9 and 14.3 ± 14.9 ($p = 0.796$), respectively. Ten (5.4%) patients had an unplanned 30-day readmission—5 for electrolyte imbalance, 4 for other medical problems, and 1 for a negative CSF leak evaluation. One hundred and twenty-six patients (67.7%) did not experience any postoperative morbidity. The rates of these morbidities were either not statistically different or favorable when compared with patients reconstructed with other techniques in our cohort and when compared with existing literature.

Conclusions: An onlay of regenerated oxidized cellulose does not increase rate of postoperative CSF leak in appropriately selected patients and is a safe and well-tolerated modality for sellar reconstruction associated with minimal postoperative morbidity.

P210. Fat as a Biological Dressing: A Novel Adjunct to Skull Base Reconstruction

John M. Byrne IV¹, Ari Stone², Margaret Tallmadge¹, Krista Brackman¹, Bhavani Kura², Juanita Celix², Amin Kassam², Sammy Khalili²

¹Aurora Research Institute, Milwaukee, Wisconsin, United States

²Aurora Neuroscience Innovation Institute, Milwaukee, Wisconsin, United States

Background: Abdominal fat is a reservoir of stem cells and growth factors that can be used to promote healing. It is routine practice amongst our skull base team to use a fat graft as a biologic dressing as an adjunct to the nasoseptal flap for reconstruction of intraoperative cerebrospinal fluid (CSF) leak.

Objective: To assess the rhinological outcomes of using an abdominal fat graft as a biologic dressing for complex skull base repairs, in addition to a nasoseptal flap.

Methods: A three-year retrospective chart review of patients who had undergone pituitary surgery between June 1st, 2016 and June 1st, 2019. Inclusion criteria included all pituitary surgeries that had a nasal septal flap and completed a Sino-Nasal Outcome Test score (SNOT-22). Preoperative and postoperative SNOT-22 scores were collected at each clinic visit. Each patient underwent an expanded endonasal approach and resection of their pituitary mass, as well as a reconstruction using a dural matrix graft, nasoseptal flap, and abdominal fat graft as a biologic dressing. They were then

packed with stented merocels bilaterally for approximately one week. Follow-up visits to clinic occurred at 1 week, 2 weeks, 4 weeks, 3 months, and 6 months from time of surgery. Debridements occurred at follow-up visits for the first month postoperatively and on an as needed basis. Surgery and follow-up were done by one skull base team at a large quaternary health system serving the area from Northern Illinois to the Upper Peninsula of Michigan. For our statistical analysis, patients were divided into two groups: those that had received a fat graft versus those who did not. Rhinologic data were then compared between the two groups.

Results: There was no significant difference in total, rhinological or quality of life SNOT-22 patient outcomes when comparing patients who had received a fat graft and those that did not ($p = 0.946, 0.6591, \text{ and } 0.4833$). Only 57 pituitary patients completed a SNOT-22, with 14 of those having an intraoperative CSF leak where both a nasoseptal flap and an abdominal fat graft were used for reconstruction. There were only two postoperative CSF leaks that required revision due to intercranial hypertension and previous radiation exposure.

Conclusion: The use of abdominal fat as a biological dressing has several advantages with limited detrimental effects. There appears to be no evidence thus far of change in longtime rhinologic outcomes as a result of its use. The technical nuances of this technique are important to ensuring successful outcomes.

P211. Management of Penetrating Anterior Skull Base Injury from Transnasal Foreign Body

Rebecca Limb¹, Martin Hunn¹

¹Alfred Hospital, Melbourne, Australia

We report the unusual case of a 35-year-old man who presented post self-insertion of a foreign body (a toothbrush with the bristled end snapped off) transnasally while suffering from a drug-induced psychosis. The tip of the retained object extended intracranially as far as the right foramen of Munro and caused unilateral obstructive hydrocephalus requiring emergency external ventricular drain insertion. There was no evidence of significant intracranial hemorrhage on initial imaging but the postcommunicating segments of both anterior cerebral arteries were significantly displaced by the object. After deliberating the safest surgical approach, we elected to perform a bifrontal craniotomy to approach the anterior fossa floor inter-hemispherically, to gain proximal control of the anterior cerebral arteries and protect them from laceration. Once this was achieved, the foreign body was removed transnasally by the ENT surgeon, who had performed prior ligation of the ipsilateral anterior ethmoidal artery to prevent catastrophic nasal hemorrhage. Nasoendoscopy revealed surprisingly little damage to the nasal cavity. The skull base defect was repaired utilizing split calvarial bone graft obtained during the craniotomy, and a vascularized pericranial flap. Postoperatively the patient did not develop a CSF leak and displayed no signs of meningitis. His psychosis self-resolved within two weeks postoperatively and he was discharged home after a 2-week course of intravenous antibiotics and with psychiatry input. A delayed postoperative MRI demonstrated no obvious abscess, empyema or cerebral infarction. On review of the literature, such extreme cases of skull base penetrating injury appear to be rare and there is little technical advice available on optimal surgical strategies. This case provides an opportunity to discuss the management of such injuries and adds to a currently scarce body of knowledge on the topic.

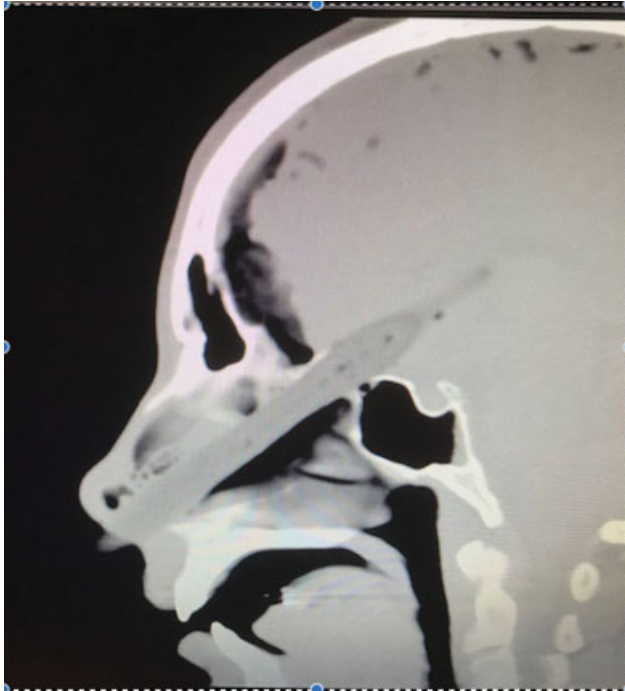


Fig. 1

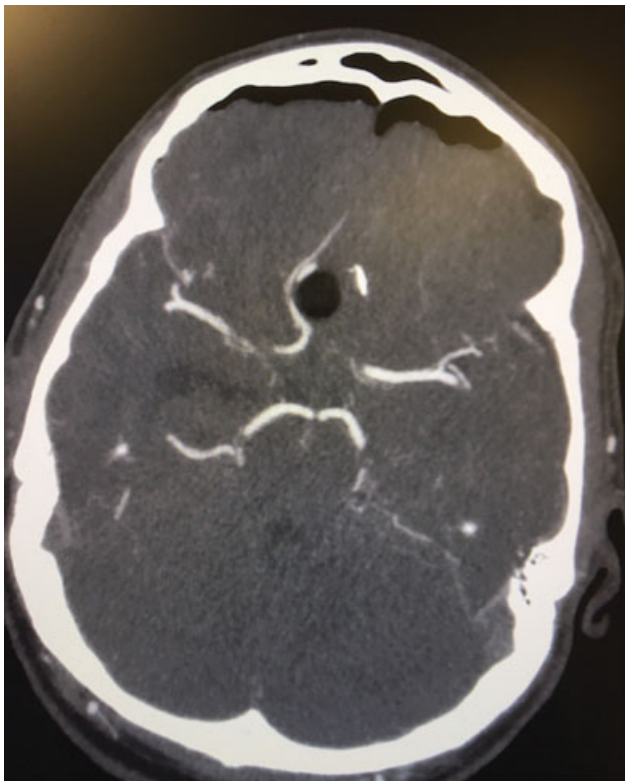


Fig. 2

P212. The Use of Resorbable and Integrative Collagen Sponges to Obliterate the Intrasellar Space and Achieve a Fatless, Spherical Dural Reconstruction Following Transsphenoidal Surgery

Won Kim¹, Sophie Peeters¹, Giyarpuram Prashant¹, Matthew Sun¹, Jasmine Dicesare¹, Marilene Wang¹, Jeffrey Suh¹, Jivianne Lee¹, Marvin Bergsneider¹

¹ University of California, Los Angeles, California, United States

Introduction: The repair of cerebrospinal fluid (CSF) leaks following transnasal transsphenoidal (TNTS) surgeries for sellar pathologies has developed considerably over the previous decades. Traditionally performed using autologous fat grafts, the advent of the nasoseptal flap (NSF) has allowed for the repair of even high flow leaks and larger skull base defects with great success. The development of improved allografts and fibrin sealants has allowed for unique ways to reconstruct the sella. However, it is unclear which materials are best suited for this task, and if autologous fat is still a necessary component of the repair.

Methods: Beginning in August of 2018, the primary author repaired grade I and II leaks without the use of autologous fat. Upon identification of a CSF leak following resection of the pituitary tumor, a piece of collagen sponge (Helistat) was cut to fill the expanded sellar cavity, while limiting extension into the suprasellar space. An oversized piece of spongy dural allograft (Duragen Plus) was then used to wrap around the intrasellar hemostatic agent, with particular care to ensure that a long length of allograft would span the entirety of the diaphragma sella. All edges were tucked intradurally and along the medial cavernous sinus and sellar floor. A Valsalva maneuver was performed to 30 mm Hg to ensure no brisk leakage of CSF was seen. A free mucosal graft or nasoseptal flap was then placed over the repair, and sealed with fibrin glue. This was then buttressed with nasopore.

Results: Eight patients from August of 2018 received sellar reconstruction in the abovementioned manner. Six were female, median age was 53 (39–68), and all had macroadenomas with an average maximum diameter of 3.1 cm (2–4.8 cm). There were two grade I leaks, and six grade II leaks. One patient had no mucosal grafting (grade I), one patient had a free mucosal graft (grade II), while all others had NSFs placed. In one case, Helistat was not available and hemostatic cellulose (Surgicel Fibrillar) was used. Tisseel was used once, while all other patients received Adherus. All patients had at least two months follow-up with no signs of CSF leak postoperatively. Postoperative MR studies demonstrate sellar lucency where the collagen sponge was placed.

Conclusion: We describe a method through which absorbable collagen sponge is used to abrogate CSF flow through the arachnoid in a semi-impermeable fashion. We believe this allows sufficient diminution of both the physical fluid pulsations transmitted from the intracranial space as well as the access of fluid to the dural repair, thereby allowing it time to seal and integrate. The use of an absorbable sponge to fill the sellar space is critical in this fatless technique as opposed to simply using dural allograft, as the latter may result in a thickened mass of dural substitute that may be challenging to traverse in cases of repeat surgeries. Future studies are needed to determine if this method is still viable without a vascularized flap or fibrin sealant.

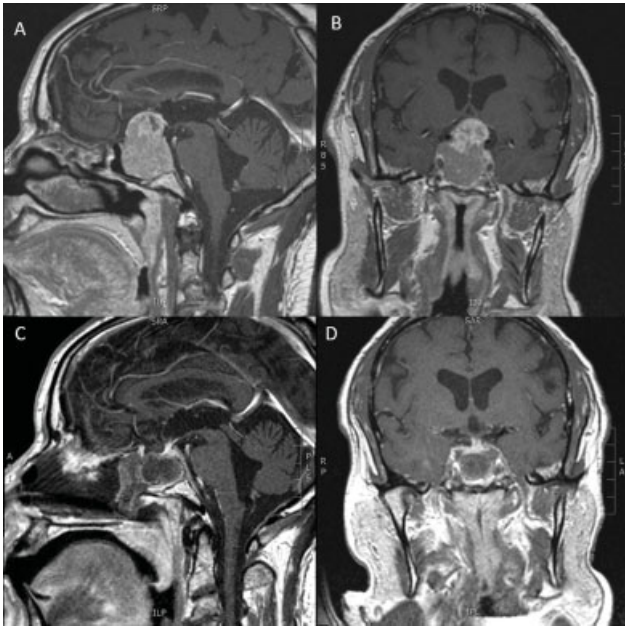


Fig. 1

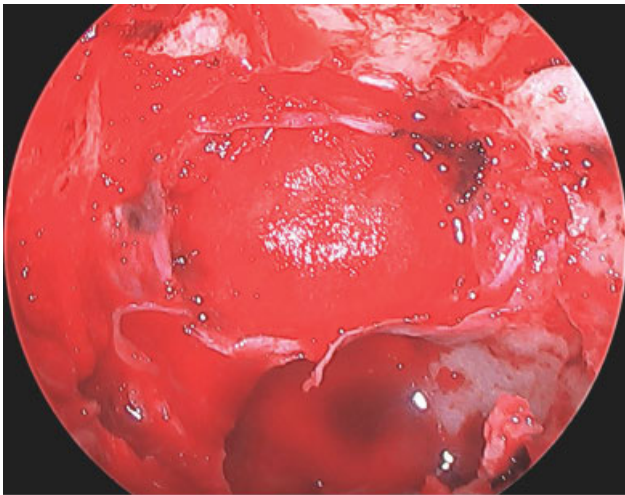


Fig. 2

P215. Ganglioneuroma of the Internal Auditory Canal

Mark E. Russo¹, Emma C. Celano², H. J. Kim¹, Amjad Anaizi², Metin Ozdemirli³

¹Department of Otolaryngology, Georgetown University, Washington, District of Columbia, United States

²Department of Neurosurgery, Georgetown University, Washington, District of Columbia, United States

³Department of Pathology, Georgetown University, Washington, District of Columbia, United States

Introduction: Ganglioneuromas are benign slow growing neurogenic tumors that are thought to originate from neural crest cells. While these tumors typically arise from sympathetic or peripheral nerves, particularly in the posterior mediastinum or retroperitoneum, there have been a few reported cases of ganglioneuroma arising at the skull base. We report another such one of these cases with a ganglioneuroma arising from the cochlear nerve in the distal

internal auditory canal (IAC). This is the second case of ganglioneuroma arising within the IAC reported in the literature.

Case Description: Our patient is a 43-year-old woman who presented with gradually worsening right-sided sensorineural hearing loss for the past five years. MRI of the IAC (Fig. 1) demonstrated a 6 × 4 mm intracanalicular enhancing lesion within the right distal IAC thought to be consistent with a vestibular schwannoma. She was deemed to have nonserviceable hearing with a pure tone average of 35dB HL and 24% word discrimination. She elected to undergo a translabyrinthine resection of the IAC lesion. Intraoperatively, the tumor appeared to be a yellowish lesion (less vascular than a schwannoma) arising from the cochlear nerve in the distal IAC. Final pathology demonstrated nerve tissue, spindle cells, fibrous stroma and adipocytes, and mature ganglion cells without atypia consistent with ganglioneuroma (Figs. 2 and 3). Immunohistochemistry revealed that the ganglion cells were positive for chromogranin and scanty positive for calretinin supporting both the neoplastic nature of the cells and the diagnosis of ganglioneuroma.

Discussion: Ganglioneuroma is a rare benign lesion in the IAC, but it should be considered on the differential diagnosis. It is important to distinguish ganglioneuroma from other more aggressive neuroblastic tumors such as ganglioneuroblastoma.

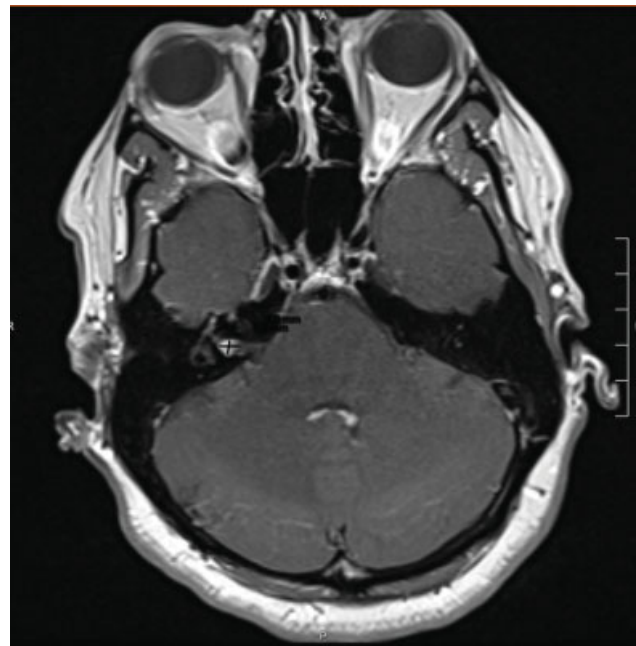


Fig. 1 Axial MRI T1 postcontrast sequence at the level of the IAC demonstrating a 6 × 4 mm enhancing intracanalicular lesion in the right internal auditory canal.

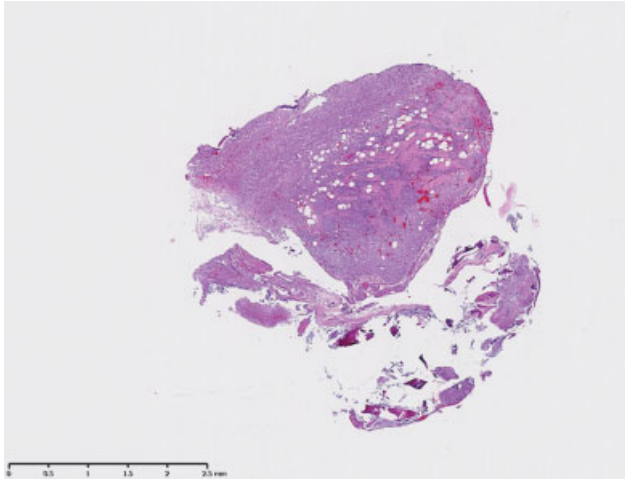


Fig. 2 Low-power magnification of hematoxylin and eosin (H&E) stain of right internal auditory canal lesion.

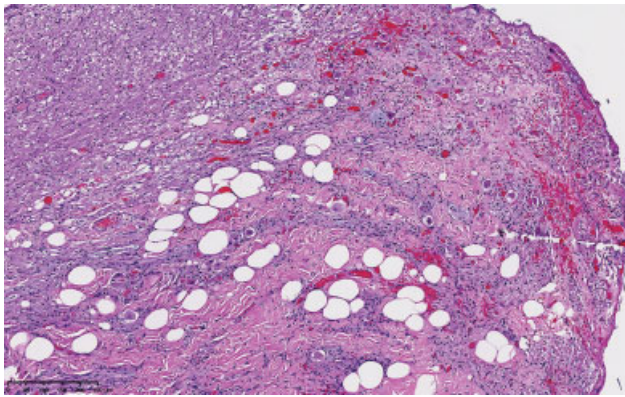


Fig. 3 High-power magnification of hematoxylin and eosin (H&E) stain of right internal auditory canal lesion. Visualized are nerve tissue, spindle cells, fibrous stroma and adipocytes. Likewise, mature ganglion cells without atypia are visualized with compact eosinophilic cytoplasm with a single eccentric nucleus.

P216. Know Your ABCS: Aneurysmal Bone Cyst of the Temporal Bone

Nitesh P. Patel¹, Lucas P. Carlstrom¹, Avital Perry¹, Collin Driscoll¹, Michael J. Link¹

¹Mayo Clinic, Rochester, Minnesota, United States

Background: Aneurysmal bone cysts (ABCs) are benign vascular bone tumors that can grow rapidly and destroy surrounding bone. These tumors are either primary (70%) or occur secondarily to other nonmalignant bone lesions. ABCs can theoretically arise in any bone but typically develop in long bones and the posterior spinal elements. Although cranial ABCs have been reported in the literature, ABCs involving the skull base are exceedingly rare. We report a case of an ABC involving the mastoid portion of the temporal bone and highlight the key imaging features and treatment options.

Methods: Case report.

Results: A 30-year-old otherwise-healthy female presented with a 1-month history of tingling in the right cheek and tongue and progressively worsening pressure-like headaches in the right occipital region. Her headaches radiated

anteriorly, worsened with dynamic head movements and Valsalva maneuvers, and were intermittently associated with right eye blurred vision. Initial CT and MR imaging revealed a multiseptated mass with fluid-fluid levels in the right lateral posterior fossa (Fig. 1). The lesion underwent surveillance imaging, and follow-up three months later revealed interval enlargement (Fig. 2). Brain MRI showed a greater degree of hyperintense T1 and T2 signal with a new central wedge-shaped area (Fig. 2A–D). Noncontrast head CT showed areas of hyperdensity consistent with blood products, and CT venogram demonstrated occlusion of the right sigmoid sinus at the level of the mass (Fig. 2E, F). Subsequent catheter angiography confirmed occlusion of the ipsilateral transverse-sigmoid sinus junction but showed no abnormal vascularity. She was taken for definitive en bloc gross total resection; intraoperatively an extradural mass was visualized emanating from the mastoid portion of the temporal bone and causing compressive occlusion, but no invasion of the ipsilateral sigmoid sinus was identified (Fig. 3A, B). Histopathology confirmed an aneurysmal bone cyst (Fig. 3C–E). FISH was negative for USP6 gene rearrangement, a marker that is observed in 70% of primary aneurysmal bone cysts but not seen in secondary cases.

Conclusion: ABCs of the skull base are rare and require nuanced review of multimodal cranial imaging for preoperative consideration. Typical MRI findings include multiple septations with fluid levels and areas of T1 and T2 hyperintensity; however, these features can also be found in other bone tumor types. Given that ABCs continue to expand until treated, surgical resection is the treatment of choice for skull base lesions that are anatomically amenable, and a gross total resection should be attempted due to high rates of recurrence.

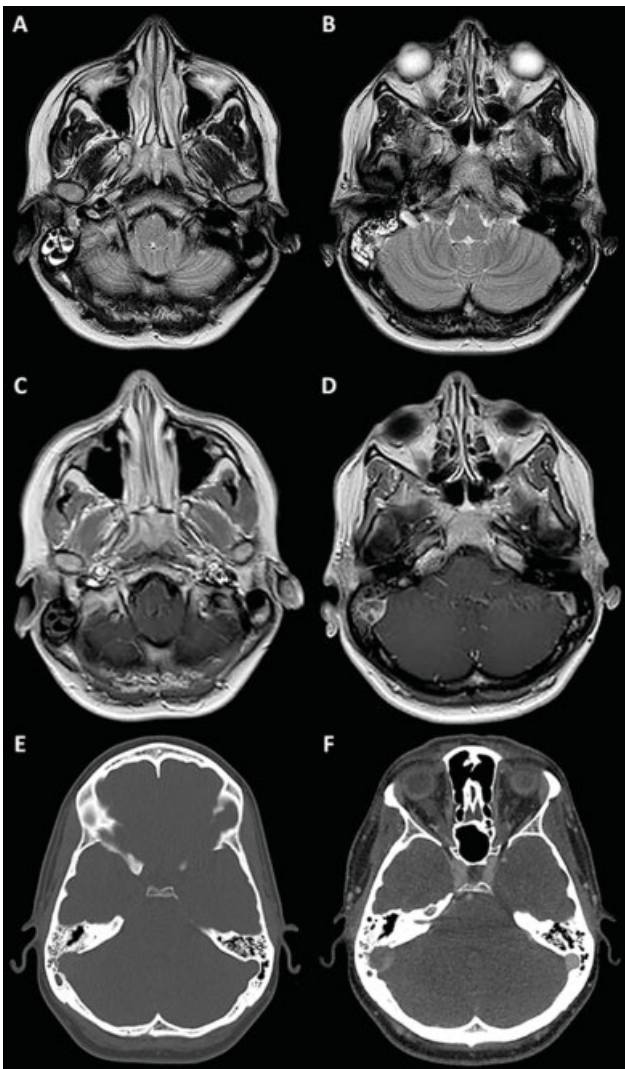


Fig. 1 Initial MRI and CT:

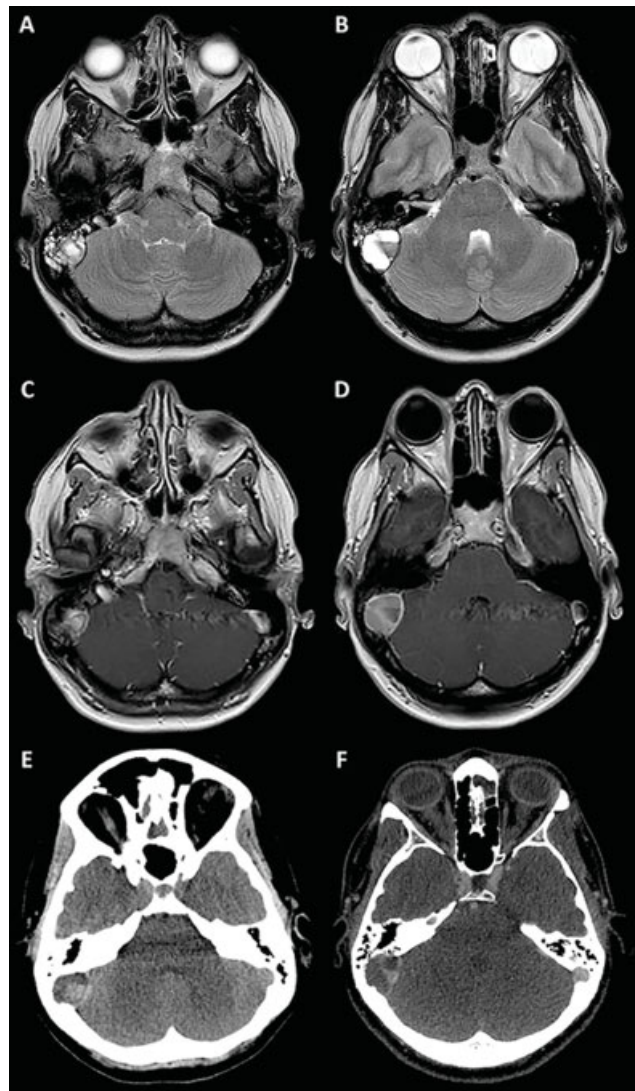


Fig. 2 Interval enlargement.

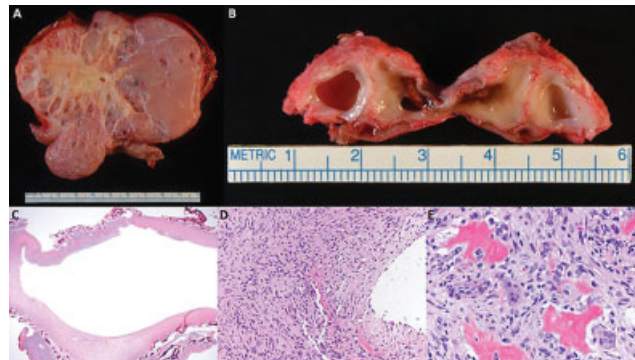


Fig. 3 Pathology.

P217. Giant Renal Cell Carcinoma Metastasis to the Skull Base with Temporal Bone Invasion: A Case Report and Review of the Literature

Lauren A. Linker¹, L. Madison Michael II², Scott Collier³, Robert J. Yawn¹

¹Department of Otolaryngology, University of Tennessee Health Science Center, Memphis, Tennessee, United States

²Department of Neurosurgery, University of Tennessee Health Science Center, Memphis, Tennessee, United States

³Department of Pathology, University of Tennessee Health Science Center, Memphis, Tennessee, United States

Objectives: To review the incidence, clinical presentation, and management of metastatic renal cell carcinoma to the lateral skull base and temporal bone, and describe a case of giant clear cell renal cell carcinoma metastasis to the skull base with temporal bone invasion.

Study Design: Case report and literature review.

Methods: The case of a patient with ear fullness, ultimately found to have metastatic renal cell carcinoma involving the posterior fossa and temporal bone, is reviewed. The clinical, radiologic, and pathologic features of the disease are discussed, with description of a transtemporal approach to the posterior fossa and mastoidectomy for surgical resection.

Results: A 67-year-old female presented to a tertiary center with recent onset decreased hearing, ear fullness, and intermittent pulsatile tinnitus on the left side. Magnetic resonance imaging revealed a $6 \times 5 \times 4$ cm posterior fossa mass with central necrosis and contrast enhancement on T1-weighted imaging (Figs. 1, 2). The mass eroded calvarial bone with extension into the retroauricular subgaleal tissue. It also eroded the posterior fossa plate with extension into the mastoid. Cranial nerve function was grossly intact. The patient had a history of renal cell carcinoma with lung and liver metastases in 2015. She underwent nephrectomy and immunotherapy until 2018, with stable hepatic and lung lesions at that time. Given this history, metastatic disease was suspected. Surgical resection via retroauricular approach to the posterior fossa with mastoidectomy was performed after preoperative embolization. Gross total resection was achieved (Fig. 3). Postoperatively, the patient was neurologically intact with no cranial nerve deficits. Pathology revealed metastatic clear cell renal cell carcinoma (Fig. 4). The patient is currently undergoing adjuvant radiation and immunotherapy.

Conclusions: Metastatic renal cell carcinoma to the temporal bone is a rare condition with few reported cases in the literature. Surgical resection with adjuvant radiation therapy is favored for large tumors. Close posttreatment surveillance is required given the aggressive nature of this tumor.

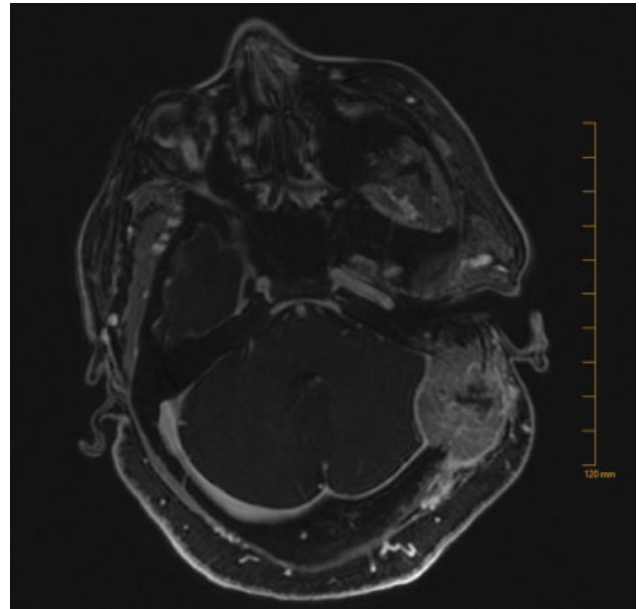


Fig. 1. Preoperative axial magnetic resonance imaging demonstrating a giant left-sided extra-axial mass with bony destruction. The mass measured $6 \times 5 \times 4$ cm in dimension with displacement of the adjacent brain parenchyma.

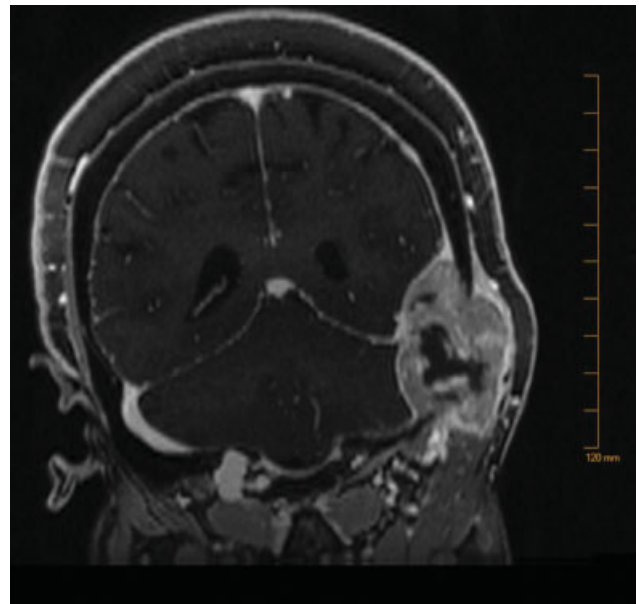


Fig. 2. Preoperative coronal magnetic resonance imaging demonstrating a giant left-sided extra-axial mass with bony destruction. The mass measured $6 \times 5 \times 4$ cm in dimension with displacement of the adjacent brain parenchyma.

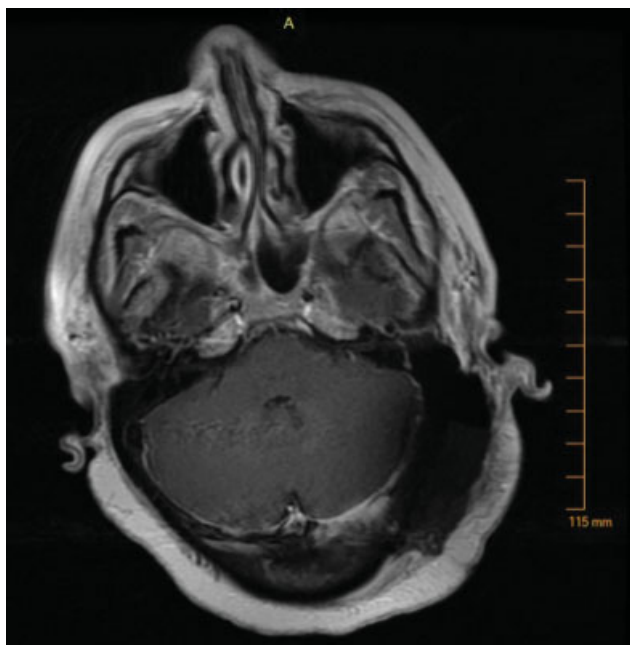


Fig. 3 Postoperative magnetic resonance imaging demonstrating gross total resection of metastatic renal cell carcinoma. Postsurgical changes are seen from left mastoidectomy and left occipital craniectomy with mass lesion resection.

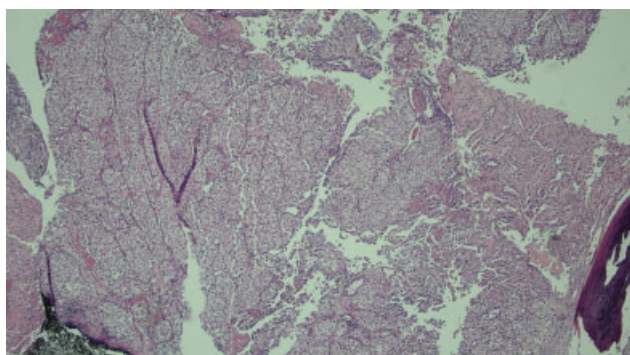


Fig. 4 Surgical pathology demonstrating metastatic clear cell renal cell carcinoma. 4× magnified view of nested pattern of tumor cells with clear cytoplasm, delicate yet distinct cell borders, with net-like array of delicate capillaries dividing cells into individual nests.

P219. Minimally Invasive Approaches: A Comparison Between Eyebrow Supraorbital Endoscopic Approach and Eyelid Transorbital Endoscopic Approach to Anterior and Middle Cranial Fossae

Ricardo A. Gomez Arroyo¹, Yury Anania¹, Shen Han¹, Carl Snyderman¹, Wang Erick¹, Georgios Zenonos¹, Paul Gardner¹
¹University of Pittsburgh Medical Center, Pittsburgh, Pennsylvania, United States

Background: In the last decades, minimally invasive surgery has gained wide popularity. The increasing application has evolved together with the advances in technology.

The purpose of this study was to compare two anterior minimally invasive approaches, namely supraorbital endoscopic approach (SEA) and transorbital endoscopic

approach (TEA), with the aim of reporting the benefits and limitations of each, based on stepwise bony work.

Methods: With the aid of image guidance, ten colored silicone-injected human cadaver head specimens (20 sides) were dissected in a stepwise fashion through a SEA or TEA. For each approach, two subsequent steps of bone drilling were analyzed. Step I was the initial craniotomy: SEA was a supraorbital 2.5 × 1.5 cm craniotomy; TEA was a lateral/posterior orbital wall craniectomy. STEP II maximized the area of exposure of each approach: SEA required lesser sphenoid wing drilling and TEA was supplemented with removal of the orbital roof.

Fixed target points along the ipsilateral anterior and middle cranial fossae were identified, and distance of each from the midpoint of the craniotomy was calculated. Moreover, each target point was classified according to their visibility/possibility to operate by two authors independently. An intraclass correlation coefficient was measured for interobserver agreement.

At the end of each step, a scan was performed to measure the resection volume. The 3D Slicer 4.10.2 program was used to calculate the volume.

Results: For either step I approaches step I SEA and TEA volume of craniotomy were 2.95 ± 0.83 cm³ and 1.82 ± 0.83 cm³, it was not possible to reach both fossae simultaneously. SEA had excellent exposure of ipsilateral anterior cranial fossa (14.7 ± 1.7 cm²), with limited to no exposure of the middle cranial fossa; TEA provided good exposure of the middle cranial fossa (10.6 ± 12.6 cm²), with no exposure of the anterior cranial fossa.

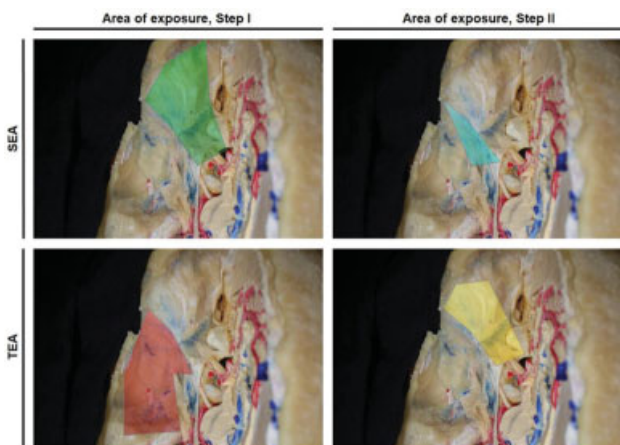
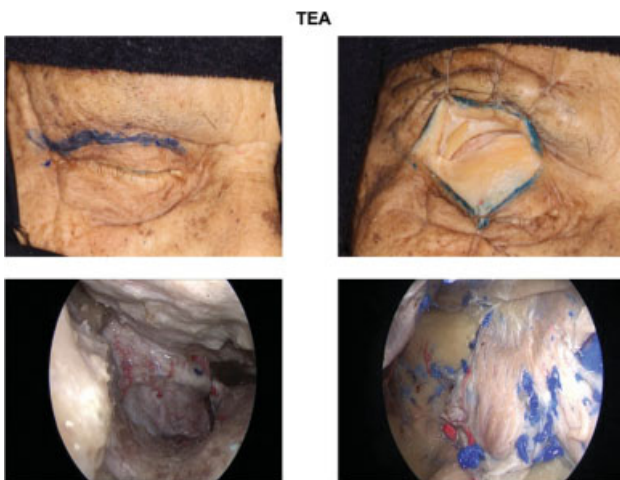
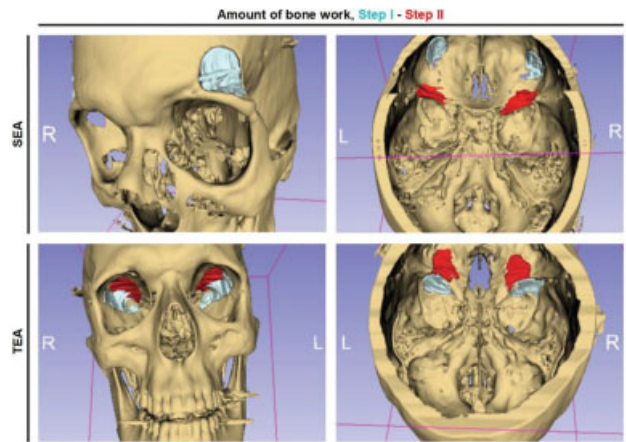
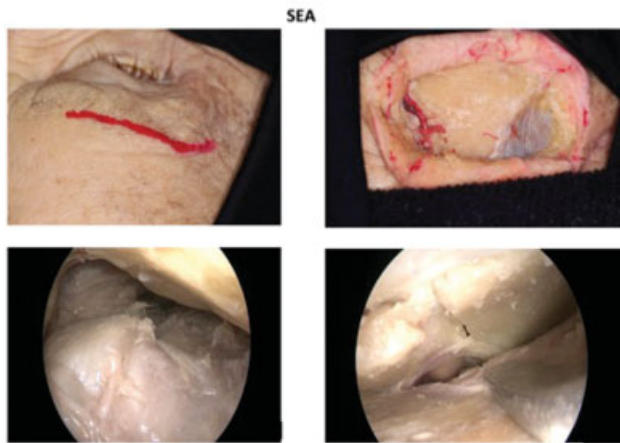
After more extensive drilling step II SEA and TEA volume of craniotomy were 0.55 ± 0.23 cm³ and 1.49 ± 1.33 cm³, respectively, access to both fossae through each approach was augmented (mean SEA and TEA areas of exposure, 17.5 ± 1.8 cm² and 18.1 ± 2.7 cm², respectively).

However, exposure of the anterior cranial fossa through a step II TEA was inferior compared with step I SEA (7.4 and 14.7 cm², respectively), and the difference was statistically significant ($p < 0.001$).

On the contrary, exposure of middle cranial fossa through a step I TEA was significantly wider ($p < 0.001$) than step II SEA (10.6 and 2.8 cm², respectively).

Conclusions: SEA and TEA are valid approaches in selected patients. Their areas of exposure have minimal overlap in their “limited” (i.e., step I) initial exposure. However, wider exposure can be achieved through drilling of deeper bony structures, with minimal increase in risk of complication. SEA is superior for anterior fossa exposure and TEA for middle fossa.

Clinical results are necessary to draw more meaningful results.



P220. Transpetrosal Translabyrinthine Approach for Obliteration of Large Perimesencephalic Dural Arteriovenous Fistula

Darshan N. Shastri¹, Nathan Quig¹, Brian Sindelar¹, Deanna Sasaki-Adams¹

¹University of North Carolina, Chapel Hill, North Carolina, United States

Introduction: Intracranial dural arteriovenous fistulas (dAVFs) are a rare cause of intracranial hemorrhage, thought to be idiopathic lesions though can be associated with trauma or previous craniotomies. Due to technical advances in endovascular techniques, the vast majority are adequately treated with embolization. The aim of this case report is to describe the surgical approach to a large perimesencephalic dAVF not amenable to endovascular therapy.

Description: This is a 47-year-old who presented with diffuse subarachnoid hemorrhage, complicated by cardiac arrest and seizures, requiring emergent external ventricular drain placement. Cerebral angiogram demonstrated a large dAVF to the basal venous plexus with arterial supply from the meningohypophyseal artery and right middle meningeal artery with multiple venous aneurysms. After multiple attempts, endovascular catheterization was unable to secure a safe transarterial route for embolization and transvenous embolization was aborted due to difficulty navigating the tortuous basilar plexus. Partial embolization of the right middle meningeal artery feeders through external carotid artery was completed, and a decision was made to proceed with surgical intervention through a right orbitozygomatic craniotomy approach. This provided adequate exposure to the superior portions of the dAVF but the venous complex just posterior to the clivus was unable to be visualized. Several small arterialized veins were coagulated and divided. An intra-op angiogram demonstrated significant reduction in blood flow to the complex structure with residual patency. Two weeks after surgery, there was a clinical decline associated with re-rupture of his dAVF. A decision was made to extend the prior right orbitozygomatic craniotomy posteriorly including transpetrosal translabyrinthine approach to provide better exposure to middle cranial fossa and more basal structures. Dura was opened lateral to the sigmoid sinus and the superior petrosal sinus coagulated allowing further extension medially along the tentorium. The fourth nerve and PCA were visualized and adequately protected. Microdissection along the middle fossa identified the prior vascular clip placed and then the cerebellopontine angle was followed,

identifying 5, 7, 8 nerves as well as multiple venous aneurysms with abnormal small arterial feeding vessels superior, inferior, and intertwined within the trigeminal nerve. Dissection was continued inferior to this nerve. The transpetrosal approach allowed for visualization of many feeding vessels lateral and anterior to the brainstem that otherwise would have been hidden by the multiple venous aneurysms. While attempting to coagulate and remove feeding dural/tentorial feeders, significant venous bleeding was encountered and hemostasis was obtained. At this point the remainder of feeders were divided and there was complete obliteration of dAVF. Postoperative angiogram at one month confirmed absence of residual dAVF. At last follow up patient was living at home and clinically improving.

Discussion: This case demonstrates a presigmoid transpetrosal translabyrinthine approach for obliteration of a complex dAVF nonamenable to standard endovascular treatment. Importance of preoperative planning and adequate exposure was vital to complete obliteration of the dAVF.

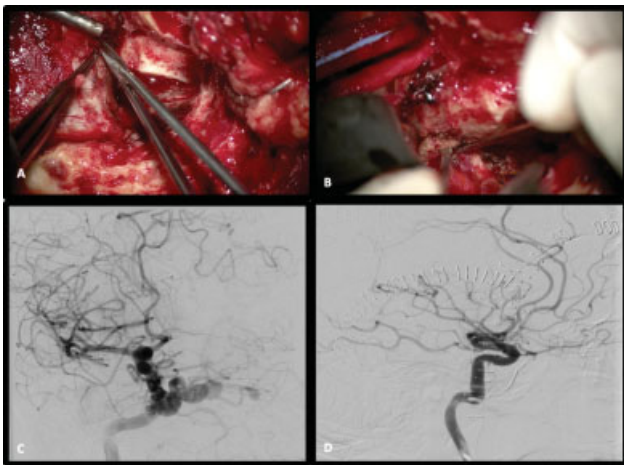


Figure 1. Dural opening shows presigmoid with middle fossa exposed (A) Trigeminal nerve with dAVF arterial feeders (B) Preoperative angiogram (C) Postoperative angiogram with obliteration of dAVF (D)

P221. Intraorbital Arteriovenous Fistula Mimicking an Anterior Cranial Fossa Dural Arteriovenous Fistula

Hae Gi Park¹

¹Severance Hospital, Yonsei University College of Medicine, Seoul, South Korea

Introduction: Intraorbital arteriovenous fistulas (AVFs) that lie purely within the orbit is quite rare and sometimes it can be misdiagnosed as an anterior cranial fossa dural AVF. The optimal treatment of intraorbital AVFs is still a matter of debate because of the small number of reported cases.

Case Presentation: A 72-year-old female patient presented a 4-month history of progressive proptosis of left eye in association with upper lid swelling and conjunctival chemosis. MRI and CT demonstrated 2 cm vascular mass-like lesion in upper superomedial aspect of globe, engorged draining left superior ophthalmic vein (SOV). Digital subtraction angiography showed an AVF, which was fed from ophthalmic artery and superior temporal artery branches and draining to SOV and it mimicked an anterior cranial fossa dural AVF. However, angiographic XperCT scan showed that the lesion located at intraorbital space and she experienced a stabbing injury near the left orbit. Finally, intraorbital AVF was diagnosed and the lesion was symptomatic, open surgical

excision was planned. After anterior orbitotomy, a thickened serpiginous thrombosed SOV was found, which was resected completely after ligation of the proximal feeding artery. Postoperative course was uneventful with good clinical outcome. CT angiography scan obtained at the time of discharge demonstrated no evidence of residual AVF.

Conclusion: Posttraumatic intraorbital AVF in association with varicose SOV, as reported here, was rare disease and mimicked an anterior cranial fossa dural AVF. In such cases, direct surgical exposure of the SOV followed by excision may accomplish complete closure of the fistula without significant risk for iatrogenic injury.

P222. Orbital Venous Malformation with Intradural Arteriovenous Shunting: Optic Nerve Compartment Syndrome

Jae Sung Park¹, Hae Gi Park¹

¹Severance Hospital, Yonsei University College of Medicine, Seoul, South Korea

Introduction: Orbital venous malformation (OVM) is common vascular malformations in the orbit. OVM can cause a functional impairment as well as a disfigured appearance of orbital and periorbital area. Rarely, it can be associated with arteriovenous (A-V) shunting, which may cause a severe neurologic impairment with visual loss, the so-called optic nerve compartment syndrome.

Case Presentation: A 49-year-old male patient with a history of congenital scalp vascular malformation presented 20-days' progressive exophthalmos and EOM limitation. MRI and CT scan showed an orbital venous malformation complicated with intraorbital thrombosis and hemorrhage. Digital subtraction angiography showed an A-V shunting, which was fed from middle meningeal artery and MCA cortical branches. Shunt flow drained into sphenoparietal sinus and intraorbital venous sac via superior orbital fissure. During the evaluation, severe orbital pain and acute visual loss occurred without direct light reflex, the so-called optic nerve compartment syndrome. Emergency surgery was performed. After orbitopterional craniotomy, orbital roof, and optic canal were extradurally grinded and optic nerve was relieved. Intradurally, A-V shunting point and its draining dural sinus was identified. These were coagulated and cut. Intraorbital venous sac was remained and second treatment was planned by a sclerotherapy. After surgery, his vision and EOM gradually recovered.

Conclusion: This report presents a rare case of OVM with A-V shunting, which cause an optic nerve compartment syndrome.

P223. Surgical Resection of Brainstem Cavernoma: A Systematic Review of the Literature

Ryan Hess¹, Ahmad Kareem Almekkawi¹, Karl R. Abi-Aad¹, Rudy J. Rahme¹, Devi P. Patra¹, Evelyn Turcotte¹, Bernard R. Bendok¹

¹Mayo Clinic, Rochester, Minnesota, United States

Introduction: Brainstem cavernomas present a unique challenge. While cavernomas are generally benign lesions, the critical location in the brainstem makes them very difficult to approach. The main treatment remains surgical resection, but is fraught with high risk of morbidity and mortality. In this paper, we present a systematic review and meta-analysis of published cases of treated brainstem cavernoma.

Methods: A review of the literature was conducted by gathering articles and textbook chapters from the Pubmed, Web of Science, Scopus, Cochrane DSR, and Embase databases. These were queried using the terms "cavernoma,"

“cavernous malformation,” “cavernous angioma,” “brainstem,” “surgery,” and their related terms. A full systematic review and meta-analysis was conducted using PRISMA guidelines.

Results: A total of 1,046 articles were found. After duplicate screening, title and abstract screening, and full-text review, 100 surgical series were selected. Across 100 series, data were available for 2,257 patients with brainstem cavernomas that were surgically treated. These patients had an average age of 38.19 years and a male:female ratio of 0.88. The majority of these lesions were located in the pons (57.6%), followed by the midbrain (25.7%) and the medulla (22.5%), with some lesions spanning multiple brainstem structures. Prior to surgery, 98% of these patients experienced one or more hemorrhagic events. Gross total resection was achieved in 92.8% of patients following initial surgery. Perioperative complications occurred in 41.9% of patients, with common complications including infection (9.8%), tracheostomy/percutaneous endoscopic gastrostomy (11.8%), CSF leak (6%), hydrocephalus (4.7%), and ventilator dependence (5.4%). In 65 studies (1,944 patients), the reported rate of postoperative cranial neuropathy was 67%. For the most part, it is unclear whether the neuropathy was transient or permanent. In regard to clinical follow-up, a total of 81 studies with 1,744 patients were reported over an average of follow-up time of 38 months weeks. At latest available follow-up, the neurological conditions compared with baseline had improved in 59.9%, remained stable in 27.7%, and worsened in 10.3%, with death attributable to the disease or procedure occurring in 1.6%.

Conclusion: Surgical treatment for brainstem cavernomas remains a reasonable treatment option. However, this procedure carries high risks and requires careful planning and patient selection.

P224. Preoperative Embolization of a Glomus Vagale Tumor Resected via the Retrosigmoid Approach

Tyler Scullen¹, Zane Freeman², Joseph Lockwood¹, Neal Jackson², Peter Amenta¹

¹Department of Neurosurgery, Tulane University, New Orleans, Louisiana, United States

²Department of Otolaryngology, Tulane University, New Orleans, Louisiana, United States

Introduction: Glomus vagale and jugulare tumors are highly vascular and locally destructive lesions that often require complex skull base approaches for surgical management. These tumors often have intra- and extracranial extension and derive their blood supply from multiple sources. Preoperative endovascular embolization decreases intraoperative blood loss, allows for a controlled and organized resection, and can facilitate brainstem separation in tumors with a large intradural component. We describe a glomus vagale tumor with primarily intradural extension and pontine compression treated with preoperative embolization prior to resection via the retrosigmoid approach.

Case Description: A 64-year-old male presented with several months of dysphagia and hoarseness and was found to have complete paralysis of the left vocal cord. Magnetic resonance imaging demonstrated an avidly enhancing tumor arising in the left jugular foramen and extending into the posterior fossa with compression of the pons. No disease was present in the middle ear and mastoid air cells and the distal cervical and petrous carotid artery was not involved. Diagnostic angiography identified an intense vascular blush with blood supply derived from branches of the left posterior inferior cerebellar artery (PICA), ascending pharyngeal artery (APA), and occipital artery (OA). The left transverse and

sigmoid sinuses and the left jugular vein were widely patent. Superselective catheterization and embolization of the APA and OA branches with 250–355 µm polyvinyl alcohol particles (PVAs) resulted in a dramatic reduction in the tumor blush. The following day, the patient underwent a left retrosigmoid craniotomy and resection of the intradural tumor. The feeding branch of the PICA was coagulated and sectioned prior to resection, resulting in near complete devascularization of the tumor. Resection proceeded with minimal blood loss and the tumor was easily debulked and separated from the brainstem. Pathology was consistent with a paraganglioma. The patient was discharged with baseline hoarseness and no additional deficits. Cranial nerve XI function was preserved. The residual tumor in the jugular foramen will be treated with stereotactic radiosurgery. A left vocal cord injection resulted in a dramatic improvement in voice quality.

Conclusion: Glomus jugulare and vagale tumors are highly vascular complex lesions that are best treated by a multidisciplinary team. Preoperative embolization is a key adjuvant therapy that reduces blood loss, improves the safety of the procedure, and facilitates resection. Embolization can be associated with significant neurologic complications due to occlusion of the blood supply to the lower cranial nerves. Additionally, dangerous anastomoses with the internal carotid and vertebral basilar circulations can result in devastating neurologic injury. Cranial base surgeons also trained in endovascular intervention provide a unique perspective and allow for a tailored embolization prior to the planned resection.

P225. Utilization of the Transotic Approach for Select Cases of Vestibular Schwannoma Resection

Scott B. Shapiro¹, Noga Lipschitz¹, Nathan Kemper¹, Gavriel Kohlberg¹, Allie Mains¹, Myles L. Pensak¹, Joseph T. Breen¹, Mario V. Zuccarello¹, Ravi N. Samy¹

¹University of Cincinnati College of Medicine, Cincinnati, Ohio, United States

Background: Vestibular schwannomas (VS) with significant intracochlear extension or extension to the anterior surface of the brainstem pose a challenge to a complete surgical resection. The transotic approach allows access to these regions via removal of the entire otic capsule without facial nerve re-routing and provides a more direct view of the basilar artery, potentially decreasing the risk of neurovascular injury. Due to these advantages, we utilize the transotic approach for vestibular schwannoma which meet these select criteria.

Objective: Examine outcomes of transotic approach to resection of VS with anterior cerebellopontine angle (CPA) or cochlear extension.

Methods: Retrospective analysis of patients managed at a tertiary care academic medical center between 2009 and 2019.

Results: Nine patients underwent transotic approach to VS resection during the study period. The indications for surgery included cochlear extension from the internal auditory canal in 5 patients, intracochlear tumor on 1 patient, and anterior CPA extension in 3 patients. Two patients had continued growth after previous stereotactic radiosurgery. Mean tumor length in the largest dimension was 40 mm. Seven patients underwent gross total resection (GTR) while two underwent subtotal resections. The facial nerve was anatomically intact at the conclusion of surgery in all cases. Eight patients had good (House-Brackmann grade I or II) facial nerve function preoperatively. Of these, 5 had a similar level of function postoperatively, while 3 had poor (grade IV–VI) function postoperatively and have undergone facial

reanimation procedures. Complications included cerebrospinal fluid leak in 2 patients, and sigmoid sinus thrombosis in one patient, which resolved without sequelae with chemical anticoagulation.

Conclusions: The transotic approach offers good rates of GTR in large and difficult-to-remove tumors that involve areas not accessed via more commonly used approaches, such as those with anterior CPA or intracochlear extension. In addition, the angle of approach may reduce the risk of injury to the basilar artery. The complication rate is comparable to other approaches for large VS.

P226. Endoscopic Third Ventriculostomy in a Patient with Giant Bilateral Vestibular Schwannomas

Ali O Jamshidi¹

¹Kaiser Permanente, Oakland, California, United States

Background: Surgical management of patients with bilateral vestibular schwannomas in the setting neurofibromatosis 2 is controversial and challenging for the physician and burdensome for the patient. There is evidence in contemporary literature that the size of these tumors can dictate hearing and facial nerve outcomes. The author presents a case of a patient with a known history of enlarging bilateral vestibular schwannomas that began to cause the patient hydrocephalus, tonsillar herniation and neurologic deterioration. Strategic interventions were necessary to avoid future complications.

Case Report: The patient is a 34-year-old female who has a 10-year history of bilateral vestibular schwannomas. She refused surgical treatment for many years and was managed with bevacizumab as a result. Ultimately, her bilateral tumors grew from 2.3 cm × 2 cm × 2.4 cm to 5 cm × 3.8 cm × 4.8 cm on the left and 1.8 cm × 1 cm × 1.3 cm to 4.2 cm × 2.2 cm × 3 cm on the right. Because of her progressive gait instability with associated severe brainstem compression, hydrocephalus, tonsillar herniation, and non-serviceable hearing on the right side, she ultimately agreed to a right translabyrinthine approach and external ventricular drain. Her surgery was complicated by a cerebellar hematoma and she had a subtotal resection. The patient remained at her neurologic baseline postoperatively and her drain remained open. She was placed on hypertonic saline to reduce the cytotoxic edema from the intraparenchymal hemorrhage. She ultimately failed a clamping trial of her drain. Because she had a significant residual tumor burden I felt that the patient would ultimately need further surgery via a retrosigmoid approach. Also because she had a large left sided tumor as well, the goal was to avoid placing ventriculoperitoneal shunt tubing in either retroauricular space. On evaluation of a head CT done related to her clamp trial, her prepontine space had opened and, consequently, an endoscopic third ventriculostomy (ETV) was suggested to the patient as a solution to the dilemma regarding CSF diversion. The patient ultimately had an ETV done and needed no further shunting procedures.

Conclusion: The patient continued to suffer from obstructive hydrocephalus after her translabyrinthine approach. Even though she had significant tumor burden that remained in her posterior fossa, an ETV was a successful and optimal strategy. This outcome proved to be beneficial as the patient would likely need both her retrosigmoid spaces available for further surgical options that may be employed during her life. An ETV should also be considered as an option for these sorts of patients.

P227. An Automated Method for Determining Vestibular Schwannoma Size and Growth

Nicholas George-Jones¹, Kai Wang¹, Jing Wang¹, Jacob B. Hunter¹

¹University of Texas Southwestern Medical Center, Dallas, Texas, United States

Vestibular schwannoma (VS) growth in the greatest linear dimension is one metric used to determine VS progression. Many studies characterizing VS growth also use manual volumetric segmentation of VS to increase the sensitivity of detecting growth and to better characterize lesions; however, high-resolution scans and radiologist-time required to make these measurements are rarely available. To create an automated means of measuring tumor size, we sought to compare manual versus automated measurements of tumor length, area, and volume in a cohort of VS patients.

Methods: We used selected cases from a database of VS cases at a tertiary care center. A total of 36 patients were selected who had at least two T1-weighted axial MRI scan with contrast at least six months after the initial scan, prior to any intervention. We manually measured the greatest linear dimension on axial imaging, in addition to manually segmenting each tumor slice. In comparison, we automatically segmented the tumor using the Chan-Vese image segmentation method. Afterwards, we calculated the area within the contour of the tumor, the major axis length of a “best-fit ellipse” around the tumor, and the tumor volume if the tumor can be contoured in more than one slice.

Results: The average age of the patients was 59.7 years (range, 35.4–76.9), with an average tumor size based on the greatest linear axial diameter was 9.0 mm, (range: 1.8–26.6). When comparing manual linear measurements with the major axis of the “best-fit ellipse,” the intraclass correlation coefficients (ICC) for the first and second measurements were 0.982 and 0.984, respectively. When comparing the absolute difference between the first and second measurements between the manual and the major axis of the “best-fit ellipse” linear measurements, the ICC was 0.918. When defining growth as an increase in tumor size ≥ 2 mm, 17/37 (45.9%) demonstrated linear growth when utilizing the manual measurement of the greatest linear dimension. However, only 4/37 (10.8%) demonstrated growth when utilizing the major axis length of the “best-fit ellipse” around the tumor, which is significantly different as compared with the manual measurement ($p = 0.002$). To date, by defining volumetric tumor growth as an increase in tumor size $\geq 20\%$, 10/19 (52.6%) of tumors demonstrate growth via semi-automated volumetric measurements. Manual segmentation of volumes will be completed and compared with semi-automated measurements.

Conclusion: With our analysis to date, manual versus automated linear measurements are in excellent agreement. However, when determining if the tumor grew, there is a significant difference in defining which tumors grew. Conclusions are pending as to volumetric measurements.

P228. Exploring the Association Between Apparent Diffusion Coefficient Values on Magnetic Resonance Imaging and the Response of Vestibular Schwannoma to Radiation

Daniel E. Killeen¹, Carlos L. Perez², Rati Chkheidze³, Samantha Moore³, Anthony M. Tolisano¹, Joe W. Kutz¹, Brandon Isaacson¹, Jacob B. Hunter¹

¹Department of Otolaryngology – Head and Neck Surgery, University of Texas Southwestern Medical Center, Dallas, Texas, United States

²Department of Radiology, University of Texas Southwestern Medical Center, Dallas, Texas, United States

³Department of Pathology, University of Texas Southwestern Medical Center, Dallas, Texas, United States

Introduction: With MRI diffusion weighted imaging (DWI), the apparent diffusion coefficient (ADC) measures the diffusion of water molecules within a tissue, and may predict the response of vestibular schwannomas (VS) to radiation. This study sought to investigate the association of pretreatment ADC values with tumor progression following radiation.

Methods: Performing a retrospective review at a single, tertiary care institution, patients with sporadic VS who were treated with gamma knife radiosurgery, had at least one pretreatment MRI with DWI with ADC values, and at least 12 months of posttreatment radiographic follow-up were identified. Demographic and clinical data were collected from the medical records. Three reviewers measured tumor diameter, tumor volume, and pretreatment ADC mean and standard deviations for all available MRI studies. Response to radiation was defined as a 20% reduction in tumor volume at last radiologic follow-up. Tumor progression was defined as either an increase in 2 mm in maximal tumor diameter or a 20% increase in tumor volume at last radiologic follow-up.

Results: A total of 27 patients with a sporadic VS treated with gamma knife radiosurgery met enrollment criteria. The cohort was composed of 52% women, with median age 67 years (range, 55–78). The median posttreatment follow-up was 36.8 months (range, 13.7–151.7). The median pretreatment maximum tumor diameter was 17.2 mm (range, 9.7–30.4) and the median pretreatment tumor volume was 0.83 cm³ (range: 0.19–5.4). A total of 66.7% of patients had a 20% reduction in tumor volume following radiation. The median ADC for responders was 1170.0 mm²/s (range 835.8–1771.6), compared with a median ADC for nonresponders of 1000.3 mm²/s (range 795.1–1423.1), which was not significantly different ($p = 0.41$). A total of 18.5% of patients demonstrated tumor progression at last follow-up following radiation. The median ADC of tumors that progressed was 1232.2 mm²/s (range 795.2–1313.7), compared with a median ADC of nonprogressing tumors of 1151.1 mm²/s (range 835.8–1771.6), which was not significant ($p = 0.80$). The median ADC was not significantly predictive of response or progression on univariate or multivariate logistic regression when controlling for age, gender, preradiation tumor greatest diameter, preradiation tumor volume.

Conclusion: While more patients will be included in the final analysis, currently in this cohort, the median ADC was not found to be predictive of radiation response or progression.

P229. Regional Variation in Patient Participation and Treatment among Acoustic Neuroma Association Survey Respondents Across the United States

John P. Marinelli¹, Samuel A. Spear¹, Debbie L. Hahs-Vaughn², Robert J. Macielak³, Michael J. Link³, Allison Feldman⁵, Chad Nye⁵, Matthew L. Carlson³

¹Department of Otolaryngology-Head and Neck Surgery, San Antonio Military Medical Center, San Antonio, Texas, United States

²Department of Learning Sciences and Educational Research, University of Central Florida, Orlando, Florida

³Department of Otolaryngology-Head and Neck Surgery, Mayo Clinic, Rochester, Minnesota, United States

⁴Department of Neurologic Surgery, Mayo Clinic, Rochester, Minnesota, United States

⁵Acoustic Neuroma Association, Cumming, Georgia, United States

Background: The Acoustic Neuroma Association (ANA) represents the largest existing patient support organization for those diagnosed with vestibular schwannoma (VS) in the United States. Despite the significant resources the ANA offers to patients, the degree to which the ANA is utilized across the country is unknown. In addition to potential regional differences in utilization of the ANA, some research suggests that treatment paradigms vary geographically across the United States.

Objectives: First, to characterize the utilization of patient support services across the United States, and second, to characterize the variation in treatment approaches by region among ANA survey respondents.

Study Design: Cross-sectional survey performed from February, 2017 through January, 2019.

Patients: ANA survey respondents diagnosed with sporadic VS.

Main Outcome Measures: ANA survey respondent participation by state and United States geographical region; regional variation in treatment approach following diagnosis.

Results: A total of 878 patients met inclusion criteria, 67% of whom were female. The majority of respondents were white ($n = 825$, 94%). The largest age group represented was those aged 61–70 years ($n = 317$, 36%), followed by 51–60 ($n = 241$, 27%) and 71–80 ($n = 135$, 15%). The District of Columbia had the largest proportion of ANA patients relative to state population (0.85 per 100,000 persons), followed by New Hampshire (0.74), Maine (0.60), and New Jersey (0.42). Mississippi (0.03), Hawaii (0.07), and Rhode Island (0.09) harbored the lowest participation rates. By region, the Northeast had the largest average number of ANA patients per 100,000 persons (mean = 0.38, SD = .19), whereas the West had the lowest (mean = 0.21, SD = 0.09). Significant treatment variations were observed across the United States: in Maine, Iowa, Missouri, Kansas, and New Hampshire, an average of 73% (range, 70–75) of patients underwent microsurgery, whereas only 24% (range, 0–35) of patients in Colorado, New York, Massachusetts, Connecticut, and West Virginia underwent microsurgery ($p < 0.001$). Similarly, a significant variation in the utilization of radiosurgery exists across the United States, with seven states averaging similarly high rates of radiosurgery at 14% of ANA survey respondents (range, 11–17) compared with 13 states with the lowest reported radiosurgery rates (average, 0%; range: 0–0) ($p < 0.001$).

Conclusions: Large regional variation exists surrounding patient participation in the ANA across the United States, with some states exhibiting over 10 times higher participation rates than low participation states. Similarly, significant treatment variation exists across the United States in the management of sporadic VS. Together, these data demonstrate geographic disparities in access to patient support

services and regional provider bias toward treatment across the United States.

P231. Impact of Petromeatal Bone Angle on Degree of Tumor Resection and Facial Nerve Injury for Vestibular Schwannomas During the Translabyrinthine Approach

Mohammad Hassan A Noureldine¹, David Aum², Gleb Zavadskiy³, Ivo Peto², Keaton Piper², Konrad Bach², Harry van Loveren², Siviero Agazzi²

¹Johns Hopkins University School of Medicine, Institute for Brain Protection Sciences, Johns Hopkins All Children's Hospital, Saint Petersburg, Florida, United States

²University of South Florida Morsani College of Medicine, Tampa General Hospital, Tampa, Florida, United States

³University of South Florida Muma College of Business, Tampa, Florida, United States

Background: The translabyrinthine approach offers a trajectory of view into the posterior fossa that is parallel to the internal acoustic canal (IAC). Visualization and work anterior to the IAC is affected by variations in the angle formed by the IAC and the posteromedial aspect of the petrous pyramid, which we will refer to as “petromeatal angle.” We postulate that varying degrees of the petromeatal angle could affect the degree of tumor resection and facial nerve outcome in vestibular schwannoma (VS) surgery. Pre-operative measurement of the petromeatal angle could then be used as a prognostic factor and guide surgical expectations in VS patients.

Methods: We conducted a retrospective review of the medical records of 39 patients who underwent a translabyrinthine approach for resection of VSs, confirmed by postoperative tissue diagnosis. The pertinent, collected data included ipsilateral petromeatal angle, petroclival angle, petrous-petrous (petrous Cobb) angle, tumor size, degree of tumor resection (gross/near-total versus sub-total), immediate postoperative cranial nerve (CN) VII deficit, and change in House–Brackmann score, calculated by subtracting the pre-operative score from the postoperative score at discharge.

The petromeatal angle is formed at the junction of two lines that are parallel to the IAM anterior edge and the posteromedial surface of the petrous bone (Fig. 1). Petrocus Cobb and petroclival angles were calculated as described by Desai et al.¹ Statistical analysis was performed using the R Statistical Software.

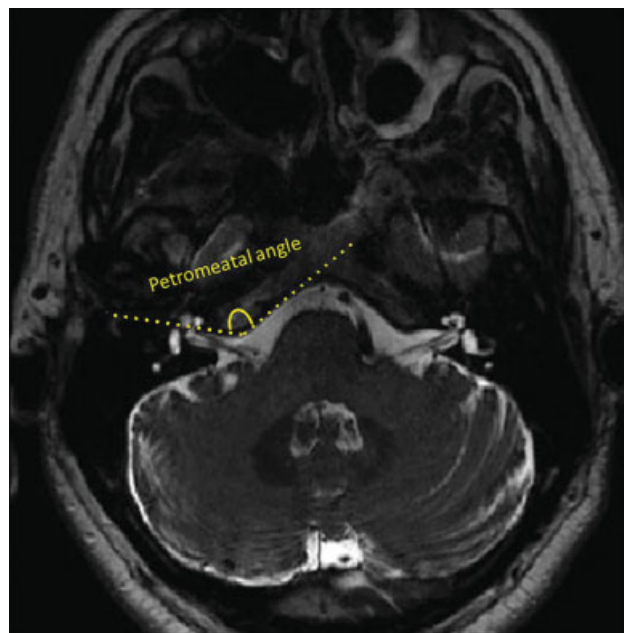


Fig. 1

Results:

Mean and 95% confidence intervals		
	Mean	CI
Ipsilateral petromeatal angle	127.4	123.3 – 131.5
Tumor size	2.9	2.6 – 3.2
Petroclival angle	129.6	127.3 – 132.0
Petrous Cobb angle	99.0	95.6 – 102.4

Table 1 Lists the mean values and 95% confidence intervals (CIs) of the pertinent data

Using the Logit statistical model to estimate the odds, our data show that every additional degree of ipsilateral petromeatal angle increases the odds of being able to accomplish gross/near-total resection by 6.63% ($p = 0.0375$). Using the same statistical model, we also found that every additional cm in tumor size decreases the odds of gross/near-total resection by 79% ($p = 0.0106$). With tumor sizes below 2.25 cm, the percentage of patients with gross/near-total resection was >87%.

No statistically significant associations were found between the ipsilateral petromeatal angle and CN VII deficit ($p = 0.366$) or change in House–Brackmann score ($p = 0.985$). No significant associations were detected between the petroclival or petrous Cobb angles and any of the three dependent variables (degree of tumor resection, immediate postop CN VII deficit, change in House–Brackmann score).

Discussion/Conclusion: With a relatively small sample of patients, our results suggest that the petromeatal angle can be a reliable predictor of gross/near-total resection during the translabyrinthine approach for VSs.

We are currently reviewing additional medical records to improve the reliability of the results and the power of this study.

This document was downloaded for personal use only. Unauthorized distribution is strictly prohibited.

Reference

- Desai SK, Baymon D, Sieloff E, et al. Computed tomography morphometric analysis of the central clival depression and petroclival angle for application of the presigmoid approach in the pediatric population. *J Pediatr Neurosci* 2016;11(2):109–111

P232. Pituitary Hemitransposition for the Resection of a Pilocytic Astrocytoma in a Middle Aged Man with Multiple Sclerosis

Ali O. Jamshidi¹

¹Kaiser Permanente, Oakland, California, United States

Background: Pilocytic astrocytomas are generally considered to be pediatric tumors. However, rarely, adults can present with them. The author discusses the case of 46-year-old male presenting with gynecomastia and a retrosellar mass with a history of multiple sclerosis and testicular cancer.

Case Discussion: The patient initially sought medical attention because of breast tenderness and gynecomastia. He had a prolactin level sent that was abnormal at 44.2 ng/mL. His MRI showed an irregular T2 hyperintense lesion without contrast enhancement in the retrosellar space. There was very mild mass effect on the posterior and dorsal aspect of the

optic chiasm and widening of the hypothalamus. He had formal visual field testing. Because the mass had grown over 12 year period and because of the contact with the optic apparatus, surgery was indicated for diagnosis and resection. The patient underwent an endoscopic, endonasal, transtubercular, transsellar, and transclival approach with resection of the left sided posterior clinoid to access the lesion. Once the dura was opened over the sella face, sharp dissection allowed for a left sided pituitary hemitransposition which allowed for visualization of the mass, which was dark gray and gelatinous. The tumor was then resected entirely. The patient experienced diabetes insipidus intraoperatively. Postoperatively, he required exogenous administration of antidiuretic hormone. He returned to clinic with concern for a low-flow spinal fluid (CSF) leak and a head CT that was showing resolving pneumocephalus. As such, he was a candidate for lumbar drain placement for primary treatment of his CSF leak. His CSF leak and breast tenderness resolved with a normalized prolactin at 17.6 ng/mL.

Conclusion: The patient was thought to have a cystic craniopharyngioma or Rathke's cleft cyst but in fact he had an intra-axial tumor of the hypothalamus. Postoperatively, the patient's hormonal abnormalities resolved and he had a gross total resection. The endoscopic, endonasal approach with pituitary hemitransposition was an effective, minimally invasive approach that provided therapeutic and oncologic benefit.

Author Index

30th Annual Meeting—North American Skull Base Society

Numbers in **bold** following author names refer to page numbers.

- Aashiq, Mohamed **S27, S65**
 Abate, Adam R. **S221**
 Abbas, Munzir **S85**
 Abdelmeguid, Ahmed S. **S26**
 Abedalthagafi, Malak **S94**
 Abel, Kathryn V. **S14**
 Abhinav, Kumar **S87, S158**
 Abi-Aad, Karl **S72, S82, S267**
 Abi-Hachem, Ralph **S15**
 Abiri, Arash **S114, S126, S133**
 Abila, Adib A. **S81, S138, S139**
 Abou-Al-Shaar, Hussam **S88**
 Abouzari, Mehdi **S114**
 Abunimer, A.M. **S43**
 Abunimer, Abdullah M. **S88**
 Abuzeid, W. M. **S219**
 Ackall, Feras Y. **S12, S15, S242**
 Adappa, Nithin D. **S241**
 Adepoju, Adedamola **S18, S80**
 Adunka, Oliver **S135**
 Agarwal, Aarti **S73**
 Agarwalla, Pankaj **S194**
 Agarwal, Nitin **S17**
 Agarwal, V. **S219**
 Agarwal, Vijay **S40**
 Agazzi, Siviero **S225, S232, S271**
 Agbi, Charles **S23, S127, S132, S133, S188**
 Aghi, Manish K. **S221**
 Agh, Manish **S171**
 Ahluwalia, Amandeep S. **S81, S138**
 Ahmadih, Tarek El **S226**
 Ahmad, Samuel **S40**
 Ahmed, Azam S. **S192**
 Aihara, Masanori **S183**
 Aizer, Ayal A. **S94**
 Akagami, Ryojo **S66**
 Akbar, N. A. **S219**
 Akiyama, Osamu **S140**
 Akobyan, Ovanes **S133**
 Alahmari, Mohammed S. **S127, S133**
 Alapati, Rahul **S107**
 Albonette-Felicio, Thiago **S165, S214**
 Albonette, Thiago F. **S141, S186, S196, S194**
 Alekseev, Andrey **S184, S198**
 Alfallaj, Muath **S213**
 Algattas, Hanna **S23**
 Alhourani, Ahmad **S142, S153, S221**
 Ali, Moustafa **S185, S186, S187**
 Aljuboori, Zaid **S142, S153, S165, S181, S212, S221**
 Alkhani, Ahmed **S85**
 Alkherayf, Fahad **S23, S127, S132, S133, S188**
 Al-Khudari, Samer **S71**
 Allen, Kyle **S232**
 Almarshad, Mody **S213**
 Almefty, Kaith K. **S60**
 Al-Mefty, Ossama **S60, S94**
 Almeida, Joao Paulo **S106, S114**
 Almekawi, Ahmad Kareem **S72, S82, S267**
 Alobaid, Abdullah **S213**
 Alonso-Basanta, Michelle **S53**
 Alonso, Pablo Perez **S206**
 Aloraidi, Ahmed **S85**
 Al-Saiegh, Fadi **S17, S69, S180**
 Alshardan, Mohammad **S127, S133**
 Altieri, Stefanie **S17**
 Alvi, Sameer **S121**
 Amano, Toshiyuki **S151**
 Amenta, Peter **S221, S255, S268**
 Amit, Moran **S27, S65**
 Anagnostopoulos, Christos **S218**
 Anaizi, Amjad **S261**
 Anand, Vijay K. **S15, S25**
 Anania, Yury **S31, S152, S237, S265**
 Andaluz, Norberto **S142, S153, S181, S221, S240**
 Anderson, Douglas **S43, S121, S170, S219**
 Anderson, Dwayne **S158**
 Anderson, Roan N. **S98**
 Anding, William J. **S55**
 Andrew, Venteicher S. **S237**
 Aoun, Salah **S226**
 Appelbaum, Eric N. **S202**
 Arai, Hajime **S140**
 Arechaga, Onditz **S248**
 Arnaout, Amel **S132**
 Arnaout, Omar **S94**
 Arriaga, Moises A. **S223**
 Arroyo, Ricardo Gomez **S152, S265**
 Arzumanov, Grant **S194, S202**
 Asha, Mohammed **S106**
 Ashayeri, Kimberly **S168**
 Asimakopoulos, Panagiotis **S144**
 Aslam, Rizwan **S221**
 Asmaro, Karam **S211**
 Aum, David **S271**
 Axon, Patrick **S43**
 Bach, Konrad **S271**
 Backous, Douglas D. **S123**
 Baglam, Tekin **S186, S187**
 Bair, Henry **S182**
 Balachandra, Sanjana **S97**
 Balchandani, Priti **S1, S2**
 Ball, Matthew K. **S110**
 Bambikidas, Nicholas C. **S138**
 Banaz, Fatmahalzahra **S127, S133**
 Bance, Mahonar **S43**
 Banks, Tim **S181**
 Banks, Timothy **S149**
 Ban, Vin Shen **S226**
 Barak, Ian **S12, S15**
 Barbagli, Giovanni **S158**
 Barbarite, Eric **S75, S111, S221**
 Barbero, Juan Manuel Revuelta **S251**
 Barker, Christopher **S27**
 Barnard, Zachary R. **S177**
 Barnett, Sam **S226**
 Barnett, Samuel L. **S132, S215**
 Bartindale, Matthew R. **S123, S170**
 Basak, Hazan **S117, S143, S189**
 Bashir, Mariah **S121**
 Basma, Jaafar **S218**
 Bates, James E. **S229**
 Batjer, Hunt **S226**
 Baumann, Brian C. **S53**
 Beahm, David **S87**
 Beaumont, Carlos **S248**
 Beaumont, Thomas L. **S32, S135**
 Bederson, Joshua B. **S1, S2, S9, S228**
 Beer-Furlan, Andre **S71**
 Belcher, Ryan **S32**
 Bell, Diana **S26, S65**
 Bellile, E. **S219**
 Belyk, Engenii **S163**
 Bender, Matthew T. **S177**
 Bendok, Bernard R. **S72, S267**
 Benjamin, Carolina G. **S93, S168, S214**
 Benner, Dimitri **S158**
 Bennett, Marc L. **S254**

- Ben-Shlomo, Nir **S43**
 Benson, Noah C. **S1**
 Berger, Mitchel S. **S221**
 Bergsneider, Marvin **S8, S34, S122, S127, S240, S260**
 Bernardo, Antonio **S76, S158, S161**
 Bertazzo-Silveira, Giuliano S. **S141, S196, S194**
 Berumen, Enrique Lopez **S154**
 Beton, Suha **S117, S143, S189**
 Bettgowda, Chetan **S46**
 Bevilacqua, Julia **S93, S214**
 Bhargava, Malika **S44, S120**
 Bhatti, Tricia **S233**
 Bien, Alexander G. **S211**
 Bilderback, Andrew **S17**
 Bilyk, Jurij R. **S82**
 Bishop, Justin **S251**
 Bi, Wenya L. **S33, S60, S94**
 Blakaj, Dukagjin **S14**
 Blue, Rachel **S19, S21, S224**
 Bly, Randall A. **S47**
 Boakye, Maxwell **S181**
 Boaro, Alessandro **S94**
 Bobinski, Matthew **S250**
 Bochkarev, Dmitriy **S184, S198**
 Bojrab II, Dennis **S55**
 Bonda, David J. **S82**
 Boon, Maurits S. **S124, S210**
 Borghei-Razavi, Hamid **S36, S206**
 Bott, Matthew **S243**
 Boucher, A. **S167**
 Boucher, Andrew B. **S183**
 Bovi, Joseph **S60**
 Bowen, Andrew J. **S65**
 Bowman, James **S219, S220**
 Bozkurt, Melih **S143**
 Brackman, Krista **S18, S259**
 Brackmann, Derald E. **S216**
 Brahimaj, Bledi **S71, S102, S121**
 Braunstein, Steve E. **S221**
 Bray, David P. **S39**
 Breen, Joseph T. **S268**
 Breese, Rebecca **S4**
 Brem, Henry **S46**
 Brown, Kevin **S64, S105**
 Brown, Paul D. **S45, S52**
 Brown, William C. **S208**
 Bruce, Jeffrey N. **S234**
 Bruch, Leslie A. **S108**
 Bruni, Margherita **S88**
 Brusko, G. D. **S128**
 Bullen, Jeniffer **S206**
 Bush, Nancy Ann Oberheim **S221**
 Buster, Bryan **S39**
 Butman, John **S131**
 Byrne, Richard W. **S102, S121**
 Byrne IV, John M. **S18, S259**
- Cabral, David T. Fernandes **S36**
 Cabrera, Claudia I. **S138**
 Cadena, Gilbert **S114, S126, S133**
 Camarata, Paul J. **S119**
 Canoll, Peter **S234**
 Cantalino, Jonathan **S60**
 Capper, David **S11**
 Cardenas, Eugenio **S86, S145, S239**
 Carle, Taylor R. **S143**
 Carlson, Matthew L. **S44, S45, S62, S63, S99, S101, S194, S270**
 Carlson, Michael L. **S65**
 Carlstrom, Lucas P. **S21, S55, S57, S62, S64, S77, S80, S95, S99, S101, S137, S149, S159, S169, S209, S217, S247, S262**
 Carrau, Ricardo L. **S3, S14, S16, S32, S48, S49, S125, S135, S141, S165, S185, S186, S187, S188, S190, S191, S196, S215, S236, S240**
 Carroll, Kate **S47, S59, S61, S96, S115, S167, S180, S217**
 Carter, Bob **S96**
 Casabella, Amanda M. **S21, S101**
 Castelnuovo, Paolo **S11**
 Catalino, Michael P. **S71, S83, S87**
 Catapano, Joshua S. **S165**
 Caulley, Lisa **S127, S133**
 Cavallo, Claudio **S60**
 Celano, Emma C. **S261**
 Celda, Maria Peris **S62, S149**
 Celix, Juanita **S18, S59, S130, S156, S259**
 Celtikci, Emrah **S36, S107**
 Celtikci, Pinar **S36**
 Cetas, Justin **S35**
 Chakravarthi, Srikant S. **S59, S85, S130, S154, S155, S156**
 Chambless, Justin Morse Lola **S245**
 Chambless, Lola B. **S96, S253**
 Chamoun, Roukoz **S87, S119**
 Champagne, Pierre-Olivier **S100, S141**
 Chan, Ann **S27**
 Chandran, Avinash **S4, S108**
 Chandra, Rakesh **S253**
 Chang, Michael T. **S16**
 Chan, Lyndon **S242**
 Chan, Stephen A. **S63**
 Charles, Marcelo **S103**
 Charlson, Emily **S182**
 Chaskes, Mark B. **S102, S258**
 Chelnis, James **S1**
 Chen, Alina **S127**
 Chen, Angela **S8**
 Cheng, Justin **S130**
 Chen, Michael **S71**
 Chen, Shao-Ching **S62, S178**
 Chiluwal, Amrit K. **S213**
- Chin, Christopher J. **S236**
 Chitguppi, Chandala **S5, S28, S29, S67, S73, S102, S107, S113, S124, S128, S231, S242**
 Chittiboina, Prashant **S129, S131**
 Chiu, Harvey K. **S143**
 Chkhaidze, Rati **S270**
 Choby, Garret **S14, S144, S194, S247**
 Choi, Jonathan **S48**
 Choi, Kevin **S242**
 Cho, Ray **S185, S186, S187**
 Cho, Sung-Woo **S143**
 Choudhury, Abrar **S221**
 Chowdhury, Naweed **S253**
 Cimino, Patrick **S61**
 Ciporen, Jeremy N. **S35, S54**
 Cocca, Paola **S71**
 Codd, Patrick **S242**
 Cognetti, David **S112**
 Cohen-Cohen, Salomon **S22, S95, S110, S144**
 Cohen-Gadol, Aaron **S173**
 Cohen, Marc **S27, S30, S69, S122, S144, S199, S243**
 Cohen, Michael A. **S62**
 Collier, Scott **S264**
 Collopy, Sarah **S107**
 Conger, Andrew **S233**
 Connelly, Jennifer **S60**
 Cools, Michael **S83**
 Coon, Alexander L. **S180**
 Corrales, C.E. **S43**
 Corrales, Carleton E. **S10**
 Costello, Joseph F. **S221**
 Couldwell, William T. **S62**
 Coumans, Jean-Valery **S96**
 Cracchiolo, Jennifer R. **S27, S69, S199**
 Craig, John **S211**
 Crowley, R. Webster **S71**
 Cruz, Ricardo José Lopes da **S190**
 Cua, Santino G. **S3**
 Curran, Kent **S18, S258**
 Curry, Joseph **S7, S112, S231**
- Dabecco, Rocco M. **S93**
 Daggubati, Lekhaj C. **S243**
 Damek, Denise **S40, S59, S74**
 Daniels, David J. **S86, S118**
 Danilov, Valeriy **S184, S198**
 Daoud, Georges **S14**
 Dasenbrock, Hormuzdiyar **S71**
 Dassi, Camila **S134**
 Dastagirzada, Yosef **S93, S214**
 Datta, Shaswati Sengupta **S203**
 David, Abel **S171**
 David, Bray P. **S183**
 David, Wyatt **S20, S119**

- Dawood, Hassan **S94**
 Day, John **S151**
 de Almeida, John **S67, S114**
 De Almeida, John **S69**
 de Andoain, Guillermo Blasco garcia **S87, S158, S161, S162**
 De Frutos, Daniel **S248**
 de Lara, Danielle **S132, S198**
 Deamont, Christos F. **S185**
 Dedmon, Matthew **S227**
 Deep, Nicholas L. **S136**
 Dehdashti, Amir R. **S82, S88, S213**
 Dejam, Dillon **S98**
 Delman, Bradley N. **S1, S2, S9**
 Demare, Benjamin **S221**
 DeMonte, Franco **S13, S27, S65**
 Devaiah, Anand K. **S71, S92**
 Devine, Conor M. **S233**
 Devlin, Phillip M. **S60**
 Dey, Jacob **S194**
 Dicesare, Jasmine **S260**
 Ding, Dale **S165, S221**
 Ding, Kevin **S98**
 Disse, Gregory D. **S250**
 Djalilian, Hamid R. **S114**
 Dobri, Georgiana **S5**
 Dodd, Robert L. **S16, S69**
 Dogan, Aclan **S35**
 Doglietto, Francesco **S30, S71**
 Domino, Joseph **S87**
 Doniz-Gonzalez, Ayoze **S87, S158, S161, S162**
 Donnelly, Neil **S43**
 Dorismond, Christina **S8**
 Dorsey, Jay F. **S53**
 Dossani, Rimmel **S149**
 Dougherty, Mark C. **S108**
 Douglas, Jennifer E. **S176**
 Doyle, Mary-Anne **S132**
 Dreyfuss, Alexandra D. **S53**
 Driscoll, Colin L. **S44, S99, S101, S137, S149, S159**
 Driscoll, Collin L. W. **S217, S262**
 Driver, Joseph **S94**
 Druce, Irene **S132**
 Dryden, Stephen C. **S212**
 Dudas, Jozsef **S11**
 Duff, Brian **S192**
 Dunn, Ian F. **S60, S94**
 Duong, Courtney **S27, S98, S118, S136**
 Dymon, Zaneta **S121**
 Dziedzic, Tomasz **S120**

 Eaton, Bree R. **S39**
 Ebert, Charles S. **S3, S8, S208, S229**
 Edem, Idara **S13**
 Eder, Adrianna **S212**

 Eguiluz-Meléndez, Aldo **S36, S76**
 Eisenberg, Mark B. **S88**
 Eliashar, Ron **S175**
 ElJalby, Mahmoud **S15**
 El-Kouri, Nadeem **S121**
 Eloy, Jean A. **S194, S202**
 El-Sayed, Ivan **S81, S138, S139, S171**
 Elsworth, Patrick J. **S41, S53, S61**
 Emerick, Kevin S. **S221**
 Emerson, Sam **S59, S61, S96, S115, S167, S180, S217**
 Emmez, Hakan **S107**
 Engel, Nils **S11**
 Enomoto, Adam **S98**
 Epping, Austin **S59, S85, S130, S154, S155, S156**
 Epps, Gregory A. **S124**
 Epsten, Madeline **S102, S121**
 Erbele, Isaac D. **S223**
 Erickson, Benjamin P. **S182, S231**
 Erick, Wang **S265**
 Ernst, Griffin **S211**
 Erson-Omay, E. Zeynep **S20, S119**
 Erson, Zeynep **S225**
 Espinoza, Jose **S148**
 Esteban, Alberto Francisco Gomez **S206**
 Evans, James J. **S5, S17, S28, S29, S67, S69, S73, S102, S107, S112, S124, S128, S177, S210, S242, S258**
 Evins, Alexander I. **S76, S158, S161**
 Ewend, Matthew **S4**
 Ewy, Joshua **S48**

 Fana, Michael **S185**
 Fan, Gaoyang **S164**
 Fang, C. H. **S219**
 Faquin, William C. **S75**
 Farrell, Christopher J. **S5, S107, S128, S256**
 Fastenberg, Judd **S124**
 Fatterpekar, Girish **S214**
 Feldman, Allison **S63, S270**
 Feldstein, Neil A. **S234**
 Felicio, Thiago Albonette **S125, S134, S188**
 Fenberg, Rachel **S13**
 Feng, Lei **S164**
 Fernandez-Miranda, Juan C. **S16, S22, S36, S69, S87, S146, S158, S161, S162**
 Fernando, Shanik **S253**
 Feroze, Abdullah **S47**
 Ferreira, Manuel **S47, S59, S61, S96, S115, S167, S180, S217**
 Filimonov, Andrey **S117, S228**
 Flanders, Adam E. **S102**
 Fleming, James C. **S212**

 Flemming, Kelly **S85**
 Fliss, Dan **S67**
 Flukes, Stephanie **S27, S30, S69, S122, S199, S243**
 Fomchenko, Elena **S20**
 Fong, Reginald **S233**
 Fontanella, Marco M. **S30, S71**
 Foote, Robert L. **S52**
 Forbes, Jonathan **S147, S169**
 Forde, Cillian **S11**
 Foreman, William **S40, S59, S74**
 Forner, David **S67**
 Forster, Martin **S11**
 Fowler, Brian T. **S212**
 Franco, Joel **S24**
 Franke, Jennifer **S37**
 Freedman, Benjamin R. **S33**
 Freeman, Zane **S255, S268**
 Frickey, Lucas **S3**
 Friedman, Gabriel **S96**
 Friedmann, David R. **S136**
 Friedman, Rick A. **S63**
 Fringuello, Anthony **S40, S59, S74**
 Frisoli, Fabio **S165**
 Fukui, Melanie B. **S59, S85, S130, S154, S155, S156**
 Fukushima, Takanori **S151**
 Fulbright, Robert K. **S20, S119**
 Fuller, Greg **S65**
 Fumagalli, Rebecca **S147**
 Funari, Abigail **S40**
 Furlan, Andre Beer **S102, S121**

 Gadkaree, Shekhar K. **S75, S111, S221**
 Galati, Lisa **S190, S191**
 Gallagher, K. Kelly **S48**
 Gallia, Gary **S46, S89, S177, S202**
 Gamblin, Austin S. **S62**
 Gamez, Mauricio **S14**
 Gandhi, Mitesh **S219, S220**
 Gandhi, Sirin **S60**
 Ganly, Ian **S27, S144**
 Garcia, Carla Fernandez **S222, S251**
 Garcia, Giancarlo A. **S182**
 Garcia, Juan Carlos **S248**
 Gardner, George **S241**
 Gardner, Paul A. **S6, S17, S22, S23, S24, S31, S36, S50, S51, S56, S67, S68, S76, S100, S141, S209, S265**
 Garrett, Samuel **S112**
 Garzon, Tomas **S17, S69, S177**
 Gattozzi, Domenico **S87, S119**
 Geer, Eliza **S69, S199**
 Gelfand, Yaroslav **S40**
 Gelpi, Mark **S56, S208**
 Geltzeiler, Mathew **S35**
 Gentili, Fred **S67, S71, S106, S114**

- George-Jones, Nicholas **S269**
Germanwala, Anand V. **S170**
Ghalib, Luma **S3**
Gheewala, Rohi **S54**
Ghosh, Satrajit **S94**
Giannini, Caterina **S86**
Gidley, Paul **S13, S27, S65**
Gilder, Hannah E. **S169**
Gill, Corey M. **S9**
Gill, Kurren S. **S107, S113**
Gil, Sebastian **S4**
Gil, Ziv **S67**
Gleber-Netto, Frederico O. **S26**
Glenn, Chad A. **S211**
Glicksman, Jeffrey **S25, S91**
Godovchik, Joseph **S112**
Goldman, Hannah G. **S209**
Goldman, Richard **S7**
Goldrich, David **S228**
Goldschmidt, Ezequiel **S17, S23**
Goldstein, David **S67, S69**
Golfinos, John G. **S93, S168, S214**
Gomez, Matías **S197, S205**
Gonen, Lior **S59**
Gonzalez-Cuyar, Luis **S61**
Gopen, Quinton **S98, S118, S136**
Gordon, Lynn **S27**
Gormley, William B. **S10**
Goshtasbi, Khodayar **S114, S126, S133**
Gossman, Mona **S225**
Govindaraj, Satish **S9, S228**
Goyal, Neerav **S51**
Gozal, Yair M. **S240**
Grady, Sean M. **S53**
Graf, Alexander **S67**
Graffeo, Christopher S. **S21, S44, S45, S52, S55, S56, S62, S64, S77, S80, S86, S89, S95, S99, S101, S118, S137, S149, S159, S169, S209, S217, S247**
Graham, Scott M. **S108**
Graner, Michael **S40, S59, S74**
Gray, Stacey T. **S75, S111, S221**
Greenlee, Jeremy D. **S108**
Griessenauer, Christoph **S233**
Grose, Elysia **S23**
Gudis, David **S230**
Guenette, J. P. **S43**
Gullane, Patrick **S67**
Gummadavelli, Abhijeet **S225**
Gunel, Murat **S225**
Gupta, Sachin **S35**
Gurewitz, Jason **S93, S214**
Gurgel, Richard **S62**
Gurrola II, Jose **S171**
Guthikonda, Bharat **S116, S149, S181, S240**
Gu, Yurong **S17, S112, S201**
Habib, Ahmed **S13**
Hachem, Ralph Abi **S12, S242, S244**
Hahs-Vaughn, Debbie L. **S63, S270**
Halderman, Ashleigh **S132, S215, S251**
Hall, Daniel **S17**
Hammrick, Forrest **S62**
Han, Daewoo **S147**
Han, Hao **S164**
Hanna, Ehab **S13, S26, S27, S50**
Hann, Christine L. **S202**
Hansen, Rosemary T. Behmer **S202**
Han, Shen **S265**
Han, Sheng **S31**
Hanson, Martin **S199, S243**
Harary, Maya **S94**
Hardesty, Douglas A. **S16, S122, S125, S134, S165, S188, S215, S236**
Hardy, David **S43**
Harn, Nick **S87**
Harper, Cierra **S10**
Harris, Elizabeth **S4**
Harris, Kendra **S221**
Harris, Thomas **S60**
Harris, William C. **S171, S199**
Harsh, Griffith R. **S16, S238**
Hartlein, Taylor **S128**
Hattab, Eyas **S221**
Hawn, V. S. **S219**
Haynes, David S. **S104, S254**
Head, Jeffery **S17, S69, S180**
Heaney, Anthony P. **S143**
Heffelfinger, Ryan **S7**
Helman, Sam **S11**
Helman, Samuel N. **S24**
Hemza, Jan **S172, S230, S242**
Henderson, Riley C. **S209**
Hendricks, Benjamin **S60, S161**
Herchenhorn, Daniel **S190**
Hermsen, Mario **S11**
Hernandez-Hernandez, Vanessa **S76**
Hernandez, Jesus Gimeno **S206, S222, S251**
Hernandez, Stephen **S229**
Herur-Raman, Aalap **S90**
Hess, Ryan **S72, S267**
Heyd, Cameron P. **S241**
Hidalgo, Diana Hernanperez **S251**
Hidayetov, Tural **S175**
Higa, Hana Caroline Morais **S190**
Higgins, Dominique **S234**
Hilz, Stephanie **S221**
Hirohata, Toshio **S200**
Hodge, Sarah **S64**
Hodson, Meghan S. **S25**
Hoffman, Samantha **S94**
Hogan, Elizabeth **S129, S131**
Hoke, Austin T. **S3**
Holcomb, Andrew **S111**
Holtzman, Adam L. **S230**
Hong, Chang Ki **S20, S95, S258**
Hong, Christopher S. **S119, S172**
Hong, Je Beom **S95**
Hong, Michelle K. **S136**
Horne, Sylvia **S241**
Howard, David **S11**
Hsueh, Wayne D. **S194, S202**
Hsu, Frank P. **S114, S126, S133**
Hsu, Liangge **S60**
Hsu, Sanford **S62, S178**
Huang, Alice E. **S194**
Huang, Gary **S138**
Huang, Kuang-Han **S1**
Hueniken, Katrina **S67**
Hughes, Joshua D. **S110**
Humala, Nelson **S234**
Hunn, Martin **S259**
Hunter, Jacob B. **S97, S269, S270**
Huntley, Colin T. **S124, S210**
Hunt, Patrick J. **S27, S65**
Huston III, John **S110**
Huttner, Anita **S20, S119**
Hutz, Michael **S43**
Hwang, Peter H. **S16, S69, S146, S231**
Ibrahim, Nour **S16**
Illing, Elisa **S173**
Iloreta, Alfred **S9, S117, S228**
Indelicato, Daniel J. **S230**
Inzucchi, Silvio **S225**
Isaacson, Brandon **S270**
Ishii, Masaru **S89, S202**
Ismail, Khaled **S32**
Issa, Khalil **S12, S15, S244**
Ivan, Michael **S105, S130**
Iyer, Charoo **S87**
Jabbour, Pascal M. **S82**
Jaboin, Jerry J. **S54**
Jack, Megan **S87**
Jackson, Christina **S37, S46**
Jackson, Neal M. **S158, S205, S221, S255, S268**
Jacobs, Rachel **S6**
Jafar, Jafar J. **S93, S168, S214**
Jameson, Mark **S73, S247**
James, Robert **S165**
Jamshidi, Ali O. **S173, S269, S272**
Jamshidi, Aria **S105**
Jang, David W. **S12, S15, S242, S244**
Janus, Jeffrey R. **S144**
Jarin, Peter **S188**
Jason, Papacostas **S74**
Jawad, Basit A. **S252**

- Jay, Amrita **S11**
 Jayender, J. **S43**
 Jean, Walter C. **S90**
 Jennings, Jonathan E. **S59**
 Jensen, Randy **S40, S59, S74**
 Jethanamest, Daniel **S136**
 Jha, R. Tushar **S225, S232**
 Jha, Roshani **S21**
 Jiam, Nicole **S171**
 Jimenez, Andres Camilo Vargas **S251**
 Jin, Lan **S20, S119**
 Jitaroon, Kawinyarat **S16, S69**
 Johnson, Chris **S11**
 Jr, Manuel Ferreira **S167, S180**
 Ju, Jianbao **S174**
 Juliano, A. **S43**
 Jung, Sin-Ho **S12, S15**
 Justo, Ness Jerold A. **S188**
 Juvekar, Parikshit **S60**
- Kacker, Ashutosh **S15, S26**
 Kaczmarzyk, Jakub **S94**
 Kaen, Ariel **S86, S145, S239**
 Kaffenberger, Thomas M. **S210**
 Kahilogullari, Gokmen **S117, S143, S189**
 Kamiyama, Hiroyasu **S85**
 Karakasis, Christopher **S206**
 Karlin, Justin N. **S73**
 Karsy, Michael **S62**
 Kasperbauer, Jan **S144**
 Kassam, Amin **S18, S59, S85, S130, S154, S155, S156, S259**
 Kassam, Mikael **S85**
 Kassir, Zachary **S56**
 Kaufman, Kenton **S55**
 Kavouridis, Vasiliou **S94**
 Kaye, Joel **S243**
 Kazi, Eman **S168**
 Keely, Erin **S132**
 Kejirwal, Sameer **S27**
 Kemper, Nathan **S268**
 Kenning, Tyler **S18, S25, S91, S103, S239, S258**
 Keole, Sameer **S72**
 Khairy, Sami **S85**
 Khalafallah, Adham M. **S21, S89**
 Khalili, Sammy **S18, S59, S130, S259**
 Khan, Hammad A. **S138**
 Khan, Nickalus R **S218**
 Khattar, Nicolas **S165**
 Khelessi, Alexander **S151**
 Khouri, Tawfiq **S5**
 Khoury, Tawfiq **S28, S29, S67, S73, S102, S107, S113, S128, S258**
 KihwanHwang, Kihwan- **S143**
 Killeen, Daniel E. **S97, S270**
- Kilty, Shaun **S23, S127, S133, S188**
 Kim, H. J. **S261**
 Kim, Hankyu **S95**
 Kim, Matthew **S178**
 Kim, Michael G. **S76, S158, S161**
 Kim, Minsoo **S22, S138**
 Kimple, Adam J. **S3, S8, S56, S208, S229**
 Kim, Won **S122, S240, S260**
 King, James **S124**
 Kircher, Matthew **S43, S170**
 Kiyofuji, Satoshi **S85**
 Kleinstern, Geffen **S62, S99**
 Knusel, Konrad K. **S41, S53, S61**
 Kocak, Mehmet **S102**
 Koester, Stefan **S165**
 Kohlberg, Gavriel **S267**
 Kojis, Nathaniel **S59**
 Kolb, Bradley **S71**
 Kolia, Nadeem R. **S50, S68**
 Komotar, Ricardo J. **S128, S130**
 Komotar, Rick **S105**
 Komune, Noritaka **S75, S151**
 Kondo, Akihideo **S140**
 Kondziolka, Douglas **S168**
 Kong, Doosik **S22**
 Kong, Keonho A. **S159**
 Konuthula, Neeraja **S47**
 Koppurapu, Srujan **S89**
 Koretsky, Alan **S131**
 Kossler, Andrea **S182**
 Kosty, Jennifer **S116, S149, S181, S240**
 Koszewski, Ian J. **S192**
 Koury, Tawfiq **S242**
 Krasnozhan, Vladimir **S198**
 Kreatsoulas, Daniel **S16, S122**
 Krein, Howard **S7**
 Krempl, Greg A. **S211**
 Krishnan, Ravindran **S118**
 Krueger, Bryan **S169**
 Kshetry, V. R. **S219**
 Kshetry, Varun **S41, S42, S53, S61, S173, S206**
 Kuan, Edward C. **S114, S126, S127, S133**
 Kumar, Jay I. **S225**
 Kunert, Przemyslaw **S120**
 Kupferman, Michael **S13, S27**
 Kura, Bhavani **S18, S59, S85, S130, S259**
 Kussyk, Dorian M. **S115**
 Kutz, Joe W. **S270**
 Kveton, John **S119**
 Kwan, Kevin **S88**
- Labarge, Donald **S185**
 Labiad, Ikrame **S147**
 Labib, Mohamed **S76, S120, S163**
- Lagman, Carlito **S138**
 Lal, Devyani **S72**
 Lamothe, Andre **S23, S127, S133**
 Lane, John I. **S65**
 Lang, Michael **S165**
 Lan, Ming-Ying **S147**
 LaRiviere, Michael J. **S53**
 Larochelle, Ryan **S231**
 Lasso, Andrea **S127, S133**
 Laufer, Ilya **S199**
 Lauretti, Liverana **S71**
 Lavergne, Pascal **S5, S17, S28, S29, S69, S73, S102, S107, S113, S128, S177, S258**
 Laws, Edward R. **S71, S87**
 Lawton, M. **S76**
 Lawton, Michael T. **S161, S163, S165**
 Le Roux, Andre A. **S236**
 Lebowitz, Rich **S214**
 Lebowitz, Rich **S93**
 Lechner, Matt **S11**
 Lechpammer, Mirna **S250**
 Lee, Eric **S117**
 Lee, Jake **S201, S256**
 Lee, Jivianne T. **S8, S122, S260**
 Lee, John Y. K. **S19, S21, S53, S176, S224**
 Lee, Jonathan **S206**
 Lee, Saangyoung E. **S208**
 Lehrich, Brandon M. **S133**
 Lehrich, Brandon M. **S114**
 Lekovic, Gregory P. **S177, S216**
 Leonard, Jeffrey **S48**
 Leonel, Luciano César P.C. **S77**
 Leonetti, John P. **S43, S121, S170, S219**
 Levine, Corinna G. **S128**
 Levy, Michael **S151**
 Lewis, Ariane **S93**
 Leyva, Oscar A. **S10**
 Liang, Kathryn M. **S209**
 Liao, Sebastian **S62, S178**
 Li, Carrie **S21**
 Li, Da **S146**
 Liebendorfer, Adam P. **S201**
 Lieberman, Seth **S93, S214**
 Li, Houyong **S17, S112, S201**
 Li, Huabin **S17**
 Li, K. L. **S219**
 Li, Lifeng **S190, S191**
 Lillehei, Kevin **S40, S59, S74**
 Lim, Rebecca **S124, S256**
 Lim, Daniel A. **S221**
 Lim, Jaejoon **S256**
 Lim, Michael **S37, S46**
 Lin, Alexander **S53**
 Lin, Charles **S74**
 Lin, Derrick T. **S75, S111, S221**

- Lindquist, Nathan R. **S202**
 Lin, Giant **S194**
 Lin, Harrison W. **S114**
 Lin, Hung-Mo **S1**
 Lin, James **S119**
 Linker, Lauren A. **S264**
 Link, Michael J. **S21, S44, S45, S52, S55, S56, S62, S63, S64, S77, S80, S85, S99, S101, S118, S137, S144, S149, S159, S169, S209, S217, S247, S262, S270**
 Lin, Theodore C. **S241**
 Lin, Yufan **S249**
 Lipinski, Katherine P. **S191**
 Lipschitz, Noga **S169, S268**
 Li, Ruichun **S165**
 Litofsky, Norman S. **S217**
 Little, Andrew S. **S60**
 Liu, Ann **S180**
 Liu, Dora **S132**
 Liu, James K. **S194, S202**
 Liu, Katherine **S117, S228**
 Liu, Quan **S17, S112, S201**
 Liu, S. John **S221**
 Li, Xiong **S139**
 Llorente, Jose L. **S11**
 Locke, Tran B. **S241**
 Lockwood, Joseph **S221, S255, S268**
 Loewenstern, Joshua **S2**
 Lohia, Shivangi **S27**
 London, Nyall **S14, S48, S49, S187, S190, S191**
 Longo, Gabriel M. **S158**
 Longo, Michael **S40**
 Long, Sallie **S144, S230**
 Lonser, Russel R. **S3**
 Lopes, Demetrius **S71**
 Lopez, Diana **S41, S42, S53, S61**
 Lopez, Enrique **S148**
 Lopez, Ricardo Ginstal **S206**
 Lovin, Benjamin **S48**
 Lucas, Carlstrom P. **S21, S55, S57, S62, S64, S77, S80, S95, S99, S101, S137, S149, S159, S169, S209, S217, S247, S262**
 Luebs, John **S56, S57, S111**
 Luginbuhl, Adam **S7, S112, S231**
 Lund, Valerie J. **S11**
 Luong, Peter Q. **S138**
 Lustig, Robert A. **S53**
 Lu, Victor M. **S44, S89, S118**
 Lysikatos-Lyssikatos, Charlampos **S129**
- Macfarlane, Robert **S43**
 Macielak, Robert J. **S270**
 Madden, John **S244**
- Madison II, Michael L. **S264**
 Madoglio, Alba **S30**
 Mady, Leila J. **S210**
 Maehara, Taketoshi **S168**
 Magill, Stephen T. **S221**
 Magliocca, Kelly **S11**
 Mahajan, Aayushi **S234**
 Mahajan, Amit **S225**
 Mahboubi, Hossein **S126**
 Mahoney, Dom E. **S218**
 Mains, Allie **S241, S268**
 Maiti, Tanmoy **S72**
 Malafronte, Patrick **S232**
 Malcolm, Janine **S132**
 Malenke, Jordan A. **S245, S253**
 Malfitano, Madison **S3**
 Mammi, Marco **S94**
 Manes, R. Peter **S11, S172**
 Manjila, Sunil V. **S141, S185, S196**
 Mankekar, Gauri **S223**
 Mannion, Richard **S43**
 Mansfield, Perry T. **S209**
 Manzoor, Nauman F. **S104, S254**
 Mao, Gordon **S115**
 Marchel, Andrzej **S120**
 Marciano, Filippo **S71**
 Marilene, Wang **S122, S127, S143, S240, S260**
 Marileo, Roberto **S205**
 Marinelli, John P. **S45, S63, S270**
 Marin, Janmais **S185**
 Marin, Janmaris **S186**
 Marino, Michael **S72**
 Markosian, Christopher **S194**
 Mark, Preul **S163**
 Marple, Bradley **S251**
 Martinez-Perez, Rafael **S125, S134, S141, S165, S188, S196, S194, S215, S240**
 Marzo, Sam **S43, S170**
 Masoudian, Pourya **S127, S133**
 Mastino, Lara **S76**
 Mathkour, Mansour **S255**
 Matsuno, Akira **S200**
 Matsuo, Satoshi **S75, S151**
 Mattavelli, Davide **S30, S71**
 Mattogno, Pier Paolo **S71**
 Mattos, Jose **S247**
 Maxwell, Anne K. **S177, S216**
 Mazza, Jacob **S17, S69, S180**
 Mazzoni, Susan **S53**
 McAree, Michael **S224**
 Mccambridge, Joshua **S102**
 McCarthy, Lily **S225**
 McCarty, Justin **S111**
 McClelland III, Shearwood **S54**
 McCoul, Edward D. **S171, S199, S252**
 McCulloch, Timothy M. **S192**
- McDermott, Michael W. **S171, S221**
 McDonald, Marin **S63**
 McDonough, Mitchell **S236**
 McDougall, Cameron G. **S180**
 McDowell, Michael **S6, S51**
 McGee, Christie **S204**
 McGill, Marlena **S144**
 McGlotten, Raven **S129**
 McInerney, James **S243**
 McKean, E. L. **S219**
 McKean, Erin L. **S13**
 McKhann II, Guy M. **S234**
 McLaughlin, Kevin **S159, S229**
 Mclaughlin, Lily **S122**
 McMenomey, Sean O. **S136**
 Meador, Andrew G. **S212**
 Meco, Cem **S117, S143, S189**
 Mehad, Mitra **S253**
 Mehta, Gautam **S65**
 Mehta, Guatam U. **S177, S216**
 Melder, Katie L. **S210**
 Mena, Laila Perez de San Roman **S130**
 Mendenhall, William M. **S230**
 Mendez, Diego **S148**
 Mendez, Humberto Reyna **S154**
 Meng, Lingzhao **S161, S162**
 Meng, Qingguo **S162, S161**
 Merkle, Hellmut **S131**
 Meybodi, Ali **S163**
 Mhaweji, Rachad **S211**
 Michael, L. Madison **S218**
 Michael, Link J. **S95**
 Mickey, Bruce **S132**
 Midwinter, Mark **S199**
 Miguel, Lopez Gonzalez **S163**
 Miles, Brett **S117**
 Miller, Craig **S47**
 Miller, David M. **S53**
 Miller, Denise **S21**
 Milton, Camille K. **S211**
 Min, Le **S87**
 Mitin, Timur **S54**
 Miyagishima, Takaaki **S183**
 Miyamatsu, Yuichiro **S151**
 Moe, Kris S. **S47**
 Moffat, David **S43**
 Mohajeri, Sepideh **S127, S133**
 Mohiuddin, Jahan J. **S53**
 Mohyeldin, Ahmed **S14, S87, S161, S162**
 Moldovan, Ioana **S23, S188**
 Moliterno, Jennifer **S20, S119**
 Momin, Arbaz **S41, S42, S53, S61**
 Monescillo, Rosario Garcia **S206**
 Monroy-Sosa, Alejandro **S59, S85, S130, S154, S155, S156**
 Monsour, Meredith A. **S96**
 Montaser, Alaa **S16**

- Monteiro, Eric **S67, S114**
 Montemagno, Kora **S147**
 Montoure, Andrew J. **S60**
 Montoya, Francisca **S205**
 Mooney, David J. **S33**
 Mooney, Michael A. **S60**
 Moon, Ju Hyung **S256**
 Moore, Dennis **S43**
 Moore, Eric J. **S144**
 Moore, Samantha **S270**
 Mora, Alfredo Espinosa **S154**
 Morcos, Jacques J. **S127, S130**
 Moreira, Leandro Borba **S60**
 Moreno, Ivan Muerte **S222**
 Moreno, Maria Cruz Iglesias **S206, S251**
 Morgenstern, Peter **S15**
 Morita, Akio **S85, S200**
 Morris, Christopher G. **S229**
 Morris, Jonathan **S56, S137**
 Morse, Justin C. **S253**
 Moshtaghi, Omid **S63**
 Moskowitz, H. S. **S219**
 Mowry, Sarah E. **S138**
 Moyheldin, Ahmed **S146**
 Mrugala, Maciej **S72**
 Muelleman, Thomas J. **S216**
 Muelleman, Tommy J. **S177**
 Muge, Luke **S134**
 Muhanna, Nidal **S67**
 Muhlestein, Whitney E. **S96**
 Muhsen, Baha`eddin A. **S206**
 Mukherjee, Debraj **S21, S89, S202, S248**
 Mullen, Reed **S168**
 Munoz, Alexander **S87**
 Murari, Keerti **S225**
 Murchison, Ann P. **S82**
 Murphy, Kira **S28, S67, S128, S231, S242**
 Myers, Jeffrey N. **S26**
- Na'ara, Shorook **S67**
 Nader, Marc-Elie **S13, S27**
 Naeem, Komal **S44, S76, S120, S163**
 Najera, Edinson **S86, S145, S239**
 Nakagawa, Takashi **S75**
 Nakamizo, Akira **S151**
 Nakatomi, Hirofumi **S85**
 Nangunoori, Raj **S93**
 Naudy, Cristian **S197**
 Nayak, Jayakar V. **S16, S69, S146**
 Nayak, Roshan **S151**
 Nebor, Ivanna **S147**
 Neff, Brian A. **S99**
 Neill, S. **S167**
 Nelson, Megan **S221**
- Newman, Jason G. **S53**
 Newman, S. **S167**
 Newman, Sarah **S183**
 Newman, Steven A. **S73, S168, S247**
 Ng, Edwin **S98**
 Nguyen, Allison A. **S209**
 Nguyen, Candice **S142, S153**
 Nicolai, Piero **S30, S71**
 Nieman, Lynnette **S129**
 Nimmanitya, Pree **S6**
 Ninan, Sen J. **S117, S228**
 Noiphithak, Raywat **S6**
 Northam, Weston **S4, S227**
 Nouby, Radwan **S32**
 Noureldine, Mohammad Hassan A. **S232, S271**
 Nouri, Mohsen **S82, S213**
 Nuss, Daniel W. **S158, S229**
 Nye, Chad **S63, S270**
 Nyquist, Gurston G. **S5, S28, S29, S67, S73, S102, S107, S113, S124, S128, S210, S242, S258**
- O'Connell, Brendan P. **S105**
 O'Connor, Mackenzie **S231, S242**
 Oemke, Holly E. **S228**
 Okafor, Somtochi **S251**
 Olivi, Alessandro **S71**
 Olson, Jeffrey J. **S39**
 O'Malley, Bert W. **S53**
 Omay, S. Bulent **S225**
 Omay, Sacit B. **S172**
 Omofoye, Oluwaseun **S238**
 Onoda, Keisuke **S200**
 Ono, Hideaki **S85**
 Onwuka, Amanda **S48**
 Ooi, Eng **S67**
 Orlov, Cinthia **S248**
 Ormond, David **S40, S59, S74**
 Orscelik, Atakan **S139**
 Ostergard, Thomas A. **S138**
 Oswari, Selfy **S106**
 Otten, Marc **S229**
 Otto, Brad A. **S16**
 Otto, Bradley A. **S3, S32, S125, S135, S185, S186, S187, S188, S236, S240**
 Oyama, Kenichi **S200**
 Oyesiku, Nelson M. **S183**
 Ozdemirli, Metin **S261**
 Ozgural, Onur **S143**
- Pacione, Donato **S93, S168, S214**
 Paez, Wencesley **S54**
 Paisan, Gabriella **S165**
 Palejwala, Ali **S211**
 Palettas, Marilly **S32**
- Palmer, James N. **S241**
 Panizza, Ben **S219, S220**
 Pardo-sanz, Melchor Saiz **S222, S251**
 Parikh, Anuraag S. **S75, S111, S221**
 Park, Hae Gi **S267**
 Park, Hun Ho **S20**
 Park, Jae Sung **S267**
 Parney, Ian F. **S52**
 Parsel, Sean M. **S252**
 Pascal, Emily **S158**
 Pashaev, Bakhtiyar **S184, S198**
 Patel, Anand **S170**
 Patel, Evan **S136**
 Patel, Jena **S124**
 Patel, Kunal S. **S27**
 Patel, Neil S. **S99**
 Patel, Nitesh P. **S262**
 Patel, Prachi **S5, S28, S29, S107, S113, S128**
 Patel, Snehal G. **S27, S144**
 Patel, Varun **S91**
 Patel, Vijay A. **S51**
 Patel, Zara M. **S16, S69, S146**
 Patil, Nirav **S138**
 Patra, Devi P. **S72, S82, S267**
 Paul, Gardner A. **S152, S237**
 Payne, Spencer **S245**
 Peeters, Sophie M. **S122, S127, S260**
 Pelargos, Panayiotis **S211**
 Peng, Kevin A. **S216**
 Pensak, Myles L. **S267**
 Perez, Carlos L. **S270**
 Peris-Celda, Maria **S18, S25, S77, S80, S91, S99, S103, S147, S159, S217, S239, S258**
 Perry, Avital **S21, S44, S45, S52, S55, S57, S62, S64, S77, S80, S86, S89, S95, S99, S101, S118, S137, S149, S159, S169, S209, S217, S247, S262**
 Peterson, Racheal **S116**
 Peto, Ivo **S88, S225, S232, S271**
 Pezzutti, Dante L. **S194, S236**
 Phan, Jack **S13**
 Phillips, H. Westley **S98**
 Phillips, Michael **S48**
 Piazza, Martin **S48**
 Pichierri, Angelo **S218**
 Pickering, Curtis **S26**
 Pinheiro-Neto, Carlos **S18, S25, S77, S80, S91, S103, S190, S191, S217, S239, S249, S258**
 Piper, Keaton **S271**
 Pipkorn, Patrik **S201, S256**
 Placantonakis, Dimitris **S93, S168, S214**
 Platt, Andrew **S184**
 Plitt, Aaron R. **S132, S215**
 Pollack, Aron **S207**

- Pollock, Bruce E. **S45, S52, S64**
 Pool, Christopher **S151**
 Porter, Alyx **S72**
 Porter, Randall W. **S44, S120**
 Possatti, Lucas **S60**
 Poturalski, Matthew **S206**
 Powell, Allison **S49**
 Powers, Martin **S151**
 Prabakaran, Prashanth J. **S192**
 Prabhu, Vikram C. **S170**
 Pradilla, G. **S167**
 Pradilla, Gustavo **S24, S79, S113, S157**
 Prakash, Swetha **S66**
 Prashant, Giyarpuram N. **S240, S260**
 Pressman, Elliot **S225**
 Press, Robert H. **S39**
 Preul, M. **S76**
 Preul, Mark C. **S158, S163**
 Prevedello, Daniel M. **S3, S16, S32, S48, S49, S125, S134, S135, S141, S165, S185, S186, S187, S188, S190, S191, S194, S196, S215, S236, S240**
 Prevedello, Luciano M. **S32, S141**
 Price, Carrie **S21**
 Prieto, Ana Sanchez **S206**
 Przepiórka, Lukasz **S76, S120, S158**
 Przybylowski, Colin J. **S60**
 Puchi, Chris **S253**
 Puram, Sidharth V. **S75**
 Purohit, Aarti **S21**
- Qazi, Shafeen **S97**
 Qazlan, Salman Al **S213**
 Quig, Nathan **S83, S108, S266**
 Quillin, Joseph W. **S39**
 Quinsey, Carolyn **S4, S48, S108**
 Qu, Xiaopeng **S145**
- Rabinowitz, Mindy **S5, S28, S29, S67, S73, S102, S107, S113, S124, S128, S210, S242, S258**
 Raefsky, Sophia **S126**
 Rafael, Jonathan Ortiz **S154**
 Raghavan, Alankrita **S206**
 Rahimi, A. **S43**
 Rahimli, Tural **S109, S175**
 Rahman, Sadiq **S40**
 Rahme, Rudy **S72, S82, S267**
 Rajasekaran, Karthik **S176**
 Raleigh, David R. **S221**
 Ramakrishna, Rohan **S5, S25**
 Ramaswamy, Uma S. **S50**
 Ramirez, Ricardo J. **S256**
 Rangarajan, Sanjeet **S218**
- Rangel, Gustavo G. **S48, S49, S125, S134, S188, S215**
 Ranti, Daniel **S2**
 Ravindran, Krishnan **S89**
 Raviv, Joseph **S255**
 Raviv, Nataly **S238**
 Raymond, Mallory J. **S32**
 Raza, Shaan **S13, S27, S65, S71**
 Recinos, Pablo F. **S41, S42, S53, S61, S173, S206**
 Reh, Douglas D. **S177**
 Reilly, Erin K. **S124, S210**
 Remon, Pablo **S86, S145, S239**
 Rennert, Robert **S151**
 Ren, Yin **S63**
 Requena, Luis **S165**
 Requena-Requena, Luis C. **S125**
 Reyes, Camilo **S11**
 Reyna, Humberto **S148**
 Reyna, Sergio **S148**
 Richardson, Angela M. **S127, S130**
 Richa, Tony **S7**
 Riechelmann, Herbert **S11**
 Rincon-Torroella, Jordina **S177**
 Rindler, R. **S167**
 Rindler, Rima S. **S24, S113**
 Ringel, Barak **S67**
 Rivas, Alejandro **S104, S254**
 Rivera, Arnaldo L. **S217**
 Rizzi, Mark D. **S233**
 Roan, Jose Roan **S222**
 Roberts, Dianna **S26**
 Rocha, Eder **S97**
 Rockhill, Jason **S60**
 Rock, Jack **S211**
 Rodrigues, Pedro Augusto Sousa **S87, S158, S162**
 Rojas, Andres **S205**
 Roland, J. Thomas **S136**
 Romiyo, Prasanth **S98**
 Ronald, Sahyouni **S127**
 Rooper, Lisa M. **S202**
 Rosen, Marc R. **S5, S28, S29, S67, S73, S102, S107, S113, S124, S128, S210, S242, S258**
 Rosito, Diego Mendez **S116, S154**
 Rosso, Casey **S119**
 Rotondo, Ronny L. **S229**
 Rotter, Juliana **S44, S169**
 Rovin, Richard A. **S59, S85, S130, S154, S155, S156**
 Rowan, Nicholas R. **S21, S89, S202, S248**
 Rubel, Kolin **S173**
 Rubio, Roberto Rodriguez **S81, S138, S139**
 Ruffner, Randall S. **S103, S190, S191**
 Rukskul, Pataravit **S6**
 Russo, Daniel **S207**
- Russomando, Alessandra Cataldo **S175**
 Russo, Mark E. **S261**
 Russo, Paolo Di **S158**
 Rutenberg, Michael S. **S229**
 Rutkowska, Wiktoria **S120**
 Rutland, John W. **S1, S2, S9**
 Ruzevick, Jacob **S47, S59, S60, S217**
 Ruzevick, Jake **S115, S167, S180**
 Ruzevik, Jacob **S96**
 Ryan, Matthew **S251**
- Sabalza, Michael N. **S188**
 Sabourin, Victor **S17, S69, S177**
 Sahyouni, Ronald **S126**
 Saito, Nobuhito **S85**
 Salcedo, Andrea Lopez **S222**
 Saleh, Laura **S46**
 Salgado-Lopez, Laura **S147, S217**
 Sami, Mairaj T. **S119**
 Samy, Ravi N. **S169, S241, S268**
 Sanai, Nader **S60**
 Sanchez, Miguel Marigil **S106**
 Santagata, Sandro **S94**
 Santarelli, Griffin D. **S8, S229**
 Santonio, Filippo Veneziani **S76**
 Sariego, Homero **S197, S205**
 Sarlls, Joelle **S131**
 Sartori, Beatriz **S198**
 Sasaki-Adams, Deanna **S4, S83, S105, S227, S266**
 Savardekar, Amey **S181**
 Schaber, Alexandra **S221**
 Schachtel, Michael **S219, S220**
 Schaefer, Eric W. **S51**
 Schartinger, Volker H. **S11**
 Schempf, Tadhg **S231**
 Scherer, Sameul **S40**
 Scherer, Samuel **S59, S74**
 Schlachter, Leslie **S228**
 Schneider, Julia R. **S82, S213**
 Schofield, Mason **S212**
 Schrader, Ignacio Martin **S86, S145, S239**
 Schreiber, Alberto **S30, S71**
 Schueller, Ulrich **S11**
 Schuster, James M. **S53**
 Schwartz, Marc S. **S63**
 Schwartz, Nofrat **S105, S227**
 Schwartz, Theodore H. **S5, S15, S25**
 Scott, Gretchen **S129, S131**
 Scullen, Tyler **S255, S268**
 Seaman, Scott C. **S108**
 Sedaghat, Ahmad **S147**
 Sekhar, Laligam **S60**
 Seldomridge, Ashlee N. **S118**
 Selleck, Anne M. **S63**

- Sen, Chandra **S93, S168, S214**
 Senior, Brent A. **S3, S208**
 Sen, Rajeev **S167, S180**
 Seo, Kyounghee **S221**
 Sepúlveda, Patricio **S197**
 Serrano, David **S121**
 Serrano, Eduardo Castillo **S222**
 Serrano, Manuel Gomez **S222, S251**
 Setty, Pradeep **S23**
 Shah, Aashish **S105**
 Shah, Akash D. **S27**
 Shahein, Mostafa **S32, S125, S134, S135, S188, S236**
 Shah, Jatin P. **S27, S144**
 Shah, Kevin **S82**
 Shah, Kushal J. **S119**
 Shahlaie, Kiarash **S250**
 Shah, Pavan **S46**
 Shah, Sumedh S. **S130**
 Shah, Varun **S16, S122**
 Shao, Jianning **S41, S42, S53, S61**
 Shapiro, Scott B. **S169, S241, S267**
 Shapiro, William H. **S136**
 Sharma, Rahul K. **S30**
 Shastri, Darshan **S83, S266**
 Shastri, Karthik S. **S190, S191**
 Shear, Brian **S20, S119**
 Shelton, Clough **S62**
 Shen, Chan **S51**
 Sheppard, John P. **S98**
 Sherry, Alexander D. **S104, S253**
 Shinnars, Michael **S100**
 Shiokawa, Yoshiaki **S85**
 Shoheit, Michael **S9**
 Shoushtari, Alexander N. **S27**
 Shrivastava, Raj K. **S1, S2, S9**
 Shukairy, Mohammad K. **S219**
 Shulev, Yury **S133**
 Silveira-Bertazzo, Giuliano **S165, S215, S240**
 Silveira, Giuliano Schmidt Bertazzo **S125, S134, S188**
 Silveira, Roberto Leal Da **S97**
 Silver, Cheyanne **S209, S247**
 Simmonds, Jonathan **S192**
 Sindelar, Brian **S266**
 Sindwani, Raj **S173**
 Slater, Patrick **S98**
 Slattery, William H. **S177**
 Smith, Alyssa J. **S14**
 Smith, William **S85**
 Smith, Timothy R. **S10, S35**
 Sneed, Penny K. **S221**
 Snyder, Jacob **S253**
 Snyderman, Carl **S6, S17, S23, S24, S31, S50, S51, S56, S57, S67, S68, S76, S101, S111, S141, S152, S178, S210, S265**
 Solares, Arturo **S219**
 Solares, C. Arturo **S11, S24, S32, S79, S113, S157**
 Solera, Pablo Sarrío **S251**
 Sommerville, Ryan **S74**
 Sonego, Thiago B. **S132, S198**
 Song, Sun H. **S16**
 Soni, Pranay **S41, S42, S53, S61**
 Sordi, Alaina E. **S198**
 Sorenson, Jeffrey **S77, S218**
 Soriano, Roberto M. **S24, S32, S79, S113, S157**
 Sosunov, Alexander A. **S234**
 Soto, Alfonso **S86, S145, S239**
 Spadola, Michael F. **S224**
 Spear, Samuel A. **S270**
 Spock, Todd **S117**
 Sprung, Susanne **S11**
 Sreenath, Satyan B. **S56**
 Sridharan, Shaum **S209**
 Srinivasan, Archana **S82**
 Staecker, Hinrich **S119**
 Stafford, Scott L. **S52**
 Stamates, Melissa **S184**
 Stastna, Daniela **S43**
 Steckl, Andrew J. **S147**
 Steele, Toby O. **S250**
 Stefanelli, Anthony **S17, S69, S177**
 Stefko, Tonya **S24**
 Steinberg, Jeffrey **S151**
 Stewart, Matthew **S7, S242**
 Stieg, Philip E. **S76, S158, S161**
 Stock, Sarah **S206**
 Stokken, Janalee K. **S194**
 Stone, Ari **S18, S259**
 Stopa, Brittany M. **S10**
 Stratakis, Constantine **S129**
 Strong, Reyanne **S108**
 Succar, Eric **S253**
 Su, Chunhai **S164**
 Sugawara, Takashi **S168**
 Suh, Jeffrey D. **S8, S122, S143, S260**
 Sung, Kyoung Su **S256**
 Sun, Matthew Z. **S34, S98, S260**
 Sun, Xicai **S17, S112, S201**
 Sun, Yanchun **S164**
 Su, Shirley **S13, S27, S50**
 Sweeney, Alex D. **S202**
 Sweis, Auddie M. **S241**
 Swendseid, Brian **S7, S112**
 Sylvester, Michael J. **S13**
 Tabae, Abtin **S25**
 Tabar, Vivian **S69, S122, S199**
 Tabar, Viviane S. **S27**
 Tabasinejad, Raha **S106**
 Taboni, Stefano **S30**
 Tahara, Shigeyuki **S200**
 Tai, Alexander X. **S90**
 Takahashi, Yoko **S26**
 Takami, Hirokazu **S86, S106**
 Talagala, Lalith **S131**
 Tallmadge, Margaret **S18, S259**
 Tamargo, Rafael **S46**
 Tanaka, Minoru **S85**
 Tanaka, Yoji **S168**
 Tang, Dennis M. **S173**
 Tassler, Andrew **S177**
 Tatman, Philip D. **S40, S59, S74**
 Tavakol, Sherwin **S94**
 Tavanaiepour, Daryoush **S229**
 Tawfik, Kareem O. **S63**
 Taylor, Tavis **S17**
 Teitelbaum, Jordan **S12, S15, S242**
 Tepedino, Miguel Soares **S190**
 Teramoto, Akira **S200**
 Teyateeti, Achiraya **S45**
 Thammachantha, Samasuk **S27**
 Tham, Tristan **S207**
 Theodosopolous, Philip **S171**
 Theodosopoulos, Philip V. **S221**
 Thomas, Andrew J. **S35**
 Thomas, Charles R. **S54**
 Thomas, Giovana **S204**
 Thomas, Pearce M. **S237**
 Thompson, Reid C. **S104**
 Thorp, Brian D. **S3, S4, S8, S48, S56, S105, S208, S229**
 Timmerman, Robert **S132, S215**
 Ting, Jonathan Y. **S173**
 Tiwari, Neelesh **S28**
 Tjoumakaris, Stavropoula I. **S82**
 Tolisano, Anthony M. **S270**
 Topf, Michael **S112**
 Tosaka, Masahiko **S183**
 Totten, Douglas J. **S104, S253**
 Tragon, Tyson **S111**
 Tran, Sophia **S97**
 Traylor, Katie **S111**
 Truman, Kyla A. **S10**
 Truong, Huy Q. **S22, S36**
 Tsankova, Nadejda **S2**
 Tsutsumi, Kazuo **S85**
 Tufaro, Anthony P. **S177**
 Tumlin, Parker **S169**
 Turcotte, Evelyn **S72, S267**
 Turner, Justin **S245, S253**
 Turner, Meghan T. **S118**
 Turri-Zanoni, Mario **S11**
 Tyler-Kabara, Elizabeth **S23, S51**
 Tysome, James **S43**
 Ugiliweneza, Beatrice **S181**
 Ullian, Erik M. **S221**

- Uluc, Deniz **S117**
 Ungerer, Heather **S241**
 Unlu, Agahan **S143**
 Upadhyayula, Pavan S. **S234**
 Urdang, Zachary D. **S229**
 Uribe-Cardenas, Rafael **S15**
- Vagapova, Gulnar **S184, S198**
 Vaitaitis, Vilija **S229**
 Valappil, Benita **S6, S67**
 Valim, Joao G. **S132**
 Valim, João G. **S198**
 van Gompel, Jamie J. **S225**
 Van Gompel, Jamie **S89, S110, S118, S144, S194**
 van Loveren, Harry **S225, S271**
 Van Ommeren, Randy **S114**
 VanKoevering, Kyle K. **S13, S49**
 Varghese, Jordan **S11**
 Vasudevan, Harish N. **S221**
 Vega, Belen **S76**
 Velasquez, Carlos **S106**
 Velázquez, Carlos Erosa **S154**
 Verma, Gaurav **S1**
 Vescan, Allan **S67, S114**
 Vickery, Thad W. **S127**
 Vidal, Aaron **S205**
 Villanueva-Meyer, Javier E. **S221**
 Villavisanis, Dillan F. **S1**
 Vimawala, Swar **S7, S29, S112, S124, S210**
 Vining, Eugenia M. **S172, S225**
 Viswanathan, Rohan **S91**
 Vora, Sujoy **S72**
- Wadehra, Madhuri **S27**
 Wagner, Katherine **S88**
 Walker, Katherine **S205**
 Walker, Patricia **S197**
 Wallace, Nathan J. **S92**
 Waltzman, Susan B. **S136**
 Walz, Patrick **S48, S49**
 Wang, Dehui **S17, S112, S201**
 Wang, Eric **S6, S23, S24, S31, S50, S51, S56, S67, S68, S76, S100, S141, S152, S209**
 Wang, Huan **S201**
 Wang, Jing **S267**
 Wang, Kai **S267**
 Wang, Marilene B. **S8, S34, S122, S143, S240, S260**
 Wang, Michele **S120**
 Wang, Simon **S11**
 Wang, Wei-Hsin **S147**
 Wangworawut, Yossawee **S69**
 Watanabe, Kentaro **S96**
- Webb, Timothy A **S227**
 Weber, Alizabeth **S47**
 Weingart, Jon **S46**
 Welz, Matthew **S72, S82**
 Wentland, Carissa **S217**
 White, Timothy G. **S88, S213**
 Whitmeyer, Max **S121**
 Wichova, Helena **S119**
 Wiet, R. Mark **S102, S121**
 Williams, Brian **S142, S153, S181, S221**
 Williams, Jeremy Clark Brian **S212**
 Willis, Shelby **S118**
 Willman, Tyler J. **S192**
 Willrich, Louise B. **S132**
 Wilson, Meghan N. **S51, S151**
 Wise, Sarah K. **S11**
 Witterick, Ian **S67, S71, S114**
 Wladis, Edward **S91**
 Wolfson, Racheal **S149**
 Wong, Amanda **S207**
 Wong, Andrew K. **S100, S255**
 Wong, Ricky H. **S100, S184, S255**
 Wongworawut, Yossawee **S16**
 Won, Tae-Bin **S143**
 Woodard, Troy D. **S173**
 Woodiwiss, Timothy **S60**
 Woodward, Eleanor **S94**
 Woo, Shiao **S221**
 Wroblewski, Tadeusz **S40, S59, S74**
 Wu, Ingrid **S206**
 Wu, Kyle C. **S33, S60**
 Wu, Tara J. **S8**
 Wu, Zhen **S146**
- Xia, Jimmy J. **S158**
 Xia, Yin **S145**
 Xie, Tong-Xin **S26**
 Xu, Alice **S147**
 Xue, Yubin **S145**
- Yamaguchi, Rei **S183**
 Yamamoto, Junichi **S83**
 Yamashita, Sojiro **S151**
 Yancey, Kristen **S104, S253**
 Yanez-Siller, Juan Carlos **S217**
 Yang, Gang **S90, S254**
 Yang, Isaac **S27, S98, S118, S136**
 Yan, Xukun **S145**
 Yarbrough, Wendell G. **S11**
 Yasaka, Tyler **S114, S133**
 Yawn, Robert J. **S104, S264**
 Ye, Donald **S17**
 Yen, Christine **S202**
 Yeo, Heegok **S142, S153**
 Yepes, Marta Vanesa Garcia **S206**
- Ye, Ting **S145**
 Yindeedej, Vich **S6**
 Yin, Ziyang **S110**
 Yoannidis, Tom **S67**
 Yong, William **S27**
 Yoo, Jihwan **S20**
 Yoshimoto, Yuhei **S183**
 Young, William F. **S52**
 Younus, Iyan **S5, S15, S25**
 Yu, Alexander **S93, S115**
 Yu, Hongmeng **S112, S201**
 Yu, Huapeng **S17**
 Yu, Justin **S48**
 Yun, In-Sik **S20**
 Yusin, Thomas **S248**
 Yusuf, Mehran **S221**
 Yusupov, Marat **S133**
- Zacharia, Brad E. **S51**
 Zachariah, Marcus A. **S3, S96, S125, S134, S188, S214**
 Zacharoulis, Stergios **S234**
 Zadeh, Gelareh **S67, S106, S114**
 Zaimoglu, Murat **S143**
 Zakaria, Jehad A. **S170**
 Zamora, Carlos **S108**
 Zanation, Adam M. **S3, S4, S8, S56, S83, S105, S208, S229**
 Zanaly, Mario **S108**
 Zanazzi, George J. **S234**
 Zappa, Francesca **S30**
 Zavadskiy, Gleb **S225, S271**
 Zazpe, Idoya **S248**
 Zeiger, Joshua **S228**
 Zenonos, Georgios **S31, S51, S57, S101, S141, S152, S265**
 Zhang, Ashley **S49**
 Zhang, Huankang **S17**
 Zhang, Jun-Ting **S146**
 Zhang, Wenying **S145**
 Zhang, Yawaei **S119**
 Zhang, Yawei **S20**
 Zhao, Kevin **S194, S202**
 Zhao, Lei **S164**
 Zhao, Tianna **S202**
 Zhao, Weidong **S201**
 Zhao, X. **S76**
 Zhao, Xiaochun **S60, S163**
 Zheng, Chunquan **S201**
 Zheng, Lijian **S164**
 Zhu, Alexander **S192**
 Zhu, Daniel **S207**
 Zhu, Hongwei **S81, S138**
 Ziegler, Andrea M. **S121, S219**
 Zimmer, Lee A. **S240**
 Zinzuwadia, Aniket **S96**
 Zoli, Matteo **S188**

Zomorodi, A.R. **S244**
Zomorodi, Ali **S242**
Zubimendi, Coro **S248**

Zuccarello, Mario **S147, S240, S241, S267**
Zuccato, Jeffrey **S114**
Zwagerman, Nathan T. **S22, S24, S60**